

High levels of carbonic anhydrase IX in tumour tissue and plasma are biomarkers of poor prognostic in patients with non-small cell lung cancer

M Ilie^{1,2,3}, NM Mazure^{3,4}, V Hofman^{1,2,3,5}, RE Ammadi^{3,6}, C Ortholan^{3,7}, C Bonnetaud⁵, K Havet¹, N Venissac^{2,3,8}, B Mograbi^{2,3}, J Mouroux^{2,3,8}, J Pouyssegur^{3,4} and P Hofman^{*,1,2,3,5}

¹Laboratory of Clinical and Experimental Pathology, Louis Pasteur Hospital, Nice, France; ²INSERM ERI-21/EA 4319, Faculty of Medicine, University of Nice Sophia Antipolis, Nice, France; ³University of Nice Sophia Antipolis, Nice, France; ⁴Institute of Developmental Biology and Cancer Research, University of Nice Sophia Antipolis and CNRS, UMR 6543, Nice, France; ⁵Human Tissue Biobank Unit/CRB INSERM, Louis Pasteur Hospital, Nice, France; ⁶Department of Mathematical Sciences, University of Nice Sophia Antipolis, Nice, France; ⁷Department of Radiotherapy, Antoine-Lacassagne Cancer Center, Nice, France; ⁸Department of Thoracic Surgery, Louis Pasteur Hospital, Nice, France

BACKGROUND: Carbonic anhydrase IX (CAIX) is an enzyme upregulated by hypoxia during tumour development and progression. This study was conducted to assess if the expression of CAIX in tumour tissue and/or plasma can be a prognostic factor in patients with non-small cell lung cancer (NSCLC).

METHODS: Tissue microarrays containing 555 NSCLC tissue samples were generated for quantification of CAIX expression. The plasma level of CAIX was determined by ELISA in 209 of these NSCLC patients and in 58 healthy individuals. The CAIX tissue immunostaining and plasma levels were correlated with clinicopathological factors and patient outcome.

RESULTS: CAIX tissue overexpression correlated with shorter overall survival (OS) ($P=0.05$) and disease-specific survival (DSS) of patients ($P=0.002$). The CAIX plasma level was significantly higher in patients with NSCLC than in healthy individuals ($P<0.001$). A high level of CAIX in the plasma of patients was associated with shorter OS ($P<0.001$) and DSS ($P<0.001$), mostly in early stage I+II NSCLC. Multivariate Cox analyses revealed that high CAIX tissue expression ($P=0.002$) was a factor of poor prognosis in patients with resectable NSCLC. In addition, a high CAIX plasma level was an independent variable predicting poor OS ($P<0.001$) in patients with NSCLC.

CONCLUSION: High expression of CAIX in tumour tissue is a predictor of worse survival, and a high CAIX plasma level is an independent prognostic biomarker in patients with NSCLC, in particular in early-stage I+II carcinomas.

British Journal of Cancer (2010) **102**, 1627–1635. doi:10.1038/sj.bjc.6605690 www.bjcancer.com

Published online 11 May 2010

© 2010 Cancer Research UK

Keywords: carbonic anhydrase IX; non-small cell lung cancer; tissue microarray; plasma; prognosis

Non-small cell lung cancer (NSCLC) comprises approximately 80% of lung cancers, and nearly 50% of patients with stage I NSCLC die within 10 years of diagnosis (Travis *et al*, 2004; Ou *et al*, 2007). Despite major advances in surgical techniques and new strategies of neoadjuvant treatment, long-term survival is achieved in only 5–10% of NSCLC patients (Stinchcombe and Socinski, 2009). In this regard, early biomarkers are urgently needed to allow better clinical management of patients with NSCLC.

Hypoxia is common in various types of solid cancers and is associated with a more aggressive phenotype (Brahimi-Horn *et al*, 2007). Stabilisation of the α -subunit of the hypoxia-inducible transcription factor 1 (HIF-1 α) is a critical step in the adaptation of tumour cells to hypoxia (Pouyssegur *et al*, 2006). One of the consequences of HIF-1 activation is upregulation of glycolysis and hence the production of lactic acid (Pastorekova *et al*, 2004).

The enzyme carbonic anhydrase IX (CAIX), which is expressed on the tumour cell surface, catalyses the hydration of cell-generated carbon dioxide into protons and bicarbonate ions (Pastorekova *et al*, 2004). This reaction contributes to an acidic extracellular microenvironment and intracellular alkalosis, allowing tumour cells to survive under hypoxic conditions, favouring tumour growth, invasion, and development (Chiche *et al*, 2009).

Subsequent studies have shown that CAIX is expressed in only a few normal tissues (mainly the gastrointestinal tract), whereas it is ectopically induced under hypoxic conditions and highly overexpressed in many different cancer cell lines and tumour tissues, where *ca9* is one of the most upregulated gene in a (HIF-1)-dependent manner (Wykoff *et al*, 2000). The expression of CAIX is strongly upregulated by hypoxia and is downregulated by the wild-type von Hippel-Lindau (pVHL) tumour suppressor protein (Ohh *et al*, 2000). CAIX has already been shown to serve as a surrogate marker of hypoxia and as a prognostic indicator for many cancers (Loncaster *et al*, 2001). In some cancer cells, the *VHL* gene is mutated leading to strong upregulation of CAIX (up to 150-fold) as a consequence of constitutive HIF-1 activation

*Correspondence: Dr P Hofman; E-mail: hofman.p@chu-nice.fr

Received 25 February 2010; revised 8 April 2010; accepted 15 April 2010; published online 11 May 2010

(Pouyssegur *et al*, 2006). A relationship between CAIX tumour tissue expression, as detected by immunohistochemistry (IHC) and patient outcome has been reported in a wide variety of tumours (Bui *et al*, 2003; Hedley *et al*, 2003; Trastour *et al*, 2007; Choi *et al*, 2008; Klatte *et al*, 2009; Korkeila *et al*, 2009). Previous studies have reported the prognostic relevance of CAIX overexpression in NSCLC indicating a potential oncogenic function of CAIX (Swinson *et al*, 2003; Kim *et al*, 2004; Kon-no *et al*, 2006). However, these studies performed only a limiting number of IHC analyses on surgical tumour samples.

Methods that use biological materials obtained by non-invasive procedures, like plasma, can be helpful in identifying possible biomarkers for early diagnosis and in the follow-up of patients with an increased cancer risk. CAIX is a multidomain protein consisting in an N-terminal proteoglycan-like (PG) domain, an extracellular catalytic domain (CA), a transmembrane segment (TM) and a C-terminal intracytoplasmic (IC) tail (Hilvo *et al*, 2008). Recent reports have provided evidence that the extracellular domain of CAIX can be released into body fluids of patients with kidney or bladder cancers and a high CAIX plasma level was associated with poor prognosis in these patients (Zavada *et al*, 2003; Hyrsil *et al*, 2009). However, the CAIX plasma level has not yet been evaluated in patients with NSCLC.

The aim of this study was to investigate the expression of CAIX in both tissue and plasma samples from a large cohort of NSCLC patients to explore the potential role of CAIX as a prognostic biomarker for NSCLC.

PATIENTS AND METHODS

Patients

Five hundred fifty-five patients who underwent surgery for NSCLC between January 2001 and January 2008 at the Pasteur Hospital (Department of Thoracic Surgery, University of Nice, France) were included in this study. The patients received the necessary information concerning the study and consent was obtained from each of them. The study was done with the approval of the ethics committee (CHU of Nice). The main clinical and histopathological data are summarised in Table 1. Morphological classification of the tumours was assigned according to the WHO criteria (Travis *et al*, 2004). The tumours were staged according to the international tumour-node-metastasis system (Mountain, 1997). The median follow-up at the time of analysis was 35 months (3–102 months) according to the method of Schemper and Smith, (1996). Among these patients, 122 of 555 (22%) died of lung cancer.

For the ELISA assay, 209 preoperative plasma samples were obtained from these patients. The main clinical and histopathological data are summarised in Table 2. The median follow-up was 15 months (1–66 months). Among these patients 14 of 209 (8%) died of lung cancer. Plasma samples from 58 healthy individuals were used as a control for the ELISA assay.

Tissue microarrays (TMAs) and immunohistochemistry

TMAs were constructed from archival paraffin-embedded, formalin-fixed tissue blocks. Representative tumour regions and adjacent normal lung tissue were selected for building TMAs and arrays were designed as previously described (Hofman *et al*, 2008). Immunohistochemistry for CAIX, HIF-1 α and Ki-67 was performed on serial 4- μ m deparaffinised TMA sections by using an automated single-staining procedure (Benchmark XT, Ventana Medical Systems, Roche Group Inc., Tucson, AR, USA). Briefly, a rabbit polyclonal anti-CAIX antibody (clone ab15086, diluted 1:2000, Abcam, Cambridge, MA, USA) was added to each slide

Table 1 Correlation of clinicopathological parameters with the CAIX expression level detected by immunohistochemistry in 555 NSCLC patients

Variables	Overall [†]	CAIX status		P-value
		Low [†]	High [†]	
Patient cohort	555			
Mean age (years) [‡]	63.9 \pm 9.3	64.5 \pm 8.4	65.3 \pm 5.6	0.196
Gender ^a				
Male	415 (75)	309 (74)	106 (26)	0.439
Female	140 (25)	111 (79)	29 (21)	
Smoking history ^a				
Never smoked	75 (14)	54 (72)	21 (28)	0.098
Former or current smokers	480 (86)	366 (76)	114 (24)	
Tumour size (cm) [‡]	3.7 \pm 2.4	3.8 \pm 2.3	4.1 \pm 2.1	0.293
Histological cell type ^a				
Adenocarcinoma	281 (50)	245 (87)	36 (13)	<0.001*
Squamous cell carcinoma	184 (33)	116 (63)	68 (37)	
Large cell carcinoma	43 (8)	27 (63)	16 (37)	
NOS	47 (9)	32 (68)	15 (32)	
pTNM stage ^a				
I	278 (50)	221 (79)	57 (21)	0.676
II	103 (19)	79 (77)	24 (23)	
III	151 (27)	116 (77)	35 (23)	
IV	23 (4)	16 (70)	7 (30)	
Histological grade ^a				
1	214 (38)	168 (78)	46 (22)	0.785
2	187 (34)	143 (76)	44 (24)	
3	137 (25)	101 (74)	36 (26)	
4	17 (3)	13 (76)	4 (24)	
Neoadjuvant therapy ^a	67 (12)	62 (92)	5 (8)	0.105

Abbreviations: NOS = not otherwise specified; TNM = tumour node metastasis. [†]Values expressed as n (%) or mean \pm s.d. ^a χ^2 -test. [‡]Mann–Whitney test. *P-value significant at the 0.05 level.

after blocking of endogenous peroxidase and proteins, and the sections were incubated with a biotinylated mouse anti-rabbit IgG (Abcam) as the secondary antibody. EDTA-pretreated sections were immunostained for HIF-1 α (mouse, clone 54; diluted 1:10; BD Biosciences, Heidelberg, Germany) and Ki-67 (rabbit, clone 30–9; diluted 1:100; Ventana Medical Systems). Paraffin-embedded sections from healthy lung tissue exposed under normoxic/hypoxic conditions were stained for BNIP3 (rabbit, clone ANa40; diluted 1:250; Sigma-Aldrich, St Louis, MI, USA) and BNIP3L (rabbit, polyclonal; diluted 1:250, Sigma-Aldrich). 3–3'-diaminobenzidine (Sigma-Aldrich) was the chromogen used in all reactions. Positive controls for CAIX were biopsy cores of head and neck squamous cell carcinoma, which has previously been established as positive for CAIX (Koukourakis *et al*, 2001).

Automated image analysis

After antibody staining, images were acquired using automated quantitative analysis (Hofman *et al*, 2008). The CAIX signal was measured on a grayscale of 0 (black) to 255 (white) and expressed as target signal intensity relative to plasma membrane compartment area. Grey values ranged between 0 and 152, and a value superior or equal to 50 was arbitrarily defined as CAIX overexpression. In addition, the cut-off values for the different markers were: \geq 35 grey levels for HIF-1 α and \geq 10% for Ki-67. Staining intensity was based on a scale from 0 to 3 and the percentage of positive cells (0 < 1%, 1 = 1–10%, 2 = 10–50%,

Table 2 Correlation of clinicopathological parameters with the CAIX plasma level detected by ELISA in 209 NSCLC patients

Variables	Overall†	Mean CAIX level (pg ml ⁻¹)	P-value
Patient cohort	209		
Mean age (years) ^a	64 ± 9.18		0.172
Gender ‡			
Male	143 (68)	45.73	0.290
Female	66 (32)	43.15	
Smoking status‡			
Never smoked	21 (10)	32.37	0.330
Former or current smokers	188 (90)	46.34	
Tumour size (cm) ^a	4.0 ± 2.4		0.042*
Histological cell type‡			
Adenocarcinoma	109 (52)	43.63	0.280
Squamous cell carcinoma	60 (29)	51.11	
Large cell carcinoma	13 (6)	39.76	
NOS	27 (13)	37.41	
pTNM stage‡			
I	102 (49)	42.25	0.448
II	40 (19)	53.21	
III	52 (25)	43.14	
IV	15 (7)	57.19	
Histological grade‡			
1	77 (37)	50.87	0.420
2	65 (31)	41.21	
3	48 (22)	36.85	
4	19 (9)	31.32	
Neoadjuvant therapy‡	23 (11)	40.04	0.124

Abbreviations: NOS = not otherwise specified; TNM = tumour node metastasis. †Values expressed as n (%) or mean ± s.d. ^aPearson test. ‡Mann–Whitney test. *P-value significant at the 0.05 level.

3 > 50%). The product of the intensity of staining and the percentage of tumour-positive cells was then calculated to produce an IHC score of 0 to 300, as previously described (Hassan *et al*, 2008). An IHC score > 40 distinguished low from high expression of CAIX (Lancaster *et al*, 2001). Nuclear staining in more than 50% of positive cells for HIF-1 α and a labeling index of Ki-67 \geq 10% defined overexpression of both markers (Zhong *et al*, 1999; Woo *et al*, 2009). The overall score used for statistical analysis was the mean value from three spots of the same tumour. In parallel, whole-tissue sections from tumour blocks of a subset of 40 cases were stained for each marker and compared with the corresponding TMA spots using the above-mentioned scoring criteria.

Cell culture and hypoxic exposure

The A549 lung cancer cell line (European Collection of Cell Cultures, ECACC; passage 90, Sigma-Aldrich) was maintained in RPMI 1640 supplemented with 10% FCS. Incubation in hypoxia at 1% O₂ was carried out at 37°C in 95% humidity and 5% CO₂/94% N₂ in a sealed anaerobic workstation (*in vivo* 400; Ruskin Technologies, Bridgend, UK).

Plasma CAIX ELISA immunoassay

Peripheral blood (5 ml) was taken before surgery and kept in a heparinised tube. Within 30 min of blood collection, the samples were centrifuged at 3000 r.p.m. at 4°C for 10 min to separate the plasma and blood cells. For detection of the soluble form of CAIX,

we used as an internal positive control, the culture medium of A549 cells incubated in hypoxic conditions for 48 h (Ruskin Technologies).

ELISA commercial kits for the quantitative determination of plasma CAIX concentrations were used according to the manufacturer's instructions (R&D Systems, Minneapolis, MN, USA). Test samples (100 μ l) were pipetted into the wells and incubated for 2 h at room temperature on a horizontal orbital microplate shaker (0.12" orbit) set at 500 \pm 50 r.p.m. The optical density of each well was determined using a spectrophotometer microplate reader (Bioelisa-iEMS Reader MF, Logiciel Ascent Software v2.6, LabSystems, Helsinki, Finland) set to 450 nm. Results were compared with standard curves. Measurements were done in duplicate.

Statistical methods

Analyses were performed using SPSS 16.0 statistical software (SPSS Inc., Chicago, IL, USA). We used the χ^2 and Mann–Whitney tests to explore the association between tissue CAIX expression and the clinicopathological variables of patients. The Mann–Whitney and the Pearson tests were applied to assess the association between clinicopathological variables and the CAIX plasma level. The coefficient of correlation (*r*) between the expression of proteins was calculated using the Spearman's Rank test. The optimal sensitivity and specificity of plasma CAIX were determined by ROC curve analysis. In addition, the χ^2 analysis was used to determine correlations between the immunohistochemical analysis of CAIX tissue tumour expression and the plasma CAIX ELISA assay. The degree of agreement between data from whole-tissue sections and the mean value of three spots was assessed using the Cohen's κ coefficient. Survival rates were estimated using the Kaplan–Meier method and were compared with the Log-Rank test to determine significance. The univariate and multivariate Cox proportional hazard models were used to determine the relative risk. Variables that were associated with survival with a *P*-value < 0.20 in the univariate analysis were included in a multivariate regression. The variables included in the model for DSS and overall survival (OS) were pTNM stage, histological cell type and grade. All statistical tests were two-sided, and a significant *P*-value was set at the 0.05 level.

RESULTS

Immunohistochemical analysis of tissue microarrays and correlation with the clinicopathological status

Negative or weak, intermediate, and strong CAIX membrane staining was revealed among the different NSCLC tumours (Figure 1A–P). In NSCLC the staining pattern for CAIX was membranous as observed in biopsy cores of head and neck carcinoma, used as positive control (Figure 1S–T). Tissue core biopsies taken from normal lung tissue were negative for CAIX expression (Figure 1Q–R).

Here, 135 of 555 (24.3%) tumours were designated as CAIX overexpressing (Table 1). High CAIX expression was significantly associated with histological subtypes (*P* < 0.001). Sixty-eight (37%) of 184 squamous cell carcinomas and 16 (37%) of 43 large cell carcinomas overexpressed CAIX, whereas 36 (13%) of 281 adenocarcinomas overexpressed CAIX (*P* < 0.001). No significant correlation was found between the CAIX status and the other clinicopathological variables (Table 1).

As for CAIX expression, the same immunostaining intensity pattern was observed for HIF-1 α and Ki-67 expression, which showed a nuclear staining (Supplementary Figure S1), where 133 of 555 (24%) tumours showed high HIF-1 α immunoreactivity (Supplementary Table S1). HIF-1 α -positive staining was associated

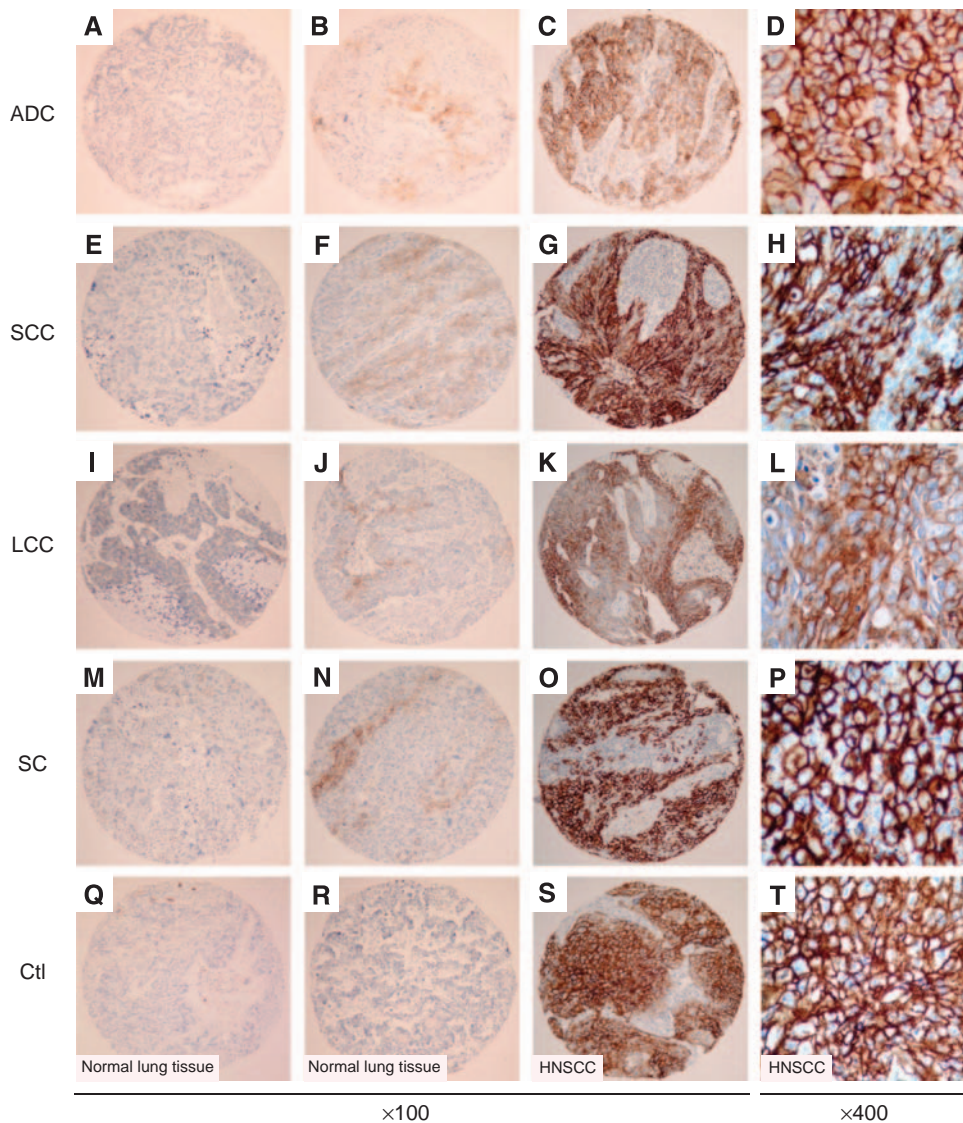


Figure 1 CAIX expression detected by immunohistochemistry in tissue microarray cores. Staining levels for CAIX in NSCLC histological subtypes: low (**A, E, I, M**), intermediate (**B, F, J, N**) and strong (**C, G, K, O**). CAIX membrane staining in adenocarcinoma (ADC) (**A–D**), squamous cell carcinoma (SCC) (**E–H**), large cell carcinoma (LCC) (**I–L**), and sarcomatoid carcinoma (SC) (**M–P**). Normal bronchial epithelium (**Q**) and alveolar tissue (**R**) are devoid of staining. Strong membrane staining in head and neck squamous cell carcinoma (HNSCC) cores used as positive control of CAIX immunostaining (**S–T**). Panels **D, H, L, P** and **T** are higher magnifications showing details of cells within the corresponding tumour shown on panels **C, G, K, O**, and **S**, respectively.

with the histological cell type, being mainly expressed in non-adenocarcinoma subtypes ($P < 0.001$) and in poorly differentiated tumours ($P = 0.0001$) (Supplementary Table S1).

CAIX, HIF-1 α , and Ki-67 expression levels observed in the TMA spots faithfully reflected the staining intensity of these proteins in whole-tissue sections from corresponding tumour blocks in a subset of 40 tumours ($\kappa = 0.89$; data not shown).

Association of CAIX tumour expression with hypoxia and proliferation

To assess the interrelationship between CAIX expression and hypoxia or proliferation, the CAIX expression level was compared with that of the HIF-1 α and Ki-67 index, respectively, by using the Spearman's Rank test (Supplementary Figure S2). High CAIX expression partially correlated with high HIF-1 α expression ($r = 0.099$, $P = 0.023$). In exchange, a χ^2 -test revealed significant

association between these categorical variables ($P = 0.036$). There was a strong positive correlation between the CAIX expression and the Ki-67 index ($r = 0.211$, $P < 0.001$).

Plasma level of CAIX in patients with NSCLC

In patients with NSCLC, the mean value of CAIX in plasma was 45.40 pg/ml (range: 0–372.89 pg ml $^{-1}$) and was significantly higher than in healthy individuals (mean = 2.48 pg ml $^{-1}$, range: 0–16.65 pg ml $^{-1}$) ($P < 0.001$) (Figure 2A).

The subtended area of the ROC curve shows a synthetic index of the overall capacity of the test in differentiating between healthy individuals and NSCLC patients (Figure 2B). The area under the ROC curve was 0.93 (CI = 0.906–0.953, $P < 0.001$). Using the results of the ROC curve, an analysis was made on the test performance with respect to the different threshold values, which showed that for a threshold equal to 11 pg ml $^{-1}$, plasma;

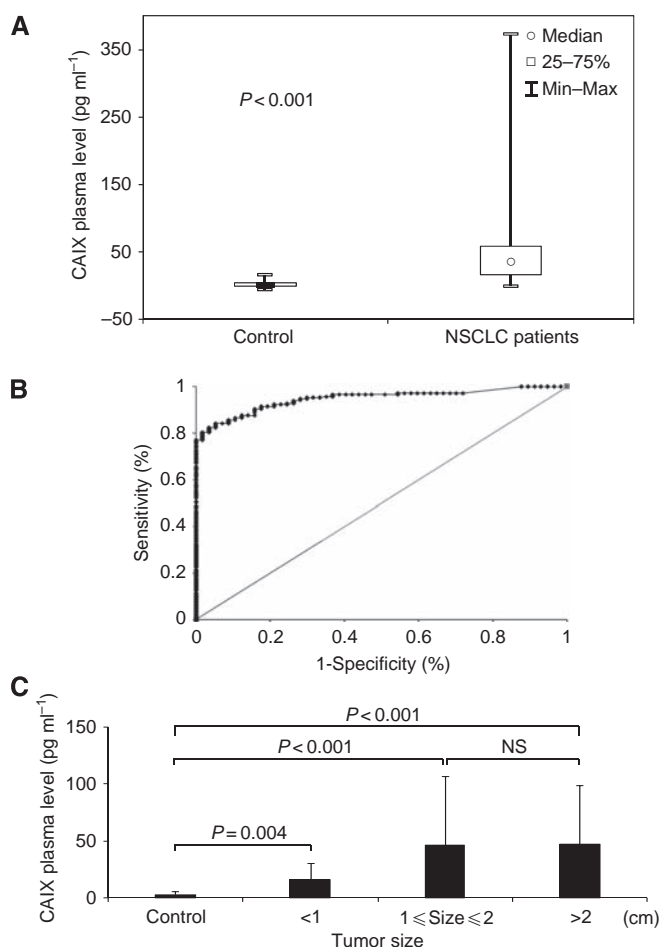


Figure 2 Quantitative evaluation of the plasma CAIX level by ELISA in patients with NSCLC and in healthy controls. **(A)** Box plots showing median (central dots), 25–75% quartile ranges (boxes), and minimum/maximum levels (whiskers) of plasma CAIX levels in healthy individuals ($n=58$) vs patients with NSCLC ($n=209$). **(B)** ROC curve analysis of CAIX as a plasma marker for NSCLC. X axis, 1-specificity; y axis, sensitivity. **(C)** Plasma concentration of CAIX according to tumour size in NSCLC and in healthy individuals. NS; non significant.

CAIX had a sensitivity of 84% and a specificity of 95% (Supplementary Table S2). Based at this cutoff we obtained a positive predictive value of 98% and a negative predictive value of 62%.

The mean value of CAIX in plasma obtained from NSCLC tumours inferior to 1 cm ($n=29$) was 28.22 pg ml^{-1} and remained significantly higher when compared with the mean value of CAIX in plasma obtained from the control group (2.48 pg ml^{-1} , $n=58$, $P=0.004$) (Figure 2C).

The CAIX plasma level was significantly correlated to tumour size ($P=0.042$) (Table 2). No significant association with age, gender, smoking status, histological subtypes, or histological grade of the tumours was noted (Table 2).

Association of the CAIX concentration in plasma with hypoxia and proliferation

The CAIX plasma level was compared with HIF-1 α expression and the Ki-67 tumour tissues index using the Spearman's Rank test. There was no significant correlation of the CAIX plasma level with these molecules (HIF-1 α ; $r=0.04$; $P=0.90$; and Ki-67; $r=-0.02$; $P=0.82$, respectively; data not shown).

Relationship between CAIX tumour expression and outcome of patients with NSCLC

The status of CAIX as determined by immunohistochemistry on TMA was evaluated by Kaplan–Meier analysis for association with OS and DSS. We found that CAIX overexpression was significantly associated with shorter OS when compared with low CAIX expression levels (median survival time; 42 vs 55 months) ($P=0.05$) (Figure 3A). The univariate analysis revealed that CAIX overexpression was significantly associated with worse DSS (median survival time; 44 vs 61 months; $P=0.002$) (Figure 3B). In addition, the OS of stage I + II tumours was significantly shorter among patients overexpressing CAIX (median survival time; 44 vs 59 months) ($P=0.034$). However, no significant difference was noted in later stage III + IV tumours (median survival time; 32 vs 37 months) ($P=0.56$). The DSS of stage I + II tumours was significantly shorter for those overexpressing CAIX (median survival time; 48 vs 75 months) ($P=0.001$). However, no significant differences were noted in later stage III + IV tumours (median survival time; 36 vs 37 months) ($P=0.290$). Subsequently, a multivariate survival analysis using the Cox's proportional hazard model was performed to examine the importance of CAIX expression in patient outcome when other prognostic factors were included (Table 3). CAIX overexpression (RR = 0.503, CI = 0.323–0.782, $P=0.002$), the disease stage (RR = 0.388, CI = 0.268–0.562, $P=0.001$) and the histological grade (RR = 0.611, CI = 0.409–0.914, $P=0.016$) were significantly independent prognostic factors of DSS. CAIX overexpression showed a trend as an independent prognostic factor of OS (RR = 0.700, CI = 0.471–1.041, $P=0.068$).

With regard to the correlation between CAIX and HIF-1 α tissue expression, the Kaplan–Meier analysis showed a trend towards worse OS and DSS for patients with both high HIF-1 α and CAIX expression ($P=0.087$ and $P=0.07$, respectively) (Supplementary Figure S3A, B). In addition, when HIF-1 α overexpression was evaluated by univariate analysis for a relationship to outcome according to different histological subtypes, there was a trend towards worse DSS in squamous cell carcinomas (median survival time; 52 vs 62 months) ($P=0.07$). In contrast, HIF-1 α overexpression was not significantly associated with survival of NSCLC patients according to the Kaplan–Meier method or by multivariate Cox analysis ($P=0.51$; $P=0.57$, respectively) (Supplementary Figure S4, Supplementary Table S3).

The CAIX level in plasma as a biomarker of poor prognosis in patients with NSCLC

Using an empirical thresholding method, we determined a threshold of 100 pg ml^{-1} (>90% plasma CAIX, as an ideal cut off for stratification of patient survival. The mean plasma CAIX level $>100 \text{ pg ml}^{-1}$ was considered as a high level of CAIX, whereas that of $\leq 100 \text{ pg ml}^{-1}$ was considered as a low CAIX level. A high plasma CAIX level significantly correlated with decreased OS ($P<0.001$) (Figure 3C) and DSS ($P<0.001$) (Figure 3D). The OS of early-stage I + II tumours was significantly shorter among those with a high CAIX plasma level ($P=0.003$), but there was no significant difference in later stage III + IV tumours ($P=0.51$). In addition, the DSS of early-stage I + II tumours was significantly shorter among those with a high level of CAIX in the plasma ($P<0.001$) when compared with later stage III + IV tumours in which high CAIX was no longer associated with survival ($P=0.23$).

Multivariate analyses correlating histological subtypes, disease stage, histological grade, and a high CAIX plasma level, showed that a high CAIX plasma level was an independent prognostic factor for OS (RR = 0.296, CI = 0.119–0.736, $P=0.009$) and DSS (RR = 0.102, CI = 0.032–0.330, $P<0.001$) (Table 3).

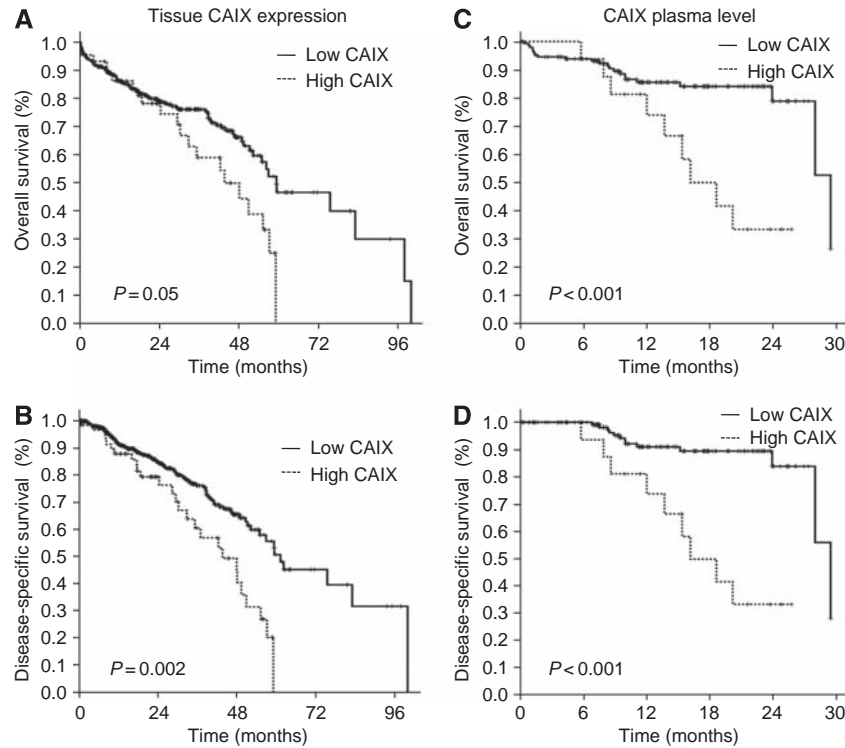


Figure 3 Kaplan–Meier curves of overall survival (top panels **A** and **C**), and disease-specific survival (bottom panels **B** and **D**) duration stratified according to the tissue CAIX expression detected by immunohistochemistry (left panels **A** and **B**) and the plasma CAIX levels as determined by ELISA (right panels **C** and **D**). The cut-off value for the CAIX immunostaining score was arbitrarily defined as superior or equal to 45 grey levels. The cut-off point for the CAIX plasma levels was empirically defined as superior or equal to 100 $\mu\text{g ml}^{-1}$. The curves are labelled with the corresponding scores.

Table 3 Multivariate Cox regression analysis of tumour tissue and plasma CAIX levels expression for OS and DSS in patients with NSCLC

Variables ^a	Overall survival			Disease-specific survival		
	RR	(95% CI)	P-value	RR	(95% CI)	P-value
Histologic cell type	0.612	0.363–1.032	0.065	0.619	0.328–1.171	0.140
pTNM stage	0.424	0.314–0.572	0.001*	0.388	0.268–0.562	0.001*
Histologic grade	0.663	0.479–0.919	0.014*	0.611	0.409–0.914	0.016*
High CAIX tissue expression	0.700	0.471–1.041	0.068	0.503	0.323–0.782	0.002*
Histologic cell type	0.391	0.114–1.345	0.136	0.497	0.105–2.364	0.380
pTNM stage	0.509	0.229–1.130	0.097	0.480	0.166–1.389	0.176
Histologic grade	0.538	0.202–1.435	0.215	0.254	0.074–0.871	0.029*
High plasma CAIX	0.296	0.119–0.736	0.009*	0.102	0.032–0.330	<0.001*

Abbreviations: CI = confidence interval; TNM = tumour node metastasis. ^aCoding of variables: Histological cell type was coded as 1 (ADC) and 2 (non-ADC). pTNM stage was coded 1 (stages I+II) and 2 (stages III+IV). Histological grade was coded 1 (grades 1 and 2) and 2 (grades 3 and 4). *P-value significant at the 0.05 level.

Expression of CAIX in tumour samples vs the level of CAIX in plasma

A χ^2 -test was used to compare CAIX immunostaining expression in tumour samples with the CAIX values in plasma from 125 patients for whom we have performed in parallel both measurements. We found no significant association ($P=0.919$) (Supplementary Table S4). Here, 90 of 125 (72%) patients had low CAIX tumour expression, but it is noteworthy that they still showed a high level of CAIX in their plasma (Supplementary Table S4). Among these patients, 28 of 90 (31%) had lymph node (pN1/pN2) or secondary metastatic sites (pM1).

DISCUSSION

Hypoxia is involved in biological processes promoting tumour progression and stabilises HIF-1 α , thereby controlling expression

of around a hundred genes involved in tumour metabolism, pH regulation, angiogenesis, migration, and invasion, including the membrane-associated CAIX protein (Semenza, 2003). CAIX was proposed as a surrogate marker of hypoxia and is strongly dependent on HIF-1 activation for expression (Beasley *et al*, 2001).

We showed that 135 of 555 (24.3%) NSCLC tumours overexpress CAIX. In a previous series concerning 134 lung adenocarcinomas, CAIX was overexpressed in 24.6% of cases (Kon-no *et al*, 2006). In this work, there was a significantly higher expression of CAIX in the non-adenocarcinoma histological subtypes ($P < 0.001$), as described (Kim *et al*, 2005). This is probably because of the fact that SCC and LCC are frequently accompanied by necrosis and CAIX is expressed predominantly around necrotic regions. This peri-necrotic expression reflects the association of tissue tumour CAIX with hypoxia (Kim *et al*, 2004). In our study, this was supported by the positive correlation between immunostaining for CAIX and HIF-1 α expression in tumour tissue ($P=0.036$).

There was no association of the CAIX level in tumour tissues with smoking status. The occurrence of mild hypoxic condition in smokers cannot be excluded and this could be the explanation of a mechanism of adaptation, and therefore no increase in CAIX expression, because of a reduced O₂ supply.

The interest into CAIX expression as a prognostic factor is currently expanding and targeted therapies directed specifically to CAIX are being developed (Supuran, 2008). We showed that CAIX tumour tissue expression is an independent prognostic factor for DSS in patients with NSCLC. High CAIX expression in tissues is a poor prognostic factor especially in early-stage I + II NSCLC for OS ($P = 0.034$), and DSS ($P = 0.001$). This is in agreement with its role in early tumourigenesis (Liao & Stanbridge, 2000). These findings are consistent with previous reports on the prognostic value of CAIX for early I/II stage resected NSCLC, in which the percentage of CAIX-positive cells was significantly associated with decreased OS (Kim *et al*, 2004). Kim *et al* (2005), reported that only a percentage of CAIX-positive cells, and not the intensity of staining, correlated with post-operative recurrence and DSS in 74 patients with early-stage NSCLC. In addition, when the perinuclear pattern of expression was considered, Swinson *et al* (2003) showed that CAIX was an independent prognostic factor for poor OS in 175 patients with NSCLC. In the same study, cytoplasmic CAIX and stromal expression were not associated with outcome, and there was only a trend towards poor prognosis for high membranous levels of CAIX in patients (Swinson *et al*, 2003). High expression of the full-length (FL) CAIX isoform was related to reduced survival of patients (Simi *et al*, 2006). Besides the expected FL mRNA, a CAIX alternative splicing isoform was detected in normal and in cancer cells, independently of the levels of hypoxia (Barathova *et al*, 2008). This alternative splicing (AS) generates a transcript lacking exons 8–9 and encodes a truncated CAIX protein lacking the transmembrane region, the intracellular tail and the C-terminal part of the catalytic domain. The expression of AS CAIX mRNA was not related to survival (Malentacchi *et al*, 2009). Overall, the antigen expression is not so homogenous and membranous CAIX expression seems to be detected more often than cytoplasmic or perinuclear CAIX expression in NSCLC. Moreover, various commercial antibodies could be the link to heterogeneous patterns of CAIX expression and therefore with a great variability in terms of outcome. Although there is a general agreement that detection of CAIX by IHC could predict poor prognosis in patients with NSCLC, most studies were limited in size and had low statistical power. The differences between our study and similar previously reported IHC studies are the large number of cases and the use of a high throughput TMA analysis with automatic quantification of signals to evaluate CAIX expression in NSCLC. We strongly believe that in a large number of NSCLC cases we were able to prove that the detection of the membranous CAIX expression on TMA can be used as a poor prognostic factor in NSCLC.

In this work, HIF-1 α positive immunolabelling significantly correlated to the histological subtype ($P < 0.001$), being mostly expressed in SCC, as already reported (Swinson *et al*, 2004). It was also related to poorly differentiated tumours ($P = 0.0001$), as already shown in different types of tumours (Couvelard *et al*, 2005; Trastour *et al*, 2007). These findings may reflect the existence of alternative regulatory modes of HIF-1 α . HIF-1 α overexpression showed a trend toward poor survival only in SCC. However, there was no significant relationship between HIF-1 α overexpression and survival of all NSCLC patients. Our findings are supported by those of Lee *et al* (2003) who showed no association between HIF-1 α expression and overall survival in 84 NSCLC patients. In contrast to our results, other groups reported a significant relationship between HIF-1 α expression and shorter survival (Swinson *et al*, 2004; Kim *et al*, 2005). Swinson *et al* (2004) reported that only when a high positive cutoff $\geq 60\%$ for HIF-1 α expression was used there was a significant relationship to poor

outcome of 172 NSCLC patients. In contrast, when a cutoff \geq median (5%) was used as a cutoff to define negative or positive HIF-1 α staining, it was no longer related to poor survival. Kim *et al* (2005) also reported a significant association between HIF-1 α overexpression with a cutoff $\geq 51.3\%$ and tumour progression in a series of 74 NSCLC patients. Taken together, HIF-1 α expression was reported to be associated with poor outcome of NSCLC patients in series that used high cut-off values and also showed a strong relationship to SCC (Swinson *et al*, 2004). These results are supported by other studies that showed a significant association between high HIF-1 α expression and shorter survival in SCC of the head and neck (Schrijvers *et al*, 2008). However, these results are in disagreement with those of Volm & Koomagi (2000) who showed that NSCLC patients with HIF-1 α -positive carcinomas had significantly longer median survival times than patients with HIF-1 α -negative carcinomas. There may be methodological and biological explanations for some discrepancies in the results observed in this study. One of the issues resides in the very short half-life of HIF-1 α (< 10 min), whereas the half-life of CAIX is more than 24 h (Rafajova *et al*, 2004). The second limitation resides in the sensitivity of antibodies used for immunohistochemistry. Anti-HIF-1 α antibodies have always been problematic, whereas the immunogenicity of the CAIX antibody is excellent with no non-specificity (Lam *et al*, 2005). Also, the variability in the results may be due to the cut-off point used to define cases as overexpressing HIF-1 α . In this study, we have used a 45 grey-levels threshold for a semi-automated analysis corresponding to a cutoff $\geq 18\%$. This is somewhat lower than that used in several studies showing a strong correlation with poor outcome.

One explanation for CAIX being discriminatory as a prognostic biomarker resides in the fact that all cells exposed to hypoxia, and therefore to a rapid proliferation, will become hypoxic and HIF-1 α positive, but not necessarily CAIX positive. In many tissues, HIF-1 α may not be sufficient to induce CAIX and only several oncogenic steps associated to epigenetic changes leading to chromatin remodeling will 'uncover' the *ca9* gene and make it permissive and inducible by HIF-1. We hypothesize that NSCLC in which CAIX is expressed present a more aggressive phenotype. This hypothesis is supported by our data on healthy lung tissue exposed to hypoxia (1% O₂) for 24 h. Although hypoxia-induced HIF-1 α stabilisation was detected by IHC on normal tissue, there was no CAIX expression (Supplementary Figure S5). Instead, we observed increased expression of BNIP3 and BNIP3L, two proteins whose expression is enhanced by HIF-1 (Guo *et al*, 2001). In this regard, further studies must be performed to check BNIP3 and BNIP3L status in the different tumour tissues. Moreover, for the subpopulation with high HIF-1 α expression, we showed that HIF-1 α required CAIX expression to predict a trend towards poor OS and DSS. This may suggest that expression of HIF-1 α alone may not be enough to affect the malignant potential of all NSCLC, but rather requires the expression of HIF-1 α -regulated genes.

Recent studies have shown that soluble CAIX is being shed from the tumour cells into the culture medium and plasma or urine of renal cancer patients (21). This corresponds to the extracellular part of the CAIX molecule, which is composed of the proteoglycan (PG)-like and CA domains that are cleaved off the plasma membrane (Zavada *et al*, 2003). Our study reports that the plasma CAIX level in NSCLC patients is significantly higher than in healthy individuals ($P < 0.001$). Nevertheless, we showed that the plasma CAIX detected in patients with NSCLC is much lower than CAIX concentrations described in renal cell carcinoma, because the very high constitutive HIF-1 α levels in these latter tumours and also differences in CAIX expression depending on the cell type (Li *et al*, 2008). Increased levels of plasma CAIX have been reported only in urological cancers (Zavada *et al*, 2003; Li *et al*, 2008; Hyrsil *et al*, 2009). Thus, our report is the first study to show evidence of high CAIX levels in the plasma of NSCLC patients. Our data show that the CAIX ELISA had a very good sensitivity

(84%) and specificity (95%). Moreover, even for tumours inferior to 1 cm in size, the mean value of CAIX was significantly higher when compared with the mean value of CAIX plasma in the control group. It appears that there is no increase in CAIX in the plasma of patients bearing tumours larger than 2 cm when compared with smaller tumours (<1 cm). This is unlikely to be explained by the loss of differentiation because in our study there was no correlation with the histological grade. In the earlier stages of tumour progression, conditions such as hypoxia or ischemia may induce a high CAIX plasma level as an adaptation to confer a proliferative advantage for tumour growth and spread. However, when this malignant potential is attained in later stages of tumour growth, continued shedding of CAIX into the plasma might no longer be required. The difference in the CAIX plasma level may reflect distinct molecular pathways and genetic alterations that impact small-sized tumours, which may determine the subsequent development and risk of progression, as already suggested for bladder cancers (Turner *et al*, 2002). On the other hand, the cumulative effects of genetic lesions involved in cancer progression could alter the pathways of the hypoxic response and therefore could affect the CAIX plasma level (Rak *et al*, 2002). This is in agreement with the lack of correlation between the plasma CAIX level and Ki-67 index observed in our study. Surprisingly, the CAIX plasma level was not related to HIF-1 α detection as observed with IHC ($r=0.04$, $P=0.90$). Moreover, there was no correlation with SCC or LCC subtypes as we observed in the case of immunodetected CAIX. With regard to the relationship between membranous CAIX and HIF-1 α detection, this finding is raising a question on whether and how HIF-1 α could influence the CAIX shedding from tumour cell surface.

Although our observations were inconsistent with the proposal that hypoxia and HIF-1 are the sole regulators of CAIX expression and thus shedding (Zatovicova *et al*, 2005), one cannot exclude that shedding occurs at hypoxic metastatic sites. Although the precise molecular mechanism of regulated CAIX shedding remains to be clarified, previous studies showed that dysregulation of HIF-1 α could be caused by mutation in the von Hippel-Lindau (*VHL*) tumour suppressor gene or activation of the epidermal growth factor receptor (EGFR) (Semenza, 2003). Mutated *VHL* prevents appropriate normoxic degradation of HIF-1 α and, as such, CAIX is highly expressed in mutated *VHL*-related tumours, independently of the extent of tumour necrosis (Swinson *et al*, 2003). *VHL* gene mutations have been previously shown in a proportion of cell lines derived from small-cell lung cancer, NSCLC, carcinoids, and mesotheliomas (Sekido *et al*, 1994). *VHL* mutations may be present in a subgroup of patients with negative

CAIX expression in tumour tissue but with a high plasma level of CAIX. With regard to EGFR signaling, *in vitro* studies showed that signaling through the EGF pathway by phosphorylation of a cytoplasmic tyrosine residue of CAIX may either activate CAIX or enhance its expression (Dorai *et al*, 2005). In addition, phosphorylation activates phosphatidylinositol 3-kinase, resulting in phosphorylation of Akt and cancer cell survival (Dorai *et al*, 2005). This suggests that EGFR activation may also increase induction of CAIX, and therefore the shedding of the CAIX ectodomain. Moreover, the basal level of tissue CAIX may be sufficient for shedding and the soluble form of CAIX may finally represent tumour progression. Our results support this hypothesis as we showed that a high plasma CAIX level was an independent prognostic factor significantly related to worse OS and DSS of early-stage I + II NSCLC when compared with later stage III + IV NSCLC.

When the correlation between CAIX expression levels as determined by ELISA and immunohistochemistry was assessed, we did not find any relationship. This indicates that the two methods are not directly interchangeable and that their value for clinical purposes may be different. Overall, when we take into account the intratumoural heterogeneity and the different controversial results regarding the value of tissue tumour CAIX expression as a prognostic factor, we postulate that the detection of the soluble form of CAIX in plasma patients can be a more reliable prognostic factor of worse OS and DSS in patients with early-stage NSCLC.

This study shows that CAIX tumour tissue expression as detected by immunohistochemistry on TMA, can serve as an important predictor for survival in patients with NSCLC. Moreover, we showed that the plasma CAIX level is an independent prognostic factor in early-stage NSCLC. Our results support the high specificity and the potentiality of plasma CAIX as a helpful clinical biomarker for detection of NSCLC at an early stage.

ACKNOWLEDGEMENTS

MI is supported by a Grant from INCa (2008). PH, VH, JM and NV are supported by a PHRC Grant (2003 CHU of Nice) and by the Canceropôle PACA (PROCAN 2008–2011, Axe II). NM and JP are supported by METOXIA (EU-FP7) and ANR.

Supplementary Information accompanies the paper on British Journal of Cancer website (<http://www.nature.com/bjc>)

REFERENCES

- Barathova M, Takacova M, Holotnakova T, Gibadulinova A, Ohradanova A, Zatovicova M, Hulikova A, Kopacek J, Parkkila S, Supuran CT, Pastorekova S, Pastorek J (2008) Alternative splicing variant of the hypoxia marker carbonic anhydrase IX expressed independently of hypoxia and tumour phenotype. *Br J Cancer* **98**: 129–136
- Beasley NJ, Wykoff CC, Watson PH, Leek R, Turley H, Gatter K, Pastorek J, Cox GJ, Ratcliffe P, Harris AL (2001) Carbonic anhydrase IX, an endogenous hypoxia marker, expression in head and neck squamous cell carcinoma and its relationship to hypoxia, necrosis, and microvessel density. *Cancer Res* **61**: 5262–5267
- Brahimi-Horn MC, Chiche J, Pouyssegur J (2007) Hypoxia and cancer. *J Mol Med* **85**: 1301–1307
- Bui MH, Seligson D, Han KR, Pantuck AJ, Dorey FJ, Huang Y, Horvath S, Leibovich BC, Chopra S, Liao SY, Stanbridge E, Lerman MI, Palotie A, Figlin RA, Belldegrun AS (2003) Carbonic anhydrase IX is an independent predictor of survival in advanced renal clear cell carcinoma: implications for prognosis and therapy. *Clin Cancer Res* **9**: 802–811
- Chiche J, Ilc K, Laferrriere J, Trottier E, Dayan F, Mazure NM, Brahimi-Horn MC, Pouyssegur J (2009) Hypoxia-inducible carbonic anhydrase IX and XII promote tumor cell growth by counteracting acidosis through the regulation of the intracellular pH. *Cancer Res* **69**: 358–368
- Choi SW, Kim JY, Park JY, Cha IH, Kim J, Lee S (2008) Expression of carbonic anhydrase IX is associated with postoperative recurrence and poor prognosis in surgically treated oral squamous cell carcinoma. *Hum Pathol* **39**: 1317–1322
- Couvelard A, O'Toole D, Turley H, Leek R, Sauvanet A, Degott C, Ruzniewski P, Belghiti J, Harris AL, Gatter K, Pezzella F (2005) Microvascular density and hypoxia-inducible factor pathway in pancreatic endocrine tumours: negative correlation of microvascular density and VEGF expression with tumour progression. *Br J Cancer* **92**: 94–101
- Dorai T, Sawczuk IS, Pastorek J, Wiernik PH, Dutcher JP (2005) The role of carbonic anhydrase IX overexpression in kidney cancer. *Eur J Cancer* **41**: 2935–2947
- Guo K, Searfoss G, Krolkowski D, Pagnoni M, Franks C, Clark K, Yu KT, Jaye M, Ivashchenko Y (2001) Hypoxia induces the expression of the pro-apoptotic gene BNIP3. *Cell Death Differ* **8**: 367–376
- Hassan S, Ferrario C, Mamo A, Basik M (2008) Tissue microarrays: emerging standard for biomarker validation. *Curr Opin Biotechnol* **19**: 19–25

- Hedley D, Pintilie M, Woo J, Morrison A, Birlle D, Fyles A, Milosevic M, Hill R (2003) Carbonic anhydrase IX expression, hypoxia, and prognosis in patients with uterine cervical carcinomas. *Clin Cancer Res* **9**: 5666–5674
- Hilvo M, Baranauskiene L, Salzano AM, Scaloni A, Matulis D, Innocenti A, Scozzafava A, Monti SM, Di Fiore A, De Simone G, Lindfors M, Janis J, Valjakka J, Pastorekova S, Pastorek J, Kulomaa MS, Nordlund HR, Supuran CT, Parkkila S (2008) Biochemical characterization of CA IX, one of the most active carbonic anhydrase isozymes. *J Biol Chem* **283**: 27799–27809
- Hofman P, Butori C, Havet K, Hofman V, Selva E, Guevara N, Santini J, Van Obberghen-Schilling E (2008) Prognostic significance of c-erbB2 levels in head and neck squamous cell carcinoma: comparison with epidermal growth factor receptor status. *Br J Cancer* **98**: 956–964
- Hyrsl L, Zavada J, Zavadova Z, Kawaciuk I, Vesely S, Skapa P (2009) Soluble form of carbonic anhydrase IX (CAIX) in transitional cell carcinoma of urinary tract. *Neoplasma* **56**: 298–302
- Kim SJ, Rabbani ZN, Dewhirst MW, Vujaskovic Z, Vollmer RT, Schreiber EG, Oosterwijk E, Kelley MJ (2005) Expression of HIF-1alpha, CA IX, VEGF, and MMP-9 in surgically resected non-small cell lung cancer. *Lung Cancer* **49**: 325–335
- Kim SJ, Rabbani ZN, Vollmer RT, Schreiber EG, Oosterwijk E, Dewhirst MW, Vujaskovic Z, Kelley MJ (2004) Carbonic anhydrase IX in early-stage non-small cell lung cancer. *Clin Cancer Res* **10**: 7925–7933
- Klatte T, Seligson DB, Rao JY, Yu H, de Martino M, Kawaoka K, Wong SG, Belldgrun AS, Pantuck AJ (2009) Carbonic anhydrase IX in bladder cancer: a diagnostic, prognostic, and therapeutic molecular marker. *Cancer* **115**: 1448–1458
- Kon-no H, Ishii G, Nagai K, Yoshida J, Nishimura M, Nara M, Fujii T, Murata Y, Miyamoto H, Ochiai A (2006) Carbonic anhydrase IX expression is associated with tumor progression and a poor prognosis of lung adenocarcinoma. *Lung Cancer* **54**: 409–418
- Korkeila E, Talvinen K, Jaakkola PM, Minn H, Syrjanen K, Sundstrom J, Pyrhonen S (2009) Expression of carbonic anhydrase IX suggests poor outcome in rectal cancer. *Br J Cancer* **100**: 874–880
- Koukourakis MI, Giatromanolaki A, Sivridis E, Simopoulos K, Pastorek J, Wykoff CC, Gatter KC, Harris AL (2001) Hypoxia-regulated carbonic anhydrase-9 (CA9) relates to poor vascularization and resistance of squamous cell head and neck cancer to chemoradiotherapy. *Clin Cancer Res* **7**: 3399–3403
- Lam JS, Pantuck AJ, Belldgrun AS, Figlin RA (2005) G250: a carbonic anhydrase IX monoclonal antibody. *Curr Oncol Rep* **7**: 109–115
- Lee CH, Lee MK, Kang CD, Kim YD, Park DY, Kim JY, Sol MY, Suh KS (2003) Differential expression of hypoxia inducible factor-1 alpha and tumor cell proliferation between squamous cell carcinomas and adenocarcinomas among operable non-small cell lung carcinomas. *J Korean Med Sci* **18**: 196–203
- Li G, Feng G, Gentil-Perret A, Genin C, Tostain J (2008) Serum carbonic anhydrase 9 level is associated with postoperative recurrence of conventional renal cell cancer. *J Urol* **180**: 510–513
- Liao SY, Stanbridge EJ (2000) Expression of MN/CA9 protein in Papanicolaou smears containing atypical glandular cells of undetermined significance is a diagnostic biomarker of cervical dysplasia and neoplasia. *Cancer* **88**: 1108–1121
- Loncaster JA, Harris AL, Davidson SE, Logue JP, Hunter RD, Wyckoff CC, Pastorek J, Ratcliffe PJ, Stratford IJ, West CM (2001) Carbonic anhydrase (CA IX) expression, a potential new intrinsic marker of hypoxia: correlations with tumor oxygen measurements and prognosis in locally advanced carcinoma of the cervix. *Cancer Res* **61**: 6394–6399
- Malentacchi F, Simi L, Nannelli C, Andreani M, Janni A, Pastorekova S, Orlando C (2009) Alternative splicing variants of carbonic anhydrase IX in human non-small cell lung cancer. *Lung Cancer* **64**: 271–276
- Mountain CF (1997) Revisions in the international system for staging lung cancer. *Chest* **111**: 1710–1717
- Ohh M, Park CW, Ivan M, Hoffman MA, Kim TY, Huang LE, Pavletich N, Chau V, Kaelin WG (2000) Ubiquitination of hypoxia-inducible factor requires direct binding to the beta-domain of the von Hippel-Lindau protein. *Nat Cell Biol* **2**: 423–427
- Ou SH, Zell JA, Zogas A, Anton-Culver H (2007) Prognostic factors for survival of stage I nonsmall cell lung cancer patients: a population-based analysis of 19 702 stage I patients in the California Cancer Registry from 1989 to 2003. *Cancer* **110**: 1532–1541
- Pastorekova S, Parkkila S, Pastorek J, Supuran CT (2004) Carbonic anhydrases: current state of the art, therapeutic applications and future prospects. *J Enzyme Inhib Med Chem* **19**: 199–229
- Pouyssegur J, Dayan F, Mazure NM (2006) Hypoxia signalling in cancer and approaches to enforce tumour regression. *Nature* **441**: 437–443
- Rafajova M, Zatovicova M, Kettmann R, Pastorek J, Pastorekova S (2004) Induction by hypoxia combined with low glucose or low bicarbonate and high posttranslational stability upon reoxygenation contribute to carbonic anhydrase IX expression in cancer cells. *Int J Oncol* **24**: 995–1004
- Rak J, Yu JL, Kerbel RS, Coomber BL (2002) What do oncogenic mutations have to do with angiogenesis/vascular dependence of tumors? *Cancer Res* **62**: 1931–1934
- Schemper M, Smith TL (1996) A note on quantifying follow-up in studies of failure time. *Control Clin Trials* **17**: 343–346
- Schrijvers ML, van der Laan BF, de Bock GH, Pattje WJ, Mastik MF, Menkema L, Langendijk JA, Kluin PM, Schuurings E, van der Wal JE (2008) Overexpression of intrinsic hypoxia markers HIF1alpha and CA-IX predict for local recurrence in stage T1-T2 glottic laryngeal carcinoma treated with radiotherapy. *Int J Radiat Oncol Biol Phys* **72**: 161–169
- Sekido Y, Bader S, Latif F, Gnarr JR, Gazdar AF, Linehan WM, Zbar B, Lerman MI, Minna JD (1994) Molecular analysis of the von Hippel-Lindau disease tumor suppressor gene in human lung cancer cell lines. *Oncogene* **9**: 1599–1604
- Semenza GL (2003) Targeting HIF-1 for cancer therapy. *Nat Rev Cancer* **3**: 721–732
- Simi L, Venturini G, Malentacchi F, Gelmini S, Andreani M, Janni A, Pastorekova S, Supuran CT, Pazzagli M, Orlando C (2006) Quantitative analysis of carbonic anhydrase IX mRNA in human non-small cell lung cancer. *Lung Cancer* **52**: 59–66
- Stinchcombe TE, Socinski MA (2009) Current treatments for advanced stage non-small cell lung cancer. *Proc Am Thorac Soc* **6**: 233–241
- Supuran CT (2008) Carbonic anhydrases: novel therapeutic applications for inhibitors and activators. *Nat Rev Drug Discov* **7**: 168–181
- Swinson DE, Jones JL, Cox G, Richardson D, Harris AL, O'Byrne KJ (2004) Hypoxia-inducible factor-1 alpha in non small cell lung cancer: relation to growth factor, protease and apoptosis pathways. *Int J Cancer* **111**: 43–50
- Swinson DE, Jones JL, Richardson D, Wykoff C, Turley H, Pastorek J, Taub N, Harris AL, O'Byrne KJ (2003) Carbonic anhydrase IX expression, a novel surrogate marker of tumor hypoxia, is associated with a poor prognosis in non-small-cell lung cancer. *J Clin Oncol* **21**: 473–482
- Trastour C, Benizri E, Ettore F, Ramaoli A, Chamorey E, Pouyssegur J, Berra E (2007) HIF-1alpha and CA IX staining in invasive breast carcinomas: prognosis and treatment outcome. *Int J Cancer* **120**: 1451–1458
- Travis WD, Brambilla E, Müller-Hermelink HK, Harris CC (2004) WHO histological classification of tumors of the lung. In *World Health Organization Classification of Tumours. Pathology and Genetics of Tumours of the Lung, Pleura, Thymus and Heart*, p 342. IARC Press: Lyon
- Turner KJ, Crew JP, Wykoff CC, Watson PH, Poulson R, Pastorek J, Ratcliffe PJ, Cranston D, Harris AL (2002) The hypoxia-inducible genes VEGF and CA9 are differentially regulated in superficial vs invasive bladder cancer. *Br J Cancer* **86**: 1276–1282
- Volm M, Koomagi R (2000) Hypoxia-inducible factor (HIF-1) and its relationship to apoptosis and proliferation in lung cancer. *Anticancer Res* **20**: 1527–1533
- Woo T, Okudela K, Yazawa T, Wada N, Ogawa N, Ishiwa N, Tajiri M, Rino Y, Kitamura H, Masuda M (2009) Prognostic value of KRAS mutations and Ki-67 expression in stage I lung adenocarcinomas. *Lung Cancer* **65**: 355–362
- Wykoff CC, Beasley NJ, Watson PH, Turner KJ, Pastorek J, Sibtain A, Wilson GD, Turley H, Talks KL, Maxwell PH, Pugh CW, Ratcliffe PJ, Harris AL (2000) Hypoxia-inducible expression of tumor-associated carbonic anhydrases. *Cancer Res* **60**: 7075–7083
- Zatovicova M, Sedlakova O, Svastova E, Ohradnova A, Ciampor F, Arribas J, Pastorek J, Pastorekova S (2005) Ectodomain shedding of the hypoxia-induced carbonic anhydrase IX is a metalloprotease-dependent process regulated by TACE/ADAM17. *Br J Cancer* **93**: 1267–1276
- Zavada J, Zavadova Z, Zat'ovicova M, Hyrs L, Kawaciuk I (2003) Soluble form of carbonic anhydrase IX (CA IX) in the serum and urine of renal carcinoma patients. *Br J Cancer* **89**: 1067–1071
- Zhong H, De Marzo AM, Laughner E, Lim M, Hilton DA, Zagzag D, Buechler P, Isaacs WB, Semenza GL, Simons JW (1999) Overexpression of hypoxia-inducible factor 1alpha in common human cancers and their metastases. *Cancer Res* **59**: 5830–5835

Overexpression of carbonic anhydrase XII in tissues from resectable non-small cell lung cancers is a biomarker of good prognosis

Marius I. Ilie^{1,2,3}, Véronique Hofman^{1,2,3,4}, Cécile Ortholan^{3,5}, Reda El Ammadi^{3,6}, Christelle Bonnetaud⁴, Katia Havet¹, Nicolas Venissac^{1,3,7}, Jérôme Mouroux^{1,3,7}, Nathalie M. Mazure^{3,8}, Jacques Pouyssegur^{3,8} and Paul Hofman^{1,2,3,4}

¹Laboratory of Clinical and Experimental Pathology, Louis Pasteur Hospital, Nice, France

²INSERM ERI-21/EA 4319, Faculty of Medicine, Nice, France

³University of Nice Sophia Antipolis, Nice, France

⁴Human Tissue Biobank Unit/CRB INSERM, Louis Pasteur Hospital, Nice, France

⁵Department of Radiotherapy, Centre Antoine-Lacassagne, Nice, France

⁶Department of Mathematical Sciences, University of Nice Sophia Antipolis, Sophia Antipolis, France

⁷Department of Thoracic Surgery, University Hospital Centre of Nice, Nice, France

⁸Institute of Developmental Biology and Cancer Research, University of Nice and CNRS UMR 6543, Nice, France

The pattern of protein expression in tumors is under the influence of nutrient stress, hypoxia and low pH, which determines the survival of neoplastic cells and the development of tumors. Carbonic anhydrase XII (CAXII) is a transmembrane enzyme that catalyzes the reversible hydration of cell-generated carbon dioxide into protons and bicarbonate. Hypoxic conditions activate its transcription and translation and enhanced expression is often present in several types of tumors. The aim of our study was to assess the prognostic significance of CAXII tumor tissues expression in patients with NSCLC. Five hundred fifty-five tumors were immunostained for CAXII on tissue microarrays (TMA) and the results were correlated with clinicopathological parameters and outcome of patients. CAXII overexpression was present in 105/555 (19%) cases and was associated with tumors of lower grade ($p = 0.015$) and histological type ($p < 0.001$), being significantly higher in squamous cell carcinoma. High CAXII expression correlated with better overall and disease-specific survival of patients with resectable NSCLC in univariate ($p < 0.001$) and multivariate survival analyses ($p < 0.001$). In conclusion, this is the first study demonstrating that a high CAXII tumor tissue expression evaluated on TMAs is related to a better outcome in a large series of patients with resectable NSCLC.

Key words: non-small cell lung cancer, tissue microarrays, prognostic biomarker, carbonic anhydrase XII, hypoxia

Abbreviations: CA: carbonic anhydrase; DSS: disease-specific survival; HIF: hypoxia-inducible factor; HRE: hypoxia-response element; IHC: immunohistochemistry; NSCLC: non-small cell lung cancer; OS: overall survival; pVHL: von Hippel-Lindau protein; TMA: tissue microarray

Additional Supporting Information may be found in the online version of this article

Grant sponsors: Canceropôle PACA; **Grant number:** PROCAN 2008-2011, Axe II; **Grant sponsors:** INCa, PHRC (2003 CHU of Nice)

DOI: 10.1002/ijc.25491

History: Received 19 Feb 2010; Accepted 27 May 2010; Online 2 Jun 2010

Correspondence to: Paul Hofman, Laboratory of Clinical and Experimental Pathology, Pasteur Hospital, 30 Avenue de la voie Romaine, 06002 Nice Cedex 01, France, Tel.: +33-4-92-03-87-49, Fax: +33-4-92-03-87-50, E-mail: hofman.p@chu-nice.fr

Lung cancer has the highest cancer-related morbidity and mortality rate in the world.¹ Non-small cell lung cancer (NSCLC) accounts for ~80% of all lung cancers and more than a half of patients with early-stage NSCLC die within 10 years of diagnosis.^{2,3} Despite major advances in surgical techniques and new strategies in chemotherapy and/or radiotherapy, long-term survival is achieved in only 5–10% of patients.^{4,5} Thus, identifying new tissue-based biomarkers that can predict the risk of progression and recurrence is warranted and urgently needed to improve the control of this deadly form of cancer.

As hypoxia-regulated molecular pathways have been analyzed in recent years, hypoxia-inducible genes are becoming interesting candidates as predictors of outcome.⁶ More than 100 genes involved in pH regulation, tumor metabolism, angiogenesis, migration and invasion, are currently known to be regulated by the hypoxia-inducible factor-1 (HIF-1), the key mediator of the cellular response to hypoxia.⁷ Among the corresponding gene products, the isoenzymes of the carbonic anhydrase (CA) family, CAIX and CAXII, are induced under hypoxic conditions in a variety of tumors and cultured tumor

cells and their expression is downregulated when returned to normoxia,^{8–11} particularly for CAIX, the most inducible isoform. CAXI and CAXII are transmembrane zinc metalloenzymes that catalyze the reversible hydration of carbon dioxide to form bicarbonate ($\text{H}_2\text{O} + \text{CO}_2 \leftrightarrow \text{H}^+ + \text{HCO}_3^-$). The enzymatic activity of these CAs is likely involved in modulating a variety of physiological processes including transport of carbon dioxide and solutes, as well as acidification of the microenvironment that can modulate the tumor malignant phenotype.^{12,13} Previous studies have described two mechanisms that control the expression of CAXII and CAIX. Regulation through hypoxia plays one of the major roles, *ca9* being directly upregulated *via* the binding of HIF to a hypoxia-response element (HRE) within the basal promoter of *ca9*.^{6,11} The other regulatory mechanism involves the protein product of the von Hippel-Lindau tumor suppressor gene (pVHL), which downregulates the expression of CAIX and CAXII.⁸ However, it is noteworthy that the expression and the tissue distribution of the CAXII protein do not correlate with the expression of CAIX.⁸ CAXII was originally identified as a protein overexpressed in renal cancer cells,⁹ but it is also known to be overexpressed in different human cancers, such as diffuse astrocytomas and colorectal, gastrointestinal, breast, pancreatic, ovarian and renal carcinomas.^{14–19} *In vitro* and *in vivo* studies revealed that both CAIX and CAXII are functionally connected to neoplastic processes, and promote tumor cell survival and growth by counteracting acidosis through the regulation of the intracellular pH.^{20–22} Moreover, recent studies showed that combined silencing of CAIX and CAXII can reduce the rate of growth of colon xenograft tumors.²⁰

Whereas tumor expression of HIF-1 α and CAIX has been shown to correlate with poor survival of NSCLC patients,^{23,24} the significance of expression of CAXII, which lacks the N-terminal proteoglycan domain of CAIX, which is implicated in cell adhesion,^{25,26} has not been examined in NSCLC.²⁷ In addition, the potential role of tumor CAXII expression as a prognostic biomarker in NSCLC has not been investigated.

In our study, we examined the expression of CAXII in a large collection of NSCLC tissue samples to assess if CAXII might serve as a predictor of outcome. Specifically, we aimed to assess the association between CAXII expression and the clinicopathological parameters of NSCLC patients and the relationship to outcome. Surprisingly, we found a relationship between CAXII overexpression and better outcome of patients. Our data suggest that CAXII expression in tumor tissue could serve as a potential biomarker to determine better prognosis in patients with resectable NSCLC.

Material and Methods

Patients

Five hundred fifty-five patients who underwent surgery for NSCLC (Department of Thoracic Surgery, Louis Pasteur Hospital, Nice, France) were included in our study between Janu-

ary 2001 and January 2008. The patients received the necessary information concerning the study and consent was obtained from each patient. The study was approved by the Ethics Committee of CHU of Nice and performed according to the guidelines of the Declaration of Helsinki. Cases were selected to build tissue microarrays (TMA) and included only if clinicopathological and survival data were available. The main clinical and histopathological data are summarized in Table 1. Morphological classification of the tumors was assigned according to the WHO criteria.² The tumors were staged according to the international tumor-node-metastasis system.²⁸ The median follow-up at the time of analysis was 35 months (range, 3–102 months). Of 555 patients, 122 (22%) died from cancer.

TMA construction and immunohistochemistry

TMA was constructed from archival paraffin-embedded, formalin-fixed tissue blocks. Representative tumor regions were selected for building TMAs and arrays were designed as previously described.²⁹ Briefly, three core tissue biopsies, 600 μm in diameter, corresponding to selected morphologically representative regions of each paraffin-embedded NSCLC, were punched and transferred to a receiver paraffin block using an automated tissue arrayer (Beecher Instruments, Sun Prairie, Wisconsin, USA). Three additional core tissue biopsies were selected from morphologically normal lung tissue adjacent to each tumor and served as a negative control. The quality of morphologically representative areas of the original lesions was assessed on each receiving paraffin block by H&E staining.

Immunohistochemistry for CAXII was performed on serial 4- μm deparaffinized TMA sections using an automated single-staining procedure (Benchmark XT, Ventana Medical Systems, Roche Group, Inc., Tucson, Arizona, USA). The protocol was completed as a one-step fully automated assay. Liquid Coverslip™ (LCS, heat resistant oil, Ventana Medical Systems) was used to control liquid evaporation and ensures complete slide coverage throughout the assay. The rabbit polyclonal anti-CAXII (dilution 1:2000, Sigma-Aldrich, St. Louis, MI) was used. Paraffin tissue sections were baked at 75°C for 4 min prior to the deparaffinization step with EZ Prep (Ventana Medical Systems) at 76°C for 4 min. Deparaffinized tissue sections were pretreated with a combination of heat treatment and the following antigen retrieval solutions Cell Conditioner #1 (CC1, EDTA buffer pH 8.4), Cell Conditioner #2 (CC2, Citrate buffer pH6) or Protease 1 (P1 0.5U/ml) to unmask antigen targets. Incubation without the primary antibody under the same condition served as a negative control. Washing steps with Reaction Buffer (Tris-based buffer pH 7.6, Ventana Medical Systems) were performed at 37°C. Finally, the signal was detected using XT iView DAB V.1 kit (Ventana Medical Systems). Incubation with a mouse/rabbit biotinylated secondary antibody was performed for 8 min at 37°C and streptavidin complexed with peroxidase was added for 8 min at 37°C. 3-3'-Diaminobenzidine (Sigma-Aldrich) was the chromogen in all reactions. Tissue sections were

Table 1. Correlation of CAXII expression as detected by immunohistochemistry on TMA with clinicopathological parameters of 555 NSCLC patients

Variables ¹	Total (n = 555) ²	CAXII status		p-value ³
		Low ² (n = 450)	High ² (n = 105)	
Age at diagnosis (years)				
Median ± SD	59.5 ± 7.3	60.5 ± 7.7	57.6 ± 6.7	0.285
Gender				
Male	415 (75)	344 (83)	71 (17)	0.08
Female	140 (25)	106 (76)	34 (24)	
Smoking history				
Never	75 (14)	55 (73)	20 (27)	0.093
Former or current	480 (86)	395 (82)	85 (18)	
Tumour size (cm)				
Median ± SD	3.7 ± 2.4	3.1 ± 2.3	4.2 ± 2.4	0.044
Histological type				
ADC	281 (50)	250 (89)	31 (11)	<0.001
SCC	184 (33)	120 (65)	64 (35)	
LCC	43 (8)	39 (91)	4 (9)	
NOS	47 (9)	41 (87)	6 (13)	
Disease stage				
I	273 (49)	216 (79)	57 (21)	0.702
II	111 (20)	92 (83)	19 (17)	
III	150 (27)	125 (83)	25 (17)	
IV	21 (4)	17 (81)	4 (19)	
Tumour grade				
1	214 (38)	163 (76)	51 (24)	0.042
2	187 (34)	151 (81)	36 (19)	
3	137 (25)	119 (87)	18 (13)	
4	17 (3)	16 (94)	1 (6)	
Neoadjuvant therapy	67 (12)	53 (79)	14 (21)	0.629

¹χ² or Mann–Whitney test when appropriate. ²Values expressed as n (%) or median ± SD. ³p-value <0.05 statistically significant.

ADC: adenocarcinoma; SCC: squamous cell carcinoma; LCC: large cell carcinoma; NOS: not otherwise specified.

counterstained with Hematoxylin II (Ventana Medical System) for 8 min and bluing reagent for 4 min. Counterstained slides were first rinsed with soap under tap water to remove LCS, rinsed with distilled water until the soap was removed completely from the slide and then dehydrated with absolute alcohol and mounted with an automatic sealing machine (Tissue-Tek® SCA, Sakura Finetek, Torrance, CA). Positive controls for CAXII were biopsy cores of breast carcinoma, which have been previously established as positive for CAXII.³⁰

Assessment of CAXII expression

After antibody staining, images were acquired using automated, quantitative analysis, as described previously.²⁹ Tissue cores were analyzed with a semiautomated tissue array image-analysis workstation (Spot Browser, version 7, Alpelhys, Paris, France). The CAXII signal was measured on

a grayscale of 0 (black) to 255 (white) and expressed as target signal intensity relative to the cell membrane. Gray values ranged between 0 and 122, and a value superior or equal to 45 was arbitrarily defined as CAXII overexpression. The degree of positive staining on the sections was assessed at high magnification (×200). In parallel, assessment of immunostaining was performed by three pathologists (M.I., V.H. and P.H.) blinded to clinicopathological parameters of patients. Staining intensity was based on a scale from 0 to 3 and the percentage of positive cells (0 < 1%, 1 = 1–10%, 2 = 10–50% and 3 > 50%). The product of the intensity of staining and the percentage of tumor positive cells was then calculated to produce an immunostaining score (IHC score) of 0–300, as previously described.³¹ An IHC score > 40 distinguished high from low expression of CAXII.³⁰ Spots were excluded from analysis if they contained no tumor tissue

(sampling error), or too few tumor cells (<10%). The overall score used for statistical analysis was the mean value from all spots of the same tumor. In parallel, whole-tissue sections from tumor blocks of a subset of 40 cases were stained for CAXII and compared to the corresponding TMA spots using the aforementioned scoring criteria. For the capture of photographs we used an image system, including a CoolSNAP EZ cooled charge-coupled device camera (Roper Scientific, Evry, France) and a Leica DMR optic microscope (Leica Microsystems Imaging Solution, Cambridge, UK).

Statistical analysis

Analyses were performed using SPSS 16.0 statistical software (SPSS, Chicago, IL). Differences between groups were evaluated using the χ^2 for categorical variables and the Mann-Whitney test for continuous variables. The degree of agreement between data from whole-tissue sections and the mean value of three spots was assessed using the Cohen's κ coefficient. Median time of follow-up was calculated with the Schemper method.³² Survival rates were estimated using the Kaplan-Meier method and were compared with the log-rank test for determining significance. Patients lost for follow-up or who died from other causes were censored at the date of death. The univariate and multivariate Cox proportional hazards models were used for determining the relative risk. Variables that were associated with survival with a p -value < 0.20 in the univariate analysis were included in the multivariate regression. The variables included in the model for disease-specific survival (DSS) and overall survival (OS) were clinical parameters (age, gender, smoking history and neoadjuvant therapy), disease stage, histological cell type and tumor grade. All statistical tests were two-sided, and the level of significance was set at $p < 0.05$.

Results

Immunohistochemical analysis of CAXII expression on TMA

The immunohistochemical labeling was successful in 92.4% (513 of 555) of the initially designed samples of TMA. Forty-two tumors (7.5%) were re-punched on a separate receiver paraffin block to complete the immunohistochemical analysis. Finally, all spots (100%) of NSCLC tumors included on TMA were then interpretable for analysis.

Negative or weak, intermediate and high CAXII immunostaining was observed among the different histological subtypes of NSCLC tumors as illustrated in Figure 1. The membranous immunolabeling pattern of CAXII in epithelial tumor cells, as revealed in sections of breast carcinoma used as positive controls, was retained for further analyses (Fig. 1). Tissue core biopsies taken from normal lung tissue were immunonegative for CAXII (Fig. 1). Furthermore, the CAXII expression levels observed in the TMA cores faithfully reflected the staining intensity of this protein in whole-tissue sections from corresponding tumor blocks in a subset of 40 tumors ($\kappa = 0.86$), as described in the "Patients and Methods" section (data not shown).

Correlation between CAXII expression and the clinicopathological status of NSCLC patients

CAXII expression was evaluated according to the clinicopathological parameters of patients. Of 555 tumors, 105 (19%) demonstrated high CAXII expression (Table 1). CAXII overexpression was significantly associated with tumor size ($p = 0.044$), the histological subtype ($p < 0.001$) and the tumor grade ($p = 0.042$). Sixty-four (35%) of the 184 squamous cell carcinomas (SCC) overexpressed CAXII, whereas 31 (11%) of 281 adenocarcinomas (ADC) had high CAXII expression ($p < 0.001$). CAXII overexpression was significantly associated with well-differentiated tumors (1 + 2 vs. 3 + 4 tumor grade, $p = 0.016$). To further analyze the relationship to tumor size, categorical variables were used in a χ^2 test. High CAXII expression was significantly correlated to tumors inferior to 7 cm in size ($p = 0.035$) (Fig. 2). Moreover, a significant association was observed between high CAXII expression in tumors inferior or equal to 3 cm in size and that observed in tumors larger than 7 cm ($p = 0.021$) (Fig. 2). In addition, there was a tendency for association between CAXII overexpression in tumors superior to 3 cm but inferior to 7 cm in size in comparison to lesions superior to 7 cm ($p = 0.069$) (Fig. 2). However, there was no significant difference between CAXII overexpression in tumors inferior or equal to 3 cm and those superior to 3 cm and inferior to 7 cm ($p = 0.194$). No significant association with other clinicopathological parameters such as age, sex, smoking status, tumor size and disease stage or neoadjuvant therapy was observed (Table 1).

High CAXII tumor expression is associated with better OS and DSS in patients with resectable NSCLC

A univariate analysis was conducted to explore the relationship of CAXII expression, as determined by the immunohistochemistry on TMA, to the survival of 555 patients with resectable NSCLC. CAXII overexpression was significantly related to better OS when compared to low CAXII expression levels (Fig. 3). For patients who had CAXII tumor overexpression, the median OS was 95 months and for those who demonstrated low CAXII tumor expression was 46 months ($p < 0.001$) (Fig. 3a). In addition, patients with I + II stage tumors who had high levels of CAXII had not reached the median OS and those with low levels of CAXII had a 52 months median OS ($p = 0.007$) (Fig. 3b). For stages III + IV, patients with high levels of CAXII had a 79 months median OS and those with low levels of CAXII had a 29 months median OS ($p = 0.011$) (Fig. 3c).

The univariate analysis revealed that CAXII overexpression was significantly associated with better DSS (median DSS was not reached for patients with high levels of CAXII vs. 50 months for patients with negative levels of CAXII) ($p < 0.001$) (Fig. 3d). In addition, patients with I + II stage tumors with high levels of CAXII the median DSS was not reached and those with low levels of CAXII the median DSS was 59 months ($p = 0.001$) (Fig. 3e). For stages III + IV,

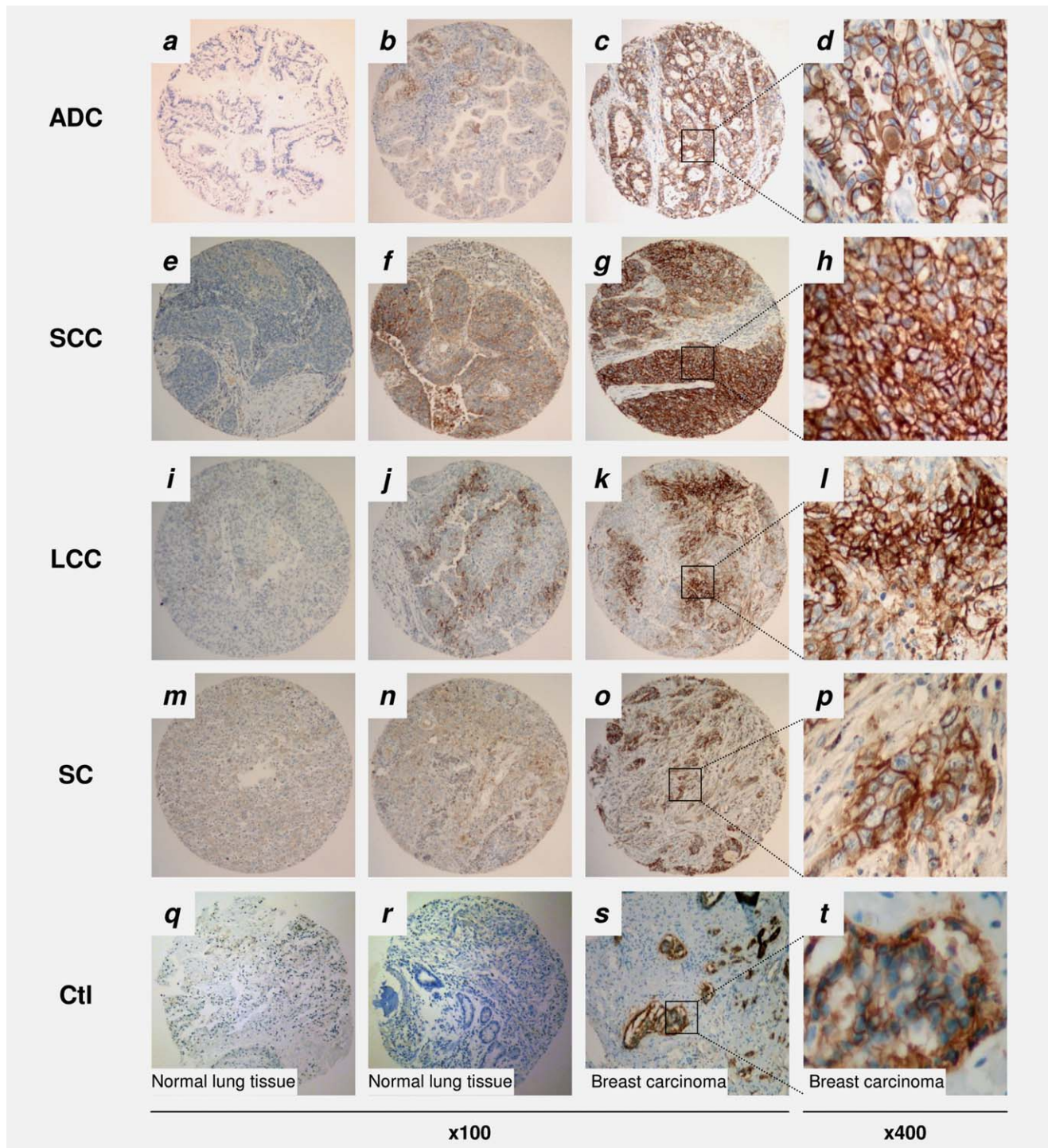


Figure 1. Representative immunohistochemical analysis of CAXII expression in NSCLC tumor TMA cores: staining levels for CAXII in NSCLC histological subtypes: low (*a–m*), intermediate (*b–n*) and strong (*c–o*) CAXII membrane immunoperoxidase staining in adenocarcinoma (ADC) (*a–d*), squamous cell carcinoma (SCC) (*e–h*), large cell carcinoma (LCC) (*i–l*) and sarcomatoid carcinoma (SC) (*m–p*). Normal alveolar tissue (*q*) and bronchial epithelium (*r*) are devoid of staining. Strong membrane staining in breast carcinoma used as positive control for CAXII immunostaining (*s, t*). Panels (*d, h, l, p* and *t*) are higher magnifications showing details of cells within the corresponding tumor shown on Panels (*c, g, k, o* and *s*).

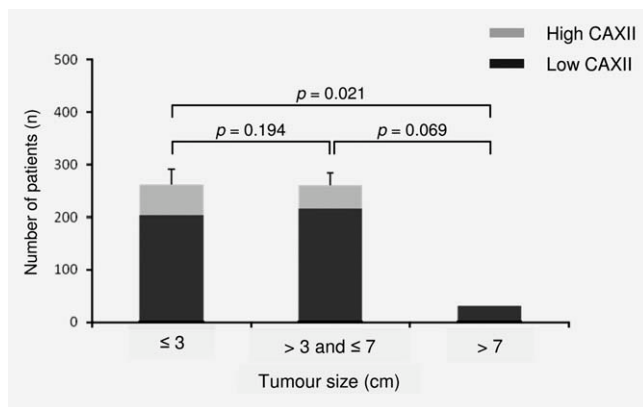


Figure 2. Distribution of CAXII expression according to tumor size as a categorical variable in 555 patients with resectable NSCLC. p value < 0.05 statistically significant.

patients with high levels of CAXII the median DSS was not reached and those with low levels CAXII had a 33 months median DSS ($p = 0.003$) (Fig. 3f).

Subsequently, a multivariate survival analysis using the Cox's proportional hazard model was performed to examine the importance of CAXII in survival when other prognostic factors were included (Table 2). High CAXII expression was a significant independent predictor of better OS (HR 2.876; 95% CI 1.765–4.687; $p < 0.001$), and DSS (HR 6.103; 95% CI 2.808–13.265; $p < 0.001$) (Table 2) when adjusted for other significant variables. In addition, the histological type and the disease stage were also independent prognostic factors for OS and DSS (Table 2).

Discussion

We showed that CAXII, evaluated by IHC in a large series of 555 resectable NSCLC, was overexpressed in 19% of these cases. Moreover, high CAXII tumor tissue expression was strongly associated with tumor size ($p = 0.044$), histological type ($p < 0.001$) and tumor grade ($p = 0.042$). We found significantly higher expression of CAXII in SCC than in other NSCLC histological subtypes ($p < 0.001$). This latter finding is consistent with previous *in vitro* observations showing that CAXII is regulated by hypoxia and responds to tumor hypoxia *in vivo*, as judged from the high amount of necrosis that characterizes SCC, which may lead to CAXII expression in peri-necrotic areas.^{10,11,30} Although a global chi-square test demonstrated that high CAXII expression was related to tumors inferior to 7 cm in size ($p = 0.035$), the subgroups related to size analysis showed significant association with smaller sized tumors (≤ 3 cm) ($p = 0.021$) and a tendency for association with mean-sized tumors (> 3 cm and ≤ 7 cm) ($p = 0.069$) when compared to large-sized tumors (> 7 cm). This finding supports the idea of a hypoxia-regulated mechanism of CAXII tumor expression since dynamic areas of progressive reoxygenation and angiogenesis in tumors of growing size might contribute to decreased CAXII expression in these

tumors (Supporting Information Fig. 1). Nevertheless, CAXII expression should not be regarded in our study as a marker of reoxygenation or angiogenesis according to tumor size. A more robust biological system should be used.

Although both isoforms, CAIX and CAXII, are known to be regulated by hypoxia, it is likely that CAXII might play a different role in tumor development and differentiation, independently of CAIX.³³ Previous studies showed that while hypoxia may influence CAXII expression in focal areas within high-grade breast tumors, the regulation of CAXII by differentiation-related factors appears to be dominant *in vivo*.³⁰ Consequently, our study demonstrated that high CAXII expression was significantly associated with well-differentiated NSCLC ($p = 0.01$). Our data are supported by former reports in which CAXII expression was shown to be higher in well-differentiated and reduced in poorly differentiated tumor lesions.¹⁶ In one previous study of 29 breast cancers there was focal expression of CAXII in normal breast tissue and 62% of invasive carcinomas overexpressed CAXII, primarily in low-grade tumors.¹⁰ Conversely, a recent study of 103 invasive breast carcinomas also demonstrated that CAXII expression is increased in well-differentiated tumors.³⁰

CAXII and CAIX demonstrate a different pattern of expression in normal versus malignant cells and distinct association with tumor differentiation. CAXII is expressed in specialized cells within normal tissues¹⁰ and in several different tumor types.^{9,14,34} CAIX is completely absent in the normal kidney tissue, while it is expressed in many renal tumors, suggesting a constitutively upregulated HIF/VHL pathway of regulation.^{35,36} Moreover, CAIX expression is rather associated with poorly differentiated tumors.³⁷ On the other hand, CAXII expression is found in epithelial cells of normal renal tubules and remains at a high level or is further increased in renal cancer.¹⁹ Similar observations, which support our findings, have been made in breast tissues, which do not belong to tissues affected by VHL disease.¹⁶ CAXII expression has been shown to be associated with lower grade breast tumors and that its regulation is influenced by a distal estrogen-responsive enhancer (ERE) region.^{11,38} Moreover, in a previous study, higher expression of CAXII was linked rather to normal colon tissues with a slight but significant decline in the associated cancers.¹⁴ However, this later study showed no obvious relationship between the levels of pVHL and either CAXII or CAIX. However, the authors did not exclude the existence of a functional connection of pVHL with its targets in normal colorectal epithelium, which may be uncoupled in tumors by hypoxia.¹⁴ This divergent expression pattern and connection to differentiation may suggest that the response of CAXII and CAIX to the HIF/pVHL pathway is modulated by different antagonistic regulatory factors and may modify the relationship between these actors in the same malignant tumor cell.

Although other members of the CA protein family have been examined in several tumor types^{39,40} and it is generally accepted that the increased expression of CAIX can predict

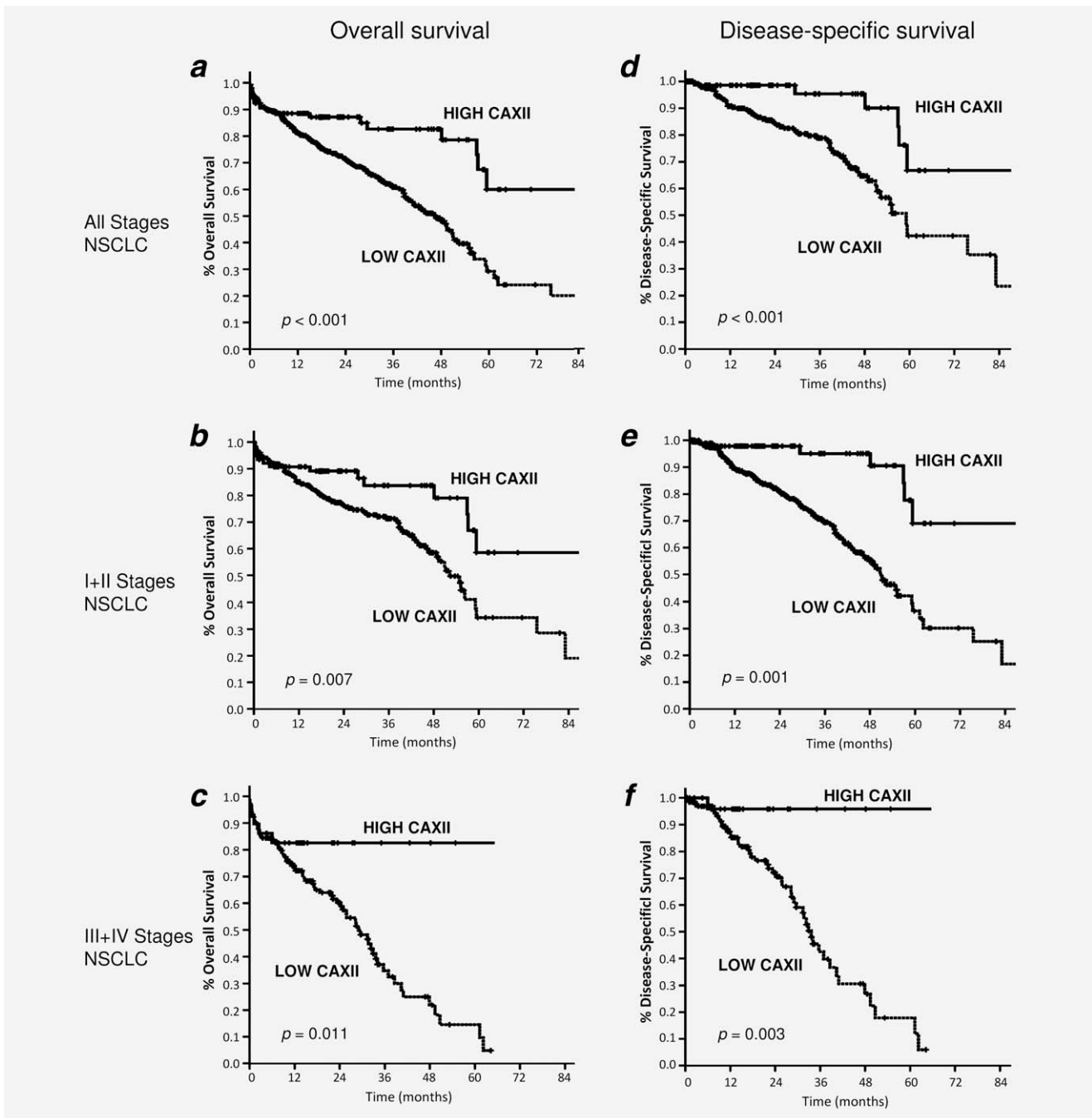


Figure 3. Kaplan–Meier estimates of (a) overall survival for the entire cohort, (b) I + II early-stages NSCLC and (c) III + IV later-stages NSCLC. NSCLC disease-specific survival for (d) all stages, (e) I + II early-stages NSCLC and (f) III + IV later-stages NSCLC. The cut-off value was arbitrarily defined as superior or equal to 45 gray levels to define high CAXII expression.

poor survival of patients, including those with lung cancer,⁴¹ a prognostic role for CAXII has not been previously identified in NSCLC. CAIX differs from the other CA isozymes in that it has a proposed dual function as an efficient enzyme⁴² and as an adhesion molecule.²⁵ This dual function appears to be related to the structure of CAIX molecule that consists of a catalytic CA domain and an extracellularly exposed N-terminal proteoglycan-like region. In tumors, the CA activity

contributes to an acidic extracellular microenvironment and intracellular alkalosis,^{20,22} allowing tumor cells to survive under hypoxic conditions, favoring tumor growth, invasion and development.^{43–45} In contrast, the role of CAXII, which lacks the extracellular proteoglycan domain of CAIX implicated in cell adhesion,^{25,26} is less well understood. Our current study showed that CAXII tumor tissue overexpression, as detected on TMA, is a prognostic factor associated with

Table 2. Multivariate Cox proportional hazard regression analysis of predicting factors for overall and disease-specific survival in 555 NSCLC patients

Prognostic factor	HR ¹	95% CI	p-value ²
Overall Survival			
Histological type			
ADC	1.430	0.256–0.729	0.002
Other subtypes	1		
Disease stage			
I + II	0.439	0.325–0.592	<0.001
III + IV	1		
Tumour grade			
1 + 2	0.731	0.529–1.012	0.059
3 + 4	1		
CAXII expression			
Low	2.876	1.765–4.687	<0.001
High	1		
Disease-Specific Survival			
Histological type			
ADC	0.348	0.184–0.657	0.001
Other subtypes	1		
Disease stage			
I + II	0.408	0.282–0.592	<0.001
III + IV	1		
Tumour grade			
1 + 2	0.709	0.475–1.058	0.092
3 + 4	1		
CAXII expression			
Low	6.103	2.808–13.265	<0.001
High	1		

¹HR, hazard ratio. ²p-value < 0.05 statistically significant. CI: confidence interval.

better OS ($p < 0.001$) and DSS ($p < 0.001$) in NSCLC, as demonstrated by both univariate and multivariate analysis. This finding was rather different to that of Haapasalo *et al.* who conducted a study on 370 astrocytomas in which CAXII was common in diffusely infiltrating astrocytomas, especially in high-grade tumors, which may have indicated a strong relation to poor prognosis.¹⁷ Hypoxia and pVHL disease or high cell density may contribute to increased CAXII expression in astrocytomas as the most malignant type (glioblastoma multiforme) represents a category of highly hypoxic

and cellular tumors.⁴⁶ Diffuse astrocytomas are also known to represent a highly malignant tumor type with extremely poor prognosis.⁴⁷ Moreover, there are two alternative splicing isoforms of CAXII and brain tumors express preferentially the shorter spliced isoform, in contrast to colon and renal carcinomas cell lines, which express the longer variant.¹⁷ As an association between differential expression of splicing isoforms and tumor progression has been shown for several proteins,^{48,49} we propose that the strong association between increased CAXII expression and poor survival in astrocytomas may be due to this splicing event.

Conversely, when an antibody recognizing both splicing isoforms was used for CAXII immunodetection, previous data supported our findings, as CAXII was a good prognostic factor in invasive breast cancer and uterine cervical carcinoma.^{30,33} Importantly, we showed that the prognostic value CAXII is even more marked in advanced stages III + IV NSCLC in comparison with early-stages I + II tumors ($p = 0.011$ for OS and $p = 0.003$ for DSS in III + IV stages, respectively). Therefore, the difference in both OS and DSS between low and high CAXII expression was more discriminant for later stages III + IV NSCLC.

The dual expression and association with survival of the related CAIX and CAXII isoforms is probably the most problematic feature in terms of therapeutic strategy against lung cancer. We strongly believe that these CA can modulate independently the growth and survival characteristics of tumors. In this regard, tumor cells expressing CAIX could acquire a particularly hostile behavior in contrast to the cell subpopulation overexpressing CAXII, which could be less aggressive. Therefore, with regard to future development of CA inhibitors, there is a need for individual targeting of these two isoforms.

In conclusion, we demonstrated in a large series of tumors that CAXII is highly expressed in 19% of NSCLC. This high expression of CAXII was mainly observed in SCC, supporting the notion that CAXII is a hypoxia regulated gene *in vivo*. Another factor influencing CAXII regulation is tumor differentiation, as higher levels of CAXII expression are associated with well-differentiated NSCLC showing better survival. In view of the contrasting clinical value observed for CAIX and XII in several types of cancer, it will be important to explore the prognostic significance of CAXII further, in concert with other CAs in larger prospective studies.

Acknowledgements

M.I.I. is supported by a Grant from INCa (2008). P.H., V.H., J.M. and N.V. are supported by a PHRC Grant (2003 CHU of Nice).

References

- Jemal A, Siegel R, Ward E, Hao Y, Xu J, Murray T, Thun MJ. Cancer statistics, 2008. *CA Cancer J Clin* 2008;58:71–96.
- Travis WD, Brambilla E, Müller-Hermelink HK, Harris CC. WHO histological classification of tumors of the lung World Health Organization Classification of Tumours. In: Pathology and genetics of tumours of the lung, pleura, thymus and heart. Lyon: IARC Press, 2004. 342.
- Ou SH, Zell JA, Ziogas A, Anton-Culver H. Prognostic factors for survival of stage I nonsmall cell lung cancer patients: a population-based analysis of 19,702 stage I patients in the California Cancer Registry

- from 1989 to 2003. *Cancer* 2007;110:1532–41.
4. Mahalingam D, Mita A, Mita MM, Nawrocki ST, Giles FJ. Targeted therapy for advanced non-small cell lung cancers: historical perspective, current practices, and future development. *Curr Probl Cancer* 2009;33:73–111.
 5. Stinchcombe TE, Socinski MA. Current treatments for advanced stage non-small cell lung cancer. *Proc Am Thorac Soc* 2009;6:233–41.
 6. Potter CP, Harris AL. Diagnostic, prognostic and therapeutic implications of carbonic anhydrases in cancer. *Br J Cancer* 2003;89:2–7.
 7. Harris AL. Hypoxia—a key regulatory factor in tumour growth. *Nat Rev Cancer* 2002;2:38–47.
 8. Ivanov SV, Kuzmin I, Wei MH, Pack S, Geil L, Johnson BE, Stanbridge EJ, Lerman MI. Down-regulation of transmembrane carbonic anhydrases in renal cell carcinoma cell lines by wild-type von Hippel-Lindau transgenes. *Proc Natl Acad Sci USA* 1998;95:12596–601.
 9. Tureci O, Sahin U, Vollmar E, Siemer S, Gottert E, Seitz G, Parkkila AK, Shah GN, Grubb JH, Pfreundschuh M, Sly WS. Human carbonic anhydrase XII: cDNA cloning, expression, and chromosomal localization of a carbonic anhydrase gene that is overexpressed in some renal cell cancers. *Proc Natl Acad Sci USA* 1998;95:7608–13.
 10. Ivanov S, Liao SY, Ivanova A, Danilkovitch-Miagkova A, Tarasova N, Weirich G, Merrill MJ, Proescholdt MA, Oldfield EH, Lee J, Zavada J, Waheed A, et al. Expression of hypoxia-inducible cell-surface transmembrane carbonic anhydrases in human cancer. *Am J Pathol* 2001;158:905–19.
 11. Wykoff CC, Beasley NJ, Watson PH, Turner KJ, Pastorek J, Sibtain A, Wilson GD, Turley H, Talks KL, Maxwell PH, Pugh CW, Ratcliffe PJ, et al. Hypoxia-inducible expression of tumor-associated carbonic anhydrases. *Cancer Res* 2000;60:7075–83.
 12. Parkkila S, Rajaniemi H, Parkkila AK, Kivela J, Waheed A, Pastorekova S, Pastorek J, Sly WS. Carbonic anhydrase inhibitor suppresses invasion of renal cancer cells in vitro. *Proc Natl Acad Sci USA* 2000;97:2220–4.
 13. Ulmasov B, Waheed A, Shah GN, Grubb JH, Sly WS, Tu C, Silverman DN. Purification and kinetic analysis of recombinant CA XII, a membrane carbonic anhydrase overexpressed in certain cancers. *Proc Natl Acad Sci USA* 2000;97:14212–7.
 14. Kivela AJ, Parkkila S, Saarnio J, Karttunen TJ, Kivela J, Parkkila AK, Bartosova M, Mucha V, Novak M, Waheed A, Sly WS, Rajaniemi H, et al. Expression of von Hippel-Lindau tumor suppressor and tumor-associated carbonic anhydrases IX and XII in normal and neoplastic colorectal mucosa. *World J Gastroenterol* 2005;11:2616–25.
 15. Kivela A, Parkkila S, Saarnio J, Karttunen TJ, Kivela J, Parkkila AK, Waheed A, Sly WS, Grubb JH, Shah G, Tureci O, Rajaniemi H. Expression of a novel transmembrane carbonic anhydrase isozyme XII in normal human gut and colorectal tumors. *Am J Pathol* 2000;156:577–84.
 16. Wykoff CC, Beasley N, Watson PH, Campo L, Chia SK, English R, Pastorek J, Sly WS, Ratcliffe P, Harris AL. Expression of the hypoxia-inducible and tumor-associated carbonic anhydrases in ductal carcinoma in situ of the breast. *Am J Pathol* 2001;158:1011–9.
 17. Haapasalo J, Hilvo M, Nordfors K, Haapasalo H, Parkkila S, Hyrskyluoto A, Rantala I, Waheed A, Sly WS, Pastorekova S, Pastorek J, Parkkila AK. Identification of an alternatively spliced isoform of carbonic anhydrase XII in diffusely infiltrating astrocytic gliomas. *Neuro Oncol* 2008;10:131–8.
 18. Hynninen P, Vaskivuo L, Saarnio J, Haapasalo H, Kivela J, Pastorekova S, Pastorek J, Waheed A, Sly WS, Puistola U, Parkkila S. Expression of transmembrane carbonic anhydrases IX and XII in ovarian tumours. *Histopathology* 2006;49:594–602.
 19. Parkkila S, Parkkila AK, Saarnio J, Kivela J, Karttunen TJ, Kaunisto K, Waheed A, Sly WS, Tureci O, Virtanen I, Rajaniemi H. Expression of the membrane-associated carbonic anhydrase isozyme XII in the human kidney and renal tumors. *J Histochem Cytochem* 2000;48:1601–8.
 20. Chiche J, Ilc K, Laferriere J, Trottier E, Dayan F, Mazure NM, Brahimi-Horn MC, Pouyssegur J. Hypoxia-inducible carbonic anhydrase IX and XII promote tumor cell growth by counteracting acidosis through the regulation of the intracellular pH. *Cancer Res* 2009;69:358–68.
 21. Svastova E, Hulikova A, Rafajova M, Zat'ovicova M, Gibadulinova A, Casini A, Cecchi A, Scozzafava A, Supuran CT, Pastorek J, Pastorekova S. Hypoxia activates the capacity of tumor-associated carbonic anhydrase IX to acidify extracellular pH. *FEBS Lett* 2004;577:439–45.
 22. Swietach P, Patiar S, Supuran CT, Harris AL, Vaughan-Jones RD. The role of carbonic anhydrase 9 in regulating extracellular and intracellular pH in three-dimensional tumor cell growths. *J Biol Chem* 2009;284:20299–310.
 23. Giatromanolaki A, Koukourakis MI, Sivridis E, Pastorek J, Wykoff CC, Gatter KC, Harris AL. Expression of hypoxia-inducible carbonic anhydrase-9 relates to angiogenic pathways and independently to poor outcome in non-small cell lung cancer. *Cancer Res* 2001;61:7992–8.
 24. Swinson DE, Jones JL, Cox G, Richardson D, Harris AL, O'Byrne KJ. Hypoxia-inducible factor-1 alpha in non small cell lung cancer: relation to growth factor, protease and apoptosis pathways. *Int J Cancer* 2004;111:43–50.
 25. Zavada J, Zavadova Z, Pastorek J, Biesova Z, Jezek J, Velek J. Human tumour-associated cell adhesion protein MN/CA IX: identification of M75 epitope and of the region mediating cell adhesion. *Br J Cancer* 2000;82:1808–13.
 26. Svastova E, Zilka N, Zat'ovicova M, Gibadulinova A, Ciampor F, Pastorek J, Pastorekova S. Carbonic anhydrase IX reduces E-cadherin-mediated adhesion of MDCK cells via interaction with beta-catenin. *Exp Cell Res* 2003;290:332–45.
 27. Pastorekova S, Zatovicova M, Pastorek J. Cancer-associated carbonic anhydrases and their inhibition. *Curr Pharm Des* 2008;14:685–98.
 28. Mountain CF. Revisions in the International System for Staging Lung Cancer. *Chest* 1997;111:1710–7.
 29. Hofman P, Butori C, Havet K, Hofman V, Selva E, Guevara N, Santini J, van Obberghen-Schilling E. Prognostic significance of cactactin levels in head and neck squamous cell carcinoma: comparison with epidermal growth factor receptor status. *Br J Cancer* 2008;98:956–64.
 30. Watson PH, Chia SK, Wykoff CC, Han C, Leek RD, Sly WS, Gatter KC, Ratcliffe P, Harris AL. Carbonic anhydrase XII is a marker of good prognosis in invasive breast carcinoma. *Br J Cancer* 2003;88:1065–70.
 31. Hassan S, Ferrario C, Mamo A, Basik M. Tissue microarrays: emerging standard for biomarker validation. *Curr Opin Biotechnol* 2008;19:19–25.
 32. Schemper M, Smith TL. A note on quantifying follow-up in studies of failure time. *Control Clin Trials* 1996;17:343–6.
 33. Kim JY, Shin HJ, Kim TH, Cho KH, Shin KH, Kim BK, Roh JW, Lee S, Park SY, Hwang YJ, Han IO. Tumor-associated carbonic anhydrases are linked to metastases in primary cervical cancer. *J Cancer Res Clin Oncol* 2006;132:302–8.
 34. Leppilampi M, Saarnio J, Karttunen TJ, Kivela J, Pastorekova S, Pastorek J, Waheed A, Sly WS, Parkkila S. Carbonic anhydrase isozymes IX and XII in gastric tumors. *World J Gastroenterol* 2003;9:1398–403.
 35. Liao SY, Aurelio ON, Jan K, Zavada J, Stanbridge EJ. Identification of the MN/CA9 protein as a reliable diagnostic

- biomarker of clear cell carcinoma of the kidney. *Cancer Res* 1997;57:2827–31.
36. Patard JJ, Fergelot P, Karakiewicz PI, Klatté T, Trinh QD, Rioux-Leclercq N, Said JW, Belldegrun AS, Pantuck AJ. Low CAIX expression and absence of VHL gene mutation are associated with tumor aggressiveness and poor survival of clear cell renal cell carcinoma. *Int J Cancer* 2008;123:395–400.
 37. Kon-no H, Ishii G, Nagai K, Yoshida J, Nishimura M, Nara M, Fujii T, Murata Y, Miyamoto H, Ochiai A. Carbonic anhydrase IX expression is associated with tumor progression and a poor prognosis of lung adenocarcinoma. *Lung Cancer* 2006;54:409–18.
 38. Barnett DH, Sheng S, Charn TH, Waheed A, Sly WS, Lin CY, Liu ET, Katzenellenbogen BS. Estrogen receptor regulation of carbonic anhydrase XII through a distal enhancer in breast cancer. *Cancer Res* 2008;68:3505–15.
 39. Haapasalo J, Nordfors K, Jarvela S, Bragge H, Rantala I, Parkkila AK, Haapasalo H, Parkkila S. Carbonic anhydrase II in the endothelium of glial tumors: a potential target for therapy. *Neuro Oncol* 2007;9:308–13.
 40. Supuran CT. Carbonic anhydrases: novel therapeutic applications for inhibitors and activators. *Nat Rev Drug Discov* 2008;7:168–81.
 41. Nakao M, Ishii G, Nagai K, Kawase A, Kenmotsu H, Kon-No H, Hishida T, Nishimura M, Yoshida J, Ochiai A. Prognostic significance of carbonic anhydrase IX expression by cancer-associated fibroblasts in lung adenocarcinoma. *Cancer* 2009;115:2732–43.
 42. Wingo T, Tu C, Laipis PJ, Silverman DN. The catalytic properties of human carbonic anhydrase IX. *Biochem Biophys Res Commun* 2001;288:666–9.
 43. Chiche J, Ilc K, Brahimi-Horn MC, Pouyssegur J. Membrane-bound carbonic anhydrases are key pH regulators controlling tumor growth and cell migration. *Adv Enzyme Regul* 2010;50:20–33.
 44. Thiry A, Dogne JM, Masereel B, Supuran CT. Targeting tumor-associated carbonic anhydrase IX in cancer therapy. *Trends Pharmacol Sci* 2006;27:566–73.
 45. Pastorekova S, Parkkila S, Pastorek J, Supuran CT. Carbonic anhydrases: current state of the art, therapeutic applications and future prospects. *J Enzyme Inhib Med Chem* 2004;19:199–229.
 46. Haapasalo JA, Nordfors KM, Hilvo M, Rantala JJ, Soini Y, Parkkila AK, Pastorekova S, Pastorek J, Parkkila SM, Haapasalo HK. Expression of carbonic anhydrase IX in astrocytic tumors predicts poor prognosis. *Clin Cancer Res* 2006;12:473–7.
 47. Boudreau CR, Yang I, Liau LM. Gliomas: advances in molecular analysis and characterization. *Surg Neurol* 2005;64:286–94.
 48. Srebrow A, Kornblihtt AR. The connection between splicing and cancer. *J Cell Sci* 2006;119:2635–41.
 49. Pajares MJ, Ezponda T, Catena R, Calvo A, Pio R, Montuenga LM. Alternative splicing: an emerging topic in molecular and clinical oncology. *Lancet Oncol* 2007;8:349–57.

Response of CAIX and CAXII to re-oxygenation: contribution to clinical outcome in NSCLC

Marius Ilie^{1,2,3}, Véronique Hofman^{1,2,3,4}, Joséphine Zangari^{2,3}, Jérôme Mouroux^{2,3,5}, Nathalie M. Mazure^{3,6}, Jacques Pouysségur^{3,6}, Patrick Brest^{2,3}, Paul Hofman^{1,2,3,4}

¹Centre Hospitalier Universitaire de Nice, Louis Pasteur Hospital, Laboratory of Clinical and Experimental Pathology, Nice, France,

²Institute of Research on Cancer and Ageing in Nice IRCAN, INSERM U1081 – CNRS UMR 7284, team 3, Nice, France,

³University of Nice Sophia-Antipolis, Faculty of Medicine, Nice, France

⁴Centre Hospitalier Universitaire de Nice, Louis Pasteur Hospital, Human Tissue Biobank Unit/CRB INSERM, Nice, France

⁵Centre Hospitalier Universitaire de Nice, Louis Pasteur Hospital, Department of Thoracic Surgery, Nice, France,

⁶Institute of Research on Cancer and Ageing in Nice IRCAN, INSERM U1081 – CNRS UMR 7284, team 7, Nice, France

Running title: re-oxygenation and NSCLC

Corresponding author: Paul Hofman MD, PhD, Laboratory of Clinical and Experimental Pathology, Pasteur Hospital, 30 avenue de la Voie Romaine, 06002 Nice Cedex 01, France. Tel: +33 4 92 03 87 49; Fax: + 33 4 92 03 87 50; E-mail: hofman.p@chu-nice.fr

Abstract

The disorganized neo-vasculature in tumours causes fluctuations in the concentration of oxygen, which contributes to tumour development and metastatic potential. Although hypoxic regulation of the expression of the carbonic anhydrases CAIX and CAXII is well established, the effect of re-oxygenation on these proteins remains to be elucidated.

A549 and H1975 human lung cancer cell lines were exposed to hypoxia for 24 h and then re-oxygenated. CAIX or CAXII expression and cell cycle progression at different time-points were monitored. We demonstrate for the first time an association between the stability of CAIX and restoration of the S/G2 phase of hypoxia-arrested cells subjected to re-oxygenation.

We previously demonstrated that CAIX expression is a poor prognostic factor and that CAXII expression is a good prognostic factor in non-small cell lung cancer (NSCLC) patients. We further detail the relevance of the combined expression of these proteins for predicting outcome in a large population of NSCLC patients after long-term follow-up. The high CAIX/low CAXII expression subgroup was associated with a high cumulative incidence of relapse and with poor overall survival of NSCLC patients ($P < 0.0001$).

Our results demonstrate a critical role for re-oxygenation on CAIX and CAXII levels that may select for an aggressive lung cancer phenotype. These findings suggest that CAIX and CAXII play dual roles in tumour progression and emphasize their significant prognostic and potential therapeutic value.

Keywords: carbonic anhydrase IX, carbonic anhydrase XII, NSCLC, prognosis, re-oxygenation

Introduction

Adaptation of tumour cells to hypoxia and acidosis is a critical driving force in tumour progression and metastasis [1]. The transcription factor hypoxia-inducible factor-1 (HIF-1) promotes cell proliferation and stimulates nutrient supply in hypoxia by mediating adaptive survival mechanisms [2]. HIF-1 also favours tumour cell survival in a hostile microenvironment *via* remediation of tumour acidosis by activating two carbonic anhydrase (CA) isoforms, carbonic anhydrase IX (CAIX) and XII (CAXII) [2-4]. Interestingly, ectopic expression of CAIX, alone, enhances cellular proliferation, while blocking its action reduces proliferation [5]. Previous *in vitro* studies demonstrated that both CAIX and CAXII are functionally involved in tumour growth and may promote tumour cell survival by counteracting acidosis through the regulation of the intracellular pH [3, 6].

In recent years, a lot of interest has been paid to the expression of hypoxia-inducible gene products as candidates to predict cancer outcome [7, 8]. Clear evidence strongly implicates CAIX as a key pro-survival enzyme of hypoxic tumours and association with poor outcome in a wide variety of cancers, including NSCLC [9-11]. Recent reports have provided evidence that the extracellular catalytic domain can be released into body fluids of patients with kidney, bladder or lung cancers [12, 13]. A high CAIX plasma level is predictive of poor prognosis in NSCLC patients [11]. Conversely, the impact of CAXII on survival remains controversial and tissue-dependent, with CAXII tumour expression being associated with either poor survival in infiltrating astrocytic gliomas or with better outcome in invasive breast carcinomas or NSCLC [14-16].

It is well known that hypoxic areas in tumours develop as a result of an imbalance between oxygen supply and consumption [17]. The oxygen concentration within a hypoxic region is therefore highly variable. The expanding tumour mass distances certain tumour areas from local blood vessels, thereby limiting the oxygen supply. Additionally, at later stages of tumour progression, when a tumour establishes an extensive vasculature to increase oxygen supply, the defects in blood vessel structure contribute to re-oxygenation of certain tumour areas [18]. Fluctuating blood flow has been proposed to promote cancer development and progression by selecting cells that survive a hypoxic-re-oxygenation

stress [19]. However, the dynamics of CAIX and CAXII expression and the relationship to cell proliferation rates on re-oxygenation has not yet been evaluated in lung cancer cells.

In our study we used human lung adenocarcinoma cell lines to explore the differential expression of *CA9/CAIX* and *CA12/CAXII* at mRNA/Protein level in hypoxia and after re-oxygenation. We demonstrate that sustained *CA9/CAIX* expression along with decreased *CA12/CAXII* levels during re-oxygenation, after initial activation by hypoxia, may lead to the restoration of the S/G2 phase of cells subjected to re-oxygenation. Moreover, this study detailed the relationship between combined CAIX and CAXII expression in a large population of NSCLC patients and questioned whether the pattern of expression may shed light on their dual potential as independent predictors of survival in NSCLC patients.

Materials and Methods

Cell Culture and Hypoxic Exposure

The human lung cancer cell lines A549 and H1975 were originally obtained from the American Type Culture Collection (ATCC). A549 cells were cultured in DMEM (Life Technologies, Invitrogen, Carlsbad, USA) supplemented with 10% FBS. H1975 cells were maintained in RPMI-1640 medium (Life Technologies) supplemented with 10% FBS. Incubation in hypoxia at 1% O₂ was carried out at 37°C in 95% humidity and 5% CO₂/94% N₂ in a sealed workstation (InVivO₂-400, Ruskinn, Leicester, UK). After 24 h of hypoxic growth, cells were incubated in a humidified incubator with 5% CO₂ and 95% room air at 37°C. Samples were collected at 0, 8, and 24 h after re-oxygenation.

RNA Extraction and Quantitative Reverse-Transcription PCR

Total RNA was extracted with TRIzol Reagent (Life Technologies) and was purified by RNeasy kit (Qiagen, Hilden, Germany) according to the manufacturer's instructions. Elimination of DNA was achieved by treating the RNA sample with RNase-free DNase I (Life Technologies) before RT-PCR. Reverse transcription of total RNA was performed with a High Capacity cDNA RT Kit (Applied Biosystems, Foster City, USA) using random primers and 1 µg total RNA as template (Supplementary Data).

Immunoblotting

Whole-cell protein extracts were prepared from cells grown to ~50% confluence (Supplementary Data). The primary antibodies included anti-CAIX (Abcam, 1:1000, Cambridge, UK), anti-HIF-1α (1:1000, R&D Systems, Minneapolis, USA), anti-CAXII (1:200, Sigma-Aldrich), and the loading control anti-Erk1/2 (1:5000, Cell Signaling technology, Boston, USA).

Flow cytometry

Harvested cells were fixed in 75% ice-cold ethanol (in PBS) for 2 h, centrifuged, washed with PBS, and treated with 0.25% Triton X-100 for 10 min at room temperature, incubated 30 min in swine serum (1% in PBS), and then overnight with anti-CAIX (Abcam) or anti-CAXII (Sigma-Aldrich) antibodies (1:200, at 4°C). Cells were incubated with FITC anti-rabbit secondary antibodies (1:200 in PBS and 1% bovine serum albumin for 2 h), washed, resuspended in 2.5 µg/mL of propidium iodide

and 250 µg/mL of RNase A in PBS, and incubated at 4°C overnight. Fluorescence intensity values FL2-A and FL2-W were quantified in a FACScalibure (Becton Dickinson). The red and green emissions from each cell were separated and quantified using standard optics.

Patients

After our previous studies showing that CAIX and CAXII tissue expression may provide valuable clinical information for the outcome of NSCLC patients, we investigated the relevance of the combined expression of these proteins on the previous described population after long-term follow-up. 552 patients diagnosed with NSCLC were included in this retrospective study and have been previously described [11, 16]. All tumours were restaged according to the 7th edition of UICC-TNM staging system [20]. Morphological classification was reassigned according to the latest recommendations of the international association for the study of lung cancer [21, 22]. The main clinical and histopathological variables are summarized in Supplementary Table 2. Immunohistochemistry for CAIX and CAXII expression and signal automated quantification were described previously [11, 16, 23].

Statistical methods

Differences between expression groups were evaluated using the χ^2 test for categorical variables, the Student's *t* test and the one way ANOVA test for continuous variables. The coefficient of correlation (ρ) between variables was calculated using the Spearman's Rank test. Survival rates were estimated using the Kaplan-Meier method. A Cox proportional hazard model was created to identify independent predictors of survival. The variables included in the model for outcome were tumour grade, histological subtype, and pTNM stage. All statistical tests were 2-sided, and *P*-values<0.05 indicated statistical significance.

Results

Unequal hypoxic activation of CA9/CAIX and CA12/CAXII in human lung adenocarcinoma cells

An increase in the mRNA and protein expression of CA9/CAIX was observed after 32 or 48 h of hypoxia in A549 and H1975 cells (Fig. 1A, B). In contrast, hypoxia induced a delayed and modest induction of CA12/CAXII in comparison with CA9/CAIX in A549 cells (Fig. 1A, C). Surprisingly, the full-length (FL) CA12/CAXII showed no induction by hypoxia in H1975 cells neither at the transcriptional nor the protein level (Fig. 1C). As previous studies showed that different forms of CAIX and CAXII are expressed, expression of the alternatively-spliced (AS) CA9 and CA12 variants in A549 and H1975 human lung adenocarcinoma cell lines was also analysed in this context. The expression of AS CA9 was hypoxia-inducible in both cell lines (Supplementary Fig. 1). Moreover, the ratio of the full-length vs. spliced form was invariable in these cells. As for the full-length variant, the expression of AS CA12 was increased in hypoxia in A549 cells in a time-dependent manner, but not in the H1975 cells (Supplementary Fig. 1).

Dynamic response of CA9/CAIX and CA12/CAXII and the proliferation cell rate upon re-oxygenation

To understand the specific regulation of CAIX and CAXII after a cycle of hypoxia/re-oxygenation, A549 and H1975 human lung adenocarcinoma cells were maintained in normoxia or hypoxia for 32 or 48 h or incubated in hypoxia for 24 h and then shifted to normoxia for either 8 or 24 h. The expression level of the transcripts and of the protein, respectively CA9/CAIX observed in hypoxia were sustained after 8 h of re-oxygenation in both A549 and H1975 cells (Fig. 1B). Although CA9/CAIX levels returned to baseline normoxic levels after an additional 24 h of re-oxygenation, the transcript and protein levels were nevertheless significantly higher than those quantified in normoxia. In contrast, the CA12/CAXII expression was only slightly induced by hypoxia and dramatically down-regulated in A549 cells after re-oxygenation (Fig. 1C). Flow cytometry of asynchronously growing A549 and H1975 cells showed arrest in G1 in hypoxia (80% vs. 68%; 82% vs. 56%, respectively; $P < 0.05$). As expected, the S/G2 phase was restored within 24 h after re-oxygenation (28% vs. 17%; 20% vs. 11%, respectively; $P < 0.05$, Fig. 2A, B). Interestingly, our results reveal that CAIX expression

is mainly restricted to growing cells (S/G2) after 32 h of hypoxia for both A549 and H1975 cells (Fig. 2C, D). Moreover, after 48 h of hypoxia both the G1 and S/G2 subpopulations demonstrated increased CAIX expression, with more staining in S/G2 cells ($P<0.05$; Fig. 2C, D). Our experiments revealed that S/G2-related CAIX expression was maintained in re-oxygenated cells relative to the normoxic control ($P<0.05$), while no effect was observed on CAXII expression (Fig. 2C, D).

CAIX and CAXII subgroup expression in patients is associated with opposite survival prognosis.

The semi-automated quantification analysis revealed 60/552 (11%) of tumours with a strong CAIX and low CAXII expression (Supplementary Table 2). 87/552 (16%) of tumours demonstrated weak CAIX and high CAXII expression. Only 17 (3%) tumours co-expressed high CAIX and high CAXII expression. There was no significant interrelationship between CAIX and the CAXII tumour expression ($\rho=1$, $P=0.994$). As shown in Supplementary Table 2, only the low CAIX/low CAXII expression subgroup significantly correlated with the smoking status of patients ($P=0.013$), the histological cell subtype ($P<0.0001$), and with well-differentiated tumours ($P=0.011$). Interestingly, the different subgroups of CAIX or CAXII expression were age, gender, tumour size, and pTNM stage independent.

At the last follow-up (range, 52 to 120 months), 214/552 (39%) patients had died, including 152/552 (28%) patients who died specifically from NSCLC progression. In the univariate analysis, clinical factors significantly associated with cumulated incidence of relapse (CIR) were the pTNM stage ($P<0.0001$), tumour grade ($P=0.075$), and the differential expression of CAIX and CAXII ($P<0.0001$) (Fig. 3). Age, gender, histological type and the smoking history were not associated with CIR (data not shown). In addition, the strong correlation between CIR and the differential expression of CAIX and CAXII was higher in early-stage I+II tumours ($P<0.0001$) than in later-stages III+IV ($P=0.006$) (Supplementary Fig. 2). Moreover, the strong impact of the differential expression of CAIX and CAXII on CIR was conserved in the most frequent NSCLC subtypes (e.g. squamous cell carcinoma, $P<0.0001$, and adenocarcinoma, $P<0.0001$) (Supplementary Fig. 3). In the multivariate analysis, the independent factors for higher CIR were stages III and IV ($P<0.0001$) and the high CAIX/low CAXII expression subgroup ($P=0.022$) (Table 1). Furthermore, the clinical factors

significantly associated with overall survival (OS) were the pTNM stage ($P<0.0001$), histological grade ($P=0.006$), histological cell type ($P=0.05$) and the CAIX and CAXII expression subgroups ($P<0.0001$) (Fig. 3). No significant correlation was observed between CIR and age, gender, or smoking history (data not shown). We also determined whether the CAIX and CAXII expression subgroups could discriminate patient outcome at each step of cancer progression. These subgroups significantly predicted OS in a more impressive manner in early-stage I+II tumours ($P<0.0001$) than in later-stages III+IV ($P=0.040$) (Supplementary Fig. 4). Moreover, the CAIX and CAXII subgroups significantly associated with OS in the most frequent NSCLC subtypes (e.g. adenocarcinoma, $P=0.003$, and squamous cell carcinoma, $P<0.0001$) (Supplementary Fig. 5). Multivariate analyses demonstrated that histology ($P=0.013$), III and IV stages ($P=0.006$), and the high CAIX/low CAXII expression subgroup ($P=0.045$) were independent prognostic factors for poor OS (Table 1).

Discussion

There is clear evidence implicating CAIX expression as a strong predictor of poor outcome in patients with a carcinoma [24, 25]. Conversely, conflicting results about the impact of CAXII tissue expression on clinical outcome of cancer patients have been reported [5, 26].

The tumour microenvironment is subjected to fluctuations in oxygen, which result from hyper-proliferation and abnormal metabolism of tumour cells as well as a disorganized neo-vasculature [27]. Re-oxygenation of tumour cells not only increases the amount of oxygen, but may induce DNA damage and potentially increased genomic instability [28]. If tumour cells survive after exposure to a hypoxia/re-oxygenation insult, they may demonstrate drug resistance and metastatic potential [27]. Although both CAIX and CAXII are known to be regulated by hypoxia, little is known about the adaptive mechanisms and dynamic responses of CAIX and CAXII upon re-oxygenation. We have therefore investigated the temporal relationship between the expression of CAIX and CAXII and hypoxia or re-oxygenation, as well as the expression in two human lung adenocarcinoma cell lines of their splicing variants. We have further investigated the frequency of expression of both CAIX and CAXII in NSCLC patients and whether the balance in expression of these two CA isoenzymes could modify the prediction of clinical outcome of these patients.

The initial response of lung adenocarcinoma cells to hypoxia was the stabilization of HIF-1 α along with marked induction of CAIX. We were not able to detect CAXII expression in H1975 cells neither in normoxia nor in hypoxia. These findings supported our immunohistochemical data that showed only a slight overlap (3%) between high CAIX and high CAXII expression in NSCLC patients. Twenty-seven % of tumours had either high CAIX with low CAXII expression or conversely low CAIX together with high CAXII expression, suggesting mutually exclusive detection of these two isoforms in NSCLC. Moreover, no significant correlation was noted between CAIX and CAXII expression in tumour tissue samples.

We hypothesized that the difference in distribution may reflect different temporal responses to cellular hypoxia and re-oxygenation. While CAIX showed marked induction in hypoxia of 32 h CAXII required 48 h of hypoxia in A549 cells. Whereas the transcript and protein levels of CAIX remained high during re-oxygenation for at least 24 h those of CAXII declined rapidly. Moreover, in

cells exposed to hypoxia we observed decreased cell cycle arrest, as previously reported [29]. Because fluctuations in oxygen pressure occur in tumours, we investigated the effect of re-oxygenation on CAIX and CAXII expression in arrested hypoxic cells. Following 8 h of re-oxygenation, the S/G2 phase was restored and the restart-associated CAIX expression was higher relative to normoxia. Our findings suggest that once CAIX is transcriptionally induced by hypoxia, lung cancer cells can maintain CAIX stability in re-oxygenated conditions, consistent with the half-life of CAIX [30]. We demonstrate for the first time a connection between the post-translational stability of CAIX and the replicative restart of hypoxia arrested cells. Furthermore, CAXII expression seemed to have a minimum effect on cell proliferation upon re-oxygenation as the mRNA and protein levels were rapidly down-regulated by the shift to normoxia. Thus, these observations strengthen our hypothesis that the dynamic CAIX and CAXII response to hypoxia-re-oxygenation may promote aggressive tumor growth. Cancer cells may therefore require hypoxia-inducible CAXII expression at early steps in oncogenesis, yet CAIX expression may be more relevant in increasing the metastatic potential of NSCLC.

Our observations were supported by our findings in NSCLC patients. The strong tumour CAIX expression associated with weak CAXII expression had an unfavourable impact on relapse and survival. Surprisingly, either the co-expression of high CAIX and high CAXII or the simultaneous low CAIX and low CAXII tumour expression had an intermediate impact on relapse and patient outcome. Conversely, low tumour CAIX expression associated with CAXII overexpression, significantly correlated with a lower level of relapse and better prognosis. When examined with a multivariate Cox proportional hazard regression model controlled for several covariates, the subgroup corresponding to high CAIX expression together with low CAXII expression was shown to be an independent predictor of higher CIR and poor OS. This study allowed us to stratify NSCLC patients into groups with different CIR and OS rates according to the tumour CAIX and CAXII expression subgroups.

Surprisingly, the subgroup co-expressing high CAXII and low CAIX had an improved outcome in NSCLC patients and this finding differs from those on astrocytomas [14, 31]. Both *CA9* and *CA12* have alternatively spliced isoforms with different distributions in response to cellular hypoxia along with a dissimilar relationship to clinical outcome [5, 14, 26, 32]. In addition to the

expected full length mRNA of *CA9*, a *CA9* alternative splicing isoform has been previously detected in normal and cancer cells, independently of the level of oxygen [32]. The AS variant generates a transcript lacking exons 8–9 and encodes a truncated CAIX protein lacking the transmembrane region, the intracellular tail and the C-terminal part of the catalytic domain. High expression of the FL-*CA9* isoform was related to decreased survival rates of lung cancer patients [33]. However, the expression of the AS-*CA9* mRNA showed no relationship to survival [34]. Like *CA9*, *CA12* has two splice variants. In astrocytomas, the shorter variant was associated with poor prognosis, in contrast to breast carcinoma cell lines that express preferentially the full-length variant [5, 14, 26]. In our study, the results of quantitative RT-PCR showed a constant FL to AS ratio in two human lung adenocarcinoma cells cultured under hypoxic or re-oxygenated conditions when compared to normoxia. In contrast, *CA12* expression seemed to be dependent on the phenotype, as both FL and AS *CA12* forms were induced by hypoxia exclusively in A549 cells.

Conclusion

This study emphasizes the importance of hypoxia-re-oxygenation in defining the pattern of CAIX and CAXII expression and the relationship with a hostile phenotype in NSCLC. The dual expression and association with survival of the related CAIX and CAXII isoforms may be an issue for determining the therapeutic strategy for NSCLC patients [35]. Thus, tumour cells expressing CAIX could acquire a particularly hostile behaviour in contrast to the CAXII overexpressing cell sub-population, which may be less aggressive. Therefore, with regard to future development of CA inhibitors, knowledge of the CA isoform phenotype of a given tumour type is required for individual effective anti-cancer treatments.

Disclosure of Potential Conflicts of Interest

No potential conflicts of interest were disclosed.

Acknowledgments

This work was partly supported by grants from the Cancéropole PACA, and by the “Fondation ARC pour la recherche sur le cancer” ARC SL220110603478 (PH, PB, MI).

References

1. Pouyssegur J, Dayan F, Mazure NM. Hypoxia signalling in cancer and approaches to enforce tumour regression. *Nature* 2006; 441: 437-443.
2. Brahimi-Horn MC, Bellot G, Pouyssegur J. Hypoxia and energetic tumour metabolism. *Curr Opin Genet Dev* 2011; 21: 67-72.
3. Chiche J, Ilc K, Laferriere J, Trottier E, Dayan F, Mazure NM, Brahimi-Horn MC, Pouyssegur J. Hypoxia-inducible carbonic anhydrase IX and XII promote tumor cell growth by counteracting acidosis through the regulation of the intracellular pH. *Cancer Res* 2009; 69: 358-368.
4. Parks SK, Chiche J, Pouyssegur J. pH control mechanisms of tumor survival and growth. *J Cell Physiol* 2011; 226: 299-308.
5. Li Y, Wang H, Oosterwijk E, Tu C, Shiverick KT, Silverman DN, Frost SC. Expression and activity of carbonic anhydrase IX is associated with metabolic dysfunction in MDA-MB-231 breast cancer cells. *Cancer Invest* 2009; 27: 613-623.
6. Swietach P, Patiar S, Supuran CT, Harris AL, Vaughan-Jones RD. The role of carbonic anhydrase 9 in regulating extracellular and intracellular pH in three-dimensional tumor cell growths. *J Biol Chem* 2009; 284: 20299-20310.
7. Potter CP, Harris AL. Diagnostic, prognostic and therapeutic implications of carbonic anhydrases in cancer. *Br J Cancer* 2003; 89: 2-7.
8. Poulsen SA. Carbonic anhydrase inhibition as a cancer therapy: a review of patent literature, 2007 - 2009. *Expert Opin Ther Pat* 2010; 20: 795-806.
9. Beketic-Oreskovic L, Ozretic P, Rabbani ZN, Jackson IL, Sarcevic B, Levanat S, Maric P, Babic I, Vujaskovic Z. Prognostic Significance of Carbonic Anhydrase IX (CA-IX), Endoglin (CD105) and 8-hydroxy-2'-deoxyguanosine (8-OHdG) in Breast Cancer Patients. *Pathol Oncol Res* 2011; 17: 593-603.

10. Nordfors K, Haapasalo J, Korja M, Niemela A, Laine J, Parkkila AK, Pastorekova S, Pastorek J, Waheed A, Sly WS, Parkkila S, Haapasalo H. The tumour-associated carbonic anhydrases CA II, CA IX and CA XII in a group of medulloblastomas and supratentorial primitive neuroectodermal tumours: an association of CA IX with poor prognosis. *BMC Cancer* 2010; 10: 148.
11. Ilie M, Mazure NM, Hofman V, Ammadi RE, Ortholan C, Bonnetaud C, Havet K, Venissac N, Mograbi B, Mouroux J, Pouyssegur J, Hofman P. High levels of carbonic anhydrase IX in tumour tissue and plasma are biomarkers of poor prognostic in patients with non-small cell lung cancer. *Br J Cancer* 2010; 102: 1627-1635.
12. Zavada J, Zavadova Z, Zat'ovicova M, Hyrsl L, Kawaciuk I. Soluble form of carbonic anhydrase IX (CA IX) in the serum and urine of renal carcinoma patients. *Br J Cancer* 2003; 89: 1067-1071.
13. Hyrsl L, Zavada J, Zavadova Z, Kawaciuk I, Vesely S, Skapa P. Soluble form of carbonic anhydrase IX (CAIX) in transitional cell carcinoma of urinary tract. *Neoplasma* 2009; 56: 298-302.
14. Haapasalo J, Hilvo M, Nordfors K, Haapasalo H, Parkkila S, Hyrskyluoto A, Rantala I, Waheed A, Sly WS, Pastorekova S, Pastorek J, Parkkila AK. Identification of an alternatively spliced isoform of carbonic anhydrase XII in diffusely infiltrating astrocytic gliomas. *Neuro Oncol* 2008; 10: 131-138.
15. Watson PH, Chia SK, Wykoff CC, Han C, Leek RD, Sly WS, Gatter KC, Ratcliffe P, Harris AL. Carbonic anhydrase XII is a marker of good prognosis in invasive breast carcinoma. *Br J Cancer* 2003; 88: 1065-1070.
16. Ilie MI, Hofman V, Ortholan C, Ammadi RE, Bonnetaud C, Havet K, Venissac N, Mouroux J, Mazure NM, Pouyssegur J, Hofman P. Overexpression of carbonic

- anhydrase XII in tissues from resectable non-small cell lung cancers is a biomarker of good prognosis. *Int J Cancer* 2011; 128: 1614-1623.
17. Vaupel P, Mayer A. Hypoxia in cancer: significance and impact on clinical outcome. *Cancer Metastasis Rev* 2007; 26: 225-239.
 18. Carmeliet P. VEGF as a key mediator of angiogenesis in cancer. *Oncology* 2005; 69 Suppl 3: 4-10.
 19. Khandrika L, Lieberman R, Koul S, Kumar B, Maroni P, Chandhoke R, Meacham RB, Koul HK. Hypoxia-associated p38 mitogen-activated protein kinase-mediated androgen receptor activation and increased HIF-1alpha levels contribute to emergence of an aggressive phenotype in prostate cancer. *Oncogene* 2009; 28: 1248-1260.
 20. Goldstraw P. The 7th Edition of TNM in Lung Cancer: what now? *J Thorac Oncol* 2009; 4: 671-673.
 21. Travis WD, Müller-Hermelink HK, Harris CC. WHO histological classification of tumors of the lung. *World Health Organization Classification of Tumours Pathology and Genetics of Tumours of the Lung, Pleura, Thymus and Heart*. ed. Lyon: IARC Press; 2004.
 22. Travis WD, Brambilla E, Noguchi M, Nicholson AG, Geisinger KR, Yatabe Y, Beer DG, Powell CA, Riely GJ, Van Schil PE, Garg K, Austin JH, Asamura H, Rusch VW, Hirsch FR, Scagliotti G, Mitsudomi T, Huber RM, Ishikawa Y, Jett J, Sanchez-Cespedes M, Sculier JP, Takahashi T, Tsuboi M, Vansteenkiste J, Wistuba I, Yang PC, Aberle D, Brambilla C, Flieder D, Franklin W, Gazdar A, Gould M, Hasleton P, Henderson D, Johnson B, Johnson D, Kerr K, Kuriyama K, Lee JS, Miller VA, Petersen I, Roggli V, Rosell R, Saijo N, Thunnissen E, Tsao M, Yankelewitz D. International association for the study of lung cancer/american thoracic

- society/european respiratory society international multidisciplinary classification of lung adenocarcinoma. *J Thorac Oncol* 2011; 6: 244-285.
23. Hofman P, Butori C, Havet K, Hofman V, Selva E, Guevara N, Santini J, Van Obberghen-Schilling E. Prognostic significance of cortactin levels in head and neck squamous cell carcinoma: comparison with epidermal growth factor receptor status. *Br J Cancer* 2008; 98: 956-964.
 24. Korkeila E, Talvinen K, Jaakkola PM, Minn H, Syrjanen K, Sundstrom J, Pyrhonen S. Expression of carbonic anhydrase IX suggests poor outcome in rectal cancer. *Br J Cancer* 2009; 100: 874-880.
 25. Brennan DJ, Jirstrom K, Kronblad A, Millikan RC, Landberg G, Duffy MJ, Ryden L, Gallagher WM, O'Brien SL. CA IX is an independent prognostic marker in premenopausal breast cancer patients with one to three positive lymph nodes and a putative marker of radiation resistance. *Clin Cancer Res* 2006; 12: 6421-6431.
 26. Hsieh MJ, Chen KS, Chiou HL, Hsieh YS. Carbonic anhydrase XII promotes invasion and migration ability of MDA-MB-231 breast cancer cells through the p38 MAPK signaling pathway. *Eur J Cell Biol* 2010; 89: 598-606.
 27. Lai LC, Su YY, Chen KC, Tsai MH, Sher YP, Lu TP, Lee CY, Chuang EY. Down-regulation of NDRG1 promotes migration of cancer cells during reoxygenation. *PLoS One* 2011; 6: e24375.
 28. Aguilera A, Gomez-Gonzalez B. Genome instability: a mechanistic view of its causes and consequences. *Nat Rev Genet* 2008; 9: 204-217.
 29. Pires IM, Bencokova Z, Milani M, Folkes LK, Li JL, Stratford MR, Harris AL, Hammond EM. Effects of acute versus chronic hypoxia on DNA damage responses and genomic instability. *Cancer Res* 2010; 70: 925-935.

30. Rafajova M, Zatovicova M, Kettmann R, Pastorek J, Pastorekova S. Induction by hypoxia combined with low glucose or low bicarbonate and high posttranslational stability upon reoxygenation contribute to carbonic anhydrase IX expression in cancer cells. *Int J Oncol* 2004; 24: 995-1004.
31. Haapasalo JA, Nordfors KM, Hilvo M, Rantala IJ, Soini Y, Parkkila AK, Pastorekova S, Pastorek J, Parkkila SM, Haapasalo HK. Expression of carbonic anhydrase IX in astrocytic tumors predicts poor prognosis. *Clin Cancer Res* 2006; 12: 473-477.
32. Barathova M, Takacova M, Holotnakova T, Gibadulinova A, Ohradanova A, Zatovicova M, Hulikova A, Kopacek J, Parkkila S, Supuran CT, Pastorekova S, Pastorek J. Alternative splicing variant of the hypoxia marker carbonic anhydrase IX expressed independently of hypoxia and tumour phenotype. *Br J Cancer* 2008; 98: 129-136.
33. Simi L, Venturini G, Malentacchi F, Gelmini S, Andreani M, Janni A, Pastorekova S, Supuran CT, Pazzagli M, Orlando C. Quantitative analysis of carbonic anhydrase IX mRNA in human non-small cell lung cancer. *Lung Cancer* 2006; 52: 59-66.
34. Malentacchi F, Simi L, Nannelli C, Andreani M, Janni A, Pastorekova S, Orlando C. Alternative splicing variants of carbonic anhydrase IX in human non-small cell lung cancer. *Lung Cancer* 2009; 64: 271-276.
35. Morris JC, Chiche J, Grellier C, Lopez M, Bornaghi LF, Maresca A, Supuran CT, Pouyssegur J, Poulsen SA. Targeting hypoxic tumor cell viability with carbohydrate-based carbonic anhydrase IX and XII inhibitors. *J Med Chem* 2011; 54: 6905-6918.

Table 1. Multivariate Cox proportional hazard regression analysis for predicting factors for the cumulative incidence of relapse and overall survival in 552 NSCLC patients.

Prognostic factor	Categories compared	Hazard Ratio	95% CI	P
<i>Cumulative Incidence of Relapse</i>				
Tumor grade	1 vs. other	1.379	0.848–3.412	0.485
Histological cell type	ADC vs. others	1.644	0.952–2.840	0.074
pTNM stage	I+II vs. III+IV	1.883	1.416–2.500	<0.0001
CAIX and CAXII expression sub-groups	High CAIX/Low CAXII vs. others	2.500	1.144–5.462	0.022
<i>Overall Survival</i>				
Tumor grade	1 vs. other	1.782	0.781–4.065	0.169
Histological cell type	ADC vs. others	2.074	1.165–3.690	0.013
pTNM stage	I+II vs. III+IV	2.673	1.328–5.376	0.006
CAIX and CAXII expression sub-groups	High CAIX/Low CAXII vs. others	2.490	1.020–6.079	0.045

Abbreviations: CI, confidence interval; CIR, Cumulative Incidence of Relapse; OS, Overall Survival; ADC, adenocarcinoma; TNM=tumor node metastasis.

Legend to Figures

Fig. 1. Dynamics of CAIX/CA9 and CAXII/CA12 expression in A549 (*left panels*) and H1975 (*right panels*) human lung adenocarcinoma cell lines cultured in normoxia (N), hypoxia 1% O₂ (H) or re-oxygenation (ReO₂) conditions for 32 h and 48 h. **(A)** Immunoblot analysis using equal protein (100 µg) detected CAIX and CAXII proteins in whole cell lysates. Total Erk is shown as loading control. **(B)** Full-length (FL) CA9 mRNA levels in A549 and H1975 cells, as determined by real-time qPCR. The results are representative of two separate experiments. The mRNA levels of CA9 were normalized to 36B4/RPLP0. **(C)** Full-length (FL) CA12 mRNA levels in A549 and H1975 cells, as determined by real-time qPCR. The results are representative of two separate experiments. The mRNA levels of CA12 were normalized to 36B4/RPLP0.

Fig. 2. CAIX and CAXII expression-dependent cell proliferation in A549 and H1975 lung adenocarcinoma cell s. **(A, B)** Cell cycle quantified by flow cytometry after propidium iodide staining. A549 **(A)** and H1975 **(B)** cells were incubated in normoxia (*left*), hypoxia (*center*) or hypoxia (24 h) and then shifted to normoxia (*right*) for 8 h (32 h ReO₂) or 24 h (48 h ReO₂). Results are from one of three experiments. **(C, D)** CAIX and CAXII expression-dependent cell viability in A549 **(C)** and H1975 **(D)** cells. Bars, SD. **P*-value significant at the level < 0.05.

Fig. 3. **(A)** Kaplan-Meier curves of the cumulative incidence of relapse stratified according to the differential expression of CAIX and CAXII in 552 NSCLC patients. **(B)** Kaplan-Meier curves of overall survival stratified according to the differential expression of CAIX and CAXII in 552 NSCLC patients.

Legend to Supplementary Figures

Supplementary Fig. 1. Expression of the alternatively-spliced (AS) *CA9* and *CA12* variants and the FL/AS ratio in A549 and H1975 human lung adenocarcinoma cells cultured under normoxic or hypoxic (1% O₂) conditions for 24 h or 48 h. The results are representative of two separate experiments. **(A) Top panel**, expression of the AS-*CA9* levels in either A549 or H1975 cells, as determined by real-time qPCR. **Bottom**, The FL/AS-*CA9* ratio in the cells. The mRNA levels of *CA9* were normalized to 36B4. **(B) Top panel**, expression of the AS-*CA12* level in either A549 or H1975 cells, as determined by real-time qPCR. **Bottom**, The FL/AS-*CA12* ratio in the cells. The mRNA levels of *CA12* were normalized to 36B4.

Supplementary Fig. 2. **(A)** Median cumulative incidence of relapse stratified according to the differential expression of the CAIX and CAXII subgroups in early-stage I+II NSCLC. **(B)** Kaplan-Meier estimates of the cumulative incidence of relapse based on the differential expression of CAIX and CAXII in early-stage I+II NSCLC. **(C)** Median cumulative incidence of relapse stratified according to the differential expression of the CAIX and CAXII subgroups in later-stage III+IV NSCLC. **(D)** Kaplan-Meier estimates of the cumulative incidence of relapse based on the differential expression of CAIX and CAXII in later-stage III+IV NSCLC.

Supplementary Fig. 3. **(A)** Kaplan-Meier estimates of the cumulative incidence of relapse based on the differential expression of CAIX and CAXII in lung squamous cell carcinomas. **(B)** Kaplan-Meier estimates of the cumulative incidence of relapse based on the differential expression of CAIX and CAXII in lung adenocarcinomas.

Supplementary Fig. 4. **(A)** Median overall survival (OS) stratified according to the differential expression of the CAIX and CAXII subgroups in early-stage I+II NSCLC. **(B)** Kaplan-Meier estimates of the OS based on the differential expression of CAIX and CAXII in early-stage I+II NSCLC. **(C)** Median overall survival stratified according to the differential expression of the CAIX and CAXII subgroups in later-stage III+IV NSCLC. **(D)** Kaplan-Meier estimates of the overall survival based on the differential expression of CAIX and CAXII in later-stage III+IV NSCLC.

Supplementary Fig. 5. **(A)** Kaplan-Meier estimates of the overall survival (OS) based on the differential expression of CAIX and CAXII in lung squamous cell carcinomas. **(B)** Kaplan-Meier

estimates of the OS based on the differential expression of CAIX and CAXII in lung adenocarcinomas.

Figure 1

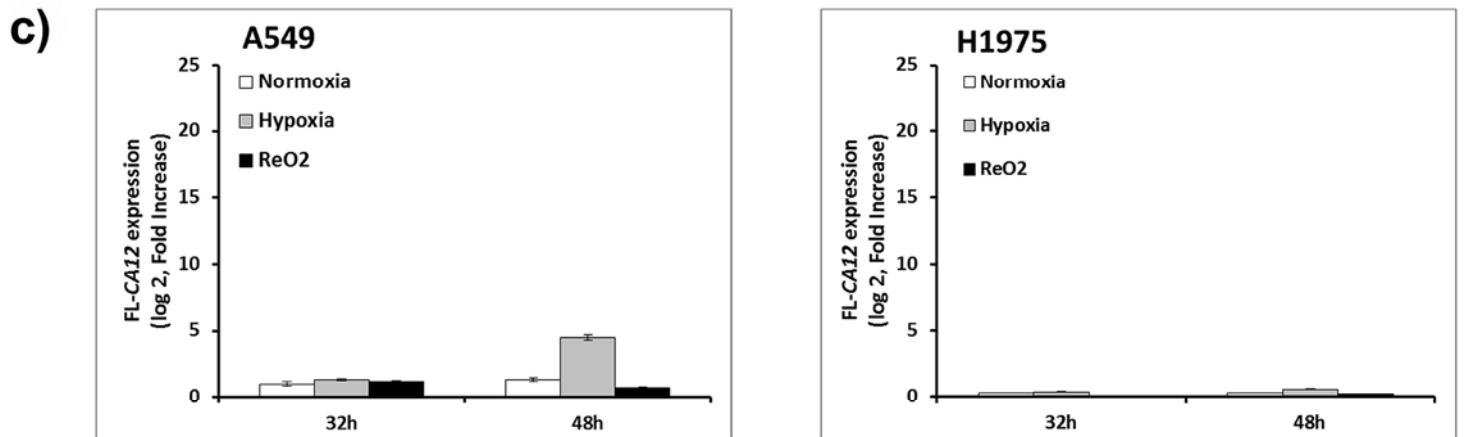
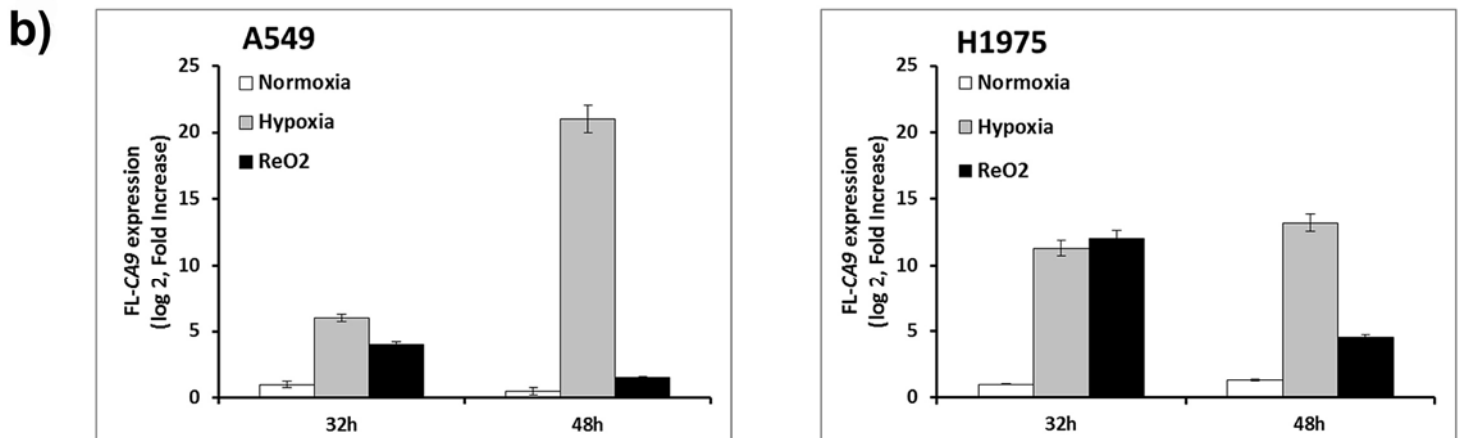
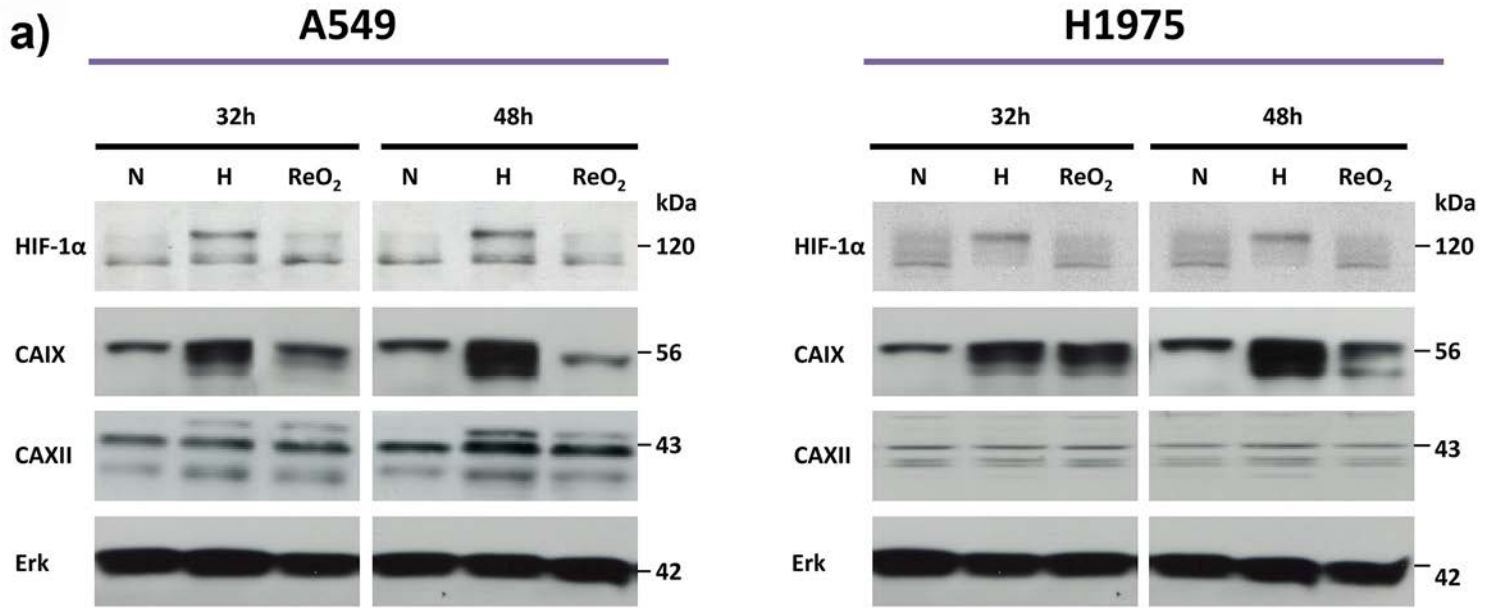


Figure 2

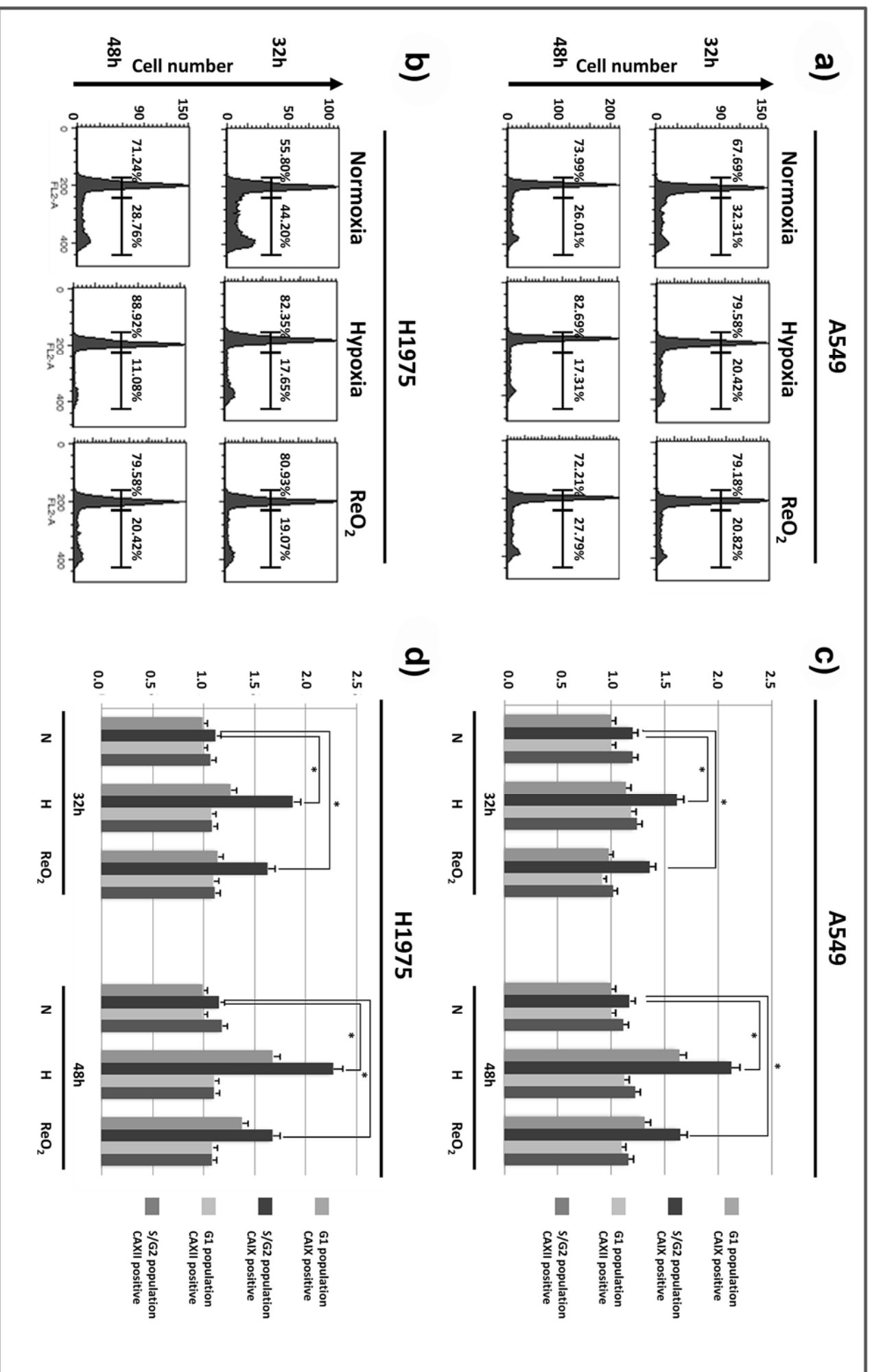
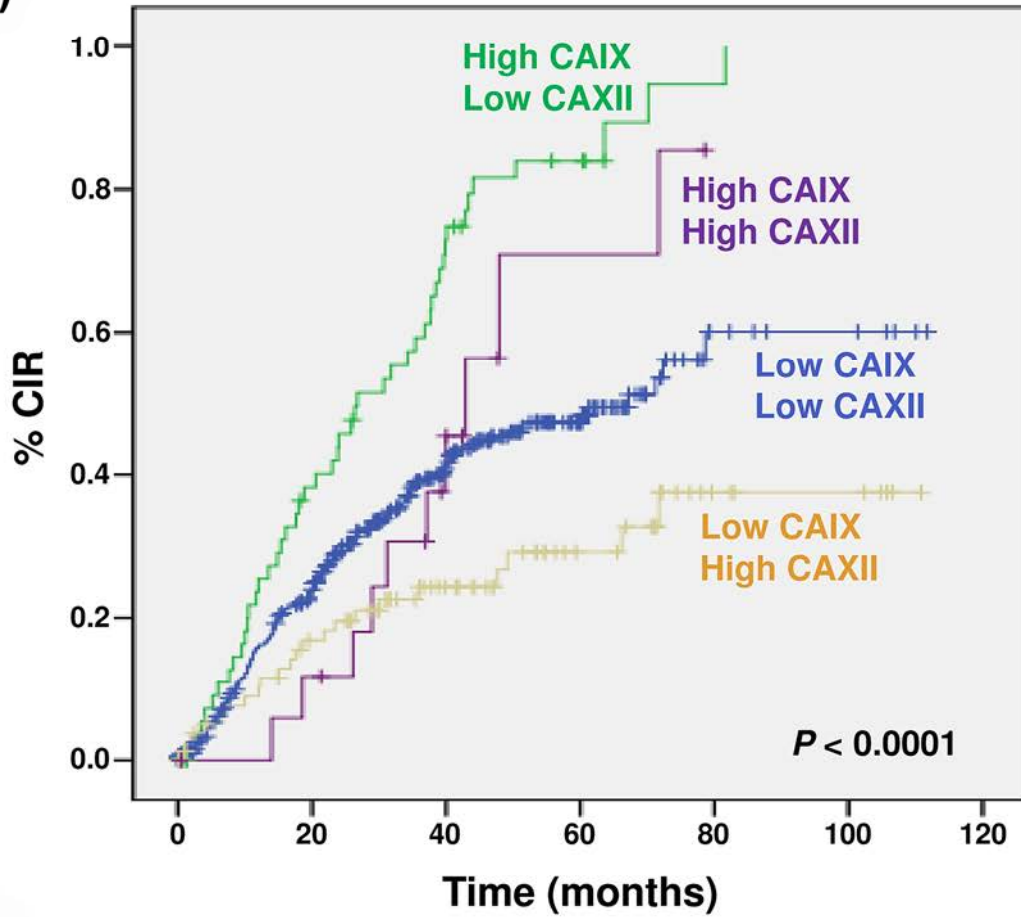
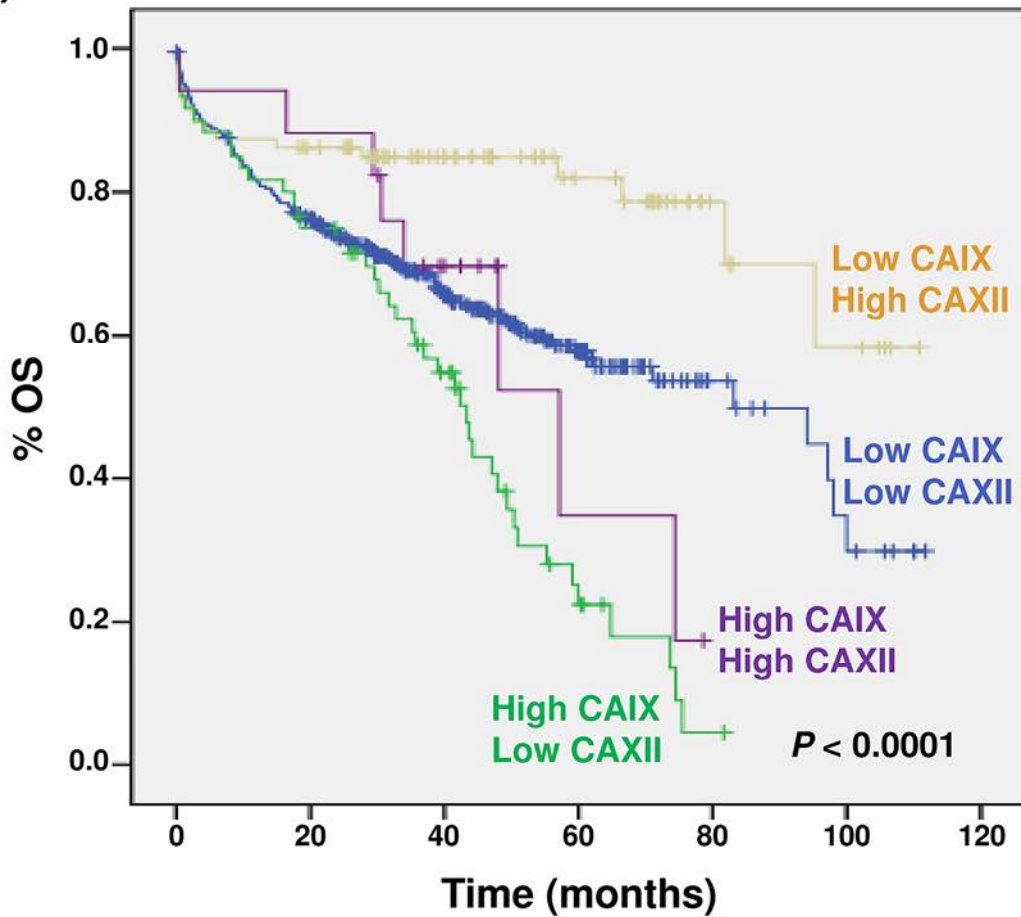


Figure 3

a)



b)



Supplementary Data

RNA Extraction and Quantitative Reverse-Transcription PCR

Total RNA was extracted with TRIzol Reagent (Life Technologies) and was purified by RNeasy kit (Qiagen, Hilden, Germany) according to the manufacturer's instructions. Elimination of DNA was achieved by treating the RNA sample with RNase-free DNase I (Life Technologies) before RT-PCR. Reverse transcription of total RNA was performed with a High Capacity cDNA RT Kit (Applied Biosystems, Foster City, USA) using random primers and 1 µg total RNA as template. The reaction mixture was incubated at 25°C for 10 min, 37°C for 2 h and 85°C for 5 min. PCR primers were designed based on the complete cDNA sequences deposited in GenBank (accession numbers: NM_001216.2 for FL CA9, EF122496.1 for AS CA9, NM_001218.3 for FL CA12, and NM_206925.1 for AS CA12; Supplementary Table 1). PCR products were detected with SYBR Green probes (Life Technologies) and PCR was performed using the ABI 7500 Fast apparatus (Life Technologies). For each cDNA sample, an internal control, human 36B4/RPLP0 was also measured. The amount of human CA9 and CA12 transcripts in the different cell lines after indicated treatments compared to 36B4 in each sample was calculated. All measurements were carried out in duplicate.

Immunoblotting

Whole-cell protein extracts were prepared from cells grown to ~50% confluence. The cells were scratched from culture plates and lysed in Laemmli buffer (60 mM Tris-Cl pH 6.8, 2% SDS, 10% glycerol, 5% β-mercaptoethanol, 0.01% bromophenol blue). The protein concentration was measured by the Lowry method (BioDC, Bio-Rad), and 50–75 µg protein was separated on 7%, 10% and 12% denaturing SDS polyacrylamide gels. The separated

proteins were electrophoretically transferred to polyvinylidene fluoride membranes (Millipore, Watford, UK) 2 h at 400 mA. The membranes were blocked with Tris-Buffered Saline Tween-20 containing 5% non-fat milk at room temperature. Detection of specific proteins was done by probing membranes with primary antibodies in 0.1% Tween-20 containing 5% nonfat dry milk overnight at 4 °C. These antibodies included anti-CAIX (Abcam, 1:1000, Cambridge, UK), anti-HIF-1 α (1:1000, R&D Systems, Minneapolis, USA), anti-CAXII (1:200, Sigma-Aldrich), and the loading control anti-Erk1/2 (1:5000, Cell Signaling technology, Boston, USA). After incubation with horseradish peroxidase-conjugated IgG secondary antibodies (1:5000), the immunoreactivity was visualized by enhanced chemiluminescence (Perkin Helmer, Buckinghamshire, UK).

Legend to Supplementary Tables

Supplementary Table 1. Primer sequences for quantitative real-time PCR used in the study

Gene	Forward primer	Reverse primer	PCR product size
<i>CA9</i>	TGACTACACCGCCCTGTGC	GCTCACACCCCCTTTGGTTC	353 bp
<i>CA9 FL</i>	TGACTACACCGCCCTGTGC	CAGGTCCCCACAGGGTGTC	108 bp
<i>CA9 FC</i>	CCAGGGCTAGGACTGCTTAGC	GCTCACACCCCCTTTGGTTC	110 bp
<i>CA12</i>	CAACTCCGGCAGGTCCAGA	CTGGACACTTGCGACACCTCAA	336 bp (isoform 1) 303 bp (isoform 2)
<i>CA12 FL</i>	TACACCTCCTTCTCCCAAGTGCAAG	TGTGGTGGTGGTGTCCATTGGC	121 bp
<i>CA12 FC</i>	CACCTCCTTCTCCCAAGGCATCATC	TGTGGTGGTGGTGTCCATTGGC	86 bp

Supplementary Table 2. Correlation of CAIX and CAXII expression subgroups as detected by immunohistochemistry on TMAs with the clinicopathological parameters of 552 NSCLC patients.

Feature	Overall	Low CAIX	High CAIX	Low CAIX	High CAIX	P
	n (%)	Low CAXII	Low CAXII	High CAXII	High CAXII	
		n (%)	n (%)	n (%)	n (%)	
Patient cohort	552 (100)	332 (60)	116 (21)	87 (16)	17 (3)	
Age (y) §						0.315
Mean ± SD	64 ± 10	63.4 ± 10.1	65.4 ± 8.6	65.3 ± 10.6	63.1 ± 10	
Gender						0.064
Male	413 (75)	253 (61)	89 (22)	56 (14)	15 (3)	
Female	139 (25)	79 (57)	27 (19)	31 (22)	2 (2)	
Smoking history						0.165
Never smoked	74 (13)	39 (53)	16 (22)	14 (19)	5 (6)	
Former or current smokers	478 (87)	293 (61)	100 (21)	73 (15)	12 (3)	
Tumor size (mean ± SD) cm	3.7 ± 2.4	3.6 ± 2.4	3.6 ± 1.7	4.1 ± 2.5	4.2 ± 2.5	0.343
Histological cell type						<0.0001
Adenocarcinoma	279 (51)	215 (77)	33 (12)	30 (11)	1 (0)	
Squamous cell carcinoma	183 (33)	60 (33)	60 (33)	55 (30)	8 (4)	
Sarcomatoid carcinoma	47 (9)	30 (64)	11 (23)	2 (4)	4 (9)	
Large cell carcinoma	43 (7)	27 (63)	12 (28)	0 (0)	4 (9)	
pTNM stage						0.237
I	292 (53)	180 (62)	52 (18)	50 (17)	10 (3)	
II	121 (22)	70 (58)	31 (26)	18 (15)	2 (1)	
III	127 (23)	78 (61)	27 (21)	17 (13)	5 (5)	
IV	12 (2)	4 (33)	6 (50)	2 (17)	0 (0)	

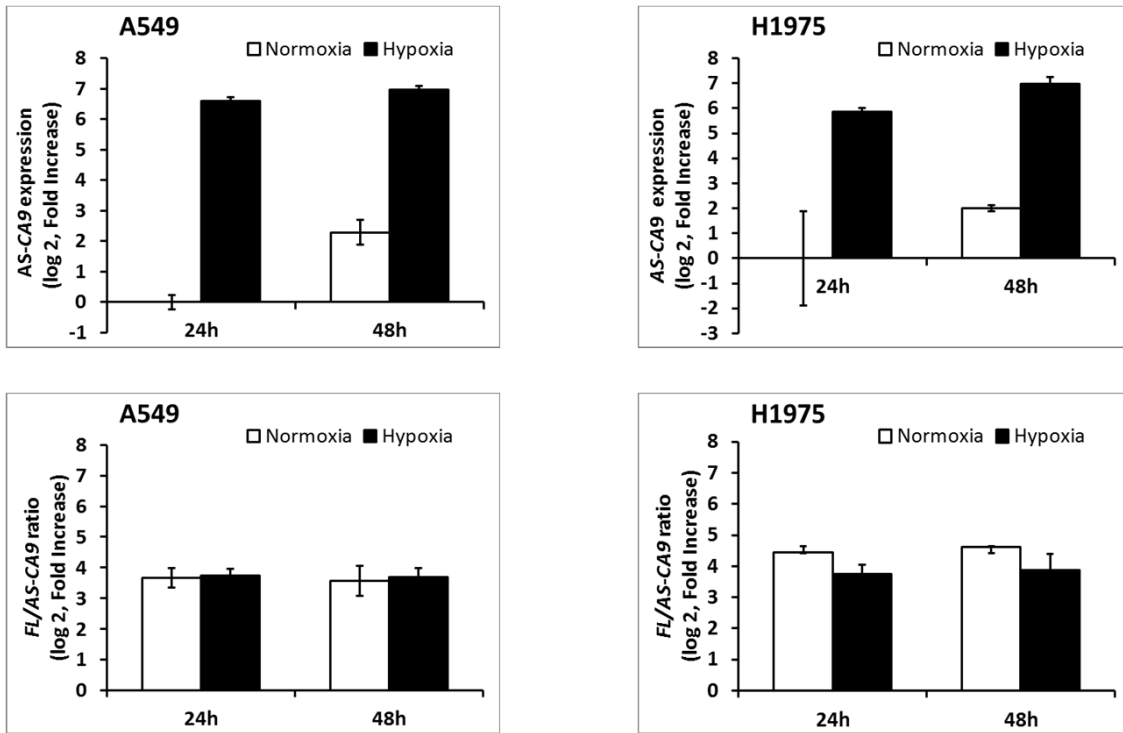
TNM = tumor node metastasis.

χ^2 test or Student's *t* test was used.

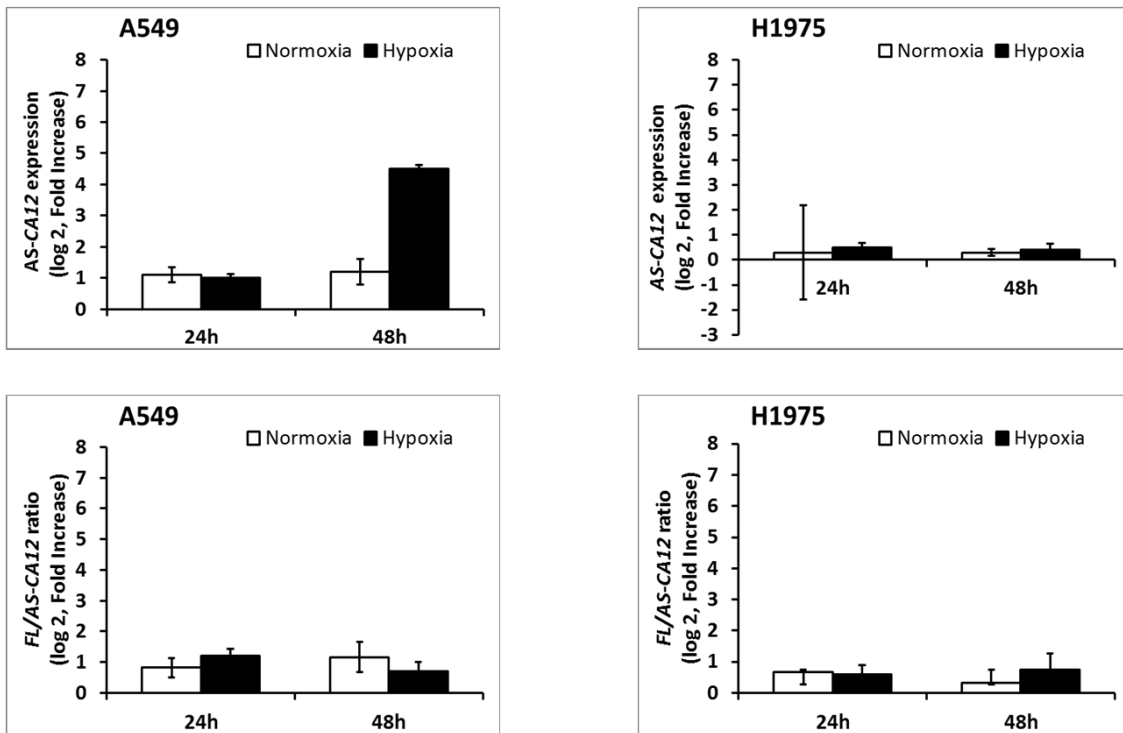
§ ANOVA test was performed.

Supplementary Figure 1

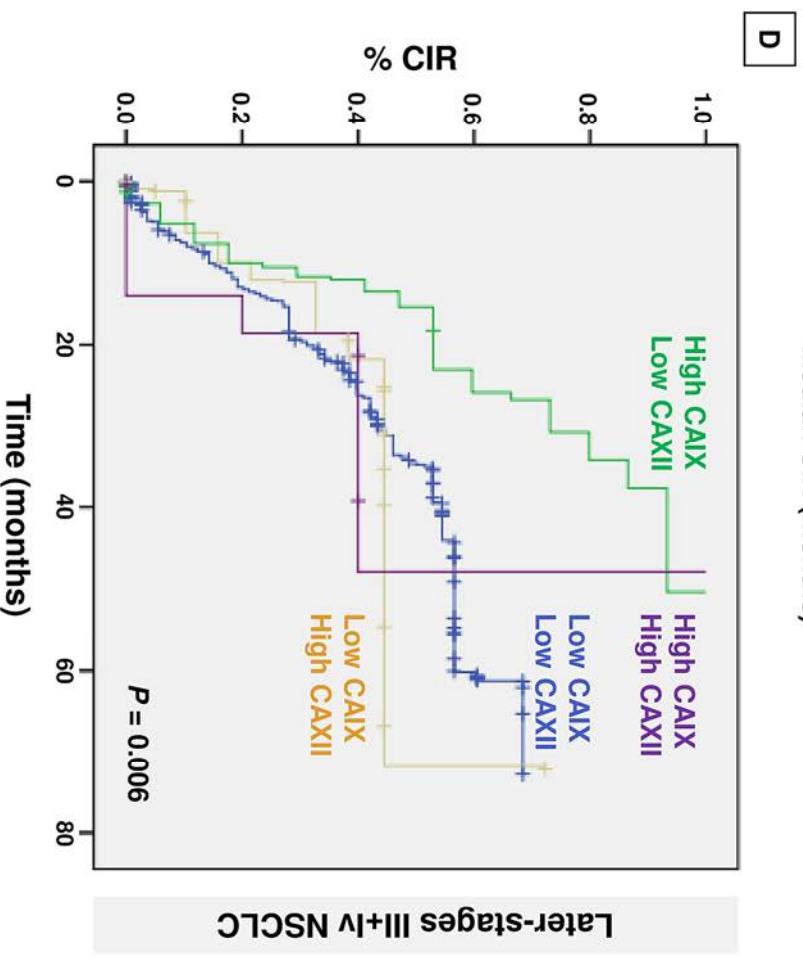
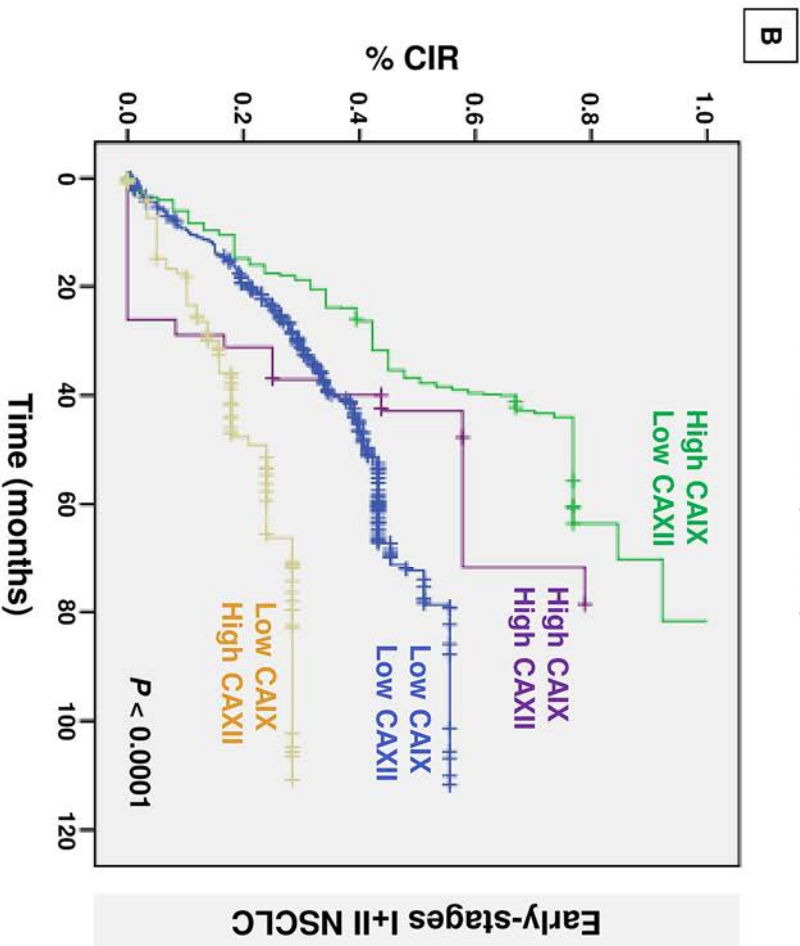
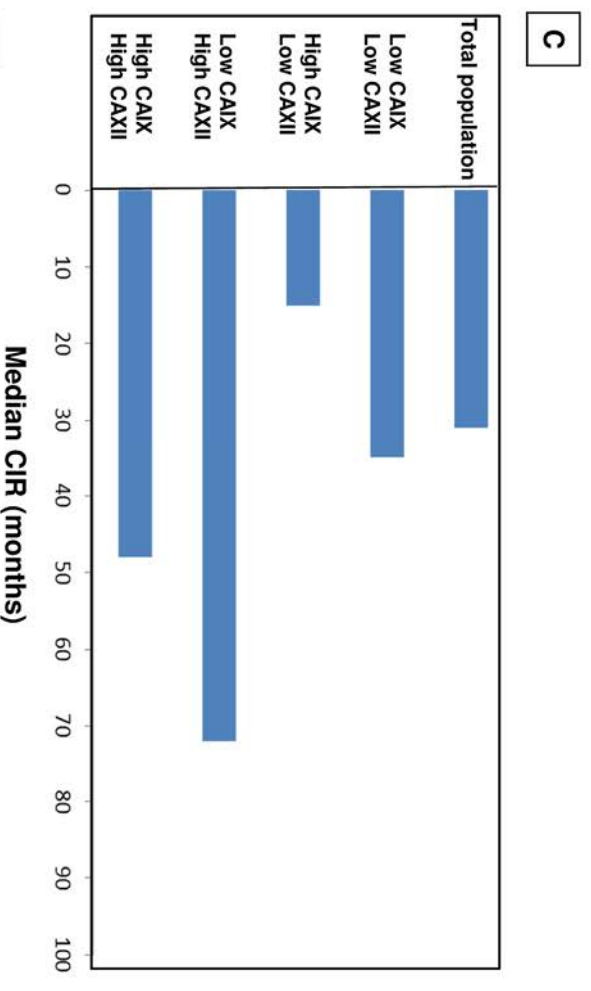
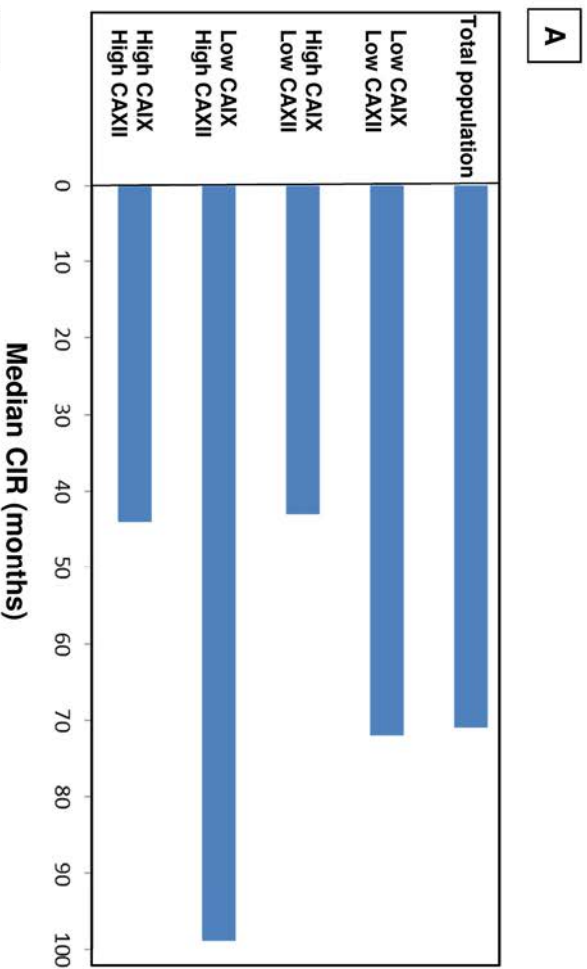
A



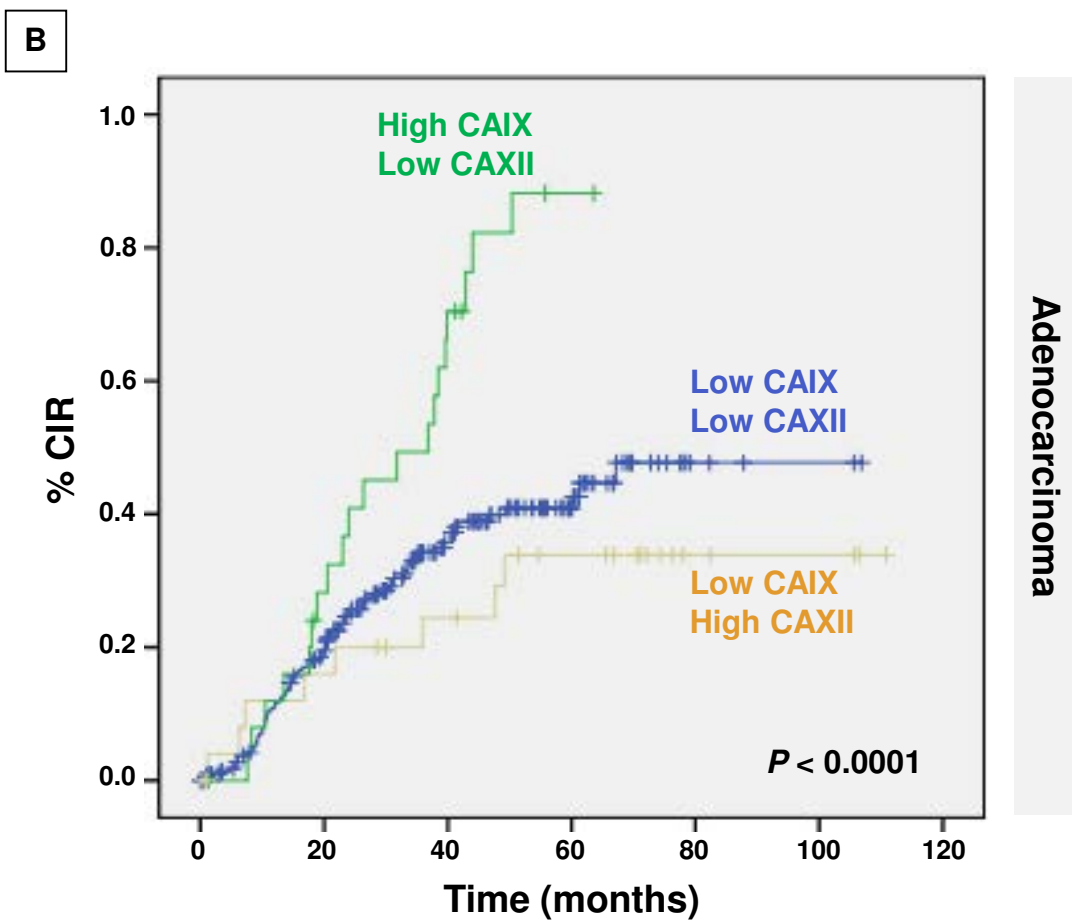
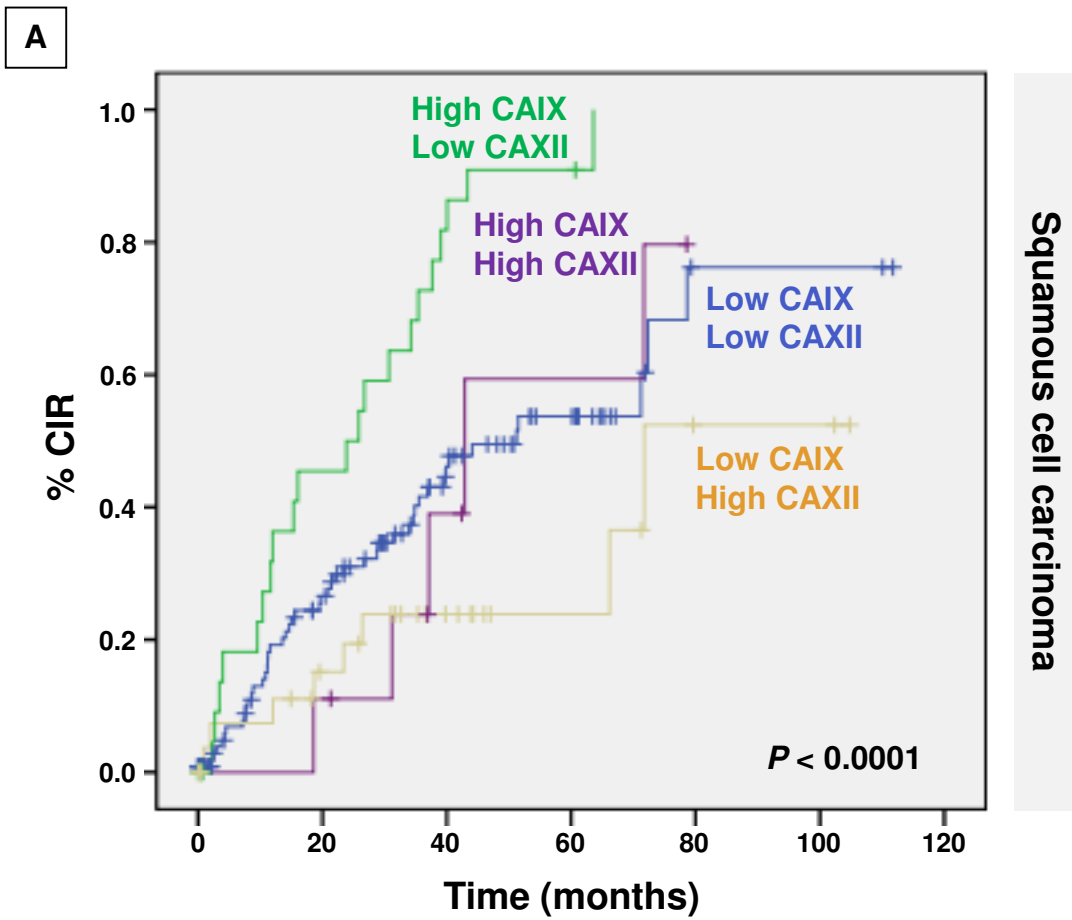
B



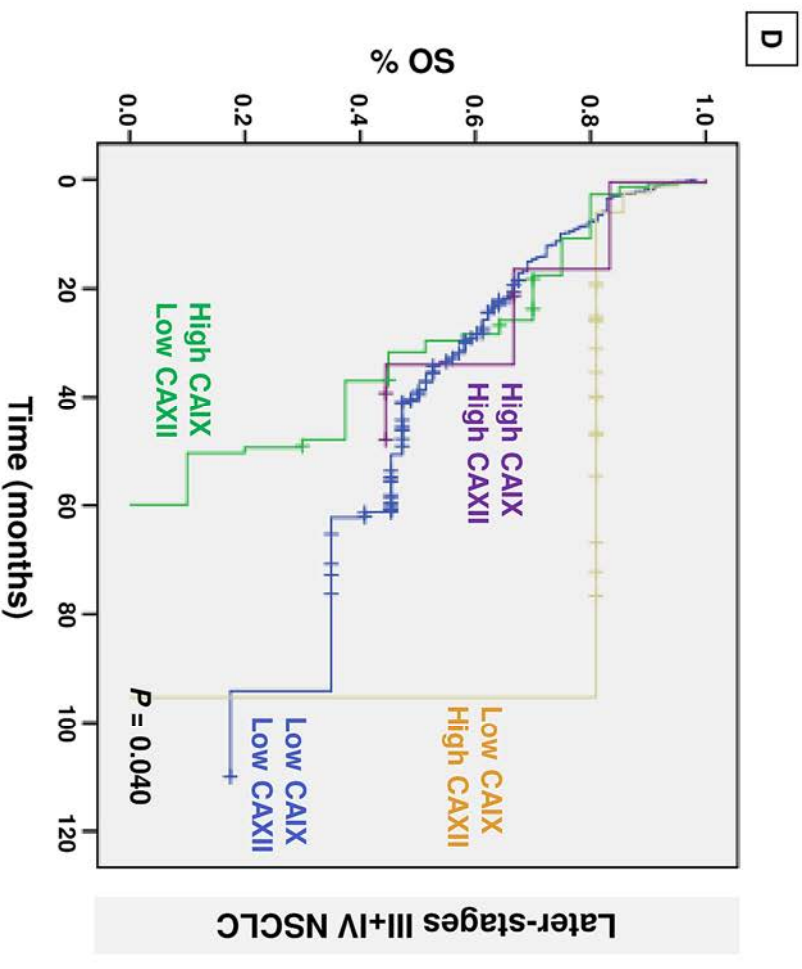
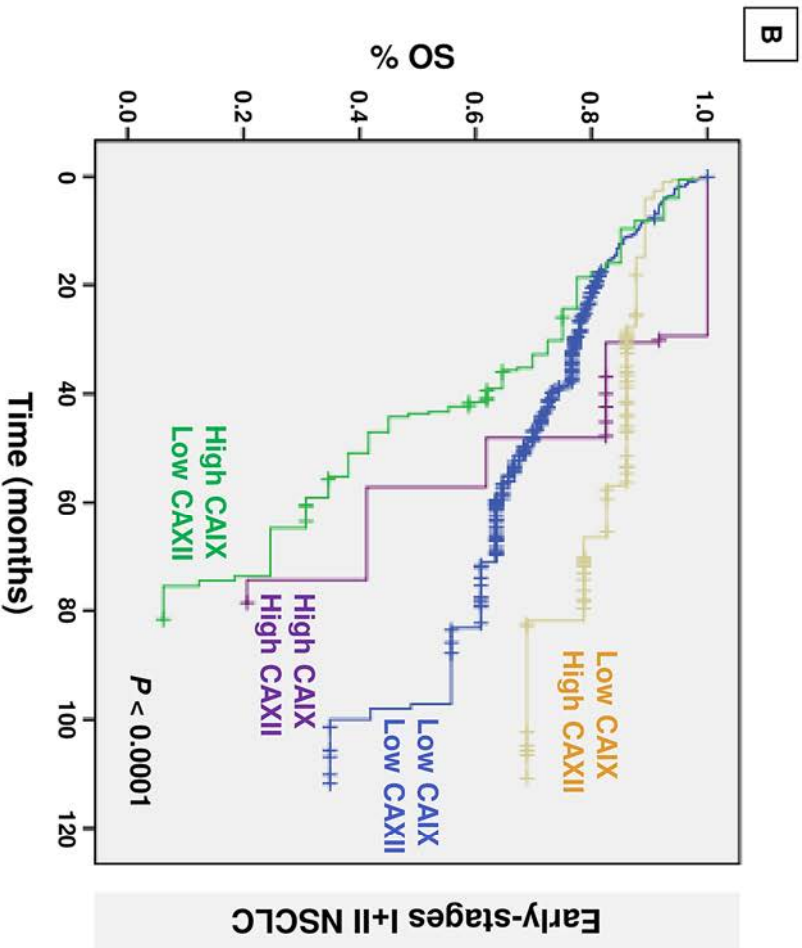
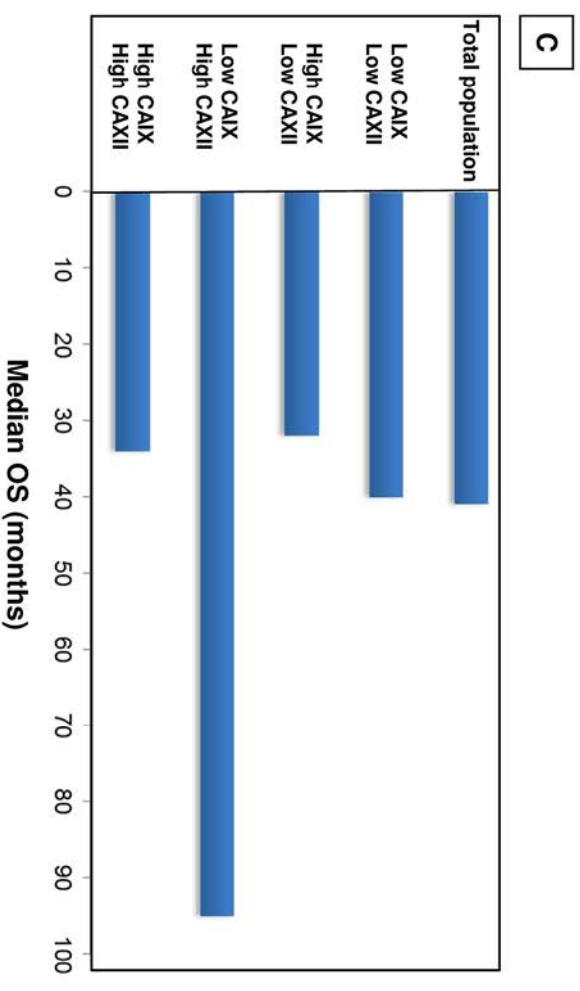
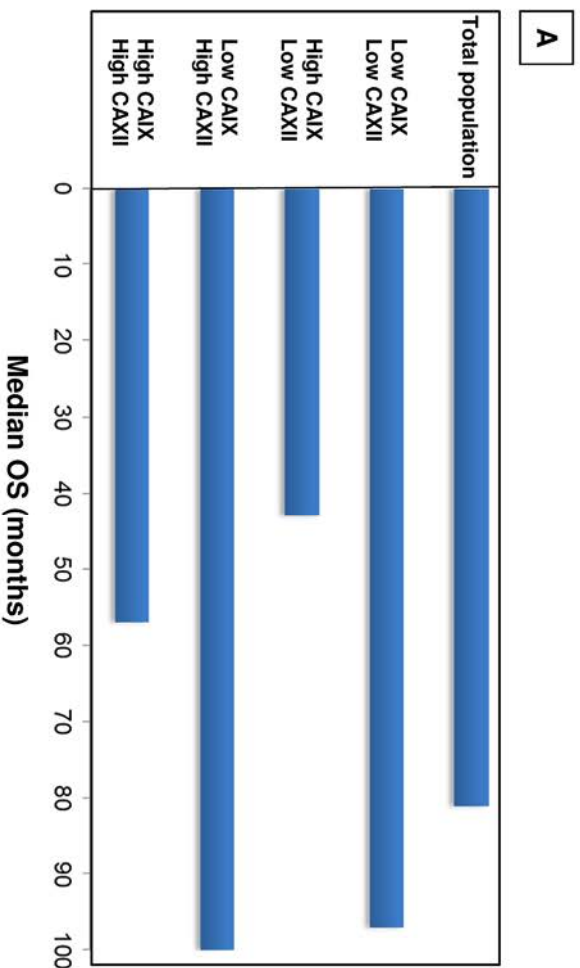
Supplementary Figure 2



Supplementary Figure 3

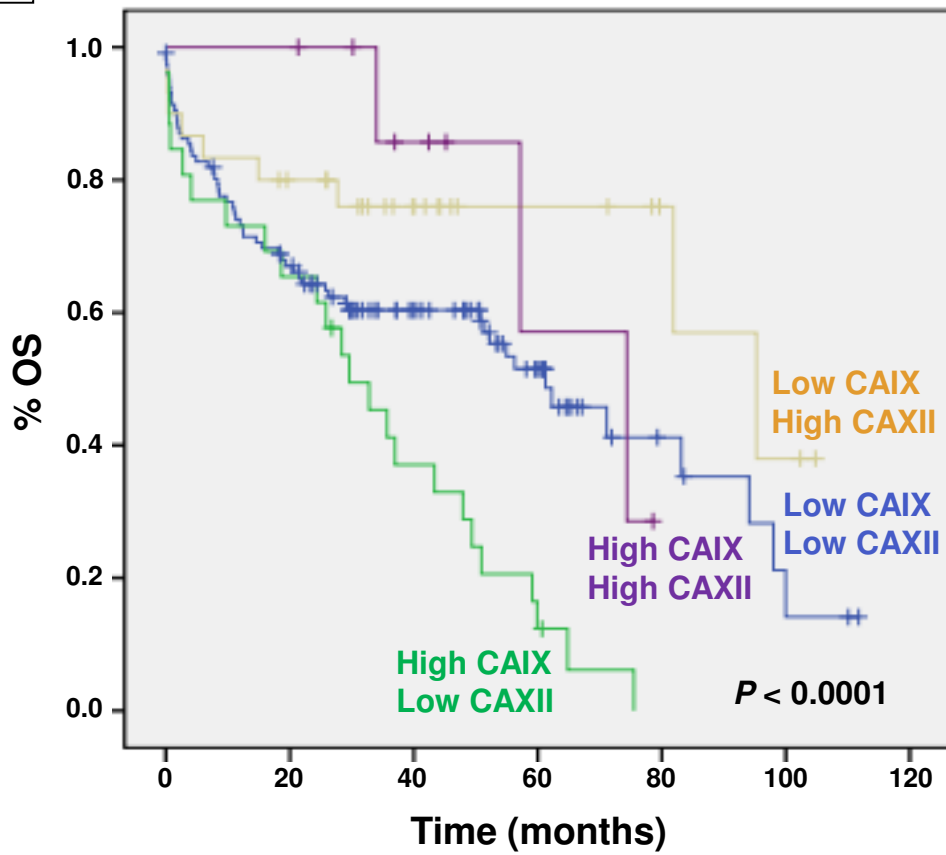


Supplementary Figure 4

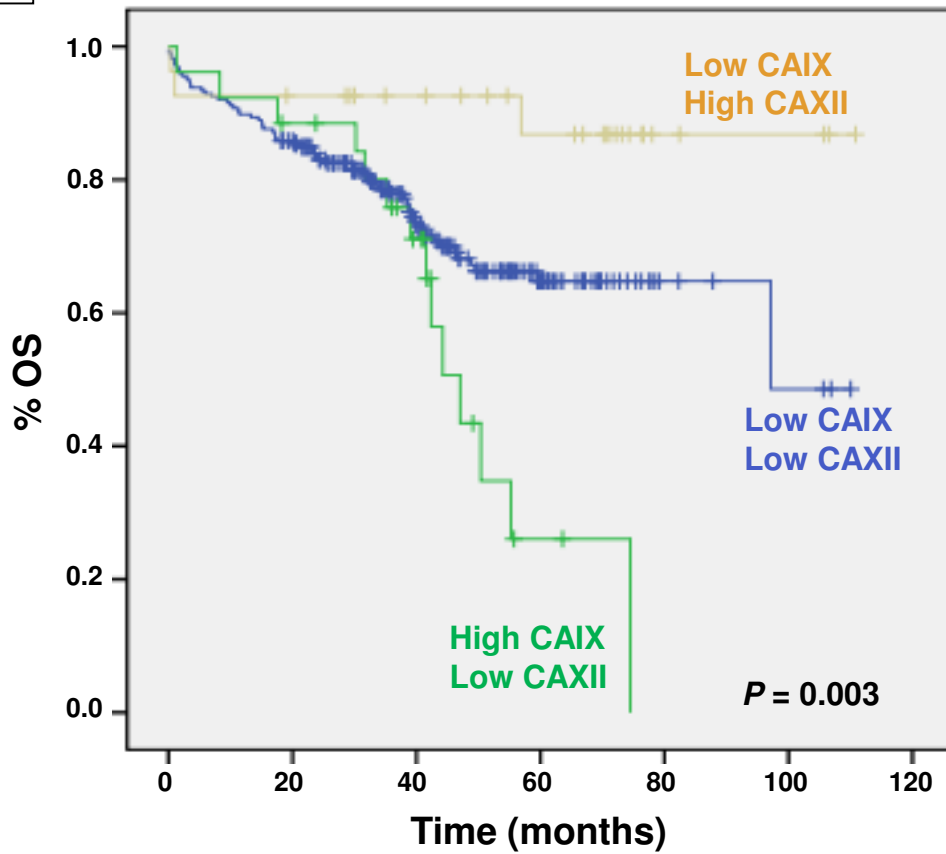


Supplementary Figure 5

A



B



Clinical Cancer Research



Preoperative Circulating Tumor Cell Detection Using the Isolation by Size of Epithelial Tumor Cell Method for Patients with Lung Cancer Is a New Prognostic Biomarker

Véronique Hofman, Christelle Bonnetaud, Marius I. Ilie, et al.

Clin Cancer Res 2011;17:827-835. Published OnlineFirst November 23, 2010.

Updated Version

Access the most recent version of this article at:
doi:[10.1158/1078-0432.CCR-10-0445](https://doi.org/10.1158/1078-0432.CCR-10-0445)

Supplementary Material

Access the most recent supplemental material at:
<http://clincancerres.aacrjournals.org/content/suppl/2011/02/17/1078-0432.CCR-10-0445.DC1.html>

Cited Articles

This article cites 35 articles, 8 of which you can access for free at:
<http://clincancerres.aacrjournals.org/content/17/4/827.full.html#ref-list-1>

Citing Articles

This article has been cited by 3 HighWire-hosted articles. Access the articles at:
<http://clincancerres.aacrjournals.org/content/17/4/827.full.html#related-urls>

E-mail alerts

[Sign up to receive free email-alerts](#) related to this article or journal.

Reprints and Subscriptions

To order reprints of this article or to subscribe to the journal, contact the AACR Publications Department at pubs@aacr.org.

Permissions

To request permission to re-use all or part of this article, contact the AACR Publications Department at permissions@aacr.org.

Preoperative Circulating Tumor Cell Detection Using the Isolation by Size of Epithelial Tumor Cell Method for Patients with Lung Cancer Is a New Prognostic Biomarker

Véronique Hofman¹⁻⁴, Christelle Bonnetaud², Marius I. Ilie³, Philippe Vielh⁵, Jean Michel Vignaud⁶, Jean François Fléjou⁷, Sylvie Lantuejoul⁸, Eric Piaton⁹, Nadine Mourad¹⁰, Catherine Butori¹⁻⁴, Eric Selva², Michel Poudoux¹¹, Stéphanie Sibon¹², Sabrina Kelhef¹², Nicolas Vénissac¹², Jean-Philippe Jais¹³, Jérôme Mouroux¹², Thierry Jo Molina¹⁴, and Paul Hofman¹⁻⁴

Abstract

Purpose: Pathologic TNM staging is currently the best prognostic factor for non-small cell lung carcinoma (NSCLC). However, even in early-stage NSCLC, the recurrence rates after surgery range from 25% to 50%. The preoperative detection of circulating tumor cells (CTC) could be useful to tailor new therapeutic strategies in NSCLC. We assessed the presence of CTC in NSCLC patients undergoing surgery, using cytologic analyses, after their isolation by size of epithelial tumor cells (ISET method). The presence and the number of CTCs were considered and correlated with clinicopathologic parameters including patient follow-up.

Experimental design: Of the 247 blood samples tested, 208 samples were from patients with resectable NSCLC and 39 from healthy subjects. The mean follow-up was 24 months. An image of detected cells with presumably nonhematologic features [initially defined as "circulating nonhematologic cells" (CNHC)] was recorded. The presence of CNHC was assessed blindly and independently by 10 cytopathologists, using cytologic criteria of malignancy on stained filters. The count of detected CNHCs was made for each filter.

Results: One hundred two of 208 (49%) patients showed CNHCs corresponding to CNHC with malignant cytopathologic features in 76 of 208 (36%) cases. CNHCs were not detected in the control group. A level of 50 or more CNHCs corresponding to the third quartile was associated with shorter overall and disease-free-survival, independently of disease staging, and with a high risk of recurrence and death in early-stage I + II-resectable NSCLC.

Conclusion: A high percentage of NSCLC patients show preoperative detection of CNHC by the ISET method. The presence and level of 50 or more CNHCs are associated with worse survival of patients with resectable NSCLC. *Clin Cancer Res*; 17(4): 827-35. ©2010 AACR.

Introduction

Lung cancer is the most prevalent neoplasm and the major cause of tumor-related mortality in the United States (1). Despite recent advances in the management of resected lung cancers and more effective treatments of metastatic tumors, the cure rate of patients with lung cancer remains low (2-6). Histologic classification of lung tumors distinguishes small and non-small cell lung carcinomas (NSCLC). Most NSCLCs display 3 histologic subtypes: adenocarcinoma, squamous cell carcinoma, and large cell carcinoma (7, 8). The prognosis of these NSCLC subtypes is quite similar (2-5).

Although pTNM staging is currently the only validated prognostic factor used in NSCLC patient follow-up and treatment, 25% to 50% of patients with early-stage NSCLC show tumor recurrence, even following extensive tumor resection, indicating the urgent need for more sensitive prognostic and predictive markers (9-11).

Authors' Affiliations: ¹INSERM (Institut National de la Santé et de la Recherche Médicale) ERI-21, Faculty of Medicine of Nice, University of Nice Sophia Antipolis; ²Human Biobank, Pasteur Hospital; ³Laboratory of Clinical and Experimental Pathology; ⁴EA 4319, Nice; ⁵Department of Biology and Pathology, Gustave Roussy Institut, Villejuif; ⁶Department of Pathology, Nancy; ⁷Department of Pathology, Saint-Antoine Hospital, Paris; ⁸Department of Pathology and INSERM U 823, A Bonniot Institut, Grenoble; ⁹Department of Pathology, Est HFME Hospital, University of Lyon 1 Claude Bernard, Lyon; ¹⁰Department of Pathology, Saint-Louis Hospital, Paris; Departments of ¹¹Pneumology and ¹²Thoracic Surgery, Pasteur Hospital, Nice; ¹³Department of Biostatistics, Faculty of Medicine Necker Enfants Malades Hospital; and ¹⁴Department of Pathology, University of Paris Descartes, AP-HP, Hôtel-Dieu Hospital, Paris, France

Note: Supplementary data for this article are available at Clinical Cancer Research Online (<http://clincancerres.aacrjournals.org/>).

V. Hofman, C. Bonnetaud, and M.I. Ilie contributed equally to this work.

Corresponding Author: Paul Hofman, INSERM ERI-21/EA 4319, Faculté de Médecine, avenue de Valombrose, 06017 Nice cedex, France. Phone: 33-4-92-03-88-55; Fax: 33-4-92-88-50; E-mail: hofman.p@chu-nice.fr

doi: 10.1158/1078-0432.CCR-10-0445

©2010 American Association for Cancer Research.

Translational Relevance

Besides pathologic tumor staging, a few prognostic biomarkers currently exist that correlate with the outcome of patients undergoing surgery for resectable non-small cell lung carcinoma (NSCLC). Therefore, improvement of relevant prognostic biomarkers, in particular for predicting recurrence, is urgently needed in lung clinical oncology. Local recurrence and metastatic dissemination of the primary tumor may arise from dissemination of circulating tumor cells (CTC) in the patient's blood prior to surgery for radical tumor resection. In this regard, early detection of CTC in patients having resectable NSCLC might be considered as a potentially relevant prognostic biomarker, which could also tailor new therapeutic strategies. We show in this study that the presence and number of CTCs detected according to their size (ISET, isolation by size of epithelial tumor cells) and then characterized by a panel of 10 cytopathologists, using a cytomorphologic analysis, are significantly correlated with shorter overall and disease-free survival in patients undergoing surgery for resectable NSCLC. We conclude that CTC detection using the ISET method in this population has a strong clinical impact.

A sizable body of evidence indicates that metastases may develop from circulating tumor cells (CTC) that spread into blood vessels before, during, and/or after surgery (12). Moreover, it has been reported that the presence of occult metastatic disease correlates with disease recurrence in stage I NSCLC patients (13). Thus, sensitive and specific detection of CTC in the blood might be considered as a potentially relevant prognostic biomarker for patients with resectable NSCLC. Indeed, the main goal for preoperative detection of CTC was to identify NSCLC patients with a high risk of recurrence after surgery in order to perform the best follow-up and therapeutic strategy.

Despite the report of a large number of studies on CTC detection, methodologic aspects concerning sensitivity, specificity, and reproducibility have prevented a clear appraisal of the clinical impact (12). While reverse transcriptase PCR (RT-PCR) and immune-mediated methods can be very sensitive, specificity remains a critical issue for these approaches, as no transcript or antigen specifically characterizing tumor cells from solid tumors is known at present (12). In this setting, cytopathologic analysis of CTC, isolated according to their size (ISET, isolation by size of epithelial tumor cells), is considered a promising approach, as CTC enrichment is very sensitive and cell morphology is not damaged (12, 14). This methodology allows "classical" cytopathologic criteria of malignancy, already used in exfoliative cytology, to be used to identify malignant tumor cells (14). Currently, ISET technology has been reported previously to allow identification of CTC in patients with liver or breast cancers (15, 16). However, the

ISET method has never been used to detect CTC in patients with NSCLC.

The aim of this study was (i) to determine the diagnostic potential of the ISET method for preoperative detection of CTC in resectable NSCLC patients and (ii) to correlate the presence and number of CTCs with different clinicopathologic parameters, in particular pathologic stages, and patient outcome. For this purpose, cytomorphologic criteria have been established by a panel of 10 cytopathologists for classification of detected circulating nonhematologic cells (CNHC) into 3 groups: (i) circulating nonhematologic cells with malignant features (CNHC-MF), (ii) CNHC with uncertain malignant features (CNHC-UMF), and (iii) CNHC with benign features (CNHC-BF).

Materials and Methods

Patients and samples

Two hundred eight consecutive patients with NSCLC undergoing surgery from September 2006 to January 2009 at the Pasteur Hospital (Department of Thoracic Surgery) University of Nice Sophia Antipolis, Nice, France, were entered into this study. All patients gave their informed consent to participate in this study. Follow-up of these patients was from 12 to 41 months (mean = 24 months). Preoperative diagnosis was made, in 50% of cases, on bronchial biopsies and/or bronchial aspirates, transbronchial or transparietal chest biopsies, or mediastinoscopy with biopsy. Biopsies were not performed for at least 15 days before surgery. Others patients underwent surgery without previous biopsy, after diagnosis based on cancer imaging and confirmation with frozen sections. The main clinicopathologic parameters of the 208 patients are summarized in Table 1. Morphologic classification was assigned according to WHO criteria (8). The tumors were staged according to the 7th edition of the international tumor-node-metastasis (TNM) system (17). Twenty-nine patients with stage IIIA disease had neoadjuvant chemotherapy. Patients with stage IV disease had solitary brain metastases and were considered as operable for their lung carcinoma (18). Among the adenocarcinomas, 90 expressed the TTF1 antigen, as determined by immunohistochemical (anti-TTF1 antibody, diluted 1:100; Dako) staining. The percentage of epithelial tumor cells in the formalin-fixed, paraffin-embedded tissue sections of the primary tumors was less than 30% (45/208 cases: 22%), between 30% and 80% (145/208 cases: 69%), and more than 80% (18/208 cases: 9%) and was defined by counting the relative proportion of tumor cells in 20 different fields of each tumor at a 200× magnification.

Blood samples from 39 healthy volunteers were used as negative controls. There were 29 men (median age = 39 years; range = 25–45 years) and 10 women (median age = 35 years; range = 22–43 years), smokers (average 11 pack-years; range = 10–17 pack-years), without knowledge of neoplastic disease.

Table 1. Main epidemiologic, clinical, and pathologic characteristics in NSCLC patients included in the study

Clinical and pathologic parameters	No of patients (%)
Overall	208 (100)
<i>Age, y</i>	
Mean	63
Range	37–84
<i>Gender</i>	
Male	141 (68)
Female	67 (32)
<i>Tobacco exposure, pack-years</i>	
Number	189 (91)
Average	41.3
Range	1–150
<i>Tumor size, cm</i>	
Mean	3.8
Range	0.4–17
<i>Histology</i>	
ADC	115 (55)
Mixed ADC	95 (46)
Acinar ADC	9 (4)
Mucinous carcinoma	5 (2)
Clear cell ADC	2 (1)
Solid ADC with mucin production	2 (1)
Papillary ADC	1 (0.5)
Bronchioloalveolar ADC	1 (0.5)
Squamous cell carcinoma	54 (26)
Large cell carcinoma	19 (9)
Sarcomatoid carcinoma	10 (5)
Adenosquamous carcinoma	5 (2.5)
Non-small cell carcinoma	5 (2.5)
<i>pTNM staging</i>	
I	86 (44)
IA	36
IB	50
II	51 (25)
IIA	26
IIB	25
III	58 (28)
IIIA	56
IIIB	2
IV	13 (6)
TTF1 antigen expression	120 (58)
Neoadjuvant therapy	29 (14)

Abbreviation: ADC, adenocarcinoma.

Methods

Ten milliliters of peripheral blood was collected in buffered EDTA before anesthesia, maintained at 4°C, and processed within 1 hour. Surgical lung specimens were taken for pTNM staging and histologic evaluation. ISET was carried out as previously described (15). The module

of filtration has 10 wells, making it possible to load and filter 10 individual samples in parallel. Briefly, after blood filtration, the membrane was then gently washed with PBS, disassembled from the filtration module, and allowed to air-dry. The membrane was cut into 2 parts, containing respectively 6 spots for staining and 4 spots stored for further potential studies. The 6 spots were stained using a modified May-Grünwald-Giemsa (MGG) staining method with the following steps: May-Grünwald (undiluted, 5 minutes), May-Grünwald (diluted 50%, 5 minutes), and Giemsa (diluted 10%, 40 minutes), followed by rinsing with PBS for 1 minute. Membranes were then air-dried and kept in the dark at room temperature. Stained spots were examined by light microscopy, using different steps: (i) observation at 100× and 200× original magnification to look for CNHC and to count these cells, and (ii) observation at 630× and 1,000× original magnification with oil immersion for detailed cytomorphologic analysis. The following criteria were taken into account to characterize the detected nonhematologic cells: irregularity and size of the nucleus, anisonucleosis, nuclear hyperchromatism, nucleocytoplasmic ratio, size and number of nucleoli, and presence of tridimensional sheets. CNHC-MFs were characterized by the presence of at least 3 of the following criteria: anisonucleosis (ratio >0.5), nuclei larger than 3 calibrated pore size of the membrane (8 μm; >24 μm), irregular nuclear borders, and presence of 3-dimensional sheets (Fig. 1A, a–c). CNHCs were defined as uncertain malignant features (CNHC-UMF) when less than 3 of these criteria were present (Fig. 1A, d–f). CNHCs with benign features (CNHC-BF) were characterized in the absence of these criteria (Fig. 1A, g–i). A semi-quantitative analysis was performed on each filter, and patients were categorized into different groups according to the number of detected CNHC: group 1, less than 10 CNHCs (Fig. 1B, a and d); group 2, between 10 and 100 CNHCs (Fig. 1B, b and e); and group 3, more than 100 CNHCs (Fig. 1B, c and f). Moreover, CNHC was expressed as the median and as the interquartile difference, when considered as a continuous variable. The third quartile of the CNHC distribution function was used as the cutoff value. Moreover, this agrees with the cytomorphologic analysis because when more than 50 CNHCs were present, they were more easily diagnosed as malignant. Both semiquantitative stratification and the cutoff point of 50 or more CNHCs were used for statistical analyses. Eight hundred sixteen photographs (average mean 8 photographs per filter, range = 1–29) were recorded, and images were digitized and collected by 2 cytopathologists (V.H. and P.H.). All images were then reviewed independently by the panel of cytopathologists (V.H., C.B., P.V., S.L., N.M., J.F.F., T.J.M., J.M.V., E.P., and P.H.) in a blind way without knowledge of the diagnosis and clinical status. Images were scored independently by the cytopathologists as CNHC-MF, CNHC-UMF, or CNHC-BF for each individual.

Statistical analysis

All calculations were performed with the statistical software R, a free language and environment for statistical

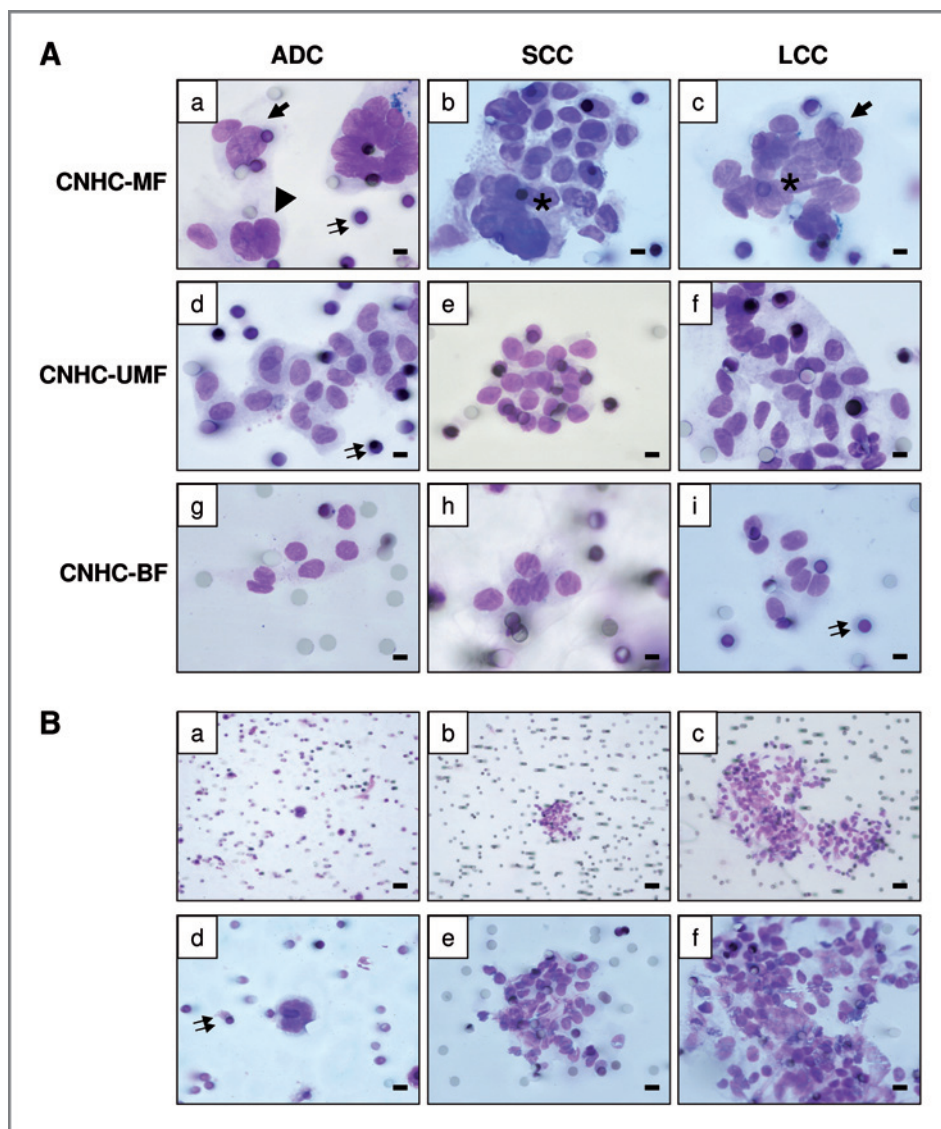


Figure 1. A, cytomorphologic criteria of CNHCs (a–c) with malignant features (CNHC-MF), (d–f) with uncertain malignant features (CNHC-UMF), and (g–i) with benign features (CNHC-BF), preoperatively isolated by the ISET method in patients with a resectable NSCLC. a–i, original magnification $\times 1,000$; MGG staining; bars, 8 μm (arrows, anisonucleosis; arrowheads, irregularity and large nuclei; asterisks, tridimensional sheets; double arrows, pores of the filter). B, a and d, isolated CNHCs (group 1, number of cells <10). b and e, small sheet of CNHCs (group 2, number of cells between 10 and 100). c and f, large sheet of CNHCs (group 3, number of cells >100); MGG; a–c, original magnification $\times 100$; d–f, original magnification $\times 630$. ADC, adenocarcinoma; SCC, squamous cell carcinoma; LCC, large cell carcinoma.

analysis and graphics (version 2.9.0). The presence or absence of CNHCs, analyzed as a binarized qualitative variable, was compared with the following clinicopathologic variables: age, gender, smoker status, neoadjuvant therapy, pTNM stages, tumor size, histologic grade, histologic subtype, percentage of tumor cells in primary tumors, and the TTF1 immunostaining status in both patients with NSCLC and healthy volunteers by the χ^2 analysis or the Mann–Whitney test when applicable. We used κ statistics, which reflect agreement between 2 measurements after removing chance agreement, as a measure of reliability (19). A value close to 1 represents almost perfect agreement, whereas values close to or below zero represent poor agreement. The ANOVA was used to explore the association between the number of CNHCs, analyzed as a continuous variable, and the pTNM stage.

Patient outcome, including overall survival (OS) and disease-free survival (DFS) comparing the presence or absence of CNHC and according to the number of CNHCs, was assessed by the Kaplan–Meier analysis with a log-rank score for determining statistical significance. OS was defined as the interval between surgery and the date of death from any cause or the last follow-up. DFS was defined as the interval between the date of surgery and the date of relapse of the disease or the date of death from any cause. Patients who did not relapse or who died (for DFS) or remained alive (for OS) at the final follow-up were censored at that time. Multivariate Cox analyses were carried out to examine whether the presence of CNHC, according to the cutoff point of 50 or more CNHCs, is an independent prognostic factor for survival with adjustment for relevant clinicopathologic covariates. Multivariate

Table 2. Correlation of the levels of CNHCs stratified by the cutoff point detected by the ISET method with disease staging in resectable NSCLC patients

pTNM stage ^a	No. of patients	Levels of CNHC, n (%)	
		<50 CNHC	≥50 CNHC
Stage I	86	65 (76)	21 (24)
IA	36	29 (81)	7 (19)
IB	50	36 (72)	14 (28)
Stage II	51	35 (67)	16 (33)
IIA	26	17 (65)	9 (35)
IIB	25	18 (72)	7 (28)
Stage III	58	38 (66)	20 (34)
IIIA	56	37 (66)	19 (34)
IIIB	2	1 (50)	1 (50)
Stage IV	13	6 (46)	7 (54)
Overall	208 (100%)	144 (69)	64 (31)

NOTE: The cutoff point for grouping was the third quartile, 50 or more CNHCs, as described in the Materials and Methods section. $P > 0.05$ for all groups. Values in parentheses are line percentages.

^a χ^2 analysis. Coding of variables: stages IA and IB were coded as 1, stages IIA and IIB were coded as 2, stages IIIA and IIIB were coded as 3, and stage IV was coded as 4. The P value for overall comparison was 0.15.

analyses using Cox regression models included all potential prognostic factors for survival with a $P < 0.2$ value in univariate analysis. The variables included in the model for OS and DFS were pTNM stage, tumor size, and histology. A $P \leq 0.05$ value was considered significant for all analyses.

Results

CNHCs were present preoperatively in 102 of 208 (49%) patients undergoing surgery for NSCLC (Supplementary Table 1). Interobserver agreement between the 2 initial cytopathologists was total ($\kappa = 1$) for detection of CNHC on filters. The mean number of CNHCs was 42 (median = 0; range = 0–500; first quartile: 0, third quartile: 50) in NSCLC patients. CNHCs were present in 88 of 179 (49%) and 14 of 29 (48%) in patients without and with neoadjuvant chemotherapy ($P = 0.86$), respectively. CNHC-MFs were characterized morphologically in 76 of 208 (37%) of cases (Fig. 1A) [in 65/179 (36%) and in 11/29 (38%) in patients without and with neoadjuvant chemotherapy ($P = 0.96$), respectively]. In all cases (100%), at least 5 of the 10 cytopathologists agreed with the final diagnosis (CNHC-MF, CNHC-UMF, or CNHC-BF) for each patient ($\kappa = 1$). CNHC-UMFs were diagnosed in 23 of 208 (11%) cases (Fig. 1A), whereas CNHC-BFs were observed in 3 of 208 (1%) of cases (Fig. 1A). The cytopathologic features of CNHC from patients with lung adenocarcinoma were not distinguishable from those of CNHCs derived from squamous cell carcinoma and large cell lung carcinoma (Fig. 1A) and the other histologic subtypes. CNHCs were not found in the blood of the 39 healthy volunteers.

No correlation was observed between the levels of CNHC ($P = 0.15$; Table 2) or according to their presence by semiquantitative grouping ($P = 0.35$; Supplementary Table 1) and the disease stage. Moreover, no correlation existed between the detection of CNHC and other clinicopathologic parameters (age, gender, tobacco exposure, tumor size, histologic subtype, histologic grade, percentage of epithelial tumor cells in the primary tumor, pleural invasion, presence of intratumoral emboli, and TTF1 staining; $P > 0.05$; data not shown). Finally, no correlation was found between the number of CNHCs and the disease stage ($P = 0.92$; Supplementary Fig. 1). Moreover, no significant relationship was noted between the number of CNHCs and the other different clinicopathologic parameters cited previously ($P > 0.05$; data not shown).

The number of CNHCs (at the level ≥ 50 cells) was significantly associated with shorter OS and DFS ($P = 0.002$, and $P = 0.001$, respectively; Fig. 2). In addition, the level of 50 or more CNHCs was significantly associated with worse DFS for both early-stage I + II- and later-stage III + IV-resectable NSCLCs ($P = 0.05$, and $P < 0.0001$, respectively; Fig. 3). Finally, the presence of CNHCs, according to semiquantitative stratification, was associated with a shorter OS and DFS (Supplementary Fig. 2).

Subsequently, multivariate survival analyses using the Cox proportional hazard model were performed to examine the importance of the level 50 or more CNHCs in patient outcome when other prognostic factors were included. Both a level of 50 or more CNHCs and the pTNM stage were significantly independent prognostic factors for OS (Table 3). In addition, a level of 50 or more CNHCs, pTNM stage, histology cell subtype, and tumor size were

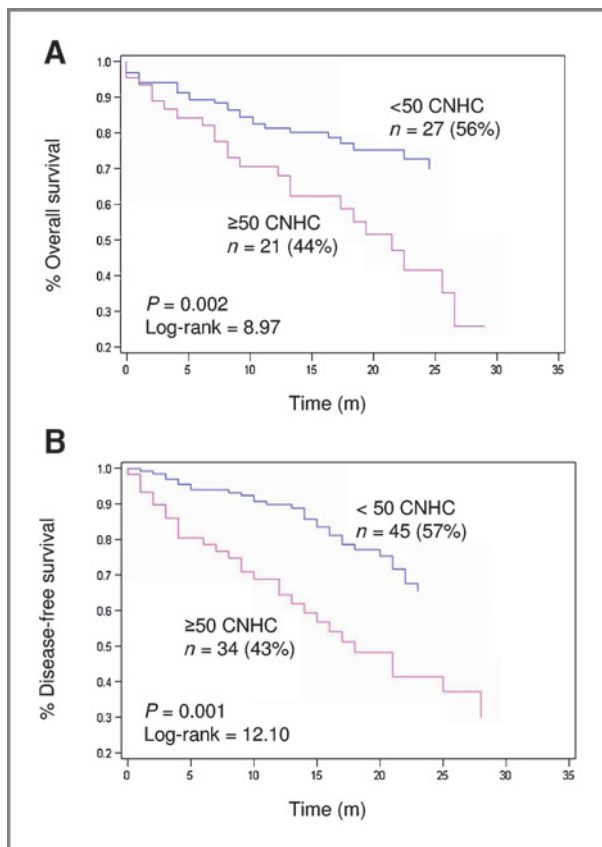


Figure 2. Kaplan–Meier curves of OS (A) and DFS (B) duration stratified according to the cutoff point of 50 or more CNHCs detected by the ISET method. The cutoff point of stratification was the third quartile, as described in the Materials and Methods section. Numbers in the legends are the number of events for each group.

significantly independent prognostic factors for DFS (Table 3).

Discussion

This study shows the feasibility of the ISET method for preoperative isolation and identification of CTC from peripheral blood samples taken from patients with resectable NSCLC. We found that around half of these patients showed detected CNHC in their blood, mainly corresponding to CNHC-MF according to cytomorphologic criteria. Moreover, in these cases, interobserver variation was low for the diagnoses of these latter cells. It is noteworthy that detection of CNHCs by ISET had a strong clinical impact, as the presence and number of CNHCs correlated with a pejorative outcome (low OS and DFS). Other clinicopathologic parameters, including pTNM staging, did not correlate with the presence and number of CNHCs. These latter results show that preoperative CNHC detection in patients with resectable NSCLC is an independent new prognostic biomarker.

Different methods have been applied in the past to detect occult CTC in patients with NSCLC (20–30). Indeed, most

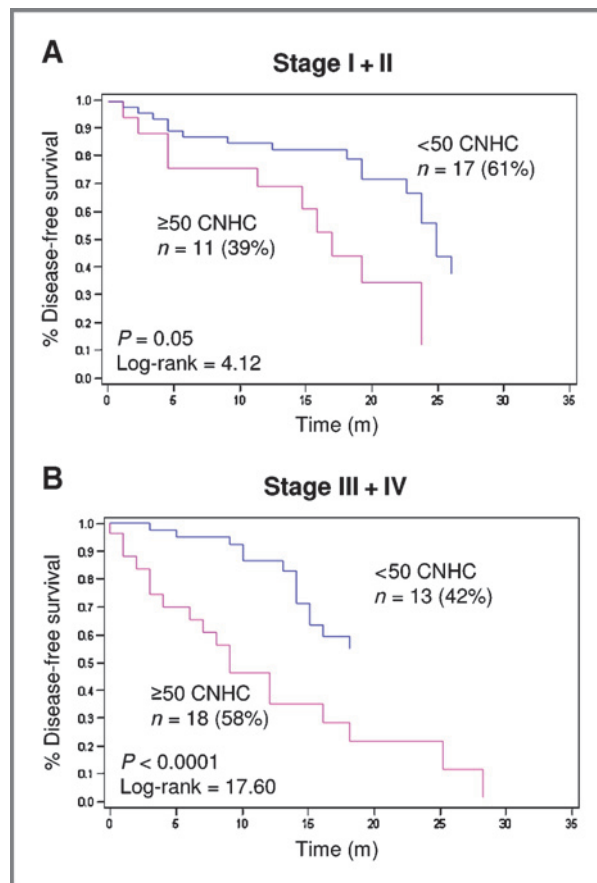


Figure 3. Kaplan–Meier curves of DFS for early-stage I + II NSCLC (A) and later-stage III + IV NSCLC (B). The cutoff value was defined as superior or equal to 50 CNHCs, as described in the Materials and Methods section, to define the presence of CNHC. Numbers in the legends are the number of events for each group.

of the previous studies have used indirect methods based on RT-PCR or quantitative RT-PCR before, during, and after surgery (21, 23, 24, 27–29) or nested RT-PCR (25) or used BErEP4-coated beads (22), magnetic bead enrichment, and laser scanning cytometric (26) and immunocytologic methods (CellSearch System; ref. 30). Different biomarkers such as the telomerase activity (22), the cytokeratin 19/carcinoembryonic antigen and c-met mRNAs (25, 27, 31), epidermal growth factor receptor (21, 32), and other different molecules of interest (23) have been used in these studies to specifically identify CTC. However, contrasting results have been obtained in all these previous studies because of technical characteristics such as marker- and method-related specificity and sensitivity and limitations such as the high cost and labor needed, which are not adapted for use in large cohorts of patients

The ISET method has been previously used in patients with liver and breast cancers (15, 16). We show here that this method can be applied to NSCLC patients. Interestingly, 49% of these patients showed preoperative CNHC in their blood. Among these CNHCs, diagnosis of CNHC-MF

Table 3. Multivariate Cox proportional hazard regression analysis of predicting factors for OS and DFS in 208 resectable NSCLC patients

Prognostic factor	HR	95% CI	P ^a
OS			
Histology			
Squamous cell carcinoma	1.610	0.909–2.850	0.10
Other subtypes	1		
pTNM stage			
I + II	0.190	0.080–0.455	<0.0001
III + IV	1		
Tumor size, cm			
≤3	0.664	0.413–1.068	0.09
>3	1		
Presence of CNHC			
≥50	2.096	1.331–3.300	0.001
<50	1		
DFS			
Histology			
Squamous cell carcinoma	2.346	1.129–4.876	0.022
Other subtypes	1		
pTNM stage			
I + II	0.225	0.604–0.840	0.0009
III + IV	1		
Tumor size, cm			
≤3	0.574	0.332–0.993	0.047
>3	1		
Presence of CNHC			
≥50	2.631	1.557–4.651	0.003
<50	1		

^aP value significant at the 0.05 level.

was made by morphologic assessment in the majority of cases. The malignant characteristics of the detected CNHCs were assessed only according to cytopathologic criteria, which are classically used by cytopathologists in exfoliative and fine-needle aspiration cytopathology.

Interestingly, a group of CNHCs in this series has been classified as having uncertain malignant features (CNHC-UMF) by the cytopathologists. A few CNHCs were also classified as benign cells only by a couple of cytopathologists, as none of malignant criteria were morphologically present. However, certain cytopathologists of the panel hypothesized that CNHCs detected in peripheral blood cannot be benign cells in NSCLC patients. Interobserver variation was low for the different subgroups of CNHCs. However, given the new domain of CTC, we cannot rule out the possibility that some specific morphologic criteria could be required in the future to precisely identify and classify CNHCs. In this regard, it is clear that markers specific for CTC should be developed in the future and combined with cytomorphologic analysis. In particular, the different CNHC groups need to be better characterized phenotypically by immunocytochemical and/or by molecular biological approaches in further studies. In this

regard, when using a morphologic method, we cannot rule out the possibility that a couple of circulating endothelial cells can be isolated or associated with CTC (33). Thus, endothelial cells could also be further identified on filters by immunocytochemistry, using different markers (34). Finally, in our study, cytomorphologic criteria did not correlate with the histologic subtype of the primary lung tumor, underlying that no features of CNHCs were representative of the histologic subtype.

No correlation was found between CNHC, as quantitative or qualitative variables, and pTNM staging. In particular, our study on the correlation between the pTNM staging and the presence of CNHC showed the presence of CNHC in a group of patients with early-stage NSCLC before surgery. It will be of great interest in the future to follow-up this group of patients and compare them with early-stage carcinoma patients without preoperative detection of CNHC by looking for relapse and/or metastasis onset. Our study shows insight into this behavior, as the level of 50 or more CNHCs was significantly associated with a higher risk of recurrence in early-stage NSCLC. Tumor cell behavior depends on interactions between nuclear genetic changes in the malignant cells and a stroma

that is favorable for growth, invasion, and metastasis, in association with angiogenesis. Thus, an increase in different stromal biomarkers has been indicative of poor outcome in patients with NSCLC (35, 36). In this regard, we thought that it would be of interest to see whether the importance of the stroma, which is considerably variable from one NSCLC to another, even at the same TNM staging, was linked to the presence of CNHC. However, we found that the percentage of tumor cells in the primary tumor did not correlate with the number of CNHCs, indicating that a substantial stroma reaction associated with carcinoma could not influence the effraction of vessels by tumor cells and then their blood dissemination. Using univariate analysis, no significant difference was noted between CNHC, as quantitative and qualitative variables, and the pathologic stage, the size of the primary tumor, the histologic subtype, and the percentage of tumor cells in the primary tumor. This finding supports the idea that the presence of CNHC is independent of the well-established prognostic factors.

We then evaluated the prognostic significance of CNHC when preoperatively detected by ISET in patients with resectable NSCLC. It is noteworthy that a level of 50 or more CNHCs detected by ISET was associated with significantly decreased OS and DFS, independently of disease staging, as determined by univariate and multivariate survival analyses. Similar results were observed for univariate survival analyses when considering the presence of detected CNHCs, according to semiquantitative group stratification.

Currently, in most of the cases, patients with early-stage NSCLC with surgically resected tumors do not have adjuvant therapy. However, among these latter patients, a group will undergo relapse and/or develop metastases. In this regard, it is of great interest to look for a biomarker that is predictive of such disease evolution. Thus, the preoperative detection of CTC by ISET in this group can allow selection

of a population with a higher risk of relapse and poorer prognosis. Although the cytomorphologic approach alone cannot assess the malignant potential of CNHC, we strongly believe that it ensures a far higher specificity than other approaches based on epithelial-related antigens or transcripts and allows the study of cells with tumor like features by complementary approaches. Thus, by combining the reference "old" cytomorphologic approach with newly developed molecular markers derived from proteomics, molecular profiling, and genetic analyses, a promising path toward better classification and treatment of patients according to their prognosis should be obtained.

In conclusion, the presence of CTCs identified by ISET in patients undergoing surgery for resectable NSCLC is associated with poor prognosis, independently of disease staging. This finding identifies CTCs detected by ISET as a very strong, independent prognostic indicator in patients with resectable NSCLC. Moreover, it might identify these CTCs as a pertinent molecular target for the development of new antitumor agents.

Disclosure of Potential Conflicts of Interest

No potential conflicts of interest were disclosed.

Acknowledgments

The authors thank the Conseil Général des Alpes Maritimes for their financial support and the PROCAN 2007–2011 (Cancerpole PACA).

Grant Support

This work received a grant from the PHRC 2008 (CHU of Nice).

The costs of publication of this article were defrayed in part by the payment of page charges. This article must therefore be hereby marked *advertisement* in accordance with 18 U.S.C. Section 1734 solely to indicate this fact.

Received February 18, 2010; revised October 15, 2010; accepted November 15, 2010; published OnlineFirst November 23, 2010.

References

- Jemal A, Siegel R, Ward E, Hao Y, Xu J, Murray T, et al. Cancer statistics, 2008. *CA Cancer J Clin* 2008;58:71–96.
- Goya T, Asamura H, Yoshimura H, Kato H, Shimokata K, Tsuchiya R, et al. Prognosis of 6644 resected non-small cell lung cancers in Japan: a Japanese lung cancer registry study. *Lung Cancer* 2005;50:227–34.
- van Rens MT, de la Riviere AB, Elbers HR, Van Den Bosch JM. Prognostic assessment of 2,361 patients who underwent pulmonary resection for non-small cell lung cancer, stage I, II, and IIIA. *Chest* 2000;117:374–9.
- Naruke T, Tsuchiya R, Kondo H, Asamura H. Prognosis and survival after resection for bronchogenic carcinoma based on the 1997 TNM-staging classification: the Japanese experience. *Ann Thorac Surg* 2001;71:1759–64.
- Pfannschmidt J, Muley T, Bulzebruck H, Hoffmann H, Dienemann H. Prognostic assessment after surgical resection for non-small cell lung cancer: experiences in 2083 patients. *Lung Cancer* 2007;55:371–7.
- Strauss GM. Adjuvant chemotherapy of lung cancer: methodologic issues and therapeutic advances. *Hematol Oncol Clin North Am* 2005;19:263–81, vi.
- el-Torky M, el-Zeky F, Hall JC. Significant changes in the distribution of histologic types of lung cancer. A review of 4928 cases. *Cancer* 1990;65:2361–7.
- Travis WD, Müller-Hermelink HK, Harris CC. WHO histological classification of tumors of the lung. In: *World Health Organization Classification of Tumours Pathology and Genetics of Tumours of the Lung, Pleura, Thymus and Heart*. Lyon: IARC Press; 2004. p. 342.
- Mountain CF. Revisions in the International System for Staging Lung Cancer. *Chest* 1997;111:1710–7.
- Blanchon F, Grivaux M, Asselain B, Asselain B, Lebas FX, Orlando JP, et al. 4-year mortality in patients with non-small-cell lung cancer: development and validation of a prognostic index. *Lancet Oncol* 2006;7:829–36.
- Mountain CF. The International System for Staging Lung Cancer. *Semin Surg Oncol* 2000;18:106–15.
- Paterlini-Brechot P, Benali NL. Circulating tumor cells (CTC) detection: clinical impact and future directions. *Cancer Lett* 2007;253:180–204.
- Coello MC, Luketich JD, Little VR, Godfrey TE. Prognostic significance of micrometastasis in non-small-cell lung cancer. *Clin Lung Cancer* 2004;5:214–25.
- Vona G, Sabile A, Louha M, Sitruk V, Romana S, Schütze K, et al. Isolation by size of epithelial tumor cells: a new method for the immunomorphological and molecular characterization of circulating tumor cells. *Am J Pathol* 2000;156:57–63.

15. Vona G, Estepa L, Beroud C, Damotte D, Capron F, Nalpas B, et al. Impact of cytomorphological detection of circulating tumor cells in patients with liver cancer. *Hepatology* 2004;39:792-7.
16. Pinzani P, Salvadori B, Simi L, Bianchi S, Distante V, Cataliotti L, et al. Isolation by size of epithelial tumor cells in peripheral blood of patients with breast cancer: correlation with real-time reverse transcriptase-polymerase chain reaction results and feasibility of molecular analysis by laser microdissection. *Hum Pathol* 2006;37:711-8.
17. Goldstraw P. The 7th Edition of TNM in Lung Cancer: what now? *J Thorac Oncol* 2009;4:671-3.
18. Modi A, Vohra HA, Weeden DF. Does surgery for primary non-small cell lung cancer and cerebral metastasis have any impact on survival? *Interact Cardiovasc Thorac Surg* 2009;8:467-73.
19. Landis JR, Koch GG. The measurement of observer agreement for categorical data. *Biometrics* 1977;33:159-74.
20. Chen TF, Jiang GL, Fu XL, Wang LJ, Qian H, Wu KL, et al. CK19 mRNA expression measured by reverse-transcription polymerase chain reaction (RT-PCR) in the peripheral blood of patients with non-small cell lung cancer treated by chemo-radiation: an independent prognostic factor. *Lung Cancer* 2007;56:105-14.
21. Clarke LE, Leitzel K, Smith J, Ali SM, Lipton A. Epidermal growth factor receptor mRNA in peripheral blood of patients with pancreatic, lung, and colon carcinomas detected by RT-PCR. *Int J Oncol* 2003;22:425-30.
22. Gauthier LR, Granotier C, Soria JC, Faivre S, Boige V, Raymond E, et al. Detection of circulating carcinoma cells by telomerase activity. *Br J Cancer* 2001;84:631-5.
23. Hayes DC, Secrist H, Bangur CS, Wang T, Zhang X, Harlan D, et al. Multigene real-time PCR detection of circulating tumor cells in peripheral blood of lung cancer patients. *Anticancer Res* 2006;26:1567-75.
24. Kurusu Y, Yamashita J, Ogawa M. Detection of circulating tumor cells by reverse transcriptase-polymerase chain reaction in patients with resectable non-small-cell lung cancer. *Surgery* 1999;126:820-6.
25. Peck K, Sher YP, Shih JY, Roffler SR, Wu CW, Yang PC. Detection and quantitation of circulating cancer cells in the peripheral blood of lung cancer patients. *Cancer Res* 1998;58:2761-5.
26. Rolle A, Gunzel R, Pachmann U, Willen B, Hoffken K, Pachmann K. Increase in number of circulating disseminated epithelial cells after surgery for non-small cell lung cancer monitored by MAINTRAC(R) is a predictor for relapse: a preliminary report. *World J Surg Oncol* 2005; 3:18.
27. Sheu CC, Yu YP, Tsai JR, Chang MY, Lin SR, Hwang JJ, et al. Development of a membrane array-based multimarker assay for detection of circulating cancer cells in patients with non-small cell lung cancer. *Int J Cancer* 2006;119:1419-26.
28. Sher YP, Shih JY, Yang PC, Roffler SR, Chu YW, Wu CW, et al. Prognosis of non-small cell lung cancer patients by detecting circulating cancer cells in the peripheral blood with multiple marker genes. *Clin Cancer Res* 2005;11:173-9.
29. Sozzi G, Conte D, Leon M, Ciricione R, Roz L, Ratcliffe C, et al. Quantification of free circulating DNA as a diagnostic marker in lung cancer. *J Clin Oncol* 2003;21:3902-8.
30. Sawabata N, Okumura M, Utsumi T, Inoue M, Shiono H, Minami M, et al. Circulating tumor cells in peripheral blood caused by surgical manipulation of non-small-cell lung cancer: pilot study using an immunocytology method. *Gen Thorac Cardiovasc Surg* 2007; 55:189-92.
31. Yamashita J, Matsuo A, Kurusu Y, Saishoji T, Hayashi N, Ogawa M. Preoperative evidence of circulating tumor cells by means of reverse transcriptase-polymerase chain reaction for carcinoembryonic antigen messenger RNA is an independent predictor of survival in non-small cell lung cancer: a prospective study. *J Thorac Cardiovasc Surg* 2002;124:299-305.
32. Maheswaran S, Sequist LV, Nagrath S, Utkus L, Brannigan B, Collura CV, et al. Detection of mutations in EGFR in circulating lung-cancer cells. *N Engl J Med* 2008;359:366-77.
33. Mancuso P, Burlini A, Pruneri G, Goldhirsch A, Martinelli G, Bertolini F. Resting and activated endothelial cells are increased in the peripheral blood of cancer patients. *Blood* 2001;97:3658-61.
34. Strijbos MH, Gratama JW, Kraan J, Lamers CH, den Bakker MA, Sleijfer S. Circulating endothelial cells in oncology: pitfalls and promises. *Br J Cancer* 2008;98:1731-5.
35. Guddo F, Fontanini G, Reina C, Vignola AM, Angeletti A, Bonsignore G. The expression of basic fibroblast growth factor (bFGF) in tumor-associated stromal cells and vessels is inversely correlated with non-small cell lung cancer progression. *Hum Pathol* 1999;30: 788-94.
36. Pirinen R, Tammi R, Tammi M, Hirvikoski P, Parkkinen JJ, Johansson R, et al. Prognostic value of hyaluronan expression in non-small-cell lung cancer: increased stromal expression indicates unfavorable outcome in patients with adenocarcinoma. *Int J Cancer* 2001;95:12-7.

Detection of circulating tumor cells as a prognostic factor in patients undergoing radical surgery for non-small-cell lung carcinoma: comparison of the efficacy of the CellSearch AssayTM and the isolation by size of epithelial tumor cell method

Véronique Hofman^{1,2,3}, Marius I. Ilie^{1,3}, Elodie Long^{1,3}, Eric Selva², Christelle Bonnetaud², Thierry Molina⁴, Nicolas Vénissac^{1,5}, Jérôme Mouroux^{1,5}, Philippe Vielh⁶ and Paul Hofman^{1,2,3}

¹EA4319, Faculty of Medicine, University of Nice Sophia Antipolis, Nice, France

²Human Biobank, Pasteur Hospital, Nice, France

³Laboratory of Clinical and Experimental Pathology, Pasteur Hospital, Nice, France

⁴Department of Pathology, Hôtel Dieu Hospital, Paris, France

⁵Department of Thoracic Surgery, Pasteur Hospital, Nice, France

⁶Department of Pathology and Translational Research Laboratory, Gustave Roussy Institute, Villejuif, Paris, France

Comparison of the efficacy of different enrichment methods for detection of circulating tumor cells (CTCs) before radical surgery is lacking in non-small-cell lung carcinoma (NSCLC) patients. Detection and enumeration of CTCs in 210 consecutive patients undergoing radical surgery for NSCLC were evaluated with the CellSearch AssayTM (CS), using the CellSearch Epithelial Cell Kit, and by the isolation by size of epithelial tumor (ISET) method, using double immunolabeling with anti-cytokeratin and anti-vimentin antibodies. CTCs were detected in 144 of 210 (69%) patients using CS and/or ISET and in 104 of 210 (50%) and 82 of 210 (39%) patients using ISET and CS, respectively. Using ISET, 23 of 210 (11%) patients had vimentin-positive cells with cytological criteria of malignancy. Disease-free survival (DFS) was worse for patients with CTCs compared to patients without CTCs detected by CS alone ($p < 0.0001$; log rank = 30.59) or by ISET alone ($p < 0.0001$; log rank = 33.07). The presence of CTCs detected by both CS and ISET correlated even better with shorter DFS at a univariate ($p < 0.0001$; log rank = 42.15) and multivariate level (HR, 1.235; 95% CI, 1.056–1.482; $p < 0.001$). CS and ISET are complementary methods for detection of CTCs in preoperative radical surgery for NSCLC. CTC detection in resectable NSCLC patients using CS and/or ISET could be a prognostic biomarker of great interest and may open up new avenues into improved therapeutic strategies for lung carcinoma patients.

Despite the different therapeutic strategies developed to date, non-small-cell lung carcinomas (NSCLC) have poor prognosis, because overall survival after 5 years is 20–25% for all stages.^{1–7} The main cause of death of NSCLC results from distant metastases. It is noteworthy that a subpopulation of patients with early-stage NSCLC, completely resected by surgery, rapidly develops metastasis. This indicates that occult micrometastases, not detectable even with high-resolution

imaging procedures, can be present before surgery.⁸ These micrometastases may be initiated by circulating tumor cells (CTCs) present in the peripheral blood, which detach from the primary tumor at an early stage.⁹ Thus, detection of CTCs before surgery might improve the treatment and the prognosis of patients with resectable NSCLC.

Different methods to detect CTCs in patients with carcinoma have been developed.^{10,11} Previous studies have used indirect molecular methods such as reverse transcription-polymerase chain reaction (RT-PCR), quantitative RT-PCR (qRT-PCR) and nested RT-PCR or have used indirect immunomediated methods using immunolabeling of cells enriched by different approaches including immunomagnetic separation with magnetic beads coated with epithelial-specific antibodies (BerEP4, EpCAM), laser scanning cytometry and, more recently, a microfluidic device (the CTC chip).^{10–12} qRT-PCR- and nested RT-PCR-based methods analyze the expression of a given transcript marker, compared to a reference marker expressed in any cell, which would be indicative of the presence of tumor cells. Moreover, the main advantage

Key words: circulating tumor cells, non-small-cell lung carcinoma, EpCAM, cytology, immunocytochemistry

Conflict of interest: Nothing to report

Grant sponsors: Conseil Général des Alpes Maritimes, Nice, France, French Ministry of Health (PHRC 2008)

DOI: 10.1002/ijc.25819

History: Received 29 Jun 2010; Accepted 15 Nov 2010; Online 2 Dec 2010

Correspondence to: Paul Hofman, EA4319, Faculté de Médecine, avenue de Valombrose, 06017 Nice cedex, France, Tel:

+33-4-92-03-88-55; Fax: +33-4-92-88-50, E-mail: hofman.p@chu-nice.fr

Table 1. Clinical and pathological characteristics of patients undergoing surgery for resectable non-small-cell lung carcinoma

Variables	Overall ¹
Patient cohort	210
Age (years)	
Mean	63
Range	33–82
Gender	
Male	152 (72)
Female	58 (23)
Smoking status	
Never smoked	24 (12)
Former or current smokers	186 (88)
Mean (range) P/Y	46 (1–75)
Tumor size (cm)	
Mean	3.8
Range	0.4–17
Histologic cell type	
Adenocarcinoma	120 (57)
Squamous cell carcinoma	57 (27)
Neuroendocrine carcinoma	7 (3)
Large cell carcinoma	9 (5)
Adenosquamous carcinoma	2 (1)
Sarcomatoid carcinoma	10 (5)
NSCLC (NOS)	5 (2)
pTNM stage	
I	91 (43)
II	40 (19)
III	60 (29)
IV	19 (9)

¹Values are expressed as *n* (%).

Abbreviations: TNM: tumor node metastasis; NSCLC: non-small-cell lung carcinoma; NOS: not otherwise specified.

of these methods is the higher sensitivity in comparison with the reported sensitivity of immune-mediated detection.¹¹ Conversely, direct methods contribute to diagnostic identification of CTCs. Given the important constraints of immune labeling and RT-PCR assays, direct diagnosis of CTCs can only be obtained by cytopathological analysis of the isolated cells and/or by the analysis of their genome, which provides clues to the neoplastic nature of the cell.¹¹ Currently, direct methods are more rarely used for CTC detection.^{13–15}

These indirect and direct methods have been used to detect CTCs before, during and after surgery.^{16–18} Some of these methods allow detection of the presence of biomarkers.^{12,19} Most of the indirect methods have been used to detect CTCs in patients with NSCLC.^{12,20–28} However, there is a considerable variability in the numbers of positive samples when using these direct and indirect techniques. More-

over, the lack of standardization of these different detection methods can act as a powerful restraint to effective implementation of CTC measurement in clinical routine practice.

Among the different indirect methods for CTC detection, the CellSearch AssayTM (CS) is currently used to detect CTCs.⁹ This method is approved by the Food and Drug Administration in the United States for the follow-up of patients with breast, colon and prostate metastatic carcinomas.⁹ CS is an EpCAM-based method for enrichment of CTCs in blood patients.⁹ This method has been used to detect CTCs in metastatic NSCLC²⁹ and, more recently, in primary NSCLC before surgery.³⁰ CS is certainly one of the most sensitive indirect methods described for CTCs detection.¹¹ However, the specificity of CS has been recently disputed.^{31–33} In particular, EpCAM expression of CTCs can be downregulated and, therefore, CS may miss detection of some CTCs.^{31,33} Among the direct methods used to detect CTCs, the isolation by size of epithelial tumor (ISET) cell technology allows substantial enrichment of circulating epithelial cells.^{14,15} Moreover, because cells are available for cytopathological analysis, the method should provide specificity and allow development of an immunocytochemical approach for phenotype identification of CTCs. However, to date, this method has not been used to detect CTCs in NSCLC patients.

Currently, there is a lack of data concerning the comparison of indirect and direct methods for detection of CTCs from the same cohort of patients undergoing radical surgery for NSCLC. Our study was designed to compare the efficacy of CS and ISET technologies to detect CTCs in blood samples taken from the same cohort of 210 patients with resectable NSCLC. In addition, each method used to detect CTCs was evaluated to correlate the presence of CTCs and the prognostic value.

Material and Methods

Patients

Two hundred and ten consecutive patients who underwent surgery for NSCLC (including 18 patients with neoadjuvant chemotherapy) between December 2007 and November 2010 at the Pasteur Hospital (Department of Thoracic Surgery, CHU of Nice, France) were included in our study. The patients received the necessary information concerning the study, and consent was obtained from each of them. The study was approved by the local ethics committees (CHU of Nice). The main clinical and pathological data are summarized in Table 1. Briefly, there were 152 (72%) men and 58 (23%) women (mean age 63 years; range 33–62 years). Eighty-eight percent of the patients were smokers (average 46 P/Y; range 1–75 PY). Patients had no transbronchial and/or transparietal chest biopsies at least 15 days before surgery. Table 1 shows morphological classification and tumor staging after surgical excision according to WHO criteria³⁴ and the international tumor-node-metastasis system.⁵ The median follow-up at the time of analysis was 15 months (1–28

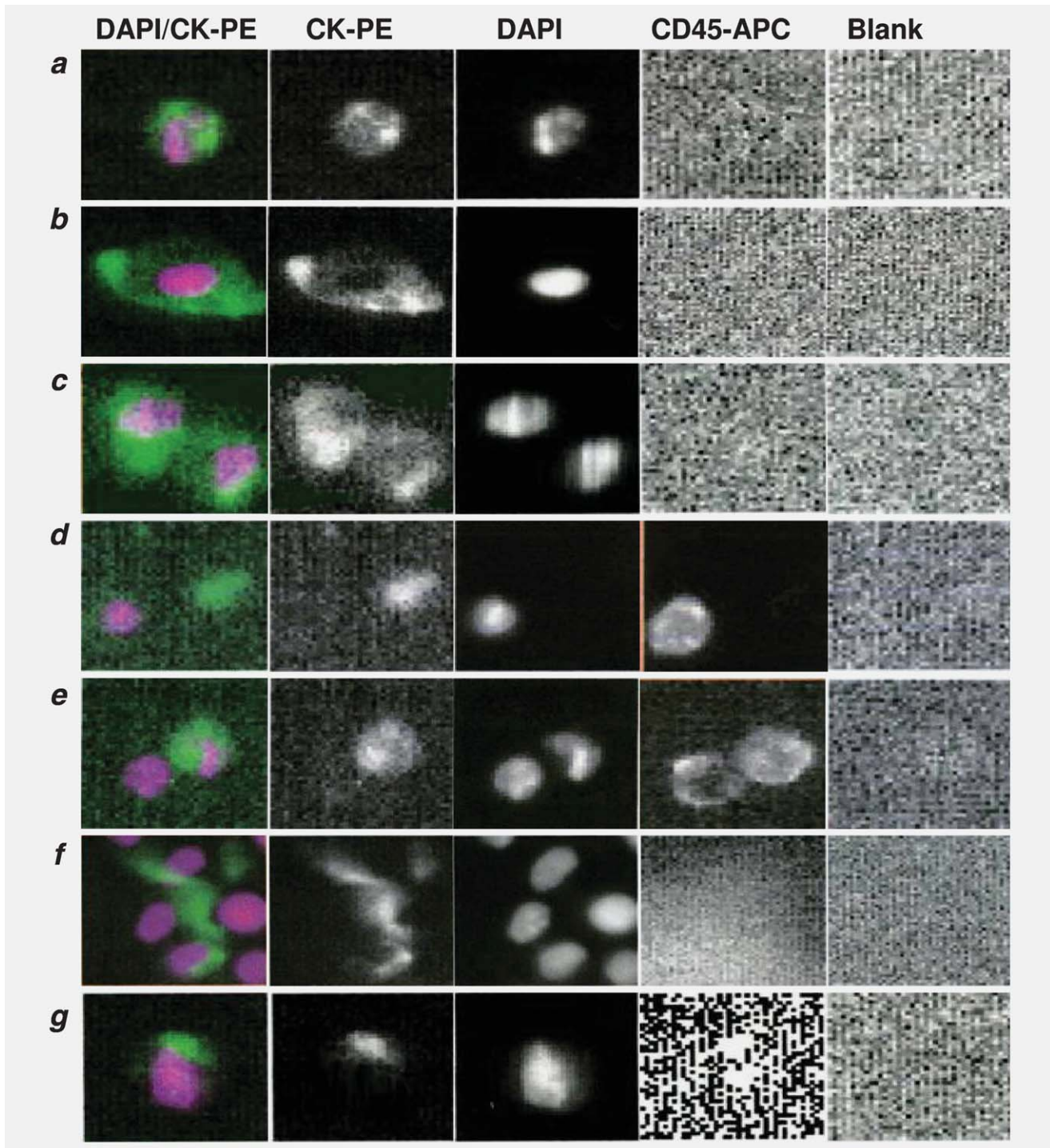


Figure 1. Gallery of circulating tumor cells (CTCs) from the CellSpotter Analyzer obtained from 7 ml of blood from patients with resectable non-small-cell lung carcinoma. Cells captured with an antiepithelial cell adhesion molecule (Ep-CAM) antibody were stained with 4',6-diamino-2-phenylindole (DAPI), with an anti-cytokeratin antibody conjugated with phycoerythrin (CK-PE) and with an anti-CD45 antibody conjugated with allophycocyanin (CD45-APC). (a, b) Cells with a round (a) to oval (b) morphology, a visible DAPI-positive nucleus, positive CK-PE staining in the cytoplasm and negative staining for CD45-APC were considered as typical intact CTC. (c) Examples of intact CTC present as clusters that are observed less frequently. (d) Contaminating leukocytes were identified as DAPI+/CK-/CD45+ cells. (e) The CD45-positive cells were not considered as CTC even when cells were positively stained for DAPI and CK-PE. (f, g) Images of cells not included in the CTC count, but frequently observed in the CTC analysis of resectable NSCLC patients. [Color figure can be viewed in the online issue, which is available at wileyonlinelibrary.com.]

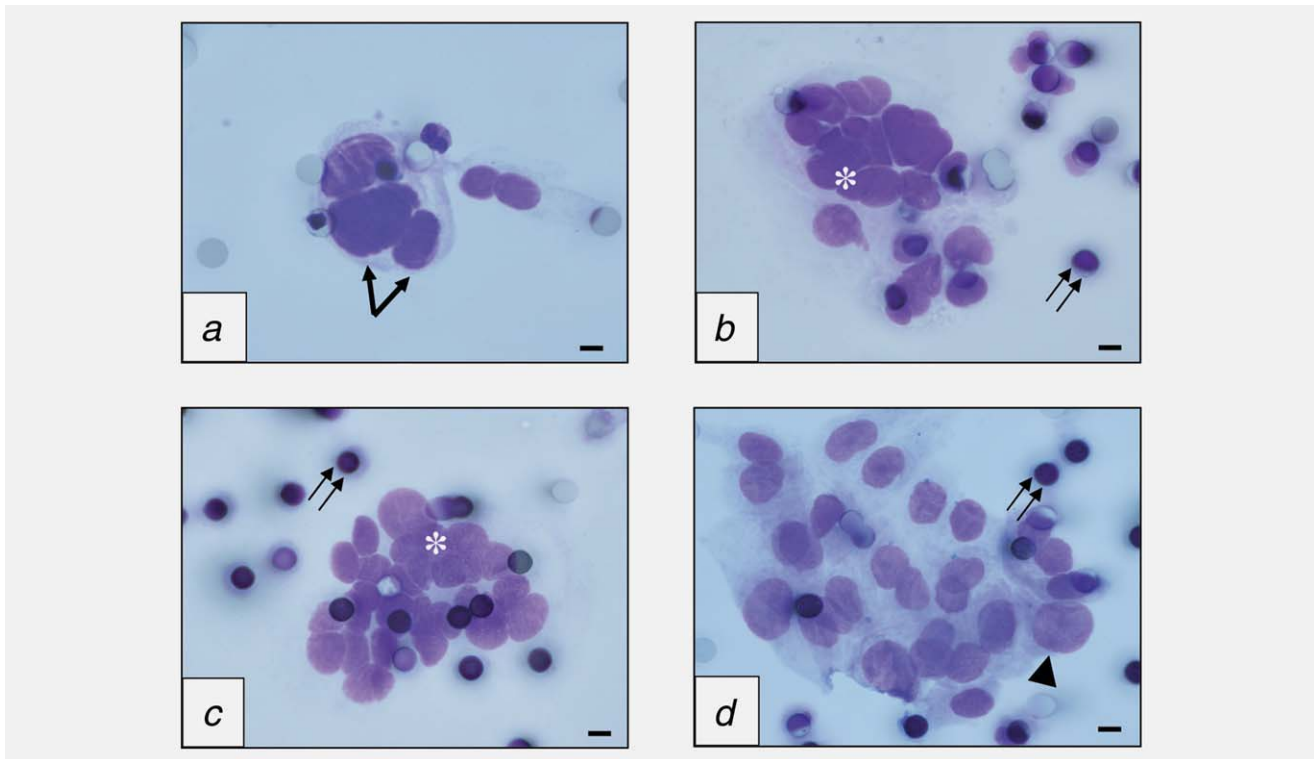


Figure 2. Cytomorphological analysis of circulating tumor cells (CTCs) detected on filtered blood using the ISET method in patients with resectable non-small-cell lung carcinoma. (a–d) Cells showing cytological malignant features isolated preoperatively by the ISET method in patients with a resectable lung adenocarcinoma (a), squamous cell carcinoma (b), large cell carcinoma (c) and sarcomatoid carcinoma (d). (a–d) Original magnification $\times 1,000$; MGG staining; bars: $8\ \mu\text{m}$ (arrows: anisonucleosis; arrows head: irregularity and large nuclei; asterisks: tridimensional sheets; double arrows: pores of the filter). [Color figure can be viewed in the online issue, which is available at wileyonlinelibrary.com.]

months) according to the method of Schemper and Smith.³⁵ The sensitivity of CTC detection was used to determine disease-free survival (DFS). A control group consisted of 40 healthy donors without previous history of cancer. There were 30 (75%) men and 10 (25%) women, all smokers (average 15 P/Y; range 2–25 PY).

Methods

CS and ISET technologies were carried out using previously described methods with slight modification.¹¹ Two consecutive blood samples were collected from each individual to serve for the two methods. The first 4 ml of peripheral blood was discarded to avoid contamination with cytokeratin-positive skin cells. For CS, 7 ml of peripheral blood was taken before anesthesia and collected in the CellSave preservative tube (Veridex LLC, Raritan, NJ). Samples were maintained at room temperature and processed within 72 hr of blood collection. Briefly, the CS system (Veridex) consists of a Cell-Prep system, the CellSearch Epithelial Cell Kit and the Cell-Spotter Analyzer. The CellPrep System is a semiautomated sample preparation system, and the CellSearch Epithelial Cell Kit consists of ferrofluids coated with epithelial cell-specific EpCAM antibodies to immunomagnetically enrich epithelial cells. In the final processing step, the cells are resuspended in

the MagNest Cell Presentation Device (Veridex). This device consists of a chamber and two magnets that orient the immunomagnetically labeled cells for analysis using the Cell-Spotter Analyzer. The criteria for definition of a CTC include a round to oval morphology, a visible nucleus (DAPI positive), positive staining for cytokeratin in the cytoplasm and negative staining for CD45 (Fig. 1). CTC enumeration was expressed as the number of positive cells per 7 ml of blood.

For the ISET method, Métagenex, Paris, France, 10 ml of peripheral blood was collected in parallel in buffered EDTA, maintained at 4°C and processed within 1 hr of blood collection. The filtration module contains ten wells, making it possible to load and filter ten individual samples in parallel. Briefly, after blood filtration, the membrane is gently washed with phosphate-buffered saline (PBS) (Sigma, Paris, France), disassembled from the filtration module and allowed to air dry. The membrane was cut into two parts containing, respectively, seven spots for immunocytochemistry and three spots for May Grünwald Giemsa (MGG) staining for further cytological analysis. Immunocytochemistry was performed using double immunolabeling with a pan-cytokeratin antibody (mouse, clone KL-1, Immunotech, Marseille, France, diluted at 1:100), which recognizes cytokeratins 2, 5, 6, 8, 10, 11, 14/15, 18 and 19, and an anti-vimentin (mouse, clone

Table 2. Analysis of the correlation between the presence of CTCs detected by isolation by size of epithelial tumor (ISET) and CellSearch assay (CS) methods

Method	CellSearch		Total	
	+	–		
ISET	+	42	62	104
	–	40	66	106
Total		82	128	210

p value = 0.7 (χ^2 test). Kappa index of agreement = 0.02.

V9, Dako, Paris, France, diluted at 1:200) antibody applied to filters for 45 min at room temperature. Filters were then washed three times with PBS at room temperature, pH 7.4, and incubated for 45 min with secondary anti-phosphatase and anti-peroxidase antibodies (Dako), respectively. Immunostained and MGG-stained spots were then examined by light microscopy using different steps: (i) observation at 100 \times and 200 \times original magnification to look for CTCs and to count these cells, and (ii) observation at 630 \times and 1,000 \times original magnification with oil immersion for detailed cytomorphological analysis. The following criteria were taken into account to characterize the detected nonhematological cells: irregularity and size of the nucleus, anisonucleosis, nuclear hyperchromatism, nucleocytoplasmic ratio, size and number of nucleoli and presence of tridimensional sheets. CTCs were characterized by the presence of at least three of the following criteria: anisonucleosis (ratio > 0.5), nuclei larger than three calibrated pore size of the membrane (8 μ m) (>24 μ m), irregular nuclei and presence of three-dimensional sheets (Fig. 2). The results of samples from 250 individuals (210 patients and 40 healthy individuals) entered into the study and processed by CS and ISET were analyzed by four operators (ES, CL, VL and VH) working blindly, without knowledge of the clinical and pathological characteristics of the patients.

A CTC was defined as a cell with an epithelial antigen detected with the CellSearch Epithelial Cell Kit. The cutoff was one detected cell per CS. When using ISET, a CTC was defined as a cell with epithelial and/or vimentin antigens detected by immunocytochemistry and showing cytological features of nonhematological circulating cells. When using the ISET method, only CTC evaluated by IHC was counted (to consider the number of CTC in the same volume of blood, *i.e.*, 7 ml for the CS and ISET methods).

Statistical analysis

The χ^2 analysis was used to evaluate whether CTCs detected by ISET correlated with CTCs detected by CS. The Cohen's kappa coefficient was used to assess the agreement between these methods. In addition, the χ^2 analysis was used to explore the association between CTCs detected by ISET and CS methods and the histological subtype and pTNM stage. Survival time was calculated using Kaplan–Meier estimates,

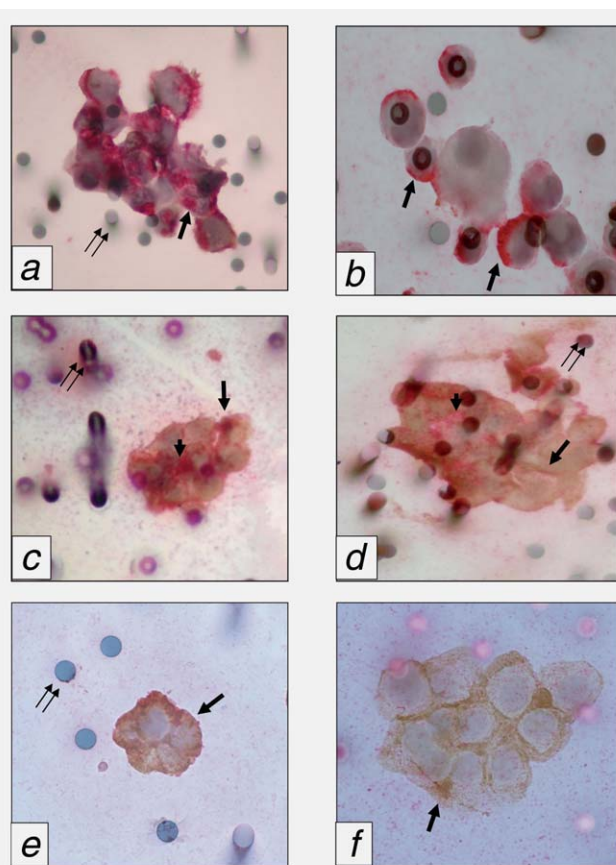


Figure 3. Clusters of immunostained circulating tumor cells (CTCs) observed on filtered blood using the ISET method in patients with resectable non-small-cell lung carcinoma. (a, b) CTCs expressing only the pan-cytokeratin antigen in patients with lung adenocarcinoma (a) and squamous cell carcinoma (b) (arrows, CTCs). (c, d) CTCs coexpressing pan-cytokeratin and vimentin antigens in patients with lung adenocarcinoma (c) and squamous cell carcinoma (d) (arrowheads: pan-cytokeratin expression; arrows, vimentin expression). (e, f) CTCs expressing only the vimentin antigen in patients with lung adenocarcinoma (e) and squamous cell carcinoma (f) (arrows: CTCs). (a–f) Original magnification \times 1,000; bars: 8 μ m; immunophosphatase staining with a pan-cytokeratin antibody (KL1) and immunoperoxidase staining with an anti-vimentin antibody (double arrows: pores of the filters). [Color figure can be viewed in the online issue, which is available at wileyonlinelibrary.com.]

and differences between survival curves were analyzed by means of the log rank test. Multivariate Cox analyses were carried out to examine whether the presence of CTC, detected either by ISET or CS method or by both methods, was an independent prognostic factor for DFS with adjustment for relevant clinicopathological covariates. Variables that were associated with survival with a p value <0.20 in the univariate analysis were included in a multivariate regression. The variables included in the model for DFS were pTNM stage and histology. Differences were considered significant when a p value was less than 0.05. All statistical

Table 3. Presence of CTCs detected by the CellSearch assay and isolation by size of epithelial tumor (ISET) methods according to pTNM staging and histological classification

Variables	ISET+	<i>p</i> value*	Cell Search +	<i>p</i> value*	ISET+ and Cell Search+	<i>p</i> value*	ISET+ or Cell Search+	<i>p</i> value*
Histologic cell type								
Adenocarcinoma	64 (53%)	0.74	51(43%)	0.3	27 (23%)	0.23	88 (73%)	0.066
Squamous cell carcinoma	23 (40%)		18 (32%)		7 (12%)		34 (60%)	
Neuroendocrine carcinoma	4 (57%)		2 (29%)		1 (14%)		5 (71%)	
Large cell carcinoma	5 (56%)		4 (44%)		2 (22%)		7 (78%)	
Adenosquamous carcinoma	1 (50%)		0 (0%)		0 (0%)		1 (50%)	
Sarcomatoid carcinoma	4 (40%)		3 (30%)		2 (20%)		5 (50%)	
NSCLC (NOS)	3 (60%)		4 (80%)		3 (60%)		4 (80%)	
pTNM stage								
I	44 (48%)	0.50	33 (36%)	0.8	13 (14%)	0.07	64 (70%)	0.59
II	24 (60%)		18 (45%)		12 (30%)		30 (75%)	
III	27 (45%)		24 (40%)		13 (22%)		38 (63%)	
IV	9 (47%)		7 (37%)		4 (21%)		12 (63%)	

**p* value significant at the 0.05 level.

Abbreviations: TNM: tumor node metastasis; NSCLC: non-small-cell lung carcinoma; NOS: not otherwise specified.

evaluations were performed using the SPSS for Windows software system, version 11.0 (SPSS, Chicago, IL).

Results

CTCs were detected in 144 of 210 (69%) patients using the CS and/or ISET method. Moreover, CTCs were detected in 104 of 210 (50%) patients using the ISET method, independently of the CS method, and in 82 of 210 (39%) patients using the CS method, independently of the ISET method, respectively ($p = 0.03$) (Table 2). CTCs were detected in 44 (21%) patients when a cutoff of two cells was considered for CS analysis (not shown). CTCs were detected in 62 of 210 (30%) patients when using the ISET method and not detected by CS and in 40 of 210 (19%) patients when using the CS method and not detected by ISET, respectively ($p = 0.01$) (Table 2). Only 42 of 210 patients (20%) showed CTCs detected both by the CS and ISET methods (Table 2). No correlation was found between CTCs detected by ISET and CS methods ($p = 0.7$; $\kappa = 0.02$), indicating that measurements assessed by these two methods are independent (Table 2). Using ISET, the majority of CTCs exhibited malignant cytopathological criteria on MGG staining (Fig. 2). Moreover, similar morphological features were noted for CTCs isolated from patients with adenocarcinoma and squamous cell carcinoma as well as other rare histological subtypes of NSCLC (Fig. 2). CTCs were isolated or grouped in sheets having between 3 and >100 CTCs (Fig. 2). Corresponding immunostained cells expressed cytokeratin alone in 27 of 210 (13%) cases or in association with vimentin in 55 of 210 cases (26%) (Fig. 3). However, in 23 of 210 (11%) patients, CTCs were only positive for vimentin (Fig. 3). These latter cells showed cytological malignant features. Moreover, the expres-

sion of TTF1 was not detected in a majority of CTCs, whereas the same primary lung adenocarcinomas expressed TTF1 (data not shown).

The number of CTCs detected by CS varied from 1 to 23 cells (mean: 12 cells), whereas the number of CTCs detected by ISET varied from 1 to 150 cells (mean: 34 cells), ($p < 0.01$; data not shown). The presence of CTCs detected by these two methods was independent of disease staging and of the histology subtypes of carcinomas (Table 3). No CTCs were detected in control individuals using the ISET and CS methods.

Patients without CTCs had a significantly longer DFS compared to patients with CTCs detected by CS alone ($p < 0.0001$; log rank = 30.59) (Fig. 4a) or ISET ($p < 0.0001$; log rank test = 33.07) (Fig. 4b). This significance was even higher in patients without CTCs compared to patients with CTCs detected by CS and/or ISET ($p < 0.0001$; log rank = 42.15) (Fig. 4c). Subsequently, the presence of CTCs as detected by the CS (HR, 1.564; 95% CI, 1.264–4.673; $p = 0.008$) or ISET (HR, 1.372; 95% CI, 1.123–3.286; $p = 0.006$) methods or by both methods (HR, 1.235; 95% CI, 1.056–1.482; $p < 0.001$) was a significantly independent prognostic factor for shorter DFS, as demonstrated by the multivariate survival analysis using the Cox's regression model (Table 4).

Discussion

Our study demonstrates that CS and ISET technologies can detect preoperative CTCs in patients with resectable NSCLC. CS and ISET present similar sensitivities for detection of CTCs, if we consider that the detection of CTCs is only based on epithelial antigen detection. Interestingly, the average number of CTCs detected by ISET in comparison to CS

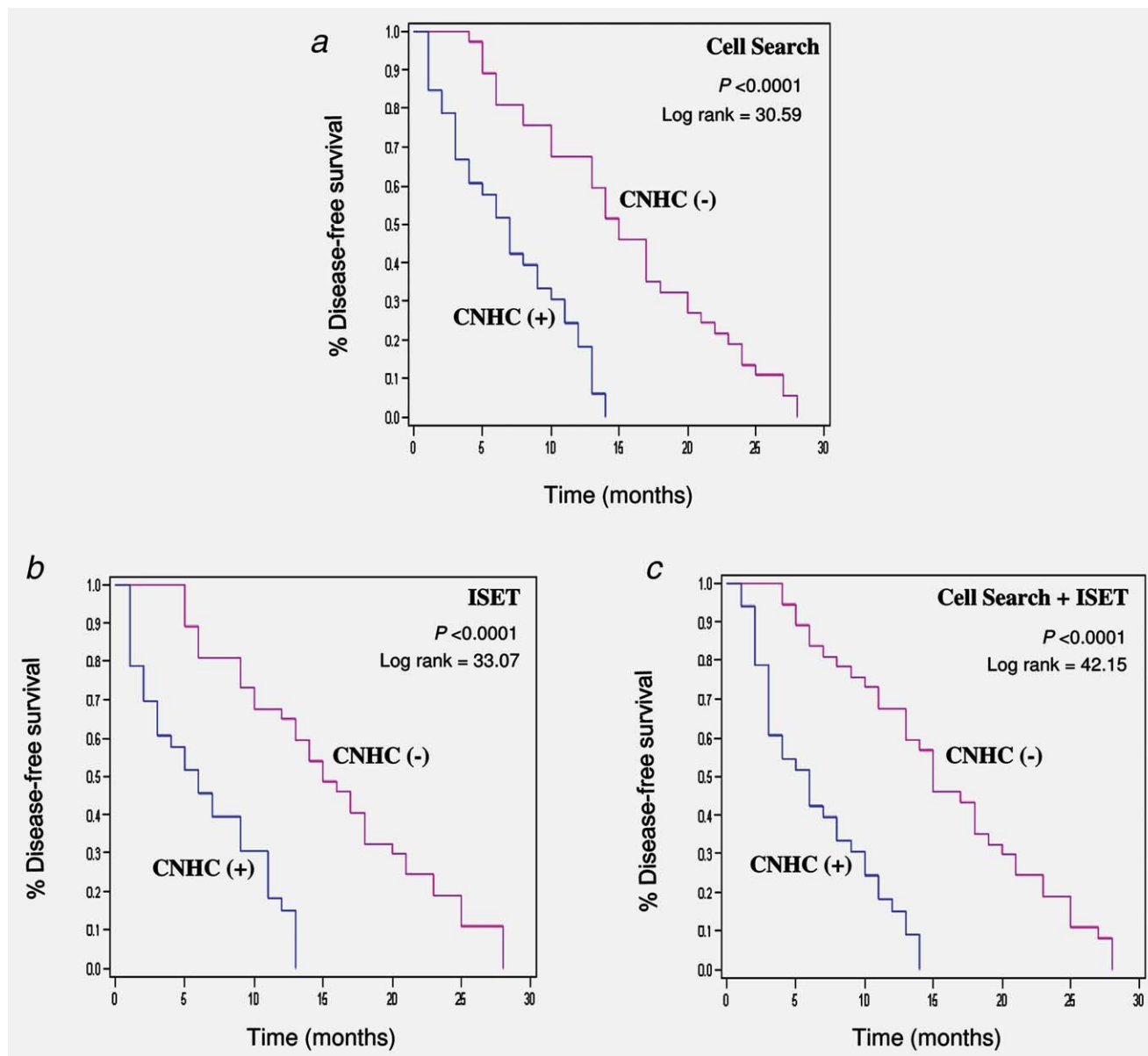


Figure 4. Kaplan–Meier curves of disease-free survival duration stratified according to the presence (+) and the absence (–) of circulating nonhematological cells (CNHC) detected by CellSearch (CS) (a) or isolation by size of epithelial tumor (ISET) (b) and by CS and ISET (c) methodology. [Color figure can be viewed in the online issue, which is available at wileyonlinelibrary.com.]

was higher. Moreover, we observed that the number of patients with detected CTCs was higher when the two methods were used in parallel compared to each method used independently. Finally, it is noteworthy that following double immunostaining of filters after ISET, we observed in a subpopulation of patients without CTCs detected by CS, some circulating cells with nonhematological features, but with cytological malignant criteria, which expressed only vimentin.

In a previous study, 34 of 168 (20%) patients with metastatic NSCLC showed two or more CTCs detected by CS.²⁹ Moreover, in our study, 14, 10 and 6% of these patients demonstrated more than 5, 10 and 50 CTCs, respectively.²⁹ In

another study using CS, CTCs were detected in peripheral blood in 5 of 30 (16.7%) patients undergoing surgery for NSCLC.³⁰ Interestingly, a good correlation of the enumeration of CTCs with the radiographic response following first-line chemotherapy administered in NSCLC patients was demonstrated in a recent study.³⁶ Using CS, we found in our series a high percentage of NSCLC patients with detection of at least one CTC (39%). However, when the cutoff was at least two CTCs, this percentage was lower (21%).

ISET technology is a direct method that allows cytomorphological analysis of CTCs.¹¹ For this reason, it offers a number of advantages, particularly for immunocytochemical

Table 4. Multivariate Cox proportional hazard regression analysis of predicting factors for disease-free survival in 210 resectable NSCLC patients

Prognostic factor	HR	95% CI	p value*
Histology			
Squamous cell carcinoma	2.764	1.223–5.342	0.023
Other subtypes	1		
pTNM stage			
I + II	0.289	0.108–0.772	0.016
III + IV	1		
CellSearch method			
CNHC+	1.564	1.264–4.673	0.008
CNHC–	1		
ISET method			
CNHC+	1.372	1.123–3.286	0.006
CNHC–	1		
CellSearch + ISET methods			
CNHC+	1.235	1.056–1.482	<0.001
CNHC–	1		

*p value significant at the 0.05 level.

Abbreviations: HR: hazard ratio; CI: confidence interval.

examination using different antibodies to better characterize the CTCs. However, some CTCs may lose a certain number of antigens normally expressed in the primary tumor. Thus, we failed to detect the expression of TTF1 in a majority of CTCs, whereas the same patients had TTF1-positive lung adenocarcinomas (data not shown). This can be explained by epithelial–mesenchymal transition (EMT), during which adenocarcinoma cells downregulate TTF1 expression.³⁷ Similarly, some CTCs may have weak or no cytokeratin expression because cell dedifferentiation inducing loss of these antigens can be present during EMT. This is in keeping with our observation of a couple of circulating cells with nonhematological features that express only vimentin. We, therefore, speculate that these cells are indeed CTCs, because they demonstrate cytological malignant criteria. Moreover, it is possible that only cells coexpressing cytokeratin and vimentin or expressing vimentin alone may have a more malignant invasive potential. Further studies using molecular biology tools are needed to better characterize these potentially different subpopulations of cells and to confirm their malignant potential. Recently, genetic abnormalities identified by an antigen-independent FISH-based assay for CTCs have been

suggested as a diagnostic and prognostic feature in patients with NSCLC.³⁸ Moreover, CTCs in combination with serological cell death assays may be used as pharmacodynamic biomarkers underlying the disease response in patients with small-cell lung cancer undergoing standard chemotherapy.³⁹

There are limitations in performing a comparison of the CS and ISET methods. In the literature, CTCs have been defined as cells detected in peripheral blood that express cytokeratin antigens. In particular, all cells positively isolated by the CS system with anti-EpCAM antibodies have been called “CTCs.” This can overestimate the real number of malignant cells present in the peripheral blood, because some monocytes can express cytokeratins and a subpopulation of epithelial cells might be nonmalignant.¹¹ Conversely, CTCs can be underestimated when using only the CS method. Thus, some CTCs probably express only vimentin because EMT allows migration of tumor cells through the stroma, to cross the endothelial barrier, and to circulate in the peripheral blood.¹¹ Consequently, CTCs that express only vimentin cannot be detected by CS. Thus, in our study, a couple of patients had CTCs expressing only vimentin when detected by ISET, whereas in the same population no CTCs were isolated by CS. However, we cannot definitively assume that all of these latter cells are “CTCs,” even though the cytomorphological analysis of most of these cells showed malignant features. Further studies are needed to better characterize these cells using a panel of antibodies raised against different antigens. Finally, some of these cells may correspond to other nonhematological circulating cells, in particular endothelial cells.^{40,41}

It is noteworthy that, in our work, the presence of CTCs detected by CS and/or ISET methods was associated with a pejorative outcome. The latter results demonstrated that preoperative CTCs detection in resectable NSCLC patients can be a prognostic biomarker in lung oncology practice.

In conclusion, CTCs can be detected by CS and ISET in NSCLC patients undergoing radical surgery. Only a fraction of this population had simultaneous detection of CTCs by ISET and CS, but the percentage of patients with detected CTCs is higher when combining the two methods. This result underlies the complementarity of the two methods for detecting CTCs preoperatively. CS failed to detect CTCs expressing only vimentin, which can be observed when using ISET.

Acknowledgements

E.L. received an ARC fellow grant.

References

- Blanchon F, Grivaux M, Asselain B, Lebas FX, Orlando JP, Piquet J, Zureik M. 4-year mortality in patients with non-small-cell lung cancer: development and validation of a prognostic index. *Lancet Oncol* 2006;7: 829–36.
- Goya T, Asamura H, Yoshimura H, Kato H, Shimokata K, Tsuchiya R, Sohara Y, Miya T, Miyaoka E. Prognosis of 6644 resected non-small cell lung cancers in Japan: a Japanese lung cancer registry study. *Lung Cancer* 2005;50:227–34.
- van Rens MT, de la Riviere AB, Elbers HR, van Den Bosch JM. Prognostic assessment of 2,361 patients who underwent pulmonary resection for non-small cell lung cancer, stage I, II, and IIIA. *Chest* 2000;117:374–9.

4. Mountain CF. Revisions in the international system for staging lung cancer. *Chest* 1997;111:1710-17.
5. Mountain CF. The international system for staging lung cancer. *Semin Surg Oncol* 2000;18:106-15.
6. Naruke T, Tsuchiya R, Kondo H, Asamura H. Prognosis and survival after resection for bronchogenic carcinoma based on the 1997 TNM-staging classification: the Japanese experience. *Ann Thorac Surg* 2001;71:1759-64.
7. Pfannschmidt J, Muley T, Bulzebruck H, Hoffmann H, Dienemann H. Prognostic assessment after surgical resection for non-small cell lung cancer: experiences in 2083 patients. *Lung Cancer* 2007;55:371-7.
8. Coello MC, Luketich JD, Litle VR, Godfrey TE. Prognostic significance of micrometastasis in non-small-cell lung cancer. *Clin Lung Cancer* 2004;5:214-25.
9. Pantel K, Brakenhoff RH, Brandt B. Detection, clinical relevance and specific biological properties of disseminating tumour cells. *Nat Rev Cancer* 2008;8:329-40.
10. Alix-Panabieres C, Riethdorf S, Pantel K. Circulating tumor cells and bone marrow micrometastasis. *Clin Cancer Res* 2008;14:5013-21.
11. Paterlini-Brechot P, Benali NL. Circulating tumor cells (CTC) detection: clinical impact and future directions. *Cancer Lett* 2007;253:180-204.
12. Maheswaran S, Sequist LV, Nagrath S, Ulkus L, Brannigan B, Collura CV, Inserra E, Diederichs S, Iafate AJ, Bell DW, Digumarthy S, Muzikansky A, et al. Detection of mutations in EGFR in circulating lung-cancer cells. *N Engl J Med* 2008;359:366-77.
13. Pinzani P, Salvadori B, Simi L, Bianchi S, Distante V, Cataliotti L, Pazzagli M, Orlando C. Isolation by size of epithelial tumor cells in peripheral blood of patients with breast cancer: correlation with real-time reverse transcriptase-polymerase chain reaction results and feasibility of molecular analysis by laser microdissection. *Hum Pathol* 2006;37:711-18.
14. Vona G, Sabile A, Louha M, Sitruk V, Romana S, Schutze K, Capron F, Franco D, Pazzagli M, Vekemans M, Lacour B, Brechot C, et al. Isolation by size of epithelial tumor cells: a new method for the immunomorphological and molecular characterization of circulating tumor cells. *Am J Pathol* 2000;156:57-63.
15. Vona G, Estepa L, Beroud C, Damotte D, Capron F, Nalpas B, Mineur A, Franco D, Lacour B, Pol S, Brechot C, Paterlini-Brechot P. Impact of cytomorphological detection of circulating tumor cells in patients with liver cancer. *Hepatology* 2004;39:792-7.
16. Biggers B, Knox S, Grant M, Kuhn J, Nemunaitis J, Fisher T, Lamont J. Circulating tumor cells in patients undergoing surgery for primary breast cancer: preliminary results of a pilot study. *Ann Surg Oncol* 2009;16:969-71.
17. Cristofanilli M, Hayes DF, Budd GT, Ellis MJ, Stopeck A, Reuben JM, Doyle GV, Matera J, Allard WJ, Miller MC, Fritsche HA, Hortobagyi GN, et al. Circulating tumor cells: a novel prognostic factor for newly diagnosed metastatic breast cancer. *J Clin Oncol* 2005;23:1420-30.
18. Sawabata N, Okumura M, Utsumi T, Inoue M, Shiono H, Minami M, Nishida T, Sawa Y. Circulating tumor cells in peripheral blood caused by surgical manipulation of non-small-cell lung cancer: pilot study using an immunocytology method. *Gen Thorac Cardiovasc Surg* 2007;55:189-92.
19. Clarke LE, Leitzel K, Smith J, Ali SM, Lipton A. Epidermal growth factor receptor mRNA in peripheral blood of patients with pancreatic, lung, and colon carcinomas detected by RT-PCR. *Int J Oncol* 2003;22:425-30.
20. Chen TF, Jiang GL, Fu XL, Wang LJ, Qian H, Wu KL, Zhao S. CK19 mRNA expression measured by reverse-transcription polymerase chain reaction (RT-PCR) in the peripheral blood of patients with non-small cell lung cancer treated by chemo-radiation: an independent prognostic factor. *Lung Cancer* 2007;56:105-14.
21. Hayes DC, Secrist H, Bangur CS, Wang T, Zhang X, Harlan D, Goodman GE, Houghton RL, Persing DH, Zehentner BK. Multigene real-time PCR detection of circulating tumor cells in peripheral blood of lung cancer patients. *Anticancer Res* 2006;26:1567-75.
22. Kurusu Y, Yamashita J, Ogawa M. Detection of circulating tumor cells by reverse transcriptase-polymerase chain reaction in patients with resectable non-small-cell lung cancer. *Surgery* 1999;126:820-6.
23. Peck K, Sher YP, Shih JY, Roffler SR, Wu CW, Yang PC. Detection and quantitation of circulating cancer cells in the peripheral blood of lung cancer patients. *Cancer Res* 1998;58:2761-5.
24. Rolle A, Gunzel R, Pachmann U, Willen B, Hoffken K, Pachmann K. Increase in number of circulating disseminated epithelial cells after surgery for non-small cell lung cancer monitored by MAINTRAC(R) is a predictor for relapse: a preliminary report. *World J Surg Oncol* 2005;3:18.
25. Sher YP, Shih JY, Yang PC, Roffler SR, Chu YW, Wu CW, Yu CL, Peck K. Prognosis of non-small cell lung cancer patients by detecting circulating cancer cells in the peripheral blood with multiple marker genes. *Clin Cancer Res* 2005;11:173-9.
26. Sheu CC, Yu YP, Tsai JR, Chang MY, Lin SR, Hwang JJ, Chong IW. Development of a membrane array-based multimarker assay for detection of circulating cancer cells in patients with non-small cell lung cancer. *Int J Cancer* 2006;119:1419-26.
27. Sozzi G, Conte D, Leon M, Ciricione R, Roz L, Ratcliffe C, Roz E, Cirenei N, Bellomi M, Pelosi G, Pierotti MA, Pastorino U. Quantification of free circulating DNA as a diagnostic marker in lung cancer. *J Clin Oncol* 2003;21:3902-8.
28. Yamashita J, Matsuo A, Kurusu Y, Saishoji T, Hayashi N, Ogawa M. Preoperative evidence of circulating tumor cells by means of reverse transcriptase-polymerase chain reaction for carcinoembryonic antigen messenger RNA is an independent predictor of survival in non-small cell lung cancer: a prospective study. *J Thorac Cardiovasc Surg* 2002;124:299-305.
29. Allard WJ, Matera J, Miller MC, Repollet M, Connelly MC, Rao C, Tibbe AG, Uhr JW, Terstappen LW. Tumor cells circulate in the peripheral blood of all major carcinomas but not in healthy subjects or patients with nonmalignant diseases. *Clin Cancer Res* 2004;10:6897-904.
30. Okumura Y, Tanaka F, Yoneda K, Hashimoto M, Takuwa T, Kondo N, Hasegawa S. Circulating tumor cells in pulmonary venous blood of primary lung cancer patients. *Ann Thorac Surg* 2009;87:1669-75.
31. Rao CG, Chianese D, Doyle GV, Miller MC, Russell T, Sanders RA Jr, Terstappen LW. Expression of epithelial cell adhesion molecule in carcinoma cells present in blood and primary and metastatic tumors. *Int J Oncol* 2005;27:49-57.
32. Sieuwerts AM, Kraan J, Bolt J, van der Spoel P, Elstrodt F, Schutte M, Martens JW, Gratama JW, Sleijfer S, Foekens JA. Anti-epithelial cell adhesion molecule antibodies and the detection of circulating normal-like breast tumor cells. *J Natl Cancer Inst* 2009;101:61-6.
33. Lu J, Fan T, Zhao Q, Zeng W, Zaslavsky E, Chen JJ, Frohman MA, Golightly MG, Madajewicz S, Chen WT. Isolation of circulating epithelial and tumor progenitor cells with an invasive phenotype from breast cancer patients. *Int J Cancer* 2010;126:669-83.
34. Travis WD, Brambilla E, Müller-Hermelink HK, Harris CC. WHO histological classification of tumors of the lung World Health Organization Classification of Tumours. Pathology and genetics of tumours of the lung, pleura, thymus and heart. Lyon: IARC Press, 2004. 342.

35. Schemper M, Smith TL. A note on quantifying follow-up in studies of failure time. *Control Clin Trials* 1996;17:343–6.
36. Wu C, Hao H, Li L, Zhou X, Guo Z, Zhang L, Zhang X, Zhong W, Guo H, Bremner RM, Lin P. Preliminary investigation of the clinical significance of detecting circulating tumor cells enriched from lung cancer patients. *J Thorac Oncol* 2009;4:30–6.
37. Saito RA, Watabe T, Horiguchi K, Kohyama T, Saitoh M, Nagase T, Miyazono K. Thyroid transcription factor-1 inhibits transforming growth factor-beta-mediated epithelial-to-mesenchymal transition in lung adenocarcinoma cells. *Cancer Res* 2009;69:2783–91.
38. Katz RL, He W, Khanna A, Fernandez RL, Zaidi TM, Krebs M, Caraway NP, Zhang HZ, Jiang F, Spitz MR, Blowers DP, Jimenez CA, et al. Genetically abnormal circulating cells in lung cancer patients: an antigen-independent fluorescence in situ hybridization-based case-control study. *Clin Cancer Res* 2010;16:3976–87.
39. Hou JM, Greystoke A, Lancashire L, Cummings J, Ward T, Board R, Amir E, Hughes S, Krebs M, Hughes A, Ranson M, Lorigan P, et al. Evaluation of circulating tumor cells and serological cell death biomarkers in small cell lung cancer patients undergoing chemotherapy. *Am J Pathol* 2009;175:808–16.
40. Mancuso P, Burlini A, Pruneri G, Goldhirsch A, Martinelli G, Bertolini F. Resting and activated endothelial cells are increased in the peripheral blood of cancer patients. *Blood* 2001;97:3658–61.
41. Strijbos MH, Gratama JW, Kraan J, Lamers CH, den Bakker MA, Sleijfer S. Circulating endothelial cells in oncology: pitfalls and promises. *Br J Cancer* 2008;98:1731–5.

Cytopathologic Detection of Circulating Tumor Cells Using the Isolation by Size of Epithelial Tumor Cell Method

Promises and Pitfalls

Véronique J. Hofman, MD, PhD,¹⁻⁴ Marius I. Ilie, MD,¹⁻⁴ Christelle Bonnetaud, MD,² Eric Selva, MD,² Elodie Long, MD,³ Thierry Molina, MD, PhD,⁵ Jean Michel Vignaud, MD, PhD,⁶ Jean François Fléjou, MD, PhD,⁷ Sylvie Lantuejoul, MD, PhD,⁸ Eric Piaton, MD,⁹ Catherine Butori, MD,¹⁻⁴ Nathalie Mourad, MD,¹⁰ Michel Poudenx, MD,¹¹ Philippe Bahadoran, MD, PhD,¹² Stéphanie Sibon, MD,¹³ Nicolas Guevara, MD,¹⁴ José Santini, MD,¹⁴ Nicolas Vénissac, MD,¹³ Jérôme Mouroux, MD,¹³ Philippe Vielh, MD, PhD,¹⁵ and Paul M. Hofman, MD, PhD¹⁻⁴

Key Words: Circulating tumor cells; Cytopathology; Diagnosis; Pitfalls

DOI: 10.1309/AJCP9X8OZBEIQWVI

Abstract

Detection of circulating tumor cells (CTCs) morphologically may be a promising new approach in clinical oncology. We tested the reliability of a cytomorphologic approach to identify CTCs: 808 blood samples from patients with benign and malignant diseases and healthy volunteers were examined using the isolation by size of epithelial tumor cell (ISET) method. Cells having nonhematologic features (so-called circulating nonhematologic cells [CNHCs]) were classified into 3 categories: CNHCs with malignant features, CNHCs with uncertain malignant features, and CNHCs with benign features. CNHCs were found in 11.1% and 48.9% of patients with nonmalignant and malignant pathologies, respectively (P < .001). CNHCs with malignant features were observed in 5.3% and in 43.1% of patients with nonmalignant and malignant pathologies, respectively. Cytopathologic identification of CTCs using the ISET method represents a promising field for cytopathologists. The possibility of false-positive diagnosis stresses the need for using ancillary methods to improve this approach.

Sensitive and specific detection of circulating tumor cells (CTCs) remains a challenge in clinical oncology.¹ Animal studies and knowledge of cell invasion processes have stimulated the development of a truly reliable method to identify CTCs. Studies performed in humans show promise for the development of clinical studies in this field.²⁻⁹ As a consequence, the potential clinical impact of CTC identification could range from early diagnosis of invasive cancers to assessment of the risk for developing recurrence or metastasis and the early detection of response or resistance to antitumor treatments.¹⁰ However, the use of different technologies and the differences among the populations tested make the clinical significance of CTC detection difficult to interpret. Thus, the clinical benefit of detecting CTCs in the blood of patients highly depends on the technical characteristics of the method used for detection and on its reliability in terms of sensitivity and specificity.¹¹⁻¹⁴ In this regard, a critical challenge in the field of CTC detection, recently highlighted by basic and clinical studies, relates to the fact that most malignant CTCs lose their “epithelial antigens” and start to express mesenchymal antigens, a process known as *epithelial to mesenchymal transition*.¹⁵

Direct and indirect methods have been proposed to detect CTCs, but their results show large variability in specificity, sensitivity, and cost.^{10,16-26} Among the direct methods, cytopathologic detection of CTCs, after substantial enrichment according to their size (isolation by size of epithelial tumor cells [ISET]), seems to be a very attractive procedure providing good specificity and sensitivity in addition to its simplicity, rapidity, and low cost.²⁶ However, although cytopathologic analysis is predictably more specific than antigen-mediated CTC capture based on antibodies

lacking specificity for tumor cells, it still has to be shown that CTCs can be recognized using the cytopathologic criteria of malignancy already used in conventional cytology (ie, in exfoliative and in fine-needle aspiration [FNA] cytopathology). Furthermore, enriching large cells from blood could also lead to the isolation of very rare hematologic (as megakaryocytes or large monocytes) or mesenchymal (as endothelial cells) cells that are undetectable by current hematologic analyses and may be difficult to distinguish from epithelial tumor cells.

For all these reasons, we planned a blinded, multicentric, cytopathologic study of blood samples obtained from patients with miscellaneous benign and malignant pathologies and from healthy subjects, processed using the ISET method. It is interesting that we found that a consensus in CTC identification can be obtained by using the same criteria as those applied to exfoliative and FNA cytology. In fact, CTCs were found neither in healthy subjects nor in the vast majority of patients with benign diseases. Strikingly, CTCs were detected in 10 (5.3%) of 190 patients with benign diseases, including thyroid and parathyroid adenomas, thus confirming that CTC identification faces the same challenges as FNA cytology in certain pathologies. Finally, these data, obtained from a national network of 10 experienced cytopathologists, confirm the interest in the ISET method and stress the need for increasing our knowledge within a potentially very important and new field in cytopathology.

Materials and Methods

Cases

A total number of 808 subjects were included in this study. They corresponded to patients with miscellaneous nonneoplastic diseases (152 cases), miscellaneous benign (38 cases) and malignant neoplasia (569 cases) diseases, and healthy volunteers (49 cases). Blood samples were obtained before surgery in 635 cases. None of the patients had undergone a biopsy or surgical excision during the month before venipuncture. The different pathologies included in this study are listed in **Table 1**. Among the patients with metastasis, 38 had breast carcinoma, 44 had colonic carcinoma, 18 had kidney carcinoma, and 5 had head and neck carcinoma. All subjects provided a signed agreement for this study, and the protocol was approved by the local ethics committee of the University of Nice, Nice, France.

Methods

For the study, 10 mL of peripheral blood was collected in buffered EDTA (before anesthesia of patients), maintained at 4°C, and processed within 1.5 hours. Surgical specimens were obtained from patients for histologic evaluation. The ISET method was carried out as previously described.²⁶ The filtration device with 10 wells makes it possible to load and filter each milliliter (of 10) in parallel. Blood filtration through a polycarbonate filter with a calibrated pore size of 8 μm is

Table 1
Number of Patients With Detected CNHCs, CNHC-MF, CNHC-UMF, CNHC-BF According to Malignant and Nonmalignant Associated Diseases*

Histologic Type	Absence of CNHCs	Presence of CNHCs	CNHC-MF	CNHC-UMF	CNHC-BF	Overall	P†
Malignant tumors	291 (51.1)	278 (48.9)	245	28	5	569 (100.0)	
NSCLC			119	4	0	394	
Miscellaneous carcinoma			11	8	2	25	
Metastatic carcinoma			56	7	0	105	
Malignant pleural mesothelioma			6	3	0	10	<.001‡
Melanoma			20	6	1	30	
Sarcoma			3	0	2	5	
Nonmalignant diseases	169 (88.9)	21 (11.1)	10	5	6	190 (100.0)	
Benign tumors			0	0	0	38	
Thyroid adenoma			7	0	0	25	
Parathyroid adenoma			3	0	0	7	
Lipoma			0	0	0	4	
Chondroma			0	0	0	2	
Nontumoral diseases			0	0	0	152	NS‡
Graves disease			0	1	0	15	
Thyroid hyperplasia			0	2	0	59	
Parathyroid hyperplasia			0	2	2	15	
Amygdalitis			0	0	2	40	
Pneumonitis			0	0	2	23	
No disease	47 (96)	2 (4)	0	0	2	49 (100)	

CNHCs, circulating nonhematologic cells; CNHC-BF, CNHCs with benign features; CNHC-MF, CNHCs with malignant features; CNHC-UMF, CNHCs with uncertain malignant features; NS, not significant; NSCLC, non-small cell lung carcinoma.

* Data are given as number (percentage) or number of cases.

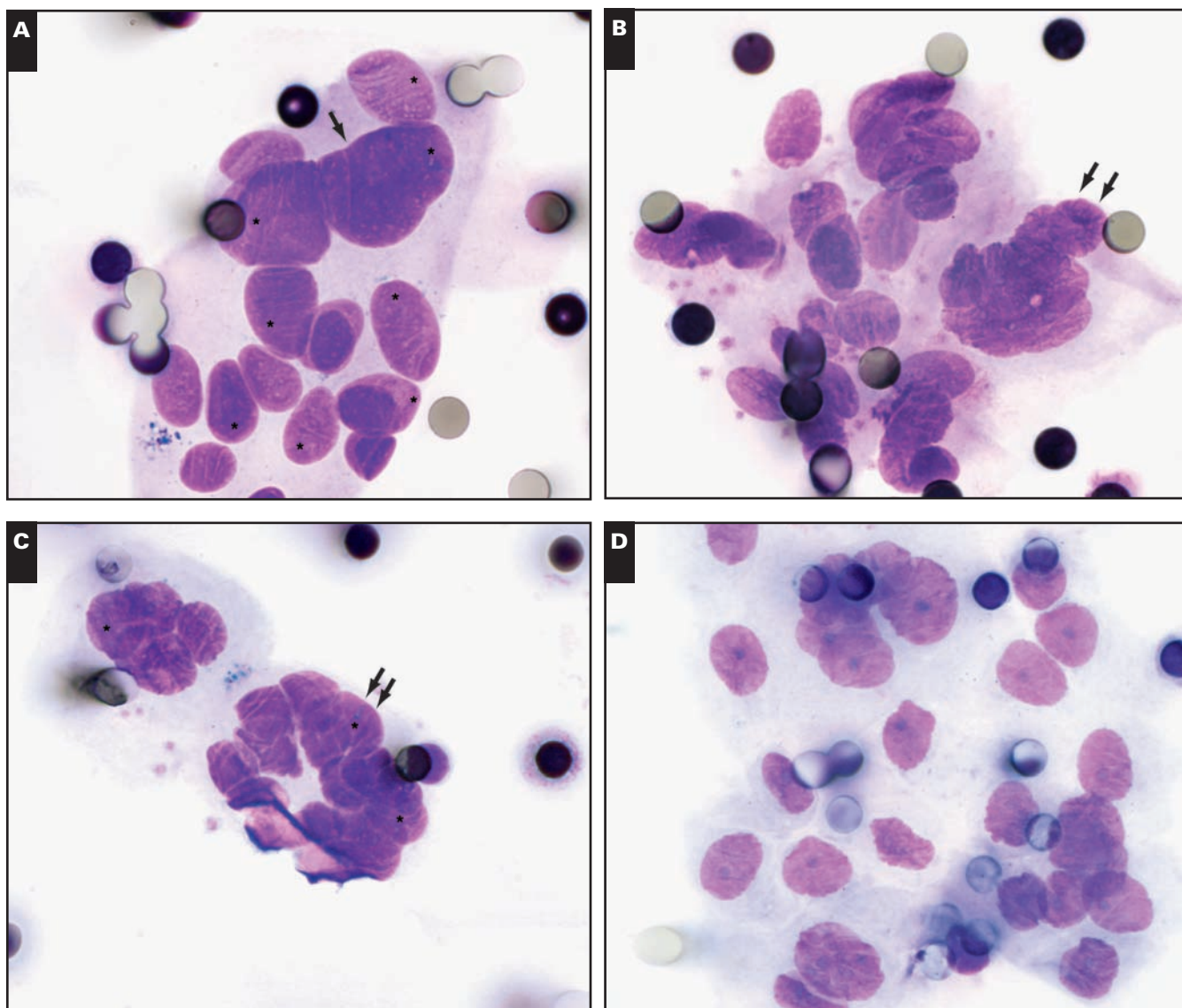
† Significant at the .05 level.

‡ Coding of variables for presence of CNHC: malignant (1) vs nonmalignant (2) diseases or benign tumors (1) vs nontumoral diseases (2).

performed. The membrane is then gently washed with phosphate-buffered saline (PBS), disassembled from the filtration device, and allowed to air dry.²⁶ The membrane was cut into 2 parts containing 6 spots to be stained and 4 spots to be stored for further studies. The spots were stained using a modified May-Grünwald-Giemsa staining method using the following steps: May-Grünwald (undiluted, 5 minutes), May-Grünwald (diluted 50% in PBS, 5 minutes), and Giemsa (diluted 10% in PBS, 40 minutes), followed by rinsing with PBS for 1 minute. Membranes were then air dried and kept in the dark at room temperature. Stained spots were examined by light microscopy using the following procedure: (1) screening at $\times 100$ and $\times 200$ to look for circulating nonhematologic cells (CNHCs)

and (2) observation at $\times 630$ and $\times 1,000$ with oil immersion for detailed cytomorphologic study.

The following criteria were taken into account: presence of cytoplasmic (only CNHCs with visible cytoplasm were considered) irregularity of the nuclear membrane, size of the nucleus, anisonucleosis, high nuclear/cytoplasmic ratio, and presence of tridimensional sheets of cells. CNHCs with malignant features (CNHC-MF = CTCs) were then characterized by the presence of at least 4 of the following criteria: anisonucleosis (ratio >0.5), nuclei larger than a 3-calibrated pore size (8 μm) (ie, $>24 \mu\text{m}$), irregular nuclei, presence of tridimensional sheets, and a high nuclear/cytoplasmic ratio ■Image 1■. CNHCs with uncertain malignant potential



■Image 1■ Cytomorphologic criteria for circulating nonhematologic cells with malignant features (CNHC-MF) obtained by the isolation by size of epithelial tumor cell method. **A**, Esophageal adenocarcinoma. **B**, Head and neck carcinoma. **C**, Malignant mesothelioma. **D**, Lung adenocarcinoma.

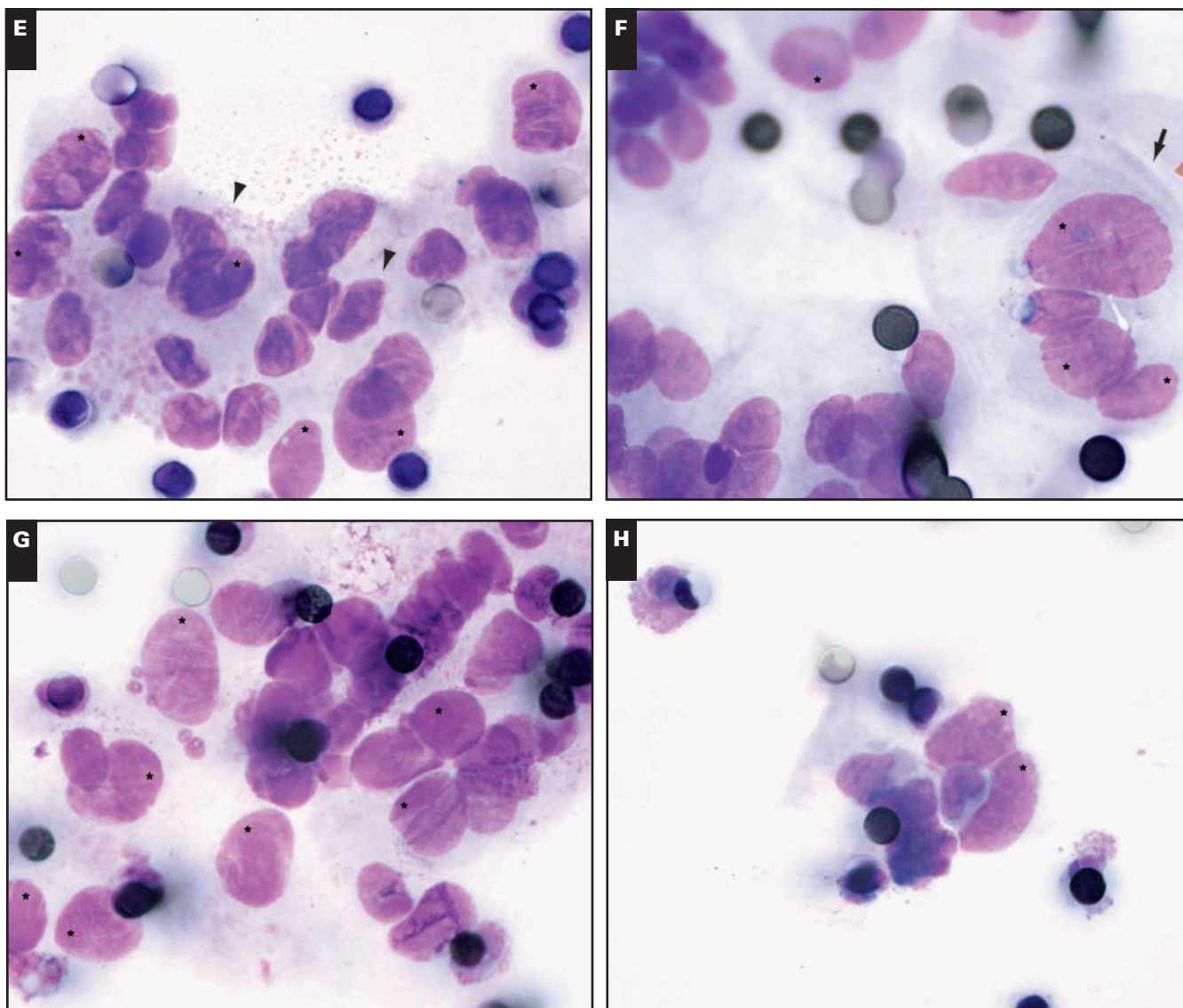
(CNHC-UMF) were defined when fewer than 2 criteria were present **Image 2**. CNHCs with benign features (CNHC-BF) were characterized by the absence of these criteria **Image 3**. A semiquantitative analysis was performed on each filter, and cases were categorized into 3 groups according to the number of CNHCs: group 1, fewer than 10 CNHCs; group 2, between 10 and 100 CNHCs; and group 3, more than 100 CNHCs. In all, 1,025 pictures (average, 5 pictures per filter; range, 1-21) were recorded, and images were digitized and collected by 3 observers (V.J.H., C.B., and P.M.H.). All images were reviewed independently by the members of the panel (V.J.H., C.B., T.M., J.M.V., J.F.F., S.L., E.P., N.M., P.V., and P.M.H.) without knowledge of the patients' clinical status and pathologic diagnosis.

Criteria for Evaluation

The presence of CNHCs was evaluated and compared in patients with nonmalignant and malignant diseases and healthy volunteers using the χ^2 statistical test. A *P* value of .05 or less was considered significant. Interobserver agreement was assessed for the diagnosis of CNHC-MF, CNHC-UMF, and CNHC-BF for CNHCs detected in patients with nonmalignant diseases and with malignant diseases using κ as the measure of agreement.

Results

Interobserver agreement for the 3 cytopathologists working in the same institution (V.J.H., C.B., and P.M.H.;



E and **F**, Thyroid adenoma. **G** and **H**, Parathyroid adenoma. Arrows, anisonucleosis; arrowhead, irregular nuclear borders and large nuclei; double arrows, 3-dimensional sheets; asterisks, cells satisfying the criteria for CNHC-MF (**A-H**, May-Grünwald-Giemsa, $\times 1,000$).

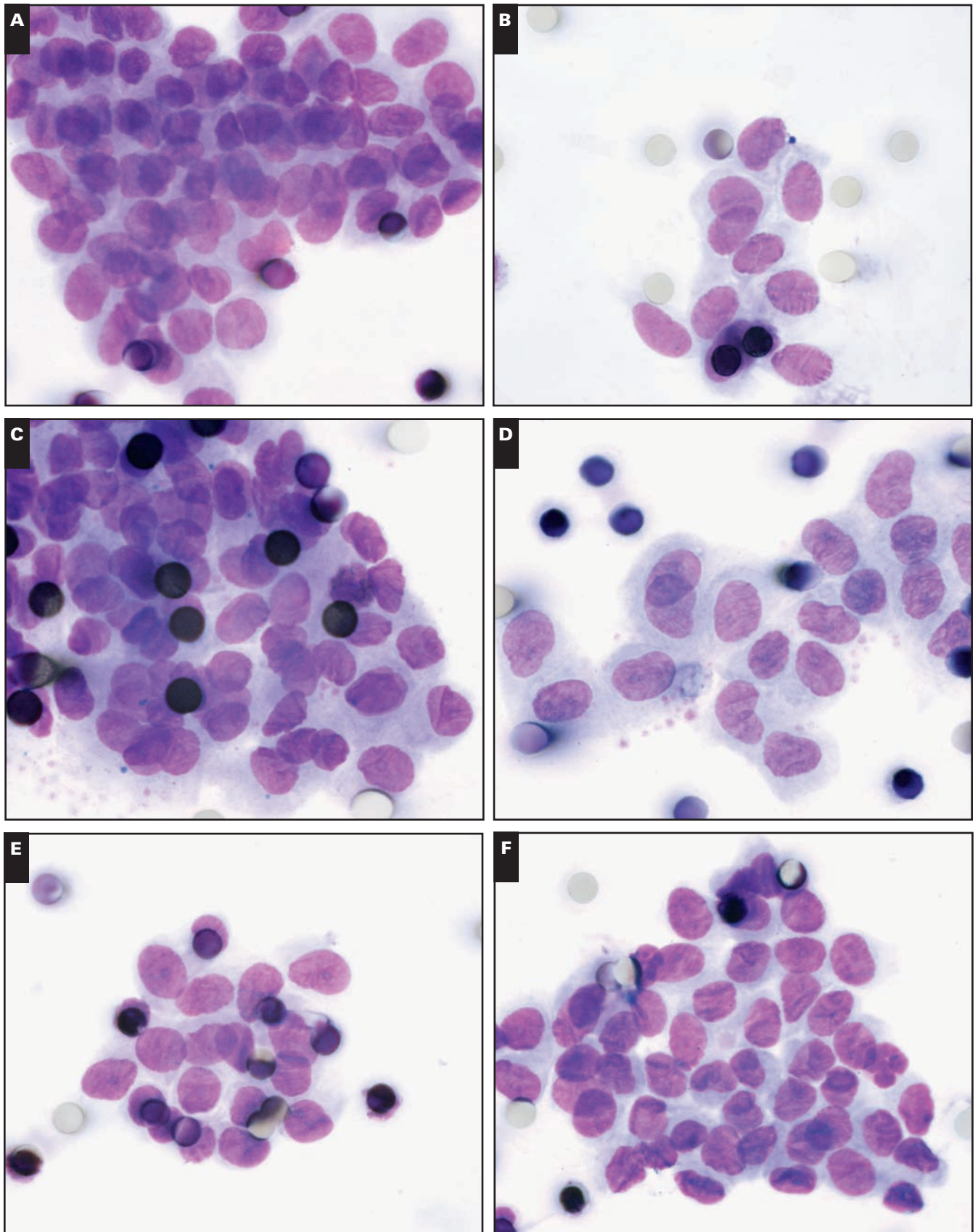


Image 2 | Cytomorphologic criteria for circulating nonhematologic cells with uncertain malignant features obtained by the isolation by size of epithelial tumor cell method. **A**, Lung epidermoid carcinoma. **B**, Malignant mesothelioma. **C**, Metastatic large bowel carcinoma. **D**, Head and neck carcinoma. **E** and **F**, Thyroid adenoma.

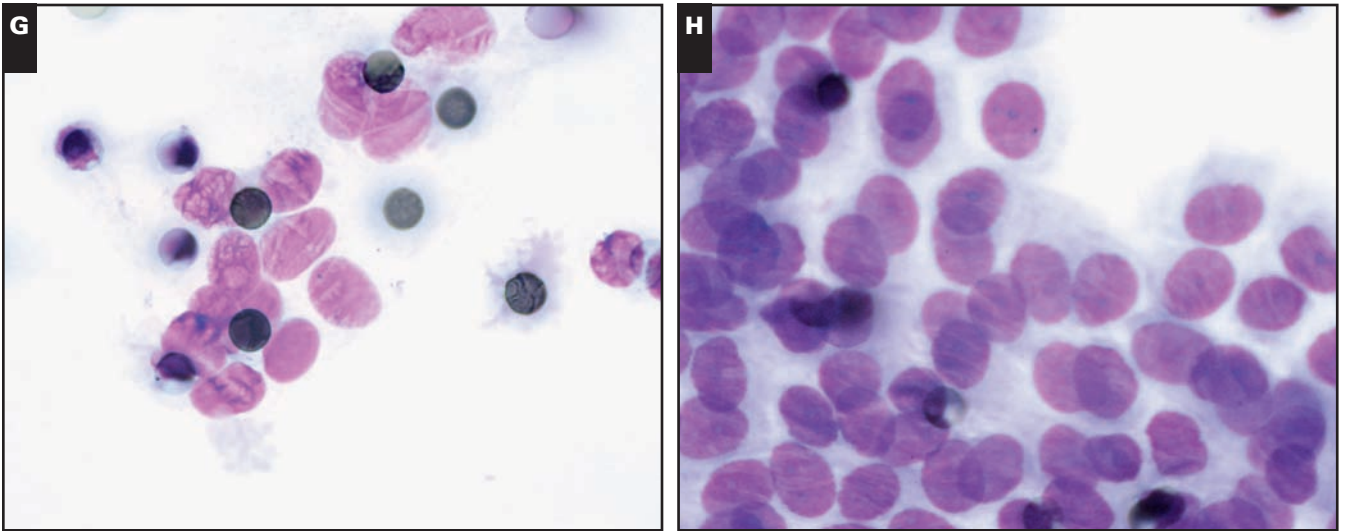


Image 2 (cont) **G** and **H**, Parathyroid adenoma (**A-H**, May-Grünwald-Giemsa, $\times 1,000$).

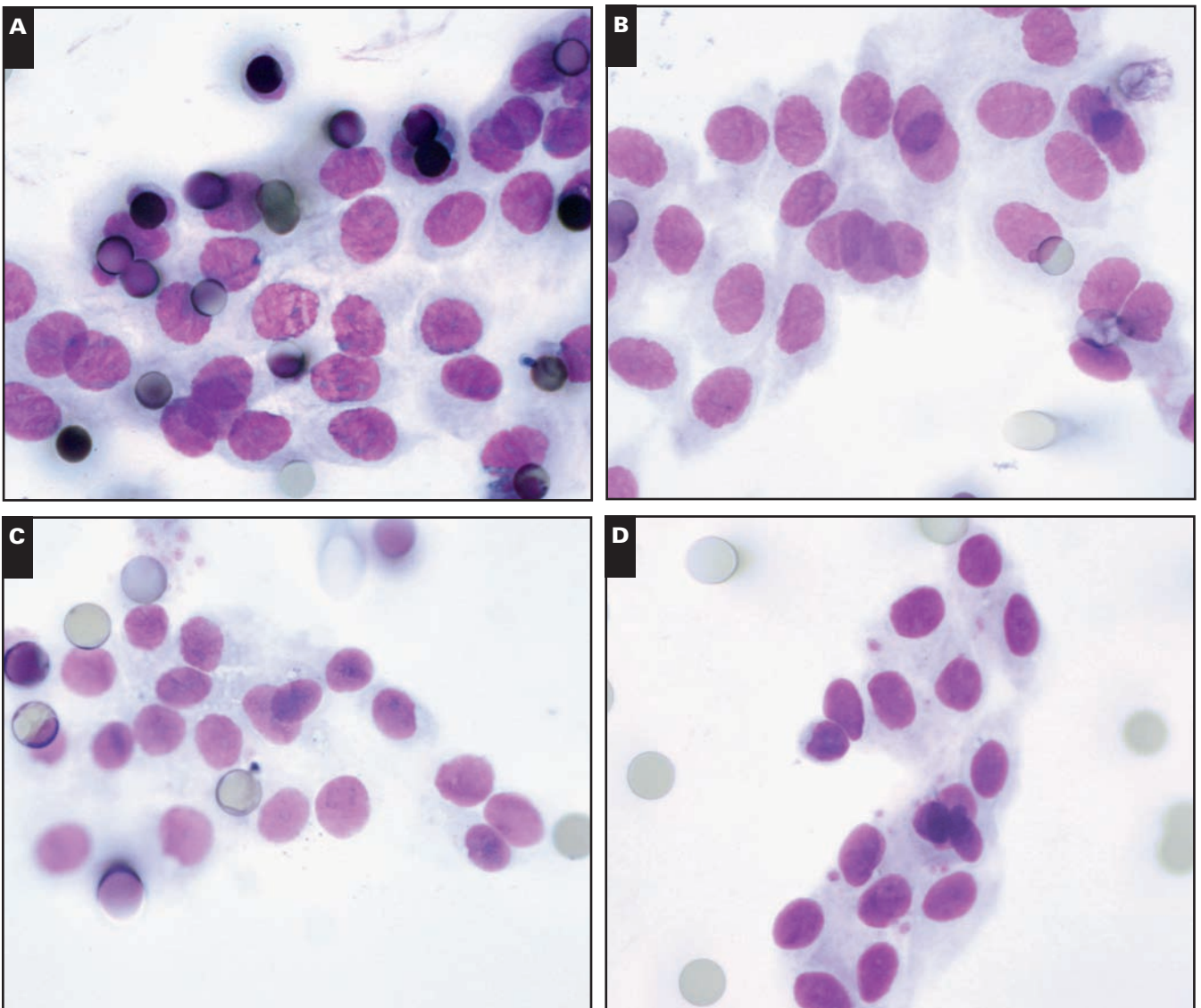


Image 3 Cytomorphologic criteria for circulating nonhematologic cells with benign features obtained by the isolation by size of epithelial tumor cell method. **A**, Lung epidermoid carcinoma. **B**, Sarcoidosis. **C**, Nodular hyperplasia of the thyroid. **D**, Thyroid adenoma.

Pasteur Hospital, Nice, France) was total ($\kappa = 1$) for detecting CNHCs on filters. According to the number of observed images among each category of CNHCs, interobserver variation was low for the diagnosis of CNHC-MF (1.9%) and relatively high for the diagnosis of CNHC-UMF (7.5%) and CNHC-BF (8.9%). Consequently, agreement of cytopathologists for the diagnosis of the different categories of CNHCs was high ($\kappa = 0.93$) for the diagnosis of CNHC-MF, moderate ($\kappa = 0.64$) for the diagnosis of CNHC-UMF, and relatively low ($\kappa = 0.35$) for the diagnosis of CNHC-BF **Table 2**. Among patients with malignant pathologies, 278 (48.9%) of 569 (Table 1) showed the presence of CNHCs that were diagnosed by all cytopathologists as CNHC-MF (Image 1), CNHC-UMF (Image 2), and CNHC-BF (Image 3) in 245 cases, 28 cases, and 5 cases, respectively. Among

the patients with benign pathologies, 21 (11.1%) of 190 had CNHCs (Table 1) that were classified by all cytopathologists as CNHC-MF (Image 1), CNHC-UMF (Image 2), and CNHC-BF (Image 3) in 10 patients (thyroid, 7 cases; parathyroid adenomas, 3 cases), 5 patients, and 6 patients, respectively. CNHCs were detected in 2 (4%) of 49 healthy volunteers, all corresponding to CNHC-BF (Table 1). Cumulatively different categories of CNHCs were observed in most patients with malignant disease. Cytopathologic features of CNHCs were similar in patients with the different pathologies (not shown). Of note, the numbers of CNHCs detected on filters were usually higher in patients with malignant diseases than the numbers observed in patients with nonmalignant diseases ($P < .001$) **Table 3** **Image 4**.

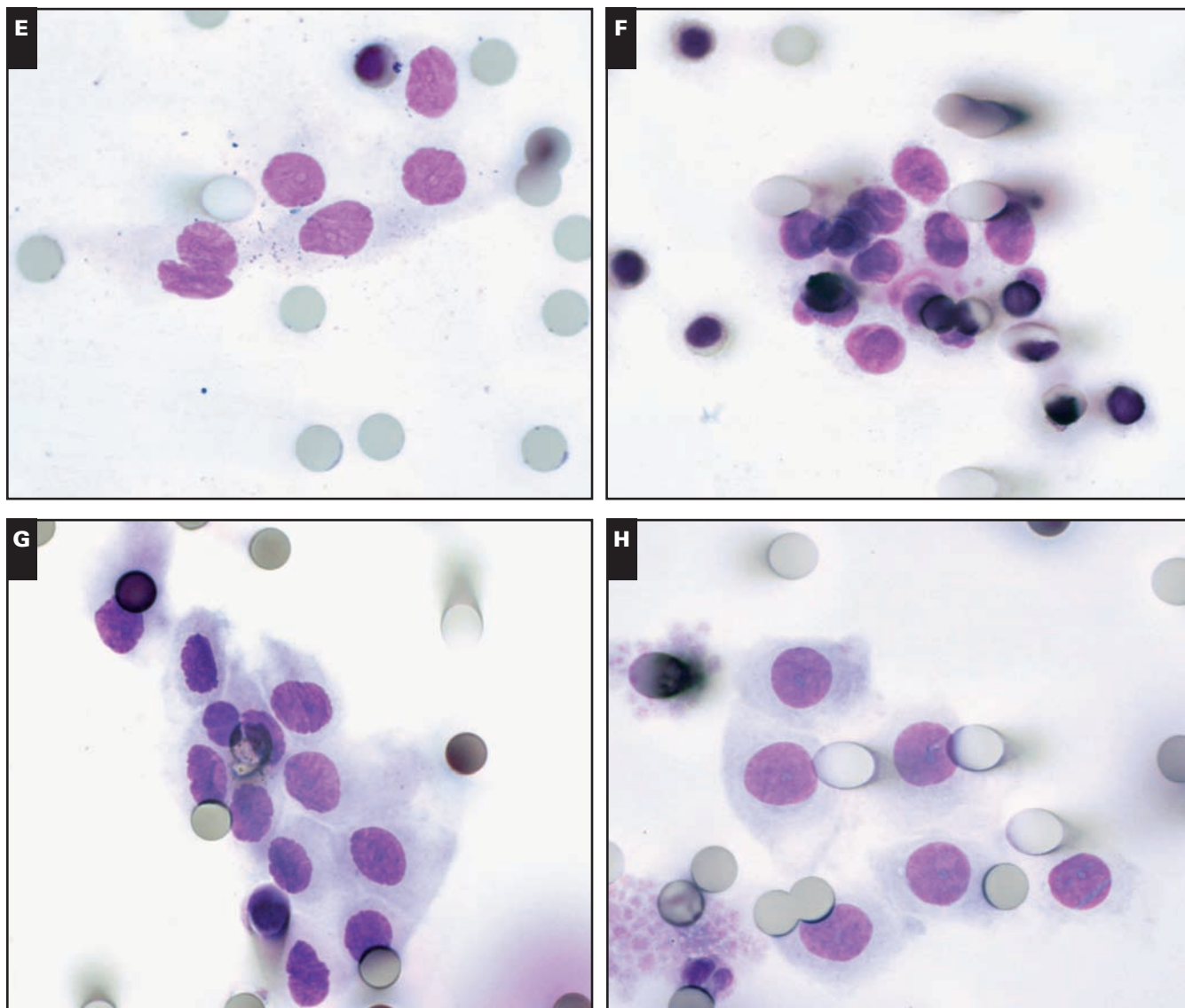


Image 3 (cont) **E**, Parathyroid hyperplasia. **F**, Amygdalitis. **G**, Pneumonitis. **H**, Parathyroid adenoma (**A-H**, May-Grünwald-Giemsa, $\times 1,000$).

Table 2
Agreement Among Cytopathologists on the Diagnosis of the Different Categories of CNHCs*

	Cytopathologist Agreement					
	10/10	9/10	8/10	7/10	6/10	5/10
Malignant tumors						
CNHCs	100% (555)	—	—	—	—	—
CNHC-MF	94% (182)	92% (134)	83% (68)	25% (31)	11% (12)	3% (3)
CNHC-UMF	52% (97)	34% (69)	22% (31)	11% (13)	5% (9)	2% (5)
CNHC-BF	29% (19)	11% (15)	9% (12)	7% (6)	4% (4)	2% (3)
Nonmalignant diseases						
CNHCs	100% (197)	0%	0%	0%	0%	0%
CNHC-MF	100% (7)	92% (2)	75% (1)	61% (1)	9% (1)	3% (1)
CNHC-UMF	61% (42)	34% (10)	26% (7)	12% (5)	8% (4)	5% (3)
CNHC-BF	61% (55)	42% (19)	14% (15)	5% (10)	2% (9)	1% (5)

CNHCs, circulating nonhematologic cells; CNHC-BF, CNHCs with benign features; CNHC-MF, CNHCs with malignant features; CNHC-UMF, CNHCs with uncertain malignant features.

* The percentages represent the positive responses made by the panel of cytopathologists for the diagnosis of the different categories of CNHC. The numbers in parentheses are the number of examined images.

Discussion

CTC detection is a highly relevant issue in clinical oncology. It is supposed to help clinicians in identifying patients with cancer with a high risk of recurrence or metastases of their solid tumors and patients with invasive tumors at a very early stage. Therefore, solving the technological challenges of sensitive and specific identification of CTCs by a noninvasive approach may represent a crucial step in modern clinical care.

An average number of 10 million leukocytes and 5 billion erythrocytes are present in 1 mL of blood. Detection of 1 single CTC per mL is expected to be clinically important, meaning that 5,000 CTCs are present in the blood circulation. Hematologic Coulter (Beckman Coulter, Fullerton, CA) automated instruments analyze blood volumes of 50 μ L or less. Thus, “rare” cells, defined in this setting, must account for at least 20 of them per milliliter. The CTC field of investigation requires a very high sensitivity combined with an “absolute” specificity of malignant cell diagnosis. Taking all these requirements into account, indirect detection of CTCs based on reverse transcriptase–polymerase chain reaction amplification of RNA markers and cell capture based on antigens lacking “absolute” specificity for malignant tumor cell identification are not expected to reach all of the mentioned clinical goals.¹⁰

Among the different reported methods for CTC detection, the ISET method allows enrichment of CNHCs in a powerful manner.²⁶ Because these isolated cells are then available for cytopathologic study, the method could also provide the specificity expected to bring advantage to patients.²⁶ However, it has never been assessed whether application of classic cytopathologic criteria, currently used in “conventional” cytopathology, to the CTC field allows pathologists to reach a consensus in patients with solid cancers and to pinpoint a cell type absent in healthy subjects.

Table 3
Number of Cases With Detected CNHCs According to Pathology

Pathology	<10 CNHCs	10-100 CNHCs	>100 CNHCs	Total
Nontumoral	5	6	0	11
Benign	5	4	1	10
Malignant	58	99	121	278
Total	68	109	122	299

CNHCs, circulating nonhematologic cells.

The present work was designed to investigate whether a national panel of 10 experienced cytopathologists, working independently and without knowledge of clinicopathologic data, could consistently and reliably identify CTCs in patients with malignant solid tumors vs in patients with benign pathologies and vs in healthy subjects. Our results clearly show the following: (1) Different morphologic subtypes of CNHCs circulate in the blood of patients, but only one, defined as CNHC-MF, represents “true” CTCs because they were never found in healthy subjects. (2) CNHC-MF were found in 10 (5.3%) of the patients with benign pathologies consisting of thyroid (7 cases) and parathyroid (3 cases) adenomas, which are known to be diagnostically challenging in FNA cytopathology. This clearly means that (1) experienced cytopathologists can reliably identify CTCs by applying classic cytopathologic criteria; (2) caution is highly recommended in the case of benign pathologies such as thyroid and parathyroid adenomas, which may give false-positive results; and (3) because CNHCs without malignant features that are easily recognized by cytopathologic analysis are indeed present in healthy subjects and in patients with nonmalignant diseases, they represent a challenge for other methods aimed at detecting CTCs using nonspecific markers for malignant cells.

These data are in favor of the use of cytopathologic methods to reliably identify CTCs and strongly encourage further

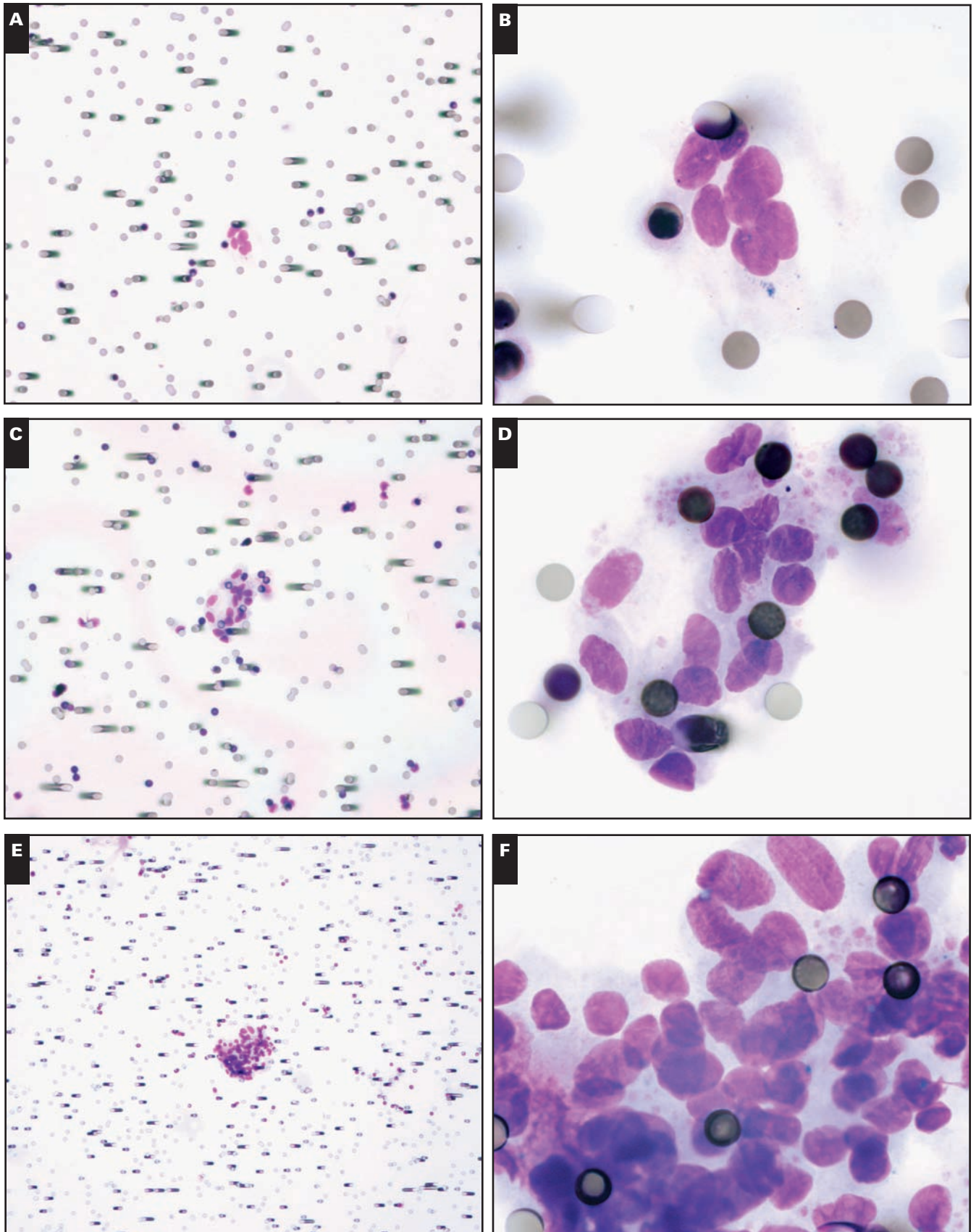


Image 4 Different numbers of circulating nonhematologic cells (CNHCs) observed in nonmalignant and malignant diseases. **A** and **B**, Isolated CNHCs or fewer than 10 CNHCs. Thyroid hyperplasia. **C** and **D**, Between 10 and 100 CNHCs. Thyroid adenoma. **E** and **F**, More than 100 CNHCs. Malignant mesothelioma (**A**, **C**, and **E**, May-Grünwald-Giemsa, $\times 200$; **B**, **D**, and **F**, May-Grünwald-Giemsa, $\times 1,000$).

studies in this field. It is interesting that in a series of 199 subjects with nonmalignant diseases, the only patient with more than 2 CTCs detected by the CellSearch system (Veridex, San Diego, CA) had a hyperthyroid disorder.²⁷ Thus, further comparison of the respective sensitivity and specificity of the ISET and CellSearch methods for CTC detection will be of great interest. Furthermore, new molecular markers should certainly be developed in the future and might help better identify and characterize CTCs. Immunocytochemical studies performed on cells obtained by the ISET method could be used to phenotype CNHCs with challenging cytopathologic features and distinguish epithelial from endothelial cells and megakaryocytes. Immunolabeling can also be of value to identify invasive CTCs and cells with an ongoing epithelial to mesenchymal transition. Studies performed on samples from patients with solid cancers at different stages and correlating immunocytochemical results with clinicopathologic data and patient follow-up need also to be planned. Most of the published studies have demonstrated that the presence of CTCs correlates with tumors of high stage and/or metastases.^{6,25,28,29} However, the different results were obtained using different methods for CTC detection.^{6,25,28,29} Further studies are needed to determine in our cohort of carcinoma patients if the presence and number of CTCs detected by ISET correlate with tumors of higher stages.

Our data show that cytomorphologic examination, the reference diagnostic method in clinical oncology, is also relevant in the field of CTC detection. However, we still have to investigate, in larger clinical studies, the potential pitfalls of this approach and its potential impact on cancer staging and follow-up. This seems to be worthwhile because combining cytomorphologic diagnosis with immunologic and molecular characterization should improve CTC detection and bring new hope to patients with solid cancers.

From ¹Inserm ERI-21, Faculty of Medicine and University of Nice Sophia Antipolis, Nice, France; ²Human Biobank, Pasteur Hospital, Nice; ³Laboratory of Clinical and Experimental Pathology, Pasteur Hospital, Nice; ⁴EA 4319, Faculty of Medicine, Nice; ⁵Department of Pathology, AP-HP, Hôtel-Dieu, University of Paris Descartes, Paris, France; ⁶Department of Pathology, Nancy, France; ⁷Department of Pathology, Saint-Antoine Hospital, Paris; ⁸Department of Pathology, la Tronche Hospital, Grenoble, France; ⁹Department of Pathology, Sud Hospital, Lyon, France, and Department of Pathology, Bron, France; ¹⁰Department of Pathology, Centre hospitalier affilié universitaire de Québec, Québec, Canada; ¹¹Department of Pneumology, Pasteur Hospital, Nice; ¹²Department of Dermatology, Archet II Hospital, Nice; ¹³Department of Thoracic Surgery, Pasteur Hospital, Nice; ¹⁴Department of Otorhinolaryngology, Pasteur Hospital, Nice; and ¹⁵Department of Biopathology and Laboratory of Translational Research,, Gustave Roussy Institute, Villejuif, France.

Supported by grants from PHRC National 2008 (CHU de Nice, France) and the Conseil Général 06, Nice, France.

Address reprint requests to Dr Paul Hofman: Inserm ERI-21/ EA 4319, Faculté de Médecine, avenue de Valombrose, 06017 Nice cedex, France.

References

- Kaiser J. Medicine: cancer's circulation problem. *Science*. 2010;327:1072-1074.
- Cristofanilli M, Hayes DF, Budd GT, et al. Circulating tumor cells: a novel prognostic factor for newly diagnosed metastatic breast cancer. *J Clin Oncol*. 2004;23:1420-1430.
- Mejean A, Vona G, Nalpas B, et al. Detection of circulating prostate-derived cells in patients with prostate adenocarcinoma through an optimized RT-PCR procedure is an independent risk factor for tumor recurrence. *J Urol*. 2000;163:2022-2029.
- Matsumura M, Niwa Y, Kato N, et al. Detection of alpha-fetoprotein mRNA, an indicator of hematogenous spreading hepatocellular carcinoma, in the circulation: a possible predictor of metastatic hepatocellular carcinoma. *Hepatology*. 1994;20:1418-1425.
- Molnar B, Sipos F, Galamb O, et al. Molecular detection of circulating cancer cells: role in diagnosis, prognosis and follow-up of colon cancer patients. *Dig Dis*. 2003;21:320-325.
- Müller V, Stahmann N, Riethdorf S, et al. Circulating tumor cells in breast cancer: correlation to bone marrow micrometastases, heterogeneous response to systemic therapy and low proliferative activity. *Clin Cancer Res*. 2005;11:3678-3685.
- Pantel K, Woelfle U. Detection and molecular characterisation of disseminated tumour cells: implications for anti-cancer therapy. *Biochim Biophys Acta*. 2005;1756:53-64.
- Sheu CC, Yu YP, Tsai R. Development of membrane array-based multimarker assay for detection of circulating cancer cells in patients with non-small cell lung cancer. *Int J Cancer*. 2006;119:1419-1426.
- Yamashita J, Matsuo A, Kurusu Y, et al. Preoperative evidence of circulating tumor cells by means of reverse transcriptase-PCR for carcinoembryonic antigen messenger RNA is an independent predictor of survival in non-small cell lung cancer: a prospective study. *J Thorac Cardiovasc Surg*. 2002;124:299-305.
- Paterlini-Bréchet P, Benali NL. Circulating tumor cells (CTC) detection: clinical impact and future directions. *Cancer Lett*. 2007;253:180-204.
- Goeminne JC, Guillaume T, Symann M. Pitfalls in the detection of disseminated non-hematological tumor cells. *Ann Oncol*. 2000;11:785-792.
- Ko Y, Grunewald E, Totzke G, et al. High percentage of false-positive results of cytokeratin 19 RT-PCR in blood: a model for the analysis of illegitimate gene expression. *Oncology*. 2000;59:81-88.
- Louha M, Poussin K, Ganne N, et al. Spontaneous and iatrogenic spreading of liver derived cells into peripheral blood of patients with primary liver cancer. *Hepatology*. 1997;26:998-1005.
- Louha M, Nicolet J, Zylberberg H, et al. Liver resection and needle liver biopsy cause hematogenous dissemination of liver cells. *Hepatology*. 1999;29:879-882.
- Weinberg RA. Twisted epithelial-mesenchymal transition blocks senescence. *Nat Cell Biol*. 2008;10:1021-1023.

16. Anker P, Mulcahy H, Stroun M. Circulating nucleic acids in plasma and serum as a noninvasive investigation for cancer: time for large-scale clinical studies? *Int J Cancer*. 2003;103:149-152.
17. Brandt B, Roetger A, Heidl S, et al. Isolation of blood-borne epithelium-derived c-erbB-2 oncoprotein-positive clustered cells from peripheral blood of breast cancer patients. *Int J Cancer*. 1998;76:824-828.
18. Chen T-F, Jiang G-L, Fu X-L, et al. CK19 mRNA expression measured by reverse-transcription polymerase chain reaction (RT-PCR) in the peripheral blood of patients with non-small cell lung cancer treated by chemo-radiation: an independent prognostic factor. *Lung Cancer*. 2007;56:105-114.
19. Clarke LE, Leitzel K, Smith J. Epidermal growth factor receptor mRNA in peripheral blood of patients with pancreatic, lung, and colon carcinomas detected by RT-PCR. *Int J Oncol*. 2003;22:425-430.
20. Gervasoni A, Monasterio Muñoz RM, Wengler GS, et al. Molecular signature detection of circulating tumor cells using a panel of selected genes. *Cancer Lett*. 2008;434:267-279.
21. Guo J, Xiao B, Jin Z, et al. Detection of cytokeratin 20 mRNA in the peripheral blood of patients with colorectal cancer by immunomagnetic bead enrichment and real-time reverse transcriptase-polymerase chain reaction. *J Gastroenterol Hepatol*. 2005;20:1279-1284.
22. Hayes DC, Secrist H, Bangur CS, et al. Multigene real-time PCR detection of circulating tumor cells in peripheral blood of lung cancer patients. *Anticancer Res*. 2006;26:1567-1575.
23. Leon SA, Shapiro B, Sklaroff DM, et al. Free DNA in the serum of cancer patients and the effect of therapy. *Cancer Res*. 1977;37:646-650.
24. Sabile A, Louha M, Bonte E, et al. Efficiency of Ber-EP4 antibody in isolating circulating epithelial tumor cells before RT-PCR detection. *Am J Clin Pathol*. 1999;112:171-178.
25. Sher YP, Shih JY, Yang PC, et al. Prognosis of non-small cell lung cancer patients by detecting circulating cancer cells in the peripheral blood with multiple marker genes. *Clin Cancer Res*. 2005;11:173-179.
26. Vona G, Sabile A, Louha M, et al. Isolation by size of epithelial tumor cells: a new method for the immunomorphological and molecular characterization of circulating tumor cells. *Am J Pathol*. 2000;156:57-63.
27. Allard WJ, Matera J, Miller MC, et al. Tumor cells circulate in the peripheral blood of all major carcinomas but not in healthy subjects or patients with nonmalignant diseases. *Clin Cancer Res*. 2004;10:6897-6904.
28. Tanaka F, Yoneda K, Kondo N, et al. Circulating tumor cell as a diagnostic marker in primary lung cancer. *Clin Cancer Res*. 2009;15:6980-6986.
29. Wang L, Wang Y, Liu Y, et al. Flow cytometric analysis of CK19 expression in the peripheral blood of breast carcinoma patients: relevance for circulating tumor cell detection. *J Exp Clin Cancer Res*. 2009;28:57. doi:10.1186/1756-9966-28-57.

Morphological analysis of circulating tumour cells in patients undergoing surgery for non-small cell lung carcinoma using the isolation by size of epithelial tumour cell (ISET) method

V. Hofman^{*†‡§1}, E. Long^{*†‡§1}, M. Ilie^{*†‡§}, C. Bonnetaud[†], J. M. Vignaud[¶], J. F. Fléjou^{**}, S. Lantuejoul^{††}, E. Piaton^{‡‡}, N. Mourad^{§§}, C. Butori^{*†‡§}, E. Selva[†], C. H. Marquette^{¶¶}, M. Poudenx^{¶¶}, S. Sibon^{***}, S. Kelhef^{***}, N. Vénissac^{***}, J. P. Jais^{†††}, J. Mouroux^{***}, T. J. Molina^{‡‡‡}, P. Vielh^{§§§1} and P. Hofman^{*†‡§1}

^{*}EA 4319, Faculty of Medicine, University of Nice Sophia Antipolis, Nice, France, [†]Human Biobank, Pasteur Hospital, Nice, France, [‡]Laboratory of Clinical and Experimental Pathology, Nice, France, [§]Inserm ERI-21, Nice, France, [¶]Department of Pathology, Nice, France, ^{**}Department of Pathology, Saint-Antoine Hospital, Paris, France, ^{††}Department of Pathology and INSERM U 823, A Bonniot Institut, Grenoble, France, ^{‡‡}Department of Pathology, Sud Hospital, Lyon, France, ^{§§}Department of Pathology, Saint-Louis Hospital, Paris, France, ^{¶¶}Department of Pneumology, Pasteur Hospital, Nice, France, ^{***}Department of Thoracic Surgery, Pasteur Hospital, Nice, France, ^{†††}Department of Biostatistics, Faculty of Medicine, Necker Enfants Malades Hospital, Paris, France, ^{‡‡‡}Department of Pathology, University of Paris Descartes, AP-HP, Hôtel-Dieu Hospital, Paris, France and ^{§§§}Department of Biology and Pathology and Histocytopathology Unit of the Translational Research Laboratory, Gustave Roussy Institute, Villejuif, France

Accepted for publication 10 November 2010

V. Hofman, E. Long, M. Ilie, C. Bonnetaud, J. M. Vignaud, J. F. Fléjou, S. Lantuejoul, E. Piaton, N. Mourad, C. Butori, E. Selva, C. H. Marquette, M. Poudenx, S. Sibon, S. Kelhef, N. Vénissac, J. P. Jais, J. Mouroux, T. J. Molina, P. Vielh and P. Hofman

Morphological analysis of circulating tumour cells in patients undergoing surgery for non-small cell lung carcinoma using the isolation by size of epithelial tumour cell (ISET) method

Background and objective: Recurrence rates after surgery for non-small cell lung cancer (NSCLC) range from 25 to 50% and 5-year survival is only 60–70%. Because no biomarkers are predictive of recurrence or the onset of metastasis, pathological TNM (pTNM) staging is currently the best prognostic factor. Consequently, the preoperative detection of circulating tumour cells (CTCs) might be useful in tailoring therapy. The aim of this study was to characterize morphologically any circulating non-haematological cells (CNHCs) in patients undergoing surgery for NSCLC using the isolation by size of epithelial tumour cell (ISET) method.

Methods: Of 299 blood samples tested, 250 were from patients with resectable NSCLC and 59 from healthy controls. The presence of CNHCs was assessed blindly and independently by 10 cytopathologists on May-Grünwald–Giemsa stained filters and the cells classified into three groups: (i) malignant cells, (ii) uncertain malignant cells, and (iii) benign cells. We assessed interobserver agreement using Kappa (κ) analysis as the measure of agreement.

Results: A total of 123 out of 250 (49%) patients showed CNHCs corresponding to malignant, uncertain malignant and benign cells, in 102/250 (41%), 15/250 (6%) and 6/250 (2%) cases, respectively. No CNHCs were detected in the blood of healthy subjects. Interobserver diagnostic variability was absent for CNHCs, low for malignant cells and limited for uncertain malignant and benign cells.

Correspondence:

P. Hofman, MD, PhD, EA 4319, Faculté de Médecine, Avenue de Valombrose, 06017 Nice Cedex, France
Tel: +33-4-92-03-88-55; Fax: +33-4-92-88-50;
E-mail: hofman.p@chu-nice.fr

¹These authors participated equally to this work.

Conclusion: Identification of CTCs in resectable NSCLC patients, using ISET technology and according to cytopathological criteria of malignancy, appears to be a new and promising field of cytopathology with potential relevance to lung oncology.

Keywords: circulating tumour cells, isolation by size of epithelial tumour cells, non-small cell lung carcinoma, diagnosis, cytopathology, interobserver agreement.

Introduction

Detection of circulating tumour cells (CTCs) in the bloodstream of cancer patients can be prognostic and may have a large impact on the development of new strategies for cancer treatment.^{1,2} CTCs can be detected during follow-up after tumour resection and in the metastatic phase.³ Moreover, these cells can be isolated in patients undergoing surgery for completely resectable tumours.⁴ CTCs can be detected using indirect or direct methodological approaches.^{2,5} Among the indirect techniques, the Cell Search method is probably the one most frequently employed, and has been authorized by the USA Food Drug Administration for the follow-up of patients with breast, colonic and prostate metastases.² Currently, direct methods for detecting CTCs, although less developed, have the advantage of allowing cytomorphological analysis, in a similar way to that performed in exfoliative cytology and in fine needle aspiration cytology.^{6,7} However, very few studies have been carried out to describe and define the cytomorphological criteria of CTCs and to examine whether the classical cytological criteria of malignancy can be applied to CTCs.^{8–11} Among the direct methods, the fibre-optical array scanning (FAST) technology has been used recently to identify CTCs using cytomorphology, in a small number of lung, colonic and prostatic cancer patients.^{9,12,13} Another direct method, called isolated by size of epithelial tumour cells (ISET) technology, first described in the field of oncology by Vona *et al.*^{7,10,11} has been used in patients with liver or breast carcinomas. This latter technique is sensitive, simple, has a low cost and allows cytomorphological analysis and characterization of CTCs.

Circulating non-haematological cells (CNHCs) can be detected in the blood of patients with non-malignant diseases, and more exceptionally in healthy individuals.² The origin of these epithelial cells is uncertain and their morphological characterization is unknown. Therefore in practice, even in cancer

patients, the detection of CNHCs could not always be considered as malignant cells, particularly if these CNHCs do not show cytological criteria of malignancy. In this regard, the cytomorphological analysis of CNHCs should be of great value in characterizing CTCs.

Lung cancer is the most prevalent neoplasm and the major cause of tumour-related mortality worldwide.^{14–16} Despite recent advances in the management of resected lung cancers and more effective treatment of metastatic tumours, the cure rate of patients with lung cancer remains low.^{14–16} In this regard, sensitive and specific detection of CTCs in the blood might be considered a potentially relevant prognostic biomarker for patients with NSCLC.¹⁷ The detection of CTCs in patients with lung carcinoma has mainly been performed with indirect methods.^{18–28} One study reported the cytomorphological details of CTCs isolated in one patient with lung adenocarcinoma using an immunofluorescent staining protocol.⁹ Moreover, we recently demonstrated an interest in prognostic biomarkers of CTCs detected by the ISET method in NSCLC patients.²⁹ However, stringent cytomorphological criteria are now needed in order to better identify the different population of CNHCs, in particular those corresponding to malignant cells. No study has been performed prior to our study for morphological characterization of CTCs by a direct method in patients undergoing surgery for resectable NSCLC. This may be of interest, since in a subpopulation of patients with complete surgical tumor resection, loco-regional and distant metastases can occur rapidly, and the preoperative detection of CTCs could allow selection of these patients with a higher risk.^{30–32}

This study was conducted in order to evaluate the usefulness and efficacy of the ISET method for preoperative detection and characterization of CTCs in NSCLC patients. For this purpose, CTCs were examined in a group of 250 patients with resectable NSCLC by a panel of 10 cytopathologists. Cytomorphological criteria had been established by this panel for classifying CNHCs into the three following categories: (i)

CNHCs with malignant features, (ii) CNHC with uncertain malignant features, and (iii) CNHC with benign features. In this paper, and for the purpose of simplicity, these categories of CNHCs were further called circulating malignant, uncertain malignant and benign cells, respectively. Interobserver agreement between these 10 cytopathologists was then studied for the three categories of CNHCs.

Methods

Patients and samples

Two hundred and fifty patients with NSCLC undergoing surgery from December 2006 to March 2010 gave their informed consent to participate in this study. Biopsies had not been performed for at least 15 days before surgery. The clinicopathological parameters of

Table 1. Epidemiological and clinico-pathological data of non-small cell lung carcinoma patients

Variables	Overall*
Patient cohort	250
Age (years)	
Mean	65
Range	33–82
Gender	
Male	172 (69)
Female	78 (31)
Smoking status	
Never smoked	30 (12)
Former or current smokers	220 (88)
Mean (range) pack years	46 (1–85)
Tumour size (cm)	
Mean	4
Range	0.4–18
Histological cell type	
Adenocarcinoma	150 (60)
Squamous cell carcinoma	67 (27)
Neuroendocrine carcinoma	7 (3)
Large cell carcinoma	9 (3)
Adenosquamous carcinoma	2 (1)
Sarcomatoid carcinoma	10 (4)
NSCLC (NOS)	5 (2)
pTNM stage	
I	111 (44)
II	70 (28)
III	50 (20)
IV	19 (8)

*Values expressed as *n* (%).

pTNM, pathological tumour node metastasis; NSCLC, non-small cell lung carcinoma; NOS, not otherwise specified.

these patients are summarized in Table 1. Among 150 adenocarcinomas, 95 expressed the TTF1 antigen, as determined by immunohistochemical (anti-TTF1 antibody, diluted 1 : 100, Dako; Glostrup, Denmark) staining. Blood samples from 59 healthy volunteers were used as negative controls. There were 39 men (median age, 39 years; range, 25–65 years) and 20 women (median age, 45 years; range, 22–53 years), who were smokers (average, 14 pack years; range, 10–47 pack years), without evidence of neoplastic disease.

Methods

Ten millilitres of peripheral blood were collected in buffered EDTA before anaesthesia, maintained at 4 °C, and processed within 1 hour. Surgical lung specimens were taken for pTNM staging and histological evaluation, according to international classifications.^{33,34} ISET was carried out as described previously.⁷ After blood filtration, the membrane was gently washed with PBS, disassembled from the filtration module and allowed to air-dry. The spots were stained using a modified May-Grünwald–Giemsa (MGG) staining method with the following steps: May-Grünwald (undiluted, 5 minute), May-Grünwald (diluted 50% in PBS, 5 minute) and Giemsa (diluted 10% in PBS, 40 minute), followed by rinsing with PBS for 1 minute. Stained spots were examined by light microscopy using different steps: (i) observation at 100× and 200× original magnification to look for non-haematological cells and to count sheets of these cells, and (ii) observation at 630× and 1000× original magnification with oil immersion for detailed cytomorphological analysis. Different criteria were taken into account to characterize the detected non-haematological cells: nucleo-cytoplasmic ratio, anisonucleosis, irregularity of the nuclear membrane and size of the nucleus, nuclear hyperchromasia, and presence of three-dimensional sheets. Cells without visible cytoplasm were not included in this study. When features corresponding to early or late apoptotic cells (nuclear shrinkage and fragmented nuclei) were noted, the corresponding cells were not counted. Circulating malignant cells were defined by the presence of at least four of the following criteria: anisonucleosis (ratio > 0.5), nuclei larger than three calibrated pore sizes of the membrane (8 µm) (i.e. >24 µm), irregular nuclei, high nucleo-cytoplasmic ratio, and presence of three-dimensional sheets (Figure 1). CNHCs were defined as circulating uncertain malignant cells when they had fewer than two criteria, but at least one was

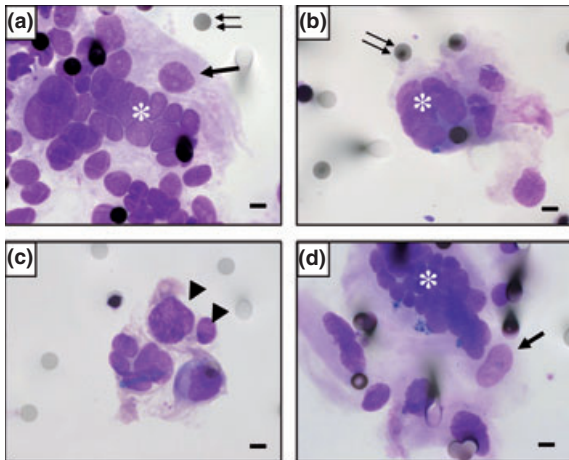


Figure 1. Cytomorphological criteria of circulating malignant cells isolated by the ISET method in patients with NSCLC. (a) Patient with T1N0 adenocarcinoma. (b) Patient with T2N1 adenocarcinoma. (c) Patient with T3N0 large cell carcinoma. (d) Patient with T2N1 large cell carcinoma. (a–d, original magnification $\times 1000$, MGG staining; bars, $8\ \mu\text{m}$; arrows, anisonucleosis; arrow heads, irregularity and large nuclei; asterisks, three dimensional sheets; double arrows, pores of filters.)

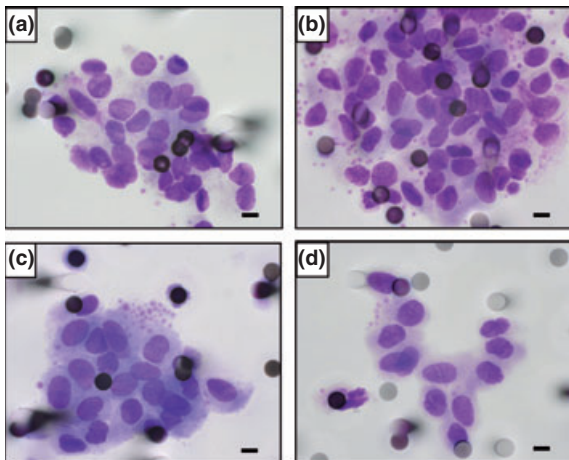


Figure 2. Cytomorphological criteria of circulating uncertain malignant cells isolated by the ISET method in patients with NSCLC. (a) Patient with T2N0 adenocarcinoma. (b) Patient with T3N1 large cell carcinoma. (c) Patient with T2N0 large cell carcinoma. (d) Patient with T1N1 squamous cell carcinoma. (a–d, original magnification $\times 1000$, MGG staining; bars, $8\ \mu\text{m}$; double arrows, pores of filters.)

present (Figure 2). CNHCs defined as circulating benign cells were characterized by the absence of these criteria (Figure 3). A total of 917 pictures (average mean, seven pictures per filter; range, 1–

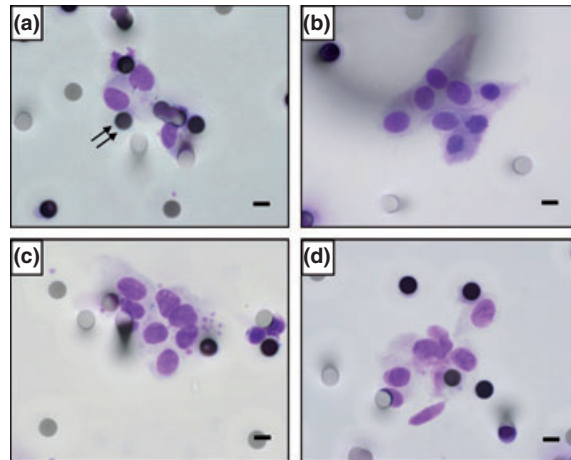


Figure 3. Cytomorphological criteria of circulating benign cells isolated by the ISET method in patients with NSCLC. (a) Patient with T2N0 adenocarcinoma. (b) Patient with T2N1 squamous cell carcinoma. (c) Patient with T2N1 large cell carcinoma. (d) Patient with T2N0 adenocarcinoma. (a–d, original magnification $\times 1000$; bars, $8\ \mu\text{m}$; double arrows, pores of filters.)

32) were recorded and images were digitized at a $\times 1000$ magnification and collected by three of the authors (VH, CB and PH). All images were then reviewed independently by the members of the panel of cytopathologists from eight different institutions (VH, CB, PV, SL, NM, JFF, TJM, JMV, EP and PH) without knowledge of the diagnosis. There were single observers in each institution, apart from at the Pasteur Hospital, Nice, where there were three observers. Images were scored independently by the cytopathologists and classified as circulating malignant, uncertain malignant or benign cells for each patient. Malignancy was confirmed if in at least one image a CTC (i.e. a circulating malignant cell) was identified and if at least five cytopathologists were in agreement. Similarly, a patient was classified in the category of patients with circulating uncertain malignant or benign cells when at least five cytopathologists agreed with this evaluation.

Statistical analysis

All calculations were performed with the statistical software R, a free language and environment for statistical analysis and graphics (version 2.9.0, Oregon State University, Corvallis, OR, USA). We used Kappa statistics, which reflect agreement between two measurements after removing chance agreement, as a

measure of reliability.^{35,36} A value close to one represents almost perfect agreement whereas values close to or below zero represent poor agreement. A useful scale for the interpretation of the Kappa estimate was developed by Landis and Koch: 0.81–1.00, 'almost perfect'; 0.61–0.80, 'substantial'; 0.41–0.60, 'moderate'; 0.21–0.40, 'fair'; 0.00–0.20, 'slight'; and <0.0, 'poor' agreement.³⁶ We computed the weighted Kappa when the classification scheme had more than two categories; greater weight was given to differences in non-adjacent categories than to differences in adjacent categories.³⁵ Conditional agreement is reported using percentages. In addition to these analyses, we examined whether the magnitude of agreement for a given pathological characteristic differed at the level of another pathological characteristic. The following criteria were evaluated and compared using the chi-square statistical test: presence or absence of CNHCs: presence or absence of CNHCs according to the pTNM stages and the histological subtype; presence or absence of circulating malignant, uncertain malignant and benign cells. The Mann–Whitney test was used to compare quantitative and qualitative variables. A *P*-value of 0.05 or less was considered to be significant.

Results

Interobserver agreement between the three cytopathologists working in the same institution (VH, CB and

PH) (Pasteur Hospital, Nice, France) was total ($\kappa = 1$) for detecting CNHCs on filters. CNHCs were present preoperatively in 123/250 (49%) patients undergoing surgery for NSCLC. In all cases (100%), five out the 10 cytopathologists agreed with the final diagnosis for each patient (circulating malignant, uncertain malignant or benign cells) ($\kappa = 1$; Table 2). Circulating malignant cells (CTC) were characterized morphologically in 102/250 (41%) of cases. It is noteworthy that interobserver variation was low for the diagnosis of malignant cells (Table 2). Patients showed circulating uncertain malignant and benign cells in only 15/250 (6%) and 6/250 (2%) cases, respectively. Among all the CNHC, circulating malignant, uncertain malignant and benign cells, represented 83% (102/123), 12% (15/123) and 5% (6/123) of cases, respectively. CNHCs were not found in the blood of the 59 healthy volunteers. Furthermore, the '5/10 cytopathologists' group was defined as a standard in order to calculate the inter-institution level of agreement (Table 3). It is noteworthy that inter-institution variability was similar, with or without stratification for the malignant features. As expected, there was higher variability between several institutions.

The frequency of detection of CNHCs in different histological subtypes was similar ($P > 0.05$) (Table 4). The cytopathological features of CNHCs from patients with lung adenocarcinoma were not distinguishable from those of CNHCs derived from the other histological subtypes (Figure 4). No correlation was

Table 2. Interobserver agreement between cytopathologists for identification of circulating malignant, uncertain malignant and benign cells

Agreement/cytopathologist	10/10	9/10	8/10	7/10	6/10	5/10
Circulating malignant cells						
Cumulative agreement/cases (%)	11 (9)	17 (14)	42 (34)	66 (54)	90 (73)	102 (83)
Circulating uncertain malignant cells						
Cumulative agreement/cases (%)	2 (1)	3 (2)	4 (3)	7 (6)	9 (7)	15 (12)
Circulating benign cells						
Cumulative agreement/cases (%)	1 (1)	2 (1)	3 (2)	4 (3)	5 (4)	6 (5)
Total						
Cumulative agreement/cases (%)	14 (11)	22 (17)	49 (39)	77 (63)	104 (84)	123 (100)

Results from the five out of 10 institutions were used as a standard for calculating Kappa level of agreement between the different institutions with or without stratification for malignant features. The percentages represent the number of positive responses made by the panel of cytopathologists for the evaluation of the different categories of circulating non-haematological cells. Numbers in brackets are the number of cases.

Table 3. Kappa values of agreement between the different institutions, with or without stratification for malignant features of cells

κ values/institution	8/8	7/8	6/8	5/8	4/8	3/8*
With stratification for malignant cells	0.12	0.19	0.45	0.68	0.89	1
Without stratification for malignant cells	0.11	0.18	0.40	0.69	0.84	1

*The 3/8-institution group was defined as a standard ($\kappa = 1$).

The results from the five out of 10 cytopathologists were defined as a standard ($\kappa = 1$) for calculating the inter-institution variability.

Table 4. Number of circulating non-haematological cells detected by isolation by the size of epithelial tumour cell method, according to histological classification of non-small cell lung carcinoma and pTNM staging

Variables	ISET (+)	ISET (-)	Total	P-value
	n (%)	n (%)	n (%)	
Histological subtype				
Adenocarcinoma	79 (53)	71 (47)	150 (100)	0.74
Squamous cell carcinoma	27 (40)	40 (60)	67 (100)	
Large cell carcinoma	5 (56)	4 (44)	9 (100)	
Neuroendocrine carcinoma	4 (57)	3 (43)	7 (100)	
Adenosquamous carcinoma	1 (50)	1 (50)	2 (100)	
Sarcomatoid carcinoma	4 (40)	6 (60)	10 (100)	
NSCLC (NOS)	3 (60)	2 (40)	5 (100)	
pTNM stage				
I	55 (49)	56 (55)	111 (100)	0.50
II	34 (48)	36 (52)	70 (100)	
III	24 (48)	26 (52)	50 (100)	
IV	10 (52)	9 (48)	19 (100)	
Overall	123 (49)	127 (51)	250 (100)	

ISET, isolation by size of epithelial tumour cell; pTNM, pathological tumor node metastasis; NSCLC, non-small cell lung carcinoma; NOS, not otherwise specified.

*P-value significant at the 0.05 level.

observed between the detection of CNHCs and the pTNM stage ($P > 0.05$) (Table 4).

Discussion

The present study shows that CNHCs can be detected using ISET, a cytomorphological technology, in around 50% of patients undergoing surgery for resectable NSCLC. The presence of these CNHCs is not correlated with pTNM or the histological subtype of the primary tumour. In most cases, these cells were identified by a large majority of the cytopathologists on the panel as having malignant cytological criteria, and hence have been classified as CTCs. However, the invasive potential of these cells, as well as their metastatic potential, cannot be correlated, to date, with their cytological features. It would therefore be of interest to correlate the presence and the number of detected CTCs with patient follow-up. The different cytological criteria of malignancy adopted to classify

the CNHCs as CTCs were those usually used in clinical cytopathology.³⁷ However, in the present study, certain criteria were more frequently observed than others. For example, anisonucleosis, increased size of nuclei and irregular nuclei were more often observed in CTCs than high nucleo-cytoplasmic ratio and three-dimensional sheets of cells. This can be explained, at least partially, by the fact that certain cytopathologists on the panel did not consider these cells as true CTCs (circulating malignant cells) and classified them as circulating uncertain malignant cells. Interestingly, isolated CNHCs in our population of patients were not diagnostic for a histological subtype of the corresponding primary NSCLC. In particular, no features of keratinization or intracytoplasmic secretory vacuoles, which could correspond to mucus secretion, were noted in these cells. This may be explained by the fact that these cells could correspond to cells pre-selected as poorly differentiated cells, which could be the only population able to cross the endothelial barrier and

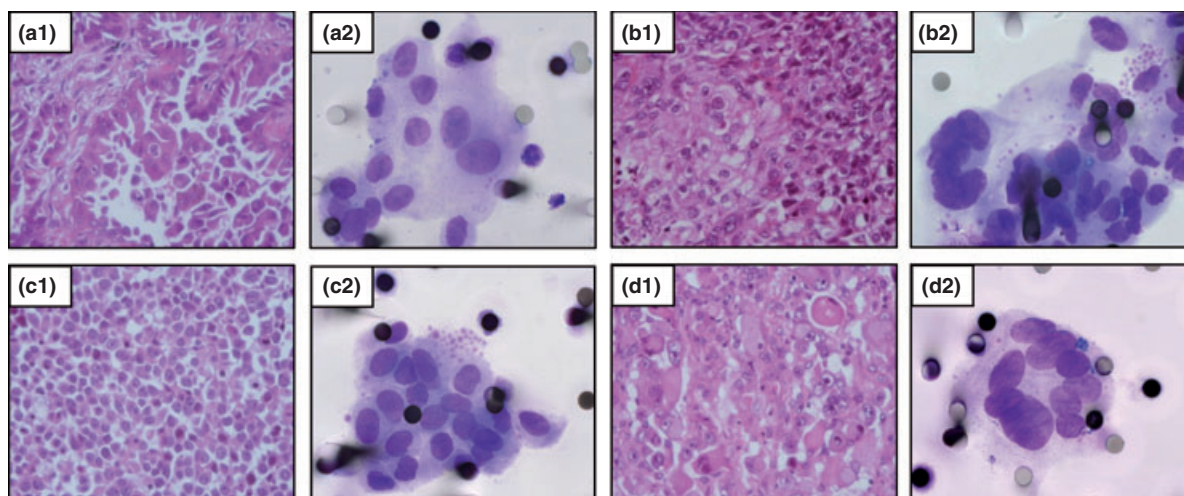


Figure 4. Comparison of the cytopathological features of circulating malignant cells and histological features of corresponding primary lung tumours. (a) Tubulo-papillary adenocarcinoma. (a1) H&E, original magnification $\times 400$. (a2) Corresponding circulating malignant cells, original magnification $\times 1000$. (b) Squamous cell carcinoma. (b1) H&E, original magnification $\times 400$. (b2) Corresponding circulating malignant cells, original magnification $\times 1000$. (c) Large cell carcinoma. (c1) H&E, original magnification $\times 400$. (c2) Corresponding circulating malignant cells, original magnification $\times 1000$. (d) Sarcomatoid carcinoma. (d1) H&E, original magnification $\times 400$. (d2) Corresponding circulating malignant cells, original magnification $\times 1000$.

migrate into the bloodstream.^{1,2,38} The presence of CNHCs without any cytological criteria of malignancy, called circulating benign cells, is questionable. They may correspond to epithelial cells detached from peritumoural areas or from other sites subjected to tissue microtrauma leading to vascular barrier disruption. However, we cannot totally exclude the possibility that they could be tumour cells without cytological atypia. This situation is rarely observed in 'conventional' cytology obtained from exfoliative or fine needle aspiration specimens, but might be potentially more frequent in the morphological analysis of CTCs. Finally, it is possible that a few of these cells could be circulating endothelial cells, as these are frequently detected in the blood of cancer patients.^{39,40} We did not consider cells with apoptotic features or naked nuclei for the diagnosis of CNHCs, although in some patients they were numerous, representing up to 30% of the isolated cells.

Some of the results of our study are not completely in keeping with some of the data on cytomorphological observations described in a recent publication.⁹ In this latter work, the authors showed a strong correlation between the cytopathological features of CTCs and the histological and cytopathological data observed in the corresponding primary lung adenocarcinoma.⁹ Moreover, the majority of CTCs detected showed a low nucleo-cytoplasmic ratio.⁹ The authors concluded that

these CTCs were not de-differentiated.⁹ This contradicts the current concept claiming that only poorly differentiated tumour cells can cross the endothelial barrier and then migrate into the blood stream.^{1,2,38} However, the results obtained by Marinucci *et al.*⁹ were observed in only one patient and used the FAST method.

Despite the importance of conventional cytopathological analysis based on MGG staining, it would certainly be of great interest to confirm these morphological criteria by an immunocytochemical study. However, immunocytochemistry of CTCs has a number of limitations because the phenotype of CTCs is usually different from that of the cells of the primary tumour.^{1,2,38} Hence, and also as a consequence of the epithelio-mesenchymal transition phenomenon, some CTCs have a low or absent level of cytokeratins.^{1,2,38} Moreover, no antibody is currently available for detecting the malignant potential of a given cell by immunocytochemistry. Recently, the detection of genomic aberrations in CTCs using an antigen-independent FISH-based assay has been suggested as a diagnostic and prognostic feature in patients with NSCLC.⁴¹ Thus different molecular biological approaches applied to CNHCs detected by ISET could be very useful in the future to improve characterization of the malignant potential of these cells.^{1,2,7,41}

In conclusion, the ISET method is a powerful approach not only for detection of CNHCs but also

for characterizing some or all of these CNHCs as CTCs. Our study shows that these CTCs are isolated in around half of patients undergoing surgery for resectable NSCLC. Whether or not their presence is related to prognosis remains to be evaluated. Quantification of these CTCs using automatic imaging devices would also be useful for looking for the prognostic impact according to the exact number of CTCs detected. Moreover, only the follow-up of our cohort of patients, with or without CTCs detected by the ISET approach, will tell us if these cells correspond to passively shed cells with little or no malignant potential, or actively migrating cells that are viable and may form further metastatic foci. The combination of 'classical' reference cytomorphological approaches with newly developed molecular markers derived from proteomic, molecular profiling and genetic analyses of the cells detected, should allow better classification and treatment of patients according to prognosis. Moreover, this might identify these CTCs as a pertinent molecular target for the development of new antitumour agents and raises the possibility that the presence of CTCs detected by ISET may guide clinicians in tailoring future therapy.

Acknowledgment

This work was supported by the Conseil Général des Alpes Maritimes and a PHRC National (2008).

References

1. Maheswaran S, Haber DA. Circulating tumor cells: a window into cancer biology and metastasis. *Curr Opin Genet Dev* 2010;**20**:96–9.
2. Paterlini-Bréchet P, Benali NL. Circulating tumor cells (CTC) detection: clinical impact and future directions. *Cancer Lett* 2007;**253**:180–204.
3. Allard WJ, Matera J, Miller MC *et al*. Tumor cells circulate in the peripheral blood of all major carcinomas but not in healthy subjects or patients with non-malignant diseases. *Clin Cancer Res* 2004;**10**:6897–904.
4. Sandri MT, Zorzino L, Cassatella MC, *et al*. Changes in circulating tumor cell detection in patients with localized breast cancer before and after surgery. *Ann Surg Oncol* 2010;**17**:1539–45.
5. Pantel K, Brakenhoff RH, Brandt B. Detection, clinical relevance and specific biological properties of disseminating tumour cells. *Nat Rev Cancer* 2008;**8**:329–40.
6. Krivacic RT, Ladanyi A, Curry DN *et al*. A rare-cell detector for cancer. *Proc Natl Acad Sci U S A* 2004;**101**:10501–4.
7. Vona G, Sabile A, Louha M *et al*. Isolation by size of epithelial tumor cells: a new method for the immunomorphological and molecular characterization of circulating tumor cells. *Am J Pathol* 2000;**156**:57–63.
8. Fetsch PA, Cowan KH, Weng DE *et al*. Detection of circulating tumor cells and micrometastases in stage II, III, and IV breast cancer patients utilizing cytology and immunocytochemistry. *Diagn Cytopathol* 2000;**22**:323–8.
9. Marinucci D, Bethel K, Lutgen M *et al*. Circulating tumor cells from well-differentiated lung adenocarcinoma retain cytomorphologic features of primary tumor type. *Arch Pathol Lab Med* 2009;**133**:1468–71.
10. Pinzani P, Salvadori B, Simi L. Isolation by size of epithelial tumor cells in peripheral blood of patients with breast cancer: correlation with real-time reverse transcriptase-polymerase chain reaction results and feasibility of molecular analysis by laser microdissection. *Hum Pathol* 2006;**37**:711–8.
11. Vona G, Estepa L, Beroud C *et al*. Impact of cytomorphological detection of circulating tumor cells in patients with liver cancer. *Hepatology* 2004;**39**:792–7.
12. Marrinucci D, Bethel K, Bruce RH *et al*. Case study of the morphologic variation of circulating tumor cells. *Hum Pathol* 2007;**38**:514–9.
13. Marrinucci D, Bethel K, Lazar D *et al*. Cytomorphology of circulating colorectal tumor cells: a small case series. *J Oncol* 2010;**2010**:861341.
14. Goya T, Asamura H, Yoshimura H *et al*. Prognosis of 6644 resected non-small cell lung cancers in Japan: a Japanese lung cancer registry study. *Lung Cancer* 2005;**50**:227–34.
15. Marcel T, van Rens M, Brutel de la Rivière A *et al*. Prognostic assessment of 2,361 patients who underwent pulmonary resection for non-small cell lung cancer, stage I, II, and IIIA. *Chest* 2000;**117**:374–9.
16. Travis WD, Lubin J, Ries L *et al*. United states lung carcinoma incidence and trends: declining for most histologic types among males, increasing among females. *Cancer* 1996;**77**:2464–70.
17. Pantel K, Riethdorf S. Pathology: are circulating tumor cells predictive of overall survival? *Nat Rev Clin Oncol* 2009;**6**:190–1.
18. Chen T-F, Jiang G-L, Fu X-L *et al*. CK19 mRNA expression measured by reverse-transcription polymerase chain reaction (RT-PCR) in the peripheral blood of patients with non-small cell lung cancer treated by chemoradiation: an independent prognostic factor. *Lung Cancer* 2007;**56**:105–14.
19. Gauthier LR, Granotier C, Soria JC *et al*. Detection of circulating carcinoma cells by telomerase activity. *Br J Cancer* 2001;**84**:631–5.
20. Hayes DC, Secrist H, Bangur CS *et al*. Multigene real-time PCR detection of circulating tumor cells in peripheral blood of lung cancer patients. *Anticancer Res* 2006;**26**:1567–75.

21. Kururu Y, Yamashita J, Ogawa M. Detection of circulating tumor cells by reverse transcriptase-polymerase chain reaction in patients with respectable non-small-cell lung cancer. *Surgery* 1999;**12**:820–6.
22. Peck K, Sher YP, Shih JY *et al.* Detection and quantitation of circulating cancer cells in the peripheral blood of lung cancer patients. *Cancer Res* 1998;**58**:2761–5.
23. Rolle A, Günzel R, Pachmann U *et al.* Increase in number of circulating disseminated epithelial cells after surgery for non-small cell lung cancer monitored by MAINTRAC is a predictor for relapse: a preliminary report. *World J Surg Oncol* 2005;**3**:1–9.
24. Sheu CC, Yu YP, Tsai JR. Development of membrane array-based multimarker assay for detection of circulating cancer cells in patients with non-small cell lung cancer. *Int J Cancer* 2006;**119**:1419–26.
25. Sher Y-P, Shih J-Y, Yang P-C *et al.* Prognosis of non-small cell lung cancer patients by detecting circulating cancer cells in the peripheral blood with multiple marker genes. *Clin Cancer Res* 2005;**11**:173–9.
26. Sozzi G, Conte D, Leon M *et al.* Quantification of free circulating DNA as a diagnostic marker in lung cancer. *J Clin Oncol* 2003;**21**:3891–3.
27. Sawabata N, Okumura M, Utsumi T *et al.* Circulating tumor cells in peripheral blood causes by surgical manipulation of non-small-cell lung cancer: pilot study using an immunocytology method. *Gen Thorac Cardiovasc Surg* 2007;**55**:189–92.
28. Yamashita J, Matsuo A, Kurusu Y *et al.* Pre-operative evidence of circulating tumor cells by means of reverse transcriptase-PCR for carcinoembryonic antigen messenger RNA is an independent predictor of survival in non-small cell lung cancer: a prospective study. *J Thorac Cardiovasc Surg* 2002;**124**:299–305.
29. Hofman V, Bonnetaud C, Ilie MI *et al.* Preoperative circulating tumor cell detection using the isolation by size of epithelial tumor cell method for patients with lung cancer is a new prognostic biomarker. *Clin Cancer Res* 2010. doi: 10.1158/1078-0432.CCR-10-0445 [Epub ahead of print].
30. Coello MC, Luketich JD, Litle VR, Godfrey TE. Prognostic significance of micrometastasis in non-small-cell lung carcinoma. *Clin Lung Cancer* 2004;**5**:214–25.
31. Naruke T, Tsuchiya R, Kondo H *et al.* Prognosis and survival after resection for bronchogenic carcinoma based on the 1997 TNM-staging classification: the Japanese experience. *Ann Thorac Surg* 2001;**71**:1759–64.
32. Pfannschmidt J, Muley T, Bülzbruck H *et al.* Prognostic-assessment after surgical resection for non-small cell lung cancer: experiences in 2083 patients. *Lung Cancer* 2007;**55**:371–7.
33. Mountain CF. The international system for staging lung cancer. *Sem Surg Oncol* 2000;**18**:106–15.
34. Travis WD, Brambilla E, Müller-Hermelink K, Harris CC. *Pathology and Genetics; Tumours of the Lung, Pleura, Thymus and Heart*. Lyon: WHO IARC; 2004.
35. Fleiss JL. *Statistical Methods for Rates and Proportions*. New York, NY: John Wiley; 1981.
36. Landis JR, Koch GG. The measurement of observer agreement for categorical data. *Biometrics* 1977;**33**:159–74.
37. Atkinson B. *Atlas of Diagnostic Cytopathology*, 2nd edn. Philadelphia, PA: W. B. Saunders Company; 2004.
38. Pantel K, Alix-Panabières C, Riethdorf S. Cancer micrometastases. *Nat Rev Clin Oncol* 2009;**6**:339–51.
39. Mancuso P, Burlini A, Pruneri G *et al.* Resting and activated endothelial cells are increased in the peripheral blood of cancer patients. *Blood* 2001;**97**:3658–61.
40. Strijbos MH, Gratama JW, Kraan J *et al.* Circulating endothelial cells in oncology: pitfalls and promises. *Br J Cancer* 2008;**98**:1731–5.
41. Katz RL, He W, Khanna A *et al.* Genetically abnormal circulating cells in lung cancer patients: an antigen-independent fluorescence in situ hybridization-based case-control study. *Clin Cancer Res* 2010;**16**:3976–87.

Predictive Clinical Outcome of the Intratumoral CD66b-Positive Neutrophil-to-CD8-Positive T-Cell Ratio in Patients With Resectable Nonsmall Cell Lung Cancer

Marius Ilie, MD^{1,2,3}; Véronique Hofman, MD, PhD^{1,2,3,4}; Cécile Ortholan, MD, PhD⁵; Christelle Bonnetaud, MD⁴; Céline Coëlle, MD⁴; Jérôme Mouroux, MD, PhD^{2,3,6}; and Paul Hofman, MD, PhD^{1,2,3,4}

BACKGROUND: The role of the interaction between tumor cells and inflammatory cells in nonsmall cell lung carcinoma (NSCLC) is unclear. In this study, the authors assessed the prognostic impact of intratumoral cluster of differentiation 66b (carcinoembryonic antigen-related cell adhesion molecule 8 [CD66b])-positive neutrophils and of the intratumoral CD66b-positive neutrophil-to-cluster of differentiation 8 (cell surface antigen T8 [CD8])-positive lymphocytes (the CD66b-positive neutrophil-to-CD8-positive lymphocyte ratio [iNTR]) in patients with resectable NSCLC. **METHODS:** Expression levels of CD66b and CD8 were evaluated by immunohistochemistry on tissue microarrays consisting of 632 NSCLC specimens from patients who underwent curative surgery. The relation between clinicopathologic variables and patient outcome was assessed. **RESULTS:** Intratumoral CD66b-positive neutrophils were elevated in 318 patients (50%). In univariate analysis, an increase in CD66b-positive cells was associated with a high cumulative incidence of relapse (CIR) (median CIR, 51 months for low CD66b-positive cell density; 36 months for high CD66b-positive cell density; $P = .002$) and trended toward worse overall survival (OS) (median OS, 57 months for low CD66b-positive cell density; 54 months for high CD66b-positive cell density; $P = .088$). The iNTR was elevated in 190 patients (30%). An increased iNTR was strongly associated with both a high CIR (median CIR: 43 months for an iNTR ≤ 1 ; 34 months for an iNTR > 1 ; $P < .0001$) and poor OS (median OS: 60 months for an iNTR ≤ 1 ; 46 months for an iNTR > 1 ; $P < .0001$). In multivariate analysis, independent prognostic factors for a higher CIR were high iNTR (hazard ratio [HR], 0.71; 95% confidence interval [CI], 0.56-0.90; $P = .005$) and tumor stage > 1 , (HR, 0.39; 95% CI, 0.30-0.52; $P < .0001$). Independent prognostic factors for worse OS were a high iNTR (HR, 0.70; 95% CI, 0.54-0.91; $P = .007$) and tumor stage > 1 (HR, 0.35; 95% CI, 0.26-0.47; $P < .0001$). **CONCLUSIONS:** The current results indicated that the iNTR is a novel, independent prognostic factor for a high rate of disease recurrence and poor OS in patients with resectable NSCLC. *Cancer* 2012;118:1726-37. © 2011 American Cancer Society.

KEYWORDS: intratumoral CD66b-positive neutrophil-to-CD8-positive T-cell ratio, nonsmall cell lung cancer, neutrophils, tissue microarrays, prognosis.

INTRODUCTION

Lung cancer is the leading cause of cancer-related deaths in the world.¹ Nonsmall cell lung cancer (NSCLC) represents 80% of lung cancers. Despite the different therapeutic strategies developed to date, patients with NSCLC have a poor prognosis, and the overall survival (OS) rate after 5 years is $< 25\%$ for all stages.² Thus, current prognostic models that include histologic subtype, tumor grade, tumor size, and pathologic tumor-lymph node-metastasis (pTNM) classification urgently need to be improved by the integration of new prognostic biomarkers.³

Increasing evidence supports the involvement of systemic inflammation in cancer development and progression.⁴ Apart from their well established function as effector cells against invading pathogens, it is certain that neutrophils are

Corresponding author: Paul Hofman, MD, PhD, Laboratory of Clinical and Experimental Pathology, Louis Pasteur Hospital, 30 Avenue de la Voie Romaine, 06002 Nice Cedex 01, France; Fax: (011) 33-4-92-03-87-50; hofman.p@chu-nice.fr

¹Laboratory of Clinical and Experimental Pathology, Louis Pasteur Hospital, University Hospital Center of Nice, Nice, France; ²National Institute for Health and Medical Research (INSERM), ERI-21, Nice, France; ³Faculty of Medicine, Nice Sophia University, Nice, France; ⁴Human Tissue Biobank Unit/Biological Resource Center (CRB) INSERM, Nice, France; ⁵Radiotherapy Department, Princess Grace Hospital Center, Radiotherapy Department, Monaco; ⁶Thoracic Surgery Department, Louis Pasteur Hospital, University Hospital Center of Nice, Nice, France

DOI: 10.1002/cncr.26456, **Received:** April 1, 2011; **Revised:** June 23, 2011; **Accepted:** June 24, 2011, **Published online** August 25, 2011 in Wiley Online Library (wileyonlinelibrary.com)

involved in carcinogenesis.⁵ The mechanisms of action involve intracellular signaling molecules and pathways, including 1) the mutagenic effect and inactivation of mismatch-repair enzymes that implicate reactive oxygen species (ROS) and nitrogen intermediates, 2) activation of the nuclear factor- κ B pathway, and 3) modulation of the expression of certain micro-RNAs.⁵ In addition, recently reported evidence also suggests a pivotal role of neutrophils in tumor progression and invasion.^{5,6} Secreted factors of neutrophils, such as neutrophil gelatinase-associated lipocalin or neutrophil elastase, are able to suppress or increase the invasion of carcinoma cells.^{7,8} Finally, neutrophils may be involved in tumor metastasis by acting on transendothelial migration of carcinoma cells,⁹ by degrading the extracellular matrix, and by enhancing angiogenesis.¹⁰ Furthermore, ROS released from activated neutrophils can generate mutations in mitochondrial DNA that regulate tumor cell metastasis.¹¹ Conversely, neutrophils can act as direct effector cells in immune surveillance against cancer by releasing cytotoxic mediators like ROS and proteolytic enzymes or through antibody-dependent, cell-mediated cytotoxicity.¹²

Moreover, emerging immune hallmarks of cancer are represented by the ability to evade immune recognition and to suppress immune reactivity. Mice with T-cell and B-cell deficiencies are more likely to develop malignant tumors.¹³ There is evidence of the existence of antitumoral immune responses in some types of cancer. For example, a high density of tumor-infiltrating cluster of differentiation 8 (cell surface antigen T8 [CD8])-positive T cells is associated with a better prognosis in patients with colorectal carcinoma.¹⁴ Moreover, cancer cells may recruit inflammatory cells, including neutrophils, which can suppress the action of cytotoxic lymphocytes. We hypothesized that the balance between conflicting inflammatory responses in tumors is likely to prove instrumental in prognosis.

Recently, the presence of intratumoral neutrophils, defined as cluster of differentiation 66b (carcinoembryonic antigen-related cell adhesion molecule 8 [(CD66b)]-positive cells, was identified as an independent prognostic factor for poor survival in patients with renal cell carcinoma.¹⁵ Moreover, a high preoperative blood neutrophil-to-lymphocyte ratio reportedly was associated with a poor outcome in various malignancies.¹⁶⁻¹⁸ However, to our knowledge, the impact of intratumoral neutrophils as a prognostic biomarker and the intratumoral neutrophil-to-lymphocyte ratio (iNTR) (ie, the ratio of CD66b-positive neutrophils to CD8-positive T lymphocytes) has not been investigated in NSCLC.

To this aim, we performed in situ immunostaining for intratumoral myeloperoxidase (MPO)-positive and CD66b-positive neutrophils and CD8-positive T lymphocytes in tumor specimens from 632 patients who had resectable NSCLC. We investigated the relation between the type and density of neutrophils and the number of CD8-positive T lymphocytes within tumors and the clinical outcome of these patients with resectable NSCLC.

Our results demonstrate that an increase in intratumoral infiltration by CD66b-positive neutrophils has prognostic value for disease recurrence. Moreover, we have identified the iNTR as an independent predictor of poor survival after resection of primary NSCLC and as a potential biomarker for the stratification of patients with early stage NSCLC according to their risk of death.

MATERIALS AND METHODS

Patients

Patients who were diagnosed with resectable NSCLC at the Department of Thoracic Surgery, University of Nice, Louis Pasteur Hospital (Nice, France) between January 2001 and April 2010 were screened for inclusion in this retrospective study. The patients received the necessary information concerning the study, and consent was obtained from each patient. The study was approved by the Ethics Committee of the University of Nice and was performed according to the guidelines of the Declaration of Helsinki. Criteria for inclusion were tumor stage I to III (according to the seventh edition of the *American Joint Committee on Cancer Staging Manual*).¹⁹ Patients underwent curative surgery of the primary tumor (wedge resection, lobectomy, or pneumonectomy) and of mediastinal lymph nodes and had clinicopathologic and outcome data available. Twelve of 632 patients (1.8%) who had tumors classified as pT4 underwent incomplete resection, and all 632 patients were included in this study. Morphologic classification was assigned according to World Health Organization criteria and also included the latest recommendations of the International Association for the Study of Lung Cancer.^{20,21} The main clinical and histopathologic parameters of the study patients are summarized in Table 1.

Tissue Microarray Construction and Immunohistochemistry

Tissue microarrays (TMAs) were constructed from archival formalin-fixed, paraffin-embedded tissue blocks. Representative tumor sections were selected for building TMAs, and arrays were designed as previously

Table 1. Correlation of intratumoral CD66b-Positive Neutrophils, CD8-Positive T-Cells, and the Intratumoral CD66b-Positive/CD8-Positive Ratio With Clinicopathologic Parameters in 632 Patients with Nonsmall Cell Lung Cancer^a

Feature	Overall	Intratumor CD66b+ Neutrophils: No. of Patients (%)		<i>P</i> ^b	CD8+ T Cells: No. of Patients (%)		<i>P</i> ^b	iNTR: No. of Patients (%)		<i>P</i> ^b
		Low	High		Low	High		Low	High	
Patient cohort	632	314 (50)	318 (50)		320 (51)	312 (49)		442 (70)	190 (30)	
Age, y				.13			.10			.52
<65	307 (49)	143 (47)	164 (53)		145 (47)	162 (53)		211 (69)	96 (31)	
≥65	325 (51)	171 (53)	154 (47)		175 (54)	150 (46)		231 (71)	94 (29)	
Sex				.71			.78			.78
Men	467 (74)	230 (49)	237 (51)		238 (51)	229 (49)		328 (70)	139 (30)	
Women	165 (26)	84 (51)	81 (49)		82 (50)	83 (50)		114 (69)	51 (31)	
Smoking history				.93			.45			.59
Never smoked	86 (14)	43 (50)	43 (50)		47 (55)	39 (45)		57 (66)	29 (34)	
Former or current smokers	546 (86)	272 (50)	274 (50)		274 (50)	272 (50)		381(70)	165 (30)	
Tumor size: Median±SD, cm	3.4 ± 2.3	3.8±2.4	3.8±2.3	.90	3.9±2.5	3.8±2.1	.32	3.8 ± 2.4	4.0 ± 2.3	.28
Histologic cell type				.35			.001			.15
Invasive adenocarcinoma	348 (55)	167(48)	181 (52)		157 (45)	191 (55)		252 (72)	96 (28)	
Squamous cell carcinoma	207 (33)	111 (54)	96 (46)		124 (60)	83 (40)		133 (64)	74 (36)	
Large cell carcinoma	29 (4)	16 (55)	13 (45)		21 (72)	8 (28)		20 (69)	9 (31)	
Sarcomatoid carcinoma	48 (8)	20 (42)	28 (58)		18 (37)	30 (63)		37 (77)	11 (23)	
pTNM stage				.39			.92			.6
I	274 (44)	137 (50)	137 (50)		137 (50)	137 (50)		197 (72)	77 (28)	
II	185 (29)	85 (46)	100 (54)		96 (52)	89 (48)		125 (68)	60 (32)	
III	173 (27)	92 (53)	81 (47)		87 (50)	86 (50)		120 (69)	53 (31)	
Tumor grade				.21			.04			.19
1	244 (39)	127 (52)	117 (48)		140 (57)	104 (43)		172 (70)	72 (30)	
2	209 (33)	92 (44)	117 (56)		100 (48)	109 (52)		137 (66)	72 (34)	
3	159 (25)	83 (52)	76 (48)		73 (46)	86 (54)		116 (73)	43 (27)	
4	20 (3)	12 (60)	8 (40)		7 (35)	13 (65)		17 (85)	3 (15)	
Neoadjuvant chemotherapy				.21			.11			.23
Yes	60 (9)	35 (58)	25 (42)		24 (40)	36 (60)		46 (77)	14 (23)	
No	572 (91)	280 (49)	292 (51)		296 (52)	276 (48)		397 (69)	175 (31)	
Adjuvant chemotherapy				.21			.15			.51
Yes	289 (46)	162 (56)	127 (44)		136 (47)	153 (53)		150 (52)	139 (48)	
No	343 (54)	174 (51)	169 (49)		182 (53)	161 (47)		168 (49)	175 (51)	

Abbreviations: +, positive; CD66b, cluster of differentiation 66b (carcinoembryonic antigen-related cell adhesion molecule 8); CD8, cluster of differentiation 8 (cell surface antigen T8); iNTR, intratumoral CD66b+ neutrophil-to-CD8+ T-cell ratio; pTNM, pathologic tumor, lymph node, metastasis classification; SD, standard deviation.

^aHigh levels of intratumoral CD66b+ neutrophils were defined as ≥49 cells/mm². High levels of CD8+ cells were ≥110 cells/mm². A high iNTR was defined as >1 cell/mm², as described in the text (see Materials and Methods).

^bChi-square tests or Student *t* tests were used to calculate *P* values.

described.²² The selection of representative tumor material (>60% tumor cells, nontumor zone or stromal reaction removal, lack of necrosis) by the pathologist guaranteed the reproducibility of the semiautomated image analysis. Twenty array blocks that contained a total of 2250 cores representing 632 tumors were built and tested by using immunohistochemistry (IHC). TMA sections were incubated for 60 minutes at room temperature with monoclonal antibodies against CD66b (clone GF10F5; 1:600

dilution; BD Biosciences, San Diego, Calif), MPO (clone RbPoAb; 1:1000 dilution; Dako, Carpinteria, Calif), and CD8 (clone C8/144B; 1:50 dilution; Dako). The clone C8/144B of the anti-CD8 antibody that was used in this study may be expressed at a lower density on a subset of CD8dim natural killer (NK) cells.

IHC was performed on serial 4-μm TMA sections that were deparaffinized in xylene and rehydrated through a graded series of ethanol concentrations. Antigen retrieval

was performed in a microwave oven in ethylene diamine tetra acetic acid buffer, pH 9.0 (Dako, Glostrup, Denmark), for 30 minutes. Intrinsic peroxidase activity was blocked with 3% hydrogen peroxide for 20 minutes. Goat serum (5%; Sigma-Aldrich, Zwijndrecht, the Netherlands) was used to block nonspecific antibody binding. An automated single-staining procedure (Benchmark XT; Ventana Medical Systems, Roche Group, Inc., Tucson, Ariz) was used to perform the staining. For visualization, the Envision+ system (horseradish peroxidase enzyme-conjugated polymer backbone coupled to secondary antibodies) and 3,3'-diaminobenzidine chromogen (Dako) were used according to the manufacturer's instructions. Tissue sections were counterstained with hematoxylin. Isotype-matched mouse or rabbit monoclonal antibodies were used as negative controls. Spleen, thymus, skin, and tonsillar sections were included as positive controls. Representative images of CD66b, MPO, and CD8 immunolabeling and of the density of cells are provided in Figure 1.

Semiautomated Image Analysis

CD66b-positive neutrophils either were localized within the blood vessels of tumors or were scattered diffusely throughout the tumor. The distinction between intratumoral CD66b-positive neutrophils and vessel-only CD66b-positive neutrophils was made by manually excluding positive cells located in vessels from tumors on selected spots by 3 pathologists (M.I., V.H., and P.H.). Slides were analyzed using an image-analysis workstation (SpotBrowser; Alphelys, Paris, France), as previously described.²³ Whole TMA slide digitalization, supported by the dedicated software tool (SpotBrowser), which allows image object quantization based on color and intensity segmentation for unbiased analysis of immunostaining results, guaranteed the reproducibility of results. The automation was monitored at every step by a single pathologist (M.I.). Polychromatic, high-resolution spot images (740 × 540 pixels; 1.181 μm/pixel resolution) were obtained (at ×100 magnification). The density was recorded as the number of positive cells per unit of tissue surface area. For each triplicate count, the mean density was used for statistical analysis. The iNTR was calculated according to the recently proposed measurement of the immune imbalance of the local microenvironment.¹⁶

Statistical Analyses

Differences between groups were evaluated using the chi-square test for categorical variables and the Student *t* test for continuous variables. The coefficient of correlation (ρ) between variables was calculated using the Spearman rank

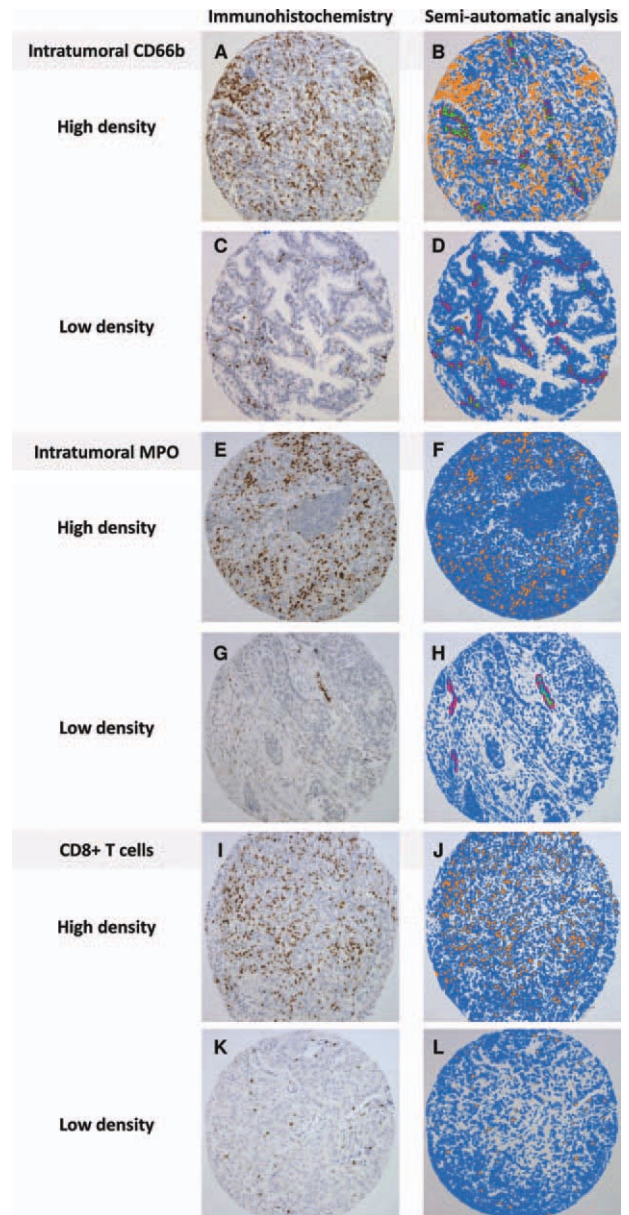


Figure 1. (A,C,E,G,I,K) These are representative examples of immunostaining of cluster of differentiation 66b (CD66b) (carcinoembryonic antigen-related cell adhesion molecule 8)-positive and myeloperoxidase (MPO)-positive neutrophils or CD8 (cell surface antigen T8)-positive T cells from adenocarcinoma tissue microarrays. Inflammatory cells (brown) and tumor cells (blue) are visible. (B,D,F,H,J,L) These digital images were analyzed with the image software SpotBrowser (Alphelys, Paris, France). Blue indicates tumor tissue; orange, intratumoral cells; green, vessel-only cells; red, blood vessels.

test. For intratumoral CD66b-positive cells and intratumoral CD8-positive T cells, the median value was used as a cutoff variable. The receiver operator characteristic curve, which plots sensitivity against a specificity of 1, was used in combination with the Youden Index (YI) as a

measure of the optimal threshold cutoff for the iNTR according to survival estimates. The median follow-up was calculated using the method described by Schemper and Smith.²⁴ Survival rates were estimated using the Kaplan-Meier method. The log-rank test was used to compare survival between groups. OS was calculated from the date of surgery to the date of either death or last follow-up. The cumulative incidence of relapse (CIR) was calculated from the date of surgery to the date of first disease recurrence (local or metastatic). A Cox proportional hazards model was created to identify independent predictors of survival. Variables that were associated with survival with a P value $< .20$ in the univariate analysis were included in the multivariate regression. Because intratumoral CD66b-positive neutrophils and CD8-positive T cells are strictly interdependent on the iNTR, these data were excluded from the multivariate analysis. Analyses were performed using the SPSS 16.0 statistical software package (SPSS Inc., Chicago, Ill). All statistical tests were 2-sided, and P values $< .05$ indicated statistical significance.

RESULTS

Analysis of Immunohistochemical Parameters

According to the semiautomatic quantification analysis, the median \pm standard deviation (SD) number of intratumoral CD66b-positive cells was 49 ± 111 cells/mm² (range, 0-577 cells/mm²), and the median \pm SD number of vessel-only cells was 0 ± 13 cells/mm² (range, 0-102 cells/mm²). The median \pm SD number of intratumoral MPO-positive cells was 117 ± 210 cells/mm² (range, 0-589 cells/mm²), and the median \pm SD number of vessel-only cells was 0 ± 45 cells/mm² (range, 0-483 cells/mm²). The median \pm SD number of CD8-positive T cells was 110 ± 142 cells/mm² (range, 1-968 cells/mm²). CD66b-positive cells and MPO-positive cells were correlated significantly ($\rho = 0.92$; $P = .001$). In contrast, high levels of intratumoral CD66b-positive cells were associated with low levels of CD8-positive cells ($\rho = 0.28$; $P = .016$). The median \pm SD iNTR was 0.4 ± 9 (range, 0-206). For each tumor, triplicate selected spots revealed a good level of homogeneity of stained cell densities.

Correlation Between CD66b-Positive, Myeloperoxidase-Positive, and CD8-Positive Cell Infiltrates and Clinicopathologic Parameters

Table 1 indicates that CD8-positive T cells were correlated significantly with histologic type, because 55% of invasive adenocarcinomas and 63% of sarcomatoid

carcinomas had high levels of CD8-positive T cells ($P = .001$). CD8-positive T cells also were correlated with poorly differentiated tumors (global chi-square test, $P = .04$; grade 1 vs grades 2-4, $P = .009$). However, no significant correlation was observed between intratumoral CD66b-positive neutrophils, the iNTR (Table 1), vessel-only CD66b-positive neutrophils, intratumoral MPO-positive neutrophils, or vessel-only MPO-positive neutrophils and clinicopathologic variables.

Survival Analysis

At the last follow-up, 269 of 632 patients (43%) had died, including 203 of 632 patients (32%) who died specifically from NSCLC progression. For the 363 patients (57%) patients who were alive at the endpoint of this study, the median follow-up was 30 months (range, 0-112 months).

The receiver operator characteristic curve and the YI were used to determine the iNTR cutoff according to the OS rate. The following 4 cutoff variables were relevant: the 25th percentile (iNTR, 0.12; sensitivity, 0.83; specificity, 0.30; YI, 0.19), the median value (iNTR, 0.4; sensitivity, 0.65; specificity, 0.61; YI, 0.26), the 75th percentile (iNTR, 1.29; sensitivity, 0.38; specificity, 0.90; YI, 0.20), and an iNTR of 1 (infiltration of CD66b-positive cells and CD8-positive T cells in equal proportions: sensitivity, 0.54; specificity, 0.82; YI, 0.60). According to this analysis, an iNTR of 1 was considered the optimal cutoff variable for further survival analyses.

The median CIR was 40 months (95% confidence interval [CI], 35-50 months). In univariate analysis, clinical factors that were associated significantly with the CIR were pTNM stage (median CIR: 57 months, 39 months, and 22 months for stage I, II, and III, respectively; $P < .0001$), tumor grade (median CIR: grade 1, 52 months; grade >1 , 33 months; $P < .001$), intratumoral CD66b-positive cells (median CIR: low CD66b-positive cell density, 51 months; high CD66b-positive cell density, 36 months; $P = .002$) (Fig. 2A), and the iNTR (median CIR: iNTR ≤ 1 , 43 months; iNTR >1 , 34 months; $P < .0001$) (Fig. 2B). Age, sex, history of smoking, histologic subtype, CD8-positive T cells, vessel-only CD66b-positive neutrophils, and intratumoral or vessel-only MPO-positive neutrophils were not associated with the CIR. In multivariate analysis, the independent factors for lower CIR were stage I disease (hazard ratio [HR], 0.39; 95% CI, 0.30-0.52; $P < .0001$) and an iNTR ≤ 1 (HR, 0.71; 95% CI, 0.56-0.90; $P = .005$) (Table 2).

When considering the whole population of patients, the median OS was 56 months (95%CI, 50-62 months).

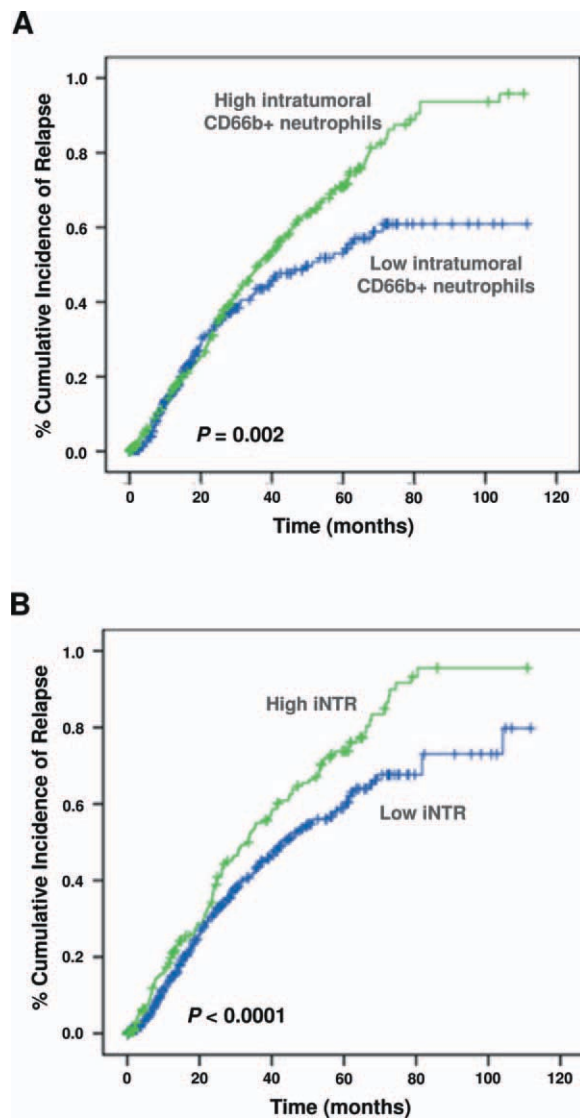


Figure 2. These Kaplan-Meier curves illustrate the cumulative incidence of relapse stratified according to (A) the level of intratumoral cluster of differentiation 66b (CD66b) (carcino-embryonic antigen-related cell adhesion molecule 8)-positive (CD66b+) neutrophils and (B) the ratio of intratumoral CD66b+ neutrophils to CD8 (cell surface antigen T8)-positive (CD8+) T cells (iNTR) (B). (A) The green curve represents patients with high intratumoral CD66b+ neutrophils (≥ 49 cells/mm²), and the blue curve represents patients with low intratumoral CD66b+ neutrophils (< 49 cells/mm²). (B) The green curve represents patients with a high iNTR (> 1), and the blue curve represents patients with a low iNTR (≤ 1).

In univariate analysis, the clinical factors that were associated significantly with OS were pTNM stage (median OS: 74 months, 57 months, and 33 months for stage I, II, and III, respectively; $P < .0001$), tumor grade (median OS: grade 1, 63 months; grade > 1 , 51 months; $P = .006$), CD8-positive cell density (median OS: low

CD8-positive cell density, 49 months; high CD8-positive cell density, 60 months; $P = .013$) (Fig. 3B), and the iNTR (median OS: iNTR ≤ 1 , 60 months; iNTR > 1 , 46 months; $P < .0001$) (Fig. 3C). Intratumoral CD66b-positive neutrophil density had a marginal effect on OS (median OS: low CD66b-positive neutrophil density, 57 months; high CD66b-positive neutrophil density, 54 months; $P = .088$) (Fig. 3A). Age, sex, history of smoking, histologic cell type, vessel-only CD66b-positive neutrophils, and intratumoral or vessel-only MPO-positive neutrophils were not associated with OS. In multivariate analysis, the independent factors that indicated better OS were stage I disease (HR, 0.35; 95% CI, 0.26-0.47; $P < .0001$) and an iNTR ≤ 1 (HR, 0.70; 95% CI, 0.54-0.91; $P = .007$) (Table 2). When considering the subgroups of patients with stage I, II, and III NSCLC, the iNTR was prognostic for patients with stage I disease (median OS, not reached vs 61 months; $P = .02$) and for patients with stage III disease (median OS, 39 months vs 25 months; $P = .009$), but it was marginal for patients with stage II disease (median OS, 59 months vs 46 months; $P = .14$) (Fig. 4).

DISCUSSION

In this study, we identify the iNTR as an independent poor prognostic factor for CIR and OS in patients with resectable stage I through III NSCLC. Patients who had high intratumoral CD66b-positive neutrophil density had a significantly increased CIR and had a trend toward decreased OS. More important, a high iNTR had better discriminatory power for identifying subgroups of patients who had a significantly increased CIR and worse OS. Thus, intratumoral CD66b-positive neutrophils and the iNTR may serve as novel biomarkers to predict the outcome of patients with resectable NSCLC.

Cancer-related inflammation is certainly a major consequence of certain environmental factors that eventually lead to increased proliferation, survival, and migration of epithelial cells as well as angiogenesis in the adjacent stroma, which promotes epithelial tumor development.²⁵⁻²⁷ Inflammatory cells operate in conflicting ways: Both tumor-antagonizing and tumor-promoting leukocytes can be identified in various proportions in most neoplastic lesions.¹³ The panel of tumor-promoting inflammatory cells includes neutrophils, macrophage subtypes, and mast cells as well as T and B lymphocytes. In addition, partially differentiated myeloid progenitors identified as myeloid-derived suppressor cells (MDSCs), which seem to represent a subpopulation of activated neutrophils, have been

Table 2. Median Cumulative Incidence of Relapse and Overall Survival Stratified According to Pathologic and Immunohistochemical Variables

Variable	Median CIR, mo	P	Median OS, mo	P
Age, y		.36		.65
<65	41		56	
≥65	39		57	
Sex		.87		.15
Men	38		54	
Women	40		67	
Smoking history		.78		.48
Never smoked	40		57	
Former or current smokers	32		53	
Tumor size, cm		.36		.48
≤3	43		57	
>3	38		53	
Histologic cell type		.97		.07
Invasive adenocarcinoma	40		59	
Squamous cell carcinoma	39		57	
Large cell carcinoma	25		35	
Sarcomatoid carcinoma	36		44	
pTNM stage		<.0001		<.0001
I	57		75	
II	39		57	
III	22		33	
Tumor grade		.003		.006
1	52		63	
2+3+4	33		51	
Intratumoral CD66b+ neutrophils		.002		.088
Low	51		57	
High	36		54	
CD8+ T cells		.158		.013
Low	46		49	
High	48		60	
iNTR		<.0001		<.0001
Low	43		60	
High	34		46	
Neoadjuvant chemotherapy		.31		.72
Yes	45		58	
No	42		56	
Adjuvant chemotherapy		.29		.68
Yes	43		59	
No	40		56	

Abbreviations: +, positive; CD66b, cluster of differentiation 66b (carcinoembryonic antigen-related cell adhesion molecule 8); CD8, cluster of differentiation 8 (cell surface antigen T8); CIR, cumulative incidence of relapse; iNTR, intratumoral CD66b+ neutrophil-to-CD8+ T cell ratio; OS, overall survival; pTNM, pathologic tumor, lymph node, metastasis classification.

identified in tumors.^{13,28,29} In this regard, growing evidence suggests that neutrophils have an important effect in reacting against the host in the setting of cancer.³⁰

Patients suffering from inflammatory pulmonary diseases, such as chronic obstructive pulmonary disease/emphysema, have an increased risk of developing lung

cancer.^{27,31} One common characteristic of many chronic inflammatory lung disorders is the influx of neutrophils. It has been suggested that the accumulation of these neutrophils in the lumen of the lung is related to the risk of lung cancer, suggesting a significant role of neutrophilic inflammation in the carcinogenic response.³²

Table 3. Multivariate Analysis of Clinicopathologic Factors and the Intratumoral CD66b-Positive/CD8-Positive Ratio with Cumulative Incidence of Relapse or Overall Survival as the Endpoint in Patients With Nonsmall Cell Lung Cancer

Prognostic Factor	Categories Compared	HR	95% CI	P
CIR				
pTNM stage	I vs other	0.39	0.30-0.52	<.0001
Tumor grade	1 vs other	0.82	0.40-1.71	.60
iNTR	Low vs high (>1)	0.71	0.56-0.90	.005
OS				
Sex	Men vs women	0.91	0.78-1.07	.25
Histologic cell type	Adenocarcinoma vs other	0.90	0.71-1.13	.35
pTNM stage	I vs other	0.35	0.26-0.47	<.0001
Tumor grade	1 vs other	0.70	0.33-1.52	.37
iNTR	High (>1) vs low	0.70	0.54-0.91	.007

Abbreviations: CI, confidence interval; CIR, cumulative incidence of relapse; HR, hazard ratio; iNTR, intratumoral CD66b-positive neutrophil-to-CD8-positive T-cell ratio; OS, overall survival.

Moreover, neutrophils have been implicated in pulmonary carcinogenesis by their genotoxic capacity.^{32,33} This may occur through the release of mutagenic ROS generated by activated neutrophils and through activation of the metabolism of environmental chemical carcinogens, which provide a growth advantage.^{34,35} Activated neutrophils are able to induce sister chromatid exchange, strand breaks, and mutations in neighboring target cells.³⁶ In addition, they are potent inhibitors of the nucleotide excision repair pathway, causing delayed removal of pro-mutagenic, bulky DNA adducts.³⁷ Alternatively, activated neutrophils may use cytokines, such as tumor necrosis factor- α , which is implicated in carcinogenesis, to stimulate ROS and nitric oxide accumulation in neighboring epithelial cells.³⁸ It is noteworthy that cancer cells in bronchioloalveolar carcinoma, a subtype of lung adenocarcinoma, are able to recruit neutrophils to the tumor microenvironment by producing interleukin-8, a chemoattractant of neutrophils.³⁹ In addition, *K-ras* mutant lung tumors in mice recruit neutrophils through CXC chemokine release.⁴⁰ With regard to the impact of *K-ras* mutations on the survival of patients with NSCLC,⁴¹ it may be of interest to perform further studies comparing *K-ras* mutations with intratumoral CD66b-positive neutrophils in a large series of NSCLC.

The tumor environment generates local conditions that prolong neutrophil survival through the production of antiapoptotic factors or pleiotropic cytokines.⁴² Recent studies demonstrated that head and neck cancer cells up-regulate the inflammatory activity and also up-regulate the production of factors in neutrophils with the possible ability to promote tumor progression.⁴³

The existence of both tumor-promoting and tumor-antagonizing inflammatory cells is generally accepted.

Therefore, another emerging hallmark of cancer is the capability to evade immune destruction.¹³ Deficiencies in the development or function of CD8-positive cytotoxic T lymphocytes, CD4-positive T cells, or NK cells each led to an increase in tumor incidence.^{13,44} However, immune surveillance is not an effective barrier to tumorigenesis or tumor progression.¹³ In this regard, the impact of CD4-positive T cells or NK cells alone on the outcome of patients with cancer has not been fully demonstrated, because several studies failed to reveal a significant association with survival.^{15,45}

Highly immunogenic cancer cells may evade immune eradication by disabling components of the immune system that have been dispatched to eliminate them.^{13,46} Subtle mechanisms operate through the recruitment of inflammatory cells that are actively immunosuppressive, including neutrophils that can suppress the action of cytotoxic lymphocytes. Recently, a dual role for neutrophils was proposed with regard to their action on lung carcinoma and mesothelioma cells.⁴⁷ It is noteworthy that 2 different populations of neutrophils may be present in tumors that are under the influence of transforming growth factor β (TGF- β), a population that favors tumor progression (tumor-associated neutrophils 2 [TAN2]) and a population that decreases tumor progression (TAN1).⁴⁷⁻⁵⁰ Infiltrating TAN2 may inhibit the cytotoxic response of CD8-positive T cells and thereby allow tumor cells to circumvent immune surveillance.⁴⁷ It is noteworthy that, after TGF- β blockade, a shift to the "N1" phenotype occurs with acquisition of antitumor activity, which is associated with increased activation of CD8-positive T cells.⁴⁷

Although the roles of the others immune cells, such as tumor-associated macrophages, regulatory T cells,

cytotoxic T lymphocytes, or mast cells, in tumor progression have been demonstrated,^{4,51,52} the impact of neutrophils is less well understood.⁴⁸ Recently, the presence of activated, intratumoral, CD66b-positive neutrophils was

described as an independent negative prognostic factor for patients with renal cell carcinoma.¹⁵ Neutrophil infiltrates within alveolar spaces in bronchioloalveolar carcinoma were associated with a poor clinical outcome.³⁹ Substantial infiltration with CD66b-positive neutrophils predicted poor survival in patients with advanced head and neck squamous cell carcinoma.⁴³

Given the major role played by tumor-promoting neutrophils in the inhibition of the cytotoxic response of the CD8-positive T cells,⁵³ the peripheral neutrophil-to-lymphocyte ratio has been correlated with a poor prognosis in several types of cancers, including NSCLC.^{17,54} Therefore, we sought to determine whether this balance in cells of the immune system is modified in a tumor tissue microenvironment. In the current study, high levels of intratumoral CD66b-positive neutrophils were associated with low levels of CD8-positive T cells. We demonstrated that the iNTR was strongly correlated with a high CIR and poor OS. These observations are in line with recent data obtained from the clinic in which the iNTR was correlated with a poor prognosis in patients with hepatocellular carcinoma.⁵⁵ Moreover, in the current study, it is noteworthy that the iNTR predicted significantly poor OS and a high CIR in early stage NSCLC. Our study raises the possibility that the recruitment of neutrophils may be doubly beneficial for the developing tumor by directly promoting tumor progression while simultaneously affording a means to evade immune destruction, as recently suggested.¹³ Given the exploratory nature of our study, further investigations are needed to clarify the mechanism of action of intratumoral neutrophils.

We observed that MPO-positive cells were greater in number than CD66b-positive cells. However, we did not observe any correlation between MPO-positive neutrophils and outcome. Only the CD66b-positive phenotype was associated significantly with poor survival,

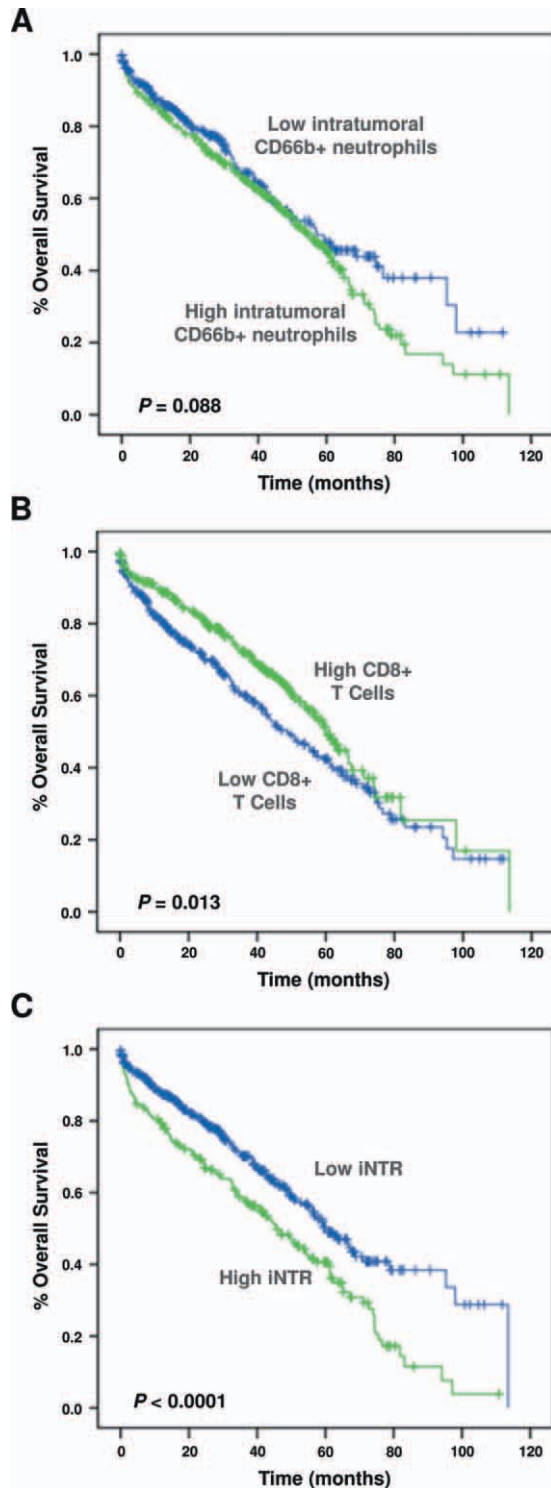


Figure 3. These Kaplan-Meier curves illustrate the overall survival probability based on (A) the number of intratumoral cluster of differentiation 66b (CD66b) (carcinoembryonic antigen-related cell adhesion molecule 8)-positive (CD66b+) neutrophils, (B) the number of CD8 (cell surface antigen T8)-positive (CD8+) T cells, and (C) the intratumoral CD66b+ neutrophil-to-CD8+ T-cell ratio (iNTR). (A) The blue curve represents patients with high intratumoral CD66b+ neutrophils (≥ 49 cells/mm²), and the green curve represents patients with low intratumoral CD66b+ neutrophils (< 49 cells/mm²). (B) The blue curve represents patients with high CD8+ T cells (≥ 110 cells/mm²), and the green curve represents patients with low CD8+ T cells (< 110 cells/mm²). (C) The blue curve represents patients with a high iNTR (> 1), and the green curve represents patients with a low iNTR (≤ 1).

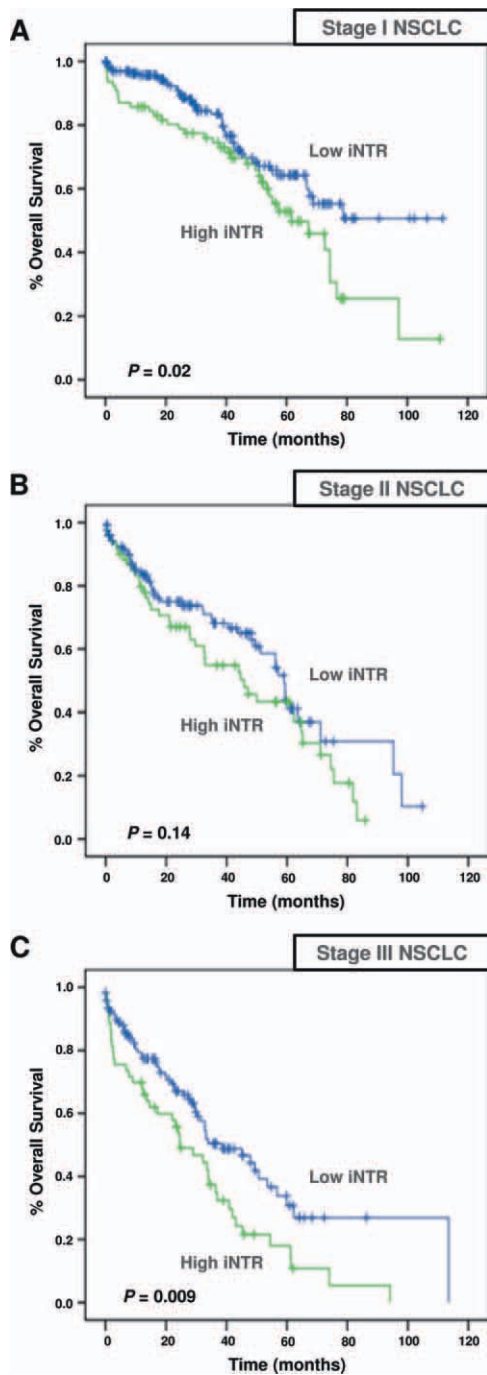


Figure 4. These Kaplan-Meier estimates illustrate the overall survival probability for patients with (A) stage I non-small cell lung cancer (NSCLC), (B) stage II NSCLC, and (C) stage III NSCLC based on the intratumoral cluster of differentiation 66b (CD66b) (carcinoembryonic antigen-related cell adhesion molecule 8)-positive neutrophil-to-CD8 (cell surface antigen T8)-positive T-cell ratio (iNTR).

because it clearly identified a subgroup of high-risk patients with NSCLC. The CD66b-positive antigen is expressed specifically on neutrophils and may be assigned to a limited, activated subtype of neutrophils.^{15,56} The CD66b antigen belongs to the family of carcinoembryonic antigen-related cell adhesion molecules that exhibit rapid up-regulation after neutrophil activation.⁵⁷ Because there are no established IHC markers to date, we do not know whether the CD66b-positive neutrophils within tumors actually are granulocytic MDSCs that were attracted to the tumor or whether they are blood-derived neutrophils that subsequently were converted to a protumor behavior by the tumor microenvironment. Recent *in vitro* studies have suggested that TGF- β blockade changes only local chemoattraction and/or the intratumoral adaptation of neutrophils rather than changing the general phenotype of myeloid cells.⁴⁷ Moreover, the functional relevance of those peripheral blood MDSCs to tumor progression in humans currently remains unclear.⁴³

MPO is one of the principal enzymes released from neutrophil azurophilic granules. For a long time, MPO has been considered a key constituent of the neutrophil's cytotoxic armament, because it catalyzes the formation of hypochlorous acid, a potent oxidant that displays bactericidal activity *in vitro*.⁵⁸ However, MPO is an enzyme contained in lysosomes of neutrophils and, to a lesser extent, in monocytes and tissue macrophages.⁵⁹ Therefore, the amount of MPO-positive cells may not be an accurate marker of activated intratumoral neutrophils. Moreover, we identified no significant correlation between MPO-positive neutrophils and the clinical outcome of patients with NSCLC.

Although they have been few in number, clinical studies that have examined TANs have demonstrated their significant potential in predicting poor clinical outcomes.^{15,43} Those studies were performed before the use of advanced IHC techniques; therefore, only hematoxylin and eosin-stained sections were examined, and that method is unreliable for distinguishing between the different inflammatory cell types.^{30,60}

In conclusion, intratumoral CD66b-positive neutrophils in patients with resectable NSCLC had prognostic value for disease recurrence. This indicates that the time to recurrence may be governed at least in part by the state of the local innate immune response. Moreover, we demonstrated that the immune balance between intratumoral CD66b-positive neutrophils and CD8-positive T cells detected on TMAs by IHC correlated better with a high CIR and poor OS. Therefore, the number of

intratumoral CD66b-positive neutrophils and the iNTR may help substantially to identify a subset of high-risk patients with resectable NSCLC, notably those with early stage I NSCLC. The benefit of active surveillance in this subpopulation of patients with a high risk of recurrence should be considered further.

FUNDING SOURCES

No specific funding was disclosed.

CONFLICT OF INTEREST DISCLOSURES

The authors made no disclosures.

REFERENCES

- Shibuya K, Mathers CD, Boschi-Pinto C, Lopez AD, Murray CJ. Global and regional estimates of cancer mortality and incidence by site: II. Results for the global burden of disease 2000 [serial online]. *BMC Cancer*. 2002; 2:37.
- Blanchon F, Grivaux M, Asselain B, et al. Four-year mortality in patients with non-small-cell lung cancer: development and validation of a prognostic index. *Lancet Oncol*. 2006; 7:829-836.
- Potti A, Mukherjee S, Petersen R, et al. A genomic strategy to refine prognosis in early-stage non-small-cell lung cancer. *N Engl J Med*. 2006;355:570-580.
- Mantovani A, Allavena P, Sica A, Balkwill F. Cancer-related inflammation. *Nature*. 2008;454:436-444.
- Hofman PM. Pathobiology of the neutrophil-intestinal epithelial cell interaction: role in carcinogenesis. *World J Gastroenterol*. 2010;16:5790-5800.
- Flavell RA, Sanjabi S, Wrzesinski SH, Licona-Limon P. The polarization of immune cells in the tumour environment by TGFbeta. *Nat Rev Immunol*. 2010;10:554-567.
- Lee HJ, Lee EK, Lee KJ, Hong SW, Yoon Y, Kim JS. Ectopic expression of neutrophil gelatinase-associated lipocalin suppresses the invasion and liver metastasis of colon cancer cells. *Int J Cancer*. 2006;118:2490-2497.
- Yang P, Bamlet WR, Sun Z, et al. Alpha1-antitrypsin and neutrophil elastase imbalance and lung cancer risk. *Chest*. 2005;128:445-452.
- Wu QD, Wang JH, Condron C, Bouchier-Hayes D, Redmond HP. Human neutrophils facilitate tumor cell transendothelial migration. *Am J Physiol Cell Physiol*. 2001; 280:C814-C822.
- Coussens LM, Werb Z. Inflammatory cells and cancer: think different! *J Exp Med*. 2001;193:F23-F26.
- Ishikawa K, Takenaga K, Akimoto M, et al. ROS-generating mitochondrial DNA mutations can regulate tumor cell metastasis. *Science*. 2008;320:661-664.
- Di Carlo E, Forni G, Lollini P, Colombo MP, Modesti A, Musiani P. The intriguing role of polymorphonuclear neutrophils in antitumor reactions. *Blood*. 2001;97:339-345.
- Hanahan D, Weinberg RA. Hallmarks of cancer: the next generation. *Cell*. 2011;144:646-674.
- Pages F, Galon J, Dieu-Nosjean MC, Tartour E, Sautes-Fridman C, Fridman WH. Immune infiltration in human tumors: a prognostic factor that should not be ignored. *Oncogene*. 2010;29:1093-1102.
- Jensen HK, Donskov F, Marcussen N, Nordmark M, Lundbeck F, von der Maase H. Presence of intratumoral neutrophils is an independent prognostic factor in localized renal cell carcinoma. *J Clin Oncol*. 2009;27:4709-4717.
- An X, Ding PR, Wang FH, Jiang WQ, Li YH. Elevated neutrophil to lymphocyte ratio predicts poor prognosis in nasopharyngeal carcinoma [serial online]. *Tumour Biol*. 2011;32:317-324.
- Cho H, Hur HW, Kim SW, et al. Pre-treatment neutrophil to lymphocyte ratio is elevated in epithelial ovarian cancer and predicts survival after treatment. *Cancer Immunol Immunother*. 2009;58:15-23.
- Ohno Y, Nakashima J, Ohori M, Hatano T, Tachibana M. Pretreatment neutrophil-to-lymphocyte ratio as an independent predictor of recurrence in patients with nonmetastatic renal cell carcinoma. *J Urol*. 2010;184:873-878.
- Goldstraw P. The seventh edition of TNM in lung cancer: what now? *J Thorac Oncol*. 2009;4:671-673.
- Travis WD, Brambilla E, Muller-Hermelink HK, Harris CC, eds. World Health Organization Classification of Tumours: Pathology and Genetics of Tumours of the Lung, Pleura, Thymus, and Heart. Lyon, France: IARC Press; 2004.
- Travis WD, Brambilla E, Noguchi M, et al. International Association for the Study of Lung Cancer/American Thoracic Society/European Respiratory Society international multidisciplinary classification of lung adenocarcinoma. *J Thorac Oncol*. 2011;6:244-285.
- Hofman P, Butori C, Haver K, et al. Prognostic significance of cortactin levels in head and neck squamous cell carcinoma: comparison with epidermal growth factor receptor status. *Br J Cancer*. 2008;98:956-964.
- Ilie M, Mazure NM, Hofman V, et al. High levels of carbonic anhydrase IX in tumour tissue and plasma are biomarkers of poor prognostic in patients with non-small cell lung cancer. *Br J Cancer*. 2010;102:1627-1635.
- Schemper M, Smith TL. A note on quantifying follow-up in studies of failure time. *Control Clin Trials*. 1996;17:343-346.
- Coussens LM, Werb Z. Inflammation and cancer. *Nature*. 2002;420:860-867.
- Nozawa H, Chiu C, Hanahan D. Infiltrating neutrophils mediate the initial angiogenic switch in a mouse model of multistage carcinogenesis. *Proc Natl Acad Sci U S A*. 2006;103:12493-12498.
- Whiteside TL. The tumor microenvironment and its role in promoting tumor growth. *Oncogene*. 2008;27:5904-5912.
- Rodriguez PC, Ernstoff MS, Hernandez C, et al. Arginase I-producing myeloid-derived suppressor cells in renal cell carcinoma are a subpopulation of activated granulocytes. *Cancer Res*. 2009;69:1553-1560.
- Qian BZ, Pollard JW. Macrophage diversity enhances tumor progression and metastasis. *Cell*. 2010;141:39-51.
- Houghton AM. The paradox of tumor-associated neutrophils: fueling tumor growth with cytotoxic substances. *Cell Cycle*. 2010;9:1732-1737.
- Gungor N, Pennings JL, Knaapen AM, et al. Transcriptional profiling of the acute pulmonary inflammatory response induced by LPS: role of neutrophils [serial online]. *Respir Res*. 2010;11:24.

32. de Visser KE, Eichten A, Coussens LM. Paradoxical roles of the immune system during cancer development. *Nat Rev Cancer*. 2006;6:24-37.
33. Stockley RA. Neutrophils and the pathogenesis of COPD. *Chest*. 2002;121(5 suppl):151S-155S.
34. Gungor N, Knaapen AM, Munnia A, et al. Genotoxic effects of neutrophils and hypochlorous acid. *Mutagenesis*. 2010;25:149-154.
35. Soo CC, Haqqani AS, Hidirolou N, Swanson JE, Parker RS, Birnboim HC. Dose-dependent effects of dietary alpha- and gamma-tocopherols on genetic instability in mouse Mutatec tumors. *J Natl Cancer Inst*. 2004;96:796-800.
36. Wistuba II. Genetics of preneoplasia: lessons from lung cancer. *Curr Mol Med*. 2007;7:3-14.
37. Gungor N, Haegens A, Knaapen AM, et al. Lung inflammation is associated with reduced pulmonary nucleotide excision repair in vivo. *Mutagenesis*. 2010;25:77-82.
38. Balkwill F. Tumour necrosis factor and cancer. *Nat Rev Cancer*. 2009;9:361-371.
39. Belloccq A, Antoine M, Flahault A, et al. Neutrophil alveolitis in bronchioloalveolar carcinoma: induction by tumor-derived interleukin-8 and relation to clinical outcome. *Am J Pathol*. 1998;152:83-92.
40. Ji H, Houghton AM, Mariani TJ, et al. K-ras activation generates an inflammatory response in lung tumors. *Oncogene*. 2006;25:2105-2112.
41. Mascaux C, Iannino N, Martin B, et al. The role of RAS oncogene in survival of patients with lung cancer: a systematic review of the literature with meta-analysis. *Br J Cancer*. 2005;92:131-139.
42. Wislez M, Fleury-Feith J, Rabbe N, et al. Tumor-derived granulocyte-macrophage colony-stimulating factor and granulocyte colony-stimulating factor prolong the survival of neutrophils infiltrating bronchoalveolar subtype pulmonary adenocarcinoma. *Am J Pathol*. 2001;159:1423-1433.
43. Trellakis S, Bruderek K, Dumitru CA, et al. Polymorphonuclear granulocytes in human head and neck cancer: enhanced inflammatory activity, modulation by cancer cells and expansion in advanced disease [serial online] [published online ahead of print December 28, 2010]. *Int J Cancer*. 2010.
44. Kim R, Emi M, Tanabe K. Cancer immunoediting from immune surveillance to immune escape. *Immunology*. 2007;121:1-14.
45. Sznurkowski JJ, Zawrocki A, Emerich J, Biernat W. Prognostic significance of CD4+ and CD8+ T cell infiltration within cancer cell nests in vulvar squamous cell carcinoma. *Int J Gynecol Cancer*. 2011;21:717-721.
46. Yang L, Pang Y, Moses HL. TGF-beta and immune cells: an important regulatory axis in the tumor microenvironment and progression. *Trends Immunol*. 2010;31:220-227.
47. Fridlender ZG, Sun J, Kim S, et al. Polarization of tumor-associated neutrophil phenotype by TGF-beta: "N1" versus "N2" TAN. *Cancer Cell*. 2009;16:183-194.
48. Mantovani A. The yin-yang of tumor-associated neutrophils. *Cancer Cell*. 2009;16:173-174.
49. Roberts AB, Wakefield LM. The 2 faces of transforming growth factor beta in carcinogenesis. *Proc Natl Acad Sci U S A*. 2003;100:8621-8623.
50. Bierie B, Moses HL. TGF-beta and cancer. *Cytokine Growth Factor Rev*. 2006;17:29-40.
51. Ju MJ, Qiu SJ, Fan J, et al. Peritumoral activated hepatic stellate cells predict poor clinical outcome in hepatocellular carcinoma after curative resection. *Am J Clin Pathol*. 2009;131:498-510.
52. Gabrilovich DI, Nagaraj S. Myeloid-derived suppressor cells as regulators of the immune system. *Nat Rev Immunol*. 2009;9:162-174.
53. Tvinnereim AR, Hamilton SE, Harty JT. Neutrophil involvement in cross-priming CD8+ T cell responses to bacterial antigens. *J Immunol*. 2004;173:1994-2002.
54. Sarraf KM, Belcher E, Raevsky E, Nicholson AG, Goldstraw P, Lim E. Neutrophil/lymphocyte ratio and its association with survival after complete resection in non-small cell lung cancer. *J Thorac Cardiovasc Surg*. 2009;137:425-428.
55. Li YW, Qiu SJ, Fan J, et al. Intratumoral neutrophils: a poor prognostic factor for hepatocellular carcinoma following resection [serial online]. *J Hepatol*. 2011;54:497-505.
56. Murdoch C, Muthana M, Coffelt SB, Lewis CE. The role of myeloid cells in the promotion of tumour angiogenesis. *Nat Rev Cancer*. 2008;8:618-631.
57. Elghetany MT. Surface antigen changes during normal neutrophilic development: a critical review. *Blood Cells Mol Dis*. 2002;28:260-274.
58. Winterbourn CC. Biological reactivity and biomarkers of the neutrophil oxidant, hypochlorous acid. *Toxicology*. 2002;181-182:223-227.
59. Krawisz JE, Sharon P, Stenson WF. Quantitative assay for acute intestinal inflammation based on myeloperoxidase activity. Assessment of inflammation in rat and hamster models. *Gastroenterology*. 1984;87:1344-1350.
60. Caruso RA, Bellocco R, Pagano M, Bertoli G, Rigoli L, Inferrera C. Prognostic value of intratumoral neutrophils in advanced gastric carcinoma in a high-risk area in northern Italy. *Mod Pathol*. 2002;15:831-837.

Table 1. Characteristics and performance of most recent tissue-based candidate biomarkers for the early detection of lung cancer

References	Specimens	Type of marker	Analyte	Clinical purpose	No. of markers	Pathologic subtype	Assay platform	Preclinical samples	BM dev. phase	Training set	Validation set	Sensitivity	Specificity	AUC
Halling (26)	Bronchial specimens	DNA	5p15, 7p12 (EGFR), 8q24 (C-MYC), CEP6	Diagnosis	4	NSCLC	FISH + cytology	n/a	I	n/a	137	61–75 ^a	83–100 ^a	n/a
Massion (27)	Bronchial biopsies	DNA	TP63, MYC, CEP3, CEP6 + sputum cytology + demographics	Diagnosis	4	NSCLC	FISH	n/a	II	n/a	70	n/a	n/a	92.6
Feng (38)	Tumors and normal tissues	DNA methylation	RAAR, BVES, CDKN2A, KCNH5, RASSF1, CDH13, RUNX, CDH1	Diagnosis	8	NSCLC	Methylation array	n/a	I	49	n/a	n/a	n/a	n/a
Anglim (22)	Tumors and normal tissues	DNA methylation	GDNF, MTHFR, OPCML, TNFRSF25, TCF21, PAX8, PTPRN2, and PITX2	Diagnosis	8	SCC	Methylation array	n/a	I	43	n/a	95.6 ^a	95.6 ^a	n/a
Schmidt (25)	Bronchial aspirates	DNA methylation	SHOX2	Diagnosis	1	NSCLC	PCR	n/a	II	n/a	523	68	95	86
Richards (24)	Tumors and normal tissues	DNA methylation	TCF21	Diagnosis	1	NSCLC	PCR	n/a	II	42	63	76	98 ^a	n/a
Spira (37)	Airway epithelium	mRNA	Gene expression signature	Diagnosis	80	NSCLC	Affy array	n/a	II	77	52	80	84	n/a
Beane (28)	Airway epithelium	mRNA	Gene expression signature + clinical factors	Diagnosis	80	NSCLC and SCLC	Affy array	n/a	II	76	62	100	91	97

(Continued on the following page)

Table 1. Characteristics and performance of most recent tissue-based candidate biomarkers for the early detection of lung cancer (Cont'd)

References	Specimens	Type of marker	Analyte	Clinical purpose	No. of markers	Pathologic subtype	Assay platform	Preclinical samples	BM dev. phase	Training set	Validation set	Sensitivity	Specificity	AUC
Kim (111)	Tumors and normal tissues	mRNA	CBLC, CYP24A1, ALDH3A1, AKR1B10, S100P, PLUNC, LOC147	Diagnosis	7	NSCLC	qRT-PCR	n/a	II	32	36 ^b	n/a	n/a	n/a
Blomquist (30)	Tumors and normal tissues	mRNA	CAT, CEBPG, E2F1, ERCC4, ERCC5, GPX1, GPX3, GSTM3, GSTP1, GSTT1, GSTZ1, MGST1, SOD1, XRCC1	Diagnosis	14	NSCLC	RT-PCR	n/a	II	n/a	49, 40	n/a	n/a	82–87
Rahman (36)	Bronchial biopsies	MALDI signature	TMLS4, ACBP, CSTA, cyto C, MIF, ubiquitin, ACBP, Des-ubiquitin	Diagnosis	9	NSCLC	MALDI/MS	n/a	II	51	60	66	88	77

NOTE: Data organized by year of publication and type of marker considered.

Abbreviations: AUC, area under the curve; BM dev. phase, biomarker development phase; n/a, not available; qPCR, quantitative real-time PCR; RT-PCR, reverse transcriptase PCR; SCC, squamous cell carcinoma; SCLC, small cell lung cancer.

^aValues derived from training set only.

^bValidation and training sets overlap.

Table 2. Characteristics and performance of most recent blood-based candidate biomarkers for the early detection of lung cancer

References	Specimens	Type of marker	Analyte	Clinical purpose	No. of markers	Pathologic subtype	Assay platform	Preclinical samples	BM dev. phase	Training set	Validation set	Sensitivity	Specificity	AUC
Zhong (60)	Serum	AutoAB	Phage peptide clones	Diagnosis	5	Lung cancer	ELISA	n/a	II	46	56	91 ^a	91 ^a	99 ^a
Chapman (64)	Serum	AutoAB	p53, cmyc, HER2, NY-ESO-1, CAGE, MUCT, GBU4-5	Diagnosis	7	Lung cancer	ELISA	n/a	I	154	n/a	n/a	n/a	n/a
Qiu (65)	Serum	AutoAB	Annexin I, 14-3-3 theta, LAMR1	Diagnosis	3	NSCLC	Protein array	170	III	170	170	51	82	73
Wu (63)	Serum	AutoAB	Phage peptide clones	Diagnosis	6	NSCLC	ELISA	n/a	II	20	180	92	92	96
Farlow (112)	Serum	AutoAB	IMPDH, PGAM1, ubiquilin, ANXA1, ANXA2, HSP70-9B	Diagnosis	6	NSCLC	ELISA	n/a	II	196	n/a	94.8 ^a	91.1 ^a	96.4 ^a
Boyle (113)	Serum	AutoAB	p53, NY-ESO-1, CAGE, GBU4-5, Annexin 1, and SOX2	Diagnosis	6	NSCLC	ELISA	n/a	II	241	255	32	91	64
Greenberg (48)	Serum	DNA methylation	S-Adenosylmethionine	Diagnosis	1	Lung cancer	HPLC	n/a	I	68	n/a	92-100 ^a	91-97 ^a	94-99 ^a
Begum (49)	Serum	DNA methylation	APC, CDH1, MGMT, DCC, RASSF1A, AIM	Diagnosis	6	NSCLC	qPCR	n/a	II	32-639	106	84	57	n/a
Chen (114)	Serum	miRNA	miRNA signature	Diagnosis	10	NSCLC	qRT-PCR	n/a	II	310	310	93	90	97
Bianchi (54)	Serum	miRNA	miRNA signature	Diagnosis	34	NSCLC	qRT-PCR	n/a	II	64	64	71	90	89
Kulpa (115)	Serum	Protein	CEA, CYFRA 21-1, SCC-Ag, NSE	Diagnosis	4	SCC	ELISA	n/a	II	420	420	20-62	95	71-90
Patz (55)	Serum	Protein	CEA, RBP4, hAAT, SCCA	Diagnosis	4	Lung cancer	ELISA	n/a	II	100	97	78	75	n/a
Takano (116)	Serum	Protein	Nectin-4	Diagnosis	1	NSCLC	ELISA	n/a	II	185	295	54	98	n/a
Yildiz (56)	Serum	Protein	MALDI/MS signature	Diagnosis	7	NSCLC	MALDI/MS	n/a	II	185	106	58	85.7	82
Pecot (19)	Serum	Protein	Model: MALDI/MS signature + clinical and imaging data	Diagnosis	7	Indeterm. lung nodule	MALDI/MS	n/a	II	100	100	n/a	n/a	72
Diamandis (117)	Serum	Protein	Penatrxin-3	Diagnosis	1	Lung cancer	ELISA	n/a	I	426	426	37-48	80-90	60-74

(Continued on the following page)

Table 2. Characteristics and performance of most recent blood-based candidate biomarkers for the early detection of lung cancer (Cont'd)

References	Specimens	Type of marker	Analyte	Clinical purpose	No. of markers	Pathologic subtype	Assay platform	Preclinical samples	BM dev. phase	Training set	Validation set	Sensitivity	Specificity	AUC
Ostroff (118)	Serum	Aptamers	<i>cadherin-1</i> , <i>CD30 ligand</i> , <i>endostatin</i> , <i>HSP90a</i> , <i>LRI/G3</i> , <i>MIP-4</i> , <i>pleiotrophin</i> , <i>PRKCI</i> , <i>RGM-C</i> , <i>SCF-sR</i> , <i>sL-selectin</i> , and <i>YES</i>	Diagnosis	6	NSCLC	Aptamers	n/a	II	985	341	89	83	90
Zhong (119)	Plasma	AutoAB	TAA signature	Diagnosis	5	NSCLC	Protein microarray	5	I	81	n/a	90 ^a	95 ^a	n/a
Kneip (120)	Plasma	DNA methylation	SHOX2	Diagnosis	1	NSCLC	qPCR	n/a	II	40	371	60	90	78
Shen (121)	Plasma	miRNA	miRNA-21, -126, -210, -486-5p	Diagnosis	4	NSCLC	qRT-PCR	n/a	II	28	87	86	97	93
Wei (122)	Plasma	miRNA	miR-21	Diagnosis	1	NSCLC	qRT-PCR	n/a	I	93	n/a	76 ^a	70 ^a	77.5 ^a
Taguchi (123)	Plasma	Protein, 2 panels	<i>EGFR</i> , <i>SFTPB</i> , <i>WFDC2</i> , <i>ANGPTL3</i> , <i>ANXA1</i> , <i>YWHAQ</i> , <i>Lmr1</i>	Diagnosis	7	NSLCL	ELISA	52	III	n/a	n/a	n/a	n/a	89
Boeri (53)	Plasma/ tissues	miRNA	miRNA signature	Diagnosis	13	Lung cancer	miRNA array and RT-PCR	n/a	II	19	22	75	100	88
Boeri (53)	Plasma/ tissues	miRNA	miRNA signature	Diagnosis	15	Lung cancer	miRNA array and RT-PCR	25	III	20	25	80	90	85

NOTE: Data organized by year of publication, specimen type, and type of marker considered.

Abbreviations: ADC, adenocarcinoma; AUC, area under the curve; AutoAB, autoantibody; BM dev. phase, biomarker development phase; HPLC, high-performance liquid chromatography; n/a, not available; qPCR, quantitative real-time PCR; RT-PCR, reverse transcriptase PCR; SCC, squamous cell carcinoma.

^aValues derived from training set only.

Table 3 - Annex

REporting recommendations for tumor MARKer prognostic studies (REMARK)

Table 1 REporting recommendations for tumor MARKer prognostic studies (REMARK).

Introduction

- 1 State the marker examined, the study objectives, and any prespecified hypotheses.

Materials and methods

Patients

- 2 Describe the characteristics (e.g. disease stage or comorbidities) of the study patients, including their source and inclusion and exclusion criteria.
- 3 Describe treatments received and how chosen (e.g. randomized or rule-based).

Specimen characteristics

- 4 Describe type of biological material used (including control samples) and methods of preservation and storage.

Assay methods

- 5 Specify the assay method used and provide (or reference) a detailed protocol, including specific reagents or kits used, quality control procedures, reproducibility assessments, quantitation methods, and scoring and reporting protocols. Specify whether and how assays were performed blinded to the study endpoint.

Study design

- 6 State the method of case selection, including whether prospective or retrospective and whether stratification or matching (e.g. by stage of disease or age) was used. Specify the time period from which cases were taken, the end of the follow-up period, and the median follow-up time.
- 7 Precisely define all clinical endpoints examined.
- 8 List all candidate variables initially examined or considered for inclusion in models.
- 9 Give rationale for sample size; if the study was designed to detect a specified effect size, give the target power and effect size.

Statistical analysis methods

- 10 Specify all statistical methods, including details of any variable selection procedures and other model-building issues, how model assumptions were verified, and how missing data were handled.
- 11 Clarify how marker values were handled in the analyses; if relevant, describe methods used for cutpoint determination.

Results

Data

- 12 Describe the flow of patients through the study, including the number of patients included in each stage of the analysis (a diagram may be helpful) and reasons for dropout. Specifically, both overall and for each subgroup extensively examined report the numbers of patients and the number of events.
- 13 Report distributions of basic demographic characteristics (at least age and sex), standard (disease-specific) prognostic variables, and tumor marker, including numbers of missing values.

Analysis and presentation

- 14 Show the relation of the marker to standard prognostic variables.
- 15 Present univariate analyses showing the relation between the marker and outcome, with the estimated effect (e.g. hazard ratio and survival probability). Preferably provide similar analyses for all other variables being analyzed. For the effect of a tumor marker on a time-to-event outcome, a Kaplan–Meier plot is recommended.
- 16 For key multivariable analyses, report estimated effects (e.g. hazard ratio) with confidence intervals for the marker and, at least for the final model, all other variables in the model.
- 17 Among reported results, provide estimated effects with confidence intervals from an analysis in which the marker and standard prognostic variables are included, regardless of their statistical significance.
- 18 If done, report results of further investigations, such as checking assumptions, sensitivity analyses, and internal validation.

Discussion

- 19 Interpret the results in the context of the prespecified hypotheses and other relevant studies; include a discussion of limitations of the study.
- 20 Discuss implications for future research and clinical value.

Table 4 - Annex

Study [ref]	Cancer cases	Control size	CTC isolation method	Sampling time	Histology	Results
Hou HW, et al. 2013	20	20	Dean Flow Fractionation	Before and after treatment	Metastatic III/IV NSCLC	Feasibility (5 to 88 CTCs/mL)
Devriese LA, et al. 2012	46	46	CellSearch and multi-marker qPCR	Before treatment	Metastatic III/IV NSCLC	Diagnostic biomarker
Hirose T, et al. 2012	33	—	CellSearch	Before treatment	Metastatic III/IV NSCLC	Predictive biomarker for the effectiveness of cytotoxic chemotherapy (gemcitabine and carboplatin)
Isobe K, et al. 2012	24	—	CellSearch	After development of EGFR-TKI resistance	Metastatic III/IV NSCLC	Presence of CTCs was correlated with the positivity of EGFR mutation in cfDNA
Ilie M, et al. 2012	87	—	ISET	Before treatment	Lung adenocarcinoma	ALK feasibility on CTCs
Das M, et al. 2012	17	—	Cytophotometry	Before and after treatment (platinum-based therapy)	Metastatic III/IV NSCLC	Low expression of ERCC1 on CTCs correlates with PFS in patients with metastatic NSCLC receiving platinum-based therapy.
Punnoose EA, et al. 2012	41	—	CellSearch	Before and after treatment (erlotinib and pertuzumab)	Metastatic III/IV NSCLC	Decreases in CTC numbers during treatment of patients with advanced NSCLC with targeted therapies are associated with clinical responses measured by FDG-PET and CT imaging
Nieva J, et al. 2012	28	—	Enrichment free fluorescent labeling with automated digital microscopy	Before chemotherapy	Metastatic IV NSCLC	Higher numbers of detected CTCs were associated with an unfavorable prognosis
Krebs MG, et al. 2012	40	—	CellSearch and ISET	Before chemotherapy	Metastatic III/IV NSCLC	Complementary dual technology approach to CTC analysis

Table 4 - Annex

Lecharpentier A, et al. 2011	6	6	ISET and triple fluorescent labeling	Unknown	Metastatic NSCLC	Exploratory study demonstrates that the majority of isolated or clusters of CTCs in patients with advanced metastatic NSCLC harbor a dual epithelial-mesenchymal phenotype
Krebs MG, et al. 2011	101	—	CellSearch	Before and after administration of one cycle of standard chemotherapy	Untreated, stage III/IV NSCLC	Prognostic and predictive biomarker
Hofman V, et al. 2012	250	59	ISET	Before surgery	Resectable NSCLC (I-IV)	Diagnostic biomarker
Hofman V, et al. 2011	210	40	CellSearch and ISET	Before surgery	Resectable NSCLC (I-IV)	Prognostic biomarker
Yoon SO, et al. 2011	79	—	Nested (for CK19) or semi-nested (for TTF-1) real-time RT-PCR	Before surgery and 1 month after surgery	Resectable NSCLC (I-III)	Prognostic biomarker
Okumura Y, et al. 2009	30	—	CellSearch	Before surgery	Resectable NSCLC	Prognostic biomarker
Wu C, et al. 2009	47	31	CellSearch	Before chemotherapy	34 NSCLC (I-IV) and 13 SCLC	Predictive biomarker
Liu L, et al. 2008	134	186	Density gradient centrifugation and nested RT-PCR assay	Before treatment	NSCLC (I-IV) without preoperative chemo- and/or radiation therapy	Diagnostic and prognostic biomarker
Sher YP, et al. 2005	54	24	Density gradient centrifugation and nested RT-PCR assay	Before treatment	NSCLC (I-IV) without preoperative chemo- and/or radiation therapy	Prognostic and predictive biomarker
Yamashita J, et al. 2002	103	Unknown	Density gradient centrifugation and RT-PCR assay for carcinoembryonic antigen	Before and after surgery	Resectable NSCLC	Prognostic biomarker

Table 4 - Annex

Yie SM, et al. 2009	143	172	RT-PCR ELISA	Before and after treatment	NSCLC (I-IV) without preoperative chemo- and/or radiation therapy	Prognostic biomarker (Survivin-expressing CTCs)
Funaki S, et al. 2011	94	—	RosetteSep® Human CD45 Depletion Cocktail (Stemcell Technologies, Inc.)	During treatment	NSCLC (I-IV) without preoperative chemo- and/or radiation therapy	Prognostic biomarker
Guo Y, et al. 2009	83	30	Nested RT-PCR	Before treatment	NSCLC NOS	Diagnostic biomarker
Sheu CC, et al. 2006	100	147	Membrane array-based multimarker assay	Before treatment	NSCLC (I-IV)	Diagnostic and prognostic biomarker
Wendel M, et al. 2012	78	—	HD-CTC technology	Before treatment	Chemotherapy-naïve NSCLC (I-IV)	Prognostic biomarker
Farace F, et al. 2011	20	—	CellSearch and ISET	Before treatment	Stage IV NSCLC	Discrepancies between the number of CTC enumerated by the CellSearch and the ISET systems
Tanaka F, et al. 2009	125	25	CellSearch	Before treatment	Chemotherapy-naïve NSCLC (I-IV)	Diagnostic and prognostic biomarker
Huang TH, et al. 2007	51	40	ICC and RT-PCR	Before treatment	Chemotherapy-naïve NSCLC (I-IV)	Diagnostic and prognostic biomarker
Hayes DC, et al. 2006	49	25	RT-PCR	Before treatment	NSCLC NOS	Diagnostic and prognostic biomarker
Sienel W, et al. 2003	62	—	ICC	During treatment	Resectable NSCLC (I-III)	Prognostic biomarker



Cancer Research

Expression of a Truncated Active Form of VDAC1 in Lung Cancer Associates with Hypoxic Cell Survival and Correlates with Progression to Chemotherapy Resistance

M. Christiane Brahim-Horn, Danya Ben-Hail, Marius Ilie, et al.

Cancer Res 2012;72:2140-2150. Published OnlineFirst March 2, 2012.

Updated version Access the most recent version of this article at:
doi:[10.1158/0008-5472.CAN-11-3940](https://doi.org/10.1158/0008-5472.CAN-11-3940)

Supplementary Material Access the most recent supplemental material at:
<http://cancerres.aacrjournals.org/content/suppl/2012/03/02/0008-5472.CAN-11-3940.DC1.html>

Cited Articles This article cites by 38 articles, 12 of which you can access for free at:
<http://cancerres.aacrjournals.org/content/72/8/2140.full.html#ref-list-1>

Citing articles This article has been cited by 1 HighWire-hosted articles. Access the articles at:
<http://cancerres.aacrjournals.org/content/72/8/2140.full.html#related-urls>

E-mail alerts [Sign up to receive free email-alerts](#) related to this article or journal.

Reprints and Subscriptions To order reprints of this article or to subscribe to the journal, contact the AACR Publications Department at pubs@aacr.org.

Permissions To request permission to re-use all or part of this article, contact the AACR Publications Department at permissions@aacr.org.

Expression of a Truncated Active Form of VDAC1 in Lung Cancer Associates with Hypoxic Cell Survival and Correlates with Progression to Chemotherapy Resistance

M. Christiane Brahimi-Horn¹, Danya Ben-Hail⁷, Marius Ilie^{2,3}, Pierre Gounon⁴, Matthieu Rouleau⁵, Véronique Hofman^{2,3}, Jérôme Doyen¹, Bernard Mari⁶, Varda Shoshan-Barmatz⁷, Paul Hofman^{2,3}, Jacques Pouyssegur¹, and Nathalie M. Mazure¹

Abstract

Resistance to chemotherapy-induced apoptosis of tumor cells represents a major hurdle to efficient cancer therapy. Although resistance is a characteristic of tumor cells that evolve in a low oxygen environment (hypoxia), the mechanisms involved remain elusive. We observed that mitochondria of certain hypoxic cells take on an enlarged appearance with reorganized cristae. In these cells, we found that a major mitochondrial protein regulating metabolism and apoptosis, the voltage-dependent anion channel 1 (VDAC1), was linked to chemoresistance when in a truncated (VDAC1-ΔC) but active form. The formation of truncated VDAC1, which had a similar channel activity and voltage dependency as full-length, was hypoxia-inducible factor-1 (HIF-1)-dependent and could be inhibited in the presence of the tetracycline antibiotics doxycycline and minocycline, known inhibitors of metalloproteases. Its formation was also reversible upon cell reoxygenation and associated with cell survival through binding to the antiapoptotic protein hexokinase. Hypoxic cells containing VDAC1-ΔC were less sensitive to staurosporine- and etoposide-induced cell death, and silencing of VDAC1-ΔC or treatment with the tetracycline antibiotics restored sensitivity. Clinically, VDAC1-ΔC was detected in tumor tissues of patients with lung adenocarcinomas and was found more frequently in large and late-stage tumors. Together, our findings show that via induction of VDAC1-ΔC, HIF-1 confers selective protection from apoptosis that allows maintenance of ATP and cell survival in hypoxia. VDAC1-ΔC may also hold promise as a biomarker for tumor progression in chemotherapy-resistant patients. *Cancer Res*; 72(8); 2140–50. ©2012 AACR.

Introduction

It is well established that cells exposed to the limiting oxygen microenvironment (hypoxia) of tumors acquire resistance to chemotherapy-induced apoptosis (1). However, the mechanisms involved and the implication of the key factor of the hypoxic response, the hypoxia-inducible factor (HIF), have not been extensively investigated (2). We recently reported that

several types of cancer cells exposed to a hypoxic microenvironment showed enlarged mitochondria with reorganized cristae; a result of modifications to fusion/fission (3). In addition, we showed that these cells were resistant to chemotherapy-induced apoptosis.

Because mitochondria regulate both metabolism and apoptosis (4–6) and that fusion/fission participates in apoptosis (7), we investigated whether certain mitochondrial proteins implicated in these processes play a role in resistance to apoptosis in a HIF-dependent manner.

The voltage-dependent anion channel (VDAC) regulates mitochondrial import and export of Ca^{2+} and metabolites including ATP and NADH and interacts with antiapoptotic proteins such as Bcl-2 and hexokinase in controlling the release of cytochrome *c* (8–11). Of note, screening by RNA interference identified VDAC1 as a protein implicated in resistance to cisplatin-induced cell death (12). In mammals VDAC is present in 3 highly homologous isoforms: VDAC1, VDAC2, and VDAC3, and VDAC1 is composed of 19 amphipathic β strands that form a β barrel and of a mobile N-terminal α helix, located inside the pore (13). Through binding to VDAC1 hexokinase, the enzyme that catalyzes the first step of glycolysis is optimally positioned for ATP capture (14) and hexokinase expression is increased by HIF (15). Thus, these interactions influence the function of

Authors' Affiliations: ¹Institute of Developmental Biology and Cancer Research, University of Nice, CNRS-UMR 6543, Centre Antoine Lacassagne; ²Human Tissue Biobank Unit/CRB and Laboratory of Clinical and Experimental Pathology, ³EA 4319, Faculty of Medicine, ⁴Centre Commun de Microscopie Appliquée, ⁵INSERM U898, University of Nice Sophia Antipolis, Nice; ⁶Institute of Molecular and Cellular Pharmacology, CNRS-UMR 6097, Valbonne, France; and ⁷Department of Life Sciences and National Institute for Biotechnology in the Negev, Ben-Gurion University of the Negev, Negev, Israel

Note: Supplementary data for this article are available at Cancer Research Online (<http://cancerres.aacrjournals.org/>).

Corresponding Authors: Nathalie M. Mazure, University of Nice, Centre Antoine Lacassagne, 33 avenue de valombrose, Nice 06189, France. Phone: 0492031230; Fax: 0492031235; E-mail: Nathalie.Mazure@unice.fr and M. Christiane Brahimi-Horn. E-mail: Christiane.Brahimi@unice.fr

doi: 10.1158/0008-5472.CAN-11-3940

©2012 American Association for Cancer Research.

both hexokinase and VDAC in cell death and metabolism. However, the role of VDAC in metabolism and apoptosis in hypoxia is not known.

Materials and Methods

Cell culture

LS174, PC3, HeLa, 786-O, SKMel, and A549 cells were grown in Dulbecco's Modified Eagle's Medium (Gibco-BRL) supplemented with 5% or 10% inactivated FBS as appropriate in penicillin G (50 U/mL) and streptomycin sulfate (50 μ g/mL). Dr. van de Wetering provided LS174 cells expressing the tetracycline repressor. A Bug-Box anaerobic workstation (Ruskin Technology Biotrace International Plc.) set at 1% oxygen, 94% nitrogen, and 5% carbon dioxide was used for hypoxia.

Transfection of short interfering RNA

The 21-nucleotide RNAs were synthesized (Eurogentec). siRNA sequences targeting SIMA (siCtl), and HIF-1 α were described previously (16). The short interfering RNA (siRNA) sequences targeting human VDAC1, VDAC2, VDAC3, and hexokinase II are given in the Supplementary Materials and Methods. HeLa cells were transfected with 40 nmol/L of siRNA 24 hours before normoxia or hypoxia, as described (3).

Reconstitution of purified VDAC1 and VDAC1- Δ C into a planar lipid bilayer, single-channel current recording and data analysis

VDAC1 and VDAC1- Δ C were purified from hypoxic HeLa cells after solubilizing in lauryldimethylamine-oxide (LDAO) and chromatography on hydroxyapatite, as described (17). Elution with increasing Pi concentrations separated VDAC1 and VDAC1- Δ C. The fractions containing either VDAC1 or VDAC1- Δ C were used for channel reconstitution into a planar lipid bilayer (PLB). A PLB was prepared from soybean asolectin dissolved in *n*-decane (50 mg/mL) and purified VDAC1 or VDAC1- Δ C was added to the *cis* chamber containing 1 mol/L NaCl and 10 mmol/L HEPES, pH, 7.4, unless otherwise indicated. After one or a few channels were inserted into the PLB, currents were recorded by voltage clamping with a Bilayer Clamp BC-525B Amplifier (Warner Instruments), the current trace duration was 4 or 10 seconds. Current was measured with respect to the *trans* side of the membrane (ground). The current was digitized on-line with a Digidata 1200 interface board and PCLAMP 6 software (Axon Instruments, Inc.).

Patients and tissue sample preparation

Forty-four patients who underwent surgery for lung adenocarcinoma between May 2007 and May 2010 at the Pasteur Hospital (Department of Thoracic Surgery, CHU de Nice, Nice, France) were selected. The patients received the necessary information concerning the study and consent was obtained. The study obtained approval of the ethics committee (CHU de Nice). The main clinical and histopathologic data are summarized in Supplementary Table S1. Morphologic classification of the tumors was assigned according to the World Health Organization (WHO) criteria (18). The tumors were staged according to the international tumor-node-metastasis system

(19). Follow-up data for all the patients were collected regularly. The median follow-up was 21 months (3.8–38.2 months). Among these patients, 13 relapsed (29.5%) and 6 (13.6%) died. Protein and miRNA were extracted from the same tissue sample using the protocol AllPrep DNA/RNA/Protein from QIAGEN.

Statistics

All values are the means \pm SD of the indicated number of determinations (*n*), and significant differences are based on the Student *t* test and *P* values indicated. All categorical data used numbers and percentages. Quantitative data were presented using the median and range or mean. Differences between groups were evaluated using the χ^2 test for categorical variables and the Student *t* test for continuous variables. SPSS 16.0 statistical software (SPSS Inc.) was used. All statistical tests were 2-sided, and *P* values less than 0.05 indicated statistical significance whereas *P* values between 0.05 and 0.10 indicated a statistical tendency.

Results

Hypoxic cells with enlarged mitochondria are resistant to chemotherapy and resistance implicates mitochondrial proteins

We reported that certain tumor-derived cell lines exposed to hypoxia showed a tubular mitochondrial network (PC3, SKMel) whereas others showed enlarged mitochondria (LS174, HeLa, A549; ref. 3). All cells showed a mitochondrial transmembrane potential ($\Delta\psi_m$) that was unchanged compared with normoxic cells but the latter group was resistant to staurosporine (STS)-induced apoptosis. We now show that when hypoxic LS174 cells with enlarged mitochondria were treated with STS, the $\Delta\psi_m$ decreased in normoxia but remained unaffected in hypoxia (Fig. 1A). In normoxia, LS174 cells released mitochondrial cytochrome *c* when incubated with STS whereas hypoxic LS174 cells with enlarged mitochondria did not (Fig. 1B). To address the implication of antiapoptotic proteins of the Bcl-2 family in hypoxic resistance to STS-induced apoptosis, we tested the effect of the BH3 domain mimetic ABT-737, an inhibitor of Bcl-2 and Bcl-X_L (20) on the apoptosis resistance of hypoxic cells. ABT-737 restored apoptosis as induced by STS in hypoxic LS174 cells (Fig. 1C), suggesting that association with a BH3 domain protein is implicated in resistance.

To better understand the molecular mechanisms behind resistance we compared the normoxic and hypoxic levels of anti- and proapoptotic proteins of the Bcl-2 family (Fig. 1D). LS174 and PC3 cells incubated in hypoxia (72 hours) were resistant or sensitive to STS-induced apoptosis, respectively. Bax and tBID were not or only slightly detected in LS174 cells (Fig. 1D) while the expression of Bak and Bcl-X_L were slightly enhanced in LS174 cells. Because Bcl-X_L has been described to interact with VDAC1 (21), we examined the level of VDAC. We observed hypoxic induction of a faster migrating SDS-PAGE form of VDAC in LS174 but not in PC3 cells (Fig. 1D). Immunoblots of mitochondrial fractions confirmed mitochondrial origin (Supplementary Fig. S1).

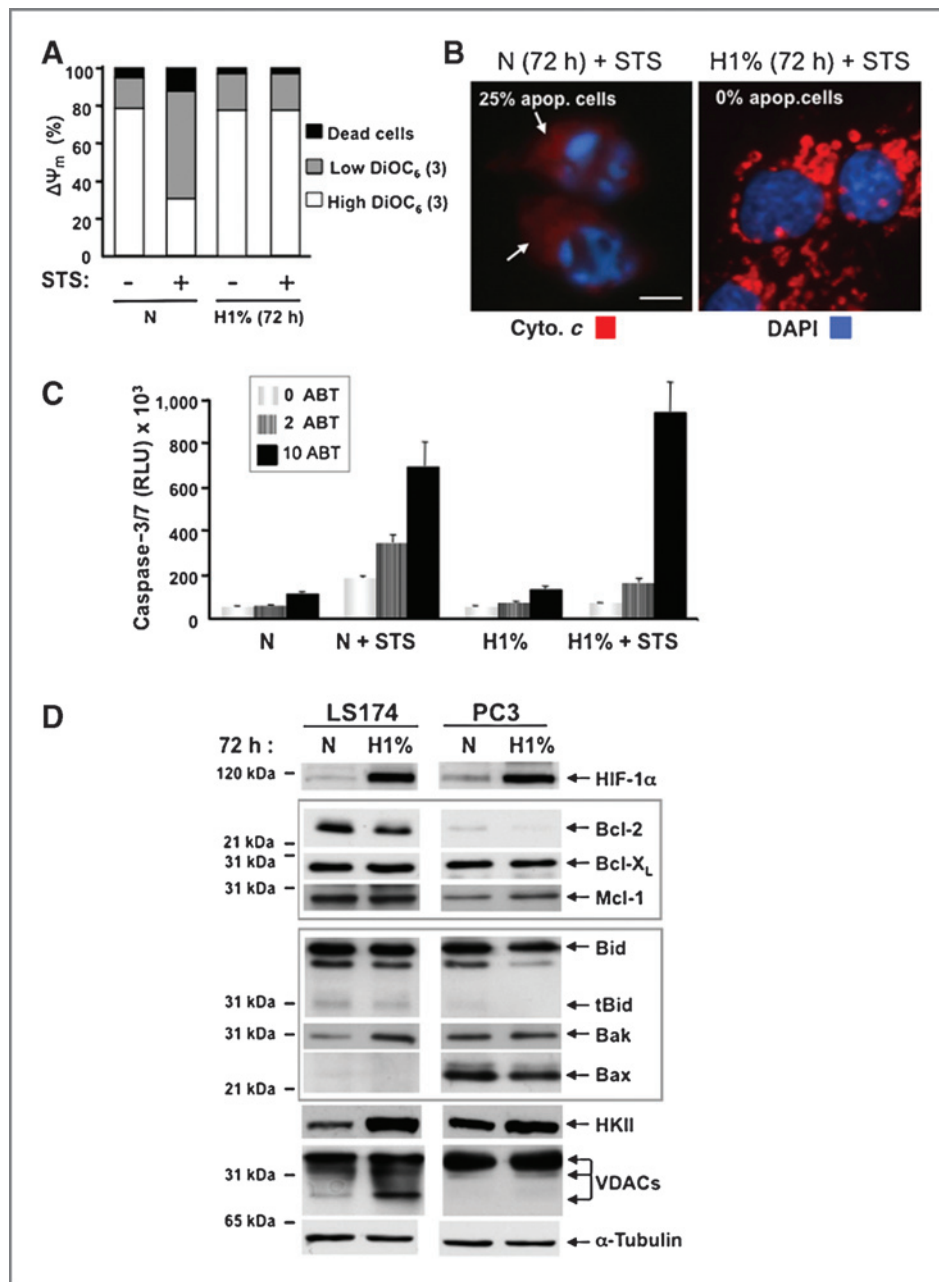


Figure 1. Anti- and proapoptotic proteins in the blockade of cytochrome c release. **A**, flow cytometric analysis of $\Delta\Psi_m$ of LS174 cells in normoxia (N) or hypoxia (H) without (–) or with (+) staurosporine (STS); 3 experiments. STS was added for 18 hours at 1 $\mu\text{mol/L}$. **B**, immunofluorescence to cytochrome c (Cyto. c) of LS174 cells in normoxia or hypoxia with STS, bar 7.3 μm . The percentage of apoptotic (apop.) cells is given. **C**, caspase activity of cells incubated in normoxia or hypoxia with or without the Bcl-2 and Bcl-X_L inhibitor ABT-737 (10 $\mu\text{mol/L}$) for the last 4 hours and without or with STS treatment for the last 4 hours ($n = 8$, 2 experiments). **D**, immunoblot of anti- and proapoptotic proteins and VDACS in LS174 and PC3 cells in normoxia or hypoxia. HK, hexokinase; DAPI, 4', 6-diamidino-2-phenylindole; RLU, relative luciferase units.

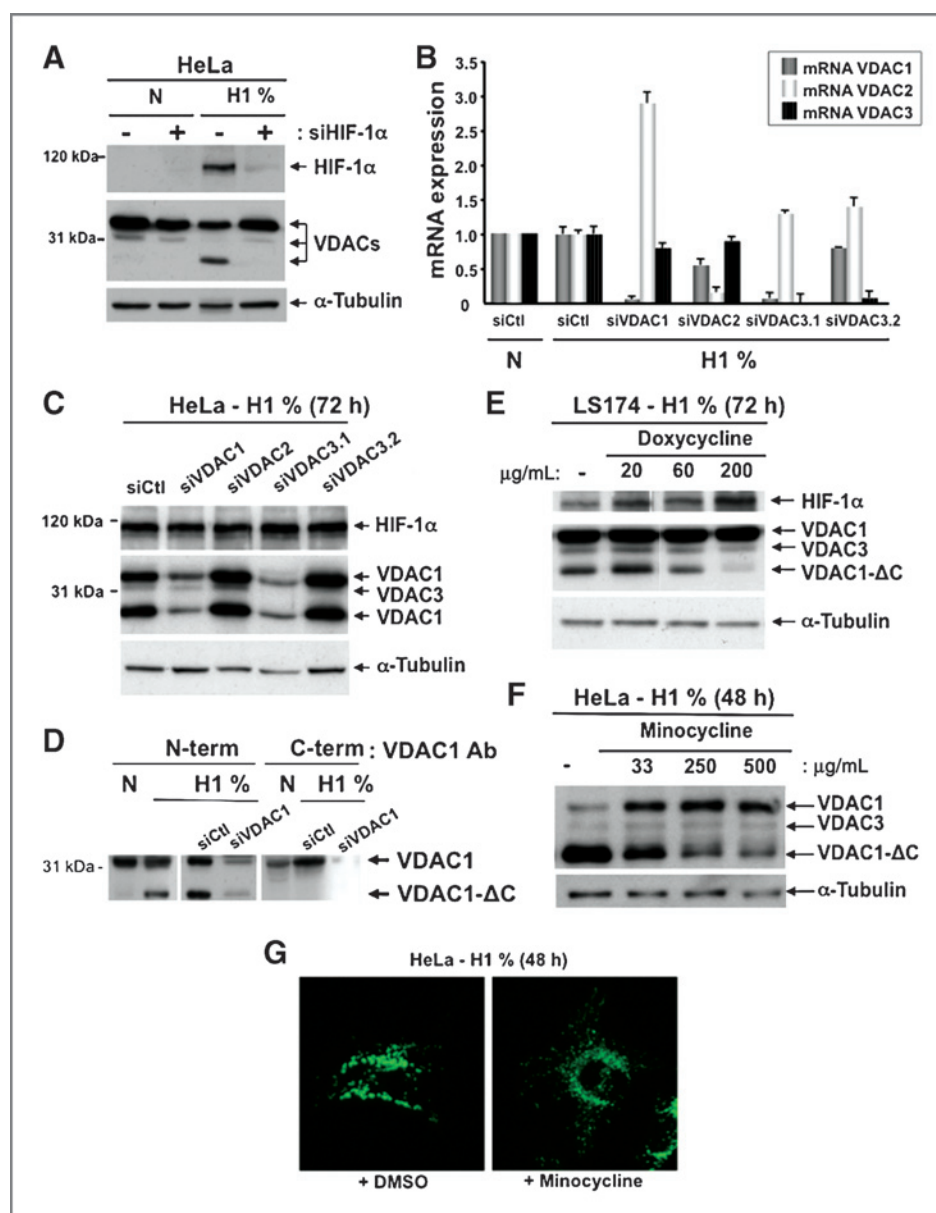
The hypoxic induction of the formation of a smaller relative molecular mass form of VDAC is dependent on HIF-1 activation

Because an additional VDAC form was observed in hypoxia-resistant cells with enlarged mitochondria, and not in sensitive cells, we focused on the hypoxic induction of this form. As HIF-1 is essential in adaptation to hypoxia, we checked whether HIF-1 was involved in the formation of this form. When HIF-1 α was silenced hypoxic cells did not contain the faster migrating form (Fig. 2A), but a normal mitochondrial morphology was restored (data not shown). Similar results were obtained for LS174 and A549 cells (data not shown). Thus HIF-1 initiates hypoxia-induced VDAC.

Expression of VDAC isoforms is not induced at the mRNA level by hypoxia and the hypoxia-mediated form of VDAC is a C-terminal-truncated VDAC1

We quantified the mRNA expression of VDAC1, VDAC2, and VDAC3 in normoxia and hypoxia but did not observe hypoxic induction of these isoforms (Fig. 2B). siRNA directed to the mRNA of the 3 isoforms gave knockdown of the corresponding VDAC isoform (Fig. 2B). Knockdown was confirmed at the protein level and identified the different isoforms (Fig. 2C). The top band corresponded to VDAC1, the intermediate band to VDAC3, and the bottom band to a faster migrating form of VDAC1. The identity of VDAC1 was confirmed with another VDAC1-specific antibody, but

Figure 2. Hypoxia induced a HIF-1 α -dependent novel form of VDAC1. **A**, induction in hypoxia of a faster migrating SDS-PAGE form of VDAC is dependent on HIF-1 α . Immunoblot of HIF-1 α and VDACS in HIF-1 α silenced HeLa cells in normoxia or hypoxia in the absence (-) or presence (+) of HIF-1 α siRNA. **B**, expression of the mRNA of VDAC1-3 in normoxia and hypoxia in HeLa cells. Expression of VDAC1, 2, and 3 after transfection with control (siCtl) or VDAC1 (siVDAC1), VDAC2 (siVDAC2), or VDAC3 (siVDAC3.1 or siVDAC3.2) siRNA, results are representative of 2 different siRNA for each isoform. **C**, immunoblot to HIF-1 α and VDAC1 (ab15895) in control (siCtl) or VDAC1 (siVDAC1), VDAC2 (siVDAC2), or VDAC3- (siVDAC3.1 or siVDAC3.2) silenced HeLa cells in hypoxia. Hypoxia-induced fast migrating VDAC1. **D**, immunoblot using antibodies against the N- or C-terminus of VDAC1 in HeLa cells incubated in normoxia or hypoxia transfected or not with siRNA. **E**, immunoblot of HIF-1 α and VDAC1 (ab15895) of LS174 cells incubated in hypoxia. Doxycycline was added for the first 24 hours of hypoxia. **F**, immunoblot of HIF-1 α and VDAC1 (ab15895) of HeLa cells in hypoxia for 48 hours. Minocycline was added for the 48 hours of hypoxia. **G**, immunofluorescence to cytochrome c of HeLa cells in hypoxia without (+DMSO) or with minocycline. DMSO, dimethyl sulfoxide.



directed to the N-terminus, and both forms were silenced with siRNA (Fig. 2D).

We considered the possibility that the fast migrating VDAC1 resulted from alternative splicing or hypoxia-mediated translation by internal ribosome entry but did not find any evidence to support either possibility (Supplementary Fig. S2).

Finally, the faster migrating VDAC1 was not detected with a VDAC1 antibody directed to the C-terminus (Fig. 2D), suggesting that the C-terminus of the protein was truncated (VDAC1- Δ C). Doxycycline, a second-generation tetracycline that has cytoprotective and metal chelator effects, was found to diminish the formation of VDAC1- Δ C (Fig. 2E). Because metal chelators increase the stability of HIF-1 α we examined the level of HIF-1 α but found only a slight increase when the fast migrating form of VDAC1 was significantly decreased (60%, 60

μ g/mL doxycycline; Fig. 2E). Minocycline, another tetracycline antibiotic, which exerts uncoupling and inhibiting effects on mitochondrial respiration (22), also inhibited formation (Fig. 2F), and partially restored normal mitochondrial morphology (Fig. 2G). Because tetracycline is an inhibitor of matrix metalloproteases we tested a number of protease inhibitors, but they did not inhibit formation of VDAC1- Δ C (data not shown). The possibility of posttranslational cleavage of VDAC1, as described previously (23), is the most likely explanation for the appearance of VDAC1- Δ C.

VDAC1- Δ C is associated with cell survival in hypoxia

We then hypothesized that VDAC1- Δ C could be involved in hypoxic resistance to apoptosis. Silencing of VDAC1 and VDAC1- Δ C decreased the number of enlarged mitochondria

and restored the tubular mitochondrial morphology (Fig. 3A). To evaluate the sensitivity to an apoptotic stimulus of normoxic and hypoxic LS174 cells, we determined the caspase-3 and -7 activity in cells exposed to STS, an inducer of mitochondrion-dependent apoptosis, and to etoposide, a topoisomerase II inhibitor used in cancer therapy (Fig. 3B). The caspase activity was the same in cells in normoxia or hypoxia, indicating that there was no induction of cell death in hypoxia. Silencing of VDAC1 in hypoxia partially reestablished the sensitivity of hypoxic LS174 cells to apoptosis (Fig. 3B).

Two additional cell lines were examined for enlarged mitochondria, VDAC1- Δ C, and resistance to STS-induced apoptosis. SKMel cells did not show any of these features whereas A549 cells showed all of them (Supplementary Fig. S3), as for HeLa cells (Figs. 2 and 3 and Supplementary Fig. S4). We then questioned which form of VDAC1 (full-length or truncated) was responsible for triggering resistance. In hypoxia, the level of VDAC1 decreased by around 50% (Fig. 3C) whereas VDAC1- Δ C increased by around 50%, which supported posttranslational cleavage of VDAC1. The silencing of *vdac1* in normoxic

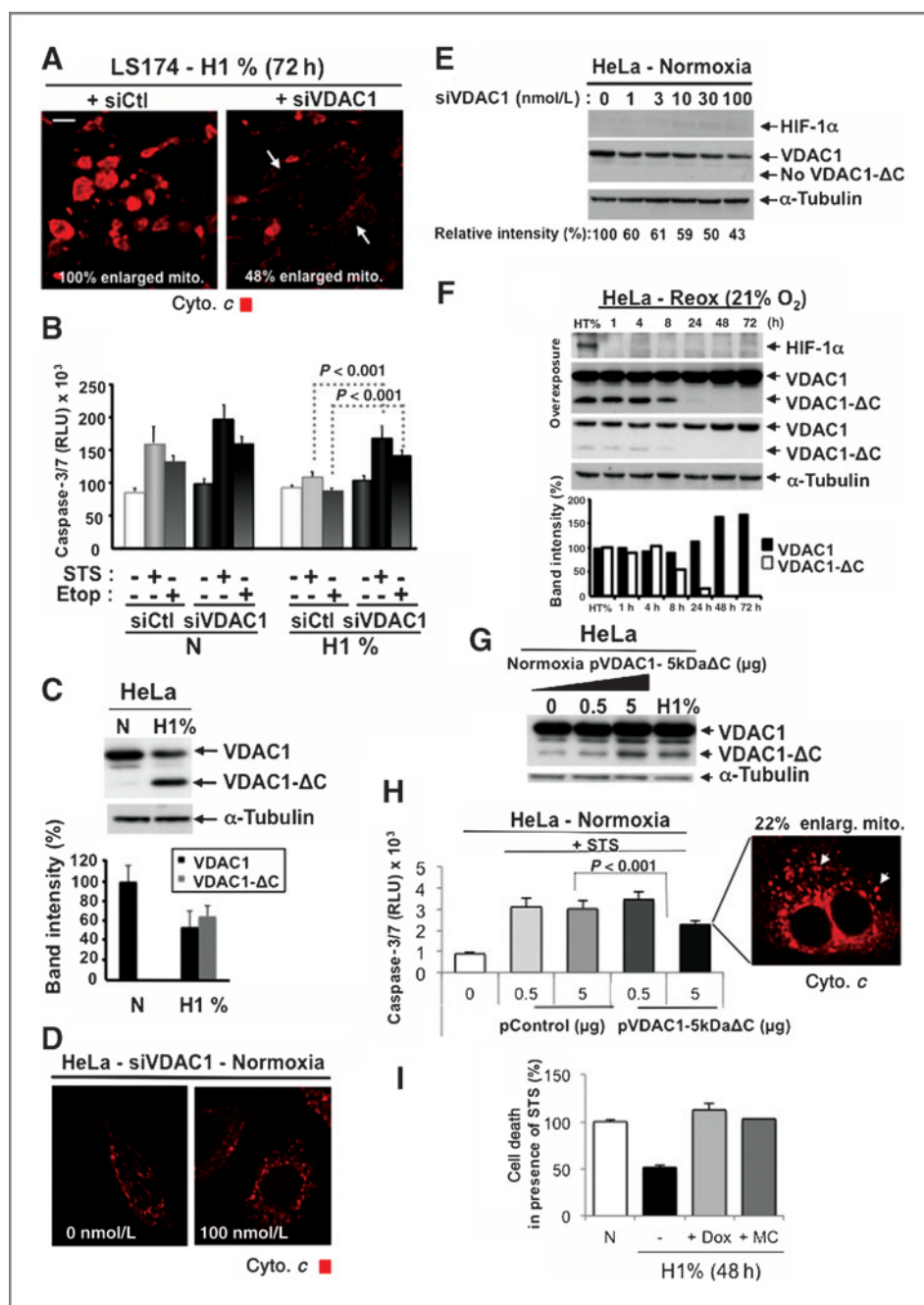


Figure 3. Hypoxic induction of VDAC1- Δ C in cells with enlarged mitochondria show protection from stimuli-induced apoptosis. **A**, immunofluorescence to cytochrome *c* in LS174 cells silenced for VDAC1 in hypoxia. Arrows indicate fragmented mitochondria; bar, 7.3 μ m. The percentage of enlarged mitochondria is given. **B**, caspase activity of control and VDAC1-silenced LS174 cells ($n = 8$; 2 experiments; *, $P < 0.001$) in normoxia or hypoxia without (-) or with (+) staurosporine (STS) or etoposide (Etop) for the last 4 hours. **C**, immunoblot of VDAC1 in HeLa cells in normoxia or hypoxia. Histograms show the quantification of the bands. **D**, immunofluorescence to cytochrome *c* of normoxic HeLa cells transfected with siRNA to VDAC1. **E**, immunoblots of HIF-1 α or VDAC1 of HeLa cells transfected with increasing concentrations of siVDAC1. **F**, immunoblots to HIF-1 α or VDAC1 of HeLa cells incubated first in hypoxia and then reoxygenated. Histograms show quantification of the signal to VDAC1 and VDAC1- Δ C. **G**, expression of pVDAC1-5kDa Δ C (0.5 and 5.0 μ g plasmid) in normoxia in HeLa cells and endogenous VDAC1- Δ C expression in hypoxia. **H**, caspase activity of HeLa cells, in normoxia, transfected with a control plasmid or a plasmid expressing a 5 kDa C-terminal-truncated VDAC1 with or without STS treatment. The percentage of cells with enlarged (enlarg.) mitochondria (mito.) is given. **I**, caspase activity (%) of HeLa cells incubated in normoxia or hypoxia with or without doxycycline (Dox) or minocycline (MC) and without or with STS for the last 4 hours ($n = 8$, 2 experiments). RLU, relative luciferase units.

cells was associated with a change in mitochondrial morphology, as visualized with anticytochrome *c* (Fig. 3D) and a decrease in VDAC1 in hypoxia (Fig. 3E). However, these cells showed an increase in apoptosis with STS (Fig. 3B), suggesting that the decrease in VDAC1 in normoxia was not responsible for the protection against apoptosis. Moreover, silencing of HIF-1 α (+Tet) in hypoxia with STS (Fig. 2A) restored sensitivity to apoptosis (data not shown). We thus concluded that resistance to apoptosis was associated with VDAC1- Δ C. To evaluate this further, cells were placed in hypoxia and then reoxygenated. The level of VDAC1- Δ C was maintained for 4 hours after reoxygenation, then progressively decreased after 8 hours and disappeared at 48 hours (Fig. 3F). As expected, the level of VDAC1 was inversely proportionate to that of VDAC1- Δ C. We showed previously that during the first 24 hours of reoxygenation, cells were protected from apoptosis (3). Transient exogenous overexpression of a small form of VDAC1 truncated by 5 kDa in the C-terminus, pVDAC1-5kDa Δ C (Fig. 3G), in cells exposed for 4 hours to STS showed a slight resistance to apoptosis (Fig. 3H). Finally, in the presence of doxycycline (Fig. 2E) or minocyclin (Fig. 2F), hypoxic cells were no longer protected from STS (Fig. 3I). Taken together, these results show that both the enlarged morphology of mitochondria and VDAC1- Δ C participate in protection against apoptosis in hypoxic LS174, A549, and HeLa cells exposed to STS or etoposide.

VDAC1- Δ C has the same channel activity and voltage dependency as VDAC1 and binds Bcl-X_L

VDAC1 and VDAC1- Δ C proteins were purified from hypoxic HeLa cells (Fig. 4A) and their channel activity was examined following reconstitution into a PLB. The current through lipid bilayer-reconstituted VDAC1 (fraction 12) or VDAC1- Δ C (fraction 22) in response to a voltage step from 0 to -10 or to -40 mV (Fig. 4B and C) was the same for the 2 proteins. At -10 mV, the channel conductance of both proteins was the same (30 pA). At a higher voltage of -40 mV, the full-length channel showed 2 major conducting states with higher occupancy at the closed substate (*S1*), whereas VDAC1- Δ C showed higher open-state occupancy (*O*) in comparison to the occupancy of low-conducting substates (*S1*, *S2*; Fig. 4C). Both channels showed similar but not identical voltage-dependent conductance. At the high voltages, VDAC1- Δ C showed slightly higher conductance than VDAC1 (Fig. 4D), in agreement with the single-channel experiments [Fig. 4B(ii) and C(ii)]. The voltage sensitivity of VDAC1- Δ C suggests the presence of the N-terminus, conferring voltage gating of the channel (8). VDAC1- Δ C showed similar Ca²⁺ conductance to VDAC1, but at higher voltages spent a longer time in its open state, as reflected in the decreased voltage sensitivity (Fig. 4E). For example, at $+40$ mV the Ca²⁺ conductance VDAC1- Δ C was about 1.4-fold higher than that of VDAC1 (Fig. 4E). VDAC1- Δ C, like VDAC1, interacted with purified Bcl-X_L(Δ C) and decreased its channel conductance (Fig. 4F). Similar results were obtained with hexokinase I from rat brain (data not shown). These results suggest that the C-terminal domain is not required for the interaction of these antiapoptotic proteins with VDAC1.

VDAC1- Δ C forms a complex with hexokinase II and is associated with cell survival in hypoxia

As hexokinase II is a major player in maintaining the highly malignant state of cancer cells (24), we focused on interaction between hexokinase II and VDACS in hypoxia. Immunoprecipitates with antihexokinase II contained VDAC1, VDAC3, and VDAC1- Δ C (Fig. 5A). In addition, the hexokinase II expression level was substantially increased in hypoxia (Fig. 5B). Silencing of more than 90% of the hypoxia-inducible expression of hexokinase II decreased considerably the level of VDAC1- Δ C (Fig. 5B). Silencing of hexokinase II in normoxia did not affect the level of VDAC1. Conversely, silencing of VDAC1 in normoxia and hypoxia decreased slightly the level of hexokinase II (Fig. 5B). These results were confirmed by immunofluorescence; no or little labeling was observed with anti-VDAC in cells silenced for either hexokinase II or VDACS (Fig. 5C). In addition, a more intense and punctate immunofluorescence was observed with anti-VDAC in VDAC1- Δ C-containing cells incubated in hypoxia than in normoxia (Supplementary Fig. S5). Clotrimazole (CTM) and bifenazole (BFN) induce apoptosis by detaching hexokinase from mitochondria (17, 25). Both agents increased mortality to a similar extent to that for VDAC silencing (Fig. 5D) and the mortality was enhanced in cells in hypoxia in their presence. This suggested that VDAC1- Δ C interacted with hexokinase II, as did purified hexokinase I, which decreased VDAC1- Δ C channel conductance. To better understand the role of VDAC1 and hexokinase II in cell survival in hypoxia, we silenced VDAC1 or hexokinase II and tested cell proliferation/death and ATP and lactate production in normoxia and hypoxia. Hypoxia does not kill cells (26), but it slows proliferation, as shown by a 3-fold decrease in the area of colonies of cells after 10 days in hypoxia (Fig. 5E). Transient silencing of VDAC1 (siVDAC1) in hypoxia had no impact on cell survival but affected proliferation ($P < 0.01$), whereas silencing of hexokinase II (siHKII) strongly inhibited survival (Fig. 5E). As hexokinase II and VDAC1 form a complex and silencing of hexokinase II decreased the level of VDAC1 in cells (Fig. 5B), we hypothesized that hexokinase II interfered with ATP transport and thereby its production via its interaction with VDAC1- Δ C. Cells produced almost 2 times more ATP in hypoxia (Fig. 5F). Silencing of VDAC1 decreased hypoxic but not normoxic production of ATP, suggesting that VDAC1- Δ C influenced ATP production (Supplementary Fig. S6). This could reflect the impact of VDAC1 silencing on hexokinase II expression. As expected the silencing of hexokinase II in hypoxia decreased ATP. Lactate production, which reflects ATP synthesis via glycolysis, was increased in hypoxia and diminished with VDAC1 or hexokinase II silencing (Fig. 5G). Taken together, these results confirm that VDAC1 is involved in energy homeostasis and points to VDAC1- Δ C as an essential actor in both glycolysis and mitochondrial energy production in hypoxia probably through interaction with hexokinase.

VDAC1- Δ C is present in tissues of patients with lung adenocarcinoma and is more frequently detected in late-stage rather than in early-stage tumors

Because we detected both VDAC1 and VDAC1- Δ C in hypoxic A549 lung carcinoma cells (Supplementary Fig. S3),

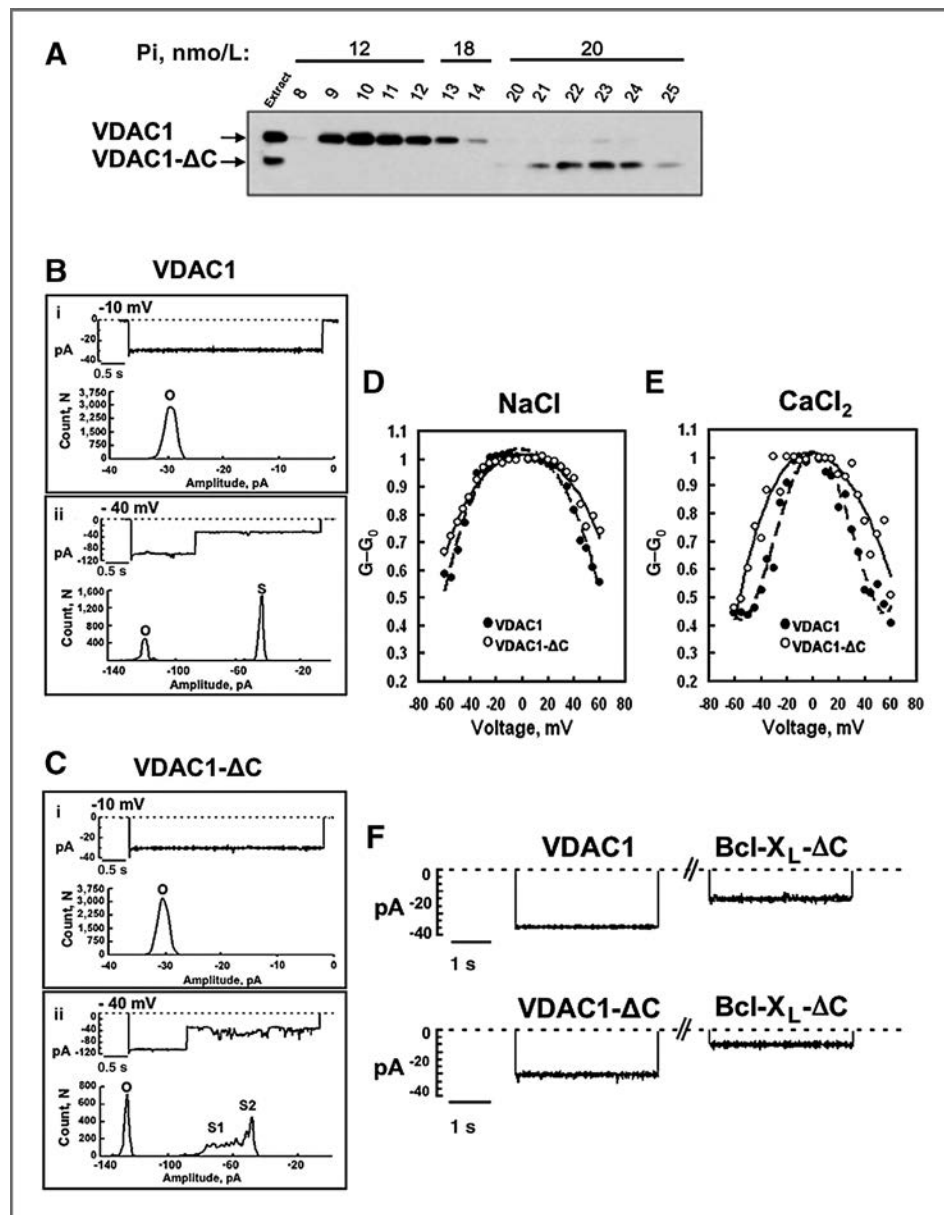


Figure 4. VDAC1- Δ C channel activity and binding of Bcl-X_L- Δ C are identical to that of VDAC1. A, VDAC1 and VDAC1- Δ C purification from HeLa cells identified by immunoblotting (anti-VDAC1; Calbiochem); fractions 21 or 22 were used. B and C, channel activity of bilayer-reconstituted purified VDAC1 or VDAC1- Δ C. Currents through bilayer-reconstituted VDAC1 or VDAC1- Δ C in response to a voltage step from 0 to -10 mV [B(i) and C(i)] or to -40 mV [B(ii) and C(ii)] were recorded. The dashed lines indicate the zero current level. The total current amplitude histogram traces (in the same recording), showing the relative occupancy of the open state (O) and closed substate (S) or, for VDAC1- Δ C, of 2 or more substates (S1 and S2) during a 4-second recording are shown (B and C). D, currents through the VDAC1 (●) or VDAC1- Δ C (○) channels were recorded in the presence of 1 mol/L NaCl and in response to a voltage step from 0 mV to voltages between -60 to $+60$ mV. Relative conductance was determined as the ratio of conductance at a given voltage (G) to the maximal conductance (G₀). The results are representative of 9 similar experiments in which the value of each voltage represents the average of 3 to 6 swipes. E, currents through VDAC1 (●) or VDAC1- Δ C (○) as recorded in the presence of 0.2 mol/L CaCl₂ and in response to a voltage step from 0 mV to voltages between -60 to $+60$ mV. The results are the average of 2 similar experiments with 3 swipes for each voltage. F, VDAC channel conductance was recorded before and 10 minutes after the addition of purified Bcl-X_L- Δ C to the cis chamber. A representative experiment of 3 similar experiments is shown.

we tested for VDAC1 and VDAC1- Δ C in lung adenocarcinomas tumor tissue from 44 patients. Tumor tissues were divided into 2 groups: stage IA and IB ($n = 25$) and stage IIIA and IIIB ($n = 19$). The clinical characteristics of the patients are listed in supplementary Table S1. The level of

VDAC1- Δ C was determined in corresponding control matched healthy (C) and tumor (T) tissue of patients with lung cancer (Fig. 6A). The tumor tissue, but not healthy tissue, contained VDAC1- Δ C and the level of VDAC1- Δ C in stage III was several fold higher than in stage I (see also

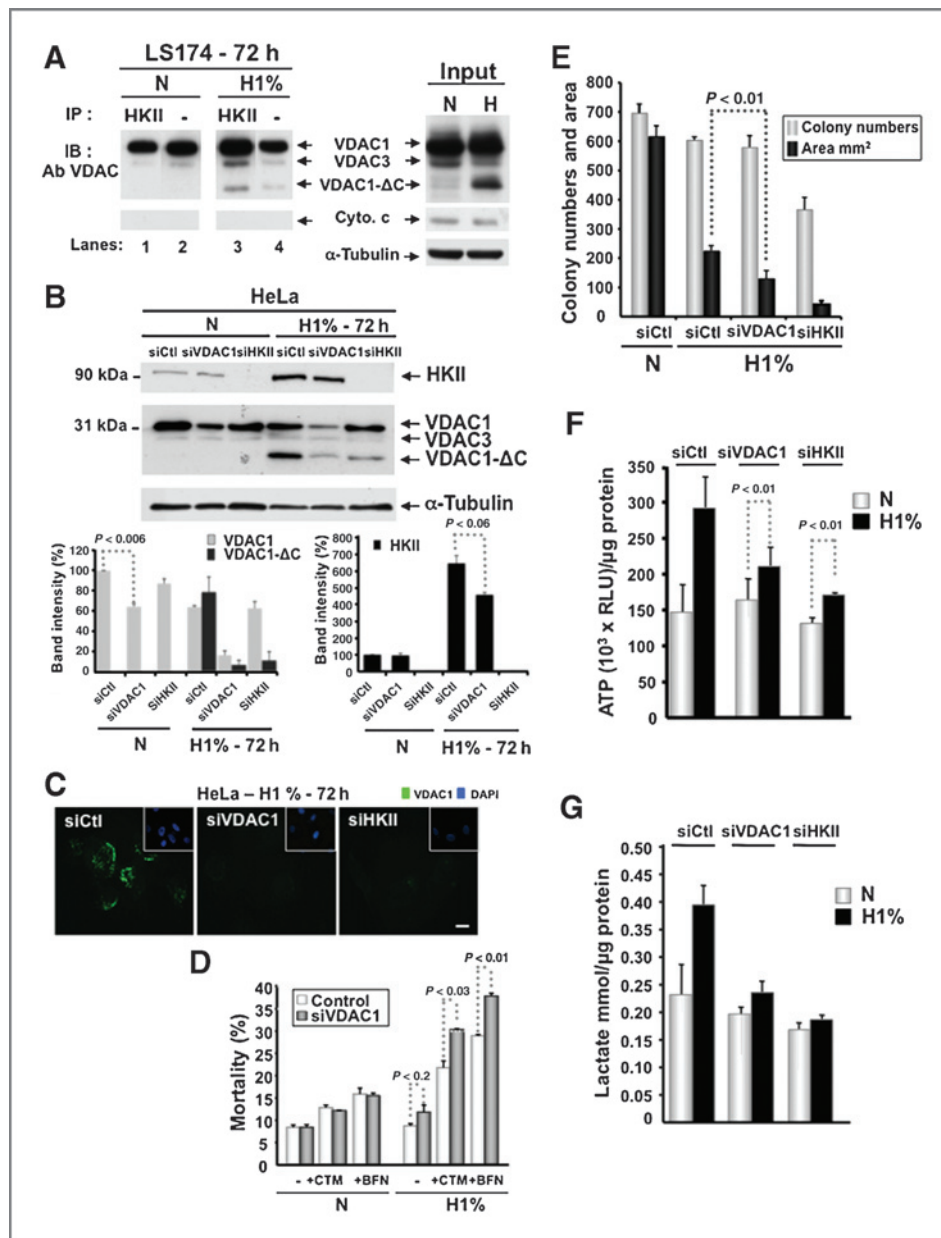


Figure 5. Hypoxic VDAC1- Δ C forms a complex with hexokinase II and cell survival in hypoxia requires VDAC1- Δ C and hexokinase II. **A**, coimmunoprecipitation of endogenous VDAC1 with hexokinase II. Lysates of hypoxic LS174 cells were immunoprecipitated with an anti-hexokinase II antibody. VDAC proteins in the lysates and the immunoprecipitates are shown (arrow). Cytochrome *c* was used as a control. IB, immunoblot; IP, immunoprecipitate. **B**, immunoblot of hexokinase II and VDAC in control (siCtl), VDAC (siVDAC1), or hexokinase II (siHKII) transfected HeLa cells in normoxia or hypoxia. Histograms show the intensities normalized to α -tubulin for VDAC1 and VDAC1- Δ C (left) and hexokinase II (right). **C**, immunofluorescence of VDAC1 in HeLa cells silenced for VDAC (siVDAC1) or hexokinase II (siHKII) in hypoxia. Bar, 7.3 μ m. **D**, percentage of mortality (Trypan blue exclusion) of HeLa cells incubated in normoxia or hypoxia. Cells were transfected with or without a siRNA to VDAC1 and incubated or not with clotrimazole (CTM-50 μ mol/L) or bifonazole (BFN-50 μ mol/L) for the last hour of normoxia or hypoxia. **E**, viability assay of HeLa cells in control (siCtl), VDAC (siVDAC1), or hexokinase II (siHKII) silenced cells in normoxia or hypoxia. Cells were transiently transfected twice with the indicated siRNA (40 nmol/L), then seeded, and incubated in normoxia or hypoxia for 10 days before staining. **F**, ATP production of HeLa cells silenced (siVDAC1) or not (siCtl) for VDAC1 or hexokinase II (siHKII; $n = 8, 3$ experiments; *, $P < 0.001$) in normoxia or hypoxia. **G**, lactate production of HeLa cells silenced (siVDAC1) or not (siCtl) for VDAC1 or hexokinase II (siHKII; $n = 2, 3$ experiments; *, $P < 0.01$) in normoxia or hypoxia. DAPI, 4', 6'-diamidino-2-phenylindole.

below). In addition, electron micrographs of mitochondria of tumor and matched normal patients' tissues showed enlarged mitochondria in only tumor samples (Supplementary Fig. S7).

The expression of carbonic anhydrase IX (CAIX; refs. 27, 28) and of miR-210 (ref. 29; Fig. 6B), 2 HIF-induced gene products, was analyzed to confirm the hypoxic status of the tissues (Fig. 6A and B). Positivity for CAIX was about 76% and 71% for tumor

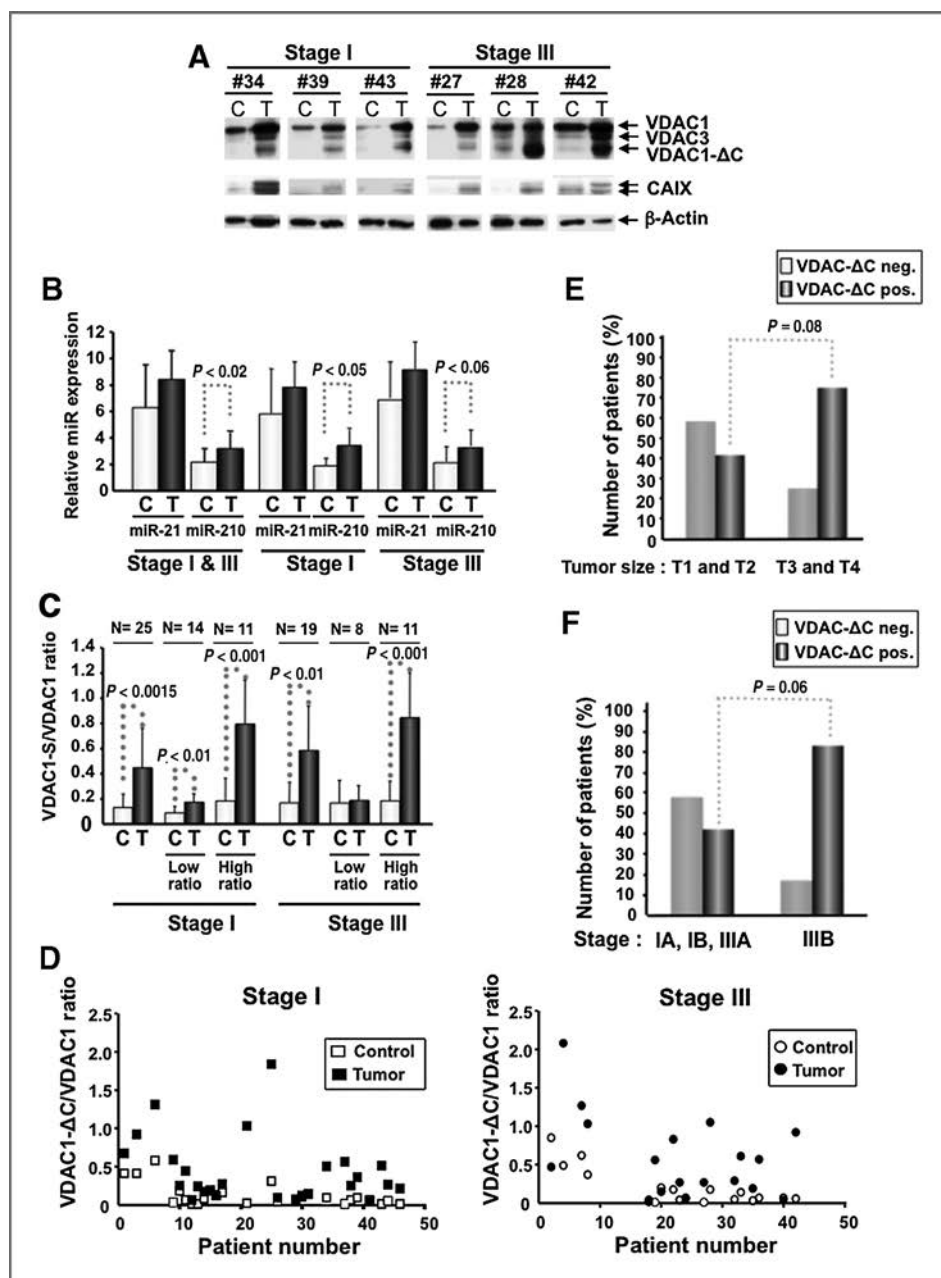


Figure 6. The ratio of VDAC1- Δ C to VDAC1 was higher in tumor tissue than in control tissue and proportionately more stage III tumors had a high ratio. **A**, representative immunoblots of VDAC in tissue extracts of healthy control (C) and tumor (T) tissue from 6 individual patients with lung cancer with either early-stage I or late-stage III tumors. CAIX was an indicator of hypoxia in tumors. **B**, the fold induction of miR-21 and miR-210 was determined for control and tumor tissues from patients with stage I and III tumors. The level of miR-21 indicated the quality of the miRNA in extracts whereas miR-210 is a hypoxia-induced miRNA. **C**, ratio of the intensity of the immunoblot signal of VDAC1- Δ C to VDAC1 for each individual patient for healthy (C) and tumor (T) tissue. Patients with lung cancer with stage I tumors (left graph) and stage III tumors (right graph). **E**, evaluation of the number of patients with lung cancer either negative or positive for VDAC1- Δ C, respectively (VDAC1- Δ C neg.) and (VDAC1- Δ C pos.), with small- (T1 and T2) or large- (T3 and T4) sized tumors. **F**, evaluation of the number of patients with lung cancer either negative or positive for VDAC1- Δ C, respectively (VDAC1- Δ C neg.) and (VDAC1- Δ C pos.), with stages IA-IB-III A or stage IIIB tumors.

tissues from stage I and stage III patients, respectively (Fig. 6A). Only rare control tissues showed minimal CAIX expression. The quality control of the miRNA in the extracts was confirmed by the level of miR-21. Significant relative expression of miR-210 was observed in tumors (Fig. 6B). The band intensity for VDAC1 and VDAC1- Δ C was determined with GeneTools software from Syngene, and the ratio of the intensity of VDAC1- Δ C to VDAC1 was evaluated for early-stage I (A and B) and late-stage III (A and B) tumors (Fig. 6A and C). The overall ratio for the early- and late-stages showed a significant increase when comparing healthy control and tumor tissue (Fig. 6A, C, and D). When patient tissues were subgrouped into tissue showing either a low or

high ratio (arbitrary threshold of 0.25) the number of patients showing a high ratio was slightly increased for stage III tumors (11 of 19 vs. 11 of 25), that is, 57.8% of stage III tumors were positive compared with 44% of stage I tumors (Fig. 6C). The difference between the matched healthy and tumor tissue was substantially higher for both early- and late-stage positive tumors (subgroup high ratio). In particular, VDAC1- Δ C was detected more frequently in larger tumors (41.7% in T1 and T2 tumors vs. 75% in T3 and T4 tumors, $P = 0.08$, statistical tendency; Fig. 6E, Table 1) and higher lung adenocarcinoma stage—patients not operated on (83.3% stage IIIB vs. 42.1% in other stages, $P = 0.06$, statistical tendency; Fig. 6F, Table 1). The level of necrosis of

Table 1. Comparison of the characteristics of the patients and their tumors with VDAC1- Δ C detection

	VDAC1- Δ C detection	χ^2 (P value)
Gender		
Female	5 (50%)	$P = 0.87$
Male	16 (47.1%)	
Age, y		
<60	13 (52%)	$P = 0.51$
≥ 60	8 (42.1%)	
Tumor size		
T1 and T2	15 (41.7%)	$P = 0.08$
T3 and T4	6 (75%)	
Node stage		
N0	14 (50%)	$P = 0.69$
N1 and N2	7 (43.8%)	
Initial stage		
IA, IB, IIIA	16 (42.1%)	$P = 0.06$
IIIB	5 (83.3%)	

the patients' tissues was neither high nor substantially different between stages I and III, 6% and 12%, respectively.

Discussion

Herein, we showed that hypoxia induces the appearance of a C-terminal truncated form of VDAC1. The mechanism regulating formation was HIF dependent and the truncated form possessed channel activity, interacted with Bcl-X_L and hexokinase I, both of which protect against apoptosis.

Interaction of VDACs with Bcl-2 family members is implicated in translocation of metabolites across the mitochondrial outer membrane (21). Nonetheless, it has been reported that the 3 isoforms are dispensable for mitochondrial-dependent cell death, but this was showed in a cellular and environmental context that was neither malignant nor hypoxic (30). In addition, VDAC2 but not VDAC1 has been shown to inhibit Bak-mediated mitochondrial apoptosis (31). It is possible to hypothesize that changes in the expression of Bcl-2 proteins are implicated directly in resistance. Cytoprotection of lung cancer cells to cisplatin correlated with suppression of activation of Bax but not Bak by cisplatin (12). However, in our study the Bax protein was not detected in LS174 cells. In addition, there exists an intricate crosstalk between the machineries of mitochondrial dynamics (fusion and fission), thus morphology, and apoptosis (32, 33). Both antiapoptotic (Bcl-2) and proapoptotic (Bak and Bax) proteins interact with proteins involved in mitochondrial fusion (mitofusins) and fission (dynamamin-related GTPases). Thus, we may speculate that modifications in the expression of Bak and Bcl-X_L correlate with the morphologic alterations observed. In addition, the increases in Bak and Bcl-X_L in hypoxic LS174 cells correlated with the morphologic alteration in hypoxia.

It may also be hypothesized that the increase in the expression of Bcl-X_L and the modification of the open configuration of the VDAC1- Δ C channel by Bcl-X_L inhibits mitochondrial ATP/ADP exchange, which favors ATP production through glycolysis. A shift toward glycolysis is a characteristic of hypoxic cancer cells and may explain survival and thus resistance when confronted with a potentially lethal agent. The observed change in organization of the cristae of the mitochondria may also rupture the interaction between VDAC and the adenine nucleotide translocase thereby leading to a change in VDAC-mediated ATP transport. In addition, if VDAC oligomerization is responsible for cytochrome *c* release in apoptosis (11), a change in its conformation may block cytochrome *c* in the mitochondrial intermembrane space and thus diminish apoptosis.

The notion that resistance of hypoxic regions of tumors to chemotherapy (34) is associated with hypoxic VDAC1- Δ C and Bcl-X_L is supported by reports showing that protection of HepG2 cells against etoposide-induced apoptosis was HIF-1 α dependent (35) and that Bcl-X_L is induced by HIF (36).

Because we detected VDAC1- Δ C in tumor tissue of patients (50%) and that the frequency of positivity for VDAC1- Δ C was higher in late-stage tumors than in early-stage tumors, we believe that VDAC1- Δ C represents a product of tumor progression. Gene expression of VDAC1 has been reported to predict poor outcome in early-stage non-small cell lung cancer (37). In addition, VDAC1 was shown to be upregulated in prednisolone-sensitive acute lymphoblastic leukemia cells but not in resistant cells (38).

In conclusion, our results point to modifications in mitochondrial dynamics and production of VDAC1- Δ C as a survival response in hypoxic cancer cells that resist apoptosis. Because agents that promote apoptosis may hold therapeutic benefit, these results may have important repercussions for combating cancer cell resistance to chemotherapy. A synthetic lethality approach targeting RAS tumor cells identified a small-molecule inhibitor of VDAC2 that induced changes in mitochondrial morphology and cell death (39). We propose that VDAC1- Δ C may be a potential biomarker to stratify patients with respect to tumor progression and that the VDAC1- Δ C/hexokinase complex may be a cancer specific target for therapy.

Disclosure of Potential Conflicts of Interest

No potential conflicts of interest were disclosed.

Acknowledgments

The authors are thankful to N. Pons for helping to extract RNA/proteins from patients' tissues and to J. Hickman for giving ABT737.

Grant Support

This research was supported by grants from the LNCC (Equipe labellisée), the ANR, the INCA, METOXIA (FP7-EU program), ARC, and Canceropôle PACA. The laboratory is funded by the Centre Antoine Lacassagne, CNRS, and INSERM.

The costs of publication of this article were defrayed in part by the payment of page charges. This article must therefore be hereby marked *advertisement* in accordance with 18 U.S.C. Section 1734 solely to indicate this fact.

Received December 5, 2011; revised February 3, 2012; accepted February 15, 2012; published OnlineFirst March 2, 2012.

References

- Wilson WR, Hay MP. Targeting hypoxia in cancer therapy. *Nat Rev Clin Oncol* 2011;11:393–410.
- Semenza GL. Defining the role of hypoxia-inducible factor 1 in cancer biology and therapeutics. *Oncogene* 2010;29:625–34.
- Chiche J, Rouleau M, Gounon P, Brahimi-Horn MC, Pouyssegur J, Mazure NM. Hypoxic enlarged mitochondria protect cancer cells from apoptotic stimuli. *J Cell Physiol* 2010;222:648–57.
- Kroemer G, Galluzzi L, Brenner C. Mitochondrial membrane permeabilization in cell death. *Physiol Rev* 2007;87:99–163.
- Galluzzi L, Kroemer G. Mitochondrial apoptosis without VDAC. *Nat Cell Biol* 2007;9:487–9.
- Kroemer G, Pouyssegur J. Tumor cell metabolism: cancer's Achilles' heel. *Cancer Cell* 2008;13:472–82.
- Suen DF, Norris KL, Youle RJ. Mitochondrial dynamics and apoptosis. *Genes Dev* 2008;22:1577–90.
- Abu-Hamad S, Arbel N, Calo D, Arzoine L, Israelson A, Keinan N, et al. The VDAC1 N-terminus is essential both for apoptosis and the protective effect of anti-apoptotic proteins. *J Cell Sci* 2009;122:1906–16.
- Abu-Hamad S, Zaid H, Israelson A, Nahon E, Shoshan-Barmatz V. Hexokinase-I protection against apoptotic cell death is mediated via interaction with the voltage-dependent anion channel-1: mapping the site of binding. *J Biol Chem* 2008;283:13482–90.
- Arzoine L, Zilberberg N, Ben-Romano R, Shoshan-Barmatz V. Voltage-dependent anion channel 1-based peptides interact with hexokinase to prevent its anti-apoptotic activity. *J Biol Chem* 2009;284:3946–55.
- Keinan N, Tyomkin D, Shoshan-Barmatz V. Oligomerization of the mitochondrial protein voltage-dependent anion channel is coupled to the induction of apoptosis. *Mol Cell Biol* 2010;30:5698–709.
- Tajeddine N, Galluzzi L, Kepp O, Hangen E, Morselli E, Senovilla L, et al. Hierarchical involvement of Bak, VDAC1 and Bax in cisplatin-induced cell death. *Oncogene* 2008;27:4221–32.
- Hiller S, Abramson J, Mannella C, Wagner G, Zeth K. The 3D structures of VDAC represent a native conformation. *Trends Biochem Sci* 2010;35:514–21.
- Pastorino JG, Hoek JB. Regulation of hexokinase binding to VDAC. *J Bioenerg Biomembr* 2008;40:171–82.
- Natsuzaka M, Ozasa M, Darmanin S, Miyamoto M, Kondo S, Kamada S, et al. Synergistic up-regulation of Hexokinase-2, glucose transporters and angiogenic factors in pancreatic cancer cells by glucose deprivation and hypoxia. *Exp Cell Res* 2007;313:3337–48.
- Berra E, Benizri E, Ginouves A, Volmat V, Roux D, Pouyssegur J. HIF prolyl-hydroxylase 2 is the key oxygen sensor setting low steady-state levels of HIF-1 α in normoxia. *Embo J* 2003;22:4082–90.
- Shoshan-Barmatz V, De Pinto V, Zweckstetter M, Raviv Z, Keinan N, Arbel N. VDAC, a multi-functional mitochondrial protein regulating cell life and death. *Mol Aspects Med* 2010;31:227–85.
- Travis WD, Brambilla E, Müller-Hermelink HK, Harris CC. WHO histological classification of tumors of the lung World Health Organization Classification of tumors. In: Pathology and genetics of tumors of the lung, pleura, thymus and heart. Vol. 10. Lyon, France: IARC; 2004.
- Mountain CF. Revisions in the International System for Staging Lung Cancer. *Chest* 1997;111:1710–7.
- Hickman JA, Hardwick JM, Kaczmarek LK, Jonas EA. Bcl-xL inhibitor ABT-737 reveals a dual role for Bcl-xL in synaptic transmission. *J Neurophysiol* 2008;99:1515–22.
- Vander Heiden MG, Li XX, Gottlieb E, Hill RB, Thompson CB, Colombini M. Bcl-xL promotes the open configuration of the voltage-dependent anion channel and metabolite passage through the outer mitochondrial membrane. *J Biol Chem* 2001;276:19414–9.
- Cuenca-Lopez MD, Karachitos A, Massarotto L, Oliveira PJ, Aguirre N, Galindo MF, et al. Minocycline exerts uncoupling and inhibiting effects on mitochondrial respiration through adenine nucleotide translocase inhibition. *Pharmacol Res* 2012;65:120–8.
- Ozaki T, Yamashita T, Ishiguro S. Mitochondrial m-calpain plays a role in the release of truncated apoptosis-inducing factor from the mitochondria. *Biochim Biophys Acta* 2009;1793:1848–59.
- Mathupala SP, Ko YH, Pedersen PL. Hexokinase II: cancer's double-edged sword acting as both facilitator and gatekeeper of malignancy when bound to mitochondria. *Oncogene* 2006;25:4777–86.
- Penso J, Beitner R. Clotrimazole and bifonazole detach hexokinase from mitochondria of melanoma cells. *Eur J Pharmacol* 1998;342:113–7.
- Bellot G, Garcia-Medina R, Gounon P, Chiche J, Roux D, Pouyssegur J, et al. Hypoxia-induced autophagy is mediated through hypoxia-inducible factor induction of BNIP3 and BNIP3L via their BH3 domains. *Mol Cell Biol* 2009;29:2570–81.
- Chiche J, Ilc K, Laferriere J, Trottier E, Dayan F, Mazure NM, et al. Hypoxia-inducible carbonic anhydrase IX and XII promote tumor cell growth by counteracting acidosis through the regulation of the intracellular pH. *Cancer Res* 2009;69:358–68.
- Ilie M, Mazure NM, Hofman V, Ammadi RE, Ortholan C, Bonnetaud C, et al. High levels of carbonic anhydrase IX in tumour tissue and plasma are biomarkers of poor prognostic in patients with non-small cell lung cancer. *Br J Cancer* 2010;102:1627–35.
- Puissegur MP, Mazure NM, Bertero T, Pradelli L, Grosso S, Robbeserment K, et al. miR-210 is overexpressed in late stages of lung cancer and mediates mitochondrial alterations associated with modulation of HIF-1 activity. *Cell Death Differ* 2011;18:465–78.
- Baines CP, Kaiser RA, Sheiko T, Craigen WJ, Molkenin JD. Voltage-dependent anion channels are dispensable for mitochondrial-dependent cell death. *Nat Cell Biol* 2007;9:550–5.
- Cheng EH, Sheiko TV, Fisher JK, Craigen WJ, Korsmeyer SJ. VDAC2 inhibits BAK activation and mitochondrial apoptosis. *Science* 2003;301:513–7.
- Brooks C, Dong Z. Regulation of mitochondrial morphological dynamics during apoptosis by Bcl-2 family proteins: a key in Bak? *Cell Cycle* 2007;6:3043–7.
- Rolland SG, Conradt B. New role of the BCL2 family of proteins in the regulation of mitochondrial dynamics. *Curr Opin Cell Biol* 2010;22:852–8.
- Brown JM, Wilson WR. Exploiting tumour hypoxia in cancer treatment. *Nat Rev Cancer* 2004;4:437–47.
- Sermeus A, Cosse JP, Crespin M, Mainfroid V, de Longueville F, Ninane N, et al. Hypoxia induces protection against etoposide-induced apoptosis: molecular profiling of changes in gene expression and transcription factor activity. *Mol Cancer* 2008;7:27.
- Chen N, Chen X, Huang R, Zeng H, Gong J, Meng W, et al. BCL-xL is a target gene regulated by hypoxia-inducible factor-1 α . *J Biol Chem* 2009;284:10004–12.
- Grills C, Jithesh PV, Blayney J, Zhang SD, Fennell DA. Gene expression meta-analysis identifies VDAC1 as a predictor of poor outcome in early stage non-small cell lung cancer. *PLoS One* 2011;6:e14635.
- Jiang N, Kham SK, Koh GS, Suang Lim JY, Ariffin H, Chew FT, et al. Identification of prognostic protein biomarkers in childhood acute lymphoblastic leukemia (ALL). *J Proteomics* 2011;74:843–57.
- Yagoda N, von Rechenberg M, Zaganjor E, Bauer AJ, Yang WS, Fridman DJ, et al. RAS-RAF-MEK-dependent oxidative cell death involving voltage-dependent anion channels. *Nature* 2007;447:864–8.

Two Panels of Plasma MicroRNAs as Non-Invasive Biomarkers for Prediction of Recurrence in Resectable NSCLC

Céline Sanfiorenzo^{1,2,3,9}, Marius I. Ilie^{1,3,4,5,9}, Amine Belaid¹, Fabrice Barlési⁶, Jérôme Mouroux^{1,3,7}, Charles-Hugo Marquette^{1,2,3}, Patrick Brest^{1,3†}, Paul Hofman^{1,3,4,5,*†}

1 Institute for Research on Cancer and Ageing in Nice IRCAN, INSERM U1081 – CNRS UMR 7284, Team 3, Nice, France, **2** University Hospital Center of Nice, Pasteur Hospital, Department of Pneumology, Nice, France, **3** University of Nice Sophia Antipolis, Faculty of Medicine, Team 3, Nice, France, **4** University Hospital Center of Nice, Pasteur Hospital, Laboratory of Clinical and Experimental Pathology, Nice, France, **5** University Hospital Center of Nice, Pasteur Hospital, Human Biobank, Nice, France, **6** Aix Marseille Université – Assistance Publique Hôpitaux de Marseille, Multidisciplinary Oncology and Therapeutic Innovations Department, Marseille, France, **7** University Hospital Center of Nice, Pasteur Hospital, Department of Thoracic Surgery, Nice, France

Abstract

The diagnosis of non-small cell lung carcinoma (NSCLC) at an early stage, as well as better prediction of outcome remains clinically challenging due to the lack of specific and robust non-invasive markers. The discovery of microRNAs (miRNAs), particularly those found in the bloodstream, has opened up new perspectives for tumor diagnosis and prognosis. The aim of our study was to determine whether expression profiles of specific miRNAs in plasma could accurately discriminate between NSCLC patients and controls, and whether they are able to predict the prognosis of resectable NSCLC patients. We therefore evaluated a series of seventeen NSCLC-related miRNAs by quantitative real-time (qRT)-PCR in plasma from 52 patients with I-IIIa stages NSCLC, 10 patients with chronic obstructive pulmonary disease (COPD) and 20-age, sex and smoking status-matched healthy individuals. We identified an eleven-plasma miRNA panel that could distinguish NSCLC patients from healthy subjects (AUC = 0.879). A six-plasma miRNA panel was able to discriminate between NSCLC patients and COPD patients (AUC = 0.944). Furthermore, we identified a three-miRNA plasma signature (high miR-155-5p, high miR-223-3p, and low miR-126-3p) that significantly associated with a higher risk for progression in adenocarcinoma patients. In addition, a three-miRNA plasma panel (high miR-20a-5p, low miR-152-3p, and low miR-199a-5p) significantly predicted survival of squamous cell carcinoma patients. In conclusion, we identified two plasma miRNA expression profiles that may be useful for predicting the outcome of patients with resectable NSCLC.

Citation: Sanfiorenzo C, Ilie MI, Belaid A, Barlési F, Mouroux J, et al. (2013) Two Panels of Plasma MicroRNAs as Non-Invasive Biomarkers for Prediction of Recurrence in Resectable NSCLC. PLoS ONE 8(1): e54596. doi:10.1371/journal.pone.0054596

Editor: Alfons Navarro, University of Barcelona, Spain

Received: July 9, 2012; **Accepted:** December 13, 2012; **Published:** January 16, 2013

Copyright: © 2013 Sanfiorenzo et al. This is an open-access article distributed under the terms of the Creative Commons Attribution License, which permits unrestricted use, distribution, and reproduction in any medium, provided the original author and source are credited.

Funding: This work was partly supported by grants from the Cancéropole PACA (Axe C, 2011 and 2012), and by the “Fondation ARC pour la recherche sur le cancer” ARC SL220110603478 (PH, PB, MI). The funders had no role in study design, data collection and analysis, decision to publish, or preparation of the manuscript.

Competing Interests: The authors have declared that no competing interests exist.

* E-mail: hofman.p@chu-nice.fr

⁹ These authors contributed equally to this work.

[†] These authors also contributed equally to this work.

Introduction

Lung cancer, predominantly non-small cell lung cancer (NSCLC), is the leading cause of cancer-related deaths worldwide [1]. Despite subtle progress over recent years in terms of treatment strategies, the high mortality rate has not decreased significantly. NSCLC is often diagnosed at advanced stages with an overall 5-year survival less than 15% [2]. The poor prognosis of NSCLC patients is largely due to the lack of routine, validated, effective and low cost screening tools that allow detection of early-stage tumors. Developing such biomarkers is a public health imperative since diagnosis and treatment of early-stage NSCLC is associated with 60–80% survival at 5 years [1,3]. One of the major clinical determinants in NSCLC prognosis is tumor extension, roughly characterized by the pTNM stage. However, a large variability in disease outcome has been observed for a subset of patients with

similar clinical and pathological features, thus the current staging system may be insufficient to consistently predict the treatment outcome of NSCLC [4]. Therefore, prognostic assessment of the patients is essential to choose the best therapeutic strategy and may be improved by the integration of new robust prognostic biomarkers.

The impact on outcome of NSCLC of screening procedures such as chest X-rays, sputum cytology, spiral computed-tomography (CT), or a combination of these, has been evaluated in large-scale clinical trials. However, these analyses have not significantly affected overall survival (OS) and have demonstrated low sensitivity [5,6]. The search for non-invasive tumor biomarkers is rapidly expanding and investigation into circulating biomarkers is the subject of intense research. Several serum tumor markers such as the carcinoembryonic antigen or Cytokeratin-21-Fragment (CYFRA 21-1) may carry some prognostic and predictive

information in NSCLC, although their use is currently limited and the biochemical methodologies used to measure them are still labor-intensive [7,8].

One of the most exciting molecular markers in tumor diagnosis and prognosis are microRNAs (miRNAs) [9]. miRNAs are small RNA molecules (18 to 24 nt) that effect substantially the expression of multiple genes at a post-transcriptional level, via mRNA destabilization or translational repression [10]. Deregulation of miRNA expression is thought to be responsible of tumor initiation and progression [11]. MiRNAs are frequently deregulated in cancer and may act as oncogenes or tumor suppressors having regulatory functions on hundreds of downstream genes with different biologic functions [12,13]. Given the fundamental role of miRNAs in tumors and their global deregulation, miRNA profiles may provide a more accurate prediction of survival than the expression of a single-marker or expression profiles of protein-coding genes [13]. In addition, recent studies have demonstrated that specific expression profiles of circulating miRNAs could be promising blood-based non-invasive biomarkers useful for cancer detection and prognosis in different types of cancer, including NSCLC [14,15,16,17,18]. Human serum or plasma contains a large amount of intact and stable miRNAs, which can be detected with a simple assay such as quantitative real-time PCR (qRT-PCR) [19]. Therefore, the high stability of miRNAs allows for efficient identification in various clinical specimens including sputum, plasma, serum, and frozen and formalin-fixed paraffin embedded tissue samples [14,20,21,22].

The aim of our study was to: 1) select a large panel of miRNAs that have been reported to be highly deregulated in NSCLC, 2) determine whether the plasma expression profiles of these miRNAs were altered in NSCLC patients compared to healthy individuals and 3) evaluate whether the miRNA profile is able to predict the prognosis of resectable NSCLC. We evaluated a panel of seventeen miRNAs by qRT-PCR in the plasma of 52 patients with resectable NSCLC and 30 controls, 10 patients with chronic obstructive pulmonary disease (COPD) and 20-age, sex and smoking status-matched healthy individuals.

Materials and Methods

Study population

Sixty-two patients hospitalized from March 2008 to March 2010 at the Pasteur Hospital (Departments of Pulmonary Medicine, and Thoracic Surgery, CHU de Nice, France) were enrolled in this study. Among these patients, 52 patients had NSCLC and 10 had COPD. COPD patients did not have symptoms of lung cancer or other malignancies. The diagnosis of NSCLC patients was based on examination of all tumor specimens using the 7th pTNM classification and on the last histological classification of NSCLC [23]. In addition, twenty-age, -sex and -smoking status-matched healthy volunteers participated in this study. Written informed consent was obtained from participants after explaining the nature of the study, which was approved by the research ethics board of the Nice University hospital and was performed according to the guidelines of the Declaration of Helsinki. The main clinical and pathological data are summarized in Table 1. Enrollment of patients in our study was conditioned by stringent criteria such as obtained signed consent, availability of resected surgical specimens along with plasma samples, good quality RNA and minimum 18 months follow-up for surviving patients.

miRNA isolation

Peripheral blood (5 ml) was taken prior to surgery and kept in an EDTA-containing tube. The samples were centrifuged at 3000 rpm at 4°C for 10 minutes within 4 hours of collection. The plasma was collected and stored at -80°C until use. Total RNA containing small RNA was extracted from 100 µl of plasma using the miRNeasy Mini Kit (Qiagen GmbH, Hilden, Germany) according to the manufacturer's protocol. The concentration and purity of the RNA were determined with a NanoDrop 1000 (Thermo Fisher Scientific, Wilmington, DE).

Selection of control genes for quantification of plasma miRNAs

To select good candidates, we used some guidelines from Exiqon company (<http://www.exiqon.com/ls/Documents/Scientific/microRNA-serum-plasma-guidelines.pdf>) Endogenous controls such as U6, RNU19, miR-16-5p, miR-192-5p, and miR-103a-3p were analyzed in these samples to identify a small RNA expressed at a similar level in equal volume of sera from both healthy subjects and patients with cancer to serve as a normalization control. Only miR-16-5p, miR-192-5p, and miR-103a-3p were expressed at a high level in the samples of this study (median Ct<30; 100%, 100% and 85% detection, respectively) and not statistically different between the analyzed classes (*t*-test; *P*>0.05), and their levels were the least variable for the miRNAs in all samples (*SD*<0.9) (data not shown). Moreover, miR-103a-3p and miR-16-5p were used as markers of hemolysis [24].

Analysis of the miRNA expression level

Normalization of the results between patients was performed by subtracting the mean of miR-192-5p and miR-16-5p levels to all data (Δ CT) as previously described for other cancers [25,26,27]. Thus, the global mean of the relative expression of each miRNA was calculated and subtracted in order to have all miRNA centered on zero for further studies ($\Delta\Delta$ CT). For diagnosis-related analysis, the mean was based on the cohort of healthy controls Δ CT. For the prognosis-related study, the control Δ CT values were removed for the analysis.

Statistical Analysis

The statistical analyses were performed with SPSS 16.0 statistical software (SPSS Inc., Chicago, IL). Hierarchical clustering and pictures were generated using MeV (TM4 Microarray Software) [28]. The receiver-operator characteristic (ROC) curve and AUC analyses were used to determine the accuracy of each miRNA profile in a specimen with a given specificity rate and to determine the optimal cut-off point. We categorized each miRNA as high or low using the median value as the cut-off. The *chi*², Student or Mann-Whitney *U*-test tests were used to analyze the correlation between the miRNA expression levels and clinicopathological features of the patients. To assess the association of miRNA expression with disease-free survival (DFS), the Kaplan-Meier method and the log-rank test were used to compare survival times between groups. A Cox proportional hazards model was created to identify independent predictors of survival. Variables that were associated with survival with a *P*-value<0.20 in the univariate analysis were included in the multivariate Cox regression. All *P*-values shown were two sided, and a *P*-value≤0.05 was considered statistically significant.

Table 1. Clinicopathological characteristics of the 52 NSCLC patients, 10 COPD patients and 20 healthy individuals included in our study.

Variables	NSCLC patients n (%)	COPD patients n (%)	Healthy subjects n (%)
Overall	52 (100%)	10 (100%)	20 (100%)
Age (years)			
Mean ± SD	65.1 ± 11.1	68.9 ± 6.7	67.5 ± 5.3
Sex			
Male	39 (75%)	8 (80%)	14 (70%)
Female	13 (25%)	2 (20%)	6 (30%)
Smoking status			
Never smoked	8 (15%)	2 (20%)	5 (25%)
Former or current smokers	44 (85%)	8 (80%)	15 (75%)
Histological type			
Adenocarcinoma	27 (52%)	n/a	n/a
Squamous cell carcinoma	25 (48%)	n/a	n/a
pTNM stage			
IA	8 (19%)	n/a	n/a
IB	14 (33%)	n/a	n/a
IIA	5 (12%)	n/a	n/a
IIB	8 (19%)	n/a	n/a
IIIA	7 (17%)	n/a	n/a
Histologic grade			
Well	22 (42%)	n/a	n/a
Moderate	19 (37%)	n/a	n/a
Poor	11 (21%)	n/a	n/a
Adjuvant treatment	21 (40%)	n/a	n/a
Life status			
Alive	40 (77%)	10 (100%)	20 (100%)
Deceased; lung cancer	9 (17%)	n/a	n/a
Deceased; other cause	3 (6%)	n/a	n/a

doi:10.1371/journal.pone.0054596.t001

Results

Levels of expression of plasma miRNAs

Based on the literature, we selected seventeen miRNAs reported to be most frequently altered in primary NSCLC patients (Table S1). To determine whether aberrations in the specified miRNAs could be confirmed in independent plasma samples, we assessed expression of the candidate miRNAs in duplicate assays by qRT-PCR for 52 NSCLC plasma samples and 30 control samples (20 healthy subjects and 10 patients with COPD).

Thirteen (76%) miRNAs including the overexpression of miR-20a-5p, miR-25-3p, miR-155-5p, miR-191-5p, miR-223-3p, miR-296-5p, and miR-320-3p along with the underexpression of let-7f-5p, miR-24-3p, miR-126-3p, miR-145-5p, miR-152-3p, miR-199a-5p, were consistently observed in all plasma samples ($\Delta\Delta CT < 32$) (Table 2). No expression was detected for miR-96-5p, miR-129-5p, miR-373-5p, and miR-516-5p, and these miRNAs were excluded from further analyses (Table 2).

MiRNA profiles of NSCLC patients and cancer-free controls

The hierarchical clustering based *t*-test along with the ROC curves were constructed to estimate the sensitivity and specificity of

the 13-plasma miRNA panel. The accuracy was 79.4% with a sensitivity of 79% and a specificity of 71% (data not shown).

However, the ANOVA test, along with the ROC curve estimation yielded a 12-miRNA signature with improved accuracy in discriminating between cancer-free controls and NSCLC patients (Figure 1). The expression of the twelve-plasma miRNA panel including miR-155-5p, miR-20a-5p, miR-25-3p, miR-296-5p, miR-191-5p, miR-126-3p, miR-223-3p, miR-152-3p, miR-145-5p, miR-199a-5p, miR-24-3p, and let-7f-5p allowed significant discrimination between controls and NSCLC patients with an accuracy of 82.1% (95% CI: 0.792–0.850; $P < 0.001$), demonstrating a sensitivity of 85% and a specificity of 75% (Figure 1). The twelve plasma miRNAs significantly discriminated between controls and stage I NSCLC patients (AUC = 0.806; Figure 1), stage II NSCLC cases (AUC = 0.849; Figure 1) and stage III NSCLC patients (AUC = 0.878; Figure 1).

Next, we carried out pairwise group comparisons to identify miRNAs that contribute significantly to the different separations, including NSCLC versus healthy controls, NSCLC versus COPD patients, and lung adenocarcinoma or squamous cell carcinoma patients versus either healthy individuals or COPD patients. There was a clear separation of the NSCLC patients from the healthy subjects based on an 11-plasma miRNA profile with an accuracy,

Table 2. Plasma expression levels of candidate miRNAs in all sample sets.

miRNA	CT Mean	SD	Deregulation in NSCLC cases
Let-7f-5p	30.76	2.99	Down-regulated
miR-20a-5p	23.08	2.39	Up-regulated
miR-24-3p	23.93	2.97	Down-regulated
miR-25-3p	24.29	1.80	Up-regulated
miR-126-3p	24.20	2.46	Down-regulated
miR-145-5p	31.18	3.01	Down-regulated
miR-152-3p	28.41	2.75	Down-regulated
miR-155-5p	30.50	1.80	Up-regulated
miR-191-5p	25.21	2.88	Up-regulated
miR-199a-5p	30.25	3.61	Down-regulated
miR-223-3p	22.54	3.21	Up-regulated
miR-296-5p	32.16	2.09	Up-regulated
miR-320-3p	22.62	2.18	Up-regulated
miR-96-5p	undetectable	undetectable	undetectable
miR-129-5p	undetectable	undetectable	undetectable
miR-373-5p	undetectable	undetectable	undetectable
miR-516-5p	undetectable	undetectable	undetectable

doi:10.1371/journal.pone.0054596.t002

sensitivity, and specificity of 87.9%, 81.1%, and 82.9%, respectively (Figure 1). In addition, the diagnostic sensitivity of the 11-plasma miRNA signature was higher for squamous cell carcinoma (91.3%) than for adenocarcinoma cases (85.7%) ($P < 0.05$; Figure S1).

Furthermore, a small subset of only six miRNAs still separated NSCLC from COPD with an accuracy, sensitivity, and specificity of 94.4%, 90.9%, and 83.3%, respectively (Figure 1). Interestingly, adenocarcinoma and squamous cell carcinoma cases shared five miRNAs when compared to COPD patients, including miR-20a-5p, miR-152-3p, miR-145-5p, miR-199a-5p, and miR-24-3p. However, miR-191-5p identified only adenocarcinoma patients versus COPD patients, and miR-25-3p, squamous cell carcinoma cases only (Figures S1 & S2). Finally, only three plasma miRNAs were differentially expressed when comparing adenocarcinoma and squamous cell carcinoma patients. Higher plasma levels of miR-20a-5p ($P = 0.034$) and miR-25-3p ($P = 0.013$) along with lower levels of miR-191-5p ($P = 0.008$) were observed in squamous cell carcinoma (Figure S2).

Correlation between plasma miRNAs and clinicopathological features of NSCLC

We then compared the plasma levels of miRNAs with patient clinicopathological parameters. Higher plasma levels of miR-20a-5p ($P = 0.012$) and miR-25-3p ($P = 0.04$) along with decreased levels of miR-191-5p ($P = 0.023$) were observed in squamous cell carcinoma (Table S2; Figure S2). No significant association was found between the levels of miRNAs and age, sex, history of smoking, tumor grade, and pathological stage ($P > 0.05$, Table S2).

Association of plasma miRNAs with DFS of NSCLC patients

We further investigated whether the expression of plasma miRNAs correlated with DFS in our group of NSCLC patients.

The mean DFS in our study population was 46 months (95% CI, 39.4 to 52.9). In the univariate analysis, the clinical factor that significantly associated with DFS was the pTNM stage ($P < 0.0001$). The unadjusted survival analysis showed that high plasma levels of miR-155-5p ($P = 0.068$) and miR-20a-5p ($P = 0.018$) along with a low level of miR-152-3p ($P = 0.049$) were associated with poor DFS of NSCLC patients (Figure S3). The remaining miRNAs such as miR-223-3p ($P = 0.348$), miR-191-5p ($P = 0.671$), miR-320-3p ($P = 0.322$), miR-126-3p ($P = 0.131$), miR-145-5p ($P = 0.705$), miR-199a-5p ($P = 0.612$), miR-24-3p ($P = 0.364$), miR-25-3p ($P = 0.816$), miR-296-5p ($P = 0.853$), and let-7f-5p ($P = 0.964$) were not associated with survival (Figure S4).

Due to the biological differences in the miRNA expression the survival analyses were conducted separately for adenocarcinoma and squamous cell carcinoma patients. Interestingly, the high plasma levels of miR-155-5p ($P = 0.008$), and miR-223-3p ($P = 0.038$) with low plasma level of miR-126-3p ($P = 0.008$; Figure 2) were significantly associated with poor DFS in lung adenocarcinoma patients. In addition, low plasma levels of miR-152-3p ($P = 0.035$) and miR-199a-5p ($P = 0.05$) along with a high plasma level of miR-20a-5p ($P = 0.001$; Figure 2) significantly correlated to decreased DFS in lung squamous cell carcinoma patients. Age, gender, history of smoking, histological subtype, and tumor grade were not associated with DFS. In a multivariate analysis, the independent factors for improved DFS were stage I ($P < 0.001$), low plasma levels of miR-155-5p ($P = 0.030$) and miR-20a-5p ($P = 0.048$) along with high plasma levels of miR-152-3p ($P = 0.029$) and miR-199a-5p ($P = 0.038$) (Table 3).

Discussion

Despite recent advances in diagnosis and treatment strategies, the prognosis of NSCLC across all stages remains unchanged and early detection and prediction of outcome is critical in improving survival. However, it can be sometimes difficult to obtain tissue for diagnosis, in particular in patients with metastatic lung cancer.

Profiling of miRNA expression in lung tumor tissues discriminated cancer patients from cancer-free individuals, and specific miRNAs correlated with disease diagnosis and clinical outcome [29]. Therefore, developing minimally invasive methods by integrating the recent advances in the field of miRNAs for early diagnosis and prognosis of NSCLC is of great interest. Accumulating reports suggest that unique patterns of circulating miRNAs may act as novel biomarkers for early detection of lung cancer and for prediction of outcome [4,19,30]. Endogenous circulating miRNAs are stable and resistant to RNases [14,21]. Because of the simplicity and reproducibility of getting a blood sample, the levels of easily testable miRNAs in plasma seem suited to surveillance of NSCLC outcome [4]. However, it seems that the expression of a single miRNA may not be a reliable biomarker for cancer diagnosis and prognosis [31,32]. Simultaneous assessment of a panel of tumor-specific circulating miRNAs may improve the sensitivity and specificity for diagnosis of lung cancer and may better predict development of the cancer. Therefore, the investigation of a plasma miRNA signature in NSCLC patients using a qRT-PCR assay, as shown in this study, may be of great clinical interest as a routine procedure.

In our study, an 11-plasma miRNAs signature significantly discriminated healthy individuals from NSCLC patients. The accuracy, sensitivity, and specificity for NSCLC detection by the 11-plasma miRNA panel are 87.9%, 85% and 82.9%, respectively, which are higher to those of blood-based single biomarker, such as CYFRA 21-1 (AUC \approx 0.84, sensitivity \approx 50%, specificity \approx 95%), tissue polypeptide specific antigen (AUC \approx 0.74, sensitivity \approx 34%,

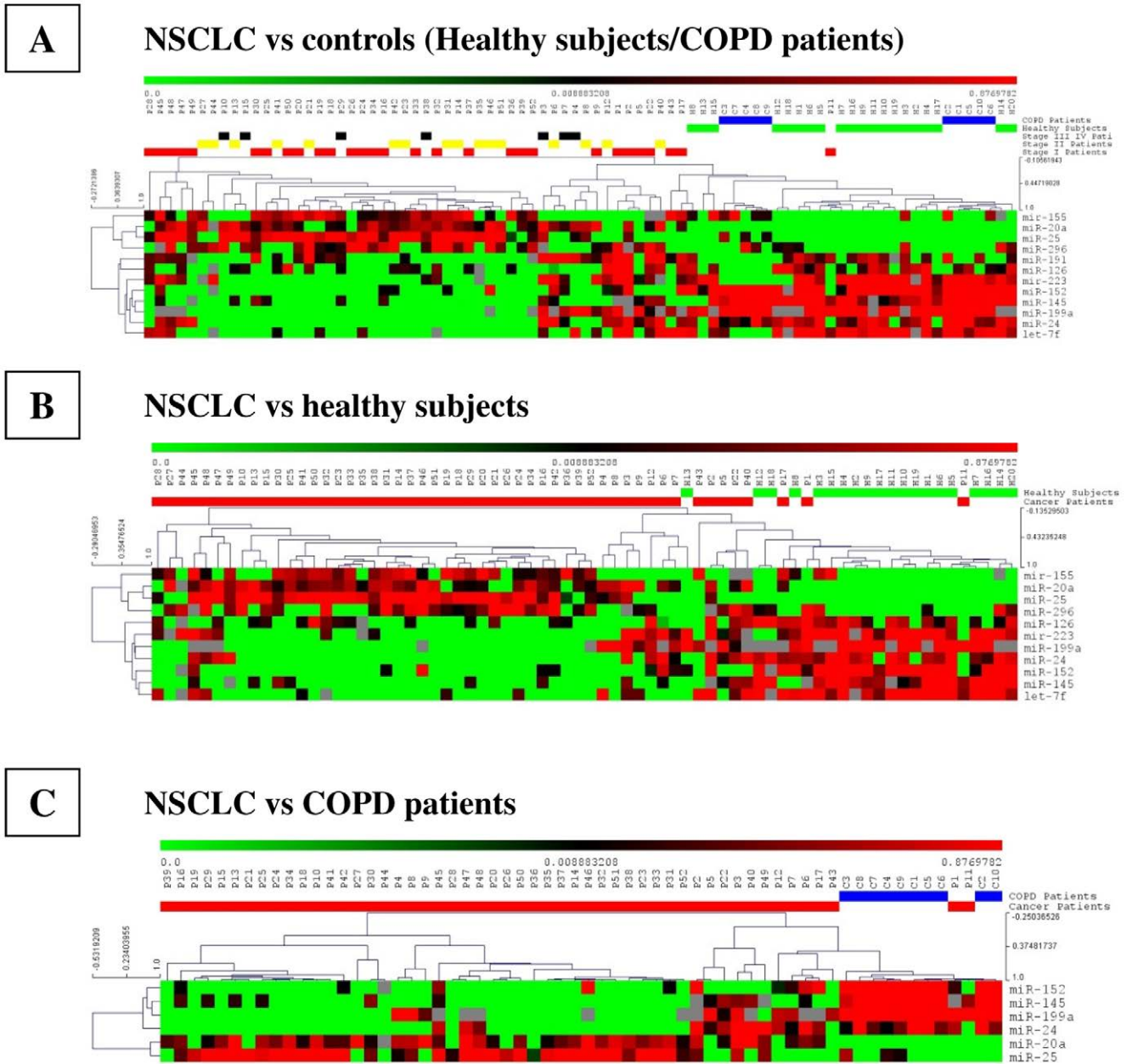


Figure 1. Heat-map clustering analysis of the deregulated miRNA expression levels of NSCLC patients, COPD patients and healthy individuals. Average linkage and 1-Pearson correlation as distance metric were used for the clustering. doi:10.1371/journal.pone.0054596.g001

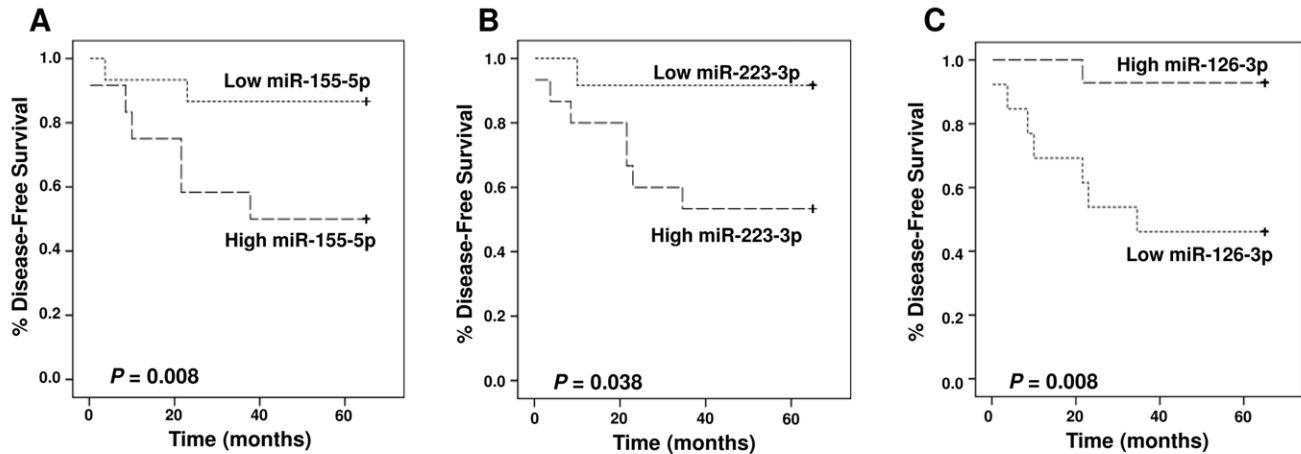
specificity≈95%), and CEA (AUC≈0.8, sensitivity≈53%, specificity≈95%) [33]. Interestingly, the diagnostic sensitivity of the 11-plasma miRNA signature was higher for squamous cell carcinoma than cases of adenocarcinoma.

It has been widely demonstrated across studies that the miRNA expression profiles strongly differentiate lung adenocarcinoma from squamous cell carcinoma [16]. However, a great number of miRNAs are shared in both histological types of NSCLC, as previously reported, which seems to be the case for our selected miRNA panel [16,34,35]. In addition, only three plasma miRNAs were differentially expressed when comparing adenocarcinoma and squamous cell carcinoma patients. In our study, higher plasma levels of miR-20a-5p and miR-25-3p along with lower levels of miR-191-5p were observed in squamous cell carcinoma, as

previously reported [16,35,36,37]. Therefore, although most miRNA expression differences were similar for both tumor types, our limited panel of miRNAs still showed fine differences that suggested that the NSCLC subtypes may follow subtle different pathways to tumorigenesis, as previously suggested [38].

Moreover, miRNA detection in plasma may be an effective procedure for the early detection of NSCLC in high-risk patients with COPD. COPD, along with tobacco smoking, is not only a common lung cancer co-morbidity but it is also associated with a higher risk of development of lung cancer [39,40]. In our study we found six miRNAs differentially expressed in plasma of NSCLC patients when compared to COPD patients, which is consistent with previous reports [39,41]. This finding could represent a powerful clinical application of the six-miRNA molecular classifier

LUNG ADENOCARCINOMA



LUNG SQUAMOUS CELL CARCINOMA

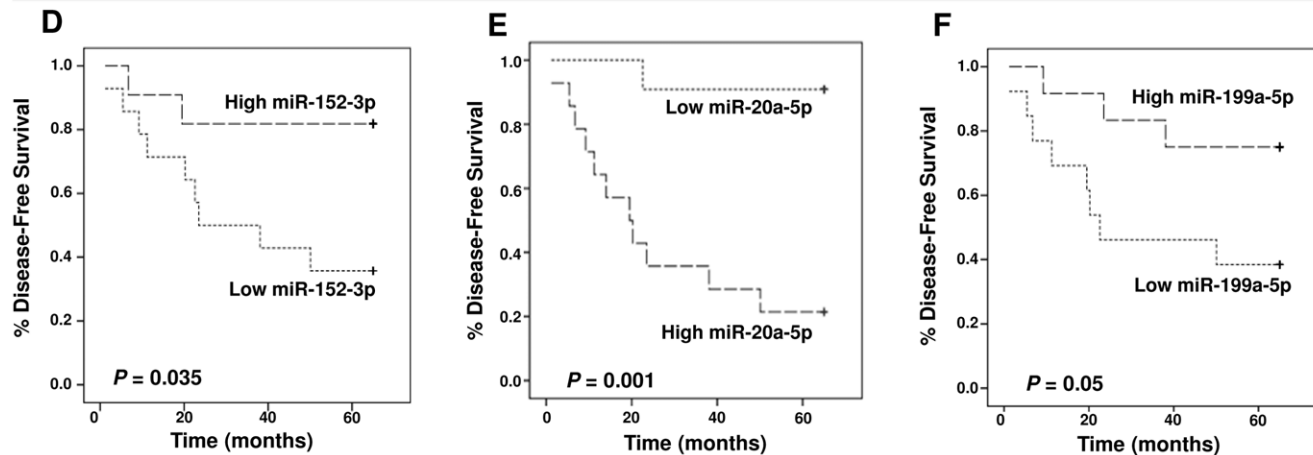


Figure 2. Kaplan-Meier DFS curves for lung adenocarcinoma patients (upper panels) and lung squamous cell carcinoma patients (lower panels) stratified according to plasma levels of miR-155-5p (A), miR-223-3p (B), miR-126-3p (C), miR-152-3p (D), miR-20a-5p (E), and miR-199a-5p (F). The *P*-values were calculated using the log-rank test between patients with high- and low-fold changes.
doi:10.1371/journal.pone.0054596.g002

in COPD patients, which has been explored as a method for early diagnosis of questionable lung densities [39,41].

Although comparison of smokers and never smokers did not demonstrate significant results in our study, possibly because of the small number of never smokers, it was interesting to note that three of the miRNA of the six-plasma miRNA panel, including miR-152-3p, miR-199a-5p and miR-20a-5p, differentially expressed between COPD patients and squamous cell carcinoma patients were able to significantly predict cancer relapse, as previously reported [16,35,36,37]. Our findings emphasize the potential role of these miRNAs as plasma biomarkers playing an important role in lung tumorigenesis and squamous cell carcinoma progression. Finally, we identified a three-plasma miRNA signature including high plasma levels of miR-155-5p and miR-223-3p with low plasma level of miR-126-3p associated with a higher risk for lung adenocarcinoma progression.

Several recent studies have proposed sets of plasma miRNAs as potential markers to monitor the development of lung cancer and its prognosis, in particular for NSCLC [4,14,17,19,30]. However the results of different studies are quite variable and often identified different miRNAs signatures. The reason for this variability is

complex, but likely arises from the differences in patients' ethnicities, sample subtypes (plasma vs. serum vs. whole blood), sample collection methods, technology platforms (microarray or qRT-PCR), as well as the bioinformatic analyses, as previously suggested [42]. We therefore carefully designed our study in order to ensure the identification of reliable miRNAs as plasma biomarkers and employed established methods that reveal valuable clinical information. We only analyzed Caucasian patients to reduce the effect of ethnicity. NSCLC patients were matched according to histology in order to minimize pathological subtype effects and to amplify the molecular homogeneity of tumor specimens. The patients were strictly selected from individuals who had not been previously treated with neoadjuvant treatment to avoid therapy bias. In addition, we demonstrated that our markers could be conveniently measured by qRT-PCR in plasma.

Interestingly, the two panels of plasma miRNAs comprising our lung squamous cell carcinoma and adenocarcinoma progression classifiers have been reported individually to have a prognostic impact in other studies.

Table 3. Multivariate analysis of prognostic factors identified in our study with DFS as the end point in patients with NSCLC.

Prognostic factor	HR ¹	95% CI ²	P-value ³
pTNM stage			
I vs. II+III	0.095	0.030–0.303	<0.001
miR-155-5p			
Low vs. high	0.060	0.005–0.767	0.030
miR-223-3p			
Low vs. high	1.449	0.581–3.614	0.426
miR-20a-5p			
Low vs. high	2.881	1.009–8.227	0.048
miR-152-3p			
High vs. low	0.333	0.125–0.892	0.029
miR-126-3p			
High vs. low	0.497	0.191–1.295	0.153
miR-199a-5p			
High vs. low	0.204	0.045–0.918	0.038

¹HR; hazard ratio. ²CI; confidence interval. ³P-value<0.05 statistically significant. doi:10.1371/journal.pone.0054596.t003

Several studies have recently validated the prognostic utility of the high plasma levels of miR-20a-5p in lung squamous cell carcinoma patients [16,35,36,37]. Furthermore, in our study, miR-199a-5p was a consistent element of the plasma miRNA signature for NSCLC diagnosis in comparison to both healthy individuals and COPD patients. This finding was in agreement with previous results obtained in a tobacco-specific carcinogen-induced lung cancer model that suggested a key role of miR-199a-5p as a part of an early-response miRNAs signature associated with pulmonary tumorigenesis [43]. Chen *et al.* reported a profiling study on serum miRNA expression among 400 NSCLC cases and 220 controls. MiR-152-3p and miR-223-3p were among the 10-serum miRNAs differentially expressed between cancer patients and control subjects in their cohort [44]. In addition, the serum expression level of miR-223 was associated with cancer-specific mortality in stage IA/B NSCLC patients [17]. Moreover, by negatively regulating tumor-suppressor genes, miR-155-5p promotes malignant transformation and cancer progression in many types of cancer, including NSCLC [45,46]. In our study, the up-regulation of miR-155-5p was found to be an independent negative prognostic factor in lung adenocarcinoma patients, as previously reported [34,47]. Shen *et al.* reported a four-miRNA panel in plasma, including miR-126 that distinguished NSCLC from healthy controls with a sensitivity and specificity of 73% and 96%, respectively [30]. One study reported the role as prognostic biomarker for miR-126-3p in NSCLC patients [48]. Finally, the fact that the six plasma miRNAs identified with prognostic utility in our study are common to other studies of NSCLC patients validates our findings.

In conclusion, we developed a robust methodology to study miRNAs in the plasma of NSCLC patients by using a clinically applicable qRT-PCR method. We identified two-plasma miRNA

signatures-histology related that are highly predictive of cancer progression. Three-plasma miRNA panel, including miR-152-3p, miR-199a-5p and miR-20a-5p, was associated with a higher risk for squamous cell carcinoma recurrence, and three-plasma miRNA signature including miR-155-5p, miR-223-3p and miR-126-3p was associated with a higher risk of lung adenocarcinoma progression. However, further studies are needed to fully validate these signatures, so as to investigate the mechanism by which miRNAs enter the bloodstream, to further elucidate the biological significance of miRNAs in the circulation and to evaluate therapeutic response.

Supporting Information

Figure S1 Heat-map clustering analysis of the deregulated miRNAs expression levels stratified according to NSCLC histology subtypes and either COPD patients or healthy individuals. Average linkage and 1-Pearson correlation as distance metric were used for the clustering. Abbreviations: ADC, adenocarcinoma; COPD, chronic obstructive pulmonary disease; SCC, squamous cell carcinoma. (TIF)

Figure S2 The expression levels of 13-plasma miRNAs included in our study and detected by qRT-PCR. Paired Student's *t*-test was performed to ascertain statistical significance between the expression levels across groups. Abbreviations: ADC, adenocarcinoma; COPD, chronic obstructive pulmonary disease; SCC, squamous cell carcinoma. (TIF)

Figure S3 Kaplan-Meier DFS curves for NSCLC patients, independently of histology, stratified according to plasma levels of miR-155-5p (A), miR-20a-5p (B), and miR-152-3p (C). The *P*-values were calculated using the log-rank test between patients with high- and low-fold changes. (TIF)

Figure S4 Kaplan-Meier DFS curves for NSCLC patients, independently of histology, stratified according to plasma levels of miR-223-3p (A), miR-191-5p (B), miR-320-3p (C), miR-126-3p (D), miR-145-5p (E), miR-199a-5p (F), miR-24-3p (G), miR-25-3p (H), miR-296-5p (I), and let-7f-5p (J). The *P*-values were calculated using the log-rank test between patients with high- and low-fold changes. (TIF)

Table S1 The panel of miRNAs included in the study. (DOC)

Table S2 Correlation of plasma miRNAs expression with clinicopathological parameters of NSCLC patients. (DOC)

Author Contributions

Conceived and designed the experiments: CS MI PB PH. Performed the experiments: CS AB MI. Analyzed the data: CS MI PB. Contributed reagents/materials/analysis tools: CHM FB JM PH. Wrote the paper: MI PB PH.

References

- Jemal A, Bray F, Center MM, Ferlay J, Ward E, et al. (2011) Global cancer statistics. *CA Cancer J Clin* 61: 69–90.
- Blanchon F, Grivaux M, Asselain B, Lebas FX, Orlando JP, et al. (2006) 4-year mortality in patients with non-small-cell lung cancer: development and validation of a prognostic index. *Lancet Oncol* 7: 829–836.
- Henschke CI, Yankelevitz DF, Libby DM, Pasmantier MW, Smith JP, et al. (2006) Survival of patients with stage I lung cancer detected on CT screening. *N Engl J Med* 355: 1763–1771.

4. Hu Z, Chen X, Zhao Y, Tian T, Jin G, et al. (2010) Serum microRNA signatures identified in a genome-wide serum microRNA expression profiling predict survival of non-small-cell lung cancer. *J Clin Oncol* 28: 1721–1726.
5. Chiriac LR, Flieder DB (2010) High-resolution computed tomography screening for lung cancer: unexpected findings and new controversies regarding adenocarcinogenesis. *Arch Pathol Lab Med* 134: 41–48.
6. Jiang F, Todd NW, Li R, Zhang H, Fang H, et al. (2010) A panel of sputum-based genomic marker for early detection of lung cancer. *Cancer Prev Res (Phila)* 3: 1571–1578.
7. Duffy MJ (2007) Role of tumor markers in patients with solid cancers: A critical review. *Eur J Intern Med* 18: 175–184.
8. Margolis ML, Hyzy JB, Schenken LL, Schepart BS (1994) Serum tumor markers in non-small cell lung cancer. A comparative analysis. *Cancer* 73: 605–609.
9. Wang QZ, Xu W, Habib N, Xu R (2009) Potential uses of microRNA in lung cancer diagnosis, prognosis, and therapy. *Curr Cancer Drug Targets* 9: 572–594.
10. Dannemann M, Pruffer K, Lizano E, Nickel B, Burbano HA, et al. (2012) Transcription Factors Are Targeted by Differentially Expressed miRNAs in Primates. *Genome Biol Evol* 4: 552–564.
11. McDermott AM, Heneghan HM, Miller N, Kerin MJ (2011) The therapeutic potential of microRNAs: disease modulators and drug targets. *Pharm Res* 28: 3016–3029.
12. Calin GA, Croce CM (2006) MicroRNA signatures in human cancers. *Nat Rev Cancer* 6: 857–866.
13. Nana-Sinkam SP, Croce CM (2011) Non-coding RNAs in cancer initiation and progression and as novel biomarkers. *Mol Oncol* 5: 483–491.
14. Chen X, Ba Y, Ma L, Cai X, Yin Y, et al. (2008) Characterization of microRNAs in serum: a novel class of biomarkers for diagnosis of cancer and other diseases. *Cell Res* 18: 997–1006.
15. Zhao H, Shen J, Medico L, Wang D, Ambrosone CB, et al. (2010) A pilot study of circulating miRNAs as potential biomarkers of early stage breast cancer. *PLoS One* 5: e13735.
16. Landi MT, Zhao Y, Rotunno M, Koshiol J, Liu H, et al. (2010) MicroRNA expression differentiates histology and predicts survival of lung cancer. *Clin Cancer Res* 16: 430–441.
17. Heegaard NH, Schetter AJ, Welsh JA, Yoneda M, Bowman ED, et al. (2012) Circulating micro-RNA expression profiles in early stage nonsmall cell lung cancer. *Int J Cancer* 130: 1378–1386.
18. Zheng D, Haddadin S, Wang Y, Gu LQ, Perry MC, et al. (2011) Plasma microRNAs as novel biomarkers for early detection of lung cancer. *Int J Clin Exp Pathol* 4: 575–586.
19. Boeri M, Verri C, Conte D, Roz L, Modena P, et al. (2011) MicroRNA signatures in tissues and plasma predict development and prognosis of computed tomography detected lung cancer. *Proc Natl Acad Sci U S A* 108: 3713–3718.
20. Xie Y, Todd NW, Liu Z, Zhan M, Fang H, et al. (2010) Altered miRNA expression in sputum for diagnosis of non-small cell lung cancer. *Lung Cancer* 67: 170–176.
21. Mitchell PS, Parkin RK, Kroh EM, Fritz BR, Wyman SK, et al. (2008) Circulating microRNAs as stable blood-based markers for cancer detection. *Proc Natl Acad Sci U S A* 105: 10513–10518.
22. Xi Y, Nakajima G, Gavin E, Morris CG, Kudo K, et al. (2007) Systematic analysis of microRNA expression of RNA extracted from fresh frozen and formalin-fixed paraffin-embedded samples. *RNA* 13: 1668–1674.
23. Travis WD, Brambilla E, Noguchi M, Nicholson AG, Geisinger KR, et al. (2011) International association for the study of lung cancer/american thoracic society/european respiratory society international multidisciplinary classification of lung adenocarcinoma. *J Thorac Oncol* 6: 244–285.
24. Kirschner MB, Kao SC, Edelman JJ, Armstrong NJ, Valley MP, et al. (2011) Haemolysis during sample preparation alters microRNA content of plasma. *PLoS One* 6: e24145.
25. Appaiah HN, Goswami CP, Mina LA, Badve S, Sledge GW Jr., et al. (2011) Persistent upregulation of U6: SNORD44 small RNA ratio in the serum of breast cancer patients. *Breast Cancer Res* 13: R86.
26. Lawrie CH, Gal S, Dunlop HM, Pushkaran B, Liggins AP, et al. (2008) Detection of elevated levels of tumour-associated microRNAs in serum of patients with diffuse large B-cell lymphoma. *Br J Haematol* 141: 672–675.
27. Vasilescu C, Rossi S, Shimizu M, Tudor S, Veronese A, et al. (2009) MicroRNA fingerprints identify miR-150 as a plasma prognostic marker in patients with sepsis. *PLoS One* 4: e7405.
28. Saeed AI, Bhagabati NK, Braisted JC, Liang W, Sharov V, et al. (2006) TM4 microarray software suite. *Methods Enzymol* 411: 134–193.
29. Yu SL, Chen HY, Chang GC, Chen CY, Chen HW, et al. (2008) MicroRNA signature predicts survival and relapse in lung cancer. *Cancer Cell* 13: 48–57.
30. Shen J, Todd NW, Zhang H, Yu L, Lingxiao X, et al. (2011) Plasma microRNAs as potential biomarkers for non-small-cell lung cancer. *Lab Invest* 91: 579–587.
31. Lu J, Getz G, Miska EA, Alvarez-Saavedra E, Lamb J, et al. (2005) MicroRNA expression profiles classify human cancers. *Nature* 435: 834–838.
32. Jay C, Nemunaitis J, Chen P, Fulgham P, Tong AW (2007) miRNA profiling for diagnosis and prognosis of human cancer. *DNA Cell Biol* 26: 293–300.
33. Nisman B, Lafair J, Heching N, Lyass O, Baras M, et al. (1998) Evaluation of tissue polypeptide specific antigen, CYFRA 21-1, and carcinoembryonic antigen in nonsmall cell lung carcinoma: does the combined use of cytokeratin markers give any additional information? *Cancer* 82: 1850–1859.
34. Yanaihara N, Caplen N, Bowman E, Seike M, Kumamoto K, et al. (2006) Unique microRNA molecular profiles in lung cancer diagnosis and prognosis. *Cancer Cell* 9: 189–198.
35. Lu Y, Govindan R, Wang L, Liu PY, Goodgame B, et al. (2012) MicroRNA profiling and prediction of recurrence/relapse-free survival in stage I lung cancer. *Carcinogenesis* 33: 1046–1054.
36. Raponi M, Dossey L, Jatkoec T, Wu X, Chen G, et al. (2009) MicroRNA classifiers for predicting prognosis of squamous cell lung cancer. *Cancer Res* 69: 5776–5783.
37. Huang W, Hu J, Yang DW, Fan XT, Jin Y, et al. (2012) Two MicroRNA Panels to Discriminate Three Subtypes of Lung Carcinoma in Bronchial Brushing Specimens. *Am J Respir Crit Care Med*.
38. McDaniels-Silvers AL, Nimri CF, Stoner GD, Lubet RA, You M (2002) Differential gene expression in human lung adenocarcinomas and squamous cell carcinomas. *Clin Cancer Res* 8: 1127–1138.
39. Leidinger P, Keller A, Borries A, Huwer H, Rohling M, et al. (2011) Specific peripheral miRNA profiles for distinguishing lung cancer from COPD. *Lung Cancer* 74: 41–47.
40. Celli BR (2012) Chronic obstructive pulmonary disease and lung cancer: common pathogenesis, shared clinical challenges. *Proc Am Thorac Soc* 9: 74–79.
41. Akbas F, Coskunpinar E, Aynaci E, Oltulu YM, Yildiz P (2012) Analysis of serum micro-RNAs as potential biomarker in chronic obstructive pulmonary disease. *Exp Lung Res* 38: 286–294.
42. Tan X, Qin W, Zhang L, Hang J, Li B, et al. (2011) A 5-microRNA signature for lung squamous cell carcinoma diagnosis and hsa-miR-31 for prognosis. *Clin Cancer Res* 17: 6802–6811.
43. Kalscheuer S, Zhang X, Zeng Y, Upadhyaya P (2008) Differential expression of microRNAs in early-stage neoplastic transformation in the lungs of F344 rats chronically treated with the tobacco carcinogen 4-(methylnitrosamino)-1-(3-pyridyl)-1-butanone. *Carcinogenesis* 29: 2394–2399.
44. Chen X, Hu Z, Wang W, Ba Y, Ma L, et al. (2012) Identification of ten serum microRNAs from a genome-wide serum microRNA expression profile as novel noninvasive biomarkers for nonsmall cell lung cancer diagnosis. *Int J Cancer* 130: 1620–1628.
45. Jiang S, Zhang HW, Lu MH, He XH, Li Y, et al. (2010) MicroRNA-155 functions as an OncomiR in breast cancer by targeting the suppressor of cytokine signaling 1 gene. *Cancer Res* 70: 3119–3127.
46. Donnem T, Eklo K, Berg T, Sorbye SW, Lonvik K, et al. (2011) Prognostic impact of MiR-155 in non-small cell lung cancer evaluated by in situ hybridization. *J Transl Med* 9: 6.
47. Takamizawa J, Konishi H, Yanagisawa K, Tomida S, Osada H, et al. (2004) Reduced expression of the let-7 microRNAs in human lung cancers in association with shortened postoperative survival. *Cancer Res* 64: 3753–3756.
48. Donnem T, Lonvik K, Eklo K, Berg T, Sorbye SW, et al. (2011) Independent and tissue-specific prognostic impact of miR-126 in nonsmall cell lung cancer: coexpression with vascular endothelial growth factor-A predicts poor survival. *Cancer* 117: 3193–3200.

Significance of circulating tumor cell detection using the CellSearch system in patients with locally advanced head and neck squamous cell carcinoma

Alexandre Bozec · Marius Ilie · Olivier Dassonville · Elodie Long · Gilles Poissonnet · José Santini · Emmanuel Chamorey · Marc Ettaiche · Damien Chauvière · Frédéric Peyrade · Christophe Hebert · Karen Benezery · Anne Sudaka · Juliette Haudebourg · Eric Selva · Paul Hofman

Received: 24 September 2012 / Accepted: 8 February 2013
© Springer-Verlag Berlin Heidelberg 2013

Abstract The objective of this study was to evaluate the potential detection of circulating tumor cells (CTCs) using the CellSearch (CS) AssayTM in patients with locally advanced head and neck squamous cell carcinoma (HNSCC) and then to identify the clinical factors predictive of the presence of CTCs. The presence and number of CTCs were determined using the CS system before treatment, and in 10 healthy individuals (control group). The CS system was able to successfully identify the presence of CTCs in 8 of 49 patients (16 %) before therapy. No CTC was found in the control group. CTCs were detected before therapy in 1 of 19 patients (5 %) with N0 tumor and in 7 of 30 patients (23 %) with N1-2c tumor ($p = 0.12$; Fisher's exact test). CTCs were identified in a relatively low proportion of patients with locally advanced HNSCC.

Keywords Head and neck squamous cell carcinoma · Oral cavity · Oropharynx · Circulating tumor cells · CellSearch system

Introduction

Head and neck squamous cell carcinomas (HNSCC) are the sixth cause of cancer deaths worldwide [1]. At diagnosis, approximately two-thirds of patients with HNSCC have locally advanced tumors and about 50 % of them will die from their cancer [1]. While locoregional recurrence is the main cause of treatment failure, distant metastases arise in around 10–20 % of cases and are associated, despite some recent improvements in palliative chemotherapy, with a very poor prognosis [2]. In addition to conventional clinical prognostic factors such as T-stage and N-stage, there is an urgent need for a reliable blood test to determine prognosis in patients with locally advanced HNSCC in order to identify those patients who may be at increased risk of locoregional recurrence and/or distant metastasis. The potential benefit of this test would be to selectively increase the intensity of treatment in a high-risk subgroup of patients [3]. The role of induction chemotherapy or molecular targeted therapies in association with conventional radiochemotherapy regimens is still to be defined in

A. Bozec (✉) · O. Dassonville · G. Poissonnet · J. Santini
Department of Surgery, Institut Universitaire de la Face
et du Cou, 31 Avenue de Valombrose, 06103 Nice, France
e-mail: alexandre.bozec@nice.unicancer.fr

A. Bozec · M. Ilie · E. Long · P. Hofman
Faculty of Medicine, IRCAN Inserm U1081 Team 3,
06107 Nice, France

M. Ilie · E. Long · P. Hofman
Laboratory of Clinical and Experimental Pathology,
Pasteur Hospital, 06002 Nice, France

M. Ilie · E. Selva · P. Hofman
Human Biobank, Pasteur Hospital, 06002 Nice, France

E. Chamorey · M. Ettaiche · D. Chauvière
Department of Statistics, Antoine Lacassagne Centre,
06189 Nice, France

F. Peyrade · C. Hebert
Department of Medical Oncology, Antoine Lacassagne Centre,
06189 Nice, France

K. Benezery
Department of Radiotherapy, Antoine Lacassagne Centre,
06189 Nice, France

A. Sudaka · J. Haudebourg
Department of Pathology, Antoine Lacassagne Centre,
06189 Nice, France

HNSCC and could be of particular interest in patients identified at high risk of treatment failure [3–5].

Circulating tumor cells (CTCs) have been identified using various technical procedures in several types of human malignancies including HNSCC [6–14]. Studies have linked CTCs to poor prognosis in particular in breast, lung, prostate and colorectal cancers [11–14]. Nevertheless, the clinical and prognosis impact of the presence of CTCs in patients with HNSCC is still elusive. Most published studies on CTCs in patients with HNSCC have enrolled a small cohort of patients and have used heterogeneous techniques of CTC isolation [6–10]. The reproducibility and reliability of these techniques is a critical issue and most of them are currently unvalidated in a clinical setting. Reverse transcriptase PCR-based analyses appear to be very sensitive methods, but are conducted without morphological cellular confirmation which may result in a high rate of false positive cases [7, 8]. The CellSearch (CS) Assay™ (Veridex, NJ, USA) is the only method of CTC identification approved by the Food and Drug Administration in the United States for the follow-up of patients with breast, colon or prostate metastatic carcinomas [11]. This is an EpCAM-based method for enrichment of CTCs in the blood of patients. Because the CS assay relies on the positive selection of EpCAM-expressing cells and the use of anti-cytokeratin antibodies, this method of CTC identification could be inadequate if cancer cells did not express this cell adhesion molecule and/or cytokeratins [8].

The objective of this study was to evaluate the detection and the number of CTCs using the CS assay in patients with locally advanced HNSCC and then to identify the clinical factors predictive of the presence of CTCs in this population.

Materials and methods

Population

Forty-nine patients diagnosed with locally advanced (stage III–IVB) HNSCC involving oral cavity or oropharynx at our institution between November 2009 and July 2011 were enrolled in our study. Patients with a previous history of cancer, severe cardiac, pulmonary, hepatic or renal dysfunction or chronic inflammatory systemic disease were excluded. The patients received the necessary information concerning the study, and consent was obtained from each of them. The study was approved by the regional ethics committees. All patients underwent a CT examination of the head, neck, chest and abdomen and panendoscopy as part of routine clinical care. Patients were staged according to the 2002 American Joint Committee on Cancer (AJCC) staging system. The treatment plan was determined by a multidisciplinary team. All patients were treated with

curative attempt with either surgery or radiotherapy (\pm chemotherapy) or both. Their main clinical characteristics are summarized in Table 1.

CTC detection

The presence of CTCs was determined in all patients prior to the initiation of therapy and in 10 healthy individuals (control group).

The CS system was used to isolate CTCs. Peripheral blood (7.5 mL) was taken and collected in the CellSave preservative tube (Veridex, NJ, USA). Samples were maintained at room temperature and processed within 72 h of blood collection. Briefly, the CS system (Veridex, NJ, USA) consists of a CellPrep system, the CellSearch epithelial cell kit and the CellSpotter Analyzer [13, 14]. The CellPrep system is a semiautomated sample preparation system, and the CellSearch epithelial cell kit consists of ferrofluids coated with epithelial cell-specific EpCAM antibodies to immunomagnetically enrich epithelial cells. In the final processing step, the cells are resuspended in the MagNest Cell Presentation Device (Veridex, NJ, USA). This device consists of a chamber and two magnets that orient the immunomagnetically labeled cells for analysis using the CellSpotter Analyzer. The criteria for definition of a CTC include a round to oval morphology, a visible nucleus (DAPI positive), positive staining for cytokeratin

Table 1 Clinical characteristics of patients

Characteristics	Number of patients (%)
Gender: male/female	34 (69)/15 (31)
Age: <60/> 60 years	24 (49)/25 (51)
Performance status: 0/1/2	36 (73)/12 (25)/1 (2)
ASA score: 1/2/3	14 (29)/30 (61)/5 (10)
Alcohol consumption	27 (84)
Tobacco consumption	19 (58)
Anemia	11 (22)
Neutropenia	1 (2)
Thrombopenia	4 (8)
Tumor site: oral cavity/oropharynx	16 (33)/33 (67)
Tumor differentiation: low/moderate/well	8 (16)/17 (35)/24 (49)
T-stage*: T1/T2/T3/T4	3 (6)/12 (24)/14 (29)/20 (41)
N-stage*: N0/N1/N2a, b or c	19 (39)/11 (22)/19 (39)
Overall tumor stage*: III/IV	15 (31)/34 (69)
Treatment characteristics:	
• Primary surgery and postoperative RT \pm CT	22 (45)
• Surgery alone	4 (8)
• Definitive RT \pm CT	23 (47)

RT radiotherapy, CT concurrent chemotherapy

*2002 American Joint Committee on Cancer (AJCC) staging system

Table 2 Predictive factors of the presence of CTCs before therapy

Clinical factors	Presence of CTCs <i>p</i> value*
Gender	1
Age	0.09
Patient's height	0.74
Patient's weight	0.46
Performance status	0.47
ASA score	0.19
Alcohol consumption	1
Tobacco consumption	0.36
Anemia	1
Thrombopenia	1
Tumor site	0.70
Tumor differentiation	0.59
T-stage	1
N-stage	0.12

* *p* values calculated by Chi-squared tests confirmed by Fisher's exact tests for qualitative factors (all factors except patient's age, height and weight), and by Student's *t* tests for quantitative factors (patient's age, height and weight)

in the cytoplasm and negative staining for CD45. CTC enumeration was expressed as the number of positive cells per 7.5 ml of blood. The results of samples from patients and healthy individuals entered in the study were analyzed by two operators working blindly, without knowledge of the clinical and pathological characteristics of the patients. The cutoff was one detected cell per CS.

Statistical analyses

Univariate analyses were performed to assess the impact of the following factors on the presence of CTCs before therapy: patient's age and gender, patient's height and weight, performance status, ASA score, alcohol and tobacco consumption, tumor site (oral cavity versus oropharynx), T-stage (T4 versus T1–3), N-stage (N > 0 versus N0), tumor differentiation, anemia and thrombopenia. Statistical analyses were done using Chi-squared tests confirmed by Fisher's exact tests for qualitative factors (all factors except patient's age, height and weight), and using Student's *t* tests for quantitative factors (patient's age, height and weight). All statistical tests were performed with the R.2.10.1 software program for Windows, with a significance threshold of 5 %.

Results

The CS system was able to successfully identify the presence of CTCs in 8/49 (16 %) patients with locally

advanced oral or oropharyngeal SCC before therapy. The number of CTCs detected per 7.5 mL of blood sample, ranged from 0 to 5 (0 CTC: *n* = 41 patients; 1: *n* = 5; 2: *n* = 1; 3: *n* = 1; 5: *n* = 1). No CTCs were found in the control group. None of the 10 healthy individuals included in the control group developed any significant disease during the study period.

Gender, patient's height and weight, performance status, ASA score, alcohol and tobacco consumption, tumor site, T-stage, tumor differentiation, anemia and thrombopenia had no impact on the presence of CTCs before therapy (see Table 2). The mean patient age was 66 years and 59 years, respectively, in patients with and without CTCs (*p* = 0.09; *t* test). CTCs were detected before therapy in 1 of 19 patients (5 %) with N0 tumor and in 7 of 30 patients (23 %) with N1-2c tumor (*p* = 0.12; Fisher's exact test).

Six months after the end of the treatment, 13 patients had recurrent or progressive disease (clinical and CT evaluation) and six patients were lost to follow-up. CTCs had been detected before therapy in two of the 13 patients (15 %) with recurrent or progressive disease 6 months after therapy. There was no significant correlation between the presence of CTCs before therapy and progressive or recurrent disease after therapy (*p* = 0.87).

Discussion

Despite aggressive multimodal therapeutic regimens, approximately 50 % of patients with locally advanced HNSCC still die from their cancer [1]. Locoregional recurrences remain the leading cause of death in HNSCC patients [2, 3]. Nevertheless, with the continuous improvement of local control rates, distant metastases represent an increasing cause of treatment failure [2, 3]. Despite some recent improvements, metastatic HNSCC patients still harbor a very poor prognosis [2]. The presence of CTCs could explain the development of metachronous distant metastasis in patients with locally advanced HNSCC even after aggressive initial therapeutic regimens [8]. CTCs and tumor cells disseminated in the bone marrow of patients probably constitute the key reservoir for the subsequent development of distant metastasis [8, 11]. Furthermore, it has recently been demonstrated that CTCs could contribute to the development of local recurrences through colonization of their primary tumor site in a "tumor self-seeding" process [15]. This phenomenon might explain the appearance of local recurrence despite ostensibly complete tumor excision. Therefore, the presence of CTCs could offer a useful marker of poor prognosis in HNSCC patients, thus predicting the development of local or metastatic recurrences.

Few studies have investigated the presence of CTCs in patients with HNSCC [6–10]. Since early-stage tumors are associated with a very low rate of distant metastasis and a favorable prognosis, patients with locally advanced disease are more likely to exhibit CTCs [3, 8]. Until now, the largest series looking for the presence of CTCs in HNSCC patients was reported by Jatana et al. [10]. This study enrolled 48 patients with HNSCC of any stage and site. Using a negative depletion method, the authors found CTCs in 71 % of the patients. Moreover, despite a limited follow-up, they reported a correlation between the presence of CTCs and disease-free survival [10]. The high rate of CTC-positive patients in this series, which included a significant proportion of patients with early-stage HNSCC, appears surprising when compared with other published studies in HNSCC patients showing CTC detection rates around 30–40 % [8]. This highlights one of the main issues when assessing the presence of CTCs in cancer patients, i.e., the reproducibility of the CTC detection technique.

As previously mentioned, the CS system is the only Food and Drug Administration-approved technique for CTC detection in the United States [13, 14]. This technology, currently used in clinical practice for patients with metastatic breast, colon and prostate cancer, is based on positive immunomagnetic enrichment of cells using surface expression of the epithelial cell adhesion molecule EpCAM [13, 14]. Till now, there was only one published study using the CS system for CTC detection in HNSCC patients [7]. This study, reported by Nichols et al. [7] identified the presence of CTCs in 6 of 15 patients with advanced HNSCC at any site. Our series is the largest published study investigating the presence of CTCs in HNSCC patients using the CS assay. We enrolled a homogeneous population of 49 patients with a locally advanced oral or oropharyngeal squamous cell carcinoma. We found CTCs in 16 % of patients before therapy. The rate of CTC-positive patients seems relatively low in our series in comparison to most published studies [6–10]. The use of the CS system, which is a positive selection method, supposes that all tumor cells express the targeted cell surface molecule EpCAM, but also cytokeratins [8]. While this system is undeniably effective for the identification of EpCAM-positive cells, it will not be adequate for those cells that do not express this marker [8]. Interestingly, in an experimental study using a panel of breast cancer cell lines, Sieuwerts et al. [16] demonstrated that some aggressive breast cancer cell lines with a low EpCAM expression were poorly recovered by the CS system. Epithelial-to-mesenchymal transition (EMT) is one of the main phenomena implicated in the invasion and metastatic process of cancer cells, particularly in HNSCC [8]. This EMT is associated with decreased expression of characteristic epithelial markers and potentially of cell adhesion molecules such as EpCAM [8]. This constitutes a substantial bias which could produce a

significant level of false-negative cases when using the CS method for CTC detection. This might explain the relatively low rate of CTC-positive patients encountered in our study. In this regard, it will be interesting, in future studies, to check the potential of other methods for CTC isolation, in particular the isolation of epithelial cells by size technology (ISET), since this method can also detect CTCs even with a mesenchymal phenotype and independently of EpCAM or cytokeratins expression [14, 17].

Our study showed that the rate of CTC-positive patients before treatment tended to increase with the patient's age and N-stage. Interestingly, the correlation between the presence of CTCs and N-stage was also reported in a study by Hristozova et al. [9]. The correlation between tumor stage (T and/or N-stage) and the presence of CTCs in HNSCC patients was not unanimously reported in recent studies [6–10]. However, previous studies had already described an association between tumor stage and the presence of disseminated tumor cells in the bone marrow of HNSCC patients [8, 18, 19].

Given the relatively low rate of CTC-positive patients in our study, assessment of the correlation between presence of CTCs and prognosis would have required including a larger number of patients. Nevertheless, there is accumulating evidence that the detection of CTCs correlates to poor survival in HNSCC patients [6–10]. Therefore, CTC identification could be a promising tool in appropriately tailoring treatment intensity to the particular prognosis of each patient.

Conclusion

The CS system identified CTCs in a low proportion of patients with locally advanced oral or oropharyngeal SCC. Although not statistically significant, our results may indicate a positive association between CTC detection, patient age and lymph node metastasis. Further studies are necessary to improve reliability and reproducibility of CTC detection technologies and to clearly determine the prognostic significance of CTCs in HNSCC patients.

Acknowledgments The authors thank Mr. Yann Chateau for his major contribution in the data management process of this study.

Conflict of interest We have no conflict of interest to declare.

References

1. Ligier K, Belot A, Launoy G et al (2011) Descriptive epidemiology of upper aerodigestive tract cancers in France: incidence over 1980–2005 and projection to 2010. *Oral Oncol* 47:302–307

2. Vermorken JB, Mesia R, Rivera F, Remenar E, Kawecki A, Rottey S (2008) Platinum-based chemotherapy plus cetuximab in head and neck cancer. *N Engl J Med* 359:1116–1127
3. Shah JP, Gil Z (2009) Current concepts in management of oral cancer—surgery. *Oral Oncol* 45:394–401
4. Bozec A, Peyrade F, Fischel JL, Milano G (2009) Emerging molecular targeted therapies in the treatment of head and neck cancer. *Expert Opin Emerg Drugs* 14:299–310
5. Lefebvre JL (2010) Candidates for larynx preservation: the next step? *Oncologist* 15(Suppl 3):30–32
6. Yang L, Lang JC, Balasubramanian P et al (2009) Optimization of an enrichment process for circulating tumor cells from the blood of head and neck cancer patients through depletion of normal cells. *Biotechnol Bioeng* 102:521–534
7. Nichols AC, Lowes LE, Szeto CC et al (2012) Detection of circulating tumor cells in advanced head and neck cancer using the cellsearch system. *Head Neck* 34:1440–1444
8. Jatana KR, Lang JC, Chalmers JJ (2011) Identification of circulating tumor cells: a prognostic marker in squamous cell carcinoma of the head and neck? *Future Oncol* 7:481–484
9. Hristozova T, Korschak R, Stromberger C et al (2011) The presence of circulating tumor cells (CTCs) correlates with lymph node metastasis in nonresectable squamous cell carcinoma of the head and neck region (SCCHN). *Ann Oncol* 22:1878–1885
10. Jatana KR, Balasubramanian P, Lang JC et al (2010) Significance of circulating tumor cells in patients with squamous cell carcinoma of the head and neck: initial results. *Arch Otolaryngol Head Neck Surg* 136:1274–1279
11. Pantel K, Brakenhoff RH, Brandt B (2008) Detection, clinical relevance and specific biological properties of disseminating tumour cells. *Nat Rev Cancer* 8:329–340
12. Cristofanilli M, Budd GT, Ellis MJ et al (2004) Circulating tumor cells, disease progression, and survival in metastatic breast cancer. *N Engl J Med* 351:781–791
13. Riethdorf S, Fritsche H, Müller V et al (2007) Detection of circulating tumor cells in peripheral blood of patients with metastatic breast cancer: a validation study of the cell search system. *Clin Cancer Res* 13:920–928
14. Hofman V, Ilie MI, Long E et al (2011) Detection of circulating tumor cells as a prognostic factor in patients undergoing radical surgery for non-small-cell lung carcinoma: comparison of the efficacy of the Cell Search Assay™ and the isolation by size of epithelial tumor cell method. *Int J Cancer* 129:1651–1660
15. Kim MY, Oskarsson T, Acharyya S et al (2009) Tumor self-seeding by circulating cancer cells. *Cell* 139:1315–1326
16. Sieuwerts AM, Kraan J, Bolt J et al (2009) Anti-epithelial cell adhesion molecule antibodies and the detection of circulating normal-like breast tumor cells. *J Natl Cancer Inst* 101:61–66
17. Vona G, Sabile A, Louha M et al (2000) Isolation by size of epithelial tumor cells: a new method for the immunomorphological and molecular characterization of circulating tumor cells. *Am J Pathol* 156:57–63
18. Ramani P, Thomas G, Ahmed S (2005) Use of Rt-PCR in detecting disseminated cancer cells after incisional biopsy among oral squamous cell carcinoma patients. *J Cancer Res Ther* 1: 92–97
19. Partridge M, Brakenhoff R, Phillips E, Ali K, Francis R, Hooper R (2003) Detection of rare disseminated tumor cells identifies head and neck cancer patients at risk of treatment failure. *Clin Cancer Res* 9:5287–5294

1999) or the components of the IL-31 receptor might be involved in the pathogenesis of sporadic PCA. Although additional work is required to translate our current finding to disease management, modulation of MCP-1 level and function, through IL-31-dependent and -independent pathways, may offer a new approach for therapeutic development for FPCA.

CONFLICT OF INTEREST

The authors state no conflict of interest.

ACKNOWLEDGMENTS

This work was funded by grants from the National Health Research Institutes (MG-099-PP-09, MG-099-PP-01), the National Science Council, Executive Yuan, Taiwan (99-2314-B-010-003-MY3), and the National Research Program for Biopharmaceuticals (101HD1006). We thank those patients who gave their consent to the skin biopsies for our research.

Yu-Ming Shiao¹, Hsiang-Ju Chung¹, Chih-Chiang Chen², Keng-Nan Chiang¹, Yun-Ting Chang^{2,3}, Ding-Dar Lee^{2,3}, Ming-Wei Lin^{4,5}, Shih-Feng Tsai^{1,6,7}, and Isao Matsuura¹

¹Institute of Molecular and Genomic Medicine, National Health Research Institutes, Zhunan, Taiwan; ²Department of Dermatology, Taipei Veterans General Hospital, Taipei, Taiwan; ³Department of Dermatology, Faculty of Medicine, National Yang-Ming University, Taipei, Taiwan; ⁴Institute of Public Health, National Yang-Ming University, Taipei, Taiwan; ⁵Office of Research and

Development, National Yang-Ming University, Taipei, Taiwan; ⁶Genome Research Center, National Yang-Ming University, Taipei, Taiwan and ⁷Department of Life Sciences and Institute of Genome Sciences, National Yang-Ming University, Taipei, Taiwan
E-mail: imatsuura@nhri.org.tw

SUPPLEMENTARY MATERIAL

Supplementary material is linked to the online version of the paper at <http://www.nature.com/jid>

REFERENCES

- Arita K, South AP, Hans-Filho G *et al.* (2008) Oncostatin M receptor-β mutations underlie familial primary localized cutaneous amyloidosis. *Am J Hum Genet* 82:73–80
- Burysek L, Syrovets T, Simmet T (2002) The serine protease plasmin triggers expression of MCP-1 and CD40 in human primary monocytes via activation of p38MAPK and Janus kinase (JAK)/STAT signaling pathways. *J Biol Chem* 277:33509–17
- Cashman JR, Ghirmai S, Abel KJ *et al.* (2008) Immune defects in Alzheimer's disease: new medications development. *BMC Neurosci* 9 (Suppl 2):S13
- Chattopadhyay S, Tracy E, Liang P *et al.* (2007) Interleukin-31 and oncostatin-M mediate distinct signaling reactions and response patterns in lung epithelial cells. *J Biol Chem* 282: 3014–26
- Cornelissen C, Marquardt Y, Czaja K *et al.* (2012) IL-31 regulates differentiation and filaggrin expression in human organotypic skin models. *J Allergy Clin Immunol* 129:426–33
- Fiala M, Lin J, Ringman J *et al.* (2005) Ineffective phagocytosis of amyloid-β by macrophages of

Alzheimer's disease patients. *J Alzheimers Dis* 7:221–32

- Jougasaki M, Ichiki T, Takenoshita Y *et al.* (2010) Statins suppress interleukin-6-induced monocyte chemo-attractant protein-1 by inhibiting Janus kinase/signal transducers and activators of transcription pathways in human vascular endothelial cells. *Br J Pharmacol* 159:1294–303
- Lin MW, Lee DD, Liu TT *et al.* (2010) Novel IL31 RA gene mutation and ancestral OSMR mutant allele in familial primary cutaneous amyloidosis. *Eur J Hum Genet* 18:26–32
- Merlini G, Bellotti V (2003) Molecular mechanisms of amyloidosis. *N Engl J Med* 349: 583–96
- Ollague W, Ollague J, Ferretti H (1990) Epidemiology of primary cutaneous amyloidosis in South America. *Clin Dermatol* 8:25–9
- Pflanz S, Kernebeck T, Giese B *et al.* (2001) Signal transducer gp130: biochemical characterization of the three membrane-proximal extracellular domains and evaluation of their oligomerization potential. *Biochem J* 356: 605–12
- Rovin BH, Lu L, Saxena R (1999) A novel polymorphism in the MCP-1 gene regulatory region that influences MCP-1 expression. *Biochem Biophys Res Commun* 7:344–8
- Tan T (1990) Epidemiology of primary cutaneous amyloidosis in Southeast Asia. *Clin Dermatol* 8:20–4
- Yagi Y, Andoh A, Nishida A *et al.* (2007) Interleukin-31 stimulates production of inflammatory mediators from human colonic subepithelial myofibroblasts. *Int J Mol Med* 19:941–6
- Zhang Q, Putheti P, Zhou Q *et al.* (2008) Structures and biological functions of IL-31 and IL-31 receptors. *Cytokine Growth Factor Rev* 19:347–56

Usefulness of Immunocytochemistry for the Detection of the BRAF^{V600E} Mutation in Circulating Tumor Cells from Metastatic Melanoma Patients

Journal of Investigative Dermatology (2013) 133, 1378–1381; doi:10.1038/jid.2012.485; published online 10 January 2013

TO THE EDITOR

Metastatic melanoma patients harboring a BRAF gene mutation on codon 600 can be treated with targeted therapies (Flaherty, 2012). Depending on the content of tumor cells and on the analytical sensitivity, BRAF mutations

are found in 50–70% of metastatic melanoma patients (Davies *et al.*, 2002). Around 80% display a valine-to-glutamic acid substitution (V600E) and ~16% harbor a valine-to-lysine substitution (V600K) causing constitutive kinase activation (Wan

et al., 2004; Rubinstein *et al.*, 2010). BRAF^{V600E} mutation analysis is currently performed in daily clinical practice on tissue samples using various molecular biology technologies. Moreover, the detection of the BRAF^{V600E} mutation in blood samples from melanoma patients in the context of translational research and clinical trials has been described (Board *et al.*, 2009; Sakaizawa *et al.*, 2012). Metastatic dissemination

Abbreviations: CMCs, circulating melanoma tumor cells; CTCs, circulating tumor cells; ICC, immunocytochemistry; IHC, immunohistochemistry; ISET, isolation by size of epithelial tumor cells

correlates with the presence of circulating tumor cells (CTCs) detected in blood samples (Paterlini-Brechot *et al.*, 2011; Alix-Panabières *et al.*, 2012). The detection of circulating melanoma tumor cells (CMCs) can be performed using different technologies, in particular by the isolation by size of epithelial tumor cells (ISET) method, a direct method that allows cytopathological analysis of CMCs (De Giorgi *et al.*, 2010). Moreover, ancillary methods for CTC characterization can be performed on cells isolated by ISET (De Giorgi *et al.*, 2010; Ilie *et al.*, 2012). Recent studies highlighted the value of immunohistochemistry (IHC) using the VE1 antibody for the detection of the BRAF^{V600E} mutation in melanoma (Capper *et al.*, 2012). The aim of this work was to combine ISET and immunocytochemistry (ICC) using the VE1 antibody to investigate the presence of BRAF^{V600E} in CMCs from metastatic melanoma patients.

Therefore, 98 metastatic melanoma patients were screened for BRAF^{V600E} both by pyrosequencing and by IHC anti-VE1. Concomitantly and blindly, ICC for the BRAF mutation was performed on CMCs isolated by ISET (See Supplementary Data). Population data are shown in Supplementary Table S1.

Of 98 patients, 53 (54%) had a BRAF^{V600E} mutation detected by pyrosequencing in tissue samples. Among these patients, 51/53 (96%) showed strong immunostaining with the VE1 antibody in tissue sections (Supplementary Table S2). Homogenous intracytoplasmic staining without associated nuclear staining was demonstrated in melanoma cells only (Figure 1). Among the tumors negative for the BRAF mutation by pyrosequencing, none had positive VE1 immunostaining (Supplementary Table S2; Figure 1). An excellent concordance was found between these two methods (Supplementary Table S2). The IHC anti-VE1 demonstrated 96% sensitivity and 100% specificity when compared with the sequencing results. CMCs were isolated in 87/98 (89%) patients. Of 87 patients, 54 (62%) demonstrated positive immunostaining on ISET filters as detected by VE1 ICC (Table 1; Figure 1). Forty-six out of fifty-four (85%) patients

Table 1. Correlation between the mutational status of the BRAF gene detected by pyrosequencing on tumor specimens and BRAF^{V600E} expression detected by ICC with the VE1 antibody on circulating melanoma cells isolated by ISET from 87 metastatic melanoma patients

Pyrosequencing (n)	ICC anti-VE1, n (%)		κ-Index	P-value ¹
	Positive	Negative		
V600E (46)	46 (85%)	0 (0%)	0.62	<0.001
V600K (5)	0 (0%)	5 (15%)		
Wild-type (36)	8 (15%)	28 (85%)		
Overall	54 (62%)	33 (38%)		

Abbreviations: ICC, immunocytochemistry; ISET, isolation by size of epithelial tumor cells.

¹A χ^2 test was used. P-value significant at the 0.05 level.

with CMCs positively stained by ICC had a BRAF^{V600E} mutation detected in tissue specimen by pyrosequencing (Table 1; Figure 1). Eight out of fifty-four (15%) patients with positive VE1-immunostained CMCs lacked BRAF^{V600E} in tumor tissues, analyzed both by pyrosequencing and IHC (Table 1; Figure 1). The ICC VE1 CMC-based assay revealed 100% sensitivity and 81% specificity when compared with the pyrosequencing results on the corresponding tumor specimens. Among the 87 patients with CMCs isolated by ISET, 5 had BRAF^{V600K} mutation in melanoma tissue, without positive staining with the VE1 antibody, both in tissue sections and in CMCs (Figure 1). Control immunostaining on CMCs using anti-CD45 was negative (not shown).

This study shows that CMCs isolated by ISET can be used to detect the BRAF^{V600E} mutation in patients with advanced melanoma by using the VE1 antibody. We demonstrated that this noninvasive approach is highly sensitive and relatively specific for the detection of BRAF^{V600E} in CMCs, having high level of concordance with results in tissue samples. In comparison with other approaches used for the detection of BRAF^{V600E} from blood samples, ISET allows cytopathological detection of CMCs before the analysis for a mutation, affording correlation of cytomorphological and ICC data and avoiding interpretation bias (Paterlini-Brechot *et al.*, 2007). Moreover, ISET is a rapid and low-cost method that can easily be repeated, thereby allowing the monitoring of CMC detection in patients on targeted therapy. The use

of ICC for the detection of the BRAF^{V600E} mutation on CMCs has advantages, but also a few potential drawbacks. Interestingly, eight patients included in the present series showed CMCs positively stained by ICC using the VE1 antibody, whereas BRAF^{V600E} was not found in the corresponding tumor tissue samples. As molecular heterogeneity is a common event in tumors, it is possible that the tissue sample used for both pyrosequencing and IHC analysis may not harbor the BRAF^{V600E} mutation (Longo, 2012). In these cases, BRAF^{V600E}-mutated CMCs derived from other parts of the tumor would have invaded the blood stream, initiating metastatic dissemination. Second, even if pyrosequencing is a sensitive technology (~5%), the presence of a small amount of mutated cells in the tissue sample may give a false negative result (Gonzalez de Castro *et al.*, 2012). It has been described previously that VE1 immunostaining may be useful for the detection of smaller amounts of BRAF^{V600E}-mutated cells in tissue sections (Capper *et al.*, 2012). The hypothesis of a false positive ICC result on CMCs can be reasonably eliminated, as negative controls made in parallel on CMCs isolated by ISET did not show any staining. Future developments on the investigation of the BRAF^{V600E} mutation in CMCs isolated by ISET, both by ICC and DNA sequencing, should add more information to this issue. For now, the low number of detected CMCs (from two to eight CMCs) in these eight patients did not allow us to obtain conclusive results by pyrosequencing performed on

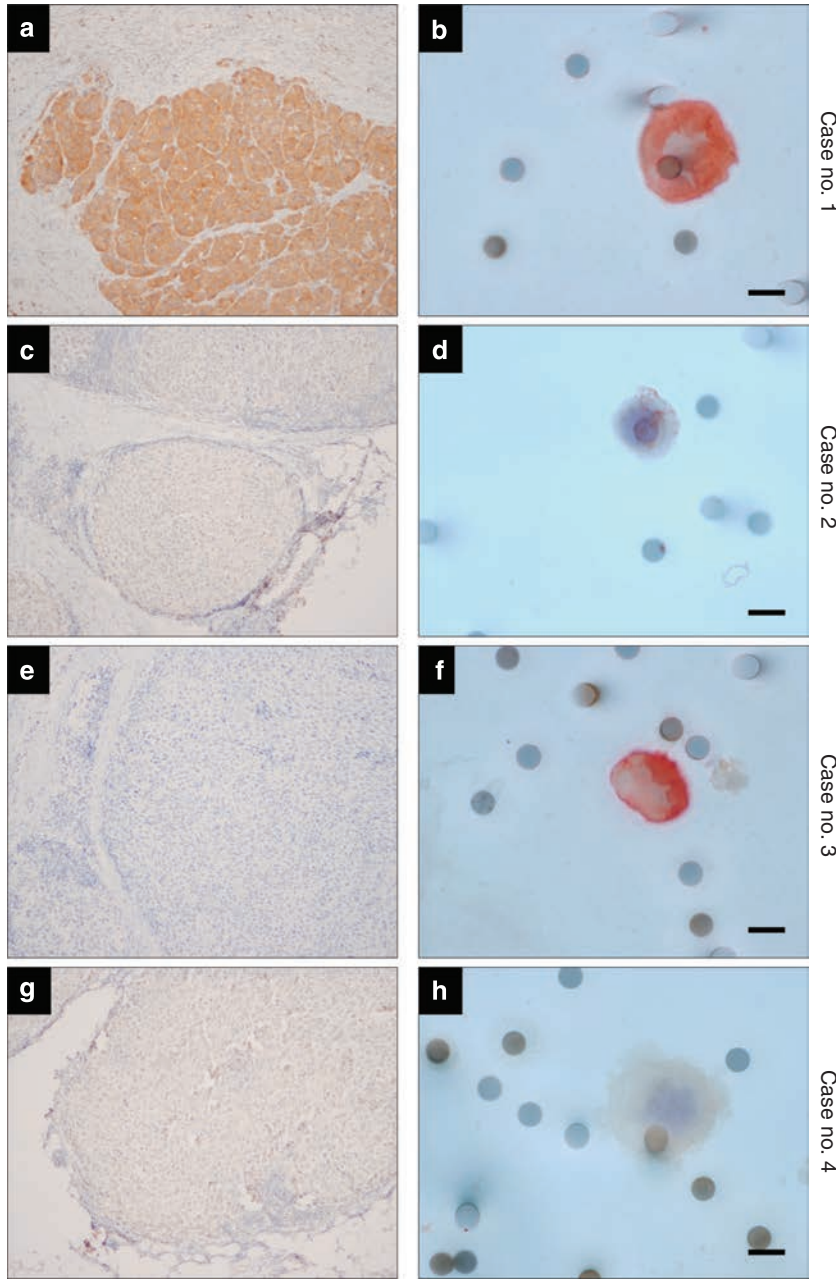


Figure 1. Immunohistochemical features of *BRAF*^{V600E}- or *BRAF*^{V600K}-mutated tumors and *BRAF* wild-type tumors. (Case no. 1) *BRAF*^{V600E}-mutated metastatic melanoma demonstrating positive immunostaining with the VE1 antibody on both (a) a tumor specimen and (b) circulating melanoma cells detected by isolation by size of epithelial tumor cells (ISET). (Case no. 2) *BRAF* wild-type metastatic melanoma showing no staining with the VE1 antibody on both a tumor specimen (c) and (d) circulating melanoma cells. (Case no. 3) *BRAF*^{V600E}-mutated metastatic melanoma displaying positive immunostaining with the VE1 clone on the tumor tissue (e) and (f) intense positive cytoplasmic staining on the circulating melanoma cells detected by ISET. (Case no. 4) *BRAF*^{V600K}-mutated metastatic melanoma demonstrating negative immunostaining with the VE1 antibody on both a tumor specimen (g) and (h) circulating melanoma cells isolated by ISET. Right figures, immunoperoxidase, original magnification $\times 200$; left figures, immunoperoxidase, original magnification $\times 1,000$; scale bar = 16 μ m.

extracted DNA from CMCs. Larger studies are now needed to determine whether the detection of *BRAF*^{V600E} in CMCs using VE1 immunostaining could

allow the selection of patients for a targeted therapy, despite the absence of detection in tissue sample. In conclusion, CMCs can be detected by ISET in

patients with advanced melanoma, and can be analyzed by using ICC with the VE1 antibody for the identification of the *BRAF*^{V600E} mutation in melanoma cells. This approach is noninvasive, rapid, very sensitive, and specific, and opens new options for taking care of metastatic melanoma patients in the era of innovative targeted treatments.

All patients enrolled in the study provided written, informed consent. The study was approved by the Ethics Committee of the Nice University Hospital Centre and was performed in adherence to the Helsinki Guidelines.

CONFLICT OF INTEREST

The authors state no conflict of interest.

ACKNOWLEDGMENTS

MI was supported by the Fondation Lefort-Beaumont de l'Institut de France through collaboration with INSERM Unit 807, Université Paris Descartes.

**Véronique Hofman^{1,2,3,7},
 Marius Ilie^{1,2,3,7}, Elodie Long-Mira^{1,3},
 Damien Giaccherio⁴, Catherine Butori³,
 Bérengère Dadone¹, Eric Selva²,
 Virginie Tanga², Thierry Passeron⁴,
 Gilles Poissonnet⁵, Jean-François
 Emile⁶, Jean-Philippe Lacour⁴,
 Philippe Bahadoran⁴ and
 Paul Hofman^{1,2,3}**

¹Laboratory of Clinical and Experimental Pathology, Pasteur Hospital, Nice, France; ²Human Biobank, Pasteur Hospital, Nice, France; ³Team 3 (Carcinogenesis-related chronic active inflammation) IRCAN, INSERM U1081—CNRS UMR 7284, Faculty of Medicine of Nice, University of Nice Sophia Antipolis, Nice, France; ⁴Department of Dermatology, Archet Hospital, Nice, France; ⁵Department of Surgery, Antoine Lacassagne Centre, Nice, France and ⁶Department of Pathology, Ambroise Paré Hospital, Paris, France
 E-mail: hofman.p@chu-nice.fr

SUPPLEMENTARY MATERIAL

Supplementary material is linked to the online version of the paper at <http://www.nature.com/jid>

REFERENCES

Alix-Panabières C, Schwarzenbach H, Pantel K (2012) Circulating tumor cells and circulating tumor DNA. *Annu Rev Med* 63:199–215
 Board RE, Ellison G, Orr MC *et al.* (2009) Detection of BRAF mutations in the tumour and serum of patients enrolled in the AZD6244 (ARRY-142886) advanced melanoma phase II study. *Br J Cancer* 101:1724–30
 Capper D, Berghoff AS, Magerle M *et al.* (2012) Immunohistochemical testing of BRAF V600E

- status in 1,120 tumor tissue samples of patients with brain metastases. *Acta Neuropathol* 123:223–33
- Davies H, Bignell GR, Cox C *et al.* (2002) Mutations of the BRAF gene in human cancer. *Nature* 417:949–54
- De Giorgi V, Pinzani P, Salviati F *et al.* (2010) Application of a filtration- and isolation-by-size technique for the detection of circulating tumor cells in cutaneous melanoma. *J Invest Dermatol* 130:2440–7
- Flaherty KT (2012) Targeting metastatic melanoma. *Annu Rev Med* 63:171–83
- Gonzalez de Castro D, Angulo B, Gomez B *et al.* (2012) A comparison of three methods for detecting KRAS mutations in formalin-fixed colorectal cancer specimens. *Br J Cancer* 107:345–51
- Ilie M, Long E, Butori C *et al.* (2012) ALK-gene rearrangement: a comparative analysis on circulating tumour cells and tumour tissue from patients with lung adenocarcinoma. *Ann Oncol* 23:2907–13
- Longo DL (2012) Tumor heterogeneity and personalized medicine. *N Engl J Med* 366:956–7
- Paterlini-Brechot P (2011) Organ-specific markers in circulating tumor cell screening: an early indicator of metastasis-capable malignancy. *Future Oncol* 7:849–71
- Paterlini-Brechot P, Benali NL (2007) Circulating tumor cells (CTC) detection: clinical impact and future directions. *Cancer Lett* 253:180–204
- Rubinstein JC, Sznol M, Pavlick AC *et al.* (2010) Incidence of the V600K mutation among melanoma patients with BRAF mutations, and potential therapeutic response to the specific BRAF inhibitor PLX4032. *J Transl Med* 8:67
- Sakaizawa K, Goto Y, Kuniwa Y *et al.* (2012) Mutation analysis of BRAF and KIT in circulating melanoma cells at the single cell level. *Br J Cancer* 106:939–46
- Wan PT, Garnett MJ, Roe SM *et al.* (2004) Mechanism of activation of the RAF-ERK signaling pathway by oncogenic mutations of B-RAF. *Cell* 116:855–67

Plasma MicroRNA-21 Is Associated with Tumor Burden in Cutaneous Melanoma

Journal of Investigative Dermatology (2013) 133, 1381–1384; doi:10.1038/jid.2012.477; published online 10 January 2013

TO THE EDITOR

In the wake of new treatments for advanced melanoma (Chapman *et al.*, 2011; Robert *et al.*, 2011), the identification of novel blood biomarkers to monitor therapeutic response and disease recurrence is timely. MicroRNAs (miRNAs) are promising because they can be assayed directly from blood. Over 1,000 of these exist (Griffiths-Jones *et al.*, 2008) showing alterations in both cancer tissue (Calin *et al.*, 2002) and blood (Mitchell *et al.*, 2008). MiR-21 is one of the most widely studied and is upregulated in many cancers (Volinia *et al.*, 2006). In melanoma, its genetic locus shows gains (Zhang *et al.*, 2006), and in histologically ambiguous melanocytic lesions it is associated with sentinel lymph node status (Grignol *et al.*, 2011) and correlates with prognosis (Jiang *et al.*, 2011). Our hypothesis was that plasma miRNAs are biomarkers of melanoma burden. We used miR-21 as a proof of concept to test this because it has been widely studied in cancer.

We analyzed 160 melanocytic tumors (Supplementary Table S1 online) and 56

blood samples. First, miR-21 expression was measured in 51 melanomas using quantitative PCR, finding a significant association with Breslow thickness and ulceration, two important prognostic features (Balch *et al.*, 2009), $P=0.02$, 0.024 , respectively, Supplementary Table S2 online. To assess independent prognostic value, another set of 79 melanomas was analyzed (Supplementary Table S1 online), 40 having disease-free survival >5 years and 39 having metastasis within 5 years. Logistic regression showed that the stage (IB/IIA versus IIB/IIC) and miR-21 (dichotomized at median) both significantly predicted progression-free survival with an odds ratio of 4.83 (confidence interval (CI), 1.79–13.04), $P=0.002$ and 2.72 (CI, 1.01–7.34), $P=0.048$, respectively. The covariates explained between 16 and 21% of the total variation (Cox and Snell R^2 and Nagelkerke R^2 , respectively). The addition of miR-21 to the American Joint Committee on Cancer (AJCC) stage increased the model accuracy ($\chi^2=4.10$, d.f. = 1, $P=0.043$). These data suggest that tissue miR-21 has independent

prognostic value. We next assessed miR-21 expression during tumor progression in 51 melanomas, 13 common nevi, and 11 congenital nevi using cultured melanocytes as calibrator (Figure 1a). Expression was significantly different ($F=5.65$, d.f. = 2, $P=0.005$). *Post hoc* analysis revealed a trend of increasing expression from common nevi and congenital nevi to melanoma ($F=11.05$, d.f. = 1, $P=0.001$). Colorimetric *in situ* hybridization confirmed tumor cell expression (Figure 1b–d). The relatively high expression in congenital nevi is intriguing, perhaps reflecting their increased risk of progressing to melanoma (Krenzel *et al.*, 2006). These data fit well with recently reported data in melanoma tissues and cell lines (Satzger *et al.*, 2012). We next looked at whether miR-21 expression in metastatic tumor tissue related to plasma levels, finding a strong correlation, $n=5$, $r=0.997$, $P=0.0002$ (Figure 2a). These data confirm that miR-21 is an important tissue biomarker in melanoma and that tissue expression reflects plasma level.

We then looked at whether plasma miR-21 correlated with melanoma burden measured by the AJCC stage. We collected blood from 18 patients

Pitfalls in Lung Cancer Molecular Pathology: How to Limit them in Routine Practice?

M. Ilie^{1,2} and P. Hofman^{*,1,2,3}

¹Laboratory of Clinical and Experimental Pathology, Louis Pasteur Hospital, Nice, France; ²IRCAN Inserm 1081, Team 3, Faculty of Medicine, University of Nice, Nice, France; ³Human Tissue Biobank Unit/CRB INSERM, Louis Pasteur Hospital, Nice, France

Abstract: New treatment options in advanced non-small cell lung carcinoma (NSCLC) targeting activating epidermal growth factor receptor (*EGFR*) gene mutations and other genetic alterations demonstrated the clinical significance of the molecular features of specific subsets of tumors. Therefore, the development of personalized medicine has stimulated the routine integration into pathology departments of somatic mutation testing. However, clinical mutation testing must be optimized and standardized with regard to histological profile, type of samples, pre-analytical steps, methodology and result reporting. Routine molecular testing in NSCLC is currently moving beyond *EGFR* mutational analysis. Recent progress of targeted therapies will require molecular testing for a wide panel of mutations for a personalized molecular diagnosis. As a consequence, efficient testing of multiple molecular abnormalities is an urgent requirement in thoracic oncology. Moreover, increasingly limited tumor sample becomes a major challenge for molecular pathology. Continuous efforts should be made for safe, effective and specific molecular analyses. This must be based on close collaboration between the departments involved in the management of lung cancer. In this review we explored the practical issues and pitfalls surrounding the routine implementation of molecular testing in NSCLC in a pathology laboratory.

Keywords: Molecular testing, non small cell lung carcinoma, pathology, pitfalls, *EGFR*, *KRAS*, *BRAF*, *ALK*, targeted therapy, quality assurance.

1. INTRODUCTION

Lung cancer is the leading cause of cancer-related deaths worldwide, with “classical” treatment options lacking adequate specificity and efficacy [1,2]. Despite these therapies, the 5-year survival rate is about 15% for patients with lung cancer across all stages of the disease [3]. However, in recent years, the treatment options have changed from cytotoxic chemotherapies alone to single-agent and combination targeted therapies [4]. Recent advances in the understanding of cancer biology have allowed the development of molecularly targeted therapies that block oncogenic signaling pathways that characterize lung cancer cells (Fig. 1). Therapeutic decisions are based on the molecular analysis of lung cancer tissue specimens. The development of personalized medicine has challenged the routine integration into pathology laboratories of somatic genetic testing, with molecular assessment being regarded as a powerful supplement to the histopathological diagnosis [5,6].

Epidermal growth factor receptor (*EGFR*) gene mutations are commonly found among molecular abnormalities analyzed in non-small-cell lung cancers (NSCLCs), particularly in lung adenocarcinomas [7,8]. The epidermal growth factor receptor (*EGFR*, *HER-1/ErbB1*) is a receptor tyrosine kinase (TK) of the ErbB family, which consists of four closely related receptors: *HER-1/ErbB1*, *HER-2/neu/ErbB2*, *HER-3/ErbB3* and *HER-4/ErbB4*. Upon ligand binding, receptor homo- or hetero-dimerization and phosphorylation activate the *EGFR* signal downstream of the *PI3K/AKT* pathway, which is involved in cell survival, or activate the *RAS/RAF/MAPK* pathway leading to cell proliferation [9,10]. Patients harboring activating *EGFR* mutations demonstrate response rates higher than 70%, 14-month progression-free survival and 27-month median overall survival when treated with *EGFR*-tyrosine kinase inhibitors (*EGFR*-TKIs; gefitinib, erlotinib) (Fig. 1) [11-13].

Since 2009, gefitinib (IressaTM, AstraZeneca, Macclesfield, Cheshire, UK) was the only licensed oral preparation for use in adult patients with locally advanced or metastatic NSCLC with activating *EGFR* mutations in all lines of therapy [11]. Recently,

erlotinib (TarcevaTM, Roche Group, Basel, Switzerland) has been granted European and US approval for the use as a first-line monotherapy in patients with locally-advanced or metastatic NSCLC with *EGFR* activating mutations. This molecule was already FDA and EMEA approved for use in maintenance and second-line treatment of NSCLC [14].

The short in-frame deletions in exon 19 and the exon 21 L858R point mutation account for approximately 90% of all *EGFR* mutations and are the most predictive of *EGFR*-TKIs efficacy in advanced lung adenocarcinomas [15-17]. However, several *EGFR* mutations contribute to primary or acquired resistance to *EGFR*-TKIs treatment [18]. The most conserved (~49% NSCLC cases) mechanism of resistance to TKIs is associated with the emergence of a single recurrent missense mutation T790M within the *EGFR* kinase domain [19]. Other secondary *EGFR* gene mutations such as D761Y, L747S, and T854A mutations have been associated to TKIs resistance, but with extremely low frequencies [18].

Intense research has led to a more detailed understanding of mechanisms of resistance in these tumors [20]. There is emerging evidence that mutations in other genes of the *EGFR* family (*HER2*) or related tyrosin-kinase receptors (*cMET*) as well as their downstream genes (in particular, *KRAS*, *BRAF*, *PIK3CA*, *AKT1*, *MEK1*) are present in NSCLC [21]. The presence of these mutations can be associated with a lack of response to the first-generation *EGFR*-TKIs in the treatment of NSCLC [22-24]. The amplification or mutation of *cMET* (20%) and *PIK3CA* gene mutations (5%) are among the most frequent “bypass mechanisms” which may determine resistance to TKIs, with continue activation of critical intracellular signaling pathways, despite continued *EGFR* inhibition. [23]. In addition, with the greater understanding of tumor biology, agents that specifically target these oncogenes are currently under development and are being evaluated into clinical trials (Fig. 1).

Recent studies have suggested that resistance to *EGFR*-TKIs may be mediated through *cMET* amplification or point mutations [25]. About 20% of patients with an *EGFR* mutation who initially respond to an oral *EGFR* inhibitor and finally progress are found to have a *cMET* amplification or somatic mutation [26]. Several agents targeting *cMET* are currently under clinical investigation as single agents as well as in combination regimens (Fig. 1) [27]. The selective, non-ATP competitive orally administered *MET* inhibitor, tivantinib (ARQ-197), has recently completed a phase II clinical trial and demonstrated an important progression-free survival

*Address correspondence to this author at the Laboratory of Clinical and Experimental Pathology, Pasteur Hospital, 30 avenue de la voie Romaine, 06002 Nice Cedex 01, France; Tel: +33 4 92 03 87 49; Fax: +33 4 92 03 87 50; E-mail: hofman.p@chu-nice.fr

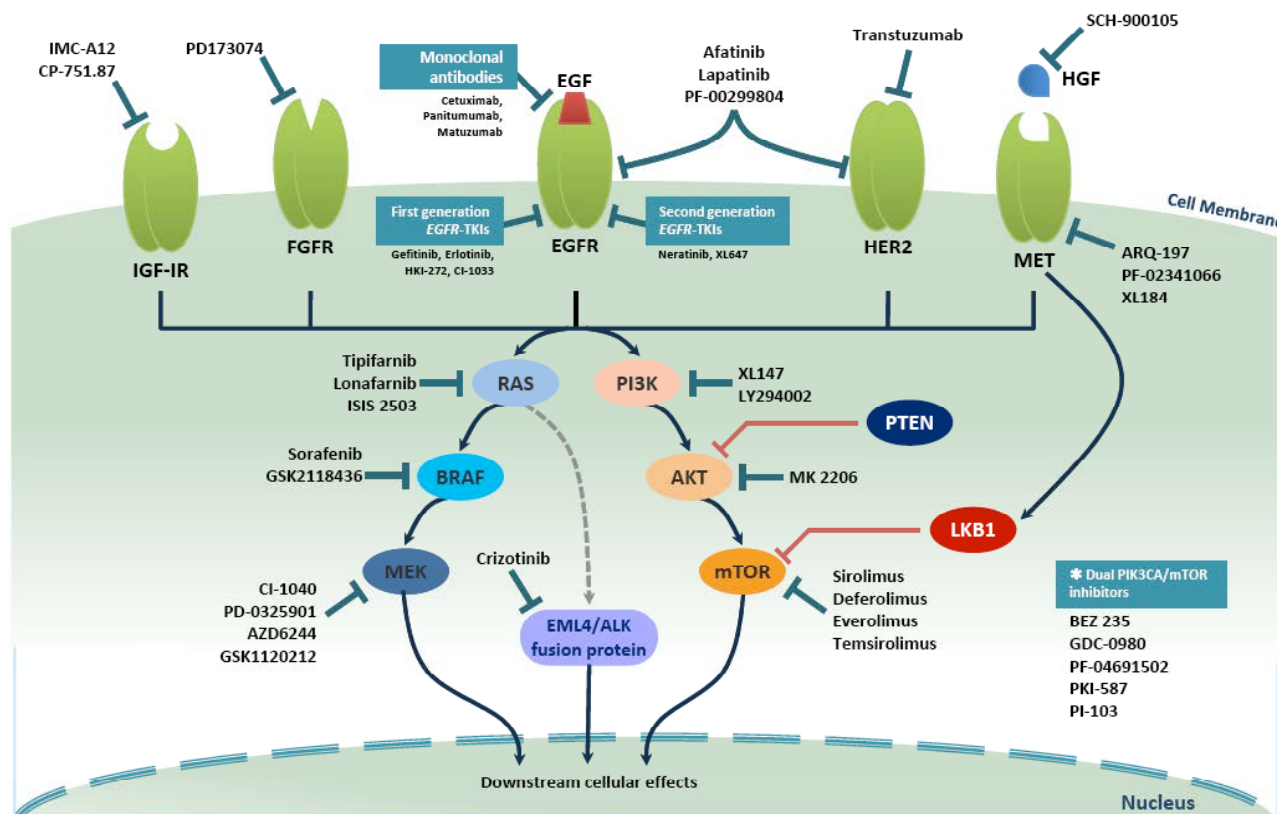


Fig. (1). Currently available therapies targeting relevant oncogenic pathways in NSCLC.

improvement when combined with erlotinib, particularly among patients with non-squamous histology, *EGFR* wild-type status and *KRAS* mutations [28]. Cabozantinib (XL184), a multikinase inhibitor that targets *cMET*, *VEGFR2*, *AXL*, *KIT*, *TIE2*, *FLT3*, and *RET*, dramatically decreased tumor cell proliferation coupled with increased apoptosis and dose-dependent inhibition of tumor growth in breast, lung, and glioma tumor *in vitro* models [29]. Finally, the dual *cMET* and *ALK* inhibitor, crizotinib (PF-02341066), demonstrated tumor and metastasis inhibitory effects in both *cMET* and *ALK*-positive patients [30,31]. This compound is under investigation in a phase I study that combines this multikinase *cMET* inhibitor with the irreversible pan-HER inhibitor PF-00299804 [32].

HER2 (*ErbB2*) gene mutations are found in approximately 2% of NSCLC [33]. The mutations are predominantly small, in-frame insertions in exon 20 and lead to constitutive activation of the mutant *HER2* kinase. In NSCLC, activating mutations of *EGFR* and *HER2* occur in a mutually exclusive manner [34]. Therefore, tumors harboring *HER2* mutations do not respond to treatment with anti-*EGFR* inhibitors or to anti-*HER2* antibody therapy alone (e.g., Trastuzumab; Fig. (1)) [33]. Instead, *HER2* insertions potentially predict sensitivity to treatment with pan-HER molecules that target *EGFR* and *HER2* (e.g., Lapatinib) [35]. Moreover, anti-tumor effects were observed when afatinib (BIBW 2992) that inhibits *EGFR* and *HER2* was used in combination with mTOR inhibitors (e.g., Sirolimus; Fig. (1)) [33]. The pan-HER inhibitor PF-00299804, with affinity for *EGFR*, *HER2*, and *HER4*, has demonstrated activity in a phase II study, and seems to have activity in preclinical models of gefitinib resistance. However, it may not overcome resistance generated by *cMET* amplification [20]. In addition, several small-molecule TKIs that inhibit receptors such as *VEGFR-2*, *EGFR*, *MET*, *PDGFR*, and *KIT* simultaneously have demonstrated clinical value over agents with single targets [26].

Additionally, intense efforts to target mutant *KRAS* are under way, including dual inhibition of the critical downstream RAS effector pathways PI3K/AKT/mTOR and RAS/RAF/MEK (Fig. 1) [36].

The frequency of *KRAS* gene mutations varies according to tumor histology (15%–35% of adenocarcinomas), patient ethnicity (more frequent in Caucasians than Asian patients) and smoking history (more frequent in smokers than never smokers). In addition, *KRAS* mutations are non-overlapping with other oncogenic mutations found in NSCLC [37]. It seems that *KRAS* mutations work better as a negative predictor of response to *EGFR*-TKIs than *EGFR* mutations do as a positive predictor [36,38]. A number of agents targeting *KRAS* have been developed and are currently under clinical investigation. Farnesyl transferase inhibitors (FTIs; tipifarnib and lonafarnib), antisense molecules (e.g. ISIS 2503), and peptide vaccines are being tested in combination with cytotoxic therapy in clinical trials in NSCLC [26].

Somatic *BRAF* mutations are associated with increased kinase activity and as part of the MAP kinase pathway, are involved in cell proliferation, differentiation, and transcriptional regulation (Fig. 1). *BRAF* mutations have been initially identified in melanomas [39]. The *BRAF* mutations prevalence in NSCLC is approximately 1–3%, most of which are adenocarcinomas [33]. In contrast to melanoma where the punctual V600E mutation in *BRAF* kinase domain is the most prevalent (~90%) somatic alteration, NSCLCs can harbor mutations at other positions V600E (50%), G469A (39%), and D594G (11%) [40]. *BRAF* mutations are non-overlapping with other oncogenic mutations found in NSCLC (e.g. *EGFR* or *KRAS* mutations, *ALK* rearrangements) [33]. In lung cancer *in vitro* models *BRAF* mutations predicted decreased sensitivity to the *EGFR*-TKIs [22]. Most of the current clinical data concerning the *BRAF* inhibitors comes from promising studies conducted with these molecules in melanoma. Improved rates of overall survival

and progression-free survival have been reported in a phase III trial comparing vemurafenib to dacarbazine in previously untreated, metastatic melanoma harboring *BRAF* V600E mutation [41]. The activity of sorafenib, the multikinase inhibitor of *BRAF*, *VEGFR-1*, *-2*, *-3*, and *PDGFR* was evaluated in NSCLC, but showed no significant difference in survival of patients [33]. However, the potential impact of *BRAF* mutations as predicting biomarkers of response to selective *BRAF* or *MEK* inhibitors is currently under investigation in NSCLC.

MEK1 (also known as *MAP2K1*) is a serine-threonine protein kinase downstream of *BRAF* and is a central mediator in the *MAP* kinase signaling pathway involved in cellular growth and proliferation (Fig. 1). The frequency of somatic *MEK1* mutations is low (~1%) in NSCLC and these are more common in adenocarcinoma than squamous cell carcinoma. *MEK1* mutations are mutually exclusive to *EGFR*, *KRAS*, *HER2*, and *BRAF* mutations [33]. The presence of *MEK1* mutations has been associated with *in vitro* resistance to *EGFR*-TKIs [24]. Inhibitors of *MEK*, which target further downstream along the *RAS*/*RAF* pathway, have recently been developed (CI-1040, PD-0325901, and AZD6244) (Fig. 1). Preclinical and clinical studies with these agents have shown promising antitumor activity in the treatment of NSCLC [24].

Phosphatidylinositol 3-kinases (PI3Ks) are lipid kinases with a key role in the mediation between growth factor receptors and intracellular downstream signaling pathways (Fig. 1). Preclinical data support the major role of the PI3K pathway in cell proliferation, growth, apoptosis, cytoskeletal rearrangement, disease progression and resistance to chemo- and radiotherapy in NSCLC cell lines [42,43]. The PI3K/*AKT*/*mTOR* signaling pathway may be activated in cancer through multiple mechanisms including mutations in *PIK3CA*, which encodes the catalytic subunit of PI3K, loss or mutation of phosphatase and tensin homolog (*PTEN*), *AKT* mutations and deregulation of mammalian target of rapamycin (*mTOR*) complexes [44,45]. Somatic mutations in *PIK3CA* have been identified in 1-4% of all NSCLC [46]. These mutations occur more frequently within two "hotspot" areas within exon 9 and exon 20 [47]. *PIK3CA* mutations appear to be increased in squamous cell carcinomas than in adenocarcinomas and occur in both never smokers and ever smokers [47]. *PIK3CA* mutations may occur concurrently with *EGFR*, *KRAS*, *BRAF* and *ALK* abnormalities [48]. Pre-clinical data demonstrated that *PIK3CA* activating mutations are sensitive to the dual *PIK3CA*/*mTOR* inhibition (Fig. 1) [45]. In exchange, recent studies suggested that coexisting *KRAS* and *PIK3CA* mutations may be associated with resistance to *PIK3CA*/*mTOR* inhibitors [49]. Multiple PI3K inhibitors are in early clinical development, but thus far the response rates to single agents are low [33]. In addition, *PIK3CA* mutations have been detected in *EGFR* mutant lung cancers with acquired resistance to *EGFR* TKIs therapy [23,50].

AKT is a downstream effector of PI3Ks and is constitutively activated in NSCLCs (Fig. 1) [51]. The prevalence of *AKT1* mutations in NSCLC is about 1%, and they have only been identified in squamous-cell carcinoma [52]. Recently, pre-clinical data suggested that the combination treatment with selective *MEK* (AZD6244) and *AKT* inhibitors (MK2206) had a significant synergistic effect on tumor growth *in vitro* and *in vivo* leading to increased survival rates in mice bearing advanced human lung tumors [53].

PTEN is a tumor suppressor gene by negatively regulating the PI3K/*AKT* signaling (Fig. 1). *PTEN* may be down regulated through several mechanisms, including mutations, loss of heterozygosity, methylation, and protein instability, which contributes to lung carcinogenesis [26]. *PTEN* somatic mutations were identified in 4.5% of all NSCLCs. *PTEN* mutations were found in ever-smokers and were significantly more frequent in

squamous cell carcinoma than in adenocarcinoma. In pre-clinical studies, *PTEN* loss in *EGFR* mutant lung tumors is associated with decreased sensitivity to *EGFR*-TKIs [54].

mTOR plays a critical role in transducing proliferative signaling mediated through the PI3K and *AKT* signaling pathways, that is essential for cancer cell growth and proliferation (Fig. 1) [20]. Its inappropriate activation is involved in the pathogenesis of numerous tumor types, including NSCLC [26]. Numerous molecules interfere with the PI3K/*AKT*/*mTOR* pathway at multiple levels. Some of them, such as the *mTOR* inhibitors temsirolimus and everolimus, are already approved by the FDA and EMEA for other indications, such as renal-cell carcinoma based on previously published phase III randomized trials. *mTOR* inhibition demonstrated promising results in *KRAS*-mutated cell lines [49].

Frequently mutated tumor suppressor genes in NSCLC include *TP53* (50%), *CDKN2A* (p16) (17%), and *LKB1* (*STK11*) (11%) [55, 56]. *TP53* mutations are more common in squamous cell carcinoma (62%) than in adenocarcinoma (39%), with the most frequent mutations occurring in exons 5–8 [55]. *TP53* mutations are more commonly found in the presence of *EGFR* mutations in never-smokers patients [56]. *LKB1* is more frequently mutated in adenocarcinoma than in squamous cell carcinoma (15% vs. 5%), in Caucasian vs. Asian patients (17% vs. 5%), and rather limited to male smokers. *LKB1* mutations may co-exist with *KRAS* or *BRAF* mutations [57,58]. Notably, cell line studies have shown that NSCLC tumors with concurrent mutations in *LKB1* and *KRAS* demonstrate sensitivity to *mTOR* and *MAPK* inhibition that is not apparent with either mutation alone [59]. Moreover, studies using gene therapy by replacement of tumor suppressors in preclinical, and in some early-phase clinical trials for NSCLC, have been performed. In this regard, the most evaluated strategy was that of restoring wild-type p53 expression in lung tumor cells [60]. In general, these trials have demonstrated safety, with low efficacy. Although, some phase I studies of p53 replacement with adenoviral vectors suggested clinical responses with a few partial responses, phase II studies failed to demonstrate difference in response rates for Ad.p53/chemotherapy-treated lesions chemotherapy alone [61]. There are no current trials ongoing in the United States or Europe using this approach in lung cancer. In the opinion of the researchers, the lack of strong bystander effects, along with the low transfection efficiency of adenoviral vectors, limited the potential application in lung cancer, unless more efficient vectors are developed [60]. In recent years, the field of gene therapy in NSCLC has shifted toward "immuno-gene therapy". This strategy requires enough gene transduction to stimulate an endogenous immune response and to create a strong bystander effect. Although these strategies seem to be successful in initiating anti-tumor immune responses, it is generally recognized that there some limits remain (e.g. large tumor volumes; significant immuno-inhibitory networks created by the tumors involving cytokines such as TGF- β , interleukin-10, prostaglandin E2, and vascular-endothelial cell growth factor; and inhibitor cells such as T-regulatory cells and myeloid-derived suppressor cells) [62].

Recent data showed that fibroblast growth factor receptor 1 (*FGFR1*) may be a new promising molecular target for the treatment of smoking-associated lung cancer [63]. *FGFR1* controls a wide range of biological functions in embryogenesis, development, wound healing, angiogenesis and metabolism, by regulating cellular proliferation, survival, migration and differentiation [64]. High-resolution genomic profiling demonstrated that the chromosomal region at 8p12 spanning the *FGFR1* gene locus is amplified in up to ~20% of squamous cell lung carcinoma, and is a rare event (1-2%) in lung adenocarcinoma [65,66]. *FGFR1* copy number aberration can be detected by several techniques, including fluorescent *in situ* hybridization (FISH) analysis [65]. The treatment of mice with *FGFR1*-amplified squamous cell lung cancer xenografts with a small anti-*FGFR1*

molecule (PD173074) resulted in significant tumor shrinkage *in vivo* [65]. In addition, this pathway may function as a mechanism of resistance to anti-EGFR and anti-VEGF treatment [67,68].

In 2007, the echinoderm microtubule-associated protein-like 4 (EML4)-anaplastic lymphoma kinase (ALK) fusion gene was identified in NSCLC [69]. *EML4-ALK* fusion results in protein oligomerization and constitutive switch on the RAS/RAF signaling pathway [49]. Transgenic mice expressing *EML4-ALK* under the control of a lung epithelial cell promoter develop multiple lung adenocarcinomas, demonstrating the oncogenic nature of this fusion gene [33]. *EML4-ALK* fusion is a rare abnormality detected in approximately 2-7% of unselected patients with NSCLC, a frequency that increases (13%) in a population of patients with at least two of the following characteristics: female sex, young adults, Asian ethnicity, never (<100 cigarettes in a life time) or light (≤ 15 pack-year) smoking history, and adenocarcinoma histology [70]. *EML4-ALK* rearrangements are generally found in tumors with wild-type *EGFR*, *KRAS* and *BRAF* [71]. As for *EGFR*-TKIs, *ALK* inhibitors have been found to be highly effective in lung cancers that have this translocation [72]. The small molecule TKI crizotinib (PF02341066; Pfizer, New York, NY, USA) is an orally *ALK* inhibitor of phosphorylation and signal transduction. This inhibition is associated with G1-S phase cell cycle arrest and induction of apoptosis in positive cells *in vitro* and *in vivo* [26]. In a phase 1-2 trial, disease control was achieved in 47 (57%) of 82 patients and 27 (33%) patients with *ALK*-fusion-positive tumors had stable disease [73]. These dramatic findings led to two subsequent clinical trials of PF-02341066. The first is a randomized phase III trial of PF-02341066 compared with standard second line chemotherapy by pemetrexed or docetaxel in *EML4-ALK* rearranged NSCLC. The second is a phase II clinical trial of single agent PF-02341066 in *EML4-ALK* positive NSCLC designed for patients not eligible for the phase III trial or patients randomized to chemotherapy who subsequently developed progressive disease [26]. Therefore, in August 2011, crizotinib (Xalkori®, Pfizer, Inc., New York, USA) was approved by the FDA for the treatment of patients with locally advanced or metastatic NSCLC that express the *ALK* rearrangement. The FDA also approved the Vysis *ALK* Break-Apart FISH Probe Kit (Abbott Molecular, Inc., Des Moines, IL, USA) concurrently with the crizotinib approval [74]. Moreover, patients who harbor this fusion gene do not benefit from *EGFR*-TKIs and should be directed to trials of *ALK*-targeted agents [70].

Finally, an area of increasing interest is the development of rationale combinations of conventional cytotoxic drugs with molecularly targeted therapies, or for combining molecular targeted alone to increase the therapeutic potential by blocking cancer cell survival mechanisms. However, at this point no general guidelines to deal with such combinations exist. Here, we reported several positive results with some combinations, although most of them were reported in pre-clinical studies. The drug interaction patterns observed *in vitro* may not be similar to those observed clinically. As previously noted, the synergy between cytotoxic and targeted therapies cannot always be reliably predicted from preclinical models and inevitably requires clinical validation [20]. Recently, in the INTACT-1, INTACT-2, TALENT, and TRIBUTE clinical trials, the addition of gefitinib or erlotinib to first-line chemotherapy failed to improve survival of NSCLC patients [75]. Some hypotheses were proposed to explain these disappointing results. First, further research efforts are necessary to select biomarkers that may predict response to targeted therapies. Second, all trials applied chemotherapy and targeted drugs simultaneously [76]. Recently, a pharmacodynamic separation model was proposed to bypass this issue: *EGFR*-TKIs primarily cause cell cycle arrest and accumulation of cells in G1; and thus, when administered concurrently with chemotherapy, may push tumor cells to the dormant phases of the mitotic cycle and render them resistant to classic cytotoxic agents [77]. Therefore, as no guidelines are

available for the moment, the definition of the optimal schedule of administration of chemotherapy with molecularly targeted therapeutic agents largely remains a controversial clinical issue.

Taken together, these molecular events define molecular subsets in NSCLC that have been identified as potentially having clinical relevance to targeted therapies [33]. Therefore, additional molecular analyses of genes other than *EGFR* have become necessary to improve patient selection for *EGFR* or other driver mutation targeted therapies. Before the implementation of *EGFR* molecular testing as a clinical practice, *EGFR* genotyping was performed within the context of experimental settings or clinical trials. In this context, tissue samples, tissue processing, and storage conditions were homogeneous, whereas in a routine setting, these different elements are more heterogeneous [78]. Currently, molecular testing for predictive biomarkers in NSCLC is neither standardized nor validated and is yet to be implemented as routine practice in a pathology laboratory. Considering the medical consequences of *EGFR* genotyping and the need to ensure high quality and reproducible analyses, technical guidelines and recommendations for *EGFR* testing in NSCLC were proposed [2,79]. These recommendations emphasize the key role of the pathologist in the selection and preparation of tissue samples, *EGFR* assay selection, and standardized reporting of results.

This review will address the need for standardization and set out the main pitfalls of molecular testing in routine practice in the management of NSCLC patients.

2. RELEVANCE OF MORPHOLOGICAL SAMPLE ASSESSMENT FOR MOLECULAR TESTING

Targeted therapies directed against specific molecular alterations require precise histological sub-classification of NSCLC [80]. Data regarding *EGFR* mutations predicting responsiveness to *EGFR*-TKIs have established the importance of histology in treatment outcome with *EGFR* inhibitors. Medical oncologists place high demands on pathologists to distinguish squamous cell carcinoma from adenocarcinoma and NSCLC not otherwise specified (NOS) in patients with advanced lung cancer [81]. However, it is noteworthy that approximately 70% of lung cancers are well diagnosed and staged by small biopsies or cytology rather than by surgical resection specimens. As expected, more limited samples will result in a less specific diagnosis, in particular with the recent increase in the use of transbronchial needle aspiration (TBNA), endobronchial ultrasound-guided TBNA and esophageal ultrasound-guided needle aspiration [82]. The latest classification of lung adenocarcinoma emphasizes the use and integration of immunohistochemical (i.e., thyroid transcription factor [TTF-1]/p63 staining), and histochemical (i.e., mucin staining) studies for more accurate diagnosis [81]. As well as helping subtype NSCLC, immunohistochemistry (IHC) is sometimes required to discriminate between primary and metastatic disease. However, the IHC profile does not always confirm diagnosis of squamous cell carcinoma or adenocarcinoma. These cases should be reported as 'NSCLC', but with the added caveat 'probably squamous cell' or 'probably adenocarcinoma' (Table 1) [83]. If there is doubt about the histological subtype then molecular testing should be performed. Performing unnecessary IHC tests wastes time, tissue, money and laboratory capacity. This is of great importance, especially when the reference pathology laboratory performs molecular testing on outsourced specimens without knowledge of the percentage of tumor cells left on the paraffin embedded tissue block after the immunohistochemical study. To evaluate tumor content, it is recommended that the pathologist assess a hematoxylin and eosin stained section of the tissue area of the paraffin block designated for mutation analysis before DNA extraction (Table 1).

Small tissue specimens have to be well managed not only for morphological diagnosis but also to maximize the amount of tissue

Table 1. Overview of Different Pitfalls and Recommendations at Each Step of Molecular Testing

Step	Pitfalls	Recommendation
Morphological sample assessment	Distinguish squamous cell carcinoma from adenocarcinoma and NSCLC NOS	Immunohistochemical (TTF1/p63 staining) and histochemical (mucin) studies May report "probably adenocarcinoma"
Material for molecular analysis	No knowledge of the percentage of tumor cells	Perform HE stain before molecular test
Time point	Extended turnaround time	At diagnosis or at disease progression if possible
Who may order?	Extended turnaround time	Treating physicians or pathologists
Sample quality	Warm ischemia time Cold ischemia time	Rapid transfer to the pathology laboratory (e.g., pneumatic air tube transport system)
Fixation	Type of fixative	10% NBF should be used. Bouin's or fixative substitutive fixatives should be avoided. Cryopreservation should be the standard method for tissue fixation and preservation
	Delay of fixation	Avoid prolonged fixation
Type of specimen	Limited size or available sample	Biopsy preferred to cytology specimens
Tumor content	Low percentage of tumor cells	Enrichment for tumor cells (macro- or microdissection)
	Minimum percentage of tumor cells required for molecular analysis	Adaptation according to the estimated analytical sensitivity of each method. Refusal if to low or absent.
Sample preparation	DNA extraction	Between 1 and 10 FFPE sections of 5- to 10- μ m thickness. Avoid contamination (e.g., separate dedicated lab areas, changing blades, sample-to-sample traceability, regular cleaning and decontamination, dedicated sterile scalpel for dissection). Fresh-frozen material should be the standard. Interfering substances removal (e.g., melanin) Test DNA quality (Control PCR amplification) Optimized and controlled reagents.
	Analysis success rate	95% of samples with successful DNA extraction.
Analysis methods	Validated methods vs. "in-house" tests	Should validate and verify each method
	Screening vs. targeted methods	According to clinical needs in agreement with physicians
	Sensitivity	The lower detection limit should be set at 1% of tumor cells for highly sensitive methods and 25-30% for direct sequencing.
	Specificity	False-negative results may occur and can be avoided by regular external quality assessment controls. Mutations should always be independently confirmed in order to avoid false-positive results.
	Reduced performance of mutation immunohistochemistry	Needs further validation
	Interpretation of positive ALK rearrangement by FISH analysis	At least two experienced pathologists should perform the reading. Use positive and negative controls.
	Analysis success rate	97% of samples with correct mutation test results.
	Quality assurance	Needs accreditation / Guidelines / External Quality Assessment Programs
	Final report	Should be reported, in conjunction with the identification of patient and health care professional, the pathology diagnosis, details on the tissue block tested, sample source, sample size and quality, estimation of the proportion of tumor cells in the sample extracted for DNA amplification, the method used, estimated test sensitivity and specificity, test results (mutant or wild-type allele) and interpretation of results in the context of the indication for testing

available for molecular studies. As 10 to 30% of tissue specimens continue to be diagnosed as NSCLC-NOS, the International Association for the Study of Lung Cancer (IASLC) has published recommendations for strategic use of the minimum amount of specimen necessary for accurate diagnosis to preserve as much tissue as possible for potential molecular studies made in a second intention [81].

3. REQUESTING MUTATIONAL STATUS

The patient *EGFR* mutational status remains the best predictor of benefit from *EGFR*-TKIs therapy [36]. *EGFR* somatic mutation testing is certainly the first molecular test prescribed in advanced stage lung adenocarcinomas [2]. *KRAS* and *EGFR* mutations are mutually exclusive molecular events [84]. Given that the *EGFR*-

KRAS signaling cascade is considered to function as unidirectional linear outside-in signaling, tumors harboring mutant *KRAS* are independent of *EGFR* activation, and are resistant to *EGFR*-targeted therapy [36]. One question surrounding *KRAS* testing is whether routine screening of *KRAS* mutations before *EGFR* testing to identify patients who do not benefit from *EGFR*-directed therapy, is worthwhile in terms of improving outcome in clinical practice, without negative consequences from delaying treatment until results are available [17,85].

In our pathology molecular laboratory (LPCE, Pasteur Hospital, Nice, France), *KRAS* testing is performed in conjunction with *EGFR* analysis. Detection of a *KRAS* mutation is a useful finding in a small-volume or poor-quality test samples, removing what may otherwise be an understandable concern regarding a false negative

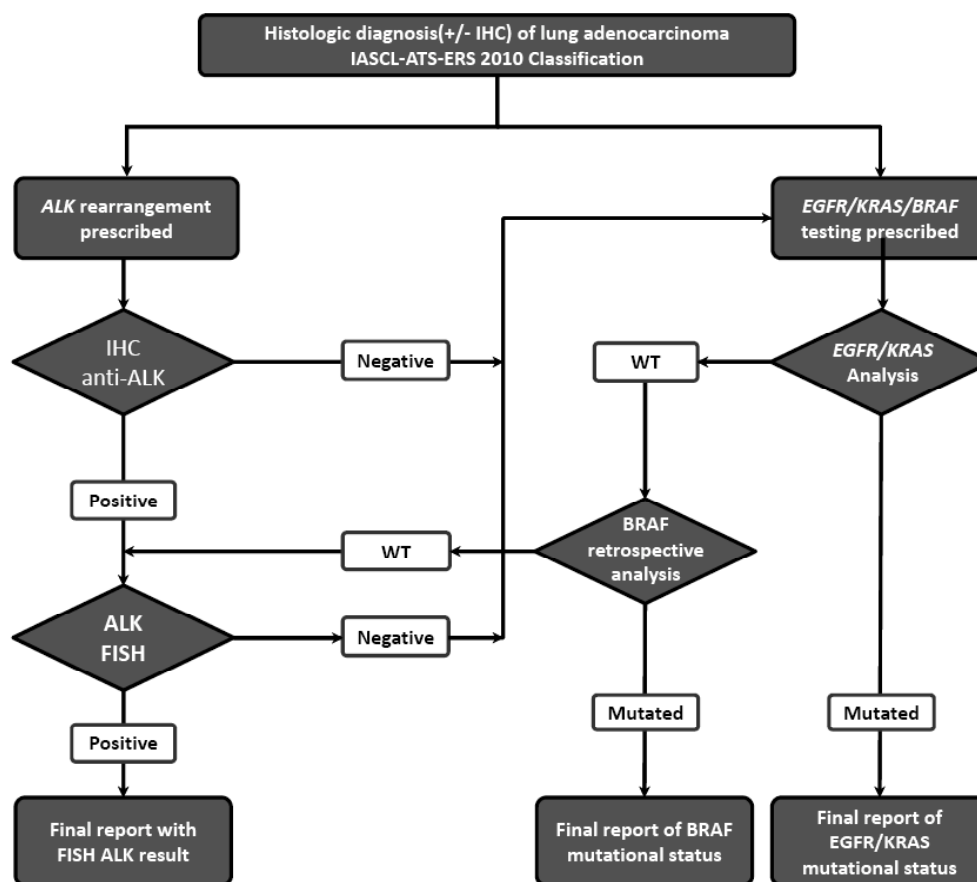


Fig. (2). Current workflow for lung adenocarcinoma molecular testing at the Laboratory of Clinical and Experimental Pathology, CHU de Nice, France.

EGFR mutation test [83]. Although *KRAS* mutation analysis is not recommended to exclude *EGFR* mutations and therefore to make *EGFR*-directed treatment decisions in clinical practice, there may be a place in the near future for this molecular test in making other treatment decisions. In this regard, the BATTLE program is assessing potential biomarkers for a variety of NSCLC treatment strategies, including the potential utility of *KRAS* for predicting treatment success with antiangiogenic agents (i.e; sorafenib) [86].

Genetic mutations in the genes encoding proteins involved in *EGFR* signaling pathways (*KRAS*, *BRAF*, *PIK3CA*, *AKT1*, *MAP2K1*, and *MET*) are mutually exclusive somatic events with exception for *PIK3CA* gene mutations [87]. Development of new therapies targeting the downstream RAS effector pathways PI3K/AKT/mTOR and RAS/RAF/MEK will probably require knowledge about the mutational status for these latter molecules [4]. The future value of testing for the *KRAS* or *BRAF* mutational status may be to exclude the possibility of an *EGFR* mutation or *ALK* translocation or to identify a molecular subset of patients with NSCLC in whom a drug development strategy that targets the *KRAS* pathway is pursued [36].

There is a need to define a standardized stepwise algorithm for molecular testing in the management of NSCLC patients in relationship to available targeted therapies. Fig. (2) shows our current workflow for routine molecular testing of advanced lung adenocarcinoma.

This algorithm has already been used by several large academic centers in the United States and Europe [4]. Moreover, pathologists may order mutational testing at the time of the diagnostic workup in order to reduce the turnaround time for molecular testing and also to provide a complete histological/ molecular diagnosis (Table 1).

Considering the multiple genetic alterations occurring in NSCLC, how pathology departments that do not have adequate molecular laboratory support will manage NSCLC specimens is a strong issue. Testing by outside laboratories brings up another challenge, such as integration of all available data about the tumor (e.g., histology, stage, and mutational profile) in the final pathology molecular report and in the patient's medical records, which is much easier if testing is performed in a single pathology laboratory [4]. Close collaboration, communication flow, and coordination between the departments involved in the management of lung cancer are essential to implement mutation testing in routine practice. Moreover, the development of the concept of integrative pathology associating a morphological pathology laboratory, a molecular pathology laboratory and a biobank in close proximity is probably a good system for optimal patient care.

4. PRE-ANALYTICAL ISSUES

4.1. Specimen Collection

As therapy for NSCLC evolves into more individualized approaches, it becomes increasingly important to optimize the collection, handling, and storage of tissues to improve the consistency and accuracy of molecular analysis. Furthermore, DNA integrity is strongly impacted by the choice of tissue sample and the method of preservation [80]. The influence of pre-analytical steps on biospecimen quality is well-recognized by tumor biobanks. Several markers of sample quality have been identified [88]. One pre-analytical variable of particular interest is the time of ischemia, which may affect the DNA integrity. This includes the time of warm ischemia (from the time of blood vessel ligation to surgical excision) and the time of cold ischemia (from excision to freezing

or fixation). Ideally, the length of both times should be kept to a minimum and both should be recorded [89]. Clearly this is more difficult for the time of warm ischemia, which depends on the surgical procedure being of absolute priority [89]. Pneumatic air tube transport systems can provide safe, efficient and rapid means to optimize the time of cold ischemia [90]. This should be implemented in pathology services, notably in those performing molecular testing.

4.2. Fixation

Another key point in the pre-analytical steps is the fixed tissue on which molecular analyses are performed in the molecular pathology laboratory. Molecular testing is generally performed on formalin-fixed paraffin-embedded (FFPE) specimens. To date, formaldehyde as 10% neutral buffered formalin (NFB) is the most widely used universal fixative as it preserves a wide range of tissues and tissue components. The acid environment of the Bouin's fixative damages both DNA and RNA, and should be definitively avoided for molecular testing [91]. The use of formalin substitute fixatives eliminates exposure of laboratory staff to formaldehyde. However, the DNA quality is somewhat variable when formalin substitute fixatives are used. In addition, the cost of formalin substitute fixatives must also be taken into consideration, and they still contain components that are potentially toxic for humans and are also inflammable [92]. Studies conducted on the preservation status of nucleic acids in FFPE tissues generally agree on the alteration of DNA [92,93]. Considerable evidence suggests that the DNA quality and PCR productivity from FFPE tissues is inferior to frozen tissue, although it may yield adequate results in many cases depending on the type of fixative solution and time of fixation before embedding. We are aware that the integration of tissue cryopreservation could be quite challenging in many pathology services due to the high cost or to the extra storage space required. Moreover, morphological control of a frozen section performed before DNA extraction is always necessary. However, immediate freezing of tumor samples in liquid nitrogen and storage at -80°C or in liquid nitrogen vapor represents the best method for tissue fixation and preservation and can be challenging in routine practice for future multiple molecular analyses and deep sequencing performed from small samples [94]. Finally, the two general rules to prevent DNA damage during storage are "low temperature" and "as dry as possible" [78].

Prolonged fixation in NFB rarely yields good quality DNA [93,95]. As a general rule, short fixation times, 6-12 hours for biopsy specimens and 8-24 hours for larger resection specimens in 10% NFB should be optimal for DNA-based tests, as well as for FISH assays [96].

5. TUMOR TISSUE SAMPLE

Many issues regarding tumor samples dedicated to molecular testing remain to be defined, notably in routine practice, such as the type of specimen, the tumor content, the area of necrosis, the biopsy site, and the reliability of molecular analyses on other specimens, such as cytology or plasma samples. To optimize molecular testing in NSCLC patients, there is a need to maximize tumor tissue acquisition, as described above. Currently, most of the NSCLCs are diagnosed at an advanced stage, and the current trends favor minimally invasive diagnostic procedures, which are challenging since it is difficult to get enough tumor tissue for molecular assessment. Cytological specimens are frequently available for diagnosis. Different methods using cell blocks, scraped cells from archival slides, and fresh cells have been used for molecular testing [97]. However, cytology specimens have not been widely used for molecular testing due to the heterogeneity within samples, and to the sparse cellularity [98-100]. Even though cytological samples may be suitable for analysis, this method needs validation for

routine molecular testing, and further research is needed to fully understand the clinical reliability of mutational data obtained from these samples. Collection and handling of cytological samples still have to be optimized for molecular testing in routine practice. Until then, clinicians should be encouraged to provide tissue biopsy samples whenever possible. In this regard, the NSCLC Working Group published recommendations indicating that FFPE tissue blocks are the preferred sample type for *EGFR* molecular assays (Table 1) [99]. Finally, imaging-guided needle biopsy seems to be satisfactory for mutation analysis. An average of 1.8 needle passes with small (18–20 gauge) core needles yields sufficient and reliable samples for mutation analysis [101].

For mutational analysis, the proportion of malignant cells within the sample is critical for the detection of gene mutations [79]. Enrichment for tumor cells may be required to improve the reliability and accuracy of the detection of tumor-specific somatic mutations, particularly for direct sequencing [79,99]. Selection of material is based upon histological examination of HE sections, and, most often, macrodissection of glass-mounted unstained sections to select for suitable tissue. Laser capture microdissection is a more elegant and accurate approach, but time-consuming, cost effective and less often available or practical and usually not required [83,102]. The minimum number of tumor cells required for adequate mutational analysis is not defined. The European *EGFR* Working Group has recommended that a sample should contain at least 200 tumor cells, with no abundant necrotic tissue, with at least 50% of tumor cells in order to reduce false negative results from sequencing [79]. Reliable results can be obtained with a tumor percentage as low as 10 to 20% when sensitive technical procedures are used. Several methods with higher analytical sensitivity than direct sequencing can detect mutations present at very low levels (1–5% gene copies mutated), allowing the possibility of detection of mutations when the tumor cell proportion is less than 10% of the test sample [103]. In any case, the analytical sensitivity of the method used must be referred to in the final molecular report, as well as the percentage of tumor cells observed in a mirror tissue sample (Fig. 3).

Although pathologists are aware that they should strive to increase the proportion of tumor cell in material for analysis to well above the threshold of the method used, they should not rely upon the sensitivity of the test to compensate for poor specimens [83]. Moreover, one question surrounding the size and the minimum tumor content is whether to exclude clinical specimens for molecular testing. We strongly believe that the refusal to do molecular analyses should be based on specific validated planned exclusion in close collaboration between the physicians and the departments involved in the management of lung cancer. Recently, the European *EGFR* Working Group recommended that rebiopsy at the time of recurrence or disease progression, or even during initial patient work-up, must be considered specifically for mutation testing if the initial samples are inadequate for mutation analysis [79].

The biopsy site, such as primary versus different metastatic tumors, may also influence the final molecular results. Several studies have demonstrated a substantial rate of discordance in results of mutational and FISH assays between primary and metastatic lesions, suggesting tumor heterogeneity at the molecular level during the process of metastasis [104-108]. This heterogeneity may depend on the gene. Usually, clinicians sample only the most easily accessible tumor tissue [79]. However, it seems more relevant to perform molecular testing on the metastatic sites and on tissue from recurrent tumors.

6. TISSUE PROCESSING FOR MOLECULAR TESTING

FFPE processing impairs the extraction efficacy and quality of DNA, thus preventing the possibility of conducting high-quality


 <p align="center">Laboratoire de Pathologie Clinique et Expérimentale Responsable : Pr P. HOFMAN Hôpital Pasteur – Pavillon J - 30 avenue de la voie Romaine - BP 69 - 06002 NICE cedex 1 Tel. - Fax</p>		<p align="right">LM XX.XXX</p>															
<p>Hosp. N° : XXXXXXXX</p> <p>PATIENT NAME : Jon Doe</p> <p>Place of birth : XXXXXXXX</p> <p>Date of birth : DD/MM/YYYY</p> <p>Sex : Male</p> <p>Prescriber : Dr. XXXXXXXX (Hospital XXXXXXXX)</p> <p>Copy to :</p>		<p align="right">Jon Doe</p>															
<p>Date received : DD/MM/YYYY</p> <p>From : Dr XXXXXXXXX</p> <p>Previous reports: Pathology report number ; Previous molecular report number</p> <p>Type of specimen</p>		<p align="center">EGFR GENE SOMATIC MUTATION DETECTION</p>															
<p>CLINICAL DATA:</p> <p>Date of surgery: DD/MM/YYYY</p> <p>Date of prescription: DD/MM/YYYY</p> <p>Prescribing physician/pathologist: Dr _____</p> <p>Pathology laboratory: _____</p> <p>ID number: SXXXXXX</p> <p>Registration date of the molecular testing demand (LPCE): DD/MM/YYYY</p> <p>Date analysis: DD/MM/YYYY</p> <p>Sample type: Surgical specimen/biopsy/TBNA/cytology/etc</p> <p>Histological diagnosis and anatomical site: Pleural metastase of pulmonary adenocarcinoma</p> <p>pTNM stage: IV</p> <p>Tumor cell percentage of the selected area: 70%</p> <p>Sample conditioning: formalin-fixed paraffin embedded tissue block</p>																	
<p>METHODS</p> <ul style="list-style-type: none"> DNA extraction: <ul style="list-style-type: none"> 10 paraffin embedded sections; After macrodissection Manual technique (Raw proteinase K lysate) DNA quantity: concentration : 2.83 µg/µl Spectrophotometer dosage (Nanodrop ND 1000) DNA quality: good Verification by PCR amplification of S26 gene Molecular biology : <ul style="list-style-type: none"> Pyrosequencing technique [PyroMark Q24 Qiagen, after PCR amplification of 18-19-20-21exons of the EGFR gene (Iberascreen EGFR Pyro Kit (ref XXXXXX))] Targeted mutations: Exon19 (p.G719S, p.G719C or p.G719A); Exon 19 (ΔDel19); Exon 20 (p.S768I, p.T790M); Exon 21 (p.L858R, p.L861Q or p.L861R) – Analytical sensitivity: 5% <p align="right">(page 1/2)</p>																	
<p>XXXXXXXXXX Engineer – Preanalytical sector XXXXXXXXXXXX Engineer – Analytical sector</p>		<p>Dr XXXXXXXXX Pathologist responsible of the morphological analysis</p> <p>Dr XXXXXXXXX Pathologist responsible of the molecular analysis</p> <p align="right">(page 2/2)</p>															
<p>Pasteur Hospital</p> <p>Report Date: DD/MM/YYYY</p> <p>Signature Chief of the Department</p> <p>ADICAP Code: OYRSAMA3</p>		<p align="center">RESULT</p> <p>- Presence of a mutation in the <i>EGFR</i> gene in exon 19: p.E746_A750del (Deletion - In frame); c.2235_2249del15.</p> <table border="1"> <thead> <tr> <th>Targeted mutations</th> <th>Therapy prediction</th> </tr> </thead> <tbody> <tr> <td>Exon 18 (p.G719S, p.G719C, p.G719A)</td> <td>Sensitive</td> </tr> <tr> <td>Exon 19 (ΔDel19)</td> <td>Very sensitive</td> </tr> <tr> <td>Exon 20 (p.T790M)</td> <td>Resistance</td> </tr> <tr> <td>Exon 20 (p.S768I)</td> <td>Sensitive</td> </tr> <tr> <td>Exon 21 (p.L858R)</td> <td>Good sensitivity</td> </tr> <tr> <td>Exon 21 (p.L861Q)</td> <td>Sensitive</td> </tr> </tbody> </table> <p><small>Note: A = de-novo + mutation p.T790M associated with an activating mutation in exons 19 or 21 may be responsible for a low-lasting response rate to TKI rather than treatment resistance. 30% of patients with exon 20 mutations (except p.T790M mutation) demonstrate sensitivity to TKIs. Current data do not allow assigning an activating role to the other mutations detected on the EGFR gene by systematic sequencing (in agreement with data published by the French National Cancer Institute – August 2010).</small></p>		Targeted mutations	Therapy prediction	Exon 18 (p.G719S, p.G719C, p.G719A)	Sensitive	Exon 19 (ΔDel19)	Very sensitive	Exon 20 (p.T790M)	Resistance	Exon 20 (p.S768I)	Sensitive	Exon 21 (p.L858R)	Good sensitivity	Exon 21 (p.L861Q)	Sensitive
Targeted mutations	Therapy prediction																
Exon 18 (p.G719S, p.G719C, p.G719A)	Sensitive																
Exon 19 (ΔDel19)	Very sensitive																
Exon 20 (p.T790M)	Resistance																
Exon 20 (p.S768I)	Sensitive																
Exon 21 (p.L858R)	Good sensitivity																
Exon 21 (p.L861Q)	Sensitive																

Fig. (3). Example of a final report of mutational analysis in the pathology molecular laboratory (LPCE, Pasteur Hospital, Nice, France)

molecular analyses and potentially affecting the results of molecular analyses. Fresh-frozen tissue represents an ideal source of archival material for molecular investigations but is not usually possible in routine practice [109].

In most pathology laboratories, DNA-extracts from FFPE samples are the most common source of template for PCR amplification. Although commercial kits for molecular pathology testing are now available, most of the current tests use in-house methods since they are much cheaper. Thus, there is a urgent need for standardization of procedures in molecular pathology, starting from nucleic acid extraction [110]. The choice of a method of nucleic acid extraction depends on several factors, including assay targets (RNA/DNA-based), specimen type, sample throughput, laboratory workflow, cost, and the performance of the extraction system. Thus, we have to keep in mind that the sample preparation processes of DNA/RNA extraction and purification are time-consuming and labor-intensive. Several steps are required, including lysis, nucleic acid extraction, impurity washes, and DNA/RNA elution.

In regard to the type of tissue preservation, the extraction methods are different when using either FFPE or fresh-frozen samples [103]. FFPE sections require a supplementary time of deparaffination. Moreover, the xylene used to remove paraffin is toxic. It can cause serious health problems and must be handled under a safety hood.

Sections cut from the FFPE tissue blocks are the standard resource for DNA extraction. Between one and ten sections of 5- to 10-µm thickness should be used (Table 1) [2]. Laboratories that use

laser capture microdissection will require thinner sections [2]. To avoid contamination or sample-to-sample carry-over, some precautions are required, such as performing extraction and amplification in separate dedicated laboratory areas (preferably a self-contained area or laminar flow hood) using dedicated material, changing blades between each paraffin block, ensure sample-to-result traceability by appropriate labeling of the container at each transfer step, regular cleaning and decontamination of all material and instruments. If the percentage of tumor cells is too low, or if the section contains necrotic tissue, fatty tissue, hemorrhagic tissue or a melanin rich area (e.g. lung metastasis of malignant melanoma), then the section must be dissected. It is highly recommended to use a dedicated sterile scalpel to select the tissue part in order to enrich the sample in tumor cells.

The DNA-extraction protocols range from homemade to commercial kits and can be divided into several groups, such as DNA extraction with or without precipitation or purification, and silica based adsorption columns. There is no consensus as to whether a single protocol is highly superior to others [110]. There is also general agreement that for molecular testing performance the quality of amplifiable DNA is more important than its quantity [79]. Most testing laboratories report a technical failure rate of 3–8%, which is often due to PCR failure as a result of poor quality DNA, most probably due to overfixation, or insufficient DNA [83]. It is highly recommended to perform a control PCR amplification to test the DNA quality and also to give the quality results to the clinician in the molecular pathology report (Fig. 3). If a sample that does not meet quality criteria has a wild-type genotype, it should be reported that a mutation was not found but that the presence of a mutation

cannot be excluded due to the poor quality of the sample [79]. We consider that no matter the method used for nucleic acid isolation, it is recommended to employ only optimized and controlled reagents in order to avoid variability in results. Some commercial nucleic acid extraction kits with automated instruments have been developed for molecular testing [111]. The automation of DNA extraction has the advantage of standardized sample treatment and avoidance of error during routine sample handling and contamination due to intermediate processes [111,112]. However, there is some debate as to the efficiency of DNA extraction by automated methods in comparison with manual extraction methods when a limited sample volume is used [113].

7. METHODS FOR MUTATION TESTING

There is a wide range of methods available for mutation detection in the oncology field. Many of these methods use laboratory-based assays and are not commercially available for use in routine molecular testing. Other methods are available as commercial test kits [114]. It is noteworthy that only a few of these tests have met the requirements of the European Directives (CE-Mark) for molecular diagnostic use.

All these methods have certain advantages and disadvantages, and there is no consensus agreement on which is the preferred method [79]. The technologies can be divided into two subgroups, screening and targeted mutation detection technologies [99]. Many of the tests available for *EGFR* molecular testing are also available for *KRAS* and *BRAF* mutation analysis, and vice versa.

EGFR gene mutations have been commonly detected by direct sequencing, this method is available in many molecular pathology laboratories. This technique allows the detection of all variants, including novel variants. The detection of unreported mutations should always be independently confirmed to avoid false-positive results due mainly to fixation and long storage conditions [78]. With sequencing there is no need for batching of samples and it provides better control of contamination as the exact, specific mutation in the sample can be determined. However, the sensitivity of direct sequencing is suboptimal in comparison with targeted methods (10-30% mutant DNA in a normal DNA background of heterogeneous tumors) [83]. In the setting of NSCLC, in which diagnosis is often based on small sized samples with a low percentage of tumor cells, detection of a mutation by direct sequencing may frequently lead to false-negative results [115]. Moreover, this method requires experienced operators and tends to be more labor-intensive, frequently resulting in an extended turnaround time for reporting results [116].

Beside this method, there are a variety of “in-house” developed screening tests. These latter methods are subject to higher inter- and intra-laboratory variability and are not always prone to adequate quality assurance, which ensures the reproducibility of the results [114]. Furthermore, highly sensitive methods were used, with the caveat that only targeted mutations are identified. The assessment of the *EGFR* mutational status has mainly focused on the detection of the most common *EGFR*-sensitizing mutations: exon 19 in-frame deletions and point mutations in exon 21 (L858R and L861Q) [117]. The technologies used may detect only the mutations assayed and therefore are less time consuming. Sensitivity is increased compared to screening tests (1 to 10% mutant DNA in a normal DNA background of heterogeneous tumors) [115]. Moreover, some of these techniques do not require a large amount of tissue and have quite equivalent performance rates for either fresh tissue or FFPE samples [116,118,119]. However, despite its low sensitivity direct sequencing is still considered the gold standard for gene mutation analysis, as some of the targeted assays require sequencing for confirmation of results. Furthermore, the significance of low-abundance mutations detected in heterogeneous samples is uncertain and these mutations need further determination of their

clinical or predictive significance [4]. Highly sensitive methods may also increase the risk of false-positive results [83]. Because of the need for mutation-specific primers, comprehensive detection of in-frame deletions in *EGFR* exon 19 may not always be possible [115]. The advantage of commercially available tests is the validation process that they have gone through, but cost factors could hamper the adoption of these kits [114]. As new targeted therapies against oncogenic targets other than *EGFR* are developed, there is an increasing need for multiple mutations testing in NSCLC. Multiplexed PCR are being developed to screen mutations in several clinically relevant genes within a single reaction. These methods seem robust and reliable in FFPE-derived DNA samples, although they are currently under evaluation [120].

Another assay that needs further validation, as it may provide a rapid and cost-effective molecular test, is IHC. IHC has the advantage of being widely available in a pathology laboratory, relatively easy to perform and retains morphological informative data [83]. Interestingly, two mutant-specific monoclonal antibodies directed against the most common mutant forms of *EGFR* have been recently developed for IHC use: the 15-bp deletion (E746_A750del) in exon 19 and the L858R point mutation in exon 21 [121]. So far, both antibodies demonstrated reduced clinically performance with sensitivities ranged between 23% and 99% for exon 19 deletions and 75%-100% for the L858R mutation [122,123]. Therefore, *EGFR* IHC is still challenging for *EGFR* testing in NSCLC in routine practice [79].

Although, until now, routine testing for *ALK* rearrangements is not currently recommended outside clinical trials, several molecular tests are available, such as FISH, reverse transcriptase-PCR (RT-PCR), multiplex PCR and IHC [124-126]. At present, the FISH assay, using commercial break-apart *ALK* probes has been the method of choice for selection of patients in the current clinical trials. However, some limitations exist. Although, the recommended type of fixative is the 10% NFB, prolonged tissue fixation may lead to progressive degradation of signal intensity. The acid fixatives damage DNA and should be definitively avoided for FISH analysis [91]. The interpretation of a positive rearrangement through the introduction of a gap between the red and green probes could be challenging. Moreover, morphological indicators of tumor cells versus non neoplastic cells are almost totally lost under fluorescence [116]. In this regard, analyses must be performed by experienced pathologists with a recommended two-person scoring approach when the percentage of positive cells is close to the cut-off (between 5% and 25%) (Table 1). It is critical to use adequate positive and negative control specimens in each assay. By FISH analysis, the actual gene rearrangement is not known, although the clinical significance between isoforms is uncertain. RT-PCR as a screening method seems to be less adapted to clinical use. Moreover, the success rate of RT-PCR on FFPE tissues is unsatisfactory, with low efficiency of RNA extraction and impaired reverse transcriptase reaction by formalin-induced degradation [4]. The IHC seems to be a relatively specific technique for identification of *ALK* rearrangements, although commercially available antibodies have demonstrated poor sensitivity [127]. Molecular pathology laboratories should test the sensitivity of immunohistochemistry in their local conditions to be made aware of its limitations in routine practice [127].

Overall, the choice of a particular molecular methodology will depend upon the available technology or what is most appropriate for individual pathology departments or cancer networks to develop [83]. This has to consider the balance between efficacy, robustness, sensitivity and specificity, method validation, analysis success rate, and costs. Testing may be developed “in-house” or in conjunction with existing local molecular pathology/genetics laboratories with the necessary expertise and technology.

8. QUALITY ASSURANCE

All molecular pathology testing must be provided and practiced under a quality assurance framework, which is subject to adaptation and interpretation by regulatory and professional organizations. Accreditation has been recognized as an effective procedure to assure the analytical and diagnostic quality for optimal patient care (Table 1) [128]. To address the need for standardized molecular mutation testing and if no legislative requirements are in place, professional societies for pathology may play an important role in forming settings for adaptation of existing accreditation systems to the needs of molecular pathology testing. This should also be the basis for international recognition of providers of external quality assessment programs. While internal quality procedures begin to be implemented in every laboratory, External Quality Assessment Programs (EQAP) are important tools to increase the analytical or diagnostic proficiency of the molecular pathology laboratory. Although there is general recognition of the necessity of EQAPs, they are usually not mandatory in EU countries. The establishment of reference laboratories in Europe may also be helpful: such laboratories exist for *KRAS* mutation testing in colorectal cancer [129,130]. Finally to prevent poor-quality mutation testing, professional organizations have developed guidelines, recommendations and checklists to which molecular pathology laboratories must comply (<http://www.oecd.org>) [2,79].

9. MUTATIONAL ANALYSIS FINAL REPORT

Accurate characterization of molecular features is crucial with the expanding role of targeted therapy in advanced NSCLC patients. The mutational analysis should be reported in conjunction with the identification of patient and health care professionals, the pathological diagnosis, details on the tissue block tested, sample source, sample size and quality, the estimation of the proportion of tumor cells in the sample extracted for DNA amplification, the method used, estimated test sensitivity and specificity, test results (mutant or wild-type allele) and interpretation of results in the context of the indication for testing (Table 1) (Fig. 3).

A turnaround time of 2 weeks from the diagnostic procedure to the final report has been suggested, but organizing a system that would include multiple departments seems to be challenging [4]. However, such an engagement cannot be completely respected especially when molecular testing is ordered on samples from external laboratories. Furthermore, in our institution, pathologists order mutational profiling at the time of diagnosis as described above, to reduce the turnaround time for molecular testing.

CONCLUSION

The emerging biomarkers may potentially modulate the sensitivity of tumors to targeted inhibitors and could therefore contribute to the improvement of predictive models and the optimization of therapeutic options. The role of pathologists in guiding treatment decisions is increasing because the molecular profiling, together with the morphological analysis, represents the future of personalizing medicine for patients with NSCLC [131].

As new therapies targeting the growing list of mutant or amplified oncogenes (e.g., *EGFR*, *KRAS*, *EML4-ALK*, *PIK3CA*, *HER2*, *BRAF*) in NSCLC are developed, it is likely that we will have to move toward a more global approach of molecular testing, such as testing for a panel of mutations or possibly using gene expression profiling to identify molecular subtypes of NSCLC [36,49]. There is no doubt, that such global gene expression screening methods will be used in the future in an attempt to identify predictive signatures. Establishing new methods of mutational analyses is an active area of research that aims to reduce time and expense with acceptable sensitivity and to use specimens other than resected tissue [3].

Routine clinical testing for molecular abnormalities in NSCLC still needs to be optimized and standardized in regard to mutational methods, specimens and tumor types, and result reporting.

CONFLICT OF INTEREST

The authors declare no conflict of interest

ACKNOWLEDGMENTS

We thank Dr M.C. Brahimi-Horn for editorial correction.

ABBREVIATIONS

AKT	=	Protein Kinase B
ALK	=	Anaplastic lymphoma kinase
AXL	=	AXL receptor tyrosine kinase
BRAF	=	v-raf murine sarcoma viral oncogene homolog B1
CDKN2A/p16Ink4A	=	Cyclin-dependent kinase inhibitor 2A
EGFR/HER-1/ErbB1	=	Epidermal growth factor receptor
EGFR-TKIs	=	EGFR tyrosine kinase inhibitors
EMEA	=	European Medicines Agency
EML4	=	Echinoderm microtubule-associated protein-like 4
EQAP	=	External Quality Assessment Programs
FDA	=	US Food and Drug Administration
FFPE	=	Formalin-fixed paraffin-embedded
FGFR1	=	Fibroblast growth factor receptor 1
FISH	=	Fluorescent in situ hybridization
FLT3	=	FMS-like tyrosine kinase receptor-3
FTIs	=	Farnesyl transferase inhibitors
HER2/neu/ErbB2	=	Human Epidermal Growth Factor Receptor 2
HER3/ErbB3	=	Human Epidermal Growth Factor Receptor 3
HER4/ErbB4	=	Human Epidermal Growth Factor Receptor 4
IASLC	=	International Association for the Study of Lung Cancer
IHC	=	Immunohistochemistry
KIT	=	Tyrosine-protein kinase Kit or Mast/stem cell growth factor receptor
KRAS	=	Kirsten rat sarcoma viral oncogene homolog
LKB1/STK11	=	Liver kinase B1 or Serine/threonine kinase 11
MAPK	=	Mitogen-activated protein kinase
MEK/MAP2K1	=	Mitogen-activated protein kinase kinase 1
MET	=	Met proto-oncogene or hepatocyte growth factor receptor
mTOR	=	Mammalian Target of Rapamycin
NFB	=	Neutral buffered formalin
NOS	=	Not otherwise specified
NSCLC	=	Non-small cell lung cancer

PDGFR	=	Platelet-derived growth factor receptor
PIK3CA	=	Phosphoinositide-3-kinase, catalytic, alpha polypeptide
PTEN	=	Phosphatase and tensin homolog
RET	=	Ret proto-oncogene/Rearranged during transfection
RT-PCR	=	reverse transcriptase-PCR
TBNA	=	Transbronchial needle aspiration
TIE2	=	Tyrosine kinase with immunoglobulin and EGF homology domains
TK	=	Tyrosine kinase
TP53	=	Tumor protein 53
TTF-1	=	Thyroid transcription factor 1
VEGFR2	=	Vascular endothelial growth factor receptor 2

REFERENCES

- Jemal, A.; Bray, F.; Center, M.M.; Ferlay, J.; Ward, E.; Forman, D. Global cancer statistics. *CA Cancer J Clin.* **2011**, *61*(2), 69-90.
- Felip, E.; Gridelli, C.; Baas, P.; Rosell, R.; Stahel, R. Metastatic non-small-cell lung cancer: consensus on pathology and molecular tests, first-line, second-line, and third-line therapy: 1st ESMO Consensus Conference in Lung Cancer; Lugano 2010. *Ann Oncol.* **2011**, *22*(7), 1507-1519.
- Moran, C. Importance of molecular features of non-small cell lung cancer for choice of treatment. *Am J Pathol.* **2011**, *178*(5), 1940-1948.
- Dacic, S. Molecular diagnostics of lung carcinomas. *Arch Pathol Lab Med.* **2011**, *135*(5), 622-629.
- Janku, F.; Garrido-Laguna, I.; Petruzella, L.B.; Stewart, D.J.; Kurzrock, R. Novel therapeutic targets in non-small cell lung cancer. *J Thorac Oncol.* **2011**, *6*(9), 1601-1612.
- Heinmoller, E.; Renke, B.; Beyser, K.; Dietmaier, W.; Langner, C.; Ruschoff, J. Pitfalls in diagnostic molecular pathology--significance of sampling error. *Virchows Arch.* **2001**, *439*(4), 504-511.
- Paez, J.G.; Janne, P.A.; Lee, J.C.; Tracy, S.; Greulich, H.; Gabriel, S.; Herman, P.; Kaye, F.J.; Lindeman, N.; Boggon, T.J.; et al. EGFR mutations in lung cancer: correlation with clinical response to gefitinib therapy. *Science.* **2004**, *304*(5676), 1497-1500.
- Lynch, T.J.; Bell, D.W.; Sordella, R.; Gurubhagavatula, S.; Okimoto, R.A.; Brannigan, B.W.; Harris, P.L.; Haserlat, S.M.; Supko, J.G.; Haluska, F.G.; et al. Activating mutations in the epidermal growth factor receptor underlying responsiveness of non-small-cell lung cancer to gefitinib. *N Engl J Med.* **2004**, *350*(21), 2129-2139.
- Herbst, R.S.; Heymach, J.V.; Lippman, S.M. Lung cancer. *N Engl J Med.* **2008**, *359*(13), 1367-1380.
- Ladanyi, M.; Pao, W. Lung adenocarcinoma: guiding EGFR-targeted therapy and beyond. *Mod Pathol.* **2008**, *21* Suppl 2, S16-22.
- Mok, T.S.; Wu, Y.L.; Thongprasert, S.; Yang, C.H.; Chu, D.T.; Saijo, N.; Sunpawaravong, P.; Han, B.; Margono, B.; Ichinose, Y.; et al. Gefitinib or carboplatin-paclitaxel in pulmonary adenocarcinoma. *N Engl J Med.* **2009**, *361*(10), 947-957.
- Mok, T.S. Personalized medicine in lung cancer: what we need to know. *Nat Rev Clin Oncol.* **2011**.
- Rosell, R.; Moran, T.; Queralt, C.; Porta, R.; Cardenal, F.; Camps, C.; Majem, M.; Lopez-Vivanco, G.; Isla, D.; Provencio, M.; et al. Screening for epidermal growth factor receptor mutations in lung cancer. *N Engl J Med.* **2009**, *361*(10), 958-967.
- Brugger, W.; Triller, N.; Blasinska-Morawiec, M.; Curescu, S.; Sakalauskas, R.; Manikhas, G.M.; Mazieres, J.; Whittom, R.; Ward, C.; Mayne, K.; et al. Prospective molecular marker analyses of EGFR and KRAS from a randomized, placebo-controlled study of erlotinib maintenance therapy in advanced non-small-cell lung cancer. *J Clin Oncol.* **2011**, *29*(31), 4113-4120.
- Sharma, S.V.; Bell, D.W.; Settleman, J.; Haber, D.A. Epidermal growth factor receptor mutations in lung cancer. *Nat Rev Cancer.* **2007**, *7*(3), 169-181.
- Yang, C.H.; Yu, C.J.; Shih, J.Y.; Chang, Y.C.; Hu, F.C.; Tsai, M.C.; Chen, K.Y.; Lin, Z.Z.; Huang, C.J.; Shun, C.T.; et al. Specific EGFR mutations predict treatment outcome of stage IIIB/IV patients with chemotherapy-naive non-small-cell lung cancer receiving first-line gefitinib monotherapy. *J Clin Oncol.* **2008**, *26*(16), 2745-2753.
- Zhu, C.Q.; da Cunha Santos, G.; Ding, K.; Sakurada, A.; Cutz, J.C.; Liu, N.; Zhang, T.; Marrano, P.; Whitehead, M.; Squire, J.A.; et al. Role of KRAS and EGFR as biomarkers of response to erlotinib in National Cancer Institute of Canada Clinical Trials Group Study BR.21. *J Clin Oncol.* **2008**, *26*(26), 4268-4275.
- Kosaka, T.; Yamaki, E.; Mogi, A.; Kuwano, H. Mechanisms of resistance to EGFR TKIs and development of a new generation of drugs in non-small-cell lung cancer. *J Biomed Biotechnol.* **2011**, *2011*, 165214.
- Godin-Heymann, N.; Ulkus, L.; Brannigan, B.W.; McDermott, U.; Lamb, J.; Maheswaran, S.; Settleman, J.; Haber, D.A. The T790M "gatekeeper" mutation in EGFR mediates resistance to low concentrations of an irreversible EGFR inhibitor. *Mol Cancer Ther.* **2008**, *7*(4), 874-879.
- Pal, S.K.; Figlin, R.A.; Reckamp, K. Targeted therapies for non-small cell lung cancer: an evolving landscape. *Mol Cancer Ther.* **2010**, *9*(7), 1931-1944.
- Ding, L.; Getz, G.; Wheeler, D.A.; Mardis, E.R.; McLellan, M.D.; Cibulskis, K.; Sougnez, C.; Greulich, H.; Muzny, D.M.; Morgan, M.B.; et al. Somatic mutations affect key pathways in lung adenocarcinoma. *Nature.* **2008**, *455*(7216), 1069-1075.
- Gandhi, J.; Zhang, J.; Xie, Y.; Soh, J.; Shigematsu, H.; Zhang, W.; Yamamoto, H.; Peyton, M.; Girard, L.; Lockwood, W.W.; et al. Alterations in genes of the EGFR signaling pathway and their relationship to EGFR tyrosine kinase inhibitor sensitivity in lung cancer cell lines. *PLoS One.* **2009**, *4*(2), e4576.
- Sequist, L.V.; Waltman, B.A.; Dias-Santagata, D.; Digumarthy, S.; Turke, A.B.; Fidias, P.; Bergethon, K.; Shaw, A.T.; Gettinger, S.; Cosper, A.K.; et al. Genotypic and histological evolution of lung cancers acquiring resistance to EGFR inhibitors. *Sci Transl Med.* **2011**, *3*(75), 75ra26.
- Marks, J.L.; Gong, Y.; Chitale, D.; Golas, B.; McLellan, M.D.; Kasai, Y.; Ding, L.; Mardis, E.R.; Wilson, R.K.; Solit, D.; et al. Novel MEK1 mutation identified by mutational analysis of epidermal growth factor receptor signaling pathway genes in lung adenocarcinoma. *Cancer Res.* **2008**, *68*(14), 5524-5528.
- Bonanno, L.; Jirillo, A.; Favaretto, A. Mechanisms of acquired resistance to epidermal growth factor receptor tyrosine kinase inhibitors and new therapeutic perspectives in non small cell lung cancer. *Curr Drug Targets.* **2011**, *12*(6), 922-933.
- Custodio, A.; Mendez, M.; Provencio, M. Targeted therapies for advanced non-small-cell lung cancer: Current status and future implications. *Cancer Treat Rev.* **2012**, *38*(1), 36-53.
- Sattler, M.; Reddy, M.M.; Hasina, R.; Gangadhar, T.; Salgia, R. The role of the c-Met pathway in lung cancer and the potential for targeted therapy. *Ther Adv Med Oncol.* **2011**, *3*(4), 171-184.
- Sequist, L.V.; von Pawel, J.; Garmey, E.G.; Akerley, W.L.; Brugger, W.; Ferrari, D.; Chen, Y.; Costa, D.B.; Gerber, D.E.; Orlov, S.; et al. Randomized phase II study of erlotinib plus tivantinib versus erlotinib plus placebo in previously treated non-small-cell lung cancer. *J Clin Oncol.* **2011**, *29*(24), 3307-3315.
- Yakes, F.M.; Chen, J.; Tan, J.; Yamaguchi, K.; Shi, Y.; Yu, P.; Qian, F.; Chu, F.; Bentzien, F.; Cancilla, B.; et al. Cabozantinib (XL184), a Novel MET and VEGFR2 Inhibitor, Simultaneously Suppresses Metastasis, Angiogenesis, and Tumor Growth. *Mol Cancer Ther.* **2011**, *10*(12), 2298-2308.
- Kijima, T.; Takeuchi, K.; Tetsumoto, S.; Shimada, K.; Takahashi, R.; Hirata, H.; Nagatomo, I.; Hoshino, S.; Takeda, Y.; Kida, H.; et al. Favorable response to crizotinib in three patients with echinoderm microtubule-associated protein-like 4-anaplastic lymphoma kinase fusion-type oncogene-positive non-small cell lung cancer. *Cancer Sci.* **2011**, *102*(8), 1602-1604.
- Ou, S.H.; Kwak, E.L.; Siwak-Tapp, C.; Dy, J.; Bergethon, K.; Clark, J.W.; Camidge, D.R.; Solomon, B.J.; Maki, R.G.; Bang, Y.J.; et al. Activity of crizotinib (PF02341066), a dual mesenchymal-epithelial transition (MET) and anaplastic lymphoma kinase (ALK) inhibitor, in a non-small cell lung cancer patient with de novo MET amplification. *J Thorac Oncol.* **2011**, *6*(5), 942-946.
- Sierra, J.R.; Tsao, M.S. c-MET as a potential therapeutic target and biomarker in cancer. *Ther Adv Med Oncol.* **2011**, *3*(1 Suppl), S21-35.
- Pao, W.; Girard, N. New driver mutations in non-small-cell lung cancer. *Lancet Oncol.* **2011**, *12*(2), 175-180.
- Perera, S.A.; Li, D.; Shimamura, T.; Raso, M.G.; Ji, H.; Chen, L.; Borgman, C.L.; Zaghlul, S.; Brandstetter, K.A.; Kubo, S.; et al. HER2YVMA drives rapid development of adenocarcinoma lung tumors in mice that are sensitive to BIBW2992 and rapamycin combination therapy. *Proc Natl Acad Sci U S A.* **2009**, *106*(2), 474-479.
- Janne, P.A.; Boss, D.S.; Camidge, D.R.; Britten, C.D.; Engelman, J.A.; Garon, E.B.; Guo, F.; Wong, S.; Liang, J.; Letrent, S.; et al. Phase I dose-escalation study of the pan-HER inhibitor, PF299804, in patients with advanced malignant solid tumors. *Clin Cancer Res.* **2011**, *17*(5), 1131-1139.
- Roberts, P.J.; Stinchcombe, T.E.; Der, C.J.; Socinski, M.A. Personalized medicine in non-small-cell lung cancer: is KRAS a useful marker in selecting patients for epidermal growth factor receptor-targeted therapy? *J Clin Oncol.* **2010**, *28*(31), 4769-4777.
- Gaughan, E.M.; Costa, D.B. Genotype-driven therapies for non-small cell

- lung cancer: focus on EGFR, KRAS and ALK gene abnormalities. *Ther Adv Med Oncol.* **2011**, 3(3), 113-125.
- [38] Riely, G.J.; Marks, J.; Pao, W. KRAS mutations in non-small cell lung cancer. *Proc Am Thorac Soc.* **2009**, 6(2), 201-205.
- [39] Davies, H.; Bignell, G.R.; Cox, C.; Stephens, S.; Edkins, S.; Clegg, S.; Teague, J.; Woffendin, H.; Garnett, M.J.; Bottomley, W.; *et al.* Mutations of the BRAF gene in human cancer. *Nature.* **2002**, 417(6892), 949-954.
- [40] Paik, P.K.; Arcila, M.E.; Fara, M.; Sima, C.S.; Miller, V.A.; Kris, M.G.; Ladanyi, M.; Riely, G.J. Clinical characteristics of patients with lung adenocarcinomas harboring BRAF mutations. *J Clin Oncol.* **2011**, 29(15), 2046-2051.
- [41] Chapman, P.B.; Hauschild, A.; Robert, C.; Haanen, J.B.; Ascierto, P.; Larkin, J.; Dummer, R.; Garbe, C.; Testori, A.; Maio, M.; *et al.* Improved survival with vemurafenib in melanoma with BRAF V600E mutation. *N Engl J Med.* **2011**, 364(26), 2507-2516.
- [42] Vivanco, I.; Sawyers, C.L. The phosphatidylinositol 3-Kinase AKT pathway in human cancer. *Nat Rev Cancer.* **2002**, 2(7), 489-501.
- [43] Marinov, M.; Fischer, B.; Arcaro, A. Targeting mTOR signaling in lung cancer. *Crit Rev Oncol Hematol.* **2007**, 63(2), 172-182.
- [44] Samuels, Y.; Wang, Z.; Bardelli, A.; Silliman, N.; Ptak, J.; Szabo, S.; Yan, H.; Gazdar, A.; Powell, S.M.; Riggins, G.J.; *et al.* High frequency of mutations of the PIK3CA gene in human cancers. *Science.* **2004**, 304(5670), 554.
- [45] Wallin, J.J.; Edgar, K.A.; Guan, J.; Berry, M.; Prior, W.W.; Lee, L.; Lesnick, J.D.; Lewis, C.; Nonomiyama, J.; Pang, J.; *et al.* GDC-0980 Is a Novel Class I PI3K/mTOR Kinase Inhibitor with Robust Activity in Cancer Models Driven by the PI3K Pathway. *Mol Cancer Ther.* **2011**, 10(12), 2426-2436.
- [46] Kawano, O.; Sasaki, H.; Endo, K.; Suzuki, E.; Haneda, H.; Yukiue, H.; Kobayashi, Y.; Yano, M.; Fujii, Y. PIK3CA mutation status in Japanese lung cancer patients. *Lung Cancer.* **2006**, 54(2), 209-215.
- [47] Sequist, L.V.; Heist, R.S.; Shaw, A.T.; Fidias, P.; Rosovsky, R.; Temel, J.S.; Lennes, I.T.; Digumarthy, S.; Waltman, B.A.; Bast, E.; *et al.* Implementing multiplexed genotyping of non-small-cell lung cancers into routine clinical practice. *Ann Oncol.* **2011**, 22(12), 2616-2624.
- [48] Chaft, J.E.; Arcila, M.E.; Paik, P.K.; Lau, C.; Riely, G.J.; Pietanza, M.C.; Zakowski, M.F.; Rusch, V.W.; Sima, C.S.; Ladanyi, M.; *et al.* Coexistence of PIK3CA and other oncogene mutations in lung adenocarcinoma - rationale for comprehensive mutation profiling. *Mol Cancer Ther.* **2011**.
- [49] Janku, F.; Stewart, D.J.; Kurzrock, R. Targeted therapy in non-small-cell lung cancer—is it becoming a reality? *Nat Rev Clin Oncol.* **2010**, 7(7), 401-414.
- [50] Zou, Z.Q.; Zhang, L.N.; Wang, F.; Bellenger, J.; Shen, Y.Z.; Zhang, X.H. The novel dual PI3K/mTOR inhibitor GDC-0941 synergizes with the MEK. *Mol Med Report.* **2012**, 5(2), 503-508.
- [51] Sun, S.; Schiller, J.H.; Spinola, M.; Minna, J.D. New molecularly targeted therapies for lung cancer. *J Clin Invest.* **2007**, 117(10), 2740-2750.
- [52] Malanga, D.; Scrima, M.; De Marco, C.; Fabiani, F.; De Rosa, N.; De Gisi, S.; Malara, N.; Savino, R.; Rocco, G.; Chiappetta, G.; *et al.* Activating E17K mutation in the gene encoding the protein kinase AKT1 in a subset of squamous cell carcinoma of the lung. *Cell Cycle.* **2008**, 7(5), 665-669.
- [53] Meng, J.; Dai, B.; Fang, B.; Bekele, B.N.; Bornmann, W.G.; Sun, D.; Peng, Z.; Herbst, R.S.; Papadimitrakopoulou, V.; Minna, J.D.; *et al.* Combination treatment with MEK and AKT inhibitors is more effective than each drug alone in human non-small cell lung cancer *in vitro* and *in vivo*. *PLoS One.* **2010**, 5(11), e14124.
- [54] Jin, G.; Kim, M.J.; Jeon, H.S.; Choi, J.E.; Kim, D.S.; Lee, E.B.; Cha, S.I.; Yoon, G.S.; Kim, C.H.; Jung, T.H.; *et al.* PTEN mutations and relationship to EGFR, ERBB2, KRAS, and TP53 mutations in non-small cell lung cancers. *Lung Cancer.* **2010**, 69(3), 279-283.
- [55] Lee, E.B.; Jin, G.; Lee, S.Y.; Park, J.Y.; Kim, M.J.; Choi, J.E.; Jeon, H.S.; Cha, S.I.; Cho, S.; Kim, C.H.; *et al.* TP53 mutations in Korean patients with non-small cell lung cancer. *J Korean Med Sci.* **2010**, 25(5), 698-705.
- [56] Sanders, H.R.; Albitar, M. Somatic mutations of signaling genes in non-small-cell lung cancer. *Cancer Genet Cytogenet.* **2010**, 203(1), 7-15.
- [57] Koivunen, J.P.; Kim, J.; Lee, J.; Rogers, A.M.; Park, J.O.; Zhao, X.; Naoki, K.; Okamoto, I.; Nakagawa, K.; Yeap, B.Y.; *et al.* Mutations in the LKB1 tumour suppressor are frequently detected in tumours from Caucasian but not Asian lung cancer patients. *Br J Cancer.* **2008**, 99(2), 245-252.
- [58] Gill, R.K.; Yang, S.H.; Meerzaman, D.; Mechanic, L.E.; Bowman, E.D.; Jeon, H.S.; Roy Chowdhuri, S.; Shakoori, A.; Dracheva, T.; Hong, K.M.; *et al.* Frequent homozygous deletion of the LKB1/STK11 gene in non-small cell lung cancer. *Oncogene.* **2011**, 30(35), 3784-3791.
- [59] Mahoney, C.L.; Choudhury, B.; Davies, H.; Edkins, S.; Greenman, C.; Haafteen, G.; Mironenko, T.; Santarius, T.; Stevens, C.; Stratton, M.R.; *et al.* LKB1/KRAS mutant lung cancers constitute a genetic subset of NSCLC with increased sensitivity to MAPK and mTOR signalling inhibition. *Br J Cancer.* **2009**, 100(2), 370-375.
- [60] Vachani, A.; Moon, E.; Wakeam, E.; Albelda, S.M. Gene therapy for mesothelioma and lung cancer. *Am J Respir Cell Mol Biol.* **2010**, 42(4), 385-393.
- [61] Schuler, M.; Herrmann, R.; De Greve, J.L.; Stewart, A.K.; Gatzemeier, U.; Stewart, D.J.; Laufman, L.; Gralla, R.; Kuball, J.; Buhl, R.; *et al.* Adenovirus-mediated wild-type p53 gene transfer in patients receiving chemotherapy for advanced non-small-cell lung cancer: results of a multicenter phase II study. *J Clin Oncol.* **2001**, 19(6), 1750-1758.
- [62] Kim, R.; Emi, M.; Tanabe, K.; Arihiro, K. Tumor-driven evolution of immunosuppressive networks during malignant progression. *Cancer Res.* **2006**, 66(11), 5527-5536.
- [63] Flemming, A. Cancer: Hope for smoking-associated lung cancer? *Nat Rev Drug Discov.* **2011**, 10(2), 98-99.
- [64] Turner, N.; Grose, R. Fibroblast growth factor signalling: from development to cancer. *Nat Rev Cancer.* **2010**, 10(2), 116-129.
- [65] Weiss, J.; Sos, M.L.; Seidel, D.; Peifer, M.; Zander, T.; Heuckmann, J.M.; Ullrich, R.T.; Menon, R.; Maier, S.; Soltermann, A.; *et al.* Frequent and focal FGFR1 amplification associates with therapeutically tractable FGFR1 dependency in squamous cell lung cancer. *Sci Transl Med.* **2010**, 2(62), 62ra93.
- [66] Dutt, A.; Ramos, A.H.; Hammerman, P.S.; Mermel, C.; Cho, J.; Sharifnia, T.; Chande, A.; Tanaka, K.E.; Stransky, N.; Greulich, H.; *et al.* Inhibitor-sensitive FGFR1 amplification in human non-small cell lung cancer. *PLoS One.* **2011**, 6(6), e20351.
- [67] Semrad, T.J.; Mack, P.C. Fibroblast Growth Factor Signaling in Non-Small Cell Lung Cancer. *Clin Lung Cancer.* **2011**.
- [68] Marek, L.; Ware, K.E.; Fritzsche, A.; Hercule, P.; Helton, W.R.; Smith, J.E.; McDermott, L.A.; Coldren, C.D.; Nemenoff, R.A.; Merrick, D.T.; *et al.* Fibroblast growth factor (FGF) and FGF receptor-mediated autocrine signaling in non-small-cell lung cancer cells. *Mol Pharmacol.* **2009**, 75(1), 196-207.
- [69] Soda, M.; Choi, Y.L.; Enomoto, M.; Takada, S.; Yamashita, Y.; Ishikawa, S.; Fujiwara, S.; Watanabe, H.; Kurashina, K.; Hatanaka, H.; *et al.* Identification of the transforming EML4-ALK fusion gene in non-small-cell lung cancer. *Nature.* **2007**, 448(7153), 561-566.
- [70] Shaw, A.T.; Yeap, B.Y.; Mino-Kenudson, M.; Digumarthy, S.R.; Costa, D.B.; Heist, R.S.; Solomon, B.; Stubbs, H.; Admane, S.; McDermott, U.; *et al.* Clinical features and outcome of patients with non-small-cell lung cancer who harbor EML4-ALK. *J Clin Oncol.* **2009**, 27(26), 4247-4253.
- [71] Wong, D.W.; Leung, E.L.; So, K.K.; Tam, I.Y.; Sihoe, A.D.; Cheng, L.C.; Ho, K.K.; Au, J.S.; Chung, L.P.; Pik Wong, M. The EML4-ALK fusion gene is involved in various histologic types of lung cancers from nonsmokers with wild-type EGFR and KRAS. *Cancer.* **2009**, 115(8), 1723-1733.
- [72] Toyooka, S.; Mitsudomi, T.; Soh, J.; Aokage, K.; Yamane, M.; Oto, T.; Kiura, K.; Miyoshi, S. Molecular oncology of lung cancer. *Gen Thorac Cardiovasc Surg.* **2011**, 59(8), 527-537.
- [73] Kwak, E.L.; Bang, Y.J.; Camidge, D.R.; Shaw, A.T.; Solomon, B.; Maki, R.G.; Ou, S.H.; Dezube, B.J.; Janne, P.A.; Costa, D.B.; *et al.* Anaplastic lymphoma kinase inhibition in non-small-cell lung cancer. *N Engl J Med.* **2010**, 363(18), 1693-1703.
- [74] Shaw, A.T.; Yeap, B.Y.; Solomon, B.J.; Riely, G.J.; Gainor, J.; Engelman, J.A.; Shapiro, G.I.; Costa, D.B.; Ou, S.H.; Butaney, M.; *et al.* Effect of crizotinib on overall survival in patients with advanced non-small-cell lung cancer harbouring ALK gene rearrangement: a retrospective analysis. *Lancet Oncol.* **2011**, 12(11), 1004-1012.
- [75] Cheng, H.; An, S.J.; Dong, S.; Zhang, Y.F.; Zhang, X.C.; Chen, Z.H.; Jian, S.; Wu, Y.L. Molecular mechanism of the schedule-dependent synergistic interaction in EGFR-mutant non-small cell lung cancer cell lines treated with paclitaxel and gefitinib. *J Hematol Oncol.* **2011**, 4, 5.
- [76] Zwitter, M. Combining cytotoxic and targeted therapies for lung cancer. *J Thorac Oncol.* **2010**, 5(10), 1498-1499.
- [77] Davies, A.M.; Ho, C.; Lara, P.N., Jr.; Mack, P.; Gumerlock, P.H.; Gandara, D.R. Pharmacodynamic separation of epidermal growth factor receptor tyrosine kinase inhibitors and chemotherapy in non-small-cell lung cancer. *Clin Lung Cancer.* **2006**, 7(6), 385-388.
- [78] Lamy, A.; Blanchard, F.; Le Pessot, F.; Sesboue, R.; Di Fiore, F.; Bossut, J.; Fiant, E.; Frebourg, T.; Sabourin, J.C. Metastatic colorectal cancer KRAS genotyping in routine practice: results and pitfalls. *Mod Pathol.* **2011**, 24(8), 1090-1100.
- [79] Pirker, R.; Herth, F.J.; Kerr, K.M.; Filipits, M.; Taron, M.; Gandara, D.; Hirsch, F.R.; Grunewald, D.; Popper, H.; Smit, E.; *et al.* Consensus for EGFR mutation testing in non-small cell lung cancer: results from a European workshop. *J Thorac Oncol.* **2010**, 5(10), 1706-1713.
- [80] West, H.; Harpole, D.; Travis, W. Histologic considerations for individualized systemic therapy approaches for the management of non-small cell lung cancer. *Chest.* **2009**, 136(4), 1112-1118.
- [81] Travis, W.D.; Brambilla, E.; Noguchi, M.; Nicholson, A.G.; Geisinger, K.R.; Yatabe, Y.; Beer, D.G.; Powell, C.A.; Riely, G.J.; Van Schil, P.E.; *et al.* International association for the study of lung cancer/american thoracic society/european respiratory society international multidisciplinary classification of lung adenocarcinoma. *J Thorac Oncol.* **2011**, 6(2), 244-285.
- [82] Shah, P.L.; Singh, S.; Bower, M.; Livni, N.; Padley, S.; Nicholson, A.G. The role of transbronchial fine needle aspiration in an integrated care pathway for

- the assessment of patients with suspected lung cancer. *J Thorac Oncol.* **2006**, *1*(4), 324-327.
- [83] Kerr, K.M. Personalized medicine for lung cancer: new challenges for pathology. *Histopathology.* **2011**.
- [84] Pallis, A.; Briasoulis, E.; Linardou, H.; Papadimitriou, C.; Bafaloukos, D.; Kosmidis, P.; Murray, S. Mechanisms of resistance to epidermal growth factor receptor tyrosine kinase inhibitors in patients with advanced non-small-cell lung cancer: clinical and molecular considerations. *Curr Med Chem.* **2011**, *18*(11), 1613-1628.
- [85] Douillard, J.Y.; Shepherd, F.A.; Hirsh, V.; Mok, T.; Socinski, M.A.; Gervais, R.; Liao, M.L.; Bischoff, H.; Reck, M.; Sellers, M.V.; *et al.* Molecular predictors of outcome with gefitinib and docetaxel in previously treated non-small-cell lung cancer: data from the randomized phase III INTEREST trial. *J Clin Oncol.* **2010**, *28*(5), 744-752.
- [86] Kim, E.S.; Herbst, H.S.; Wistuba, I.; Lee, J.; Blumenschein, G.J.; Tsao, A.; Stewart, D.; Hicks, M.; Erasmus, J.; Gupta, S.; *et al.* The BATTLE Trial: Personalizing Therapy for Lung Cancer. *Cancer Discovery.* **2011**, *1*, 44-53.
- [87] Linardou, H.; Dahabreh, I.J.; Bafaloukos, D.; Kosmidis, P.; Murray, S. Somatic EGFR mutations and efficacy of tyrosine kinase inhibitors in NSCLC. *Nat Rev Clin Oncol.* **2009**, *6*(6), 352-366.
- [88] Hewitt, R.E. Biobanking: the foundation of personalized medicine. *Curr Opin Oncol.* **2011**, *23*(1), 112-119.
- [89] Riegman, P.H.; Morente, M.M.; Betsou, F.; de Blasio, P.; Geary, P. Biobanking for better healthcare. *Mol Oncol.* **2008**, *2*(3), 213-222.
- [90] Bussolati, G.; Chiusa, L.; Cimino, A.; D'Armento, G. Tissue transfer to pathology labs: under vacuum is the safe alternative to formalin. *Virchows Arch.* **2008**, *452*(2), 229-231.
- [91] Bonin, S.; Petretera, F.; Rosai, J.; Stanta, G. DNA and RNA obtained from Bouin's fixed tissues. *J Clin Pathol.* **2005**, *58*(3), 313-316.
- [92] Lassalle, S.; Hofman, V.; Marius, I.; Gavric-Tanga, V.; Brest, P.; Havet, K.; Butori, C.; Selva, E.; Santini, J.; Mograbi, B.; *et al.* Assessment of morphology, antigenicity, and nucleic acid integrity for diagnostic thyroid pathology using formalin substitute fixatives. *Thyroid.* **2009**, *19*(11), 1239-1248.
- [93] Ferrer, I.; Armstrong, J.; Capellari, S.; Parchi, P.; Arzberger, T.; Bell, J.; Budka, H.; Strobel, T.; Giaccone, G.; Rossi, G.; *et al.* Effects of formalin fixation, paraffin embedding, and time of storage on DNA preservation in brain tissue: a BrainNet Europe study. *Brain Pathol.* **2007**, *17*(3), 297-303.
- [94] Jewell, S.D.; Srinivasan, M.; McCart, L.M.; Williams, N.; Grizzle, W.H.; LiVolsi, V.; MacLennan, G.; Sedmak, D.D. Analysis of the molecular quality of human tissues: an experience from the Cooperative Human Tissue Network. *Am J Clin Pathol.* **2002**, *118*(5), 733-741.
- [95] Srinivasan, M.; Sedmak, D.; Jewell, S. Effect of fixatives and tissue processing on the content and integrity of nucleic acids. *Am J Pathol.* **2002**, *161*(6), 1961-1971.
- [96] Williams, C.; Ponten, F.; Moberg, C.; Soderkvist, P.; Uhlen, M.; Ponten, J.; Sitbon, G.; Lundeberg, J. A high frequency of sequence alterations is due to formalin fixation of archival specimens. *Am J Pathol.* **1999**, *155*(5), 1467-1471.
- [97] da Cunha Santos, G.; Saieg, M.A.; Geddie, W.; Leigh, N. EGFR gene status in cytological samples of nonsmall cell lung carcinoma: controversies and opportunities. *Cancer Cytopathol.* **2011**, *119*(2), 80-91.
- [98] Smouse, J.H.; Cibas, E.S.; Janne, P.A.; Joshi, V.A.; Zou, K.H.; Lindeman, N.I. EGFR mutations are detected comparably in cytologic and surgical pathology specimens of nonsmall cell lung cancer. *Cancer.* **2009**, *117*(1), 67-72.
- [99] Eberhard, D.A.; Giaccone, G.; Johnson, B.E. Biomarkers of response to epidermal growth factor receptor inhibitors in Non-Small-Cell Lung Cancer Working Group: standardization for use in the clinical trial setting. *J Clin Oncol.* **2008**, *26*(6), 983-994.
- [100] Sequist, L.V.; Bell, D.W.; Lynch, T.J.; Haber, D.A. Molecular predictors of response to epidermal growth factor receptor antagonists in non-small-cell lung cancer. *J Clin Oncol.* **2007**, *25*(5), 587-595.
- [101] Solomon, S.B.; Zakowski, M.F.; Pao, W.; Thornton, R.H.; Ladanyi, M.; Kris, M.G.; Rusch, V.W.; Rizvi, N.A. Core needle lung biopsy specimens: adequacy for EGFR and KRAS mutational analysis. *AJR Am J Roentgenol.* **2010**, *194*(1), 266-269.
- [102] Donati, V.; Lupi, C.; Ali, G.; Corsi, V.; Viti, A.; Lucchi, M.; Mussi, A.; Fontanini, G. Laser capture microdissection: a tool for the molecular characterization of histologic subtypes of lung adenocarcinoma. *Int J Mol Med.* **2009**, *24*(4), 473-479.
- [103] Hofman, V.; Ilie, M.; Gavric-Tanga, V.; Lespinet, V.; Mari, M.; Lassalle, S.; Butori, C.; Coelle, C.; Bordone, O.; Selva, E.; *et al.* [Role of the surgical pathology laboratory in the pre-analytical approach of molecular biology techniques]. *Ann Pathol.* **2010**, *30*(2), 85-93.
- [104] Park, S.; Holmes-Tisch, A.J.; Cho, E.Y.; Shim, Y.M.; Kim, J.; Kim, H.S.; Lee, J.; Park, Y.H.; Ahn, J.S.; Park, K.; *et al.* Discordance of molecular biomarkers associated with epidermal growth factor receptor pathway between primary tumors and lymph node metastasis in non-small cell lung cancer. *J Thorac Oncol.* **2009**, *4*(7), 809-815.
- [105] Bozzetti, C.; Tiseo, M.; Lagrasta, C.; Nizzoli, R.; Guazzi, A.; Leonardi, F.; Gasparro, D.; Spiritelli, E.; Rusca, M.; Carbone, P.; *et al.* Comparison between epidermal growth factor receptor (EGFR) gene expression in primary non-small cell lung cancer (NSCLC) and in fine-needle aspirates from distant metastatic sites. *J Thorac Oncol.* **2008**, *3*(1), 18-22.
- [106] Italiano, A.; Vandenbos, F.B.; Otto, J.; Mouroux, J.; Fontaine, D.; Marcy, P.Y.; Cardot, N.; Thyss, A.; Pedeutour, F. Comparison of the epidermal growth factor receptor gene and protein in primary non-small-cell-lung cancer and metastatic sites: implications for treatment with EGFR-inhibitors. *Ann Oncol.* **2006**, *17*(6), 981-985.
- [107] Kalikaki, A.; Koutsopoulos, A.; Trypaki, M.; Souglakos, J.; Stathopoulos, E.; Georgoulas, V.; Mavroudis, D.; Voutsina, A. Comparison of EGFR and K-RAS gene status between primary tumors and corresponding metastases in NSCLC. *Br J Cancer.* **2008**, *99*(6), 923-929.
- [108] Monaco, S.E.; Nikiforova, M.N.; Cieply, K.; Teot, L.A.; Khalbuss, W.E.; Dacic, S. A comparison of EGFR and KRAS status in primary lung carcinoma and matched metastases. *Hum Pathol.* **2010**, *41*(1), 94-102.
- [109] Solassol, J.; Ramos, J.; Crapez, E.; Saifi, M.; Mange, A.; Vianes, E.; Lamy, P.J.; Costes, V.; Maudelonde, T. KRAS Mutation Detection in Paired Frozen and Formalin-Fixed Paraffin-Embedded (FFPE) Colorectal Cancer Tissues. *Int J Mol Sci.* **2011**, *12*(5), 3191-3204.
- [110] Bonin, S.; Hlubek, F.; Benhattar, J.; Denkert, C.; Dietel, M.; Fernandez, P.L.; Hoffer, G.; Kothmaier, H.; Kruslin, B.; Mazzanti, C.M.; *et al.* Multicentre validation study of nucleic acids extraction from FFPE tissues. *Virchows Arch.* **2010**, *457*(3), 309-317.
- [111] Lee, J.H.; Park, Y.; Choi, J.R.; Lee, E.K.; Kim, H.S. Comparisons of three automated systems for genomic DNA extraction in a clinical diagnostic laboratory. *Yonsei Med J.* **2010**, *51*(1), 104-110.
- [112] Moss, D.; Harbison, S.A.; Saul, D.J. An easily automated, closed-tube forensic DNA extraction procedure using a thermostable proteinase. *Int J Legal Med.* **2003**, *117*(6), 340-349.
- [113] Riemann, K.; Adamzik, M.; Frauenrath, S.; Egensperger, R.; Schmid, K.W.; Brockmeyer, N.H.; Siffert, W. Comparison of manual and automated nucleic acid extraction from whole-blood samples. *J Clin Lab Anal.* **2007**, *21*(4), 244-248.
- [114] van Krieken, J.H.; Jung, A.; Kirchner, T.; Carneiro, F.; Seruca, R.; Bosman, F.T.; Quirke, P.; Flejou, J.F.; Plato Hansen, T.; de Hertogh, G.; *et al.* KRAS mutation testing for predicting response to anti-EGFR therapy for colorectal carcinoma: proposal for an European quality assurance program. *Virchows Arch.* **2008**, *453*(5), 417-431.
- [115] Pao, W.; Ladanyi, M. Epidermal growth factor receptor mutation testing in lung cancer: searching for the ideal method. *Clin Cancer Res.* **2007**, *13*(17), 4954-4955.
- [116] Mino-Kenudson, M.; Mark, E.J. Reflex testing for epidermal growth factor receptor mutation and anaplastic lymphoma kinase fluorescence in situ hybridization in non-small cell lung cancer. *Arch Pathol Lab Med.* **2011**, *135*(5), 655-664.
- [117] da Cunha Santos, G.; Shepherd, F.A.; Tsao, M.S. EGFR mutations and lung cancer. *Annu Rev Pathol.* **2011**, *6*, 49-69.
- [118] Hoshi, K.; Takakura, H.; Mitani, Y.; Tatsumi, K.; Momiyama, N.; Ichikawa, Y.; Togo, S.; Miyagi, T.; Kawai, Y.; Kogo, Y.; *et al.* Rapid detection of epidermal growth factor receptor mutations in lung cancer by the SMart-Amplification Process. *Clin Cancer Res.* **2007**, *13*(17), 4974-4983.
- [119] Tanaka, T.; Nagai, Y.; Miyazawa, H.; Koyama, N.; Matsuoka, S.; Sutani, A.; Huqun; Udagawa, K.; Murayama, Y.; Nagata, M.; *et al.* Reliability of the peptide nucleic acid-locked nucleic acid polymerase chain reaction clamp-based test for epidermal growth factor receptor mutations integrated into the clinical practice for non-small cell lung cancers. *Cancer Sci.* **2007**, *98*(2), 246-252.
- [120] Dias-Santagata, D.; Akhavanfard, S.; David, S.S.; Vernovsky, K.; Kuhlmann, G.; Boisvert, S.L.; Stubbs, H.; McDermott, U.; Settleman, J.; Kwak, E.L.; *et al.* Rapid targeted mutational analysis of human tumours: a clinical platform to guide personalized cancer medicine. *EMBO Mol Med.* **2010**, *2*(5), 146-158.
- [121] Yu, J.; Kane, S.; Wu, J.; Benedetti, E.; Li, D.; Reeves, C.; Innocenti, G.; Wetzel, R.; Crosby, K.; Becker, A.; *et al.* Mutation-specific antibodies for the detection of EGFR mutations in non-small-cell lung cancer. *Clin Cancer Res.* **2009**, *15*(9), 3023-3028.
- [122] Simonetti, S.; Molina, M.A.; Queralt, C.; de Aguirre, I.; Mayo, C.; Bertran-Alamillo, J.; Sanchez, J.J.; Gonzalez-Larriba, J.L.; Jimenez, U.; Isla, D.; *et al.* Detection of EGFR mutations with mutation-specific antibodies in stage IV non-small-cell lung cancer. *J Transl Med.* **2010**, *8*, 135.
- [123] Ilie, M.I.; Hofman, V.; Bonnetaud, C.; Havet, K.; Lespinet-Fabre, V.; Coelle, C.; Gavric-Tanga, V.; Venissac, N.; Mouroux, J.; Hofman, P. Usefulness of tissue microarrays for assessment of protein expression, gene copy number and mutational status of EGFR in lung adenocarcinoma. *Virchows Arch.* **2010**, *457*(4), 483-495.
- [124] Camidge, D.R.; Kono, S.A.; Flacco, A.; Tan, A.C.; Doebele, R.C.; Zhou, Q.; Crino, L.; Franklin, W.A.; Varella-Garcia, M. Optimizing the detection of lung cancer patients harboring anaplastic lymphoma kinase (ALK) gene

- rearrangements potentially suitable for ALK inhibitor treatment. *Clin Cancer Res.* **2010**, *16*(22), 5581-5590.
- [125] Takeuchi, K.; Choi, Y.L.; Soda, M.; Inamura, K.; Togashi, Y.; Hatano, S.; Enomoto, M.; Takada, S.; Yamashita, Y.; Satoh, Y.; *et al.* Multiplex reverse transcription-PCR screening for EML4-ALK fusion transcripts. *Clin Cancer Res.* **2008**, *14*(20), 6618-6624.
- [126] Mino-Kenudson, M.; Chirieac, L.R.; Law, K.; Hornick, J.L.; Lindeman, N.; Mark, E.J.; Cohen, D.W.; Johnson, B.E.; Janne, P.A.; Iafrate, A.J.; *et al.* A novel, highly sensitive antibody allows for the routine detection of ALK-rearranged lung adenocarcinomas by standard immunohistochemistry. *Clin Cancer Res.* **2010**, *16*(5), 1561-1571.
- [127] Hofman, P.; Ilie, M.; Hofman, V.; Roux, S.; Valent, A.; Bernheim, A.; Alifano, M.; Leroy-Ladurie, F.; Vaylet, F.; Rouquette, I.; *et al.* Immunohistochemistry to identify EGFR mutations or ALK rearrangements in patients with lung adenocarcinoma. *Ann Oncol.* **2011**.
- [128] Orlando, C.; Verderio, P.; Maatman, R.; Danneberg, J.; Ramsden, S.; Neumaier, M.; Taruscio, D.; Falbo, V.; Jansen, R.; Casini-Raggi, C.; *et al.* EQUAL-qual: a European program for external quality assessment of genomic DNA extraction and PCR amplification. *Clin Chem.* **2007**, *53*(7), 1349-1357.
- [129] van Krieken, H.; Tol, J. Setting future standards for KRAS testing in colorectal cancer. *Pharmacogenomics.* **2009**, *10*(1), 1-3.
- [130] Bellon, E.; Ligtenberg, M.J.; Tejpar, S.; Cox, K.; de Hertogh, G.; de Stricker, K.; Edsjo, A.; Gorgoulis, V.; Hofler, G.; Jung, A.; *et al.* External quality assessment for KRAS testing is needed: setup of a European program and report of the first joined regional quality assessment rounds. *Oncologist.* **2011**, *16*(4), 467-478.
- [131] Kulesza, P.; Ramchandran, K.; Patel, J.D. Emerging concepts in the pathology and molecular biology of advanced non-small cell lung cancer. *Am J Clin Pathol.* **2011**, *136*(2), 228-238.

Usefulness of tissue microarrays for assessment of protein expression, gene copy number and mutational status of EGFR in lung adenocarcinoma

Marius I. Ilie · Véronique Hofman · Christelle Bonnetaud · Katia Havet ·
Virginie Lespinet-Fabre · Céline Coëlle · Virginie Gavric-Tanga · Nicolas Vénissac ·
Jerôme Mouroux · Paul Hofman

Received: 31 May 2010 / Revised: 17 July 2010 / Accepted: 11 August 2010 / Published online: 28 August 2010
© Springer-Verlag 2010

Abstract Specific inhibitors targeting the epidermal growth factor receptor (EGFR) can increase survival rates in certain lung adenocarcinoma patients with mutations in the *EGFR* gene. Although such EGFR-targeted therapies have been approved for use, there is no general consensus among surgical pathologists on how the EGFR status should be tested in lung adenocarcinoma tissues and whether the results of immunohistochemistry (IHC), fluorescence in situ hybridization (FISH), and mutational analysis by molecular methods correlate. We evaluated the EGFR status in 61 lung adenocarcinomas by IHC (using total and mutant-specific antibodies against EGFR), by FISH analysis on tissue microarrays (TMAs), and by direct sequencing. The results of each method were compared using χ^2 and kappa statistics. The sensitivity and negative

predictive value estimating the presence of abnormal EGFR for each test was calculated. The results show that, with respect to expression patterns and clinicopathological parameters, the total and mutant-specific EGFR detected by immunohistochemistry and FISH analysis on TMAs are valid and are equivalent to conventional methods performed on whole-tissue sections. Abnormal EGFR was detected in 52.4% of patients by IHC, FISH, and sequencing. The best sensitivity (100%) and negative predictive value (100%) was determined by evaluating the EGFR status with all methods. Testing for molecular changes in EGFR using a single test is likely to underestimate the presence of EGFR abnormalities. Taken together, these results demonstrate the high potential of TMAs to test for the major mechanisms of EGFR activation in patients with lung adenocarcinoma.

M. I. Ilie · V. Hofman · K. Havet · P. Hofman (✉)
Laboratory of Clinical and Experimental Pathology,
Louis Pasteur Hospital,
30 Avenue de la Voie Romaine,
06002 Nice Cedex 01, France
e-mail: hofman.p@chu-nice.fr

M. I. Ilie · V. Hofman · N. Vénissac · J. Mouroux · P. Hofman
INSERM ERI-21/EA 4319, Faculty of Medicine,
University of Nice Sophia Antipolis,
Nice, France

M. I. Ilie · V. Hofman · C. Bonnetaud · V. Lespinet-Fabre ·
C. Coëlle · V. Gavric-Tanga · P. Hofman
Human Tissue Biobank Unit/CRB INSERM,
Louis Pasteur Hospital,
Nice, France

N. Vénissac · J. Mouroux
Department of Thoracic Surgery, Louis Pasteur Hospital,
Nice, France

Keywords EGFR · Lung adenocarcinoma ·
Tissue microarrays · Immunohistochemistry · FISH ·
Sequencing

Epidermal growth factor receptor (EGFR) tyrosine kinase inhibitors (TKIs) such as gefitinib (Iressa®, Astra-Zeneca, UK) and erlotinib (Tarceva®, OSI/ Genentech, USA) show objective responses in 10% to 27% of patients with advanced non-small-cell lung cancer (NSCLC) after failure of standard chemotherapy [1, 2]. Moreover, recent clinical trials demonstrated substantial benefit of gefitinib administration in selected patients with advanced NSCLC with *EGFR* mutation-positive tumors [3]. Therefore, the European Medicines Agency (EMA) supported the approval of gefitinib for patients with locally advanced or metastatic NSCLC with activating mutations of EGFR, across all lines of therapy (<http://www.ema.europa.eu/>

humandocs/Humans/EPAR/iressa/iressa.htm. Accessed 24 April 2010). In this regard, the French National Institute of Cancer (INCa) launched, at the end of 2009, a national program financing the detection by sequencing of *EGFR* mutations in patients with lung adenocarcinoma.

EGFR (HER-1/ErbB1) is a TK receptor of the ErbB family that plays a major role in tumor development and progression [4]. EGFR activation on the surface of cancer cells promotes the activation of the Ras-antiapoptotic cascade, cell growth, survival, and cell cycle progression, differentiation, and angiogenesis [5–7]. Together with its ligands, it is expressed in 40–80% of patients with NSCLC [8]. However, it appears that certain patients obtain more benefit from EGFR-TKIs than others. A higher probability of response appears to be associated with clinical characteristics, such as gender (female), never smoking status, Asian ethnic origin, and adenocarcinoma sub-type [9]. Nevertheless, strategies for patient selection using molecular diagnostics of EGFR activation increase the efficacy of EGFR-targeted therapies and greatly optimize response to treatment in patients with lung adenocarcinoma. Various mechanisms of EGFR activation in cancer cells have been demonstrated: overexpression of ligands and receptors, gene amplification, and activating mutations [10]. For these reasons, selection of patients who will benefit from EGFR inhibition according to their genetic status is an important issue in EGFR-targeted therapy in NSCLC.

The relationship between EGFR protein expression and tumor sensitivity to TKIs is currently unclear [11–15]. Retrospective studies failed to demonstrate a predictive value for EGFR overexpression measured by immunohistochemistry (IHC) in patients with NSCLC who are treated with TKIs [12, 13]. However, other recent trials found a relationship between EGFR protein expression and better overall survival in patients with relapsed or refractory NSCLC who received TKI therapy [11, 14, 15]. Conversely, some studies showed that high polysomy or amplification of the *EGFR* gene analyzed by fluorescence in situ hybridization (FISH) tended to be the best predictor of response, even better than detection of gene mutations in *EGFR* [11, 16, 17]. Finally, other studies assert the superiority of the detection of *EGFR* mutations for prediction [18, 19]. The two most frequent *EGFR* mutations are short in-frame deletions of exon 19 and a point mutation (CTG to CGG) in exon 21 at nucleotide 2573, which results in substitution of leucine by arginine at codon 858 (L858R) [20]. Together, these two mutations account for almost 90% of all *EGFR* mutations in NSCLC [20]. Response rates to EGFR-TKIs range from 48% to 90% for patients with *EGFR* mutations, while responses are less common in patients without a mutation (5–31%) [21]. Interestingly, two mutant-specific antibodies directed against the most common mutant forms of the EGFR oncoprotein have been recently developed for IHC

use: 15-bp deletion (E746_A750del) in exon 19 and the L858R point mutation in exon 21 [22].

Limited studies have analyzed the possible correlation between different EGFR abnormalities measured by IHC, for total protein expression or for the two mutants (specific antibodies), FISH and sequencing [23–27]. The variability in the results of trials that tested these methods of detection of the EGFR status may reflect variations in the methodology and the interpretation of the test results, as well as patient demographics and cohorts [26, 28, 29].

This study was conducted to demonstrate the potential interest of the tissue microarray (TMA) method to assess protein expression, gene amplification, and mutational status of EGFR in a retrospective cohort of lung adenocarcinoma patients. For this purpose, the relationship between protein expression, gene copy number, and mutational status of EGFR (using mutant-specific antibodies) was evaluated in TMA built with 61 lung adenocarcinomas. Results were then compared with direct sequencing of exons 19, 20, and 21 of *EGFR*, performed in parallel from DNA extracted from mirror frozen tumor tissues. Finally, the correlation between the genetic status and clinicopathological parameters of patients was evaluated. The results show that the TMA method could be useful in detecting EGFR overexpression, mutational status, or gene amplification and may be suitable in a larger series of NSCLC patients.

Patients and methods

Patients

Selected paraffin blocks of formalin-fixed tissues from 61 patients diagnosed with lung adenocarcinoma from January 2007 to November 2009 were retrieved from the archives of the Laboratory of Clinical and Experimental Pathology (Pasteur Hospital, Nice, France). Patients were all Caucasians and were matched for gender and smoking status. The median age was 67 years (range, 42–83 years). Tumors were histologically classified according to WHO guidelines [30]. They included 29 mixed adenocarcinomas with a bronchioloalveolar component, 27 mixed adenocarcinomas, and 5 bronchioloalveolar carcinomas. All tumors were staged according to the international Tumor–Node–Metastasis (TNM) classification [31]. There were 32 I-stage, 9 II-stage, 15 III-stage, and 5 IV-stage tumors. To build TMAs, selection of the cases to be included in the study was based on parameters such as collection by rigorous adherence to banking protocols [32], the absence of neoadjuvant treatment, and the availability of sufficient tissue to examine molecular abnormalities and protein expression by IHC. A well-qualified sample is one where

there is over 60% cancer cells and no necrosis [33]. The study was done with the approval of the ethics committee (CHU of Nice). The patients received the necessary information concerning the study, and informed signed consent was obtained from each patient.

Preparation of tissue microarrays

Representative tumor regions were selected for building TMAs after thorough evaluation of H&E slides, and arrays were designed as previously described [34]. Three core tissue biopsies, 600 μm in diameter, corresponding to the selected morphologically representative region of each paraffin-embedded tumor, were transplanted onto a recipient block using an automated tissue arrayer (Beecher Instruments, Silver Spring, MD, USA and Alphelys, Paris, France). Moreover, the cores were selected from different tumor regions, including the center and the periphery of the lesion. Three additional core tissue biopsies were selected from morphologically normal lung tissue adjacent to each tumor and served as a negative control.

Immunohistochemistry

IHC for total EGFR was performed on serial 4 μm deparaffinized TMA sections, as described [34], using an automated single-staining procedure (Benchmark XT, Ventana Medical Systems, Roche Group, Inc., Tucson, AZ). A mouse monoclonal antibody anti-EGFR (clone 3C6; Ventana, Strasbourg, France) was used according to the manufacturer's instructions. Sections were blindly and independently analyzed by two observers (MI and VH) at low magnification ($\times 200$). Total EGFR protein overexpression was evaluated on TMA cores using an IHC scoring system as described: 0, no membrane staining; 1+, faint, partial membrane staining; 2+, weak, complete membrane staining in $>10\%$ of tumor cells; 3+, intense complete membrane staining in $>10\%$ of tumor cells [25].

IHC with the two mutation-specific antibodies, one recognizing the exon 21 L858R *EGFR* mutation and the other the E746-750 15-bp deletion in exon 19, was done manually as described [22]. Briefly, after deparaffinization, antigen retrieval was performed using EDTH pH 9 (Dako, Glostrup, Denmark) for 30 min, and the primary antibody (1:100, rabbit, monoclonal, Cell Signalling, Danvers, USA) was applied. For detection, the EnVision FLEX kit (Dako) was used. The intensity of EGFR mutant-specific IHC was scored as previously described: 0 = no or faint staining in $<10\%$ of tumor cells; 1+ = faint staining in $>10\%$ of tumor cells; 2+ = moderate staining; 3+ = strong staining [35]. Total EGFR overexpression was considered as 2+ and 3+ and positive mutant-specific EGFR expression as between 1+ and 3+. Whole-tissue sections from tumor blocks of all

cases were stained for total EGFR and compared with the corresponding TMAs spots using the above-mentioned scoring criteria. IHC with the mutant-specific antibodies was performed on whole sections of all positive cases by direct sequencing. In parallel, seven randomly selected negative cases were evaluated on whole-tissue sections.

Fluorescence in situ hybridization

Fluorescence in situ hybridization (FISH) was performed on paraffin-embedded TMAs and whole-tissue 4- μm sections according to a protocol described previously [36]. At least 100 non-overlapping interphase nuclei per core were analyzed blindly and independently by two pathologists (MI and VH). Patients were classified into two strata according to previously described criteria [16]: (1) FISH-negative, with no or low genomic gain (≤ 4 copies of EGFR in $>40\%$ of cells) or (2) FISH-positive with either high polysomy (≥ 4 copies of EGFR in $>40\%$ of cells) or with gene amplification. Gene amplification was considered positive when tight gene clusters were present and a gene/chromosome ratio per cell of ≥ 2 or homogeneously staining regions with ≥ 15 copies in $\geq 10\%$ of cells were detected. A FISH analysis was performed in parallel on whole-tissue sections corresponding to all the positive cases and on seven randomly selected negative cases on TMA and compared with the corresponding TMA spots using the above-mentioned scoring criteria.

DNA extraction and direct sequencing of the *EGFR* gene

Genomic DNA was extracted from frozen tissue samples with $>60\%$ tumor cells using the MagNA Pure Compact Nucleic Acid Isolation Kit Large Volume (Roche Group, Inc., Tucson, AR) according to the manufacturer's instructions. After initial denaturation at 94°C for 5 min, gDNA (100 ng) for exons 19, 20, and 21 of EGFR analysis was subjected to 35 cycles of polymerase chain reaction (PCR) (94°C for 30 s, 56°C for EGFR exon 20, 60°C for EGFR exons 19 and 21 for 30 s, and 72°C for 30 s) using Taq platinum (Invitrogen), followed by a final extension at 72°C for 10 min. Primer pairs used for amplification were those described by Choong et al. [37]. Aliquots of all PCR products were examined by 2% agarose gel electrophoresis. After amplification, post-PCR purification was performed using ExoSAP-IT (GE Healthcare Life Sciences) according to the manufacturer's procedures. All samples were bidirectionally sequenced on an ABI Prism 310 sequencer using the Applied Big Dye Terminator v1.1 kit (Applied Biosystems, Inc., Foster City, CA). Mutations in the *EGFR* gene in patients were reanalyzed with the BioEdit software program [38] by additional amplification and sequencing.

Statistical analysis

Analyses were performed using SPSS 16.0 statistical software (SPSS Inc., Chicago, IL). The degree of agreement between data from whole-tissue sections and the mean value of the three spots corresponding to each case on TMAs was assessed using the Cohen's κ coefficient. The optimal sensitivity and the negative predictive value of the EGFR test were determined by ROC curve analysis. The χ^2 and Mann–Whitney tests were used to explore the association between EGFR test results and the clinicopathological variables of patients. All statistical tests were two-sided, and a significant p value was set at 0.05.

Results

EGFR mutations were detected by direct sequencing in 16.4% (10 of 61) of cases. All cases had an exon 19 mutation (100%). Among the ten *EGFR* mutations in exon 19, there were 15-bp deletions ($n=8$), 18-bp deletions ($n=1$),

and insertion/duplication of 18 bp ($n=1$) (Fig. 1). No mutation was identified in exons 20 and 21 of *EGFR*.

Positive immunolabeling for total EGFR detected by IHC on TMAs was noted in 36% (22 of 61) of all cases and in 40% (4 of 10) of mutant cases (Fig. 2a; Table 1). The EGFR expression levels observed on the TMA spots faithfully reflected the staining intensity of the protein on whole-tissue sections from corresponding tumor blocks ($\kappa=0.92$). Although total EGFR overexpression strongly correlated with the mutational positive status detected by direct sequencing ($p=0.024$), there was poor agreement between these two latter methods ($\kappa=0.03$; Table 1). Six mutant tumor samples (60%) stained faintly on IHC, whereas 35% (18 of 51) of wild-type cases overexpressed EGFR (Table 1).

Thirteen of 61 (21.3%) cases demonstrated high polysomy and amplification by FISH analysis in both whole-tissue sections and corresponding TMA cores (Fig. 3; Table 2). The kappa index was used to measure the agreement between these two methods, and a total concordance was found ($\kappa=1$; $p<0.0001$). Moreover, the

Fig. 1 Mutations in the *EGFR* gene detected by direct sequencing of the cohort. **a** Three representative nucleotide patterns of mutations in *EGFR* exon 19. **b** Three representative electropherograms of mutations in *EGFR* exon 19



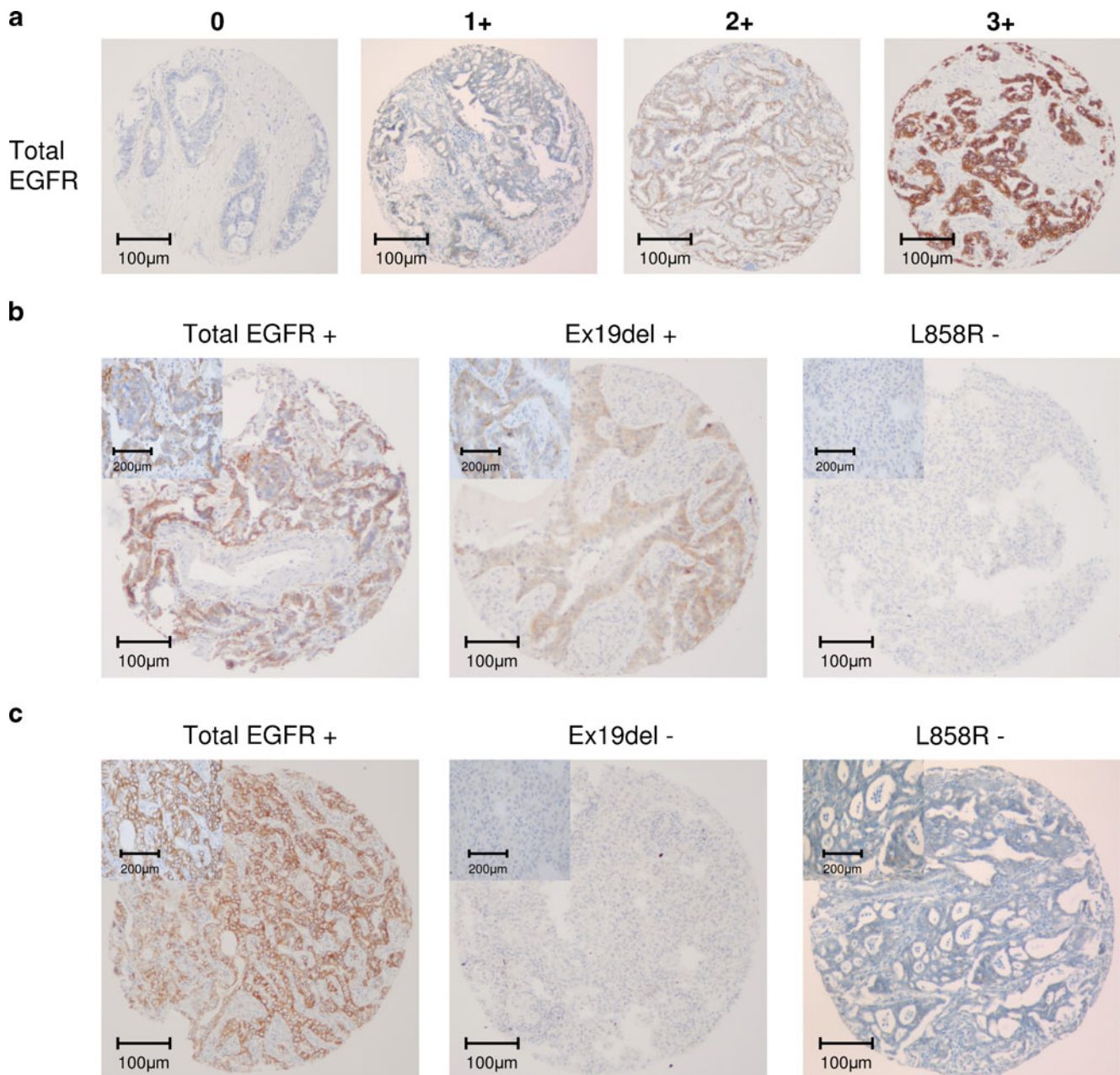


Fig. 2 Lung adenocarcinomas with different levels of immunohistochemical staining. **a** From absent to high total EGFR protein expression. **b** A tumor sample showing positive immunolabelling to the exon 19 mutant-specific and total EGFR antibodies and negative staining to the *EGFR* L858R mutant-specific antibody. **c** Wild-type

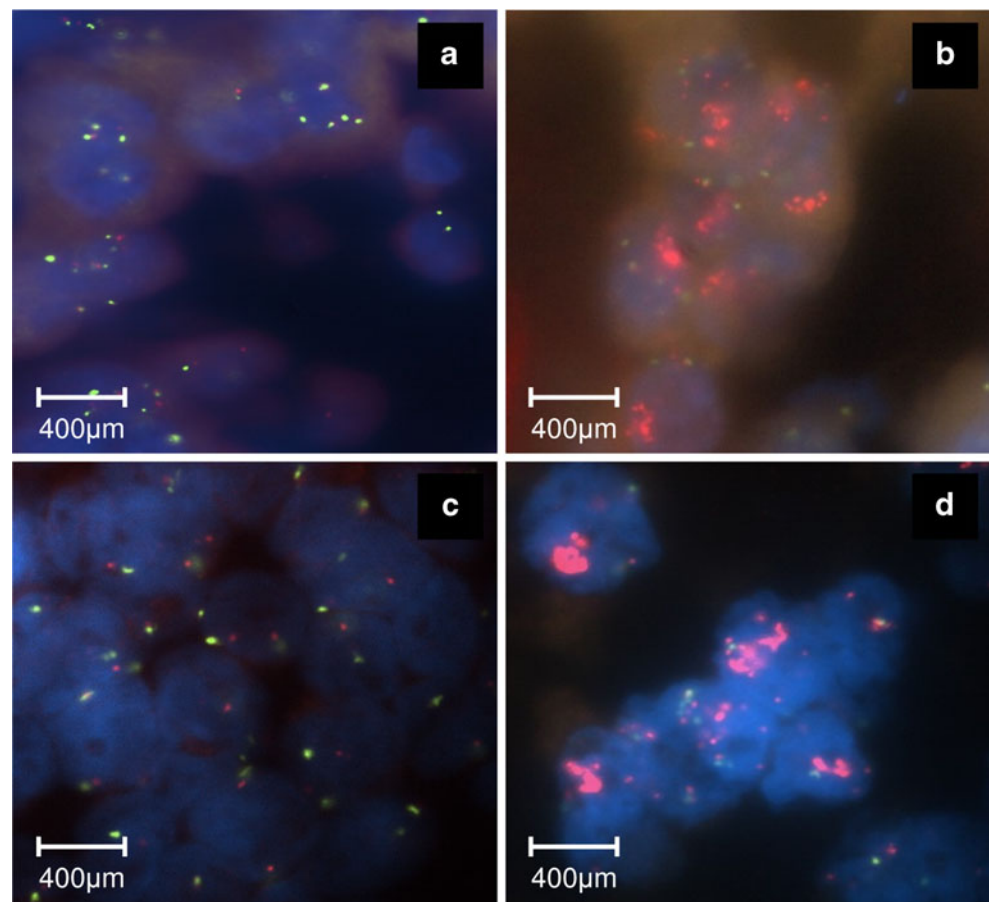
tumor sample showing positive staining to total EGFR and negative staining to the two mutant-specific antibodies (exon 21, L858R and exon 19, E746-750 15-bp deletion). Scale bar in **a–c**, 100 μ m and in **b** and **c** inserts, 200 μ m

Table 1 Correlation between the mutational status of *EGFR* obtained by direct sequencing and of total EGFR protein expression obtained by immunohistochemistry on TMAs

Sequencing	Total EGFR IHC				K index	p value*
	0	1+	2+	3+		
Wild-type (n=51)	15 (29.4%)	18 (35.2%)	14 (27.4%)	4 (7.8%)	0.03	0.024
Exon 19 mutations (n=10)	3 (30%)	3 (30%)	0 (0%)	4 (40%)		

* $p=0.05$; a χ^2 test was used

Fig. 3 Detection of the copy number of the *EGFR* gene by FISH (red signal *EGFR*, green signal CEP 7) in lung adenocarcinomas. Negative FISH test (a) and clustered gene amplification (b) on a whole-tissue section (top). Negative FISH analysis (c) and increased copy numbers of *EGFR* (d) showing gene amplification on TMA cores (bottom). Scale bar 400 μ m



FISH-positive status was strongly related to total EGFR overexpression when performed on TMAs ($p=0.013$), and we found fair agreement between the two tests ($\kappa=0.33$; Table 2). The relationship between mutational status obtained by direct sequencing and *EGFR* gene copy number analyzed by FISH on TMAs was evaluated. There was a significant correlation between these two methods ($p=0.045$) and fair agreement between them ($\kappa=0.30$; Table 3).

Out of all cases, 13 were positive with the exon 19 *EGFR* mutant-specific antibody when performed on TMAs (Fig. 2b, c; Table 4). Similar expression levels were

observed in whole-tissue sections from corresponding tumor blocks in a subset of 20 tumors ($\kappa=0.91$). The staining was both cytoplasmic and membranous. There was no significant correlation to total EGFR protein overexpression ($p=0.23$) and the kappa index showed slight agreement ($\kappa=0.18$; Table 4). All the eight cases (100%) with a 15-bp deletion in exon 19, detected by direct sequencing, were positive for IHC with the EGFR mutant-specific antibody (Table 5). However, positive immunostaining with the exon 19 mutant-specific antibody was also observed in four cases without mutations and in one case with an 18-bp deletion. The EGFR exon 19

Table 2 Correlation between the total EGFR protein expression obtained with TMAs by immunohistochemistry and the *EGFR* gene copy number obtained by FISH analysis

Total EGFR IHC	FISH		K index	p value*
	FISH + (n)	FISH - (n)		
Positive	9	13	0.33	0.013
Negative	4	35		

* $p=0.05$; a χ^2 test was used

Table 3 Correlation between the mutational status obtained by direct sequencing and the *EGFR* gene copy number obtained with TMAs by FISH analysis

Sequencing	FISH		K index	p value*
	FISH + (n)	FISH - (n)		
Wild-type	5	5	0.30	0.045
Exon 19 mutations	8	43		

* $p=0.05$; a χ^2 test was used

Table 4 Relationship between *EGFR* exon 19 mutant-specific TMA immunohistochemistry and total TMA *EGFR* protein expression

EGFR mutant-specific IHC	Total EGFR IHC		<i>K</i> index	<i>p</i> value*
	Positive (<i>n</i>)	Negative (<i>n</i>)		
Positive	7	6	0.18	0.23
Negative	15	33		

* $p=0.05$; a χ^2 test was used

mutant-specific antibody detected 90% of exon 19 mutants with a specificity of 92%. Furthermore, these two methods demonstrated strong statistical correlation ($p<0.001$) and substantial concordance ($\kappa=0.73$ and $\kappa=0.76$, respectively; Table 5). Finally, we found a significant relationship ($p=0.004$) with fair agreement ($\kappa=0.41$) between a high *EGFR* gene copy number and an exon 19 mutational status as determined by mutant-specific IHC, where both analyses were performed on TMAs (Table 6). However, when the 15-bp deletion cases were considered for analysis, the kappa index was lower ($\kappa=0.26$), and there was only a tendency for association with the positive FISH status ($p=0.09$; Table 6).

Among the 61 cases, 26 of 61 (43%) were negative with all four methods. Using the method described by Gupta et al. to define a “true positive result” by identifying a positive result with any of these methods, we found that total *EGFR* IHC demonstrated the highest percentage of positivity (36%) when *EGFR* tests were individually considered (Fig. 4a). By adding the results of the gene copy number analysis to the mutational status, we found larger benefit, which was higher when IHC for total *EGFR* was performed with either three of the methods (Fig. 4b). Finally, the highest percentage of positive *EGFR* tests was obtained with all four methods taken together (Fig. 4c).

Table 5 Relationship between *EGFR* exon 19 mutant-specific TMA immunohistochemistry and mutational status obtained by direct sequencing

EGFR mutant-specific IHC	Sequencing		<i>K</i> index	<i>p</i> value*
	Exon 19 mutations (<i>n</i>)	Wild-type (<i>n</i>)		
Exon 19 mutations				
Positive	9	4	0.73	<0.001
Negative	1	47		
15-bp deletion cases				
Positive	8	4	0.76	<0.001
Negative	0	47		

* $p=0.05$; a χ^2 test was used

Table 6 Relationship between *EGFR* exon 19 mutant-specific TMA immunohistochemistry and the *EGFR* gene copy number as detected by FISH analysis of TMAs

EGFR mutant-specific IHC	FISH		<i>K</i> index	<i>p</i> value*
	FISH + (<i>n</i>)	FISH – (<i>n</i>)		
Exon 19 mutations				
Positive	7	6	0.41	0.004
Negative	6	42		
15-bp deletion cases				
Positive	4	4	0.26	0.09
Negative	9	44		

* $p=0.05$; a χ^2 test was used

When the results of a single method were evaluated, IHC had the highest sensitivity (62.86%; Table 7). *EGFR* protein expression detected by IHC and the mutational status determined either by direct sequencing or by mutant-specific IHC together demonstrated an acceptable sensitivity (80%) and a negative predictive value (79%; Table 7). Finally, we found a total sensitivity (100%) and a total negative predictive value (100%) when all methods were evaluated (Table 7).

We performed statistical analysis to evaluate a possible relationship between the results of these three methods and the clinicopathological variables of patients. The results obtained by direct sequencing alone were used to define the mutational status, with regard to its strong correlation with mutant-specific IHC. The proportion of *EGFR* exon 19 deletions detected by direct sequencing was significantly associated with the never smoking status ($p=0.01$) and with female sex ($p=0.01$; Table 8). No other correlation was found with age, histological sub-type, or pathologic tumour-node-metastasis (pTNM) stage.

Discussion

There is urgent need for methods that allow the high-throughput analysis of the *EGFR* status in biopsy samples using IHC markers and FISH analysis based markers. Some studies have focused on validation of immunohistochemical analysis of *EGFR* expression on TMAs, while only limited reports have validated FISH analysis or recently developed mutant *EGFR*-specific antibodies for IHC using TMAs in several types of cancer [35, 36, 39]. We are aware of the limited interest in TMA technology as a daily routine test. However, given the rising interest in new prognostic and theranostic biomarkers, our study, although quite limited in the number of cases, demonstrates the potential of detecting such biomarkers in larger studies for efficient translational research [40].

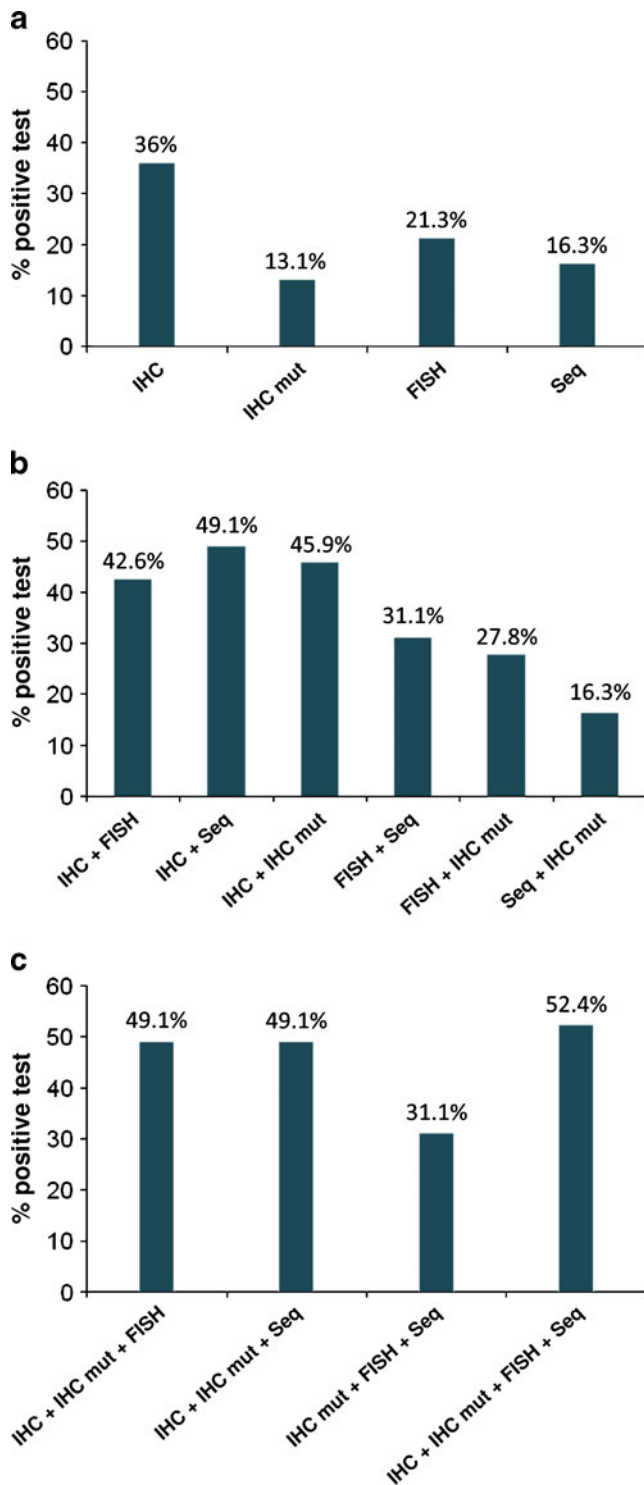


Fig. 4 Percentage of EGFR-positive tests obtained by immunohistochemistry with total EGFR and *EGFR* exon 19 mutant-specific antibodies, fluorescence in situ hybridization, and direct sequencing in 61 lung adenocarcinomas. **a** Test results with one method. **b** Test results with two methods. **c** Test results with three or all methods together

We show that total EGFR IHC, mutant-specific IHC, and FISH analyses performed on whole-tissue sections can be performed with TMAs. Previous studies revealed a variable level of concordance between whole-tissue sections and assessable TMAs when other markers, like HER2, MYC, CCND1, and MDM2, were tested by FISH [41–43]. Since the intratumor heterogeneity would have the most significant impact on the results in tumors with low levels of protein expression or gene amplification, we compared both whole sections and TMA. We recently validated the TMA methodology in lung oncology for analysis of the expression of other proteins in a large series of 555 NSCLC cases [44]. We found an excellent correlation between FISH analysis on whole-tissue sections in comparison with corresponding TMAs. Intratumor variation in the EGFR gene copy number can be more dramatic at higher levels of EGFR gene amplification. However, this variation would have a minimal impact on the designation of a tumor as being EGFR amplified or not amplified in most cases on whole-tissue sections [43]. EGFR-FISH analysis on TMAs in lung adenocarcinoma may therefore be suitable for evaluation of the EGFR gene copy number in a large series of lung adenocarcinoma. In addition, we found fair concordance between total EGFR IHC staining and FISH analysis on TMAs, as EGFR protein overexpression is often associated with *EGFR* gene amplification [45]. Moreover, our results indicate that *EGFR* amplification, preferentially of the mutant allele, often accompanies *EGFR* mutation, as already suggested [25]. Thus, TMAs

Table 7 Sensitivity and negative predictive value of immunohistochemistry, FISH analysis, or direct sequencing for evaluation of the EGFR status

Method	Sensitivity (%)	NPV (%)
IHC	62.86	67
IHC mut	22.86	49
FISH	37.14	54
Seq	28.57	51
IHC+IHC mut	80	79
IHC+FISH	74.29	74
IHC+Seq	80	79
IHC mut+FISH	48.57	59
IHC mut+Seq	51.43	60
FISH+Seq	51.43	60
IHC+IHC mut+FISH	85.71	84
IHC+IHC mut+Seq	97.14	96
IHC mut+FISH+Seq	62.86	67
All methods	100	100

NPV negative predictive value, IHC total EGFR immunohistochemistry, IHC mut EGFR mutant-specific immunohistochemistry, Seq sequencing

Table 8 Clinicopathological characteristics of 61 patients with lung adenocarcinoma according to EGFR protein expression detected by TMA immunohistochemistry, the gene copy number determined by FISH analysis, and mutational status determined by direct sequencing

Variables ^a	FISH		<i>p</i> value*	IHC		<i>p</i> value*	Seq		<i>p</i> value*
	+	–		+	–		+	–	
Age									
>65 years	7	27	0.99	13	21	0.99	7	27	0.51
≤65 years	5	22		7	20		3	24	
Sex									
Female	9	21	0.093	11	19	0.99	9	21	0.01
Male	3	28		9	22		1	30	
Smoking history									
Never smoked	7	17	0.23	10	14	0.36	9	15	0.01
Former or current smokers	5	32		10	27		1	36	
Histologic sub-type									
Mixed ADC	9	18	0.50	8	19	0.17	3	24	0.24
Mixed ADC+BAL	4	25		12	17		7	22	
BAL	0	5		0	5		0	5	
pTNM stage									
I+II	8	33	0.87	16	25	0.68	7	34	0.87
III+IV	5	15		6	14		3	17	

Seq sequencing, ADC adenocarcinoma, BAL bronchioloalveolar carcinoma, TNM tumor node metastasis

^a χ^2 or Mann–Whitney tests when appropriate

**p* value significant at the 0.05 level

can be an appropriate tool for analyzing EGFR protein expression and *EGFR* gene amplification, allowing a more precise evaluation of these mechanisms of activation in a larger series of patients [46–48].

Having validated immunostaining for the total EGFR protein and FISH analysis of the *EGFR* gene copy number on TMAs, we evaluated the mutational status either by using a recently developed mutant EGFR-specific antibody on TMAs or by direct sequencing. Our results show that EGFR exon 19 mutant-specific IHC on TMAs highly correlated with whole-tissue section analysis. Because the large sections may be much more frequently considered as mutant-specific IHC-positive than TMA spots, it might be assumed that false positives on large sections may represent either biologically irrelevant focal findings or local artificial staining, as described [43]. Because of the size of the tissue area to be stained, artificial staining results can be a greater problem on large sections than on TMAs. Although there was a strong correlation between IHC staining on TMAs and results obtained by direct sequencing, false positive results (8%) and the 92% specificity emphasize the need for further molecular validation in routine use. Moreover, *EGFR* gene amplification was associated with IHC staining for mutant-specific exon 19 EGFR on TMAs but not for the 15-bp deletion. Although *EGFR* amplification occurs preferentially on the mutated allele [25], this may suggest that there is no amplification of a specific type of mutation.

We found that *EGFR* genomic gain and mutations were much less frequent cellular events than EGFR overexpression, as previously described [24]. However, the highest

percentage of positive EGFR tests was obtained with all four methods taken together. Furthermore, we evaluated the sensitivity of these methods. Total EGFR IHC had the highest sensitivity, which was not surprising considering the high frequency (34–84%) of EGFR protein overexpression, as already reported in NSCLC [49–51]. Total EGFR protein expression and the mutational status gave a very good negative predictive value (96%) according to a recent report [26]. However, only the evaluation by all four methods reached a high 100% sensitivity and a 100% negative predictive value in detecting EGFR abnormalities. Therefore, great attention should be made when choosing less than three or four methods for EGFR testing in routine clinical practice. This latter finding suggests that the presence of EGFR abnormalities, which might significantly predict response to TKIs, may be underestimated when using direct sequencing alone.

Although IHC staining for total EGFR statistically correlated with a positive mutational status, there was poor agreement between these two methods. In addition, IHC could not predict the *EGFR* mutational status since, in our study, it missed 60% of mutant tumors, as previously shown [25]. Moreover, a large number of IHC-positive tumors lacked mutations. However, we believe that this test should not be completely proscribed as it demonstrated the best sensitivity (62.86%) and negative predictive value (67%). When considered along with *EGFR* molecular modifications (i.e., gene amplification and mutations), we found an even higher negative predictive value (96%). Previous studies have reported the lack of correlation between an *EGFR* mutation and IHC positivity [11, 52]

and *EGFR* mutant tumors with an absence of IHC positivity [14] in TKIs-treated NSCLC patients.

There are many published reports attempting to correlate *EGFR* protein overexpression and benefit of TKIs in lung adenocarcinoma patients [11–15]. However, the data regarding the role of *EGFR* expression in predicting the tumor sensitivity to TKIs are inconsistent and confusing [29]. In this regard, retrospective analyses of patients with NSCLC who received TKIs therapy found no obvious relationship between the amount of *EGFR* protein, assessed by immunohistochemistry (IHC), and the objective response rate [12, 13]. Perez-Soler et al. suggested that the detection of *EGFR* overexpression by IHC may not offer predictive information [13], although Tsao et al. have shown a significant correlation between *EGFR* overexpression detected by IHC and response to TKIs therapy [15]. Similarly, in the ISEL phase III study that compared gefitinib treatment with placebo, patients with *EGFR*-positive tumors who received gefitinib demonstrated significantly prolonged survival compared with patients with *EGFR*-negative tumors [14]. Among the patients whose tumors were negative for *EGFR* protein expression, a trend toward decreased overall survival was observed for the 83 patients treated with gefitinib compared with those treated with placebo. The lack of consensus regarding the predictive value of *EGFR* protein expression might reflect the use of a variety of antibodies, the different protocols, or the quantification criteria and the subjectivity in interpretation. In addition, this might be a result of a lack of clarity surrounding the definition and biological implication of protein expression vs overexpression, with the latter implying a pathological state.

Inconsistent results have also been reported regarding a correlation between detection of *EGFR* gene amplification/polysomy as detected by FISH and benefit of TKIs. Hirsch et al. and others have proposed that detection of polysomy and gene amplification by FISH analysis provides a valuable predictive test [23]. Sone et al., in a study of 59 patients, showed a correlation between *EGFR* mutations detected by PCR and amplification detected by FISH [53]. In contrast, Cappuzzo et al. did not show similar results [11]. Bell et al. and Endo et al. did not find a correlation between the results of FISH and molecular analysis and proposed that *EGFR* kinase mutations and gene amplification appear to identify different genetic subsets of pulmonary adenocarcinoma [17]. The study of Bell et al. is of particular interest since they used quantitative PCR, a precise method to evaluate the *EGFR* gene copy number and to distinguish specific amplification from non-specific aneuploidy [17]. However, this study did not evaluate the results with statistical methods [17]. A recent study by Li et al. using PCR to detect deletions within exon 19 and the L858R mutation in exon 21, IHC for expression of *EGFR*,

and chromogenic in situ hybridization for *EGFR* amplification showed that *EGFR* amplification is often associated with an *EGFR* mutation [25]. *EGFR* mutations were predictive biomarkers in 78% of studies, but there was no consensus concerning the methodology [28]. Most studies have evaluated exon 19 in-frame deletions, exon 18 and 21 single nucleotide substitutions, and exon 20 in-frame duplications [28]. Mitsudomi et al. [54] suggested that patients with point mutations at the *EGFR* 19 locus have a lower response rate to gefitinib than individuals with deletions in the same exon, whereas Sasaki et al. have reported that exon 19 deletions offer no predictive value [55]. In addition, the mutant and wild-type *EGFR* could be influenced by mutations in genes coding for proteins associated with downstream *EGFR* pathways. Therefore, different patterns of phosphorylation are associated with *EGFR* mutations and may be used as surrogate markers for therapeutic decisions. Moreover, even the wild-type *EGFR* pathway may be active through these alternative routes, and these patients may benefit from treatment with TKIs [56]. Therefore, it may be of great interest to study the functional activity of these proteins and their relationship to a TKIs response.

Three major recent clinical trials, BR.21, IDEAL, and IPASS concluded that *EGFR* protein overexpression was not predictive of response to erlotinib or gefitinib therapy and that these drugs provided maximum benefit in patients with TK mutations [3, 17, 53]. However, a recent meta-analysis of 5,000 lung adenocarcinoma patients reported in 27 studies showed that IHC, FISH, and sequencing were all associated with a significant response to TKIs therapy [28]. This latter review also identified considerable variability in the methodologies used in the different studies and in the predictive value of the results for response to gefitinib and erlotinib therapy [28]. Regarding the methodology used for *EGFR* analysis, the TMA methodology could be a good approach to reduce such variability, as we showed that all the major mechanisms of *EGFR* activation can be detected and analyzed on TMAs. For this purpose, a stringent quality control of samples is needed, as awareness of the importance of preanalytical factors is becoming apparent [33, 57]. High-quality tumor tissue is the key to optimal molecular and proteomic analysis. Therefore, the collection, processing, storage, and shipment of biosamples for analysis must be performed under well-documented and rigorously quality-controlled procedures as each of one of these critical steps can modify the nucleic acid and protein structures [33]. Moreover, new fixatives may improve such analyses. A recent study addressed this issue and showed that non-aldehyde fixatives were less convenient for TMA construction [58]. Moreover this study showed that non-aldehyde fixatives can increase the DNA integrity of fixed samples [58]. Intratumoral heterogeneity is the major issue for

consideration when using TMAs to analyze for biomarkers. The key to obtaining a high concordance between analysis of whole paraffin sections and TMA core samples is the selection of representative tumor material (>60% tumor cells, non-tumor zone or stromal reaction removal, lack of necrosis) by the surgical pathologist. Loss of material during pretreatment stages can be another limitation. For this purpose, a minimum of three cores from each tumor sample is recommended [59].

Considering the complexity and redundancy of the EGFR pathway, it is natural to assume that one cannot expect a sole determinant for clinical benefit of EGFR-TKIs [60]. In the present study we evaluated the EGFR status in 61 patients with lung adenocarcinoma by IHC staining for total EGFR and for exon 19 mutant-specific EGFR by FISH on TMAs and by direct sequencing. We demonstrate the high potential of the TMA methodology in detecting the abnormal EGFR status. We showed that the test results are independent variables, suggesting that there is a need to develop evidence-based and consensus standardization guidelines for the performance and interpretation of EGFR tests in routine clinical practice.

Acknowledgement M.I. Ilie was supported by a fellowship from Institut National du Cancer (INCa). P. Hofman, V. Hofman, and J. Mouroux were supported by a PHRC 2003 Grant (CHU of Nice).

Conflict of interest statement We declare that we have no conflict of interest.

References

- Hirsch FR, Witta S (2005) Biomarkers for prediction of sensitivity to EGFR inhibitors in non-small cell lung cancer. *Curr Opin Oncol* 17:118–122
- Reck M (2009) Gefitinib in the treatment of advanced non-small-cell lung cancer. *Expert Rev Anticancer Ther* 9:401–412. doi:10.1586/era.09.1
- Mok TS, Wu YL, Thongprasert S et al (2009) Gefitinib or carboplatin-paclitaxel in pulmonary adenocarcinoma. *N Engl J Med* 361:947–957
- Jorissen RN, Walker F, Pouliot N, Garrett TP, Ward CW, Burgess AW (2003) Epidermal growth factor receptor: mechanisms of activation and signalling. *Exp Cell Res* 284:31–53. doi:10.1016/S0014-4827(02)00098-8
- Sato M, Shames DS, Gazdar AF, Minna JD (2007) A translational view of the molecular pathogenesis of lung cancer. *J Thorac Oncol* 2:327–343. doi:10.1097/01.JTO.0000263718.69320.4c
- Ono M, Kuwano M (2006) Molecular mechanisms of epidermal growth factor receptor (EGFR) activation and response to gefitinib and other EGFR-targeting drugs. *Clin Cancer Res* 12:7242–7251. doi:10.1158/1078-0432.CCR-06-0646
- Herbst RS, Heymach JV, Lippman SM (2008) Lung cancer. *N Engl J Med* 359:1367–1380. doi:10.1056/NEJMra0802714
- Mendelsohn J, Baselga J (2003) Status of epidermal growth factor receptor antagonists in the biology and treatment of cancer. *J Clin Oncol* 21:2787–2799
- Ciardiello F, Tortora G (2008) EGFR antagonists in cancer treatment. *N Engl J Med* 358:1160–1174. doi:10.1056/NEJMra0707704
- Sequist LV, Lynch TJ (2008) EGFR tyrosine kinase inhibitors in lung cancer: an evolving story. *Annu Rev Med* 59:429–442. doi:10.1146/annurev.med.59.090506.202405
- Cappuzzo F, Hirsch FR, Rossi E et al (2005) Epidermal growth factor receptor gene and protein and gefitinib sensitivity in non-small-cell lung cancer. *J Natl Cancer Inst* 97:643–655. doi:10.1093/jnci/dji112
- Parra HS, Cavina R, Latteri F, Zucali PA, Campagnoli E, Morengi E, Grimaldi GC, Roncalli M, Santoro A (2004) Analysis of epidermal growth factor receptor expression as a predictive factor for response to gefitinib ('Iressa', ZD1839) in non-small-cell lung cancer. *Br J Cancer* 91:208–212. doi:10.1038/sj.bjc.6601923
- Perez-Soler R, Chachoua A, Hammond LA et al (2004) Determinants of tumor response and survival with erlotinib in patients with non-small-cell lung cancer. *J Clin Oncol* 22:3238–3247. doi:10.1200/JCO.2004.11.057
- Hirsch FR, Varella-Garcia M, Bunn PA Jr et al (2006) Molecular predictors of outcome with gefitinib in a phase III placebo-controlled study in advanced non-small-cell lung cancer. *J Clin Oncol* 24:5034–5042. doi:10.1200/JCO.2006.06.3958
- Tsao MS, Sakurada A, Cutz JC et al (2005) Erlotinib in lung cancer—molecular and clinical predictors of outcome. *N Engl J Med* 353:133–144
- Hirsch FR, Varella-Garcia M, McCoy J et al (2005) Increased epidermal growth factor receptor gene copy number detected by fluorescence in situ hybridization associates with increased sensitivity to gefitinib in patients with bronchioloalveolar carcinoma subtypes: a Southwest Oncology Group Study. *J Clin Oncol* 23:6838–6845. doi:10.1200/JCO.2005.01.2823
- Bell DW, Lynch TJ, Haserlat SM et al (2005) Epidermal growth factor receptor mutations and gene amplification in non-small-cell lung cancer: molecular analysis of the IDEAL/INTACT gefitinib trials. *J Clin Oncol* 23:8081–8092. doi:10.1200/JCO.2005.02.7078
- Han SW, Kim TY, Hwang PG et al (2005) Predictive and prognostic impact of epidermal growth factor receptor mutation in non-small-cell lung cancer patients treated with gefitinib. *J Clin Oncol* 23:2493–2501. doi:10.1200/JCO.2005.01.388
- Morita S, Okamoto I, Kobayashi K et al (2009) Combined survival analysis of prospective clinical trials of gefitinib for non-small cell lung cancer with EGFR mutations. *Clin Cancer Res* 15:4493–4498. doi:10.1158/1078-0432.CCR-09-0391
- Sharma SV, Bell DW, Settleman J, Haber DA (2007) Epidermal growth factor receptor mutations in lung cancer. *Nat Rev Cancer* 7:169–181. doi:10.1038/nrc2088
- Ellis PM, Morzycki W, Melosky B et al (2009) The role of the epidermal growth factor receptor tyrosine kinase inhibitors as therapy for advanced, metastatic, and recurrent non-small-cell lung cancer: a Canadian national consensus statement. *Curr Oncol* 16:27–48
- Yu J, Kane S, Wu J et al (2009) Mutation-specific antibodies for the detection of EGFR mutations in non-small-cell lung cancer. *Clin Cancer Res* 15:3023–3028. doi:10.1158/1078-0432.CCR-08-2739
- Hirsch FR, Varella-Garcia M, Cappuzzo F et al (2007) Combination of EGFR gene copy number and protein expression predicts outcome for advanced non-small-cell lung cancer patients treated with gefitinib. *Ann Oncol* 18:752–760. doi:10.1093/annonc/mdm003
- Hirsch FR, Varella-Garcia M, Bunn PA Jr, Di Maria MV, Veve R, Bremmes RM, Baron AE, Zeng C, Franklin WA (2003) Epidermal growth factor receptor in non-small-cell lung carcinomas: corre-

- lation between gene copy number and protein expression and impact on prognosis. *J Clin Oncol* 21:3798–3807. doi:10.1200/JCO.2003.11.069
25. Li AR, Chitale D, Riely GJ, Pao W, Miller VA, Zakowski MF, Rusch V, Kris MG, Ladanyi M (2008) EGFR mutations in lung adenocarcinomas: clinical testing experience and relationship to EGFR gene copy number and immunohistochemical expression. *J Mol Diagn* 10:242–248. doi:10.2353/jmoldx.2008.070178
 26. Gupta R, Dastane AM, Forozan F, Riley-Portuguez A, Chung F, Lopategui J, Marchevsky AM (2009) Evaluation of EGFR abnormalities in patients with pulmonary adenocarcinoma: the need to test neoplasms with more than one method. *Mod Pathol* 22:128–133. doi:10.1038/modpathol.2008.182
 27. El-Zammar OA, Zhang S, Katzenstein AL (2009) Comparison of FISH, PCR, and immunohistochemistry in assessing EGFR status in lung adenocarcinoma and correlation with clinicopathologic features. *Diagn Mol Pathol* 18:133–137. doi:10.1097/PDM.0b013e3181857ea9
 28. Gupta R, Dastane AM, McKenna R Jr, Marchevsky AM (2009) The predictive value of epidermal growth factor receptor tests in patients with pulmonary adenocarcinoma: review of current “best evidence” with meta-analysis. *Hum Pathol* 40:356–365. doi:10.1016/j.humpath.2008.08.008
 29. Eberhard DA, Giaccone G, Johnson BE (2008) Biomarkers of response to epidermal growth factor receptor inhibitors in non-small-cell lung cancer working group: standardization for use in the clinical trial setting. *J Clin Oncol* 26:983–994. doi:10.1200/JCO.2007.12.9858
 30. Travis WD, Brambilla E, Muller-Hermelink HK, Harris CC (2004) World health organization classification of tumours. Pathology and genetics of tumours of the lung, pleura, thymus and heart. IARC Press, Lyon
 31. Mountain CF (1997) Revisions in the international system for staging lung cancer. *Chest* 111:1710–1717. doi:10.1378/chest.111.6.1710
 32. Betsou F, Lehmann S, Ashton G et al (2010) Standard preanalytical coding for biospecimens: defining the sample PREanalytical code. *Cancer Epidemiol Biomark Prev* 19:1004–1011. doi:10.1158/1055-9965.EPI-09-1268
 33. Hofman V, Ilie M, Gavric-Tanga V et al (2010) Rôle du laboratoire d’anatomie pathologique dans l’approche pré-analytique des examens de biologie moléculaire réalisés en pathologie tumorale. *Ann Pathol* 30:85–93
 34. Hofman P, Butori C, Havet K, Hofman V, Selva E, Guevara N, Santini J, Van Obberghen-Schilling E (2008) Prognostic significance of cortactin levels in head and neck squamous cell carcinoma: comparison with epidermal growth factor receptor status. *Br J Cancer* 98:956–964. doi:10.1038/sj.bjc.6604245
 35. Brevet M, Arcila M, Ladanyi M (2010) Assessment of EGFR mutation status in lung adenocarcinoma by immunohistochemistry using antibodies specific to the two major forms of mutant EGFR. *J Mol Diagn* 12:169–176. doi:10.2353/jmoldx.2010.090140
 36. Koynova DK, Tsenova VS, Jankova RS, Gurov PB, Toncheva DI (2005) Tissue microarray analysis of EGFR and HER2 oncogene copy number alterations in squamous cell carcinoma of the larynx. *J Cancer Res Clin Oncol* 131:199–203. doi:10.1007/s00432-004-0627-y
 37. Choong NW, Dietrich S, Seiwert TY et al (2006) Gefitinib response of erlotinib-refractory lung cancer involving meninges—role of EGFR mutation. *Nat Clin Pract Oncol* 3:50–57. doi:10.1038/nponc0400
 38. Hall TA (1999) BioEdit: a user-friendly biological sequence alignment editor and analysis program for Windows 95/98/NT. *Nucl Acids Symp Ser* 41:95–98
 39. Park K, Han S, Shin E, Kim HJ, Kim JY (2007) EGFR gene and protein expression in breast cancers. *Eur J Surg Oncol* 33:956–960. doi:10.1016/j.ejso.2007.01.033
 40. Sauter G, Simon R, Hillan K (2003) Tissue microarrays in drug discovery. *Nat Rev Drug Discov* 2:962–972
 41. Al-Kuraya K, Schraml P, Torhorst J et al (2004) Prognostic relevance of gene amplifications and coamplifications in breast cancer. *Cancer Res* 64:8534–8540. doi:10.1158/0008-5472.CAN-04-1945
 42. Giltman JM, Molinaro A, Cheng H, Robinson A, Turbin D, Gelmon K, Huntsman D, Rimm DL (2008) Comparison of quantitative immunofluorescence with conventional methods for HER2/neu testing with respect to response to trastuzumab therapy in metastatic breast cancer. *Arch Pathol Lab Med* 132:1635–1647
 43. Bhargava R, Lal P, Chen B (2004) Feasibility of using tissue microarrays for the assessment of HER-2 gene amplification by fluorescence in situ hybridization in breast carcinoma. *Diagn Mol Pathol* 13:213–216
 44. Ilie M, Mazure NM, Hofman V et al (2010) High levels of carbonic anhydrase IX in tumour tissue and plasma are biomarkers of poor prognostic in patients with non-small cell lung cancer. *Br J Cancer* 102:1627–1635
 45. Suzuki S, Dobashi Y, Sakurai H, Nishikawa K, Hanawa M, Ooi A (2005) Protein overexpression and gene amplification of epidermal growth factor receptor in non small cell lung carcinomas. An immunohistochemical and fluorescence in situ hybridization study. *Cancer* 103:1265–1273. doi:10.1002/cncr.20909
 46. Bubendorf L, Nocito A, Moch H, Sauter G (2001) Tissue microarray (TMA) technology: miniaturized pathology archives for high-throughput in situ studies. *J Pathol* 195:72–79. doi:10.1002/path.893
 47. Sato-Kuwabara Y, Neves JJ, Fregnani JH, Sallum RA, Soares FA (2009) Evaluation of gene amplification and protein expression of HER-2/neu in esophageal squamous cell carcinoma using Fluorescence in situ Hybridization (FISH) and immunohistochemistry. *BMC Cancer* 9:6. doi:10.1186/1471-2407-9-6
 48. Nocito A, Kononen J, Kallioniemi OP, Sauter G (2001) Tissue microarrays (TMAs) for high-throughput molecular pathology research. *Int J Cancer* 94:1–5. doi:10.1002/ijc.1385
 49. Brabender J, Danenberg KD, Metzger R, Schneider PM, Park J, Salonga D, Holscher AH, Danenberg PV (2001) Epidermal growth factor receptor and HER2-neu mRNA expression in non-small cell lung cancer is correlated with survival. *Clin Cancer Res* 7:1850–1855
 50. Nakamura H, Kawasaki N, Taguchi M, Kabasawa K (2006) Survival impact of epidermal growth factor receptor overexpression in patients with non-small cell lung cancer: a meta-analysis. *Thorax* 61:140–145. doi:10.1136/thx.2005.042275
 51. Franklin WA, Vee R, Hirsch FR, Helfrich BA, Bunn PA Jr (2002) Epidermal growth factor receptor family in lung cancer and premalignancy. *Semin Oncol* 29:3–14. doi:10.1053/sonc.2002.31520
 52. Pinter F, Papay J, Almasi A et al (2008) Epidermal growth factor receptor (EGFR) high gene copy number and activating mutations in lung adenocarcinomas are not consistently accompanied by positivity for EGFR protein by standard immunohistochemistry. *J Mol Diagn* 10:160–168. doi:10.2353/jmoldx.2008.070125
 53. Sone T, Kasahara K, Kimura H et al (2007) Comparative analysis of epidermal growth factor receptor mutations and gene amplification as predictors of gefitinib efficacy in Japanese patients with nonsmall cell lung cancer. *Cancer* 109:1836–1844. doi:10.1002/cncr.22593
 54. Mitsudomi T, Kosaka T, Endoh H et al (2005) Mutations of the epidermal growth factor receptor gene predict prolonged survival after gefitinib treatment in patients with non-small-cell lung cancer with postoperative recurrence. *J Clin Oncol* 23:2513–2520. doi:10.1200/JCO.2005.00.992

55. Sasaki H, Endo K, Okuda K et al (2008) Epidermal growth factor receptor gene amplification and gefitinib sensitivity in patients with recurrent lung cancer. *J Cancer Res Clin Oncol* 134:569–577
56. VanMeter AJ, Rodriguez AS, Bowman ED et al (2008) Laser capture microdissection and protein microarray analysis of human non-small cell lung cancer: differential epidermal growth factor receptor (EGFR) phosphorylation events associated with mutated EGFR compared with wild type. *Mol Cell Proteomics* 7:1902–1924
57. Yu YY, Zhu ZG (2010) Significance of biological resource collection and tumor tissue bank creation. *World J Gastrointest Oncol* 2:5–8. doi:[10.4251/wjgo.v2.i1.5](https://doi.org/10.4251/wjgo.v2.i1.5)
58. Lassalle S, Hofman V, Marius I et al (2009) Assessment of morphology, antigenicity, and nucleic acid integrity for diagnostic thyroid pathology using formalin substitute fixatives. *Thyroid* 19:1239–1248
59. Piqueras M, Navarro S, Castel V, Canete A, Llombart-Bosch A, Noguera R (2009) Analysis of biological prognostic factors using tissue microarrays in neuroblastic tumors. *Pediatr Blood Cancer* 52:209–214
60. Uramoto H, Mitsudomi T (2007) Which biomarker predicts benefit from EGFR-TKI treatment for patients with lung cancer? *Br J Cancer* 96:857–863. doi:[10.1038/sj.bjc.6603665](https://doi.org/10.1038/sj.bjc.6603665)

Immunohistochemistry to identify *EGFR* mutations or *ALK* rearrangements in patients with lung adenocarcinoma

P. Hofman^{1,2,3,4}, M. Ilie^{1,2,3}, V. Hofman^{1,2,3,4}, S. Roux⁵, A. Valent⁶, A. Bernheim^{5,6}, M. Alifano⁷, F. Leroy-Ladurie⁸, F. Vaylet⁹, I. Rouquette¹⁰, P. Validire¹¹, M. Beau-Faller¹², L. Lacroix¹³, J. C. Soria^{14,15} & P. Fouret^{5,16*}

¹Laboratory of Clinical and Experimental Pathology, Pasteur Hospital, CHU Nice, Nice; ²ERI-21, INSERM, Nice; ³EA4319, Medical School, Nice Sophia University, Nice, France; ⁴Human Tissue Bio bank Unit/CRB, INSERM, Nice; ⁵U985 Tumour Genetic, INSERM, Villejuif; ⁶Molecular Pathology, Biology and Pathology Department, Institut Gustave Roussy, Villejuif; ⁷Thoracic Surgery Department, CHU Hôtel-Dieu, APHP, Paris; ⁸Thoracic Surgery Department, Marie-Lannelongue Surgical Centre, Le Plessis-Robinson; ⁹Pneumology Department, HIA Percy, Clamart; ¹⁰Pathology Department, Rangueil Hospital-CHU Toulouse, Toulouse; ¹¹Pathology Department, Institut Mutualiste Montsouris, Paris; ¹²Biochemistry and Molecular Biology Department, CHU Strasbourg, Strasbourg; ¹³Translational Research Laboratory; ¹⁴Medicine Department, Gustave-Roussy Institute, Villejuif; ¹⁵Paris XI University, Villejuif; ¹⁶Pierre et Marie Curie University, Paris, France

Received 25 August 2011; revised 3 October 2011; accepted 5 October 2011

Background: Immunohistochemistry has been proposed as a specific and sensitive method to identify *EGFR* mutations or *ALK* rearrangements in lung tumours.

Patients and methods: We assessed *EGFR* and *KRAS* by direct sequencing in 154 patients with lung adenocarcinoma. *ALK* rearrangements were assayed by FISH and RT-PCR. Immunohistochemistry was carried out and evaluated closely following published methods using recommended monoclonal rabbit or mouse antibodies.

Results: Thirteen of 36 exon 19 *EGFR*-mutated tumours (36%)—including 12 of 22 with p.Glu746_Ala750del (55%)—were positive with the 6B6 antibody that was raised against p.Glu746_Ala750del. One hundred eleven of 114 *EGFR* exon 19 wild-type tumours (97%) were negative with 6B6. Four of 21 exon 21 *EGFR*-mutated tumours (19%)—including 4 of 17 with p.Leu858Arg (24%)—were positive with the 43B2 antibody that was raised against p.Leu858Arg. One hundred twenty-two of 124 (98%) *EGFR* exon 21 wild-type tumours were negative with 43B2. Two of four *ALK* rearrangements—including two of three with *ELM4-ALK* fusion transcripts—were identified with the 5A4 antibody. Eleven of 13 tumours without *ALK* rearrangement (85%) were negative with 5A4.

Conclusions: Immunohistochemistry is a specific means for identification of *EGFR* mutations and *ALK* rearrangements. It suffers, however, from poor sensitivity.

Key words: ALK, *EGFR*, immunohistochemistry, lung cancer, mutation

introduction

One of the clinical distinctions of lung cancer in never smokers (NS) is the observed response to tyrosine kinase inhibitors (TKI) that target the epidermal growth factor receptor (*EGFR*) [1]. Compared with ever smokers (ES), NS treated with *EGFR*

TKI have higher response rates to treatment [2, 3]. The response to *EGFR* TKI is linked to constitutional activation of *EGFR* signalling in tumour cells [4]. Lung cancer in NS is characterised by a high frequency of activating *EGFR* mutations that are exclusive of *KRAS* mutations [5, 6].

Rearrangements of the *anaplastic lymphoma kinase (ALK)* have been identified in 2%–7% of all non-small-cell lung carcinoma [7–11]. *ALK* rearrangements are more frequent in NS or light ES with lung adenocarcinomas that are wild type

*Correspondence to: Prof. P. Fouret, INSERM Génétique des tumeurs U985, Institut Gustave-Roussy, 114 rue E. Vaillant, 94805 Villejuif Cedex, France. Tel: +33-1-42-17-77-82; Fax: +33-1-42-17-77-77; E-mail: pierre.fouret@igr.fr

for both *EGFR* and *KRAS* [12]. Oncogenic fusion genes consisting of *ALK* and *echinoderm microtubule associated protein like 4 (EML4)* encode chimeric proteins with constitutive kinase activity, which confers sensitivity to ALK TKI [7]. Inhibition of ALK signalling benefits most patients with *ALK* rearrangements [11].

Based on these findings, it has been proposed to use *EGFR* and *ALK* genetic analyses to guide treatment decisions in patients with advanced-stage lung adenocarcinoma. In order to increase the yield of genetic assays, investigators have proposed to use immunohistochemical assays, which are conveniently carried out on the formalin-fixed paraffin-embedded biopsy samples that are examined for pathological diagnosis. The results of several such studies support that immunohistochemistry is a sensitive and specific method to identify *EGFR* mutations [13–16] or *ALK* rearrangements [10, 17, 18] in paraffin-embedded lung adenocarcinoma specimens.

In this paper, we report the results of immunohistochemical assays to identify mutated *EGFR* or *ALK* rearrangements in patients with lung adenocarcinoma belonging to a cohort that was designed primarily to study lung cancer in NS. The higher prevalence of *EGFR* mutations or *ALK* translocations in NS compared with ES was expected to facilitate the evaluation of immunohistochemistry as a mean to assess genetic status.

methods

patients

All patients had been treated by surgery for lung adenocarcinoma. No patient had received chemotherapy before surgery. Patients belonged to two cohorts based on their smoking status. NS had a lifetime exposure of < 100 cigarettes. ES were matched with NS by centre, sex and stage. Formalin-fixed paraffin-embedded tumour samples were available for 154 patients, including 80 NS and 74 ES. This study was part of the Lung Genes (LG) project, which was approved by the Institut National du Cancer Review Board (Programme National d'Excellence Spécialisé Poumon).

sequencing of *EGFR* and *KRAS*

Genomic DNA was extracted from frozen samples containing at least 50% tumour cells (Qiagen, Courtaboeuf, France). Direct sequencing was carried out after on amplified *EGFR* exons 18, 19, 20, 21 (NM_005228.3) and *KRAS* codons 12 and 13 of exon 2 (NM_033360.2), respectively. Purified DNA was sequenced using BigDye® Terminator Cycle Sequencing Kit (Applied Biosystems, Foster City, CA). Sequencing reactions were analysed on 16-capillary ABI3130 or on 48-capillary 3730 DNA Analyzer® in both sense and antisense directions from two independent amplifications. Sequences reading and alignment were carried out with SeqScape® software (Applied Biosystems). Sequencing data had been published for 46 NS [19].

FISH study

FISH to detect *ALK* rearrangements was carried out on paraffin-embedded sections using Vysis LSI *ALK* dual colour split probe (Abbott Molecular, Des Plaines, IL). Deparaffinised slides were immersed in pretreatment solution (Dako, Glostrup, Denmark) for 10 min at 95°C. After cooling, the pepsin solution was applied for 6–8 min at room temperature and then stopped in wash buffer. The *ALK* probe was heated for 5 min at 84°C and applied overnight at 44°C. Slides were washed with a stringent buffer for 10 min at 65°C, air-dried and counterstained with DAPI.

One hundred tumour cells were analysed for each case. The number of fluorescent signals within the nuclear boundary of each interphase tumour cell was counted using an Axiophot-ZEISS fluorescent microscope at ×1000 magnification. Only nuclei with unambiguous signals were scored. The normal pattern of the *ALK* probe was seen as two yellow (or red and green overlapping) signals. The rearrangement was identified by split signals in > 15% tumour cells: only one yellow signal was detected and well separated green and red signals were seen. Samples were also deemed FISH positive in case of isolated 3' signals (red) representing partial deletion of the 5' part of *ALK* (green) in > 15% tumour cells [11]. The chromosome 2/*ALK* polysomy was detected if > 2 yellow signals were visible in one nucleus.

reverse transcription–polymerase chain reaction

RNA was extracted (Qiagen) and qualified using Agilent Bioanalyzer (Agilent, Massy-Palaiseau, France). Reverse transcription and PCR amplification was carried out using the published primers and protocol [11].

mutant *EGFR* immunohistochemistry

Immunohistochemistry was carried out using two mutation-specific rabbit monoclonal antibodies that were raised against peptides matching the E746-750 exon 19 15-bp deletion mutant sequence (clone 6B6; Cell Signalling Technology, Denver, CO) or the exon 21 L858R mutant sequence (clone 43B2; Cell Signalling Technology) of human *EGFR* [13].

Preliminary assays showed no difference in staining intensity and proportion of labelled cells when the primary antibodies were incubated overnight or for 1 h, following the protocols described by Yu et al. [13] or Brevet et al. [16] and Simonetti et al. [15], respectively. The preliminary study included mismatching cases (e.g. immunohistochemistry negative with both incubation times and sequencing positive). We selected 1 h incubation time such that the procedure could be fully automated.

Deparaffinised slides were subjected to antigen retrieval by microwave boiling in 1 mmol/l EDTA pH 9.0 (Dako) for 30 min. The staining procedure was carried out using an automate (Benchmark XT; Ventana Medical Systems, Roche Group Inc., Tucson, AR). Intrinsic peroxidase activity was blocked by 3% hydrogen peroxide for 20 min. Goat serum (5%; Sigma, St Louis, MO) solution was used for blocking non-specific antibody binding. The primary antibodies were applied at the recommended 1 : 100 dilution. Slides were washed in PBS before incubation with labelled polymer-horseradish peroxidase anti-rabbit secondary antibody for 30 min at room temperature. For visualisation, the iVIEW DAB Detection kit was used according to the manufacturer's instructions (Ventana Medical Systems, Faulquemont, France).

The intensity of staining as well as percentages of positive cells were assessed semi-quantitatively as previously described [13, 16]: 0 = no or faint staining in < 10% of tumour cells; 1+ = faint staining in > 10% of tumour cells; 2+ = moderate staining; 3+ = strong staining. Positive mutant-specific *EGFR* expression was considered as between 1+ and 3+ [13, 16]. Immunohistochemical staining in specimens was independently assessed by two pathologists (MI and PH) blinded to clinical and genotype data. When discrepancy between the two pathologists was noted, the slides were reviewed in order to obtain a consensus.

The level of discordance between the two pathologists was 3% (4/139) for the E746_A750 deletion antibody and 5% (7/137) for the L858R point mutation antibody.

ALK immunohistochemistry

Immunohistochemistry was carried out using the mouse monoclonal antibody 5A4, which was raised against a recombinant protein corresponding to a region which spans the tyrosine kinase catalytic domain

and part of the C-terminus of NPM-ALK transcript (419–520 aa) (Abcam, Cambridge, UK).

An increased sensitivity was obtained using the intercalated antibody-enhanced polymer method as developed by Takeuchi et al. [17]. Briefly, slides were heated in Target Retrieval Solution (pH 9.0; Dako) for 40 min at 97°C. They were incubated at room temperature with Protein Block Serum-free Ready-to-Use solution (Dako) for 10 min. Then anti-ALK 5A4 antibody was applied for 30 min at a recommended dilution of 1 : 50. Slides were incubated at room temperature with EnVision FLEX + Mouse Linker (Dako) for 15 min. The immune complexes were then detected with the dextran polymer reagent.

The percentage of labelled tumour cells and intensity of staining was recorded for each specimen. Immunohistochemical staining in specimens was independently assessed by two pathologists (MI and PH) blinded to clinical and genotype data. No discordance was noted between the two pathologists.

statistical analysis

The frequencies of *EGFR* and *KRAS* mutations were compared using the two-tailed chi-square test.

results

clinicopathological characteristics

The 154 patients were predominantly women (88%). The median age was 65 years (interquartile range = 55–73 years). The stages according to UICC classification [20] were stage I for 87 patients, stage II for 19 patients and stage III for 48 patients. The adenocarcinomas comprised 119 mixed, 23 acinar, 5 papillary and 7 solid histological subtypes. NKX2-1 was expressed in 92% tumours.

EGFR mutations

EGFR status could be assessed in 151 tumours. Mutations were found in 62 cases (41%). They were more frequent ($P = 0.0002$) in NS (49 of 78, or 63%) than in ES (13 of 73, or 18%).

Mutations were found mainly in exon 19 (36 tumours, or 58%) and in exon 21 (21 tumours, or 34%). Mutations in exon 19 and mutations in exon 21 were exclusive. Five tumours harboured mutations in exons other than exon 19 or exon 21: two tumours in exon 18, two tumours in exon 20 and one tumour in both exon 18 and exon 20. All mutations were in frame.

The 36 mutations in exon 19 included 22 c.2235_2249 or c.2236_2250 deletions, p.Glu746_Ala750del (61%), 12 small indels (33%) and 2 small insertions. The 21 mutations in exon 21 included 17 c.2373 substitutions, p.Leu858Arg (81%), 2 c.2582 substitutions, p.Leu861Gln and 2 c.2582 substitutions, p.Leu861Glu.

KRAS mutations

KRAS status could be assessed in 151 tumours. Mutations were found in 36 cases (24%). They were more frequent ($P < 0.0001$) in ES (30 of 73, or 41%) than in NS (6 of 78, or 7.5%). Mutations were found in codon 12 (33 tumours, or 92%) and in codon 13 (3 tumours, or 8%) of exon 2. *KRAS* mutations were exclusive of *EGFR* mutations.

ALK rearrangements

Tumours wild type for both *EGFR* and *KRAS* in NS were selected for assaying *ALK* rearrangements using FISH. Among 20 tumours that could be analysed, 4 (20%) displayed *ALK* rearrangements: 3 had split *ALK* 5' and 3' probe signals in > 50% cells and 1 had isolated 3' signals in > 50% cells. Representative examples of these signals are shown in supplemental Figure S1 (available at *Annals of Oncology* online). Table 1 summarises the clinicopathological characteristics of the four patients with *ALK* rearrangement.

Ten tumours demonstrated chromosome 2 trisomy or polysomy, including one case with high-level polysomy (more than six copies).

EML4-ALK fusion transcripts

EML4-ALK fusion transcripts were found in 3 among 19 tumours wild type for both *EGFR* and *KRAS* that could be analysed by RT-PCR. Those three tumours had the *ALK* rearrangement as shown by the split *ALK* 5' and 3' probe signals. The fourth tumour with a rearrangement as shown by the 3' isolated signal did not contain *EML4-ALK* fusion transcripts.

expression of EGFR proteins

Table 2 summarises the immunohistochemical data according to exon 19 or exon 21 *EGFR* status. Representative examples of immunohistochemical staining are shown in supplemental Figure S2 (available at *Annals of Oncology* online).

Using the described criteria [13, 16], 16 (9%) tumours were positive (1 + : 5 cases; 2 + : 7 cases; 3 + : 4 cases) with the 6B6 clone that was generated using a peptide containing the p. Glu746_Ala750del mutation, while 6 (4%) tumours were positive (1 + : 2 cases; 2 + : 3 cases; 3 + : 1 case) with the 43B2 clone that was generated using a peptide containing the p. Leu858Arg mutation.

Among 36 tumours harbouring exon 19 mutations, 13 (36%) were positive with 6B6, including 5 cases with 1 + positivity. Among 22 tumours harbouring the c.2235_2249 or c.2236_2250 deletion, p.Glu746_Ala750del mutation, 12 (54.5%) were positive with the 6B6 clone. Among 114 tumours

Table 1. Clinicopathological characteristics in four never smokers with *ALK* rearrangements

Sample ID	Sex	Age (years)	TNM	Histological subtype	Differentiation	NKX2-1 expression
26	Female	77	IB	Mixed	Poor	Positive
66	Female	57	IIIa	Mixed	Poor	Positive
86	Female	47	IIIB	Acinar	Intermediate	Positive
220	Female	46	IB	Solid	Poor	Positive

wild type for exon 19, 111 (97%) were negative with the 6B6 clone.

Among 21 tumours harbouring exon 21 mutations, 4 (19%) were positive with 43B2, including 1 case with 1 + positivity. Among 17 tumours harbouring c.2573 substitution, p.Leu858Arg mutation, 4 (23.5%) were positive with the 43B2 clone. Among 124 tumours wild type for exon 21, 122 (98%) were negative with the 43B2 clone.

Table 2. Immunohistochemical reactivity according to *EGFR* mutation in exon 19 and in exon 21

	Immunohistochemical reactivity			
	6B6 clone		43B2 clone	
	Positive	Negative	Positive	Negative
Exon 19				
Mutation				
p.Glu746_Ala750del	12	10	1 ^a	19
indels	0	12	0	12
insertions	1	1	0	2
all	13	23	1	33
Wild type	3	111	5	106
Exon 21				
Mutation				
p.Leu858Arg	0	17	4	13
p.Leu861Gln	0	2	0	2
p.Leu861Glu	0	2	0	2
all	0	21	4	17
Wild type	16	113	2	122

^aWas positive for both antibodies

One tumour harbouring the c.2236_2250del, p.Glu746_Ala750del mutation was positive with the 43B2 clone, whereas none of the tumours harbouring exon 21 mutations was positive with the 6B6 clone. None of the five tumours harbouring only mutations in exon 18 or exon 20 was positive with the antibodies.

expression of ALK protein

Table 3 summarises the results of FISH, RT-PCR and immunohistochemistry to identify *ALK* rearrangements in tumours wild type for both *EGFR* and *KRAS*.

Four samples displayed moderate staining in 70%–90% of tumour cells, while 16 other samples displayed no staining. The four samples displaying diffuse staining were deemed positive.

Among four tumours harbouring *ALK* rearrangement as determined by FISH, two were positive with the 5A4 clone. Among 13 tumours without *ALK* rearrangement that could be analysed with the 5A4 clone, 11 (85%) were negative.

Representative examples of immunohistochemical staining for *ALK* rearrangement are shown in supplemental Figure S3 (available at *Annals of Oncology* online).

discussion

We studied lung adenocarcinomas by means of immunohistochemistry with monoclonal antibodies that were reported to be specific and sensitive tools to identify *EGFR* or *ALK* mutations. The procedures were carried out by closely following published protocols including steps that were developed to increase sensitivity [13, 15–17]. The results were

Table 3. Results of FISH, RT-PCR and immunohistochemistry in patients with wild-type *EGFR* and *KRAS*

ID sample	<i>ALK</i> break apart FISH	RT-PCR for <i>EML4-ALK</i> fusion transcripts	Immunohistochemistry <i>ALK</i> with 5A4 clone
3	Normal	Negative	Positive
21	2p23 trisomy	Negative	Negative
25	Na	Negative	Negative
26	Split signal	Positive	Positive
28	2p23 trisomy	Negative	Na
31	2p23 trisomy	Negative	Negative
36	2p23 trisomy	Negative	Na
52	Normal	Negative	Negative
53	2p23 polysomy	Negative	Negative
62	2p23 polysomy	Negative	Negative
66	Split signal	Positive	Positive
67	2p23 trisomy	Negative	Negative
86	Isolated 3' signal	Negative	Negative
87	Normal	Na	Negative
92	Normal	Negative	Negative
169	Normal	Negative	Negative
186	Na	Na	Negative
196	Normal	Negative	Negative
218	2p23 high-level polysomy	Na	Negative
220	Split signal	Positive	Negative
222	2p23 polysomy	Negative	Positive
237	2p23 polysomy	Negative	Negative

analysed using previously reported criteria [13, 16]. The classification into positivity and negativity was straightforward as positive cases had a large proportion of reacting tumour cells, while no or minimal background staining could be seen in negative cases. In our hands, the specificity of immunohistochemistry could be considered good (from 85% to 98%), indicating that the antibodies were indeed able to specifically react in paraffin-embedded material with the peptides against which they were raised and that we used these antibodies with appropriate technical care. The sensitivity of immunohistochemistry, however, was clearly less than expected by previous reports [10, 13–18]: less than half of all the genetic alterations were identified by immunohistochemistry in our study. This was disappointing as genetic analyses of unselected patients with lung cancer yield few positive results.

The frequency of *EGFR* mutations was high (41% for the whole cohort and 63% for NS), consistent with the high prevalence of *EGFR* mutations that were recently reported in European [21] or Asian [22] NS with lung non-small-cell carcinoma. The frequency of *ALK* rearrangements (~20%) in NS with both wild-type *EGFR* and *KRAS* validates the selection of this subpopulation to increase the likelihood of finding *ALK* rearrangements [12]. Moreover, among the four patients with *ALK* rearrangements, the adenocarcinomas were of the solid subtype in one case and of the mixed subtype with low differentiation in two cases, which implies a substantial solid histological component. Our data are thus consistent with the histology seen in patients with *ALK* rearrangements [11].

In our study, immunohistochemistry was carried out in surgical samples that may be less homogeneously preserved by fixation procedure than biopsy samples. This does not seem to be a confounding factor as the measures of sensitivity as sensitivities previously reported in immunohistochemical studies using surgical samples were acceptable for *EGFR* exon 19 mutation (79%) or exon 21 mutation (83%) [14] and excellent for *ALK* translocation (100%) [10]—proportions not very different from those recorded using biopsy samples [13, 15, 16, 18]. Moreover, the whole section of each sample in our series was carefully screened by both pathologists. Overnight incubation with primary antibodies may increase sensitivity of immunohistochemistry on surgical samples. However, in our preliminary study, there was no difference of immunolabeling results in *EGFR*-mutant cases, including mismatching cases, between 1 h and overnight incubation. The cut-off for positivity is also important. Cases with faint positivity in > 10% cells were all truly positive, validating the use of this low cut-off. It cannot be ruled out that few samples were not optimally fixed, thus preventing detection of fragile epitopes. Although suboptimal fixation of few samples could not explain the low sensitivity in the whole cohort, it could have been a major problem had the results of immunohistochemistry been used in the context of personalised medicine.

We report a sensitivity of 36% and 19% for immunohistochemistry when considering all exon 19 or 21 *EGFR* mutations, respectively. When restricting the analysis to the common mutations translating into peptides against which antibodies were generated, the sensitivity increased to 54.5% with 6B6 (p.Glu746_Ala750del) and to 23.5% with 43B2 (p.Leu858Arg). With one exception, the antibodies almost

completely failed to recognise the other less common *EGFR* mutations, which accounted for 31% of exon 19 mutations and 19% of exon 21 mutations. The failure to recognise the less common *EGFR* mutations is evidence of specificity, but it may have contributed to low sensitivity. The 54.5% sensitivity reported here using 6B6 to detect p.Glu746_Ala750del is at the lower range of the confidence interval around the 69% sensitivity reported by Simonetti et al. [15] for exon 19 mutations. These authors also reported that most of the uncommon *EGFR* mutations in exon 19 were negative with 6B6. This is an unavoidable limitation of immunohistochemistry using currently available antibodies, as those less common mutations are able to activate *EGFR* signalling.

Our results with the *ALK* antibody also suggest a lack of sensitivity for immunohistochemistry as two of four rearrangements were missed by immunohistochemistry. It is easily explained by the fact that *ALK* rearrangements in lung cancer are usually associated with low levels of *ALK* expression in contrast to anaplastic lymphomas with *ALK* rearrangements where the protein is robustly detected by immunohistochemistry [23]. We selected the 5A4 mouse monoclonal antibody that was reported to give the best results among five monoclonal antibodies that were compared in a comprehensive study [17]. One could argue that an increase in sensitivity can be achieved using a higher affinity antibody such as the rabbit monoclonal antibody used by Mino-Kenudson et al. [18], although it is not currently commercially available.

RT-PCR also failed to identify one *ALK* rearrangement, presumably because not every *ALK* rearrangement leads to *EML4-ALK* fusion genes [11].

In conclusion, our results support that immunohistochemistry is a relatively specific means for identification of *EGFR* mutations and *ALK* rearrangements. In our hands, however, it suffers from poor sensitivity. As patients in our study were all treated by surgery, it is clear that the results of the genetic analyses would have not guided therapeutic decisions. Nevertheless, the surgical samples were very convenient to evaluate the actual performance of the antibodies in routinely fixed and paraffin-embedded lung tumours. We strongly recommend that laboratories should test the sensitivity of immunohistochemistry in their local conditions to be aware of its limitation in their routine practise.

acknowledgement

The following investigators participated to the Lung Genes (LG) project: Centre Chirurgicale Marie-Lannelongue, Le Plessis-Robinson: P. Darteville, E. Dulmet, F. Leroy-Ladurie, V. de Montpreville; CHI Créteil, Créteil: I. Monnet; CHU Dijon, Dijon: A. Bernard, F. Piard; CHU Hôtel-Dieu, Paris: M. Alifano, S. Camilleri-Broët, J. F. Régnaud; CHU Nice, Nice: P. Hofman, V. Hofman, J. Mouroux; CHU Saint-Louis, Paris: J. Trédaniel; CHU Strasbourg, Strasbourg: M. Beau-Faller, G. Massard, A. Neuville; CHU Tenon, Paris: M. Antoine, J. Cadranet; CHU Toulouse: L. Brouchet, J. Mazières, I. Rouquette; HIA Percy, Clamart: P. Saint-Blancard, F. Vaylet; Institut Gustave-Roussy, Villejuif: A. Berhneim, P. Dessen,

F. Dufour, N. Dorvault, P. Fouret, B. Job, L. Lacroix, V. Lazar, C. Richon, J. C. Soria, V. Roux, P. Saulnier, E. Taranchon, S. Toujani, A. Valent; Institut Mutualiste Montsouris, Paris; P. Girard, D. Gossot, P. Validire; Ligue Nationale contre le Cancer, Paris; J. Laffaire.

funding

This work was supported by Institut National du Cancer (Programme National d'Excellence Spécialisé Poumon) and by Association pour la Recherche sur le Cancer (SFI20101201740).

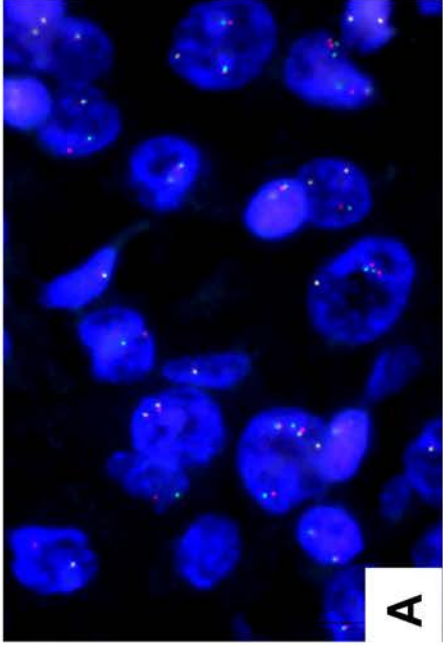
disclosure

The authors declare no conflict of interest.

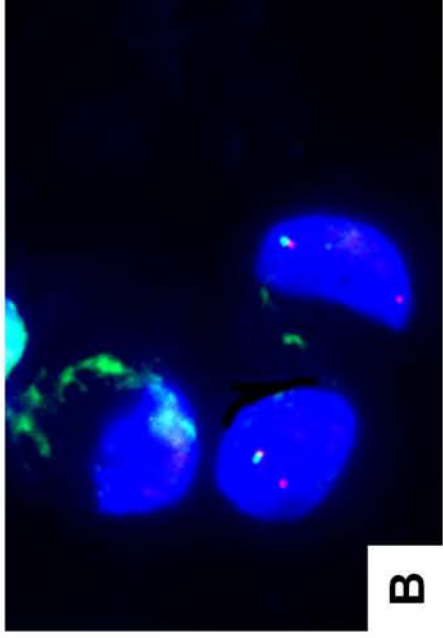
references

- Subramanian J, Govindan R. Lung cancer in never smokers: a review. *J Clin Oncol* 2007; 25: 561–570.
- Shepherd FA, Rodrigues Pereira J, Ciuleanu T et al. Erlotinib in previously treated non-small-cell lung cancer. *N Engl J Med* 2005; 353: 123–132.
- Thatcher N, Chang A, Parikh P et al. Gefitinib plus best supportive care in previously treated patients with refractory advanced non-small-cell lung cancer: results from a randomised, placebo-controlled, multicentre study (Iressa Survival Evaluation in Lung Cancer). *Lancet* 2005; 366: 1527–1537.
- Gazdar AF, Shigematsu H, Herz J, Minna JD. Mutations and addiction to EGFR: the Achilles 'heel' of lung cancers? *Trends Mol Med* 2004; 10: 481–486.
- Pao W, Miller V, Zakowski M et al. EGF receptor gene mutations are common in lung cancers from "never smokers" and are associated with sensitivity of tumors to gefitinib and erlotinib. *Proc Natl Acad Sci U S A* 2004; 101: 13306–13311.
- Tam IYS, Chung LP, Suen WS et al. Distinct epidermal growth factor receptor and KRAS mutation patterns in non-small cell lung cancer patients with different tobacco exposure and clinicopathologic features. *Clin Cancer Res* 2006; 12: 1647–1653.
- Soda M, Choi YL, Enomoto M et al. Identification of the transforming EML4-ALK fusion gene in non-small-cell lung cancer. *Nature* 2007; 448: 561–566.
- Takeuchi K, Choi YL, Soda M et al. Multiplex reverse transcription-PCR screening for EML4-ALK fusion transcripts. *Clin Cancer Res* 2008; 14: 6618–6624.
- Koivunen JP, Mermel C, Zejnullahu K et al. EML4-ALK fusion gene and efficacy of an ALK kinase inhibitor in lung cancer. *Clin. Cancer Res* 2008; 14: 4275–4283.
- Wong DW-S, Leung EL-H, So KK-T et al. The EML4-ALK fusion gene is involved in various histologic types of lung cancers from nonsmokers with wild-type EGFR and KRAS. *Cancer* 2009; 115: 1723–1733.
- Kwak EL, Bang Y-J, Camidge DR et al. Anaplastic lymphoma kinase inhibition in non-small-cell lung cancer. *N Engl J Med* 2010; 363: 1693–1703.
- Camidge DR, Kono SA, Flacco A et al. Optimizing the detection of lung cancer patients harboring anaplastic lymphoma kinase (ALK) gene rearrangements potentially suitable for ALK inhibitor treatment. *Clin Cancer Res* 2010; 16: 5581–5590.
- Yu J, Kane S, Wu J et al. Mutation-specific antibodies for the detection of EGFR mutations in non-small-cell lung cancer. *Clin Cancer Res* 2009; 15: 3023–3028.
- Kawahara A, Yamamoto C, Nakashima K et al. Molecular diagnosis of activating EGFR mutations in non-small cell lung cancer using mutation-specific antibodies for immunohistochemical analysis. *Clin Cancer Res* 2010; 16: 3163–3170.
- Simonetti S, Molina MA, Queralt C et al. Detection of EGFR mutations with mutation-specific antibodies in stage IV non-small-cell lung cancer. *J Transl Med* 2010; 8: 135.
- Brevet M, Arcila M, Ladanyi M. Assessment of EGFR mutation status in lung adenocarcinoma by immunohistochemistry using antibodies specific to the two major forms of mutant EGFR. *J Mol Diagn* 2010; 12: 169–176.
- Takeuchi K, Choi YL, Togashi Y et al. KIF5B-ALK, a novel fusion oncokine identified by an immunohistochemistry-based diagnostic system for ALK-positive lung cancer. *Clin Cancer Res* 2009; 15: 3143–3149.
- Mino-Kenudson M, Chirieac LR, Law K et al. A novel, highly sensitive antibody allows for the routine detection of ALK-rearranged lung adenocarcinomas by standard immunohistochemistry. *Clin Cancer Res* 2010; 16: 1561–1571.
- Job B, Bernheim A, Beau-Faller M et al. Genomic aberrations in lung adenocarcinoma in never smokers. *PLoS ONE* 2010; 5: e15145.
- Bootz F, Hermanek P, Howaldt HJ et al. TNM Atlas. Guide illustré de la classification TNM/pTNM des tumeurs malignes, 4th edition. Paris, France: Springer-Verlag France 1998.
- Rosell R, Moran T, Queralt C et al. Screening for epidermal growth factor receptor mutations in lung cancer. *N Engl J Med* 2009; 361: 958–967.
- Mok TS, Wu Y-L, Thongprasert S et al. Gefitinib or carboplatin-paclitaxel in pulmonary adenocarcinoma. *N Engl J Med* 2009; 361: 947–957.
- Kutok JL, Aster JC. Molecular biology of anaplastic lymphoma kinase-positive anaplastic large-cell lymphoma. *J Clin Oncol* 2002; 20: 3691–3702.

Supplementary figure S1



Split signals

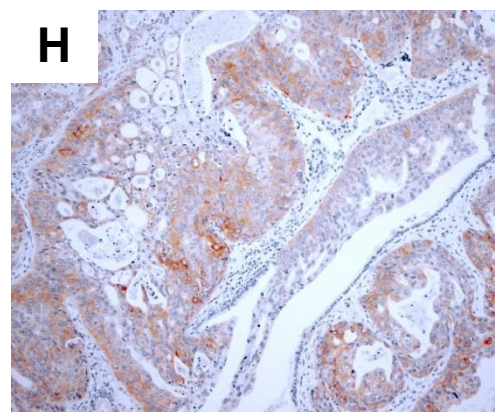
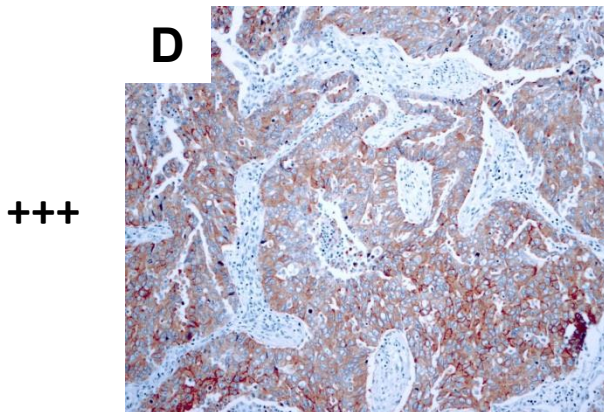
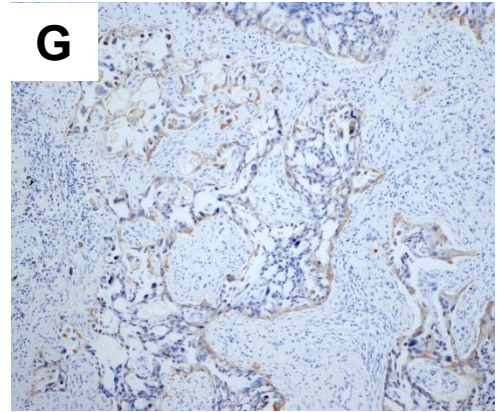
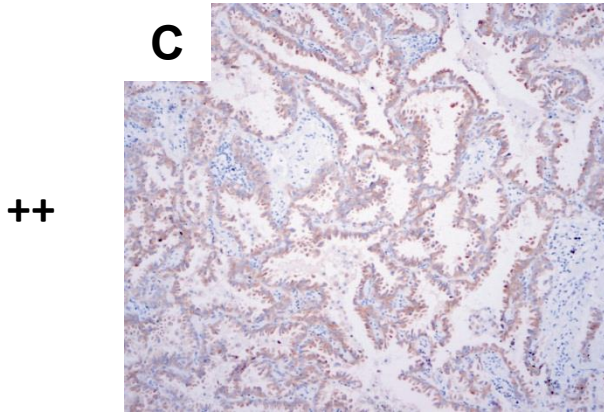
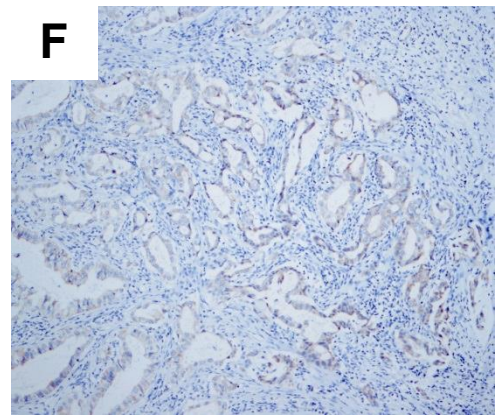
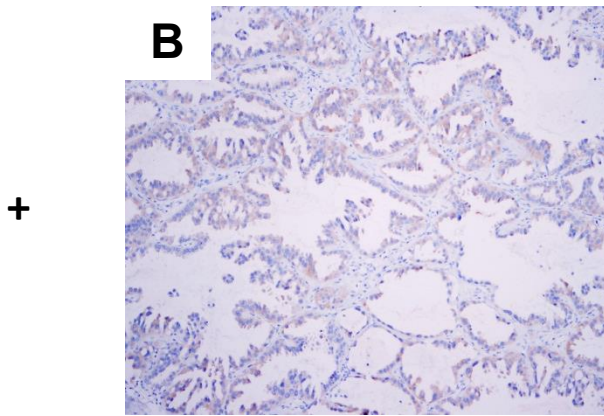
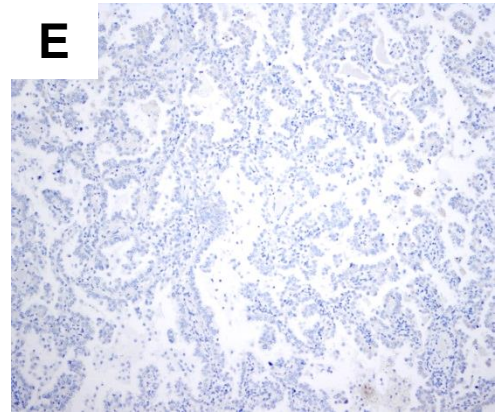
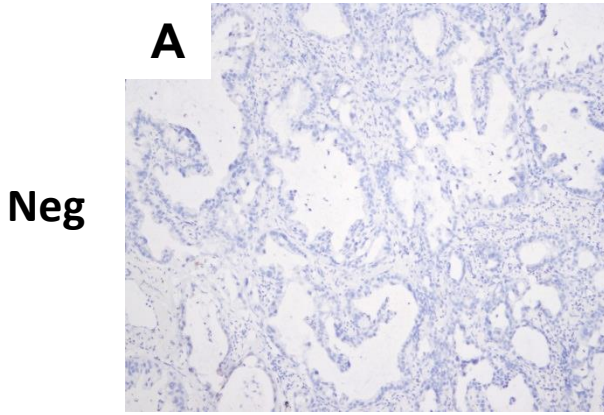


Isolated 3' signals

Supplementary Figure S2

6B6

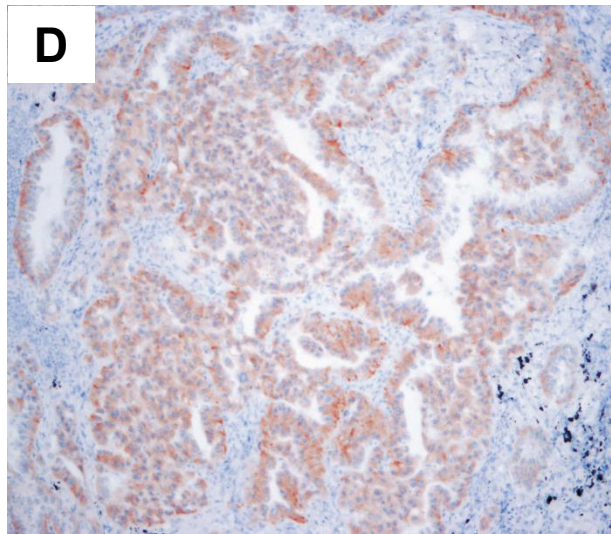
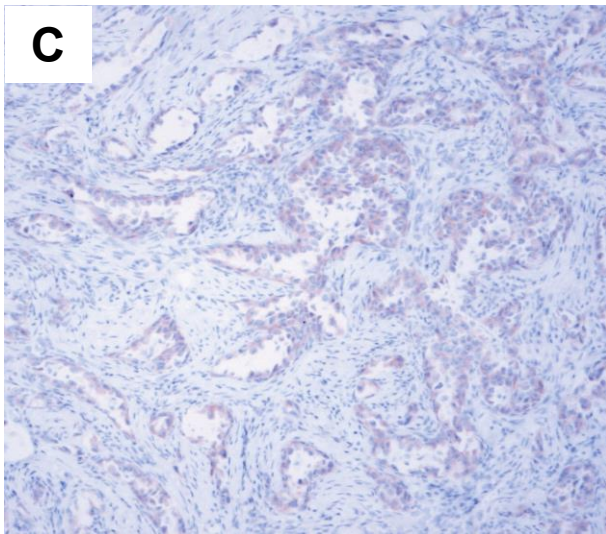
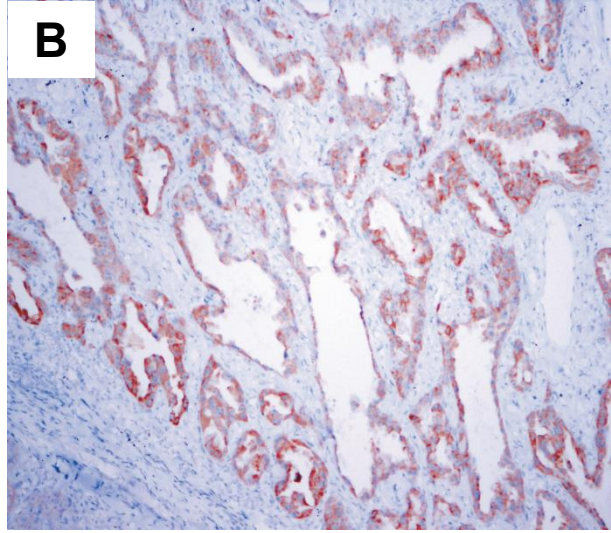
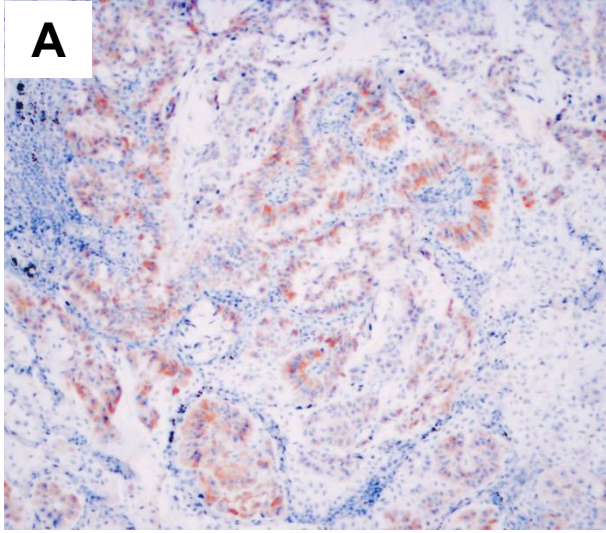
43B2



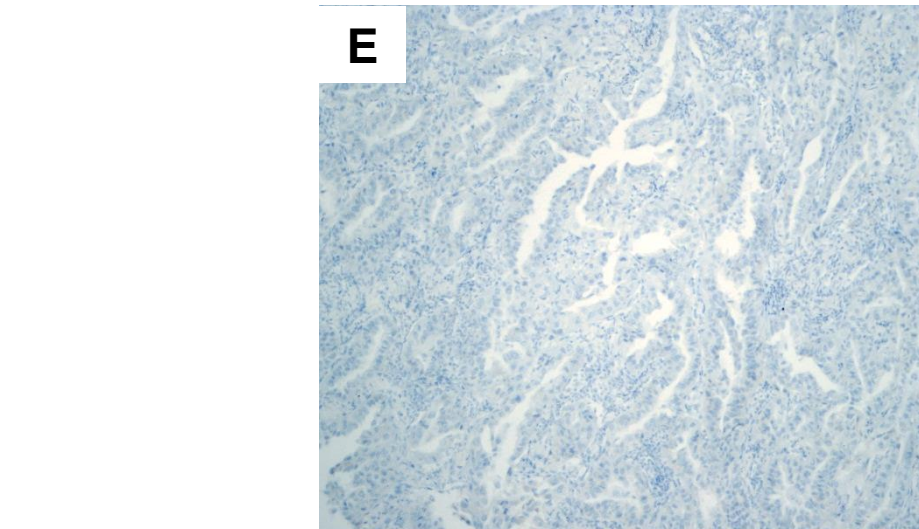
Supplementary Figure S3

Positive ALK IHC

Positive ALK IHC



Negative ALK IHC



REVIEW ARTICLE

The Potential Value of Immunohistochemistry as a Screening Tool for Oncogenic Targets of Personalized Lung Cancer Therapy

Marius Ilie, MD., and Paul Hofman, MD., Ph.D.

ABSTRACT

From the Laboratory of Clinical and Experimental Pathology, Louis Pasteur Hospital, University of Nice Sophia Antipolis Nice, Nice, France (M.I., P.H.); Human Tissue Biobank Unit/CRB INSERM, Louis Pasteur Hospital, Nice, France (M.I., P.H.); and Team 3, Faculty of Medicine of Nice, IRCAN, INSERM U1081 – CNRS UMR 7284, Nice, France (M.I., P.H.). Correspondence: Paul Hofman, M.D., Ph.D., Laboratory of Clinical and Experimental Pathology, Louis Pasteur Hospital, 30 Avenue De La Voie Romaine, 06002 Nice Cedex 01, France (hofman.p@chu-nice.fr).

TJOP 2013;00:1–11

Copyright © 2013 Optimal Clinical (Doctors.MD).

The advent of personalized molecular therapeutics in routine clinical practice for nonsmall cell lung cancer (NSCLC) has revolutionized the field of thoracic oncology. Strong evidence now shows that molecular pathology has become the driving force for optimal management in personalized oncology. The development of this field has greatly stimulated the integration into pathology departments of routine molecular testing for a wide panel of oncogenic targets. Although DNA-based assays are the standard methods for detection of molecular alterations in NSCLC, they are probably not ready for immediate integration into all pathology laboratories. However, immunohistochemistry (IHC) is a well-established and cost-effective method, which is used broadly for routine lung biopsy tissue diagnosis in the daily clinical practice. The extended diagnostic requirement from increasingly limited material provided by minimally invasive biopsy techniques and the cost-effectiveness of the DNA-based assays are major challenges for pathology departments. There is a need for efficient diagnostic screening algorithm method of molecular alterations using the IHC method. The IHC may provide an efficient screening tool for "druggable" genomic alterations by taking advantage of a growing list of available mutation-specific antibodies. This article reviews the use of immunohistochemical assays for the detection of driving molecular alterations in NSCLC, including epidermal growth factor receptor (EGFR), anaplastic lymphoma kinase (ALK), BRAF, ROS1, and MET, as an alternative or supplemental tool to molecular biology techniques.

Keywords: immunohistochemistry; mutation-specific antibody; molecular testing; NSCLC; targeted therapy; molecular pathology; *EGFR*; *BRAF*; *ALK*; *ROS1*; *MET*

The major advances made, in the last few years, in the understanding of the pathophysiology of lung carcinoma have shifted the traditional way of treatment toward personalized targeted therapy.¹ Based on these advances, small molecules that inhibit tumor growth through targeting specific genomic alterations have been rapidly developed.² The most consistent targeted therapeutic advances in nonsmall cell lung cancer (NSCLC) have been made in lung adenocarcinoma (ADC). The current treatment of lung ADC patients is now orientated toward the administration of several effective molecular-targeted therapies, because there is an urgent need to improve the poor outcome of this

cancer.¹ The overall survival of a subset of patients with advanced-stage IIIB/IV lung ADC can be improved by treatment specifically targeting activating mutations of the epidermal growth factor receptor (*EGFR*) gene and rearrangements of the anaplastic lymphoma kinase (*ALK*) gene. Additional therapies targeting somatic mutations on other oncogenes, such as the *BRAF*, *ROS1*, or *MET* genes, are currently under development or being studied in clinical trials.^{3,4} Moreover, pulmonary ADCs that are initially responsive to *EGFR*-tyrosine kinase inhibitors (TKIs) or *ALK* inhibition eventually develop acquired resistance due to one or more of several possible mechanisms. Therefore, there is a need of predictive biomarker tests for lung cancers that develop resistance to current first-generation *EGFR* or *ALK* inhibition therapies.³

The vast majority of lung cancers are diagnosed in an advanced stage of disease that cannot potentially undergo surgical resection. In this regard, about 70% of lung cancers are diagnosed on small-sized biopsies and/or cytological specimens, and additional tissue samples may not be obtained.³ Therefore, the introduction of targeted molecular therapies has added a strong value and introduced a new role for pathologists in the care of lung cancer patients, as therapeutic decisions are now mostly based on the molecular analysis of lung cancer tissue specimens.^{5,6} Moreover, according to the latest World Health Organization classification of lung ADC, the morpho-molecular characterization of lung ADC is now critical for the optimal selection by oncologists of several of these new therapies.^{3,7}

The current hot molecular targets such as *EGFR*, *ALK*, *ROS1*, or *BRAF* alterations are rather rare molecular events in Caucasian lung ADC patients. We, and others, question the optimal management of patients having a probability of less than 5–10% of carrying somatic mutations on these targets.^{8,9} A large number of methods can be performed on formalin-fixed paraffin-embedded biopsies that allow morphological and immunohistochemical characterization, as well as gene-based assays. However, it is questionable as to whether the majority of lung cancer patients will be assessed for these genomic alterations due to financial and logistic restrictions. Similar restrictions also overshadow the accessibility of cancer patients to exome/genome sequencing followed by targeted therapy for most drugs still to be developed.⁸ Thus, the management of small

specimens must be optimized and a decision algorithm, taking into consideration the current ancillary methods, must be strictly defined to efficiently select targeted therapies. Although the DNA-based assay is the standard method of determining the altered genomic status in lung ADC, it is quite expensive and not available in all pathology laboratories. The extended diagnostic requirement from increasingly limited material provided by minimally invasive biopsy techniques and the cost-effectiveness of the DNA-based assays are major challenges for pathology departments. There is a need for efficient diagnostic screening algorithm method of "druggable" molecular alterations using the immunohistochemistry (IHC) method.

IHC may provide a rapid and cost-effective molecular test in most routine diagnostic pathology laboratories. IHC has the advantage of being widely available in clinical pathology laboratories. It is relatively easy to perform and retains informative morphological data. Currently, there is ongoing debate in the oncology community regarding the adequacy of samples obtained for molecular analysis from NSCLC patients. Although initial data suggested that cytological samples were not adequate for molecular analysis, recent findings suggest that minimally invasive techniques might suffice.¹⁰ Potentially, IHC may be more adapted to small tissue samples, fine needle aspiration cytology, and cell blocks from body fluids.^{11,12} Overall, there is a need to integrate and develop screening algorithms by using IHC and DNA-based assays.

This review addresses the recent advances in the development of mutation-specific antibodies, the description, and performances of different testing methodologies with their advantages and disadvantages, provides a suggested screening algorithm using IHC and DNA-based assays for somatic mutational status in personalized lung cancer therapy, and puts forward a proposal for an external quality assessment program in IHC, with an emphasis on the *EGFR*, *ALK*, and *BRAF* genes.

DETECTION OF *EGFR* MUTATIONS BY IHC

The discovery of the strong association between activating mutations in the tyrosine kinase domain of the *EGFR* gene and the clinical response with TKIs has revolutionized the field of thoracic oncology. Although there are several activating mutations in the *EGFR* gene, the two

most common mutations accounting for approximately 85–90% of *EGFR* mutations are the L858R point mutation in exon 21 and the short 15-bp (E746_750A) in-frame deletion in exon 19. These mutations are the most predictive of *EGFR*-TKI efficacy in advanced lung NSCLC.^{13–15}

Yu et al. generated 2 monoclonal antibodies (mAbs) against the E746_A750del (6B6 clone) and L858R point mutations (43B2 clone; Cell Signaling Technology) in the *EGFR* gene, which were evaluated by Western blotting, immunofluorescence, and IHC.¹⁶ The authors tested these antibodies in a series of different cell lines and in tumor tissues from 340 patients with primary NSCLC, comparing the IHC results with DNA sequencing. They reported a sensitivity of 92% and a specificity of 99% for the IHC assay.¹⁶

Several studies examined further the presence of *EGFR* mutations in NSCLC by IHC using these 2 mAbs. The range of the overall sensitivity and specificity varied from 23% to 100% and from 85% to 99%, respectively, across studies using the same antibodies^{17–24} (Fig. 1).

A first-pass screening of NSCLC patients with these antibodies would rapidly identify 90% of patients responsive to *EGFR*-TKIs.¹⁶ However, these antibodies cannot recognize the other less common *EGFR* mutations, which account for 10% of mutations. When keeping in mind the fact that these less common mutations are also able to activate the *EGFR*-signaling pathway, the methodology using the currently available

mutation-specific antibodies against *EGFR* has its limits. The detection of the remaining mutations will require the development of additional mutation-specific antibodies or DNA-based assays.^{21,23} Moreover, no antibodies have been generated to date against mutations associated with resistance to *EGFR*-TKI. Considering that a negative result for IHC does not necessarily indicate the absence of an *EGFR* mutation, all negative cases should be tested by molecular analysis to confirm the mutational status. Including basic clinical and histological parameters in a screening algorithm may improve the prediction of response to *EGFR*-TKI therapy, which may be of value if *EGFR* mutation status is not available.²⁵ Moreover, an algorithm integrating a screening step by IHC was recently proposed for this purpose.¹⁷

Although the IHC approach can support the routine assessment of specific *EGFR* mutations, different scoring schemes of the immunostaining have been adopted. Most of the studies have used an intensity scoring method based on membranous and cytoplasmic intensity staining of more than 2+, avoiding the false-positive results.^{17,26,27} In contrast, the University of Colorado's IHC H-score criteria and Kozu et al. adopted a different scoring system.^{19,28} However, no statistical methodology has been used to validate the optimal scoring method of IHC intensity. A recent study has suggested that the ratio between the histological score, based on

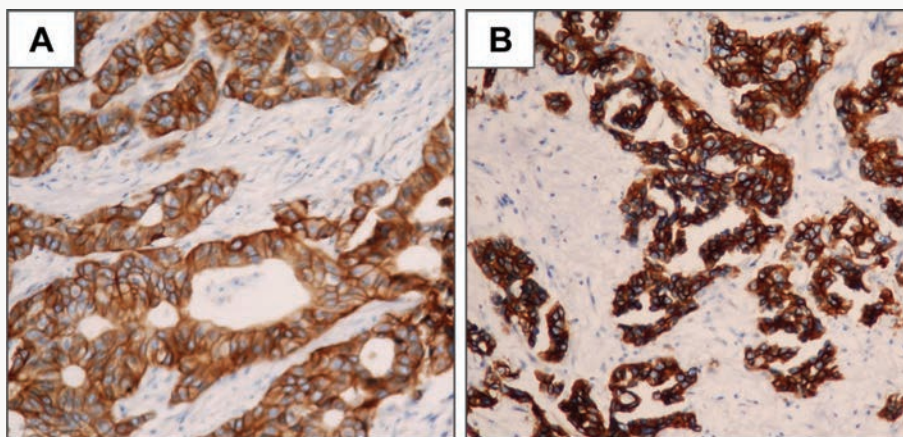


Figure 1. Representative Immunostaining with *EGFR*-Mutation-Specific Antibodies in Lung ADC.

The 6B6 clone against the E746_A750del (A) and the 43B2 clone against the L858R point mutation (B) directly visualized the location of lung ADC cells with the *EGFR* mutation (immunoperoxidase, original magnification $\times 200$).

the estimation of the percentage of positive cells and the intensity of the staining of the mutant, EGFR protein and EGFR expression may improve the sensitivity of the test.²⁶ However, this score system is not readily applied to cytological material and small biopsies. The relatively low sensitivity of these antibodies due to the high cutoff of 2+ for positive cases should not represent an obstacle to implementation in the clinical practice, since cases interpreted as negative by IHC should still be analyzed by molecular testing according to the previously recommended algorithm.²² Therefore, it is necessary to use a stringent cutoff for the interpretation of a positive IHC test, as patients with a false-positive result can show adverse effects if given TKI instead of chemotherapy.²⁵

Immunostaining to detect specific mutant EGFR shows a good correlation with mutation analysis and can be used as a screening method to identify patients for TKI therapy. IHC methodology is potentially useful when molecular analysis is not available and for use in small biopsies when material is too scant for molecular tests. Importantly, mutation-specific antibodies are useful in determining EGFR status in tissues obtained from bone biopsy as decalcification processes used in molecular-based studies often result in DNA degradation hindering mutation detection.²²

However, considering the overall performance of IHC assays across studies in terms of sensitivity and specificity, it cannot be ruled out that some samples may not be optimally fixed, thus preventing detection of fragile epitopes. Suboptimal fixation of tumor samples could be a major problem in particular for multicentric independent validation in the context of personalized medicine.

Furthermore, immunocytochemistry (ICC) with these antibodies is of great interest for cytological specimens. Because minimally invasive diagnostic procedures are most often used in a diagnostic setup for lung cancer, and because only 30% of patients with NSCLC present as surgical candidates, small-sized tissue and cytological samples are the main sources of tissue for molecular testing to date. Moreover, studies using DNA-based sequencing on cytological samples have shown a rather good correlation with results from surgically obtained tissue.¹² However, a small but significant proportion of cytological specimens has given inconclusive results or failure of EGFR molecular analysis. Preservation and

quality of the extracted DNA seem to matter more than the actual number of tumor cells present in the samples. However, major issues still reside in the amount of material, the interference from background nonneoplastic cells, and standardization of parameters for cytological samples.^{12,27,29} This may lead to "rebiopsy" in order to obtain more biological material for the molecular analysis. In this context, small tissue specimens have to be well managed not only for morphological diagnosis but also to maximize the amount of tissue available for molecular studies. Moreover, the effective number of tumor cells present in the samples may alter the recovery rate and may constitute a problem in obtaining sufficient material for molecular analysis.¹² Therefore, in these situations, immunohistochemical or immunocytochemical staining with the mutation-specific antibodies against EGFR may be of great clinical utility.

Although, recommendations for strategic use of the minimal tissue sample necessary for diagnosis have been recently made, there will still be cases with scant material. There is a need for every institution to develop a multidisciplinary strategy to obtain these small specimens and process them not only for diagnosis but also for molecular testing.³⁰

DETECTION OF THE ALK REARRANGEMENT BY IHC

Recently, the echinoderm microtubule-associated protein-like 4 (EML4)-ALK fusion gene was identified in NSCLC.³¹ The ALK rearrangement is a rare molecular event that is detected in approximately 5% of unselected patients with NSCLC, a frequency that increases to 22% in a subset of patients including males, young patients, never or light smokers, patients with an advanced stage at presentation, and an ADC histology with solid architecture and signet ring cell features. Among never/light smokers without EGFR mutation, the frequency of EML4-ALK may be as high as 33%.³² ALK rearrangements are generally mutually exclusive events with EGFR and KRAS gene mutations.³³

The dual ALK and MET inhibitor Xalkori (crizotinib) demonstrated strong efficacy in treating patients with ALK-positive lung ADC.³⁴ Moreover, the ALK fusion gene seems to be associated with EGFR-TKI resistance in patients with metastatic disease.³²

Several methods may be used for the detection of *ALK* in ADC samples including the reverse transcriptase polymerase chain reaction (RT-PCR), fluorescent in situ hybridization (FISH), and IHC for the *ALK* protein. Because each method inevitably has both advantages and disadvantages, we should be aware of their characteristics before applying them to clinical samples.³⁵ Analysis by RT-PCR requires good quality RNA and multiple primers because of the multiple break points and the large number of partner genes of *ALK*.^{27,36} Currently, FISH is the gold standard procedure for the detection of an *ALK* rearrangement allowing the retention of tumor morphology. However, this method is expensive and time consuming, has a limited availability, can be a more labor-intensive technique than IHC, and requires well-trained pathologists for the interpretation. Therefore, the development of a robust screening method for detecting of cases of *ALK* fusion is essential for successful treatment using the *ALK* inhibitor. *ALK* IHC may represent a cost-effective and efficient means of screening for an *ALK* rearrangement in ADC. This assay holds the advantages of using archival tissue and the ability to detect any partner gene. Although IHC does not detect the *ALK* fusion gene itself, *ALK* is not detectable in any normal tissues other than the brain.³⁵ Therefore, an *ALK*-positive reaction is associated with dysregulated expression of the gene, due to

the altered promoter activity that is highly characteristic of an *ALK* inversion.³⁵

Several *ALK* antibodies are currently available, including the *ALK*1 clone (Dako, Glostrup, Denmark), the 5A4 clone (Novocastra, Leica Biosystems, Abcam, CliniSciences), and the D5F3 clone (Ventana, Roche Group). Immunohistochemical analysis using the monoclonal antibody *ALK*1 has been successfully used to detect the *ALK* fusion protein in anaplastic large cell lymphoma (ALCL) and inflammatory myofibroblastic tumors. The early studies with IHC using the *ALK*1 antibody reported difficulty in detection with background interference. The *ALK* mRNA transcriptional activity seems to be lower in lung cancer compared to that in ALCL; therefore, the false-negative results appear to be caused by lower sensitivity.³⁵ The two clones 5A4 and D5F3 were reported to be high-affinity antibodies with sensitivity rates ranging from 92% to 100% and specificity from 75% to 100%^{23, 37-44} (Table 1).

Moreover, when highly sensitive detection systems were used, either clone correctly identified *ALK*-rearranged lung ADCs with high reproducibility, although D5F3 may demonstrate pseudomembranous staining in some *ALK*-negative tumors (Fig. 2).³⁵

Interestingly, our group recently demonstrated the feasibility of detection of an *ALK*-gene rearrangement by ICC and FISH on circulating tumor cells (CTCs), thus, paving the way for a

Table 1. Sensitivity and Specificity of the *ALK*-Rearrangement Antibodies Across Studies.

Study	Number of Patients	<i>ALK</i> Clone	Sensitivity (%)	Specificity (%)
Conklin et al. ³⁷	337 NSCLC	5A4 (Novocastra)	100	87.5
		D5F3 (Cell Signaling Technology)	100	75
		5A4 (Leica) <i>ALK</i> 1	100	62.5
		<i>ALK</i> 1 (Dako; FLEX)	66	100
		<i>ALK</i> 1 (Dako; ADVANCE)	66	87.5
Hofman et al. ²³	154 lung ADC	5A4 (Abcam)	100	89
McLeer-Florin et al. ³⁸	441 lung ADC	5A4 (Abcam)	95	100
Park et al. ⁴³	1166 NSCLC	5A4 (Novocastra)	100	98.7
Paik et al. ⁴⁰	465 NSCLC	5A4 (Novocastra)	100	95.8
Yi et al. ⁴⁰	101 lung ADC	<i>ALK</i> 1 (Dako; ADVANCE)	90	97.8
		<i>ALK</i> 1 (Dako)	67	97
Mino-Kenudson et al. ³⁹	174 lung ADC	D5F3 (Cell Signaling Technology)	100	99
		5A4 (Abcam)	100	100

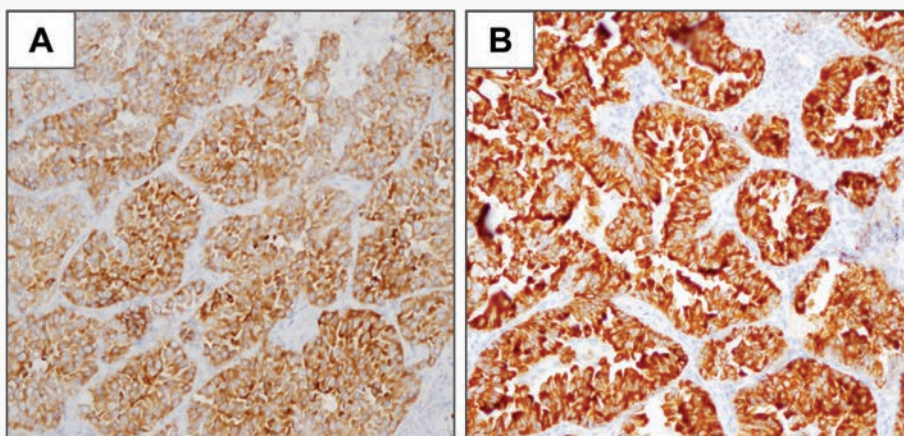


Figure 2. Representative Immunostaining with ALK Antibodies.

Diffuse cytoplasmic staining with the 5A4 clone (Abcam) (A) and the D5F3 clone (Cell Signaling Technology) (B) in ALK-rearranged lung ADC (immunoperoxidase, original magnification $\times 200$).

CTC-based predictive approach for noninvasive ALK status prescreening of lung cancer patients (Fig. 3).⁴⁵

Because IHC does not directly demonstrate an ALK fusion, certain pitfalls have been described previously.³⁵ Certain small cell lung cancers and hepatocellular carcinomas may show positive reactions, without an ALK translocation.³⁵ This positive reaction did not appear to be associated with gene amplification, and the reason for the positive reaction was unknown. Another caveat is a certain rate of false-negative results in ADC with signet ring cell features, even when using a high-affinity antibody with a highly sensitive detection method. A large amount of cytoplasmic mucin can often push the cytoplasm into the rim, and the thinned cytoplasm demonstrates a weak positive reaction in certain cases.³⁵ However, pure signet ring cell carcinoma is extremely uncommon in lung cancer, and the other tumor components can show positive reactions, or a FISH analysis can be used instead.³⁵

Overall, IHC seems to be a reliable screening tool for the identification of an ALK rearrangement in lung ADC. Moreover, several studies have demonstrated that adenosquamous lesions may also harbor EGFR mutations and ALK rearrangements.^{33,46} Although large cohort studies have not demonstrated EGFR mutations or ALK rearrangements in a significant proportion of squamous cell carcinoma, isolated reports have described these alterations in squamous cell carcinoma.⁴⁷

As for mutant EGFR IHC, Lung Cancer Societies have reported guidelines for ALK testing.³⁵ The standard procedure may involve screening with IHC and confirmation with FISH. IHC should be performed concurrent with EGFR mutation testing in ADCs, large cell carcinomas, poorly differentiated carcinoma and NSCLC not otherwise specified (NOS). Lesions diagnosed on a small sample with histological subtypes other than ADC may be considered for testing, because

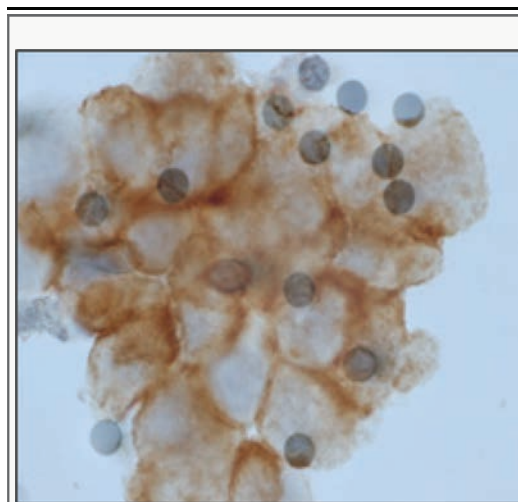


Figure 3. Cluster of Circulating Tumor Cells Showing an Intense Cytoplasmic and Pseudomembranous ALK Immunostaining Using 5A4mAb (Abcam, Immunoperoxidase, Original Magnification $\times 1000$; Bar: 16 μm).

Source: adapted from Ilie et al.⁴⁵

limited sampling does not effectively exclude an adenocarcinomatous component. FISH analysis should then be used to confirm positive cases (1+ to 3+) as well as negative cases in a subset of patients on clinical (age lower than 40years, patients with no or a minimal history of smoking), or histological considerations (mucinous cribriform pattern, signet ring cells, and Thyroid Transcription Factor-1 (TTF)-1 positivity in mucinous ADCs). Although histologic findings may help to identify cases for *ALK* testing, none of the histologic parameters are completely sensitive or specific to *ALK* rearrangement, and morphology should not replace confirmatory molecular or immunohistochemical studies.⁴⁷ Because each method has advantages and disadvantages, the use of more than one method to detect *ALK* fusion is recommended. More data on a large independent series and parallel testing with different antibodies are needed for successful validation of IHC as a screening method.⁴⁸

DETECTION OF THE *BRAF* MUTATION BY IHC

With the advent of specific inhibitors active against *BRAF*-mutated cancers, the detection of the single point mutation at codon 600 of the *BRAF* gene (*V600E*) has become of great clinical relevance. The prevalence of the *BRAF* mutation in lung ADC is approximately 3%.⁴ In contrast to melanoma where the *BRAFV600E* mutation is

the most prevalent somatic alteration, the *BRAFV600E* mutation represents approximately 50% of the *BRAF* mutations detected in lung ADCs.⁴⁹ Notably, 39% of *BRAF* mutations involve the G469A point mutation, which may reflect a tobacco-related carcinogenic effect.⁴⁹ This lower incidence of *V600E* mutations is important, as current second-generation RAF inhibitors, in light of the near ubiquity of the *V600E* mutation in melanoma, have been tailored to have specific activity against the *V600E* mutant kinase. *BRAF* mutations are nonoverlapping with other oncogenic mutations found in NSCLC (eg, *EGFR* or *KRAS* mutations, *ALK* rearrangements).⁴ So far, the *BRAF* mutation status is assessed using DNA-based methods, which are expensive and labor-intensive, and thus suboptimal for routine diagnostic applications.⁵⁰ Recently, a monoclonal antibody specifically recognizing the *V600E* mutation (clone VE1; Spring Bioscience, Roche Group) was generated.⁵¹ Thus, the *BRAFV600E* mutation has been successfully detected by IHC using the novel mutation-specific antibody VE1 on different types of cancer.⁵⁰⁻⁵⁴ Several studies have shown that this antibody is highly sensitive and specific (Table 2).

A recent study demonstrated that VE1 IHC was able to detect *BRAFV600E*-positive tumor cells in 66.6% cases with inconclusive gene-sequencing results including several cases with minute small cell aggregates embedded in healthy tissue evading recognition by sequencing

Table 2. Sensitivity and Specificity of the *BRAFV600E* Mutation-Specific Antibody VE1 Across Different Studies.

Study	Type of Cancer	Number of Patients	VE1 Sensitivity (%)	VE1 Specificity (%)
Long et al. ⁵⁵	Melanoma	100	97	98
Colomba et al. ⁵⁶	Melanoma	111	100	100
Feller et al. ⁵⁷	Melanoma	35	100	100
Capper et al. ⁵¹	Melanoma, papillary thyroid cancer	47 (melanoma) 21 (papillary thyroid cancer)		
		100		
Capper et al. ⁵⁰	Brain metastasis (melanoma, ovarian, colorectal, lung, thyroid, choriocarcinoma)	1120	97	97
Bosmuller et al. ⁵⁸	Serous ovarian carcinoma	141	100	100
Ilie et al. ⁵⁹	Lung ADC	450	90.5	100
Andrulis et al. ⁵³	Hairy cell leukemia	52	100	91
Sahm et al. ⁵⁴	Langerhans cell histiocytosis	89	95	97

due to insufficient copy number of mutant alleles.^{8,50} Moreover, the antibody seems to be able to identify single cells with the V600E mutation. Recently, an ICC assay using the VE1 antibody was used for the detection of the BRAFV600E mutation in circulating melanoma cells (CMCs) isolated from metastatic melanoma patients and demonstrated a high concordance between the tissue samples and the corresponding CMCs. Interestingly, a subset of patients showed CMCs positively stained with the VE1 antibody, whereas the corresponding tumor tissue was BRAFV600E-negative.⁶⁰ This finding opens a range of novel opportunities and questions about the origin and evolution of tumors. VE1 immunostaining is relatively easy to interpret with positivity being considered when a distinct, strong, and homogenous signal is observed in the cytoplasm of all carcinoma cells (Fig. 4).⁵⁰

A false-positive interpretation may be given by untrained pathologists, possibly due to a faint to moderate cytoplasmic staining with any type of isolated nuclear staining in tumor cells with a scant cytoplasm. Nuclear staining, as well as staining of monocytes/macrophages, and a weak staining of single interspersed cells have been described as the most frequent artifacts. The analysis should be done with caution in the presence of nuclear staining even if moderate cytoplasmic staining is present.^{50,59} Capper et al. observed a strong reduction in the staining intensity in postcryofixed tissue compared with directly formalin-fixed tissue that might have led

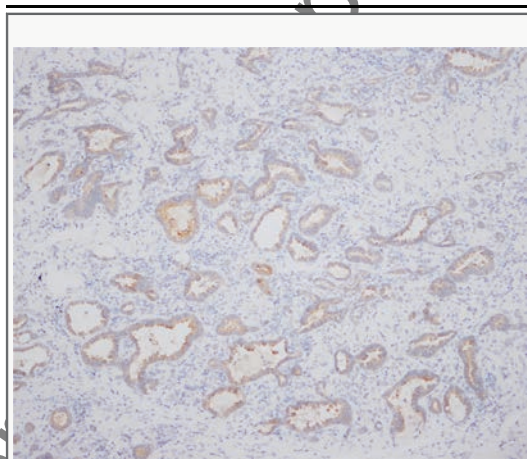


Figure 4. Representative Immunostaining with the VE1 Clone of a BRAFV600E-Mutated ADC (Immunoperoxidase, Original Magnification $\times 100$).

to a negative interpretation of the IHC with VE1.⁵¹

The use of a specific and sensitive antibody should provide a rapid and cost-effective method for the detection of the BRAFV600E mutation. However, the VE1 antibody does not detect BRAF non-V600E mutations, which are relatively frequent in lung ADC.⁵⁹ Currently, a strategy involving IHC-based screening for the BRAFV600E mutation supplemented by molecular biology analysis of negative, doubtful, or interpretable cases can be recommended.⁸

PERSPECTIVES AND CONCLUSIONS

New molecular targets such as MET expression or ROS1 protein tyrosine kinase fusions are continuously emerging in NSCLC. A recent report described early evidence of clinical response to crizotinib in ROS1-rearranged NSCLCs.⁶¹ Rimkunas et al. recently developed a ROS1 rabbit mAb (clone D4D6) and evaluated it by Western blotting and IHC.⁶² They first validated ROS1 D4D6 on cell lines and xenograft models and then screened 556 primary NSCLC tumors, comparing the IHC results with those of FISH and RT-PCR. They reported a sensitivity of 100% and a specificity of 98% for the IHC D4D6 assay.⁶² This is the first study describing a ROS1 IHC assay, and further validation needs to be performed. However, the utility of such a method is underlined by the expansion of the clinical utility of crizotinib in patients with NSCLC who express ROS1 fusions.

Finally, MET expression occurs in about 25–75% of NSCLC and has been associated with poor prognosis.⁶³ Whereas amplification of the gene coding for MET is rare in baseline tumor samples from EGFR-TKI naive patients, preclinical data suggest that MET-gene amplification may be responsible for approximately 20% of acquired resistance to EGFR-TKI of patients with EGFR-mutant tumors.⁶⁴ In addition to blocking ALK and ROS1, crizotinib is also a potent MET inhibitor, which demonstrates strong responses in MET-amplified NSCLC patients.⁶⁵ Moreover, several MET inhibitors are currently being tested in phase II/III trials. Increased MET expression may be detected by IHC, gene expression analysis, or FISH.⁶⁶ Although, several antibodies directed against the total MET protein (phosphorylated and nonphosphorylated), a particular effort is ongoing with the aim of discovering the

optimal companion diagnostic associated with MET treatment efficacy and patient selection.⁶⁷

In conclusion, detection of predictive molecular biomarkers is the most reliable basis for selecting NSCLC patients who are likely to respond to selective inhibitors. With a growing list of emerging mutant or amplified oncogenes in NSCLC, we will have to move toward stepwise strategies for molecular testing. Despite a plethora of molecular biology methods, these tests may not be widely available due to high costs, technical complexity, and the requirement of highly trained personnel. Although the DNA-based assays (eg, sequencing, FISH) are the gold standard methods in determining an altered genomic status in lung ADC, they are relatively expensive for routine use in clinical laboratories and are not available in all pathology laboratories. In addition, they depend greatly on the quality of the tumor samples. Moreover, the evolution of sequencing technologies with the development of the next-generation sequencing (NGS) approach complicates the scene. NGS holds a number of potential advantages over the traditional molecular methods, including the ability to fully sequence large numbers of genes in a single test.⁶⁸ However, significant challenges, particularly with respect to extensive computational expertise, infrastructure, and massive costs, or high turnaround time, will have to be overcome to bring NGS into a clinical context.⁶⁸

However, IHC may provide a rapid and cost-effective molecular test in most routine diagnostic pathology laboratories. IHC has the advantage of being a standardized assay, which is widely available in clinical pathology laboratories, and relatively easy to perform. Of most importance, it retains informative morphological data and demonstrates high sensitivity and specificity. Moreover, it can also be applied to small tissue

samples, fine needle aspiration cytology, and cell blocks from body fluids.^{11,12} However, there is a need for mutation-specific antibodies to be extensively evaluated by Western blotting, immunofluorescence, and IHC to determine their sensitivity and specificity in NSCLC patient tumor samples. However, as for the molecular biology methods, implementation in the routine clinical context requires that high-quality molecular IHC be performed by meeting good laboratory practices or accreditation guidelines set by regulatory and professional organizations in certain countries.^{9,69,70}

An immunohistochemical approach for the detection of mutant proteins should be considered as an alternative or complement to molecular techniques, in particular for small formalin-fixed biopsies and cytological samples. This assay has the potential to be widely available in most pathology laboratories. In addition, it has the advantage of a rapid turnaround time in comparison with the more time-consuming molecular tests.

More importantly, the use of mutation-specific antibodies has the benefit of detecting the mutant protein at the single-cell level with very high sensitivity for diagnosis. Thus, IHC using antibodies targeting different molecular genetic alterations may be useful in molecular diagnosis. Finally, IHC with mutation-specific antibodies may be used as a substitute for genetic testing in cases where the diagnostic material is unsatisfactory for molecular use such as in scant cellular preparations and/or when there is no tumor DNA available.

CONFLICT OF INTEREST

Authors declare that they have no conflict of interest.

REFERENCES

- Cheng L, Alexander RE, MacLennan GT, et al. Molecular pathology of lung cancer: key to personalized medicine. *Mod Pathol*. 2012;25(3):347–369.
- Yousem SA. Role of molecular studies in the diagnosis of lung adenocarcinoma. *Mod Pathol*. 2012;25(suppl 1):S11–S17.
- Cagle PT, Allen JC. Lung cancer genotype-based therapy and predictive biomarkers: present and future. *Arch Pathol Lab Med*. 2012;136(12):1482–1491.
- Pao W, Girard N. New driver mutations in non-small-cell lung cancer. *Lancet Oncol*. 2011;12(2):175–180.
- Janku F, Garrido-Laguna I, Petruzella LB, Stewart DJ, Kurzrock R. Novel therapeutic targets in non-small cell lung cancer. *J Thorac Oncol*. 2011;6(9):1601–1612.
- Heinmoller E, Renke B, Beyser K, Dietmaier W, Langner C, Ruschoff J. Pitfalls in diagnostic molecular pathology – significance of sampling error. *Virchows Arch*. 2001;439(4):504–511.
- Travis WD, Brambilla E, Noguchi M, et al. International Association for the Study of Lung Cancer/American Thoracic Society/European Respiratory Society: international multidisciplinary classification of lung adenocarcinoma: executive summary. *Proc Am Thorac Soc*. 2011;8(5):381–385.
- von Deimling A, Sahn F, Capper D. Mutation specific antibodies: tool or dinosaur? *Oncotarget*. 2012;3(9):907–908.
- Ilie M, Hofman P. Pitfalls in lung cancer molecular pathology: how to limit them in routine practice? *Curr Med Chem*. 2012;19(16):2638–2651.
- Lozano MD, Zulueta JJ, Echeveste JJ, et al. Assessment of epidermal growth factor receptor and K-ras mutation status

- in cytological stained smears of non-small cell lung cancer patients: correlation with clinical outcomes. *Oncologist*. 2011;16(6):877–885.
11. Kerr KM. Personalized medicine for lung cancer: new challenges for pathology. *Histopathology*. 2011;60(4):531–546.
 12. da Cunha Santos G, Saieg MA, Geddie W, Leigh N. EGFR gene status in cytological samples of non-small cell lung carcinoma: controversies and opportunities. *Cancer Cytopathol*. 2011;119(2):80–91.
 13. Sharma SV, Bell DW, Settleman J, Haber DA. Epidermal growth factor receptor mutations in lung cancer. *Nat Rev Cancer*. 2007;7(3):169–181.
 14. Yang CH, Yu CJ, Shih JY, et al. Specific EGFR mutations predict treatment outcome of stage IIIB/IV patients with chemotherapy-naïve non-small-cell lung cancer receiving first-line gefitinib monotherapy. *J Clin Oncol*. 2008;26(16):2745–2753.
 15. Zhu CQ, da Cunha Santos G, Ding K, et al. Role of KRAS and EGFR as biomarkers of response to erlotinib in National Cancer Institute of Canada Clinical Trials Group Study BR.21. *J Clin Oncol*. 2008;26(26):4268–4275.
 16. Yu J, Kane S, Wu J, et al. Mutation-specific antibodies for the detection of EGFR mutations in non-small-cell lung cancer. *Clin Cancer Res*. 2009;15(9):3023–3028.
 17. Brevet M, Arcila M, Ladanyi M. Assessment of EGFR mutation status in lung adenocarcinoma by immunohistochemistry using antibodies specific to the two major forms of mutant EGFR. *J Mol Diagn*. 2010;12(2):169–176.
 18. Kitamura A, Hosoda W, Sasaki E, Mitsudomi T, Yatabe Y. Immunohistochemical detection of EGFR mutation using mutation-specific antibodies in lung cancer. *Clin Cancer Res*. 2010;16(13):3349–3355.
 19. Kato Y, Peled N, Wynes MW, et al. Novel epidermal growth factor receptor mutation-specific antibodies for non-small cell lung cancer: immunohistochemistry as a possible screening method for epidermal growth factor receptor mutations. *J Thorac Oncol*. 2010;5(10):1551–1558.
 20. Nakamura H, Mochizuki A, Shinmyo T, et al. Immunohistochemical detection of mutated epidermal growth factor receptors in pulmonary adenocarcinoma. *Anticancer Res*. 2010;30(12):5233–5237.
 21. Simonetti S, Molina MA, Queralt C, et al. Detection of EGFR mutations with mutation-specific antibodies in stage IV non-small-cell lung cancer. *J Transl Med*. 2010;8:135.
 22. Hasanovic A, Ang D, Moreira AL, Zakowski MF. Use of mutation specific antibodies to detect EGFR status in small biopsy and cytology specimens of lung adenocarcinoma. *Lung Cancer*. 2012;77(2):299–305.
 23. Hofman P, Ilie M, Hofman V, et al. Immunohistochemistry to identify EGFR mutations or ALK rearrangements in patients with lung adenocarcinoma. *Ann Oncol*. 2012;23(7):1738–1743.
 24. Ilie MI, Hofman V, Bonnetaud C, et al. Usefulness of tissue microarrays for assessment of protein expression, gene copy number and mutational status of EGFR in lung adenocarcinoma. *Virchows Arch*. 2010;457(4):483–495.
 25. Mok TS, Wu YL, Thongprasert S, et al. Gefitinib or carboplatin-paclitaxel in pulmonary adenocarcinoma. *N Engl J Med*. 2009;361(10):947–957.
 26. Wu SG, Chang YL, Lin JW, et al. Including total EGFR staining in scoring improves EGFR mutations detection by mutation-specific antibodies and EGFR TKIs response prediction. *PLoS One*. 2011;6(8):e23303.
 27. Moreira AL, Hasanovic A. Molecular characterization by immunocytochemistry of lung adenocarcinoma on cytology specimens. *Acta Cytol*. 2012;56(6):603–610.
 28. Kozu Y, Tsuta K, Kohno T, et al. The usefulness of mutation-specific antibodies in detecting epidermal growth factor receptor mutations and in predicting response to tyrosine kinase inhibitor therapy in lung adenocarcinoma. *Lung Cancer*. 2011;73(1):45–50.
 29. Smouse JH, Cibas ES, Janne PA, Joshi VA, Zou KH, Lindeman NI. EGFR mutations are detected comparably in cytologic and surgical pathology specimens of non-small cell lung cancer. *Cancer*. 2009;117(1):67–72.
 30. Travis WD, Rekhtman N. Pathological diagnosis and classification of lung cancer in small biopsies and cytology: strategic management of tissue for molecular testing. *Semin Respir Crit Care Med*. 2011;32(1):22–31.
 31. Soda M, Choi YL, Enomoto M, et al. Identification of the transforming EML4-ALK fusion gene in non-small-cell lung cancer. *Nature*. 2007;448(7153):561–566.
 32. Shaw AT, Yeap BY, Mino-Kenudson M, et al. Clinical features and outcome of patients with non-small-cell lung cancer who harbor EML4-ALK. *J Clin Oncol*. 2009;27(26):4247–4253.
 33. Wong DW, Leung EL, So KK, et al. The EML4-ALK fusion gene is involved in various histologic types of lung cancers from nonsmokers with wild-type EGFR and KRAS. *Cancer*. 2009;115(8):1723–1733.
 34. Toyooka S, Mitsudomi T, Soh J, et al. Molecular oncology of lung cancer. *Gen Thorac Cardiovasc Surg*. 2011;59(8):527–537.
 35. Murakami Y, Mitsudomi T, Yatabe Y. A screening method for the ALK fusion gene in NSCLC. *Front Oncol*. 2012;2:24.
 36. Choi YL, Soda M, Yamashita Y, et al. EML4-ALK mutations in lung cancer that confer resistance to ALK inhibitors. *N Engl J Med*. 2010;363(18):1734–1739.
 37. Conklin CM, Craddock KJ, Have C, Laskin J, Couture C, Ionescu DN. Immunohistochemistry is a reliable screening tool for identification of ALK rearrangement in non-small-cell lung carcinoma and is antibody dependent. *J Thorac Oncol*. 2013;8(1):45–51.
 38. McLeer-Florin A, Moro-Sibilot D, Melis A, et al. Dual IHC and FISH testing for ALK gene rearrangement in lung adenocarcinomas in a routine practice: a French study. *J Thorac Oncol*. 2012;7(2):348–354.
 39. Mino-Kenudson M, Chirieac LR, Law K, et al. A novel, highly sensitive antibody allows for the routine detection of ALK-rearranged lung adenocarcinomas by standard immunohistochemistry. *Clin Cancer Res*. 2010;16(5):1561–1571.
 40. Paik JH, Choe G, Kim H, et al. Screening of anaplastic lymphoma kinase rearrangement by immunohistochemistry in non-small cell lung cancer: correlation with fluorescence in situ hybridization. *J Thorac Oncol*. 2011;6(3):466–472.
 41. Takeuchi K, Choi YL, Togashi Y, et al. KIF5B-ALK, a novel fusion oncogene identified by an immunohistochemistry-based diagnostic system for ALK-positive lung cancer. *Clin Cancer Res*. 2009;15(9):3143–3149.
 42. Yi ES, Boland JM, Maleszewski JJ, et al. Correlation of IHC and FISH for ALK gene rearrangement in non-small cell lung carcinoma: IHC score algorithm for FISH. *J Thorac Oncol*. 2011;6(3):459–465.
 43. Park HS, Lee JK, Kim DW, et al. Immunohistochemical screening for anaplastic lymphoma kinase (ALK) rearrangement in advanced non-small cell lung cancer patients. *Lung Cancer*. 2012;77(2):288–292.
 44. Jokoji R, Yamasaki T, Minami S, et al. Combination of morphological feature analysis and immunohistochemistry is useful for screening of EML4-ALK-positive lung adenocarcinoma. *J Clin Pathol*. 2010;63(12):1066–1070.
 45. Ilie M, Long E, Butori C, et al. ALK-gene rearrangement: a comparative analysis on circulating tumour cells and tumour tissue from patients with lung adenocarcinoma. *Ann Oncol*. 2012;23(11):2907–2913.
 46. Klemptner SJ, Cohen DW, Costa DB. ALK translocation in non-small cell lung cancer with adenocarcinoma and squamous cell carcinoma markers. *J Thorac Oncol*. 2011;6(8):1439–1440.
 47. Yoshida A, Tsuta K, Nakamura H, et al. Comprehensive histologic analysis of ALK-rearranged lung carcinomas. *Am J Surg Pathol*. 2011;35(8):1226–1234.
 48. Thunnissen E, Bubendorf L, Diel M, et al. EML4-ALK testing in non-small

- cell carcinomas of the lung: a review with recommendations. *Virchows Arch.* 2012;461(3):245–257.
49. Paik PK, Arcila ME, Fara M, et al. Clinical characteristics of patients with lung adenocarcinomas harboring BRAF mutations. *J Clin Oncol.* 2011;29(15):2046–2051.
50. Capper D, Berghoff AS, Magerle M, et al. Immunohistochemical testing of BRAF V600E status in 1,120 tumor tissue samples of patients with brain metastases. *Acta Neuropathol.* 2012;123(2):223–233.
51. Capper D, Preusser M, Habel A, et al. Assessment of BRAF V600E mutation status by immunohistochemistry with a mutation-specific monoclonal antibody. *Acta Neuropathol.* 2011;122(1):11–19.
52. Koperek O, Kornauth C, Capper D, et al. Immunohistochemical detection of the BRAF V600E-mutated protein in papillary thyroid carcinoma. *Am J Surg Pathol.* 2012;36(6):844–850.
53. Andrulis M, Penzel R, Weichert W, von Deimling A, Capper D. Application of a BRAF V600E mutation-specific antibody for the diagnosis of hairy cell leukemia. *Am J Surg Pathol.* 2012;36(12):1796–1800.
54. Sahm F, Capper D, Preusser M, et al. BRAFV600E mutant protein is expressed in cells of variable maturation in Langerhans cell histiocytosis. *Blood.* 2012;120(12):e28–e34.
55. Long GV, Wilmott JS, Capper D, et al. Immunohistochemistry is highly sensitive and specific for the detection of V600E BRAF mutation in melanoma. *Am J Surg Pathol.* 2013;37(1):61–65.
56. Colomba E, Helias-Rodzewicz Z, Von Deimling A, et al. Detection of BRAF p.V600E mutations in melanomas: comparison of four methods argues for sequential use of immunohistochemistry and pyrosequencing. *J Mol Diagn.* 2013;15(1):94–100.
57. Feller JK, Yang S, Mahalingam M. Immunohistochemistry with a mutation-specific monoclonal antibody as a screening tool for the BRAFV600E mutational status in primary cutaneous malignant melanoma. *Mod Pathol.* 2013;26(3):414–420.
58. Bosmuller H, Fischer A, Pham DL, et al. Detection of the BRAF V600E mutation in serous ovarian tumors: a comparative analysis of immunohistochemistry with a mutation-specific monoclonal antibody and allele-specific PCR. *Hum Pathol.* 2013;44(3):329–335.
59. Ilie M, Long E, Hofman V, et al. Diagnostic value of immunohistochemistry for the detection of the BRAFV600E mutation in primary lung adenocarcinoma Caucasian patients. *Ann Oncol.* 2013;24(3):742–748.
60. Hofman V, Ilie M, Long-Mira E, et al. Usefulness of immunocytochemistry for the detection of the BRAF(V600E) mutation in circulating tumor cells from metastatic melanoma patients. *J Invest Dermatol.* 2013 Jan 10. doi: 10.1038/jid.2012.485.
61. Bergethon K, Shaw AT, Ou SH, et al. ROS1 rearrangements define a unique molecular class of lung cancers. *J Clin Oncol.* 2012;30(8):863–870.
62. Rimkunas VM, Crosby KE, Li D, et al. Analysis of receptor tyrosine kinase ROS1-positive tumors in non-small cell lung cancer: identification of a FIG-ROS1 fusion. *Clin Cancer Res.* 2012;18(16):4449–4457.
63. Cappuzzo F, Marchetti A, Skokan M, et al. Increased MET gene copy number negatively affects survival of surgically resected non-small-cell lung cancer patients. *J Clin Oncol.* 2009;27(10):1667–1674.
64. Sequist LV, Waltman BA, Dias-Santagata D, et al. Genotypic and histological evolution of lung cancers acquiring resistance to EGFR inhibitors. *Sci Transl Med.* 2011;3(75):75ra26.
65. Ou SH, Kwak EL, Siwak-Tapp C, et al. Activity of crizotinib (PF02341066), a dual mesenchymal-epithelial transition (MET) and anaplastic lymphoma kinase (ALK) inhibitor, in a non-small cell lung cancer patient with de novo MET amplification. *J Thorac Oncol.* 2011;6(5):942–946.
66. Belalcazar A, Azana D, Perez CA, Raez LE, Santos ES. Targeting the MET pathway in lung cancer. *Expert Rev Anticancer Ther.* 2012;12(4):519–528.
67. Vincent MD, Kuruvilla MS, Leigh NB, Kamel-Reid S. Biomarkers that currently affect clinical practice: EGFR, ALK, MET, KRAS. *Curr Oncol.* 2012;19(suppl 1):S33–S44.
68. Cronin M, Ross JS. Comprehensive next-generation cancer genome sequencing in the era of targeted therapy and personalized oncology. *Biomark Med.* 2011;5(3):293–305.
69. Long E, Hofman V, Ilie M, et al. Accreditation of the activity of molecular pathology according to ISO 15189: key steps to follow and the main potential pitfalls. *Ann Pathol.* 2013; in press.
70. Hofman V, Ilie M, Gavric-Tanga V, et al. Role of the surgical pathology laboratory in the pre-analytical approach of molecular biology techniques. *Ann Pathol.* 2010;30(2):85–93.

Copyright © 2013 Optimal Clinical (Doctors.MD).



Cancer Research

Autophagy plays a critical role in the degradation of active RHOA, the control of cell cytokinesis and genomic stability

Amine Belaid, Michael Cerezo, Abderrahman Chargui, et al.

Cancer Res Published OnlineFirst May 23, 2013.

Updated version	Access the most recent version of this article at: doi: 10.1158/0008-5472.CAN-12-4142
Supplementary Material	Access the most recent supplemental material at: http://cancerres.aacrjournals.org/content/suppl/2013/05/23/0008-5472.CAN-12-4142.DC1.html
Author Manuscript	Author manuscripts have been peer reviewed and accepted for publication but have not yet been edited.

E-mail alerts [Sign up to receive free email-alerts](#) related to this article or journal.

Reprints and Subscriptions To order reprints of this article or to subscribe to the journal, contact the AACR Publications Department at pubs@aacr.org.

Permissions To request permission to re-use all or part of this article, contact the AACR Publications Department at permissions@aacr.org.

Molecular and Cellular Pathobiology

Autophagy plays a critical role in the degradation of active RHOA, the control of cell cytokinesis and genomic stability

Amine Belaid^{1,2,3}, Michaël Cerezo^{1,2,4}, Abderrahman Chargui^{1,2,3}, Elisabeth Corcelle–Termeau⁵, Florence Pedeutour^{1,2,6,7}, Sandy Giuliano^{2,4}, Marius Ilie^{1,2,3,6,8}, Isabelle Rubera^{2,9}, Michel Tauc^{2,9}, Sophie Barale^{2,10}, Corinne Bertolotto^{2,4}, Patrick Brest^{1,2,3}, Valérie Vouret-Craviari^{1,2,3}, Daniel J. Klionsky¹¹, Georges F. Carle^{2,10}, Paul Hofman^{1,2,3,6,8,12}, Baharia Mograbi^{1,2,3}✉

1. Institute of Research on Cancer and Ageing of Nice (IRCAN), INSERM U1081, CNRS UMR7284, Centre Antoine Lacassagne, Nice, F-06107, France.
2. Université de Nice-Sophia Antipolis, Faculté de Médecine, Nice, F-06107, France.
3. Equipe Labellisée par l'ARC 9 rue Guy Môquet F- 94803 Villejuif, France.
4. INSERM U895 / C3M, Nice, F-06204, France.
5. Cell Death and Metabolism Unit, Danish Cancer Society Research Center, DK-2100 Copenhagen, Denmark.
6. Centre Hospitalier Universitaire de Nice, Pasteur Hospital, Nice, F-06107, France
7. Laboratory of Solid Tumors Genetics, Nice, France.
8. Laboratory of Clinical and Experimental Pathology, Nice, F-06002, France.
9. TIANP, UMR 6097, Nice, F-06108, France.
10. Laboratoire TIRO-MATOs UMR E4320, Commissariat à l'Energie Atomique, Centre Antoine Lacassagne, Nice, France.
11. University of Michigan, Life Sciences Institute, Ann Arbor, Michigan, 48109 USA.
12. Human Biobank, Nice, F-06002, France.

Corresponding Author: Baharia Mograbi; Institute of Research on Cancer and Ageing of Nice (IRCAN); Centre Antoine Lacassagne, Avenue de Valombrose; 06107 Nice Cedex 02, France; Tel: +33.4.92.03.12.45. Fax: +33.4.92.03.12.41; E. mail: mograbi@unice.fr.

Short title: Control of the RHOA pathway by Autophagy

Keywords: Autophagy; RHOA; tumor suppression; cytokinesis; aneuploidy

Conflicts of Interest disclosure statement: No potential conflicts of interest were disclosed.

Abstract

Degradation of signaling proteins is one of the most powerful tumor suppressive mechanisms by which a cell can control its own growth. Here, we identify RHOA as the molecular target by which autophagy maintains genomic stability. Specifically, inhibition of autophagosome degradation by the loss of the v-ATPase $\alpha 3$ (*TCIRG1*) subunit is sufficient to induce aneuploidy. Underlying this phenotype, active RHOA is sequestered *via* p62 (SQSTM1) within autolysosomes, and fails to localize to the plasma membrane or to the spindle midbody. Conversely, inhibition of autophagosome formation by *ATG5* shRNA dramatically increases localization of active RHOA at the midbody, followed by diffusion to the flanking zones. As a result, all of the approaches we examined that compromise autophagy (irrespective of the defect: autophagosome formation, sequestration or degradation) drive cytokinesis failure, multinucleation, and aneuploidy, processes that directly have an impact upon cancer progression. Consistently, we report a positive correlation between autophagy defects and the higher expression of RHOA in human lung carcinoma. We therefore propose that autophagy may act in part as a safeguard mechanism that degrades and thereby maintains the appropriate level of active RHOA at the midbody for faithful completion of cytokinesis and genome inheritance.

Abbreviations: Atg, autophagy-related; bafA1, bafilomycin A1; CQ, chloroquine; GAP, GTPase-activating protein; GEF, guanine nucleotide exchange factor; LAMP, lysosomal-associated membrane protein; LC3, microtubule-associated protein 1 light chain 3; PCT, proximal convoluted tubule; \oplus -MLC, phosphomyosin light chain; RHOGDI, RHO guanine nucleotide-dissociation inhibitor-1; shRNA, short hairpin RNA; v-ATPase, vacuolar-ATPase.

Introduction

Cells are faced with the tasks of dividing, of keeping the genome intact, and even of dying when appropriate. At their heart, these cell fates are dictated by tumor-suppressor mechanisms. One such mechanism is autophagy, which is commonly mutated or downregulated in human cancers (1). Indeed, the essential autophagy gene *BECN1* is deleted or mutated in 40 to 75% of breast, ovarian, colon and prostate cancers. Consistently, the notion that autophagy suppresses tumor development came from the demonstration that allelic loss of *Becn1* predisposes mice to lymphomas, hepatocellular carcinomas, and lung carcinomas (2, 3). Likewise, defects in other autophagy genes (*Atg4c*, *Atg5*, *Uvrag*, *Ambra1*, and *Bif-1/Sh3glb1*) render cells or mice tumor prone (4-8).

Physiologically, autophagy ensures in all cell types the turnover of all organelles and most long-lived proteins by a pathway, which begins with the formation of a double-membrane compartment, termed a “phagophore” that sequesters them. The phagophore expands into a completed vesicle, an “autophagosome”, and subsequently, the autophagosome rapidly fuses with a lysosome to become an “autolysosome” where the content is finally degraded. Originally identified as a housekeeping process, emerging data suggest that constitutive autophagy (*i.e.*, under nutrient-rich conditions) might also fight cancer by limiting inflammation (9), facilitating senescence (10) or clearing signaling proteins (11). Likewise, recent studies reveal that both *BECN1* and *ATG5* function as 'guardians' of cellular genome. Epithelial cells with loss of *Becn1* or *Atg5*, display gene amplification, and aneuploidy (7, 8). In support, activation of autophagy was demonstrated to reduce genomic instability within hepatocarcinoma cells (12). However, despite the importance of aneuploidy in cancer development (13, 14), the mechanisms underlying how autophagy deficiency compromises genomic stability are still unknown.

To address this issue, we explored the possibility that signaling proteins essential for cell growth might be degraded by autophagy. Whereas significant advances have been made in the discovery of

autophagy machinery, less is known about the nature of the autophagy substrates. Therefore, a key feature of our strategy was to inhibit the autophagy pathway at the degradation step, in order to achieve sequestration and accumulation of substrates within autolysosomal structures (**Fig. S1A**).

Materials and Methods

Cell culture and treatments

To inhibit the maturation of autophagosomes into degradative autolysosomes, renal cells derived from proximal convoluted tubules of wild-type (WT, $a3^{+/+}$) or the lysosomal v-ATPase $a3/TCIRG1$ -null mice ($a3^{-/-}$) were isolated and immortalized with the pSV3 neo vector. The renal epithelial cell lines that do or do not express $a3$ were referred to as WT and $a3^{-/-}$ cells, respectively. As controls, cells were stimulated with an inhibitor of v-ATPase activity, bafilomycin A1 (100 nM, bafA1; Sigma); or a weak base that raises intralysosomal pH, chloroquine (100 μ M, CQ; Sigma). Alternatively, the formation of autophagosomes was inhibited at the initiation step by *Atg5* or *Atg7* short hairpin RNA (shRNA). As a further control, we analyzed the phenotype of *Atg5* KO MEFs (provided by N. Mizushima) (15), and *ATG5*-depleted A549 lung epithelial cells. We also prevented the sequestration of autophagy substrates within the autophagic vesicles by *p62* shRNA. For details on cell culture and shRNA sequences see supplemental information.

Clinical samples

Primary NSCLC (pairs of pathological and control tissues from the same patient) were obtained from patients in Nice (France) and collected by the Tumor Biobank of Nice Hospital (Nice CHU, agreement 2010–06).

Analysis of autophagy

The activity of the autophagy pathway was monitored by four hallmarks: *i*) the formation of autophagic vesicles; and the degradation of three well-established autophagy substrates: *ii*) membrane-associated LC3-II; *iii*) p62/SQSTM1; and *iv*) long-lived proteins.

Ploidy determination and chromosomal abnormalities by metaphase spread

At 70% confluency, cells were arrested with colchicine (Invitrogen) in metaphase. Chromosomes were stained with giemsa and ~150 mitotic figures per cell line were photographed and the number of chromosomes was counted by Metafer M-Search Metaphase Finder and Ikaros softwares (Metasystems).

Time-lapse video microscopy

For monitoring cell progression through mitosis, exponentially growing cells cultured in complete growth medium were imaged every 5 min during 18 h on an inverted microscope (Carl Zeiss) equipped with a CO₂-equilibrated chamber.

Analysis of the RHOA pathway

The activity of RHOA pathway was monitored by *i*) the levels of active GTP-bound RHO (RHOTEKIN RHO Binding Domain Pull-down and ELISA-based G-LISA assays, Cytoskeleton Inc.); *ii*) the recruitment of RHOA to membranes; and *iii*) the downstream phosphorylation of myosin regulatory light chain (P-MLC) and reticulation of ACTIN cytoskeleton.

RHOA immunoprecipitation

Cells were lysed in RIPA and RHOA was immunoprecipitated with anti-RHOA antibody followed by western blotting with anti-ubiquitin, anti-p62, anti-LC3 and anti-RHOA antibodies.

RHOA stability

HEK 293 cells and A549 cells (Control, *ATG5*, or *p62* shRNA transduced cells) were transfected with FuGene^{HD} (Promega) and plasmids encoding the active (RHOA Q63) or inactive (RHOA N19) RHOA mutants. 20 h after transfection, cells were treated with cycloheximide (CHX; Sigma; C-4859; 10-20

$\mu\text{g/mL}$) to stop *de novo* protein synthesis for 7-57 h, alone or in combination with proteasomal (MG132, Sigma; 10 μM) and lysosomal (CQ; 100 μM) inhibitors and the drop in the levels of RHOA mutants was assayed by anti-myc western blotting (Millipore; P01106; 1:1000).

Complete and detailed description of all methods employed are available as Supplementary Data.

Statistical analysis

When adequate, results are presented as means \pm SD from the indicated number *n* of separate experiments. Statistical comparisons were done using Khi2 or Student T tests as appropriate. A *p* value <0.05 was considered significant.

Results

The V-ATPase $\alpha 3$ -dependent autophagy defect is characterized by the formation of giant multinucleate cells

To gain a deeper insight into the role of autophagy, we established cell-lines from v-ATPase $\alpha 3/TCIRG1$ -null mice (16). PCT (proximal convoluted tubule) cells were chosen as they express the highest level of v-ATPase (17); the $\alpha 3$ subunit is localized in the lysosomal limiting membrane (18). In agreement with the other reported defect of v-ATPase (19, 20), we show that the $\alpha 3$ loss increased autophagy sequestration and simultaneously impaired autophagic degradation, as evidenced by the accumulation of ATG12–ATG5 conjugate, of autolysosomes and of autophagic substrates (long-lived proteins, LC3-II, and p62) (Fig. 1A and S1B). In contrast, $\alpha 3$ -null cells seemed to have functionally intact proteasomes (Fig. S1C). Remarkably, this $\alpha 3$ -dependent autophagy defect was characterized by an increase in cell size and a flattened morphology with the accumulation of vesicles and nuclei (Fig. 1B-C), supporting the importance of autophagy in maintaining cell size (21, 22). By using different approaches, we excluded a role for senescence as a cause of enlarged morphology (Fig. S2). Consistently, FACS analysis revealed that $\alpha 3^{-/-}$ cells were dividing and displayed increased DNA content (3–4 N, Fig. S2C). Of interest, no subdiploid or subtetraploid cells were detected, indicating that the $\alpha 3$ loss did not induce cell death. Subsequent karyotypes of $\alpha 3^{-/-}$ cells confirmed a near-triploid karyotype (group average, 131; Fig. 1D). Therefore, despite aneuploidy, the $\alpha 3^{-/-}$ cells continued to proliferate, and escaped apoptosis or senescence. All these abnormalities, which are hallmarks of cancer cells, were reminiscent of that reported for $Atg5^{-/-}$ or $Becn1^{-/+}$ cells (8). Collectively, these data support the notion that defects of the entire autophagy pathway [*i.e.* either at the step of formation ($Atg5^{-/-}$ or $Becn1^{-/+}$) or degradation (herein, V-ATPase $\alpha 3^{-/-}$) of autophagosomes] could result in aneuploidy.

The multinucleate phenotype of $a3^{-/-}$ cells arises from cytokinesis failure

We hypothesized that the aneuploidy of $a3^{-/-}$ cells might arise through cytokinesis failure. Multiple mitotic defects leading to aneuploidy were indeed identified in $a3^{-/-}$ cells, as these cells often showed multipolar spindles and several chromosome segregation defects: improper attachment of chromosomes to spindle microtubules, lagging chromosomes, chromosome bridges connecting daughter cells, and micronuclei. Strikingly, a large proportion of $a3^{-/-}$ cells were connected *via* an asymmetric bridge, in contrast to the short intracellular bridge observed in the middle of the two WT daughter cells (Fig. S3).

Using real-time imaging, we showed that the WT cells completed cytokinesis in only 15 min (Fig. 2A, Movie S1). By contrast, the cytokinesis was incomplete upon v-ATPase inhibition by bafilomycin A1 treatment (Fig. 2B) or $a3$ loss (Fig. 2C-G, Movies S2-S5). 72% of $a3^{-/-}$ cells that entered mitosis normally failed abscission (Fig. 2C) and instead remained connected by an intracellular bridge for up to eight h before separating (Fig. 2D, Movie S2), re-entering mitosis synchronously (still bound to the sister cell, Fig. 2E Movie S3) or collapsing back, forming a single binucleate cell (Fig. 2F-G, Movies S4-S5). Moreover, we did not observe cell-cell fusion, cell engulfment and endoreplication during live-cell imaging (n=200). Thus, impairment of cytokinesis at the membrane abscission step was the key event responsible for the formation of multinucleate $a3^{-/-}$ cells.

The inhibition of autophagy degradation by v-ATPase $a3$ loss stabilizes RHOA-GTP within autolysosomes

We then explored which signaling proteins might be degraded by autophagy and could underlie this phenotype. One candidate was the small GTPase RHOA, that dictates cell shape and completion of cytokinesis *via* F-ACTIN reticulation (23). In this regard, a striking hallmark of $a3^{-/-}$ cells was a dramatic remodeling of ACTIN cytoskeleton with the loss of stress fibers and the formation of ACTIN patches (Fig. 3A and S4A,B). The current consensus is that fine-tuning of RHO activity involves the guanine nucleotide

exchange factors (GEFs) that activate them, the GTPase-activating proteins (GAPs) that inactivate them, and the guanine nucleotide-dissociation inhibitors (GDIs) that maintain RHO inactive within the cytoplasm (23). Exciting findings have revealed that RHO GTPases, their upstream regulators and downstream targets might also be subjected to irreversible proteasome-dependent degradation (24-32).

Instead of proteasome, however, we determined that active RHOA was constitutively maintained at low levels by autophagy. Indeed, the active RHOA was barely detected at the plasma membrane of $\alpha 3^{-/-}$ cells but instead accumulated intracellularly, within autolysosomes positive both for the autophagy marker LC3 and lysosomal marker LAMP1 (Fig. 3B, S4B *inset*). Notably, the level of RHOA-GTP was elevated in resting $\alpha 3^{-/-}$ cells, as evidenced by the RHOTEKIN-binding pull-down assay, the recruitment of RHOA to cellular membranes and the downstream phosphorylation of myosin regulatory light chain (P-MLC, Fig. 3C and S4B).

A role for autophagy in controlling RHOA-GTP level was then suggested by the shRNA-mediated inhibition of autophagosome formation: expression of *Atg5* shRNA increased the localization of active RHOA at the plasma membrane of $\alpha 3^{-/-}$ cells, which allowed ACTIN polymerization into filaments (Fig. 3D). Consistently, the *Atg5* shRNA-transduced $\alpha 3^{-/-}$ cells displayed a smaller size and tight cohesion within the colony (Fig. 3D). Importantly, the control of RHOA by autophagy was remarkably specific, as the related GTPase RAC (Fig. S4E), as well as the RHOA regulator, RHOGDI, were not affected (Fig. 3C). Together, these data highly suggest a working model in which autophagy might sequester and degrade active RHOA. Inhibition of v-ATPase by $\alpha 3$ loss would stabilize RHOA-GTP within autolysosomal structures, protecting it from autophagy degradation, and at the same time this would preclude reticulation of ACTIN cytoskeleton (Fig. S1A).

p62-dependent autophagy specifically degrades active RHOA

As proof-of-concept, pharmacological inhibition of autophagy degradation by bafA1 or chloroquine (CQ) treatment similarly increased the levels of membrane-bound RHOA together with the autophagy substrates LC3-II and p62 (Fig. S5). This occurred in multiple cell types, including fibroblast, kidney, and lung epithelial cells (Fig. S5A). In contrast, impairment of proteasome by MG132 failed to alter the levels of the membrane-bound RHOA in every cell line tested (Fig. S5A). As expected, all features of $a3^{-/-}$ cells (*i.e.*, RHOA autolysosomal recruitment, F-ACTIN depolymerization, and increased cell size) were mimicked by bafA1, but not MG132 treatment, further supporting the model that activity of the RHOA pathway can be controlled by the autophagy-lysosome pathway (Fig. S5B–C). Consistently, the active, but not inactive, RHOA mutants were long-lived proteins selectively degraded by autophagy (Fig. 4). Indeed, upon inhibition of protein synthesis with cycloheximide (CHX), the active RHOA (RHOA⁺, Q63) was degraded within 28 h and stabilized by inhibiting lysosomal degradation (CQ, Fig. 4A), or autophagosome formation (*ATG5* shRNA, Fig. 4B and S6A-B) but not proteasomal activity (MG132, Fig. 4A). Inversely, the inactive form of RHOA (RHOA⁻, N19) was unstable and as expected stabilized by inhibition of proteasome, but not by inhibition of lysosomal activity or of autophagy (Fig. 4A-B), in agreement with previous reports (24-30).

At this stage, it was of interest to address how autophagy may specifically targets the active RHOA. One adaptor by which autophagy acquires specificity is p62 (SQSTM1) that targets ubiquitinated substrates to the autophagy machinery (33). Of interest, p62 appears as a prime candidate for regulating RHOA as it is the sole autophagy adaptor involved in cell mitosis (34), cell spreading (35) and tumor growth (36-38). We observed that p62 not only co-immunoprecipitated (Fig. 4C) and co-localized (Fig. 4D) with ubiquitinated RHOA and LC3-II in CQ-treated cells but also was essential in the selective clearance of active RHOA by autophagy (Fig. 4B and D). Upon p62 silencing and CQ treatment, autophagosomes formed normally (as evidenced by LC3-II conversion, Fig. S6A), but the autophagic

sequestration (Fig. 4D) and degradation (Fig. 4B) of active RHOA were defective. Collectively, these results strongly suggest a new signaling role for p62-dependent autophagy in the control of RHOA pathway.

Regulation of the amount of active RHOA at the midbody during cytokinesis by autophagy

The multinucleate phenotype of $a3^{-/-}$ cells raised the question of whether autophagy may control cytokinesis through regulation of RHOA. Autophagy was suggested to clear the midbody ring after cytokinesis completion (39, 40). Likewise, the depletion of several autophagy genes (*Atg5*, *Becn1*, *Uvrag*, *Bif-1* And *Vps34*) was demonstrated to lead to polynucleation, but the role of autophagy in controlling RHOA activation during cytokinesis was not documented (8, 41).

Although several key RHOA activators have been identified (42), little is known about the mechanisms that confine active RHOA at the midbody. Using the $a3^{-/-}$ cells, we observe that little, if any, active RHOA was at the equatorial furrow and was instead sequestered within autolysosomes, close to the midbody (Fig. 5A), likely as a result of increased sequestration. Inversely, when we blocked autophagosome formation by *ATG5* shRNA (Fig. S6A), RHOA was highly enriched at the equatorial furrow of cytokinetic A549 lung cancer cells (Fig. 5B and S7A). Notably, the RHO activity zone in *ATG5*-depleted cells was three times as wide and bright as in controls (control shRNA = $3.7 \pm 0.8 \mu\text{m}$; *ATG5* shRNA = $11.4 \pm 2.6 \mu\text{m}$; mean \pm SD, Fig. 5C–D). Outside the cell equator, RHOA activity was also abnormally high at the cell cortex (Fig. 5B and S7). Accordingly, *Atg5* knockdown in mouse embryonic fibroblasts (Fig. 5E), and *ATG7* or *p62* depletion in A549 cells (Fig. S6) faithfully recapitulated the same phenotype with regard to the RHOA pathway. Likewise, closer examination indicated that the upstream regulators required for narrowed activation of RHOA such as the kinesin MKLP1, the RHOA GEF ECT2 and spindle microtubules concentrated at the midbody of cytokinetic cells (Fig. S8A-B) (43). It is also highly likely that the loss of

ATG5 would create defects in the generation and the delivery of new membranes to the cleavage furrow, a process that is central to cytokinesis. As shown in Figure S8C, the delivery of endosomes to the midbody appeared not to be affected by *ATG5* depletion: the endosomes were delivered to the cleavage furrow and clustered on either side of midbody of *ATG5*-depleted cells, as observed in control cells. By contrast, *ATG5*-depleted cells exhibited in addition to RHOA a broader distribution of downstream F-ACTIN that triggers the formation of actomyosin ring (Fig. S7B). Our data therefore suggest that the degradation of RHOA by autophagy may function as a key, but hitherto uncharacterized, mechanism concentrating active RHOA at midbody.

Autophagy defects fuel chromosomal instability in lung cancer cells

Considering the apparent connection between autophagy and RHOA, a key issue is how defects in autophagy might affect cell behavior in a way relevant for cancer progression. Maintaining the appropriate amount of active RHOA at midbody is critical for faithful cytokinesis as it dictates the position, the formation and the contraction of actomyosin ring (42, 44). If our model were correct, one would expect that the inhibition of autophagy sequestration in autophagy-competent A549 tumor cells would be sufficient to disturb cytokinesis and thereby drive the genomic instability required for tumor progression. As shown in Figure 6, in control A549 cells, the clustering of RHOA in a narrow zone resulted in the formation of a unique and compact ring whose position and size remained constant throughout furrow ingression (Fig. 6A-B, upper panels). As a result, control cells successfully completed cytokinesis (Movie S6). Without functional autophagy, the subsequent hyperactivation of RHOA zone would jeopardize the assembly of an efficient contractile ring, as expected from the cytokinesis defects observed for active RHOA mutants (Fig. S4C). Indeed, *ATG5*-depleted A549 cells progressed through mitosis until the furrow started to constrict, then 52% of the cells demonstrated unstable and loose furrowing that suddenly fell apart, reformed and constricted more slowly than control furrows, delaying

cytokinesis completion (Fig. 6A-B, lower panels, Movie S6). As result of cytokinesis failure, these autophagy compromises (*ATG5* shRNA and *p62* shRNA) were sufficient to increase the percentage of cells with multiple nuclei (Fig. 6C), and the frequency of chromosomal gains and losses in nearly all of the chromosomes (Fig. 6D), one hallmark of aggressive cancer. Together, these findings highly suggested that autophagy may act in part as a master safeguard mechanism of active RHOA localization during cytokinesis for faithful genome inheritance.

Overexpression of RHOA is correlated with autophagy defects in lung carcinomas

The biochemical, cellular, and genomic changes (increased RHOA activity, increased cellular sizes, and aneuploidy) we consistently observed herein following autophagy inhibition (irrespective of particular autophagy defects) are noteworthy because they accompany the onset and progression of cancers. RHOA overexpression has been observed in many aggressive cancers, such as breast, colon, prostate, and lung cancers, but has been attributed largely to increased *RHOA* transcription (45). Consistent with a role of autophagy in RHOA degradation, we found that RHOA, together with p62 and LC3-II were overexpressed in late stages of non-small cell lung cancers (NSCLC; T; pTNM stage IIIA), compared to normal epithelia (N) and stage I adenocarcinomas (Fig. 7A-B). An impaired autophagic degradation rather than an increased transcription was correlated with RHOA overexpression, as the levels of RHOA expression and activity increased progressively with the accumulation of the autophagy substrates p62 and LC3-II (Fig. 7A), and no significant changes in *RHOA* mRNA expression were measured (Fig. 7A, right panel). Of interest, the inactivation of autophagy and the subsequent RHOA upregulation were not early events, but instead were late events in the progression of lung cancer, when these cancers acquire a more genomic instability. All tumor cells positive for p62 were also RHOA-positive (Fig. 7B). p62 overexpression, as a readout of an autophagy defect, was associated with a reduced or absent RHOA

membrane localization, which instead displayed intracellular localization (T, right panels). In sharp contrast, normal bronchial epithelial cells that barely expressed p62 showed strong membrane expression of RHOA primarily at their apical ciliated cell surface (N, left panels).

Discussion

So far, most studies suggest that signal termination and irreversible progression through cell-cycle depend largely on the proteasomal degradation of key regulatory proteins (46). Recently, Gao et al. provide the first evidence that autophagy negatively regulates Wnt signaling by degrading Dishevelled; however, this occurs under nutrient starvation (11). Therefore, the ability of autophagy to degrade signaling proteins under basal conditions and thereby to ensure tumor suppressive functions remains to be established.

We show here that autophagy promotes the degradation of active RHOA. In support of this, (i) RHOA-GTP was elevated in cells deficient in autophagosome clearance; (ii) importantly, RHOA failed to localize to midbody and instead accumulated within autolysosomes; (iii) a role for autophagy in regulating RHOA-GTP was then suggested by the shRNA-mediated inhibition of autophagosome formation: *ATG5* shRNA dramatically increased the localization of RHOA-GTP at the equatorial furrow of cytokinetic cells. One related RHO GTPase, RAC, was not targeted by autophagy. As a result, defects of the entire autophagy pathway [*i.e.* either at the formation (*ATG5* or *ATG7* shRNA), sequestration (*p62* shRNA) or degradation of autophagosomes (v-ATPase *a3*^{-/-} cells)] similarly drive the formation of unstable and loose furrowing, disturbing cytokinesis completion and genome inheritance; processes that directly contribute to cancer development.

The regulation of RHOA is unique in that it involves GEF, GAP, and GDI proteins, along with the proteasome (47) and autophagy. Depending on its activation state, we provide the first lines of evidence that RHOA used distinct routes for degradation: while the proteasome degraded the cytosolic and inactive forms, the autophagy pathway specifically degraded the membrane-associated and active pool of RHOA. This is consistent with the recently reported degradation of two constitutively active RHO, RHOH and RHOB, within lysosomes (48, 49) and the redistribution of active RHOA to undefined

perinuclear localization after treatment of enterocytes with an autophagy inducer, LPS (50). We therefore propose that autophagy may act as a tumor suppressor pathway in part by turning off RHOA activation (Fig. 7C). In this model, the remarkable dynamics of autophagy together with its integration of extracellular cues might dictate the time and place where a RHOA is active, and able to interact with its downstream substrates. Accordingly, we reported the targeting of autolysosomes at midbody during cytokinesis, the same subcellular and temporal localizations where RHOA should be controlled. Therefore, autophagy might be critical for localized degradation of active RHOA at midbody and thereby proper ACTIN dynamics during accurate completion of cytokinesis and faithful genome inheritance.

The development of a cancer depends on the ability of tumor cells to acquire growth advantages. Whatever the mutations, deletions, and epigenetic silencing of autophagy genes, our findings provide new information on how autophagy defects can drive tumor progression through deregulation of RHOA pathway. As autophagy is commonly downregulated in cancers (1) where RHOA is overexpressed (47), this new paradigm may be a general mechanism for the acquisition of aneuploidy and progression of human cancer cells.

Authors' Contributions

Conception and design: AB and BM.

Development of methodology: AB, MC, AC, FP, SG, CB and BM conducted experiments; IR, MT, SB, and GFC established the PCT cell-lines from WT and v-ATPase $\alpha 3^{-/-}$ mice. **NSCLC diagnosis and collection:** MI and PH.

Administrative, technical, or material support (i.e., reporting or organizing data): ECT, PB, VVC, DJK, PH and BM.

Writing, review, and/or revision of the manuscript: BM and DJK.

Study supervision: BM.

Acknowledgments

We thank Nathalie Rochet, Nathalie Singer, Etienne Boulter, Jean Albregues, and Emmanuel Lemichez for helpful discussions. We are grateful to Laurence Cailleteau, Thibault Fabas, Annie-Claude Peyron, Valérie Pierrefite-Carle, Isabelle Mothe, Adrien Botta, and Virginie Tanga-Gavric for their technical assistance. We acknowledge Pr Mouroux and Pr Vénissac (thoracic surgery department, Nice, France) and Dr N. Mizushima (Tokyo, Japan) for providing us with surgical lung specimens and *Atg5* KO MEFs, respectively.

Grant support

This work was supported by grants from “Institut National de la Santé et de la Recherche Médicale”, “Agence de l'Environnement et de la Maîtrise de l'Energie” (AB and AC: ADEME n° 0862C0044), Agence régionale santé Provence Alpes Côte d'Azur and Direction régionale de l'Environnement, de l'aménagement et du logement (AB: plan régional santé environnement PRSE PACA n°6.3.3.3 et 6.3.3.4), “Association pour la Recherche contre le Cancer” (ARC Grants no SL220110603478), “Programme

Hospitalier De Recherche Clinique" (PH: PHRC Nice CHU 2003), "Cancéropole PACA" (PROCAN 2007, axe II), "Institut National du Cancer" (PH: PNES POU MON INCa), NIH (DJK: GM053396).

References

1. Mathew R, Karantza-Wadsworth V, White E. Role of autophagy in cancer. *Nat Rev Cancer*. 2007;7:961-7.
2. Qu X, Yu J, Bhagat G, Furuya N, Hibshoosh H, Troxel A, et al. Promotion of tumorigenesis by heterozygous disruption of the beclin 1 autophagy gene. *J Clin Invest*. 2003;112:1809-20.
3. Yue Z, Jin S, Yang C, Levine AJ, Heintz N. Beclin 1, an autophagy gene essential for early embryonic development, is a haploinsufficient tumor suppressor. *Proc Natl Acad Sci USA*. 2003;100:15077-82.
4. Fimia GM, Stoykova A, Romagnoli A, Giunta L, Di Bartolomeo S, Nardacci R, et al. Ambra1 regulates autophagy and development of the nervous system. *Nature*. 2007;447:1121-5.
5. Takahashi Y, Coppola D, Matsushita N, Cuaing HD, Sun M, Sato Y, et al. Bif-1 interacts with Beclin 1 through UVRAG and regulates autophagy and tumorigenesis. *Nat Cell Biol*. 2007;9:1142-51.
6. Mariño G, Salvador-Montoliu N, Fueyo A, Knecht E, Mizushima N, Lopez-Otin C. Tissue-specific autophagy alterations and increased tumorigenesis in mice deficient in Atg4C/autophagin-3. *J Biol Chem*. 2007;282:18573-83.
7. Karantza-Wadsworth V, Patel S, Kravchuk O, Chen G, Mathew R, Jin S, et al. Autophagy mitigates metabolic stress and genome damage in mammary tumorigenesis. *Genes Dev*. 2007;21:1621-35.
8. Mathew R, Kongara S, Beaudoin B, Karp CM, Bray K, Degenhardt K, et al. Autophagy suppresses tumor progression by limiting chromosomal instability. *Genes Dev*. 2007;21:1367-81.
9. Degenhardt K, Mathew R, Beaudoin B, Bray K, Anderson D, Chen G, et al. Autophagy promotes tumor cell survival and restricts necrosis, inflammation, and tumorigenesis. *Cancer Cell*. 2006;10:51-64.
10. Young AR, Narita M, Ferreira M, Kirschner K, Sadaie M, Darot JF, et al. Autophagy mediates the mitotic senescence transition. *Genes Dev*. 2009;23:798-803.
11. Gao C, Cao W, Bao L, Zuo W, Xie G, Cai T, et al. Autophagy negatively regulates Wnt signalling by promoting Dishevelled degradation. *Nat Cell Biol*. 2010;12:781-90.
12. Xie R, Wang F, McKeehan WL, Liu L. Autophagy enhanced by microtubule- and mitochondrion-associated MAP1S suppresses genome instability and hepatocarcinogenesis. *Cancer Res*. 2011;71:7537-46.
13. Geigl JB, Obenauf AC, Schwarzbraun T, Speicher MR. Defining 'chromosomal instability'. *Trends Genet*. 2008;24:64-9.
14. Fujiwara T, Bandi M, Nitta M, Ivanova EV, Bronson RT, Pellman D. Cytokinesis failure generating tetraploids promotes tumorigenesis in p53-null cells. *Nature*. 2005;437:1043-7.
15. Kuma A, Hatano M, Matsui M, Yamamoto A, Nakaya H, Yoshimori T, et al. The role of autophagy during the early neonatal starvation period. *Nature*. 2004;432:1032-6.
16. Scimeca JC, Franchi A, Trojani C, Parrinello H, Grosgeorge J, Robert C, et al. The gene encoding the mouse homologue of the human osteoclast-specific 116-kDa V-ATPase subunit bears a deletion in osteosclerotic (oc/oc) mutants. *Bone*. 2000;26:207-13.
17. Hurtado-Lorenzo A, Skinner M, El Annan J, Futai M, Sun-Wada GH, Bourgoin S, et al. V-ATPase interacts with ARNO and Arf6 in early endosomes and regulates the protein degradative pathway. *Nat Cell Biol*. 2006;8:124-36.
18. Toyomura T, Murata Y, Yamamoto A, Oka T, Sun-Wada GH, Wada Y, et al. From lysosomes to plasma membrane: localization of vacuolar type H⁺-ATPase with the a3 isoform during osteoclast differentiation. *J Biol Chem*. 2003;278:22023-30.
19. Lee JH, Yu WH, Kumar A, Lee S, Mohan PS, Peterhoff CM, et al. Lysosomal proteolysis and autophagy require presenilin 1 and are disrupted by Alzheimer-related PS1 mutations. *Cell*. 2010;141:1146-58.

20. Juhasz G. Interpretation of bafilomycin, pH neutralizing or protease inhibitor treatments in autophagic flux experiments: Novel considerations. *Autophagy*. 2012;8:1875-6.
21. Hosokawa N, Harab Y, Mizushima N. Generation of cell lines with tetracycline-regulated autophagy and a role for autophagy in controlling cell size. *FEBS Lett*. 2006;580:2623-9.
22. Lum JJ, Bauer DE, Kong M, Harris MH, Li C, Lindsten T, et al. Growth factor regulation of autophagy and cell survival in the absence of apoptosis. *Cell*. 2005;120:237-48.
23. Jaffe AB, Hall A. RHO GTPases: biochemistry and biology. *Annu Rev Cell Dev Biol*. 2005;21:247-69.
24. Doye A, Mettouchi A, Bossis G, Clément R, Buisson-Touati C, Flatau G, et al. CNF1 exploits the ubiquitin-proteasome machinery to restrict RHO GTPase activation for bacterial host cell invasion. *Cell*. 2002;111:553-64.
25. Wang HR, Zhang Y, Ozdamar B, Ogunjimi AA, Alexandrova E, Thomsen GH, et al. Regulation of cell polarity and protrusion formation by targeting RHOA for degradation. *Science*. 2003;302:1775-9.
26. Ozdamar B, Bose R, Barrios-Rodiles M, Wang HR, Zhang Y, Wrana JL. Regulation of the polarity protein Par6 by TGF β receptors controls epithelial cell plasticity. *Science*. 2005;307:1603-9.
27. Chen Y, Yang Z, Meng M, Zhao Y, Dong N, Yan H, et al. Cullin mediates degradation of RHOA through evolutionarily conserved BTB adaptors to control actin cytoskeleton structure and cell movement. *Mol Cell*. 2009;35:841-55.
28. Bryan B, Cai Y, Wrighton K, Wu G, Feng XH, Liu M. Ubiquitination of RHOA by Smurf1 promotes neurite outgrowth. *FEBS Lett*. 2005;579:1015-9.
29. Asanuma K, Yanagida-Asanuma E, Faul C, Tomino Y, Kim K, Mundel P. Synaptopodin orchestrates actin organization and cell motility via regulation of RHOA signalling. *Nat Cell Biol* 2006;8:485-91.
30. Boulter E, Garcia-Mata R, Guilluy C, Dubash A, Rossi G, Brennwald PJ, et al. Regulation of RHO GTPase crosstalk, degradation and activity by RHOGDI1. *Nat Cell Biol*. 2010;12:477-83.
31. Su L, Agati JM, Parsons SJ. p190RHOGAP is cell cycle regulated and affects cytokinesis. *J Cell Biol*. 2003;163:571-82.
32. Lynch EA, Stall J, Schmidt G, Chavrier P, D'Souza-Schorey C. Proteasome-mediated degradation of Rac1-GTP during epithelial cell scattering. *Mol Biol Cell*. 2006;17:2236-42.
33. Johansen T, Lamark T. Selective autophagy mediated by autophagic adapter proteins. *Autophagy*. 2011;7:279-96.
34. Linares JF, Amanchy R, Greis K, Diaz-Meco MT, Moscat J. Phosphorylation of p62 by cdk1 controls the timely transit of cells through mitosis and tumor cell proliferation. *Mol Cell Biol*. 2011;31:105-17.
35. Kadandale P, Stender JD, Glass CK, Kiger AA. Conserved role for autophagy in RHO1-mediated cortical remodeling and blood cell recruitment. *Proc Natl Acad Sci USA*. 2010;107:10502-7.
36. Mathew R, Karp CM, Beaudoin B, Vuong N, Chen G, Chen HY, et al. Autophagy suppresses tumorigenesis through elimination of p62. *Cell*. 2009;137:1062-75.
37. Duran A, Linares JF, Galvez AS, Wikenheiser K, Flores JM, Diaz-Meco MT, et al. The signaling adaptor p62 is an important NF-kappaB mediator in tumorigenesis. *Cancer Cell*. 2008;13:343-54.
38. Inami Y, Waguri S, Sakamoto A, Kouno T, Nakada K, Hino O, et al. Persistent activation of Nrf2 through p62 in hepatocellular carcinoma cells. *J Cell Biol*. 2011;193:275-84.
39. Pohl C, Jentsch S. Midbody ring disposal by autophagy is a post-abscission event of cytokinesis. *Nat Cell Biol*. 2009;11:65-70.
40. Kuo TC, Chen CT, Baron D, Onder TT, Loewer S, Almeida S, et al. Midbody accumulation through evasion of autophagy contributes to cellular reprogramming and tumorigenicity. *Nat Cell Biol*. 2011;13:1214-23.
41. Sagona AP, Nezis IP, Pedersen NM, Liestøl K, Poulton J, Rusten TE, et al. PtdIns(3)P controls cytokinesis through KIF13A-mediated recruitment of FYVE-CENT to the midbody. *Nat Cell Biol*. 2010;12:362-71.

42. Piekny A, Werner M, Glotzer M. Cytokinesis: welcome to the RHO zone. *Trends Cell Biol.* 2005;15:651-8.
43. Yüce O, Piekny A, Glotzer M. An ECT2-centralspindlin complex regulates the localization and function of RHOA. *J Cell Biol.* 2005;170:571-82.
44. Miller AL, Bement WM. Regulation of cytokinesis by RHO GTPase flux. *Nat Cell Biol.* 2009;11:71-7.
45. Chan CH, Lee SW, Li CF, Wang J, Yang WL, Wu CY, et al. Deciphering the transcriptional complex critical for RHOA gene expression and cancer metastasis. *Nat Cell Biol.* 2010;12:457-67.
46. Kerscher O, Felberbaum R, Hochstrasser M. Modification of proteins by ubiquitin and ubiquitin-like proteins. *Annu Rev Cell Dev Biol.* 2006;22:159-80.
47. Sahai E, Marshall CJ. RHO-GTPases and cancer. *Nat Rev Cancer.* 2002;2:133-42.
48. Perez-Sala D, Boya P, Ramos I, Herrera M, Stamatakis K. The C-terminal sequence of RHOB directs protein degradation through an endo-lysosomal pathway. *PLoS ONE.* 2009;4:e8117.
49. Schmidt-Mende J, Geering B, Yousefi S, Simon HU. Lysosomal degradation of RHOH protein upon antigen receptor activation in T but not B cells. *Eur J Immunol.* 2009;40:525-9.
50. Cetin S, Ford HR, Sysko LR, Agarwal C, Wang J, Neal MD, et al. Endotoxin inhibits intestinal epithelial restitution through activation of RHO-GTPase and increased focal adhesions. *J Biol Chem.* 2004;279:24592-600.

Figure Legends

Figure 1. The $\alpha 3$ -dependent autophagy defect is characterized by the formation of giant multinucleate cells.

A, Accumulation of autolysosomes (LC3-II and LAMP1 positive; fluorescence images) that were defective in the degradation of long-lived proteins (upper left inset), LC3-II and p62 (right insets). Right: note the accumulation of the ATG12–ATG5 conjugate (a marker of autophagosome formation) in response to the $\alpha 3$ loss. (See Fig. S1).

B, Cell and nuclei area of WT and $\alpha 3^{-/-}$ cells (n = 400).

C, Representative photomicrographs showing that the WT cells were all small ($200 \pm 47 \mu\text{m}^2$) with one nucleus, while the $\alpha 3$ -null cells were heterogeneous in size. 30-40% of $\alpha 3^{-/-}$ cells showed a gigantic size ($200\text{-}7,300 \mu\text{m}^2$), and a flattened shape with the accumulation of vesicles and nuclei.

D, Representative karyotype figures showing aneuploidy and structural abnormalities in $\alpha 3^{-/-}$ cells.

Figure 2. Cytokinesis is specifically impeded by v-ATPase inactivation.

Control (A, treated with DMSO, Movie S1; *inset*: high magnification of the last frame where the daughter WT cells are outlined in white to help visualize their successful division), bafA1-treated WT cells (B, 100 nM, 8 h after the addition of bafA1) or $\alpha 3^{-/-}$ cells (C-G, Movies S2–S5), all under complete medium were followed for 18 h using phase-contrast time-lapse microscopy.

C, Frequency of cytokinesis failure in $\alpha 3^{-/-}$ cells (n = 125).

D, Still images of a mitotic $\alpha 3^{-/-}$ cell that remained connected by an intracellular bridge for up to eight h before abscission (Movie S2).

E, Pairs of $\alpha 3^{-/-}$ cells that entered mitosis synchronously are outlined in white (Movie S3). Lower panel: two mitotic cells (white arrows) remained connected by an intracellular bridge (empty arrow).

F, Still-images of an $\alpha 3^{-/-}$ cell that exited mitosis as a binucleated cell after 18 attempts of cleavage furrow formation. Note that this cell developed ectopic furrows, which led to the formation of anuclear fragments (white filled arrows) that fused back to the cell (Movie S4).

G, Still-images of a mononucleate $\alpha 3^{-/-}$ cell that formed a tetranucleate cell after two rounds of abortive mitoses (Movie S5).

Both giant and small $\alpha 3^{-/-}$ cells failed cytokinesis, resulting in multinucleation and differentially sized daughter cells. All daughter cells were viable throughout imaging (up to 18 h). White empty arrows indicate cleavage furrow formation, arrowheads indicate nuclei, and time points are in h:min from the initiation of metaphase (zero time point).

Figure 3. The inhibition of autophagy degradation by v-ATPase $\alpha 3$ loss stabilizes RHOA-GTP within autolysosomes.

A, Phalloidin labeling showed the loss of stress fibers in $\alpha 3^{-/-}$ cells that instead developed ACTIN patches (empty arrows).

B, Intracellular ring of RHOA (arrows) that colocalized with LC3-II and LAMP1 (*insets*, see also the color images in Fig. S4B left) in $\alpha 3^{-/-}$ cells in contrast to the WT cells that displayed RHOA at their plasma membrane (arrowhead).

C, Accumulation of RHOA-GTP in $\alpha 3^{-/-}$ cells was evidenced by RHOTEKIN binding (pull-down assay and G-ELISA kit; left and middle panels, respectively); the recruitment of active RHOA proteins to Triton X-100 insoluble cell membranes; and the downstream phosphorylation of myosin regulatory light chain (P-MLC ; lower panels). Bound proteins (upper panel) and total cell lysates (lower panels) were analyzed by western blotting. Note that $\alpha 3$ loss increased the ratio of activated (membrane-associated):total RHOA from 2% (WT) to 4% ($\alpha 3^{-/-}$ cells). Western blots are representative of three independent experiments.

RT-PCR analysis showing that RHOA-GTP accumulation was not due to an increased *RHOA* transcription (right panel).

D, *Atg5* shRNA rescues RHOA localization at the plasma membrane (arrowhead) of *a3*^{-/-} cells. Cells were infected with *Atg5* shRNA lentivirus and selected with media containing puromycin for 72 h. Shown are representative images where DAPI marks nucleus and F-ACTIN denotes the filamentous ACTIN stained by phalloidin.

Figure 4. p62-dependent autophagy controls the levels of active RHOA.

A, The active RHOA is specifically degraded by a lysosomal pathway. HEK cells were transfected with plasmids encoding the active (Q63, RHOA⁺) or inactive RHOA (N19, RHOA⁻) mutants, and incubated with cycloheximide (CHX; 10 µg/mL) for the indicated time in the presence or absence of CQ (100 µM) or MG132 (10 µM) to inhibit the lysosomal or proteasomal functions, respectively. Expression of RHOA mutants was analyzed by anti-myc western blotting. (See Fig. S5).

B, Inhibiting autophagy sequestration in A549 cells by *ATG5* or *p62* depletion stabilized the active but not the inactive RHOA mutant. Control, *ATG5*, or *p62* shRNA-transduced-A549 cells were transfected with the RHOA mutants, and treated with CHX (20 µg/mL) for 57 h. Equal protein loading was verified by anti-TUBULIN immunoblotting. The data are representative of at least 3 independent experiments. (See Fig. S6A–B).

C, The ubiquitin-binding protein p62/SQSTM1 acts as a receptor that targets the active RHOA to autophagy. Ubiquitinated RHOA species (gray arrowheads) formed a complex with p62 and LC3-II in CQ-treated A549 cells.

D, p62 affects RHOA localization. Left: RHOA colocalized with p62, LC3-II, and LAMP1 upon autophagy inhibition by CQ. Right: decreasing p62 levels by shRNA reduced colocalization of RHOA with LC3-II and rescued RHOA localization at the plasma membrane of CQ-treated cells.

Figure 5. Autophagy defects disturb the clustering of active RHOA at the midbody during cytokinesis.

A, Confocal images of cytokinetic $a3^{-/-}$ PCT cells showing that RHOA failed to localize to midbody (arrowhead) and instead accumulated within autolysosomes (LC3 and LAMP1 positive). *Inset:* RHOA-positive vesicles were not degraded and accumulated within the luminal space of autolysosomes.

B, *ATG5* depletion in A549 tumor cells caused aberrant RHOA diffusion along the cell cortex during cytokinesis. RHOA, normally detected in a narrow zone at midbody of control cells, accumulated within a looser equatorial zone (arrows) and outside (arrowheads) of cleavage furrow of *ATG5*-depleted cells. (See Fig. S6A and S7).

C, RHOA staining at similar stages of furrowing in *control* (left) and *ATG5*-depleted (right) A549 cells. Representative intensity profile that measures RHOA zone width along the cell edge (middle).

D, The increases in the RHOA zone width ($P=5.34 \times 10^{-8}$) and RHOA intensity (area under curve, $P=0.000266995$) reflect a net increase in RHOA activation at equatorial region of *ATG5*-depleted cells. Results are mean \pm SD; n=15.

E, Compared to WT cells, *Atg5*^{-/-} MEF cells showed severe RHOA diffusion over the entire cell surface, ectopic furrowing during cytokinesis, as well as enlarged nuclei and cell morphology, and enhanced F-ACTIN polymerization.

Figure 6. Autophagy defects cause genomic instability in lung cancer cells.

A, Persistent ectopic furrowing as *ATG5*-depleted A549 cells entered cytokinesis. Phase-contrast images of control and *ATG5*-depleted A549 cells were acquired at the indicated times (h:min; Movie S6). Virtually all control cells showed normal compact furrowing during cytokinesis (85%; n=100, upper inset), whereas the majority (52%; $P=2.8 \times 10^{-19}$; n=50) of telophase *ATG5*-depleted cells exhibited unstable and loose furrowing. The black arrowheads indicate ectopic furrows and the bar marks the width of the equatorial furrow.

B, Representative picture of a telophase *ATG5*-depleted cell that exhibited unstable furrowing, with numerous cortical constrictions and blebs (arrowheads), in contrast to the unique and compact furrow of a control cell. (See Fig. S7).

C, Defects at the stage of autophagosome formation (*ATG5* or *ATG7* shRNA) or the recruitment of autophagy substrates (*p62* shRNA) resulted in a seven- to ten-fold increase of multinucleate cells compared with *control* shRNA-transduced cells. The different autophagy defects are indicated on the x axis (n=900). The y axis shows the percentage of multinucleate cells. (See Fig. S6C).

D, Frequency of whole chromosome gains (black) and losses (grey) in *control*, *ATG5*-depleted, and *p62*-depleted A549 cells (n = 7). Chromosome numbers are indicated on the x axis. Note that the chromosomal gains or losses occurred with low frequency in the autophagy-competent A549 tumor cells and were limited to fewer chromosomes in comparison with *ATG5*-depleted cells and *p62*-depleted cells, which showed widespread chromosomal gains and losses in nearly all of the chromosomes. Chromosome 2 loss (n=7) and chromosome 19 gain (n=5) were recurrent in *p62*-depleted A549 cells.

Figure 7. Correlation between RHOA protein levels and autophagy in human lung cancers.

A, Immunoblotting of NSCLC samples (T, tumor: early stage n=4; late stage n=4; see Table S1) versus normal peritumoral tissues (N, normal) using the indicated antibodies. p62 serves as a positive control for autophagy impairment (36), and ACTIN as a loading control. Similar *RHOA* mRNA levels in tumor and normal tissues (right panel, not statistically significant).

B, Immunohistochemical staining revealed a high overexpression of RHOA and p62 in late stages of NSCLC. In line with *a3^{-/-}* cell results (Fig. 3), the defect in lung cancer samples was a defect in autophagosome degradation with the concomitant accumulation of the three autophagy substrates LC3, p62, and active RHOA (RHOA recruitment to intracellular cell membranes; and downstream \oplus -MLC).

C, Proposed model by which autophagy sequesters and degrades the active RHOA that would otherwise diffuse from midbody to flanking zones. Together with RHO GEF, autophagy seems essential to confine RHOA activation at midbody, allowing the assembly of a unique and compact contractile ring, for successful cytokinesis and faithful genome inheritance.

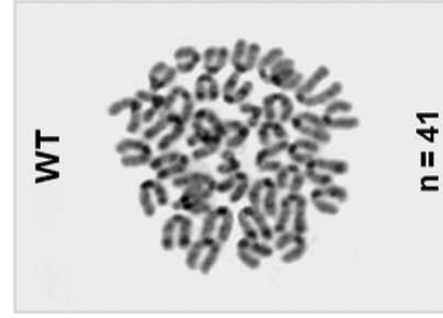
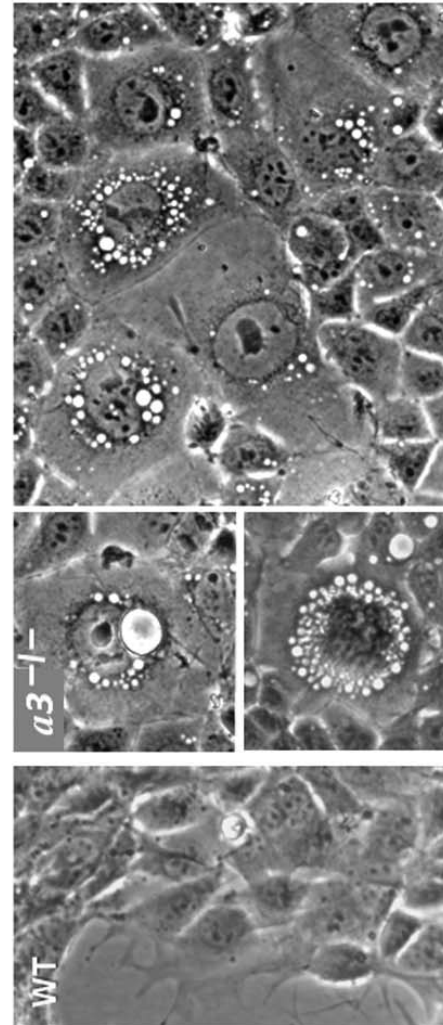
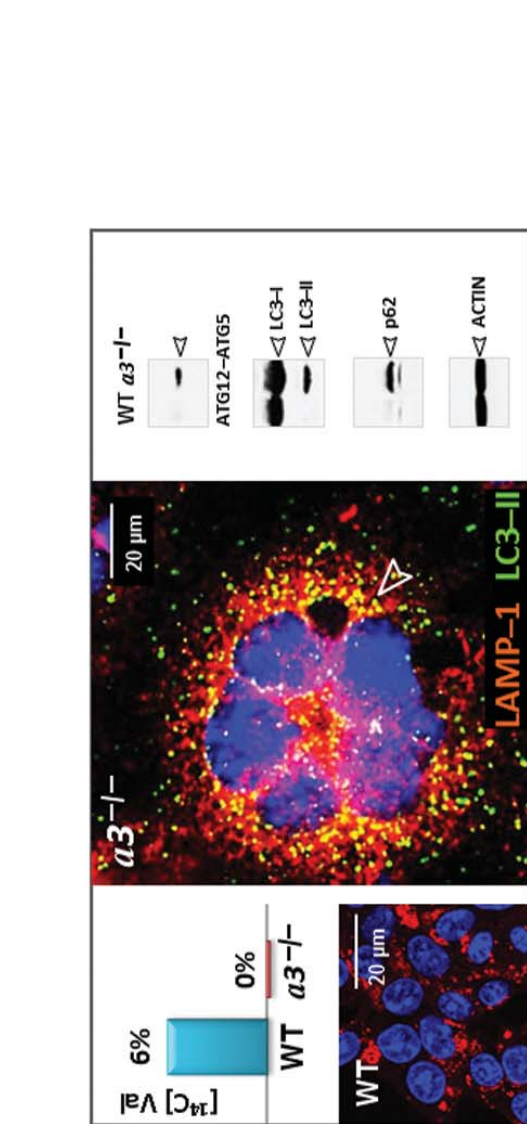
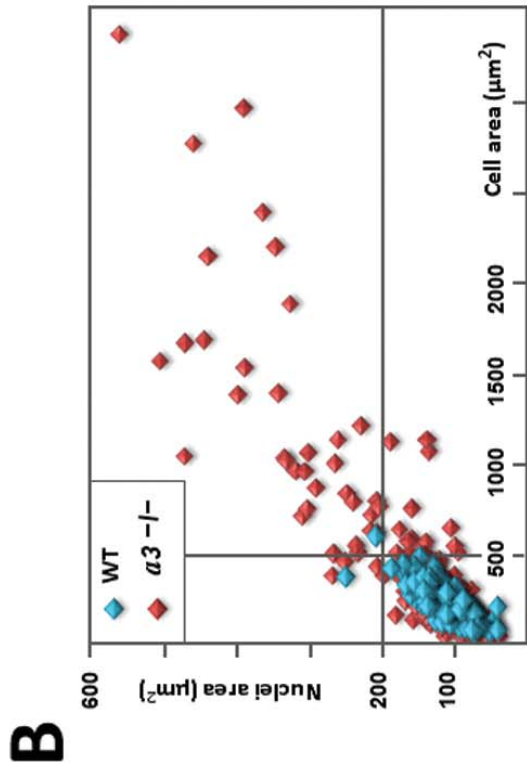
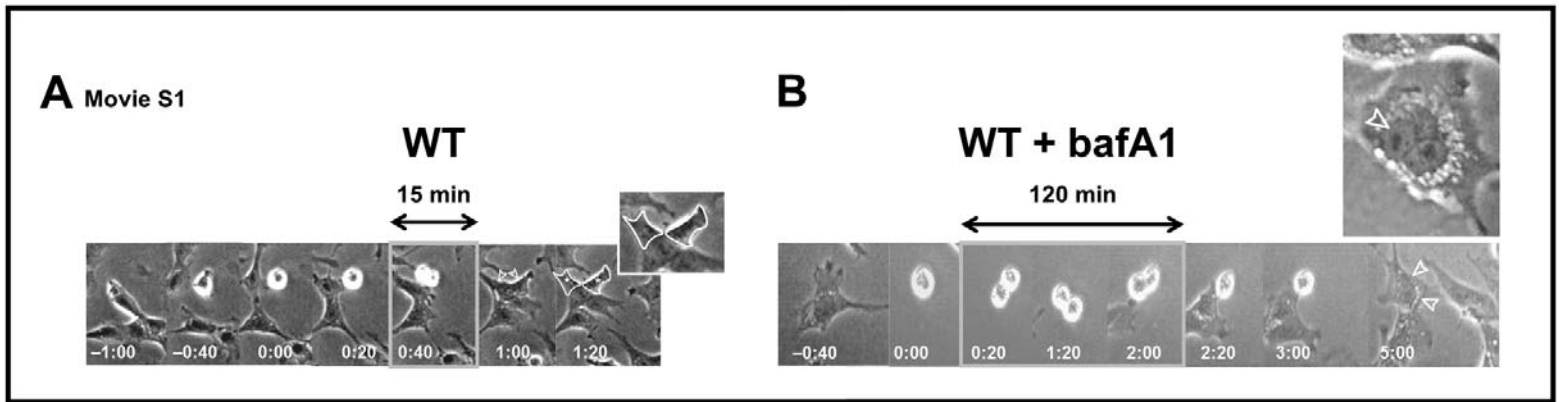


Figure 1 – Belaid *et al.* 2013

WT



V-ATPase $\alpha 3^{-/-}$

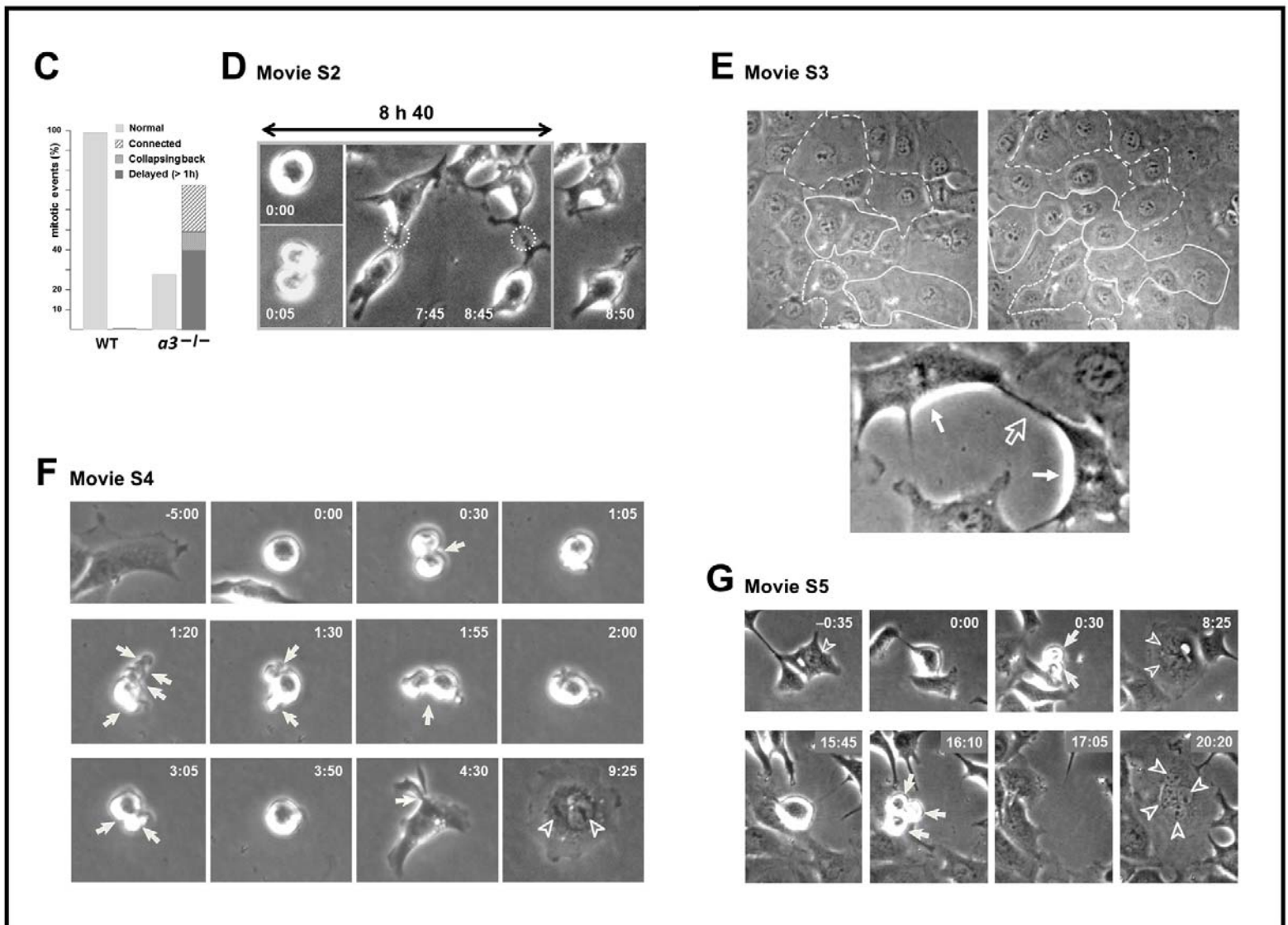


Figure 2 – Belaid *et al.* 2013

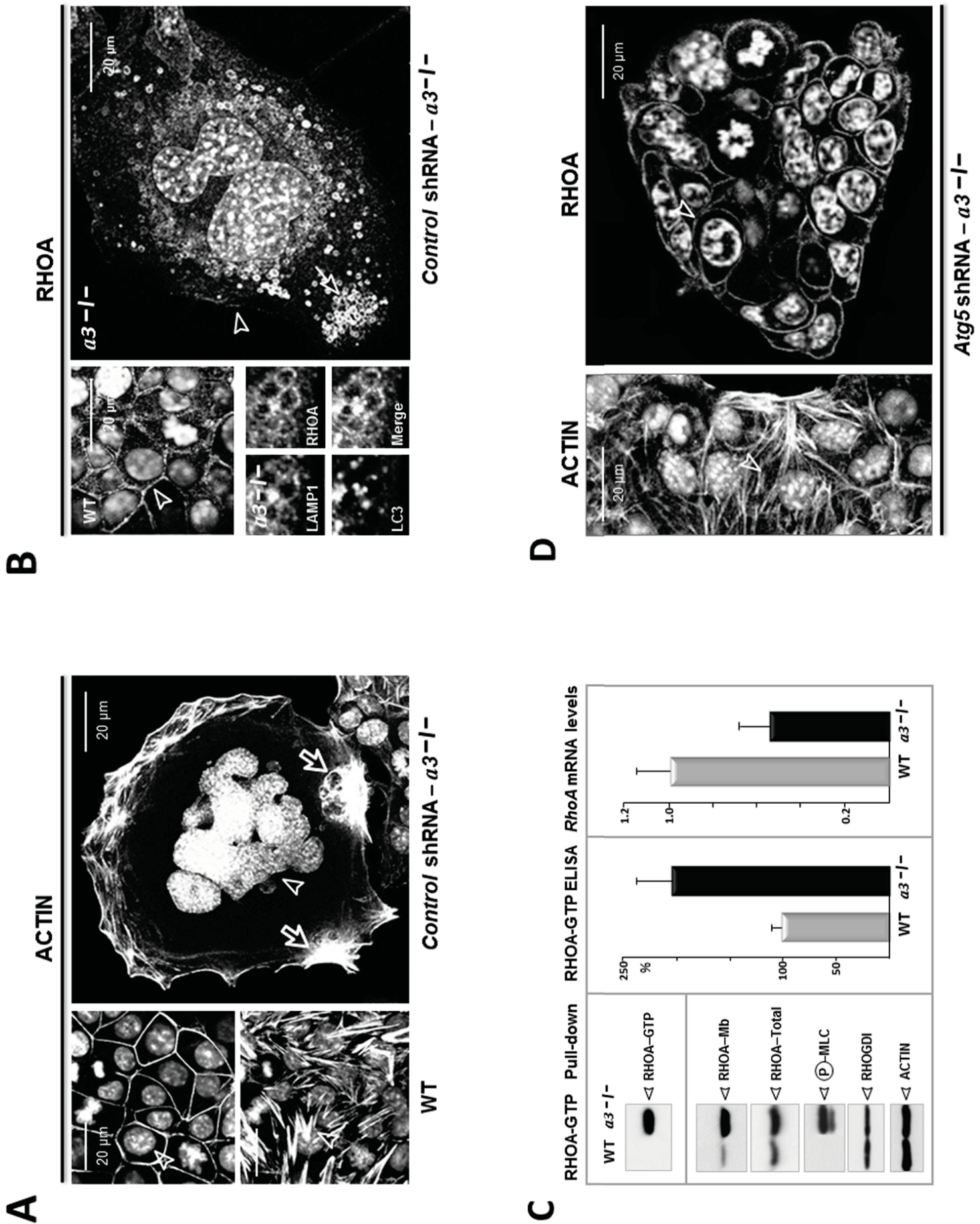


Figure 3 – Belaid *et al.* 2013

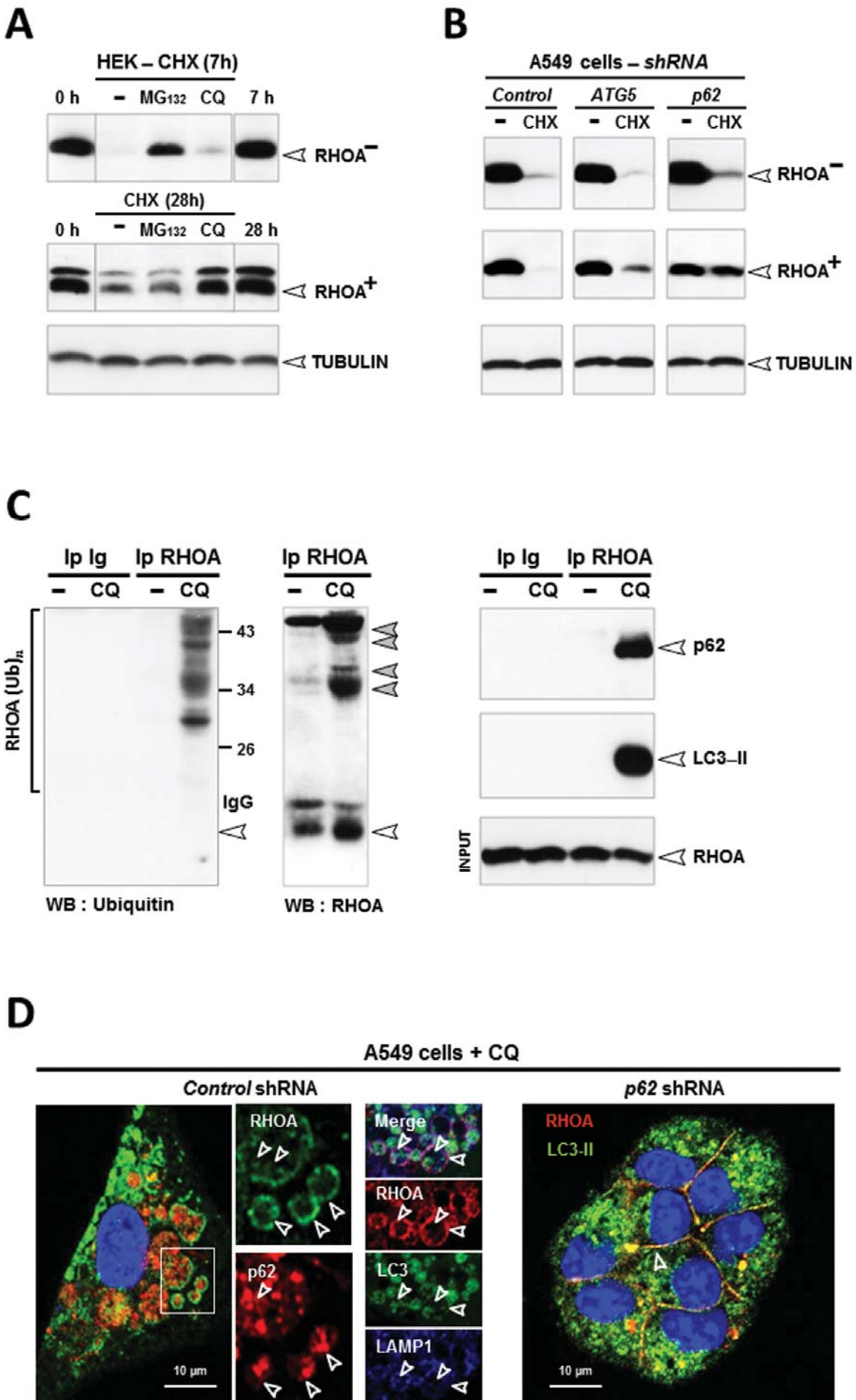


Figure 4 – Belaid *et al.* 2013

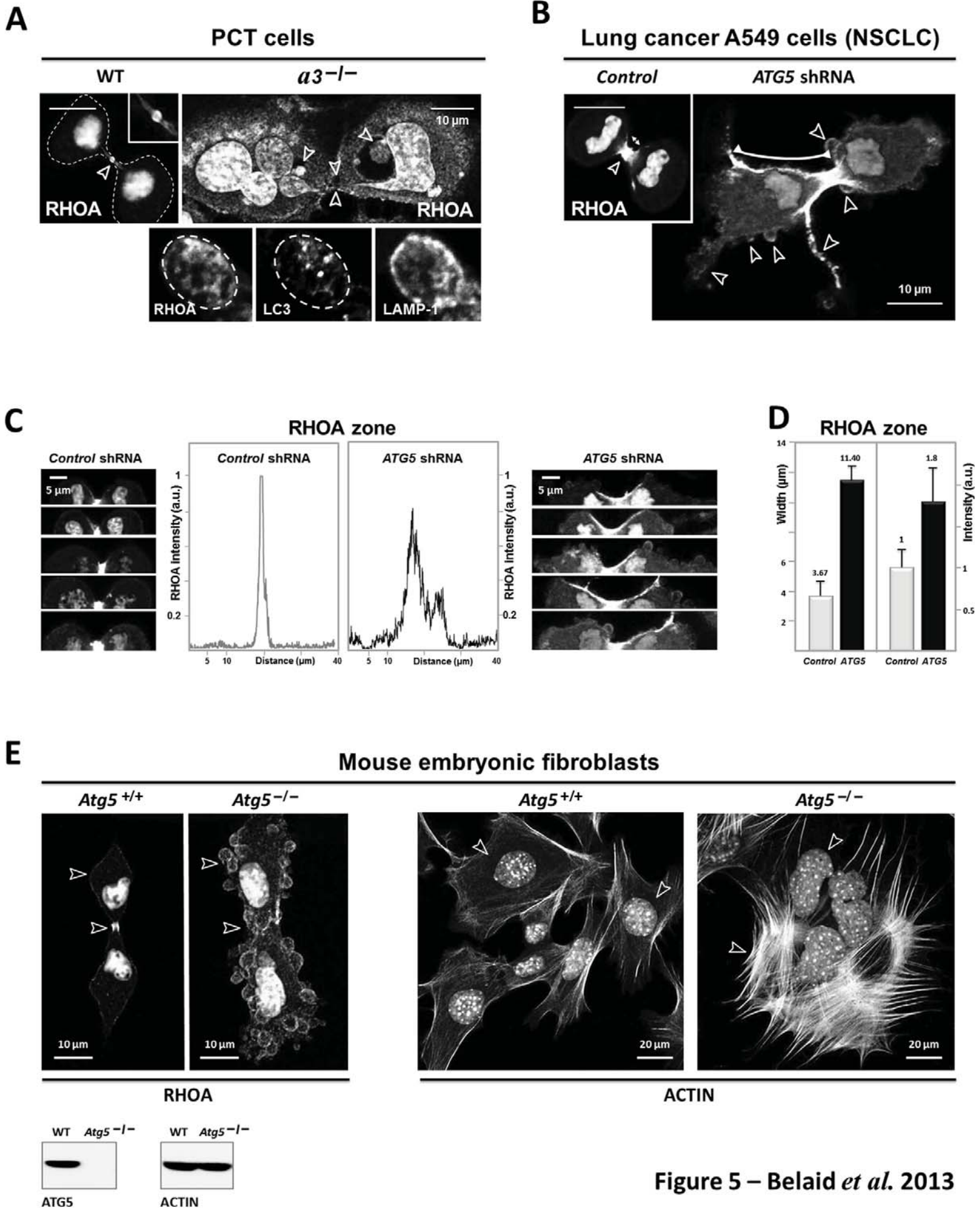


Figure 5 – Belaid *et al.* 2013

A Lung cancer A549 cells (NSCLC)

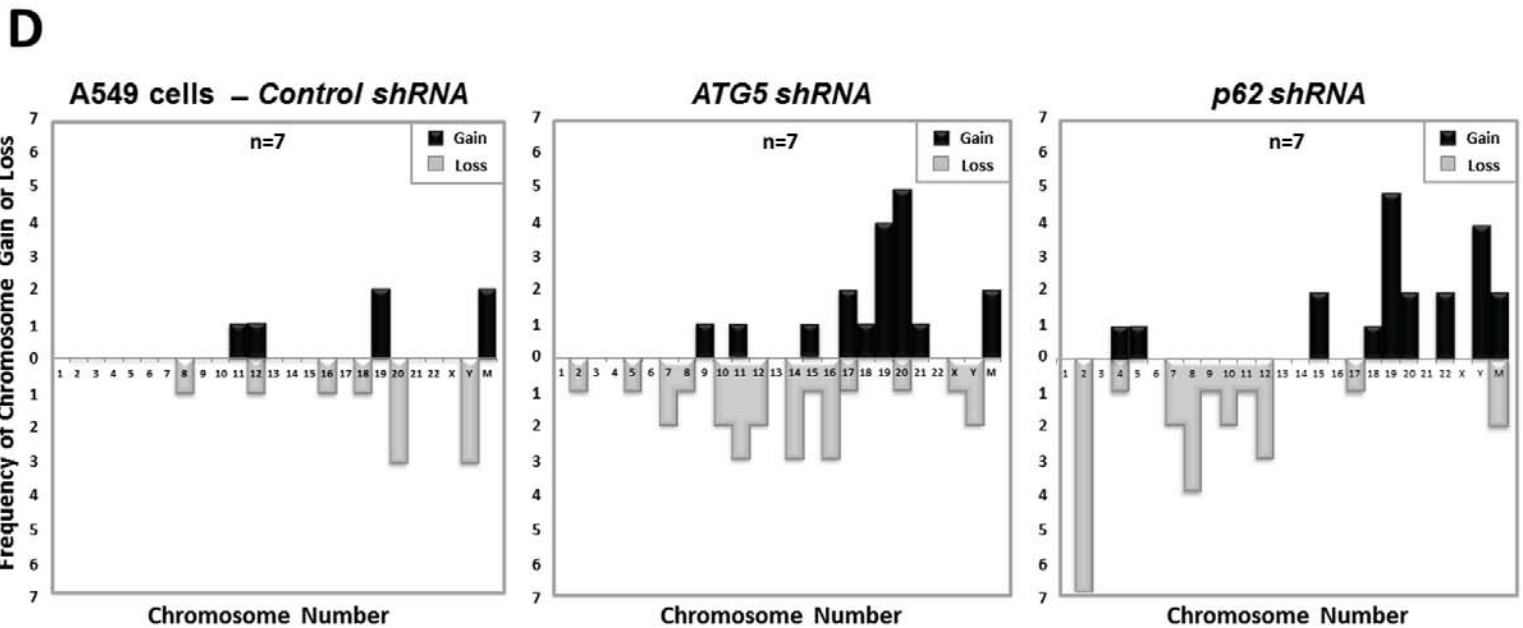
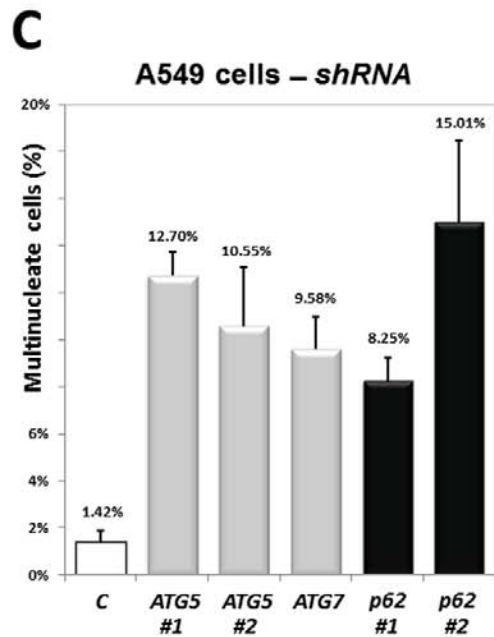
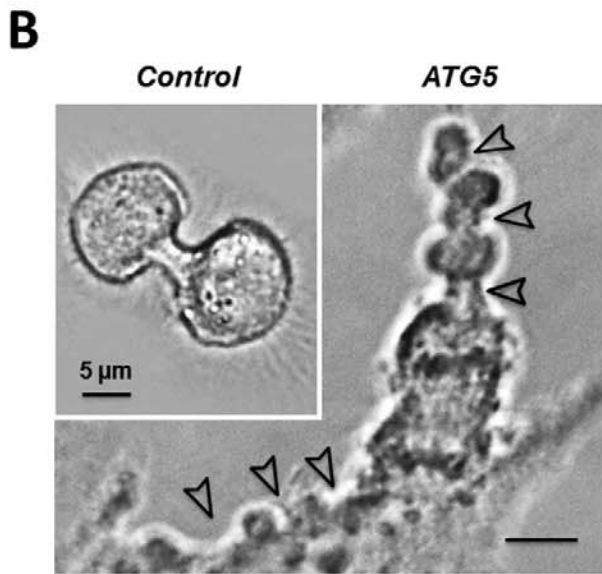
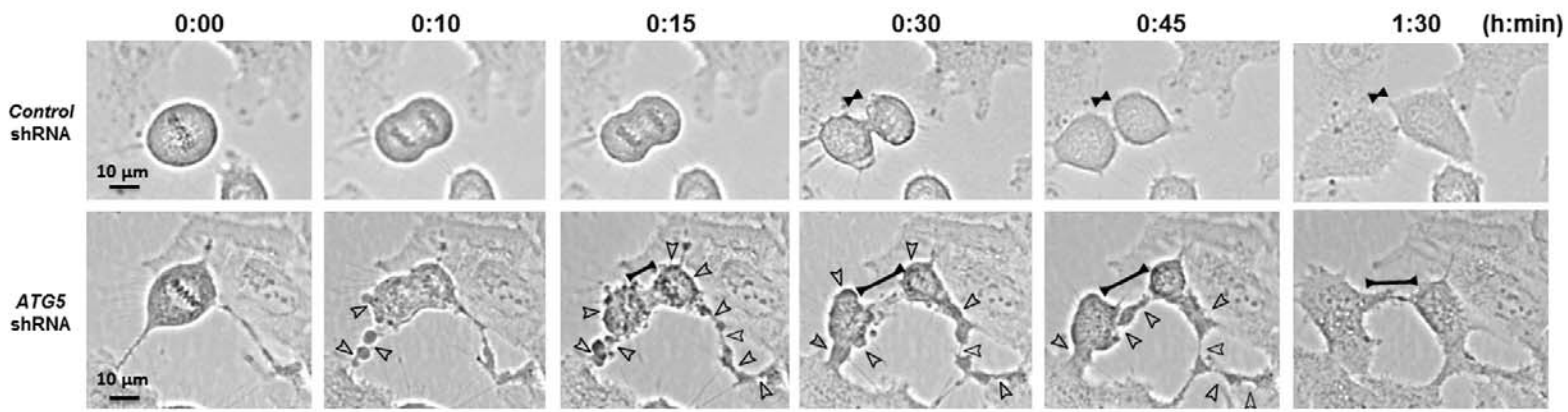
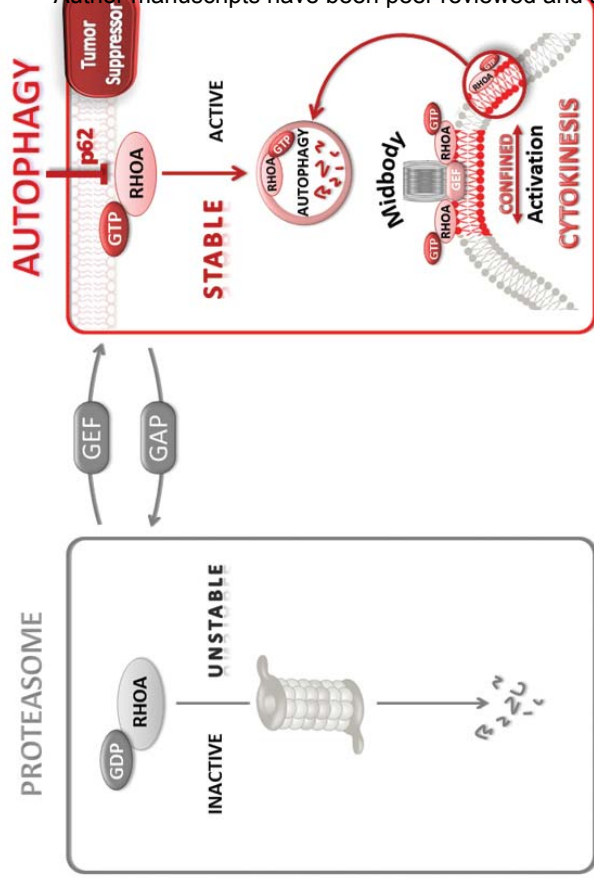
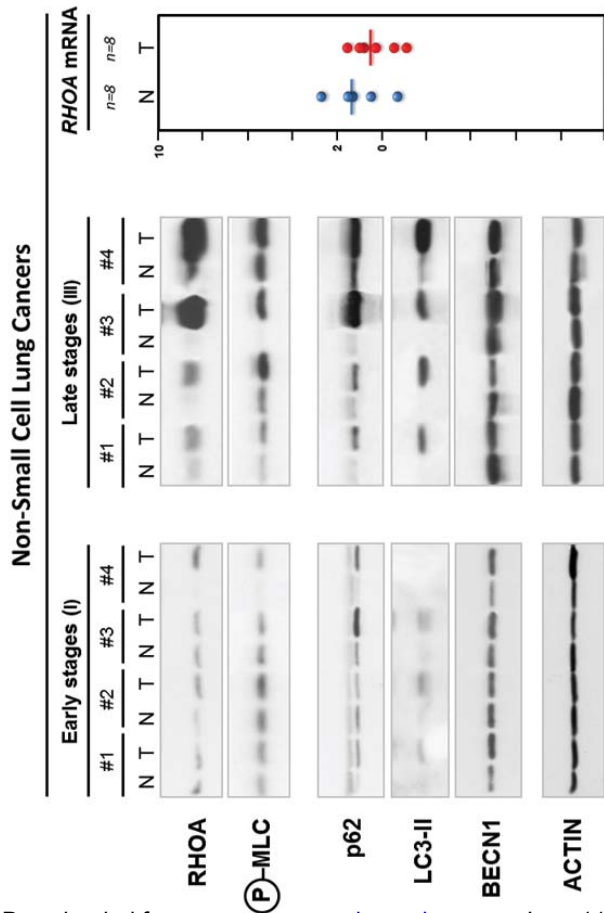


Figure 6 – Belaid et al. 2013

C



A



B

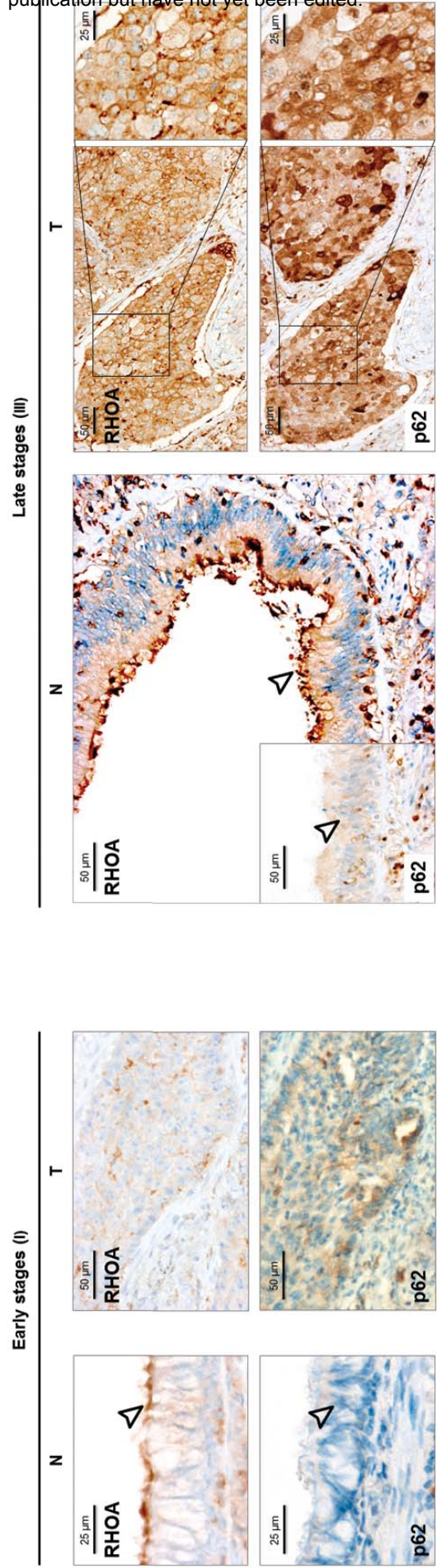


Figure 7 – Belaid et al. 2013